ACKNOWLEDGEMENTS

Numerous individuals, firms, and government agencies from the ground-water, petroleum, and logging industries in Texas and several other states contributed to the success of this study. They provided well files, rig time, logging services, technical advice, and logistical support valued in excess of $2,000,000. Without their assistance, the project would never have been completed. I want to acknowledge and say thank you to everyone who contributed to the study . My apology to anyone whom I have overlooked.

Special thanks are due to the Board of the Texas Water Development Board for funding the study and to the staff of the TWDB for their encouragement, patience, and assistance. David Thorkildsen initiated the whole process in 1986, when he contacted me regarding an in-house logging school for the TWDB. Since the submittal of the grant proposal in 1986, Henry Alvarez and Tommy Knowles have been very helpful with various aspects of the grant. Bob Bluntzer, serving as contract manager, was a constant source of encouragement. He provided valuable technical and logistical assistance. Phil Nordstrum assisted with deciphering water analyses. Marc Berryman and Paul McElhaney plotted the TDS-Cw graphs in Volume II. Doug Crim logged a number of wells.

One of the main objectives of the project was to evaluate the applicability of new logging technology to ground-water studies. Critical to the success of this goal was access to uncased boreholes in different aquifers throughout the state. Several drilling contractors were gracious enough to provide rig time to log eleven boreholes: Alsay, Inc. (Harl Barlitt and A.C. England), Layne Western (James Crouch, Jack Waldron, Don Campbell, Otis Larson, and David Bardsley), McKinley Drilling (Don, Murray, and Ike Mc Kinley), and J.L. Myers Co. (Joe Dillard and Kenneth Watson). These contractors also contributed the majority of the well files used to construct the data base in Volume II. Marion Striegler and his TWDB drilling crew drilled several test holes that were critical to the study. The Edwards Underground Water District (Diane Poteet and John Hoyt) provided rig time, access to boreholes, and logging services for five wells at New Braunfels and San Marcos.

Also critical to the success of the study was the assistance provided by several logging companies: Bee-Line Services (Gerald Bauer), Comprobe

(Bill Hawkins), Halliburton (Dan Arnold), Schlumberger and Schlumberger Doll-Research (Georger Coates and Stefan Luthi), Tejas Well Logging (T.C. and Mike Largent), and USGS (Ticie Taylor). These companies provided logging services and valuable technical assistance.

Well files used to construct the data base in Volume II, some of the logging examples in Voume I, and various types of other information were provided by the following: Alsay, Inc., Atlas Wireline, BP (Mark Alberty), Tom Cliett (El Paso Water District), CoLog, Crowell Drilling Co., Edwards Underground Water District, J.F. Fountaine and Associates, Bill Goodsey, Jr. (RRC), Jim Griffith, William F. Guyton Associates, Ron Hardin and Associates, Dusty Jeter (TWC), John Doveton (Kansas Geological Survey), Lanford Drilling, Joe Reed, Alvin Schultz, StrataData, W.K. Sumners (Albuquerque Public Works Department), Welenco (Joe Newman), John Williamson Drilling, and Wisenbaker, Fix, and Associates.

ResTech, Charlie Harrison in particular, provided computer processing of logs during the first half of the project. ResTech was very supportive of the project and I want to especially thank Bob Truman and Bill Johnson. Terrasciences provided their TerraLog software, which was invaluable in processing several of the logs found in Volume I. The Terrasciences staff, especially John Sherrill, provided considerable technical support.

Encouragement and technical assistance was also provided by the staff of the Texas Water Commission and the Railroad Commission, as well as Andrew Williams, Jr., Don Jorgenson (USGS), Baroid Drilling Fluids, John Davis (Kansas Geological Survey), Lee Etnyre (ARCO), John Hem (USGS), and Leroy Goodson (TGWA). Emma McPherson (USGS) analyzed several water samples which were very important to evaluating the quality of water analyses in Texas.

Over the course of the project, a number of ACU students (Julie Howard, Lynette Dunn, Carole Harris, Lisa McLeroy, Becky Cundiff, Elsa Cavazos, Summer Richards, Lori Blue, and Patricia Hart) provided able part-time assistance with secreterial and data processing tasks. Julie Howard later worked full-time and did an excellent job with the loin's share of the typing and data manipulation. My wife, Gail, stepped in at the home stretch to assist in finishing the manuscript. Our children, Aaron, Nathan, and Daniel, did an excellent job as office organizers (or more precisely disorganizers).

My thanks also to ACU for administering the grant; especially to Shirley Riley for keeping the books. Bill Hilton, Vice President of Finance, and Glen Davis, Dean of the College of Natural and Applied Sciences, were very supportive.

Finally, I want to thank those who have reviewed all or parts of the manuscript. They have all provided numerous comments that have improved the clarity and accuracy of the report. Bob Bluntzer and James Carter (UTD) have suffered through the entire document. Doug Hilchie reviewed all the logging chapters and Bill Powell reviewed some of them. John Hem reviewed the chapters dealing with water analyses. Lee Etnyre reviewed the chapter on curve-fitting routines. Lynette Dunn reviewed the report for typographical and grammatical errors.

Dedicated to
Robert (Bob) P. Alger
May 4, 1913 - March 1, 1989

This report is dedicated to the memory of Bob Alger. Bob was an integral part of this study from its inception until the day of his death. Bob, along with his wife Louise, were very supportive and hospitable during the two years Bob worked on the project. Bob was instrumental in the success of the project.

Bob's career in log interpretation spanned six decades. He was hired conditionally by Schlumberger after his graduation from Missouri School of Mines in 1938. He stayed with Schlumberger until his retirement. Bob's career coincided with the period during which quantitative log interpretation evolved and he was instrumental in the development of several interpretation techniques. He authored over two dozen technical papers and was granted five patents on logging techniques.

Although Bob's career focused on pertroleum logging, he had a long-standing interest in the application of logging technology to ground-water studies. In 1966 he authored one of the first papers on the subject, "Interpretation of Electric Logs in Fresh Water Wells in Unconsolidated Formations". The paper is still an important reference on the subject. After his retirement in 1976, Bob pursued his interest in ground-water logging with ResTech.

When this author met Bob in 1986 , he was putting the finishing touches on a follow-up paper to his 1966 publication. He was seeking additional data on ground-water logging and jumped at the chance to participate in this study. Bob recognized the importance of ground-water resources to the citizens of Texas and wanted to close out his career contributing to the subject.

It was a privilege to work with Bob Alger during the first two years of this project. He had a keen mind and was a diligent, meticulous researcher. Bob was a gentleman of high integrity and a good teacher. He will be sorely missed.

BOREHOLE GEOPHYSICAL TECHNIQUES FOR DETERMINING THE WATER QUALITY AND RESERVOIR PARAMETERS OF FRESH AND SALINE WATER AQUIFERS IN TEXAS

VOLUME I

LIST OF TABLES

LIST OF FIGURES

BOREHOLE GEOPHYSICAL TECHNIQUES FOR DETERMINING THE WATER QUALITY AND RESERVOIR PARAMETERS OF FRESH AND SALINE WATER AQUIFERS IN TEXAS

VOLUME II

TEXAS WATER DEVELOPMENT BOARD
REVIEW COPY

Preliminary Draft Manuscript Report
September 1992

BOREHOLE GEOPHYSICAL TECHNIQUES FOR DETERMINING THE WATER QUALITY AND RESERVOIR PARAMETERS OF FRESH AND SALINE WATER AQUIFERS IN TEXAS

VOLUME [illegible] — INTERPRETATIONS

BY

[illegible]
ASSISTANT PROFESSOR, [illegible]
ABILENE CHRISTIAN UNIVERSITY

[illegible] Texas Water Development Board
[illegible]
[illegible] Christian University
[illegible]

THIS IS A PRELIMINARY DRAFT WHICH IS SUBJECT TO REVISION

Add to, or modify, Title page

(Should carry this to the next & other more -- this is the "official" title page)

suggest add something like this to Title page)

Some of the materials in this report are taken with permission from copyrighted sources. Such materials may not be again reproduced without further permissions from the respective copyright holders.

IMPORTANT Caution: Both the author and publisher need to protect themselves in this. Do not hang up on precisely how it's worded. -- but it's important that the author and publisher keep a permanent, written proof of these permissions.

Check needs to be made that every copyrighted item is properly labeled as such in this report & that permissions are on file.

(Requires a search through the prefatory pages of every document regardless of where from, as well as looking at each item.)

John White
10-22-92

ACKNOWLEDGEMENTS

Numerous individuals, firms, and government agencies from the ground-water, petroleum, and logging industries in Texas and several other states contributed to the success of this study. They provided well files, rig time, logging services, technical advice, and logistical support valued in excess of $2,000,000. Without their assistance, the project would never have been completed. I want to acknowledge and say thank you to everyone who contributed to the study . My apology to anyone whom I have overlooked.

(TWDB) Special thanks are due to the Board of the Texas Water Development Board for funding the study and to the staff of the TWDB for their encouragement, patience, and assistance. David Thorkildsen initiated the whole process in 1986, when he contacted me regarding an in-house logging school for the TWDB. Since the submittal of the grant proposal in 1986, Henry Alvarez and Tommy Knowles have been very helpful with various aspects of the grant. Bob Bluntzer, serving as contract manager, was a constant source of encouragement. He provided valuable technical and logistical assistance. Phil Nordstrum assisted with deciphering water analyses. Marc Berryman and Paul McElhaney plotted the TDS-Cw graphs in Volume II. Doug Crim logged a number of wells.

One of the main objectives of the project was to evaluate the applicability of new logging technology to ground-water studies. Critical to the success of this goal was access to uncased boreholes in different aquifers throughout the state. Several drilling contractors were gracious enough to provide rig time to log eleven boreholes: Alsay, Inc. (Harl Barlitt and A.C. England), Layne Western (James Crouch, Jack Waldron, Don Campbell, Otis Larson, and David Bardsley), McKinley Drilling (Don, Murray, and Ike Mc Kinley), and J.L. Myers Co. (Joe Dillard and Kenneth Watson). These contractors also contributed the majority of the well files used to construct the data base in Volume II. Marion Striegler and his TWDB drilling crew drilled several test holes that were critical to the study. The Edwards Underground Water District (Diane Poteet and John Hoyt) provided rig time, access to boreholes, and logging services for five wells at New Braunfels and San Marcos.

Also critical to the success of the study was the assistance provided by several logging companies: Bee-Line Services (Gerald Bauer), Comprobe

(Due to printing convention, all right-hand pages are odd-numbered; left pages numbers will work out.)

, and also the U.S. Geological Survey -- USGS (Ticie Taylor),

(Bill Hawkins), Halliburton (Dan Arnold), Schlumberger and Schlumberger Doll-Research (Georger Coates and Stefan Luthi), Tejas Well Logging (T.C. and Mike Largent) ~~and USGS (Ticie Taylor)~~. These companies provided logging services and valuable technical assistance.

Well files used to construct the data base in Volume II, some of the logging examples in Voume I, and various types of other information were provided by the following: Alsay, Inc., Atlas Wireline, BP (Mark Alberty), Tom Cliett (El Paso Water District), CoLog, Crowell Drilling Co., Edwards Underground Water District, J.F. Fountaine and Associates, Bill Goodsey, Jr. (~~BWC~~), Jim Griffith, William F. Guyton Associates, Ron Hardin and Associates, Dusty Jeter (~~BWC~~), John Doveton (Kansas Geological Survey), Lanford Drilling, Joe Reed, Alvin Schultz, StrataData, W.K. Sumners (Albuquerque Public Works Department), Welenco (Joe Newman), John Williamson Drilling, and Wisenbaker, Fix, and Associates.

ResTech, Charlie Harrison in particular, provided computer processing of logs during the first half of the project. ResTech was very supportive of the project and I want to especially thank Bob Truman and Bill Johnson. Terrasciences provided ~~their~~ TerraLog software, which was invaluable in processing several of the logs ~~found~~ in Volume I. The Terrasciences staff, especially John Sherrill, provided considerable technical support.

Encouragement and technical assistance ~~was~~ were also provided by the staff of the Texas Water Commission and the Railroad Commission, as well as Andrew Williams, Jr., Don Jorgenson (USGS), Baroid Drilling Fluids, John Davis (Kansas Geological Survey), Lee Etnyre (ARCO), John Hem (USGS), and Leroy Goodson (TGWA). Emma McPherson (USGS) analyzed several water samples which were very important to evaluating the quality of water

Abilene Christian University (ACU)

of the project, a number of ~~ACU~~ students (Julie Carole Harris, Lisa McLeroy, Becky Cundiff, Elsa ards, Lori Blue, and Patricia Hart) provided able part- creterial and data processing tasks. Julie Howard -time and did an excellent job with the lion's share of the typing and data manipulation. My wife, Gail, stepped in at the home stretch to assist in finishing the manuscript. Our children, Aaron, Nathan, and Daniel, did an excellent job as office organizers (or more precisely disorganizers).

~~iii~~
iv

My thanks also to ACU for administering the grant; especially to Shirley Riley for keeping the books. Bill Hilton, Vice President of Finance, and Glen Davis, Dean of the College of Natural and Applied Sciences, were very supportive.

Finally, I want to thank those who have reviewed all or parts of the manuscript. They have all provided numerous comments that have improved the clarity and accuracy of the report. Bob Bluntzer and James Carter (UTD) have suffered through the entire document. Doug Hilchie reviewed all logging chapters and Bill Powell reviewed some of them reviewed the chapters dealing with water analyses. chapter on curve-fitting routines. Lynette Dunn rev. typographical and grammatical errors.

Dedicated to
Robert (Bob) P. Alger
May 4, 1913 - March 1, 1989

This report is dedicated to the memory of Bob Alger. Bob was an integral part of this study from its inception until the day of his death. Bob, along with his wife Louise, were very supportive and hospitable during the two years Bob worked on the project. Bob was instrumental in the success of the project.

Bob's career in log interpretation spanned six decades. He was hired conditionally by Schlumberger after his graduation from Missouri School of Mines in 1938. He stayed with Schlumberger until his retirement. Bob's career coincided with the period during which quantitative log interpretation evolved and he was instrumental in the development of several interpretation techniques. He authored over two dozen technical papers and was granted five patents on logging techniques.

Recommend keep this as a right-hand page, = odd-numbered page number, even if it means that its facing page is blank)

Although Bob's career focused on petroleum logging, he had a long-standing interest in the application of logging technology to ground-water studies. In 1966 he authored one of the first papers on the subject, "Interpretation of Electric Logs in Fresh Water Wells in Unconsolidated Formations". The paper is still an important reference on the subject. After his retirement in 1976, Bob pursued his interest in ground-water logging with ResTech.

When this author met Bob in 1986 , he was putting the finishing touches on a follow-up paper to his 1966 publication. He was seeking additional data on ground-water logging and jumped at the chance to participate in this study. Bob recognized the importance of ground-water resources to the citizens of Texas and wanted to close out his career contributing to the subject.

It was a privilege to work with Bob Alger during the first two years of this project. He had a keen mind and was a diligent, meticulous researcher. Bob was a gentleman of high integrity and a good teacher. He will be sorely missed.

TABLE OF CONTENTS

BOREHOLE GEOPHYSICAL TECHNIQUES FOR DETERMINING THE WATER QUALITY AND RESERVOIR PARAMETERS OF FRESH AND SALINE WATER AQUIFERS IN TEXAS

VOLUME I

LIST OF TABLES (CONTINUED)

LIST OF TABLES (CONTINUED)

LIST OF TABLES

LIST OF TABLES

LIST OF TABLES (CONTINUED)

LIST OF TABLES (CONTINUED)

LIST OF FIGURES

LIST OF FIGURES (CONTINUED)

LIST OF FIGURES (CONTINUED)

LIST OF FIGURES (CONTINUED)

LIST OF FIGURES (CONTINUED)

LIST OF PLATES

SCOPE OF THIS STUDY

Chapter 1

Introduction

Texas is becoming a water-short state, and techniques are needed to accurately assess the quality and quantity of its fresh and saline ground-water resources. In determining the water quality of an aquifer there is certainly nothing equal to a laboratory analysis of the water. Unfortunately, however, water samples are frequently not available. This is true for fresh as well as brackish and saline water aquifers throughout Texas. Aquifers have not been sampled for a variety of reasons:

1. In most water wells only the screened interval is sampled. Financial constraints and/or lack of proper planning result in other water-bearing intervals not being sampled.

2. Most water supply wells are deliberately not drilled deep enough to penetrate brackish and saline water aquifers.

3. Oil wells penetrate aquifers of all salinities, but water samples are rarely taken. Samples that are taken are often of questionable value due to sampling and/or testing procedures.

In the absence of a water analysis, water quality can be estimated from borehole geophysical logs. This is the best, and usually the only, alternative. Relative to water analyses, logging data are abundant and easily accessible. In Texas tens of thousands of geophysical logs are available in the files of various government agencies, commercial log libraries, ground-water consulting firms, water well drilling contractors, and oil companies.

Data such as pump tests, core analyses, and sample descriptions for quantifying aquifer properties (e.g. lithology, porosity, and bed thickness) are scarce. Again, geophysical logs are the best data base.

Water conductivity (C_w) and total dissolved solids (TDS) are the water quality parameters of chief concern to the ground-water industry. Total dissolved solids is the most important and most often cited parameter, since it serves as the basis for drinking water standards (Table 1-1). Water

TABLE 1-1. GROUND-WATER CLASSIFICATION BASED ON TOTAL DISSOLVED SOLIDS

Class	Total Dissolved Solids (mg/l)	Examples of Use
Fresh Water	Zero to 1000	Drinking and all other uses
Slightly Saline Water	More than 1000 to 3000	Drinking if fresh water is unavailable, livestock watering, irrigation, industrial, mineral extraction, oil and gas production
Moderately Saline Water	More than 3000 to 10,000	Potential future drinking and limited livestock watering and irrigation if fresh or slightly saline water is unavailable; Industrial, mineral extraction, oil and gas production
Very Saline Water	More than 10,000 to 100,000	Mineral extraction, oil and gas production
Brine Water	More than 100,000	Mineral extraction, oil and gas production

(Modified from Freeze and Cherry, 1979 and Texas Water Commission, 1991.)

conductivity is frequently cited because it is a good indicator of total dissolved solids ~~that~~ and can be quickly and easily measured.

Determining water quality from borehole geophysical logs has long been a subject of interest to log analysts. However, most logging research has been conducted by the petroleum industry. Their efforts have concentrated on techniques to determine the resistivity (Rw) of very saline and brine waters. Little research has been conducted on applications of borehole geophysical techniques to ground-water studies and the logging problems which are unique to water and monitoring wells. Only two books have been written on ground-water logging (Keys, 1988, and Repsold, 1989), and both contain only a minimal treatment on methods of determining water quality from logs.

A few papers have addressed the subject of ground-water quality determination from logs. Significant methodology papers are Jones and Buford (1951), Turcan (1962 and 1966), Guyod (1966), Alger (1966), and Alger and Harrison (1988). Published case studies include Vonhof (1966),

Brown (1971), Dyck, et al. (1972), Emerson and Haines (1974), Evers and Iyer (1975a), MacCary (1978 and 1980), McConnell (1983, 1985, and 1989), Kwader (1982, 1984, and 1985), Hansen and Wilson (1984), Guo (1986), Fogg and Blanchard (1986), Weiss (1987), Brown (1988), Jorgensen (1989) and Repsold (1989).

Objectives

In 1987 the Texas Water Development Board entered into contract 8-483-511 with Abilene Christian University and Hughbert Collier as the principal investigator to research applications of openhole borehole geophysical techniques for characterizing ground-water resources in Texas. The project studied the following types of aquifers:

1. Aquifers with TDS's ranging from near zero to 50,000 milligrams per liter, which approaches the upper limit of water suitable for desalinization.

2. Carbonate, unconsolidated clastic, and consolidated clastic aquifers.

3. Major aquifers such as the Edwards, Gulf Coast, Carrizo-Wilcox, and Trinity.

Data on existing wells was collected from the files of water well drilling contractors, ground-water consultants, government agencies, and oil companies. Twenty-one new wells were logged during the course of this study (Table 1-2). Drilling contractors across the state provided free access to the wells and rig time. Logging service companies provided free or discounted services. A variety of logging tools, from state-of-the-art petroleum-type logs to simple, older ground-water logging suites, was run in each well.

The objectives of the study were:

1. To evaluate the applicability of various logging tools to ground-water studies.

2. To evaluate existing borehole geophysical techniques for determining water quality and aquifer parameters.

TABLE 1-2. WELLS LOGGED FOR THIS STUDY

County	Well Name	Drilling Contractor
Cameron	Public Test Site F BY 88-59-410	Texas Water Development Board
Cameron	Public Test Site F BY 88-59-411	Texas Water Development Board
Comal	EUWD New Braunfels A-1 DX 68-23-616	Layne Western
Comal	EUWD New Braunfels B-1 DX 68-23-617	Layne Western
Comal	EUWD New Braunfels C-1 DX 68-23-619	Layne Western
Ellis	Bristol #2	J.L. Myers
Falls	Tri County WSC #5	J.L. Myers
Fannin	Ladonia #2	J.L. Myers
Grayson	Van Alstyne #3	J.L. Myers
Harris	Cypress Creek #3	Alsay
Harris	Kingwood #B-3	Alsay
Harris	MUD 275 #1	Layne Western
Harris	NW Harris MUD 21 & 22 #2	Alsay
Hays	EUWD San Marcos B LR 67-01-812	Layne Western
Hays	EUWD San Marcos C LR 67-01-813	Layne Western
McClennan	Hercules RWSS #1	Alsay
McCulloch	Brady Test Hole 42-62-909	Texas Water Development Board
McCulloch	Brady Test Hole 42-62-910	Texas Water Development Board
McMullen	Fox Creek #2	McKinley
Travis	Balcones Research Center Test Well 58-35-721	Texas Water Development Board
Webb	George Strait #1	McKinley

3. To develop new borehole geophysical techniques for determining water quality and reservoir parameters.

4. To evaluate the accuracy of TDS and specific conductance measurements performed by laboratories in Texas.

5. To quantify the relationship between water conductivity and TDS for aquifers in Texas.

6. To document the differences between logging petroleum and ground-water wells.

7. To establish guidelines for logging ground-water wells.

8. To determine the differences between slimhole ground-water/environmental and petroleum logging tools.

This study focused on calculating total dissolved solids derived water conductivity values. The procedure has three two data sets (log data and a TDS-Cw relationship) and a calculate the resistivity of the formation water (Rw) from 1 outlines the procedure.

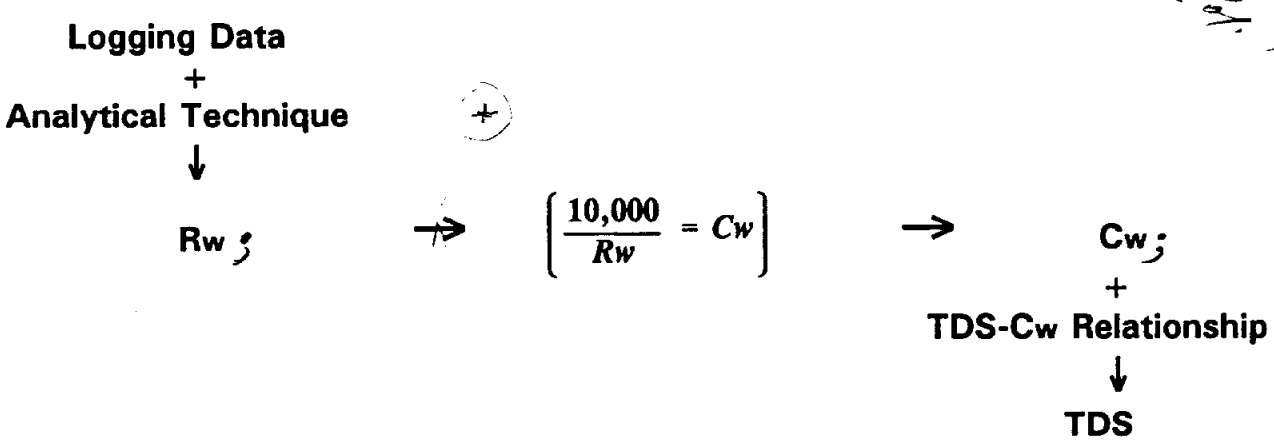

Figure 1-1. flow diagram of the three steps in calculating TDS from wireline logs.

Chapter 2 discusses water conductivity and Chapter 3 discusses total dissolved solids. Chapter 4 reviews how to establish the TDS-Cw relationship. Chapters 5 through 13 cover the acquisition and analysis of

logging data. Chapter 14 outlines the techniques to calculate water conductivity from log data. Additional supporting documentation of the basic data used in this study, including calculations and graphs, is provided in Volume II.

This study is specifically for waters that have 50,000 parts per million (ppm) or less total dissolved solids. For waters having greater than 50,000 ppm total dissolved solids, and especially for brines, modifications may need to be made to some of the following statements.

Recommend a reference to Volume II within Volume I somewhere -- this seems a good spot for it.

SPECIFIC CONDUCTANCE MEASUREMENTS

Chapter 2

Establishing a valid TDS-Cw relationship requires an accurate water conductivity measurement. This chapter contains a discussion of water conductivity, the factors controlling the measurement, a survey of how accurately laboratories in Texas measure water conductivity, and an analysis of the accuracy of computed water conductivities.

Virtually all of the water analyses examined during this study were from six laboratories: Texas Department of Health, Pope Testing, Edna Wood (formerly Microbiology Service Laboratories), United States Geological Survey (USGS), Curtis (out of business), and Texas Testing (out of business). These laboratories have analyzed most of the ground-water samples taken in Texas. The following comments, while principally addressed to water analyses from these laboratories, apply to all water analyses.

Units of Measurement

Water conductivity (Cw), also known as **specific conductance** or **specific conductivity**, is the ability of water to conduct an electric current. The unit of measurement is micromhos per centimeter (μmhos/cm) at 25° C (77° F). It is often shortened to simply micromhos (μmhos). In accordance with the International System of Units (SI) the unit of conductivity has been renamed siemens (S). A microsiemens (μS) is equal to a micromho. The term micromho still dominates the ground-water literature.

In petroleum logging literature conductivity is expressed as millimhos per meter (mmhos/m) or simply mmhos. The relationship between mmhos and μmhos is as follows:

$$mmhos/m = 10 \times \mu mhos/cm \qquad (2\text{-}1)$$

The petroleum logging community prefers to use the reciprocal of conductivity, **resistivity**. The names for the units of measurement are also "reciprocals"- mho and ohm. Resistivity is measured in ohm-meter^2 per

meter. This is usually simplified to ohm-m. The relationship between the two is as follows:

$$Resistivity\ (ohm\text{-}m) = \frac{10{,}000}{Specific\ Conductance}\ (\mu mhos/cm) \qquad (2\text{-}2)$$

Techniques for Measuring Specific Conductance

Specific conductance is usually measured in the laboratory and/or in the field with a conductivity meter. With properly calibrated equipment, a conductivity measurement will be within ±2 to ±5 percent of the actual value (Hem, 1985, p. 69). Unfortunately, the accuracy of conductivity measurements varies widely among laboratories (e.g. Summers, 1972; Moore and Kaufman, 1983). Table 2-1 and its accompanying discussion quantifies the differences for the principal, present-day ground-water laboratories in Texas.

This study found that problems exist with specific conductance measurements for a number of reasons:

1. A laboratory may not routinely and/or properly calibrate its conductivity meters.

2. A laboratory may not use suitable equipment and/or analytical techniques.

3. The Texas Department of Health and Pope Testing laboratories only consider their measurements of specific conductance to be a gross estimate, and only use such estimates as a quality control indicator for evaluating the accuracy of their total dissolved solids measurements (personal communication, Texas Department of Health and Pope Testing Laboratories, 1990).

Another possible problem with some laboratories is that they are only set up to analyze fresh waters. They therefore make no adjustments to their lab techniques on the infrequent occasions when they measure saline waters. The same calibration solution (generally 1000 mg/l KCl) and cell constant are used for all waters[1]. For high salinity waters, the accuracy of

[1] Worthington, et al. (1990) has an excellent discussion of conductivity meters and cell constants.

TABLE 2-1. COMPARISON OF SPECIFIC CONDUCTANCE MEASUREMENTS FROM VARIOUS TEXAS LABORATORIES

Sample	USGS Austin	Edna Wood	Pope Testing	%var.[1]	USGS San Antonio	Schlumberger Resistivity Meter	TWDB shaken	TWDB unshaken	%var.[2]	Mean[3]	Range[3]	Texas Department of Health Measured	%var.[4]	Texas Department of Health Average	%var.[4]	Texas Department of Health Diluted	%var.[4]
BRC 58-35-721 Travis Co. 398'																	
1a	1220	1300	1300				1179	1173	<1%	1250			-13%		-2.5%		8%
											1176-1300	1089		1219		1350	
1b	1220	1250	1200				1176	1168	<1%	1212			-10%		<1%		11%
variation between a & b	-0-	4%	8%				<1%	<1%									
Petrolero Corp. #4-3 McMullen Co. 4030'																	
2a	1620	1650	1500	-7%			1564	1503	4%	1620[5]			-9%		<-1%		8%
					1603	1661					1500-1700	1470		1619		1768	
2b	1620	1650	1700				1562	1489	5%	1632			-10%		<-1%		8%
variation between a & b	-0-	-0-	12%				<1%	1%									
Quintana #C-9 McMullen Co. 3845'																	
3a	3930	4000	4000				3810	—		3922			-22%		-2%		18%
					3800	3994					3800-4000	3060		3839		4619	
3b	3930	4000	4000				3820	3750	2%	3923			-22%		-2%		18%
variation between a & b	-0-	-0-	-0-				<1%										
Skinner & Newman #C-10 McMullen Co. 4660'																	
4a	7200	7150	7600				7440	7420	<1%	7311			-30%		-6%		18%
					7100	7377					7100-8000	5120		6872		8624	
4b	7230	7500	8000	9%			7440	7350	1%	7329[5]			-30%		-6%		18%
variation between a & b	<1%	5%	5%				-0-	1%									
Skinner & Newman #A-11 McMullen Co. 4634'																	
5a	7420	7350	9000	20%			7670	7550	1.6%	7477[5]			-31%		-6%		20%
					7300	7625					7300-9000	5150		7055		8960	
5b	7450	7350	9000	21%			7570	7550	<1%	7459[5]			-31%		-5%		20%
variation between a & b	<1%	-0-	-0-				1%	-0-									
Petroleum Corp. #1-3 McMullen Co. 5533'																	
6	33,600	33,500	48,000	42%	33,500	34,262	34,300	33,800	1.5%	33,832[5]	33,500-48,000	12,000	-65%	28,848	-15%	45,696	35%

%var. = Percent variation

All measurements are in μmhos/cm @ 25° C.

Samples a and b are duplicates.

"Measured" Texas Department of Health values are determined with a procedure that gives only a rough estimate of the actual value.

"Diluted" Texas Department of Health values are obtained from samples which are diluted with distilled water. The reading is then multiplied by the dilution factor to yield diluted conductance.

[1] % variation for Pope Testing values that vary by more than 6% from the mean.

[2] Percent variation between the shaken and the unshaken sample.

[3] USGS San Antonio and Schlumberger resistivity values were included in both the a & b averages. All Texas Department of Health and the Texas Water Development Board unshaken values were excluded.

[4] Percent variation from the mean.

[5] The Pope Testing sample was not included in this average.

EXPLANATION OF TABLE 2-1:

COMPARISON OF SPECIFIC CONDUCTANCE MEASUREMENTS FROM VARIOUS TEXAS LABORATORIES

Methodology

During the course of this study, questions emerged as to the accuracy and repeatability of specific conductance measurements made by various laboratories in Texas. The differences were quantified for the three principal, present-day labs (Edna Wood, Pope Testing, and the Texas Department of Health). Each lab analyzed samples of six different waters. A sample of each water was analyzed by four labs (United States Geological Survey in Austin, Edna Wood, Pope Testing, and the Texas Department of Health), two field conductivity meters (USGS San Antonio and the Texas Water Development Board), and a Schlumberger resistivity meter. USGS Austin, Edna Wood, Pope Testing, and Texas Water Development Board analyzed duplicate sets of water samples 1 to 5. The duplicates were not labeled as such; each of the four labs measured the same containers of water.

The samples in Table 2-1 span a wide range of conductivities: 1,200 to 33,800 μmhos/cm. Sample 1 is from the Edwards aquifer in Travis County. Samples 2 to 5 are from the Carrizo aquifer in McMullen County. Sample 6 is from the lower portion of the Wilcox aquifer in McMullen County. Samples 3 to 6 are from oil producing intervals; samples 1 and 2 are from intervals that produce only water.

An average (mean) specific conductance was calculated for each of the eleven samples. The USGS San Antonio and Schlumberger resistivity meter measurements were averaged with both the a and b samples. The unshaken Texas Water Development Board values and the Texas Department of Health values were not averaged. Values differing by more than 6 percent of the mean have unacceptable accuracy and were not averaged. The percent variation from the mean is noted beside the unacceptable measurements.

Repeatability is expressed as percent variation between a and b samples. Acceptable repeatability is less than $\pm$5 percent variation between duplicate samples.

Results

Comparison of the measurements reveals that:

1. Most of the samples have excellent repeatability. Pope Testing had unacceptable repeatability for samples 1 and 2.

2. Most labs were within acceptable accuracy tolerances. Pope Testing had five samples that exceeded accuracy tolerances. These samples deviated from 7 to 42 percent from the mean.

3. Repeatability does not insure accuracy. Pope Testing sample 5 has perfect repeatability, but is inaccurate.

4. Field conductivity meters and the Schlumberger resistivity meter give acceptable accuracy.

5. Shaking a sample before measuring specific conductance increases the reading by 0.3 to 5 percent.

   a. For samples having 4000 or less μmhos/cm, the shaken sample is closer to the mean specific conductance.
   b. For samples having greater than 4000 μmhos/cm, the unshaken sample reads closer to the mean specific conductance.

6. For the Texas Department of Health measurements, neither "measured" nor diluted values are accurate.

   a. "Measured" values are less than actual specific conductance.
   b. Diluted values are greater than actual specific conductance.
   c. "Measured" values are less accurate than diluted measurements.
   d. Accuracy decreases as conductivity increases.
   e. Averaging the two measurements gives accurate specific conductance values for waters up to about 7000 μmhos/cm.
   f. The average of the two measurements is less than the actual value. The difference increases as conductivity increases.

7. Edna Wood and USGS Austin values are very close. This is in spite of the fact that Edna Wood uses only 1000 mg/l KCl as a calibration standard, while USGS Austin uses KCl solutions that are similar to the water conductivity being measured.

Conclusions

1. Pope Testing should improve its calibration procedures.

2. Field conductivity meters and the Schlumberger resistivity meter give acceptable specific conductance values.

3. The Texas Department of Health should change its procedure for determining specific conductance. The present method of using diluted conductance is a waste of time and money. The Texas Department of Health needs to determine actual specific conductance by using appropriately calibrated conductivity meters.

4. For existing Texas Department of Health water analyses, use the average of diluted and "measured" values.

a. The average value will have acceptable accuracy up to 7000 μmhos/cm.
b. Beyond 7000 μmhos/cm the accuracy of the average diminishes, but it is still far better than either diluted or "measured" values.

5. Texas Department of Health diluted conductivities should not be used to establish TDS-Cw relationships.

   a. Unfortunately, most of the specific conductances in the Texas Water Development Board Ground-Water Data Base are Texas Department of Health measurements. These conductivities should be recalculated from ionic concentrations (See Appendix I, **GUIDELINES FOR VERIFYING THE ACCURACY OF WATER ANALYSES** for a description of the calculation).
   b. Since 1988 both field conductivities and diluted conductivities are in the Ground-Water Data Base. Prior to 1988 the Texas Water Development Board did not routinely measure field conductivity, so few of the water analyses have both conductivities (Bob Bluntzer, personal communication,1991). Field conductivities are the more accurate of the two and should be used to establish TDS-Cw relationships.
   c. Water analyses from laboratories other than the Texas Department of Health will not be diluted conductivities and can therefore be used. A few of these analyses are scattered throughout the data base (Bob Bluntzer, personal communication, 1991).

the conductivity measurements can be improved by using a more conductive KCl solution and a larger cell constant (Hem, 1982, p. 147). However, comparison of the Edna Wood (1000 mg/l KCl standard) and USGS Austin (standards of varying KCl concentrations) data in Table 2-1 shows that the difference in accuracy is not necessarily significant.

Techniques for Calculating Specific Conductance

In addition to measuring specific conductance, it can be calculated from some chemical analysis reports. There are two occasions when calculated conductances are useful:

1. When a water analysis does not include a conductivity measurement (old Pope Testing, some Curtis, and some oilfield laboratory reports).

2. As a quality control check on the accuracy of a measured specific conductance.

Specific conductance can be calculated by using either a TDS-Cw relationship, the ionic concentration in mg/l, or the sum of the anions in meq/l. Each of the techniques is detailed in Appendix I, **GUIDELINES FOR VERIFYING THE ACCURACY OF WATER ANALYSES**. The accuracy of the ionic concentration and the sum of the anions methods is quantified in Tables 2-2 and 2-3. Comparison of the two methods (Table 2-4) demonstrates that specific conductances calculated from ionic concentrations are much more accurate than those calculated from anion sums. The accuracy of specific conductances calculated from the TDS-Cw relationship varies widely according to the water type.

The conclusions drawn from Tables 2-1 to 2-4 are based on a limited data base: eleven samples for Table 2-1 and thirty-one water analyses for Tables 2-2 to 2-4. To better substantiate these conclusions, an analysis was made of the entire data base compiled during this study. The data base contains 771 entries, but only 440 were suitable. Water analyses had to be complete and include a measured specific conductance to be usable. All 440 analyses are from the principal currently operating laboratories (Edna Wood, formerly Microbiology Service; Pope Testing; and Texas Department of Health) and laboratories no longer operating in Texas (Curtis and Texas Testing).

TABLE 2-2. SPECIFIC CONDUCTANCES COMPUTED FROM IONIC CONCENTRATIONS (MG/L)

Well Name	Na or Na + K	Cl	CO_3	HCO_3	SO_4	Mg	Ca	K	TDS 100% HCO_3[1]	$NaCl_{Calc.}$	$Cw_{Calc.}$	$Cw_{Measured}$	% variation
Tyron Road WSC #1 Gregg Co. 243'	113	22	0	246 x .36 = 89	24 x .72 = 17	1 x 1.75 = 2	3 x 1.2 = 4	--	409	247	500	470	6
BRC 58-35-721 Travis Co. 396'	177	145	13 x .95 = 12	268 x .35 = 94	152 x .7 = 106	24 x 1.7 = 41	41 x 1.13 = 46	10 x .91 = 9	841	629	1,250	1,231	1.5
Test Hole #1 540' Chambers Co.	299	190	24 x .95 = 23	450 x .35 = 158	29 x .7 = 20	4.5 x 1.6 = 7	15 x 1.1 = 17	--	1,014	714	1,400	1,390	<1
Petroleo Corp. #4-3 McMullen Co. 4030'	373	117	10 x .93 = 9	659 x .34 = 230	133 x .68 = 90	1 x 1.6 = 2	10 x 1.08 = 11	--	1,303	832	1,610	1,626	-1
Test Hole #1 818' Chambers Co.	422	355	25 x 1.05 = 26	559 x .34 = 190	0	3 x 1.58 = 5	11.5 x 1.06 = 12	--	1,397	1,030	2,000	1,970	1.5
Seaville #8 1290' See Co.	635	561	0	750 x .34 = 255	0	2 x 1.5 = 3	7 x 1 = 7	--	1,955	1,461	2,750	2,720	1
Quintana #C-9 McMullen Co. 3845'	1,064	232	79 x .8 = 63	2273 x .32 = 727	15 x .6 = 9	1 x 1.44 = 1.44	3 x .89 = 3	5 x .92 = 5	3,659	2,086	4,000	3,922	2
Edinburg Ice #1 Hidalgo Co. 393'	932	1,248	0	336 x .32 = 108	460 x .6 = 276	54 x 1.41 = 76	106 x .88 = 93	--	3,136	2,733	5,100	5,350	-5
Test Hole #1 1060' Chambers Co.	1,266	1,650	24 x .9 = 22	632 x .32 = 202	0	13 x 1.45 = 19	32 x .9 = 29	--	3,623	3,186	5,900	6,000	-2
Skinner & Newman #C-10 McMullen Co. 4660'	1,771	1,433	34 x .7 = 24	2279 x .31 = 706	17 x .57 = 10	3 x 1.38 = 4	6 x .82 = 5	12 x .9 = 11	5,590	3,964	7,200	7,320	2
Skinner & Newman #A-11 McMullen Co. 4634'	1,857	1,409	0	2596 x .3 = 779	17 x .56 = 10	2 x 1.37 = 3	10 x .8 = 8	14 x .9 = 13	5,942	4,079	7,600	7,470	2
Test Hole #1 1140' Chambers Co.	2,000	3,000	0	503 x .31 = 156	0	27 x 1.37 = 37	73 x .82 = 60	--	5,605	5,253	9,500	9,740	-2.5
Test Hole #1 1340' Chambers Co.	2,730	4,300	0	429 x .3 = 129	0	48 x 1.32 = 63	113 x .8 = 90	--	7,643	7,313	13,000	13,000	--
Mobil Oil #3 Jefferson Co. 520'	2,511	4,146	0	295 x .3 = 89	10 x .54 = 5	62 x 1.31 = 81	154 x .8 = 123	--	7,178	6,955	12,300	10,200	21
Petroleo Corp. #1-3 McMullen Co. 5533'	8,316	12,363	0	1068 x .28 = 299	6 x .46 = 3	24 x 1.13 = 27	64 x .82 = 52	39 x .91 = 35	21,905	21,095	36,000	33,832	6
Mobil Oil #1 Jackson Co. 4136'	22,400	41,000	0	120 x .2 = 24	0	540 x .79 = 427	2825 x .78 = 2204	--	66,914	66,055	00,500	91,700	10

Table 2-2 continued on next page.

TABLE 2-2 (CONTINUED). SPECIFIC CONDUCTANCES COMPUTED FROM IONIC CONCENTRATIONS (MG/L)

Well Name	Na or Na + K	Cl	CO_3	HCO_3	SO_4	Mg	Ca	K	TDS 100% HCO_3[1]	$NaCl_{calc.}$	$C_{w_{calc.}}$	$C_{w_{measured}}$	% variation
Milam WC & ID #1 Milam Co.													
1610'	2,003	1,050	0	334 x .3 = 100	3175 x .55 = 1746	62 x 1.34 = 83	180 x .8 = 144	--	6,808	5,126	9,100	8,700	5
1810'	1,962	1,100	26 x .79 = 20	303 x .3 = 91	3200 x .54 = 1728	82 x 1.34 = 110	230 x .8 = 184	--	6,908	5,195	9,400	9,160	3
3192'	547	156	0	333 x .34 = 113	889 x .66 = 587	18 x 1.63 = 28	62 x 1 = 62	--	2,014	1,493	2,800	2,725	3
3373'	569	174	0	372 x .34 = 126	882 x .65 = 573	18 x 1.5 = 27	63 x .96 = 60	--	2,083	1,529	2,900	2,854	2
City of Huntington #7 Angelina Co.													
495'	194	50	24 x .98 = 24	361 x .36 = 130	18 x .72 = 13	.3 x 1.7 = 1	1.3 x 1.22 = 2	--	648	414	820	765	7
636'	190	64	18 x .98 = 18	360 x .36 = 130	0	.2 x 1.7 = 0	1.2 x 1.2 = 2	--	634	404	800	752	6
1153'	5,433	8,500	0	464 x .28 = 130	0	63 x 1.2 = 76	116 x .8 = 93	--	14,576	14,232	25,000	24,500	2
1772'	677	580	36 x .89 = 32	732 x .34 = 249	0	1 x 1.53 = 2	3 x 1 = 3	--	2,031	1,543	2,950	3,080	-4
KGS Haberer #1 Kansas													
Upper Dakota 176'	4,700	5,610	NA	1184 x .29 = 343	1960 x .5 = 980	273 x 1.2 = 328	168 x .8 = 134	28 x .9 = 25	13,951	12,120	21,000	22,000	-5
Lower Dakota 276'	5,030	6,250	NA	1277 x .29 = 370	2020 x .5 = 1010	291 x 1.2 = 349	182 x .8 = 146	33 x .9 = 30	15,109	13,185	23,000	23,200	-1
KGS Braun #1 Kansas													
Upper Dakota 651'	10,600	14,250	NA	1690 x .25 = 423	3980 x .43 = 1711	705 x 1.05 = 740	252 x .82 = 206	80 x .94 = 75	31,588	28,005	48,000	43,200	11
Upper Dakota 651'	9,940	13,560	NA	1470 x .26 = 382	3570 x .44 = 1571	620 x 1.07 = 676	188 x .82 = 154	81 x .93 = 75	29,477	26,358	45,000	41,400	9
Lower Dakota 772'	8,340	11,500	NA	892 x .27 = 241	3340 x .46 = 1536	557 x 1.1 = 612	72 x .82 = 59	86 x .91 = 78	24,813	22,363	38,000	35,700	6
Cheyene 835'	10,300	14,600	NA	1070 x 25 = 268	4110 x .43 = 1767	713 x 1.05 = 749	64 x .82 = 52	65 x .94 = 61	30,953	27,797	48,000	43,700	9
Cedar Hills 1185'	11,500	16,100	NA	1690 x .25 = 423	4610 x .42 = 1936	801 x 1 = 801	182 x .82 = 149	76 x .96 = 73	34,999	30,982	52,000	49,100	6

NA = not available

[1]Silica was not included in the TDS value. Silica did not exceed 34 mg/l in any of the samples.

EXPLANATION OF TABLE 2-2:

ACCURACY OF SPECIFIC CONDUCTANCES COMPUTED FROM IONIC CONCENTRATIONS (MG/L)

Table 2-2 lists thirty-one water analyses from various parts of Texas and Kansas. The calculations used to compute specific conductance from ionic concentrations are listed ($Cw_{Ion\ Conc.}$), along with a laboratory measured specific conductance ($Cw_{Measured}$). The Mobil Oil #3, Jefferson County well is not included in the tabulations due to apparent error in $Cw_{Measured}$.

The following conclusions can be drawn from the data:

1. Specific conductance computed from ionic concentrations is accurate.
   a. $Cw_{Ion\ Conc.}$ varies ±5 percent from $Cw_{Measured}$ for all but five samples up to 35,700 μmhos/cm (24,813 TDS). The remaining five samples have 6 to 7 percent variation.
   b. Samples with greater than 35,700 μmhos/cm vary 6 to 11 percent.

2. $Cw_{Ion\ Conc.}$ normally exceeds $Cw_{Measured}$.
   a. $Cw_{Ion\ Conc.}$ is always greater than $Cw_{Measured}$ for Cw greater than 30,000 μmhos/cm.
   b. Below 30,000 μmhos/cm either value may be greater, although $Cw_{Ion\ Conc.}$ is usually larger.

3. A NaCl equivalent must be used to calculate specific conductance for waters with Cw less than about 8000 μmhos/cm (about 6000 ppm TDS). Due to abundant bicarbonate and/or sulfate ions, these waters are significantly less conductive than a NaCl water with the same TDS.

4. There is no need to calculate a NaCl equivalent for ground waters with Cw greater than 8000 μmhos/cm. These waters are usually NaCl type waters. The TDS value can be input directly into Figure AI-2 in Appendix I, unless sulfate ions are abundant.

5. Specific conductances computed from ionic concentrations are excellent checks on the accuracy of $Cw_{Measured}$. A case in point is the Mobil Oil #3, Jefferson County. $Cw_{Measured}$ is 10,200 μmhos/cm. Conductivities computed by ionic concentrations and anion sum (Table 2-3) agree at 12,300 and 12,200 μmhos/cm. $Cw_{Measured}$ is probably too low.

6. Specific conductance computed from ionic concentrations can be used to correct and/or verify the Cw's in the Texas Water Development Board Ground-Water Data Base.

TABLE 2-3. SPECIFIC CONDUCTANCES COMPUTED FROM SUM OF THE ANIONS (MEQ/L)

Well Name	MEQ/L cations	MEQ/L anions	Cw from anion MEQ/L	$Cw_{measured}$	% variation
Tyron Road WSC #1 Gregg Co. 243'	5.15*	5.15	515	470	10
BRC 58-35-721 Travis Co. 398'	12.03	12.2	1,220	1,231	<-1
Test Hole #1 540' Chambers Co.	14.14*	14.14	1,414	1,390	2
Petrolero Corp. #4-3 McMullen Co. 4030'	16.92	17.26	1,726	1,626	6
Test Hole #1 818' Chambers Co.	20.0*	20	2,000	1,970	1.5
Beeville #8 1290' Bee Co.	28.13*	28.13	2,813	2,720	3
Quintana #C-9 McMullen Co. 3845'	46.89	47.01	4,701	3,922	20
Edinburg Ice #1 Hidalgo Co. 393'	50.27*	50.27	5,027	5,350	-6
Test Hole #1 1060' Chambers Co.	57.69*	57.69	5,769	6,000	-4
Skinner & Newman #C-10 McMullen Co. 4660'	77.87	79.51	7,951	7,320	9
Skinner & Newman #A-11 McMullen Co. 4634'	81.8	82.84	8,284	7,470	11
Test Hole #1 1140' Chambers Co.	92.84*	92.84	9,284	9,740	-5
Test Hole #1 1340' Chambers Co.	128.29*	128.29	12,829	13,000	-1
Mobil Oil #3 Jefferson Co. 520'	122.0*	122	12,200	10,200	20
Petrolero Corp. #1-3 McMullen Co. 5533'	367.7	366.5	36,650	33,832	8
Mobil Oil #1 Jackson Co. 4136'	1159.0*	1159	115,900	91,700	26
Milam WC & ID #1 Milam Co.					
1510'	101.5*	101.5	10,150	8,700	17
1810'	104.0*	104	10,400	9,160	13.5
3192'	28.4*	28.4	2,840	2,725	4
3373'	29.0*	29	2,900	2,854	2
City of Huntington #7 Angelina Co.					
495'	8.5*	8.5	850	765	11
636'	8.3*	8.3	830	752	10
1153'	247.6*	247.6	24,760	24,500	1
1772'	29.6*	29.6	2,960	3,080	-4
KGS Haberer #1 Kansas					
Upper Dakota 176'	235	219	21,900	22,000	<-1
Lower Dakota 276'	252	240	24,000	23,200	3
KGS Braun #1 Kansas					
Upper Dakota 651'	531.6	515	51,500	43,200	19
Upper Dakota 651'	492	478	47,800	41,400	15.5
Lower Dakota 772'	412.2	411	41,100	35,700	15
Cheyene 835'	510	517	51,700	43,700	18
Cedar Hills 1185'	575	580	58,000	49,100	18

* Na by difference, so cation and anion sums equal.

EXPLANATION OF TABLE 2-3:

ACCURACY OF SPECIFIC CONDUCTANCES COMPUTED FROM SUM OF THE ANIONS (MEQ/L)

Table 2-3 lists the sum of the anions and cations for thirty-one water analyses from various parts of Texas and Kansas. A computed conductivity ($Cw_{Anion\ Sum}$) was calculated by multiplying the anion sum by 100. Anion-cation balances were within acceptable limits (less than 5 percent) for all but one analysis, which was 7 percent. Seventeen samples calculated sodium by difference, which made the ions balance perfectly. The Mobil Oil #3, Jefferson County well is not included in the tabulations due to an apparent error in $Cw_{Measured}$.

The following conclusions can be drawn from the data:

1. Specific conductances computed from the sum of the anions should be used only as a gross estimation of conductivity.
   a. $Cw_{Anion\ Sum}$ varies less than ±5 percent from $Cw_{Measured}$ for 43 percent of the samples.
   b. The variation is 10 percent or less for all but five of the twenty-five samples up to 33,832 μmhos/cm (21,905 mg/l TDS). Five samples vary 11 to 20 percent.
   c. $Cw_{Anion\ Sum}$ varies 15 to 19 percent from $Cw_{Measured}$ for samples from 35,700 to 49,100 μmhos/cm.
   d. The variation is 26 percent for the 91,700 μmhos/cm sample.

2. $Cw_{Anion\ Sum}$ normally exceeds $Cw_{Measured}$.
   a. $Cw_{Anion\ Sum}$ is always greater than $Cw_{Measured}$ for Cw's greater than 30,000 μmhos/cm.
   b. Below 30,000 μmhos/cm either value may be greater, although $Cw_{Anion\ Sum}$ is usually larger.

TABLE 2-4. COMPARISON OF SPECIFIC CONDUCTANCES CALCULATED BY IONIC CONCENTRATION, ANION SUM, AND DILUTED CONDUCTIVITY

Well Name	TDS 100% HCO_3	$Cw_{Ion\ Conc.}$	% variation[1]	$Cw_{Measured}$	Cw from anion MEQ/L	% variation[1]	Diluted Cw	% variation[1]
Tyron Road WSC #1 Gregg Co. 243'	409	500	6	470	515	10		
BRC 58-35-721 Travis Co. 398'	841	1,250	1.5	1,231	1,220	<-1	1,350	10
Test Hole #1 540' Chambers Co.	1,014	1,400	<1	1,390	1,414	2		
Petrolero Corp. #4-3 McMullen Co. 4030'	1,303	1,610	-1	1,626	1,726	6	1,768	9
Test Hole #1 818' Chambers Co.	1,397	2,000	1.5	1,970	2,000	1.5		
Beeville #8 1290' Bee Co.	1,955	2,750	1	2,720	2,813	3		
Quintana #C-9 McMullen Co. 3845'	3,659	4,000	2	3,922	4,701	20	4,619	18
Edinburg Ice #1 Hidalgo Co. 393'	3,136	5,100	-5	5,350	5,027	-6		
Test Hole #1 1060' Chambers Co.	3,623	5,900	-2	6,000	5,769	-4		
Skinner & Newman #C-10 McMullen Co. 4660'	5,590	7,200	-2	7,320	7,951	9	8,624	18
Skinner & Newman #A-11 McMullen Co. 4634'	5,942	7,600	2	7,470	8,284	11	8,960	20
Test Hole #1 1140' Chambers Co.	5,605	9,500	-2.5	9,740	9,284	-5		
Test Hole #1 1340' Chambers Co.	7,643	13,000	-0-	13,000	12,829	-1		
Mobil Oil #3 Jefferson Co. 520'	7,178	12,300	21	10,200	12,200	20		
Petrolero Corp. #1-3 McMullen Co. 5533'	21,905	36,000	6	33,832	36,650	8	45,696	35
Mobil Oil #1 Jackson Co. 4136'	66,914	100,500	10	91,700	115,900	26		
Milam WC & ID #1 Milam Co.								
1510'	6,808	9,100	5	8,700	10,150	17		
1810'	6,908	9,400	3	9,160	10,400	13.5		
3192'	2,014	2,800	3	2,725	2,840	4		
3373'	2,083	2,900	2	2,854	2,900	2		
City of Huntington #7 Angelina Co.								
495'	648	820	7	765	850	11		
636'	634	800	6	752	830	10		
1153'	14,576	25,000	2	24,500	24,760	1		
1772'	2,031	2,950	-4	3,080	2,960	-4		
KGS Haberer #1 Kansas								
Upper Dakota 178'	13,951	21,000	-5	22,000	21,900	<-1		
Lower Dakota 276'	15,109	23,000	-1	23,200	24,000	3		
KGS Braun #1 Kansas								
Upper Dakota 651'	31,588	48,000	11	43,200	51,500	19		
Upper Dakota 651'	29,477	45,000	9	41,400	47,800	15.5		
Lower Dakota 772'	24,813	38,000	6	35,700	41,100	15		
Cheyene 835'	30,953	48,000	9	43,700	51,700	18		
Cedar Hills 1185'	34,999	52,000	6	49,100	58,000	18		

[1] Percent variation from $Cw_{Measured}$

EXPLANATION OF TABLE 2-4:

COMPARISON OF SPECIFIC CONDUCTANCES CALCULATED BY IONIC CONCENTRATION, ANION SUM, AND DILUTED CONDUCTIVITY

Table 2-4 is a summary of Tables 2-2 and 2-3, along with six Texas Department of Health diluted conductances. The data demonstrate that:

1. Specific conductance calculated from ionic concentrations is by far the most accurate of the three methods.

2. Specific conductance calculated from ionic concentrations is the only method that consistently gives acceptable accuracy.

3. Diluted conductance never gives acceptable accuracy.

4. Diluted conductance is always greater than the actual value and the difference increases with increasing salinity. This is in keeping with the principle of interionic interference. (See the section **Factors Controlling Water Conductivity** in this chapter).

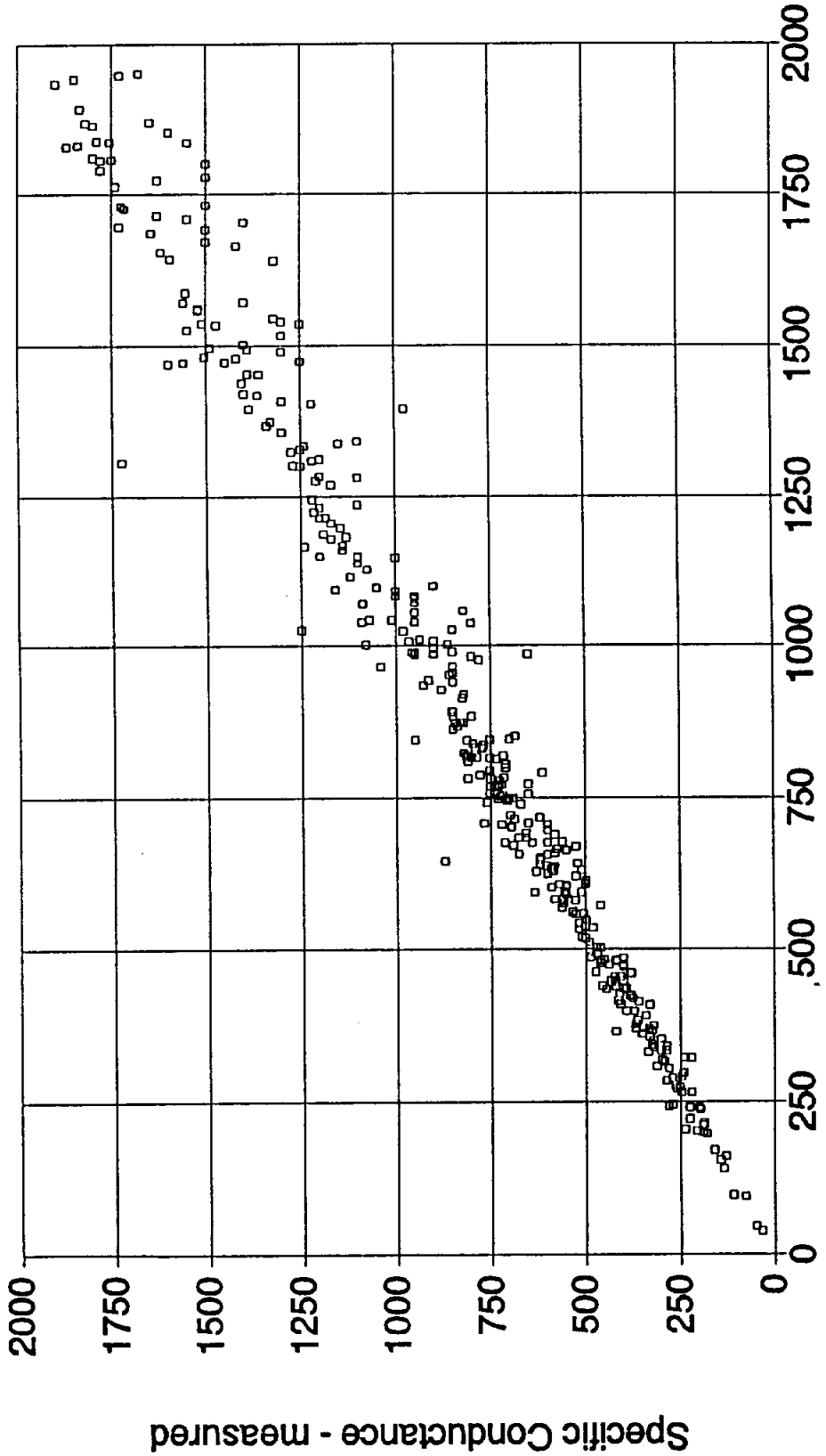

Figure 2-1. Graph of $Cw_{Measured}$ versus $Cw_{Ion\ Conc.}$ values ranging between 0 and 2,000 μmhos/cm. The data are from water analyses performed by Curtis, Edna Wood, Microbiology Service, Pope Testing, Texas Testing, and Texas Department of Health Laboratories.

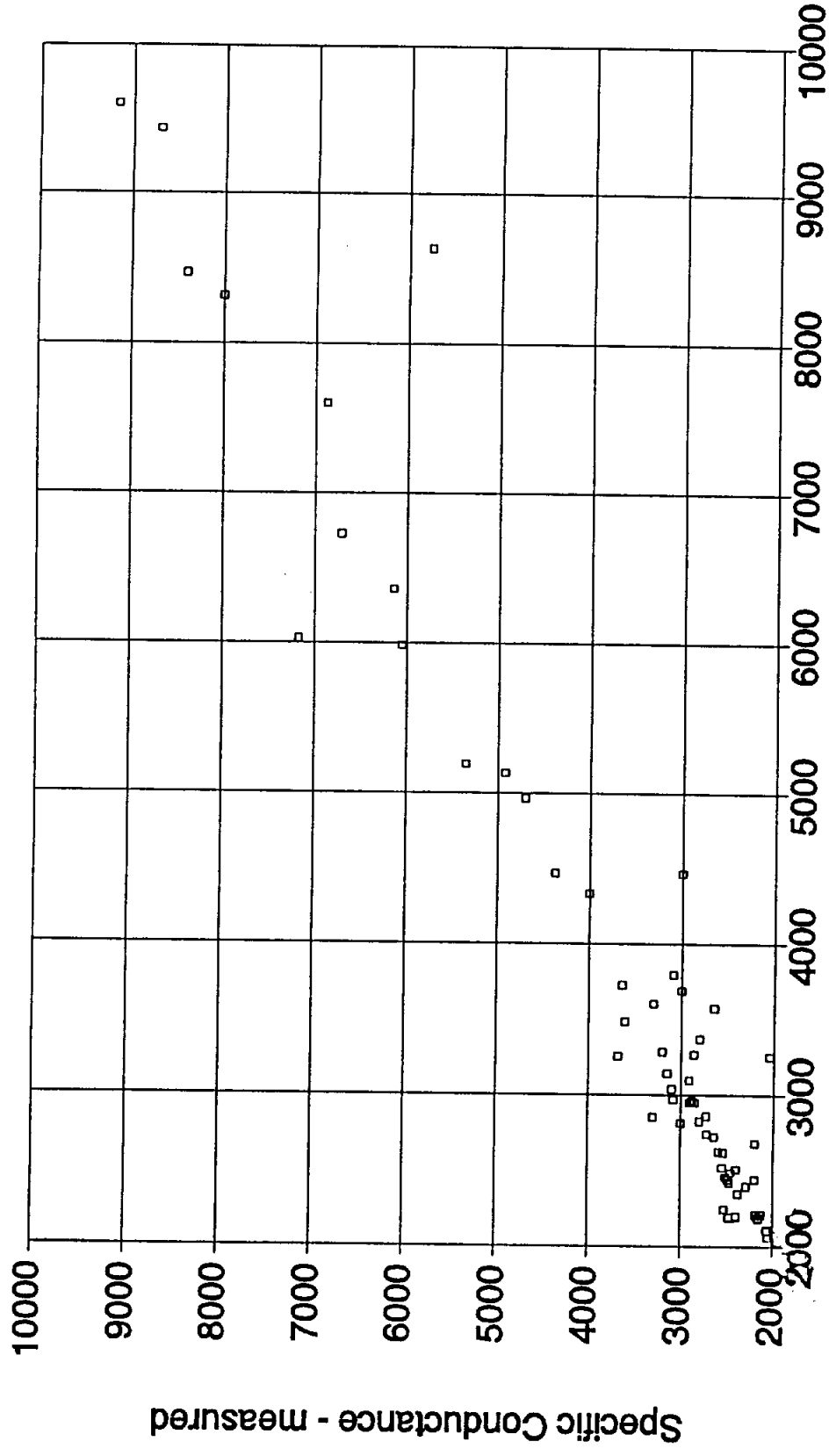

Figure 2-2. A graph of $Cw_{Measured}$ versus $Cw_{Ion\ Conc.}$ values ranging between 2,000 and 10,000 μmhos/cm. The data are from water analyses performed by Curtis, Edna Wood, Microbiology Service, Pope Testing, Texas Testing, and Texas Department of Health Laboratories.

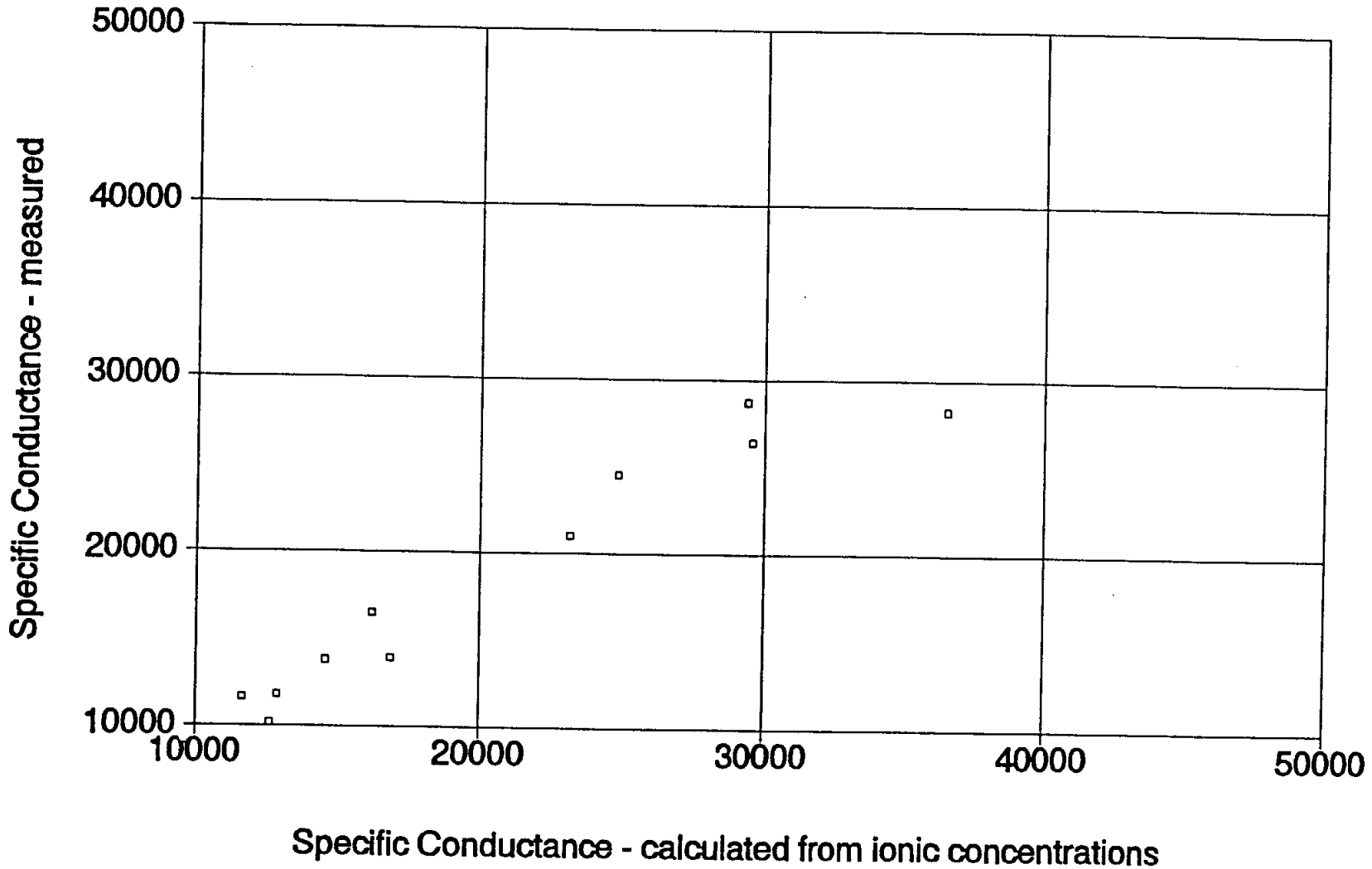

Figure 2-3. A graph of $Cw_{Measured}$ versus $Cw_{Ion\ Conc.}$ values ranging between 10,000 and 50,000 μmhos/cm. The data are from water analyses performed by Curtis, Edna Wood, Microbiology Service, Pope Testing, Texas Testing, and Texas Department of Health Laboratories.

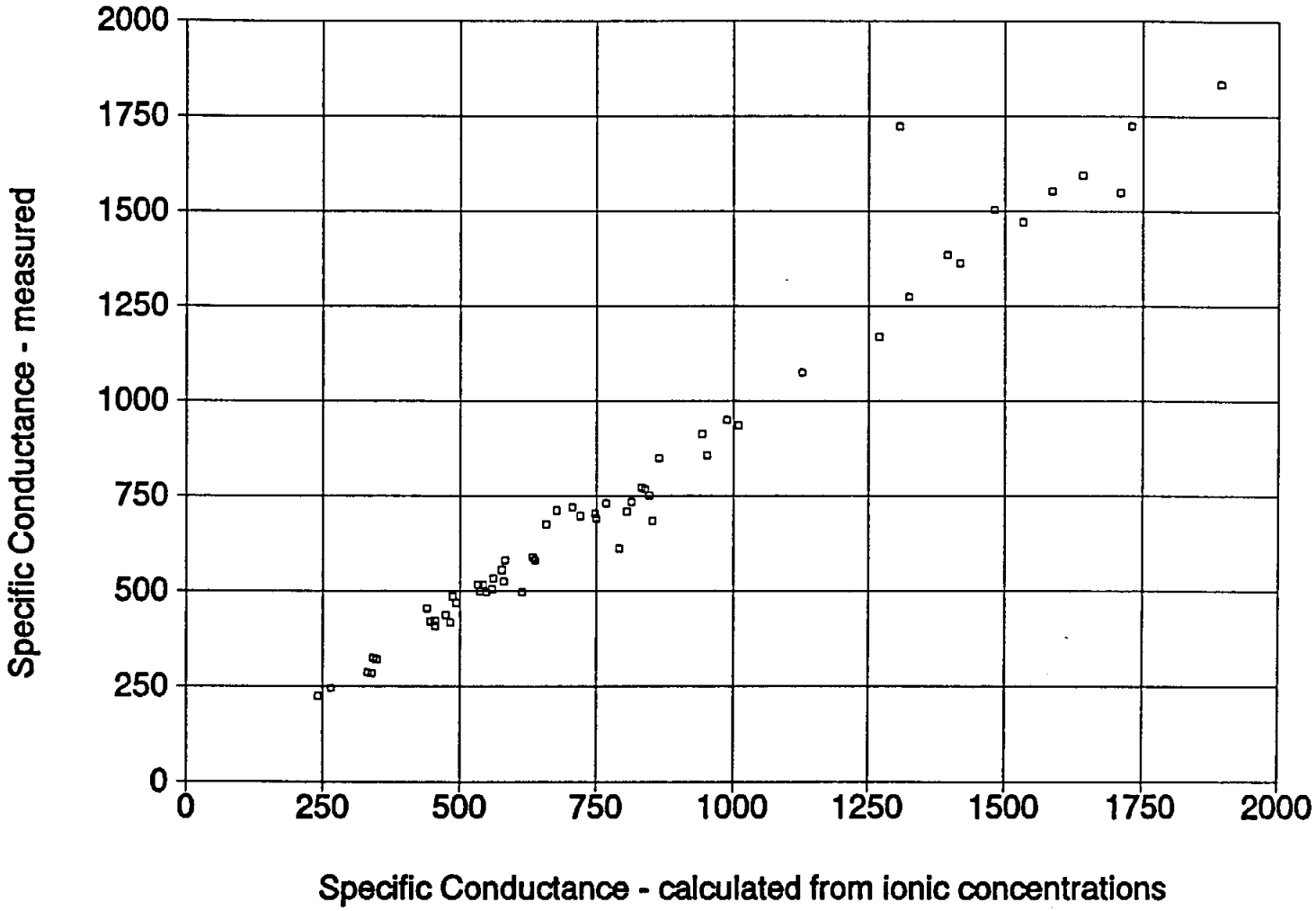

Figure 2-4. A graph of $Cw_{Measured}$ versus $Cw_{Ion\ Conc.}$ values ranging between 0 and 2,000 μmhos/cm. The data are from water analyses performed by Curtis Laboratories.

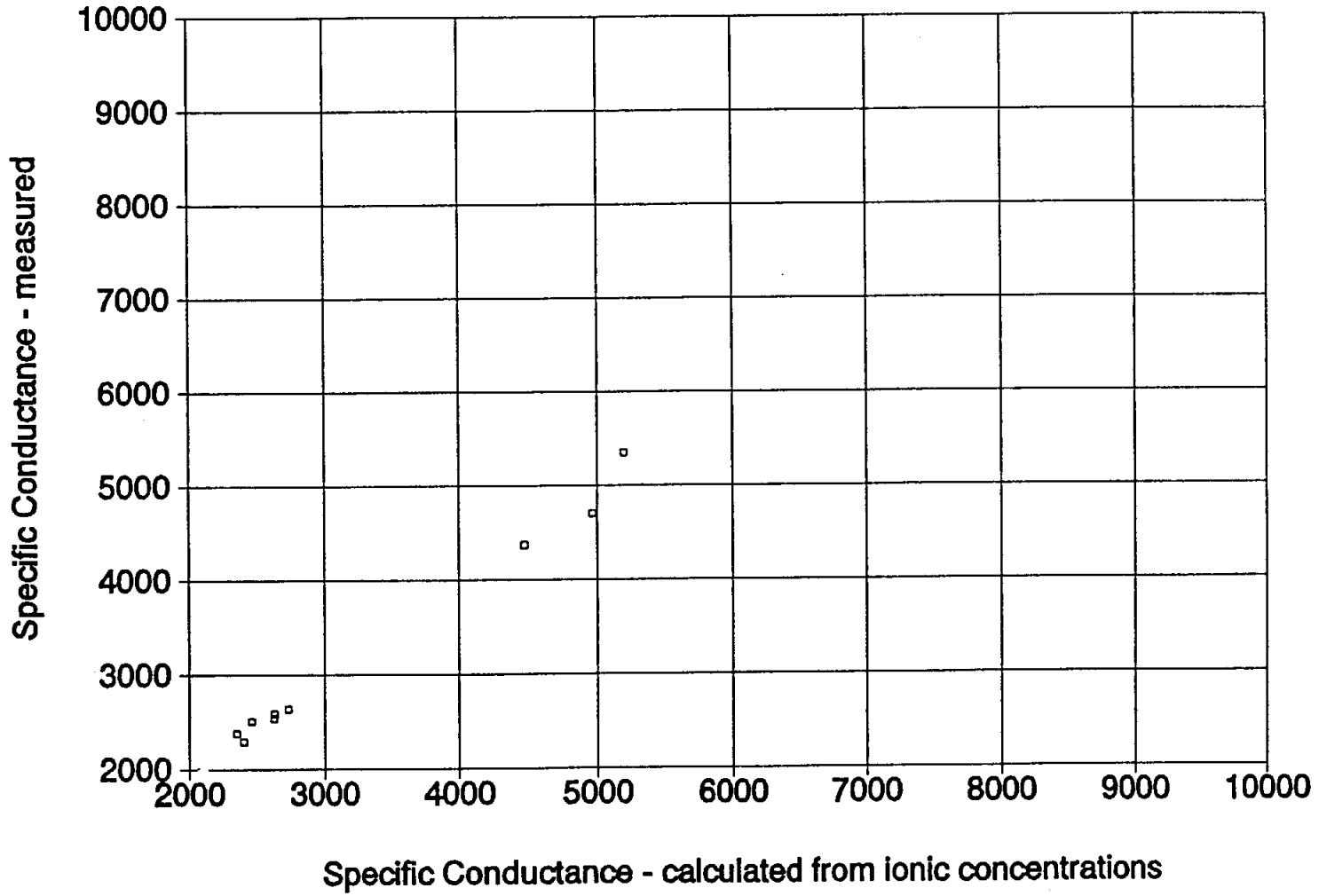

Figure 2-5. A graph of $Cw_{Measured}$ versus $Cw_{Ion\ Conc.}$ values ranging between 2,000 and 10,000 μmhos/cm. The data are from water analyses performed by Curtis Laboratories.

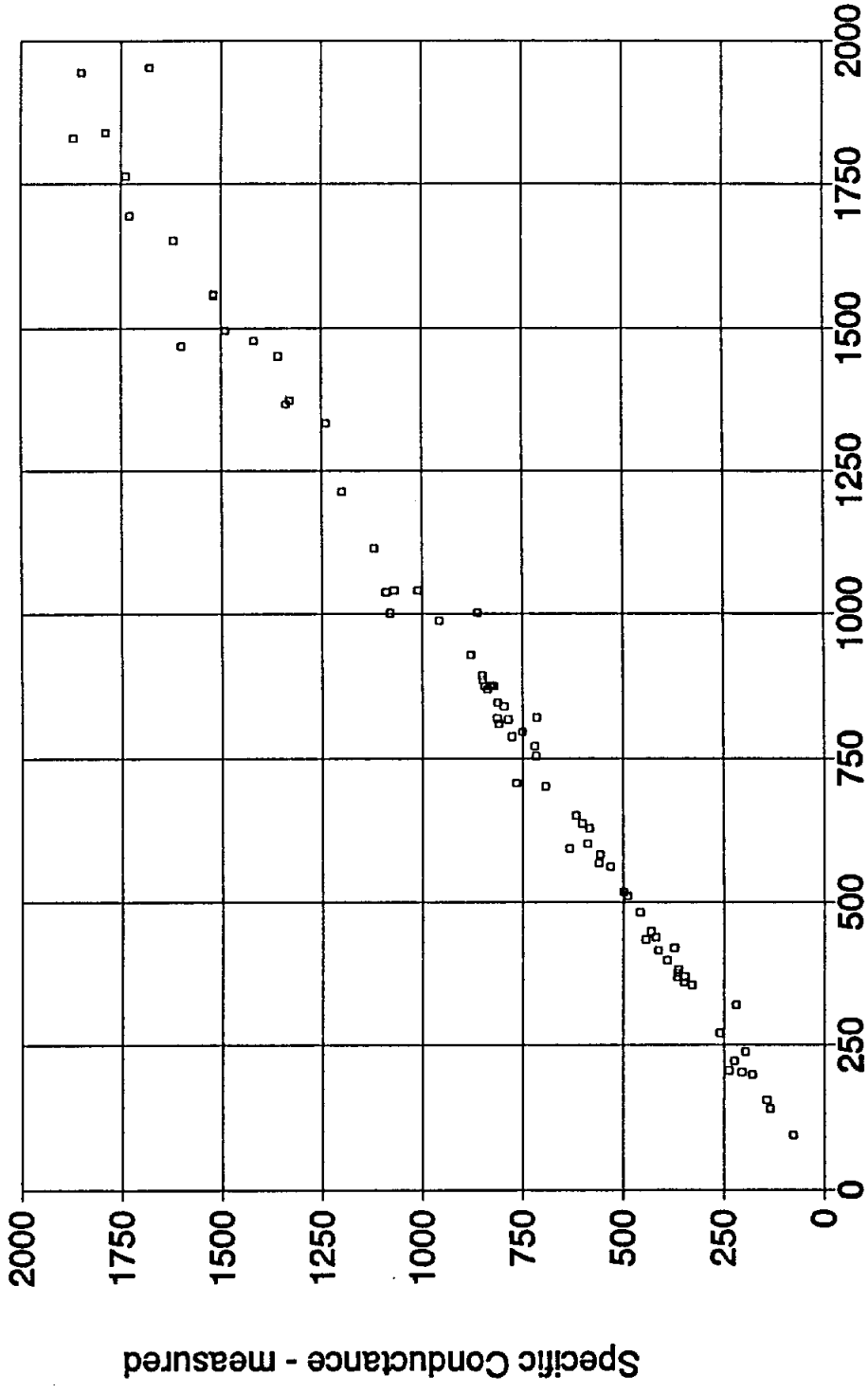

Figure 2-6. Graph of $Cw_{Measured}$ versus $Cw_{Ion\ Conc.}$ values ranging between 0 and 2,000 μmhos/cm. The data are from water analyses performed by Edna Wood Laboratories.

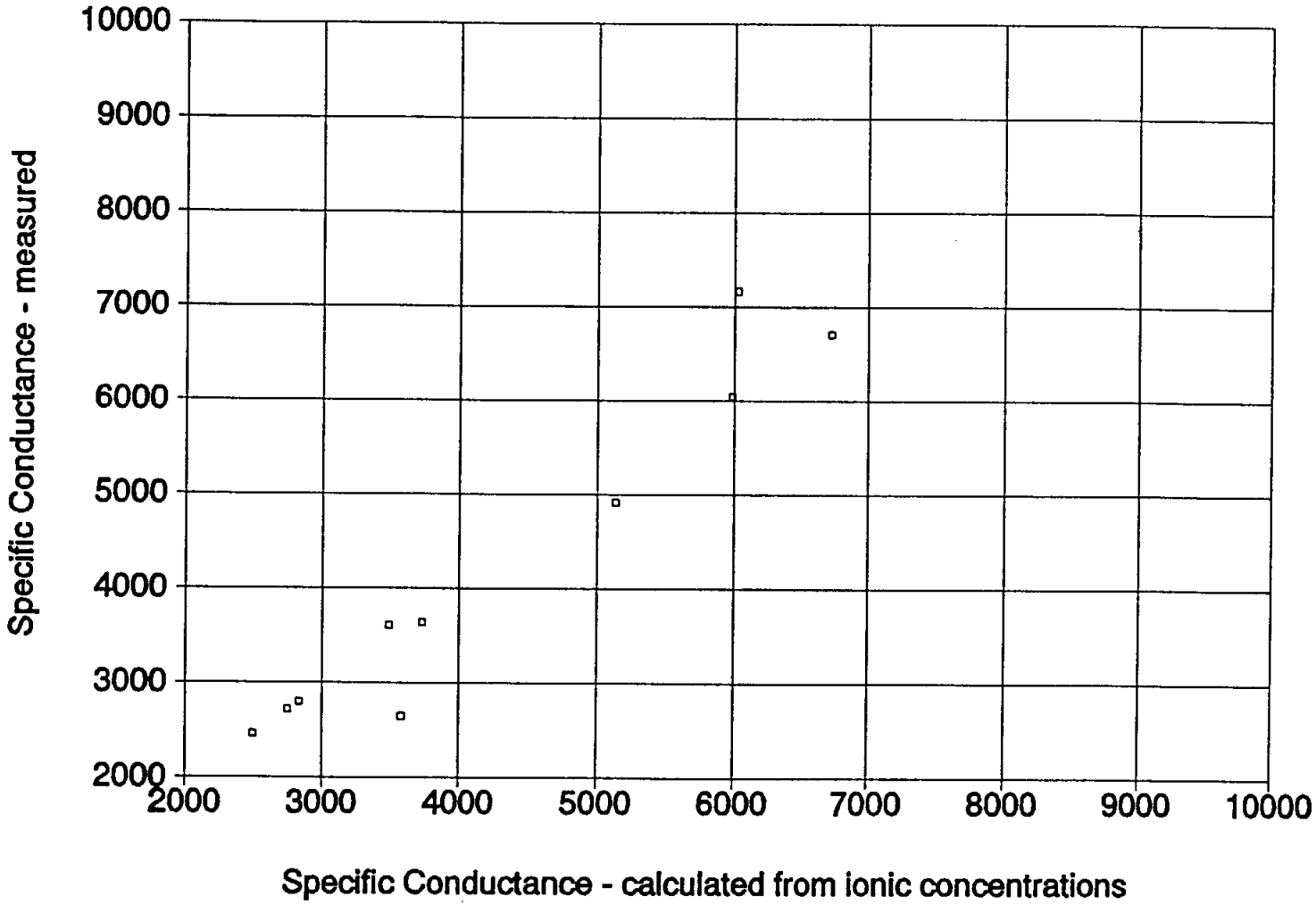

Figure 2-7. A graph of $Cw_{Measured}$ versus $Cw_{Ion\ Conc.}$ values ranging between 2,000 and 10,000 μmhos/cm. The data are from water analyses performed by Edna Wood Laboratories.

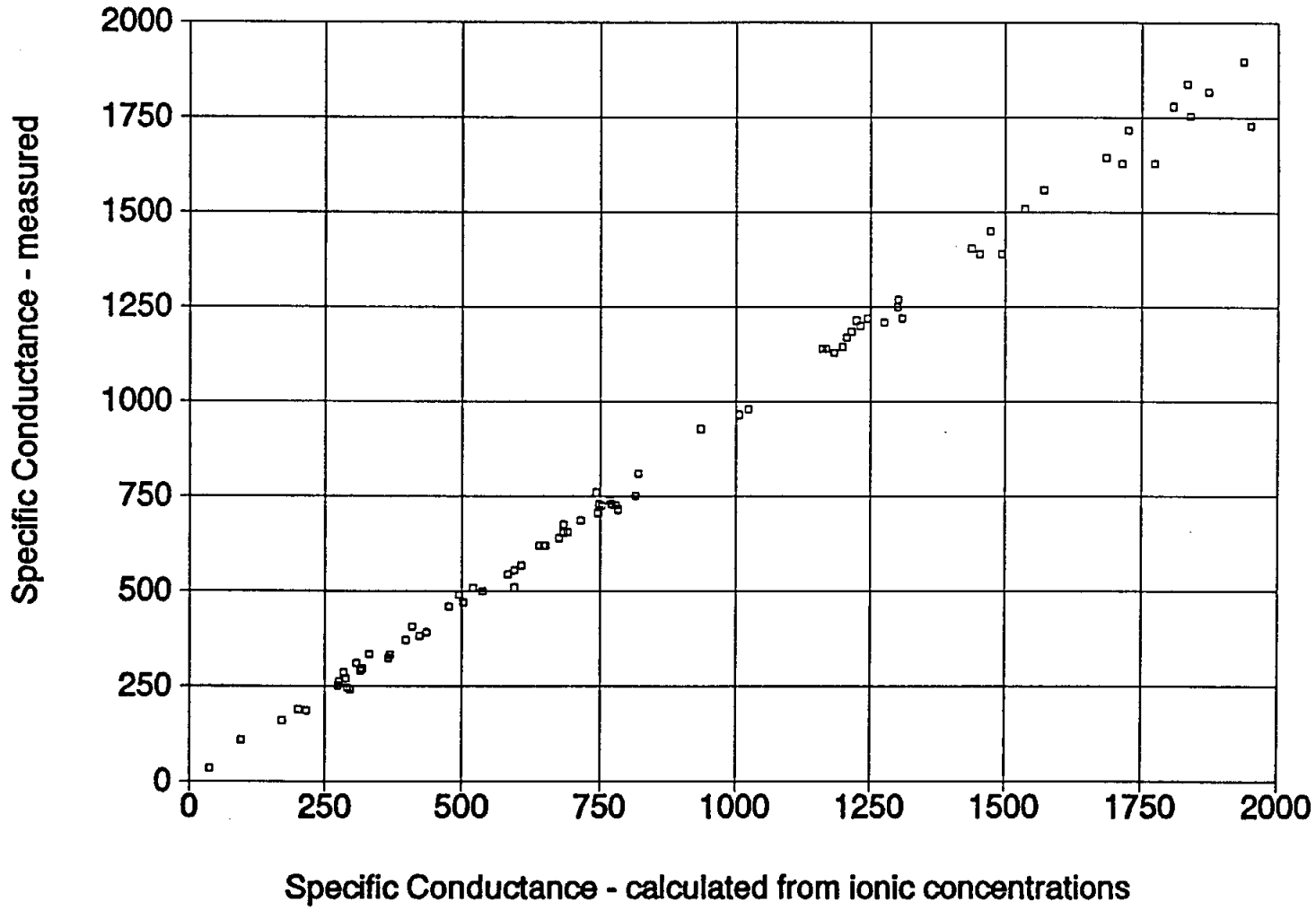

Figure 2-8. A graph of $Cw_{Measured}$ versus $Cw_{Ion\ Conc.}$ values ranging between 0 and 2,000 μmhos/cm. The data are frrom water analyses performed by Microbiology Service Laboratories.

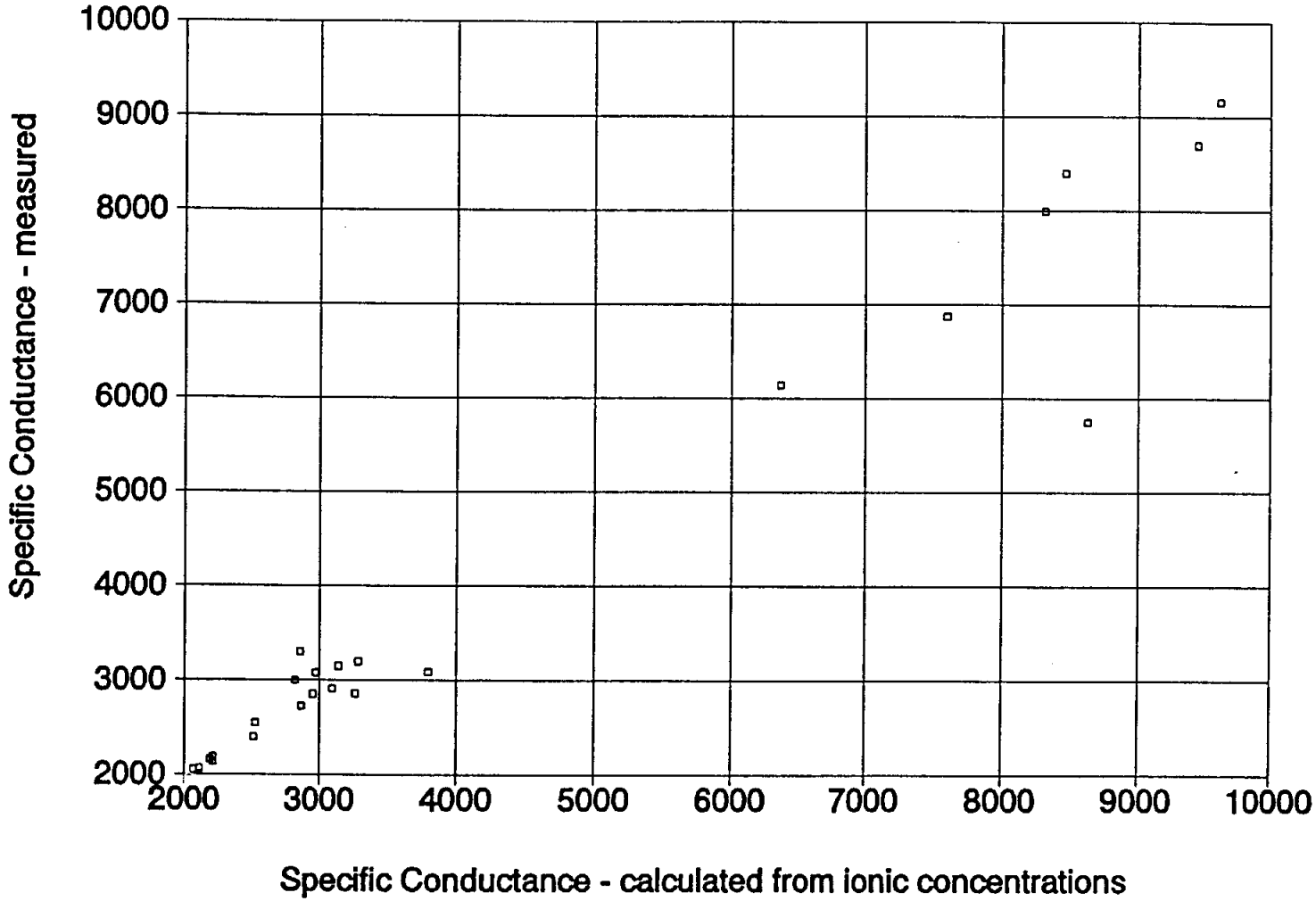

Figure 2-9. A graph of $Cw_{Measured}$ versus $Cw_{Ion\ Conc.}$ values ranging between 2,000 and 10,000 μmhos/cm. The data are from water analyses performed by Microbiology Service Laboratories.

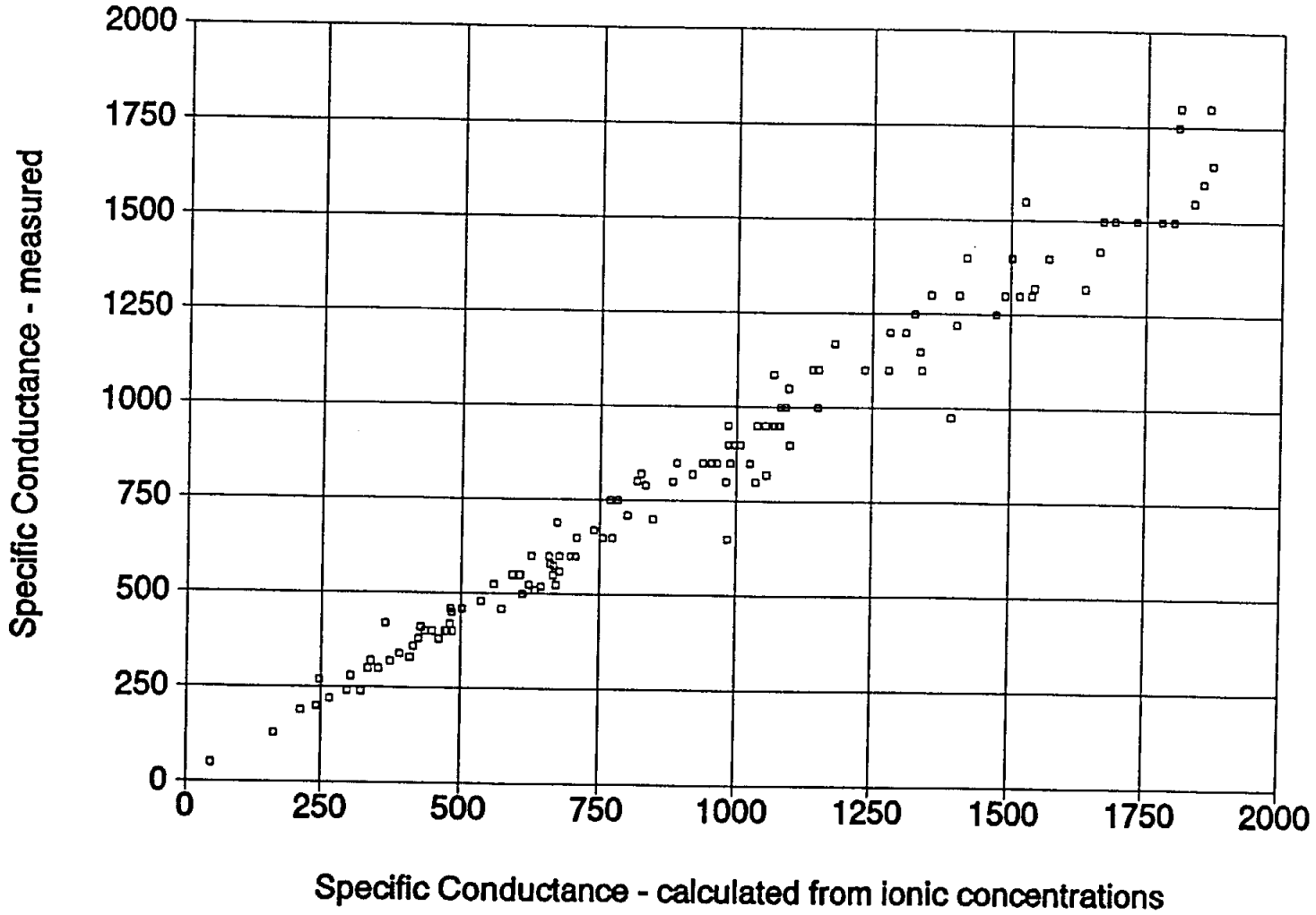

Figure 2-10. A graph of $Cw_{Measured}$ versus $Cw_{Ion\ Conc.}$ values ranging between 0 and 2,000 μmhos/cm. The data are from water analyses performed by Pope Testing Laboratories.

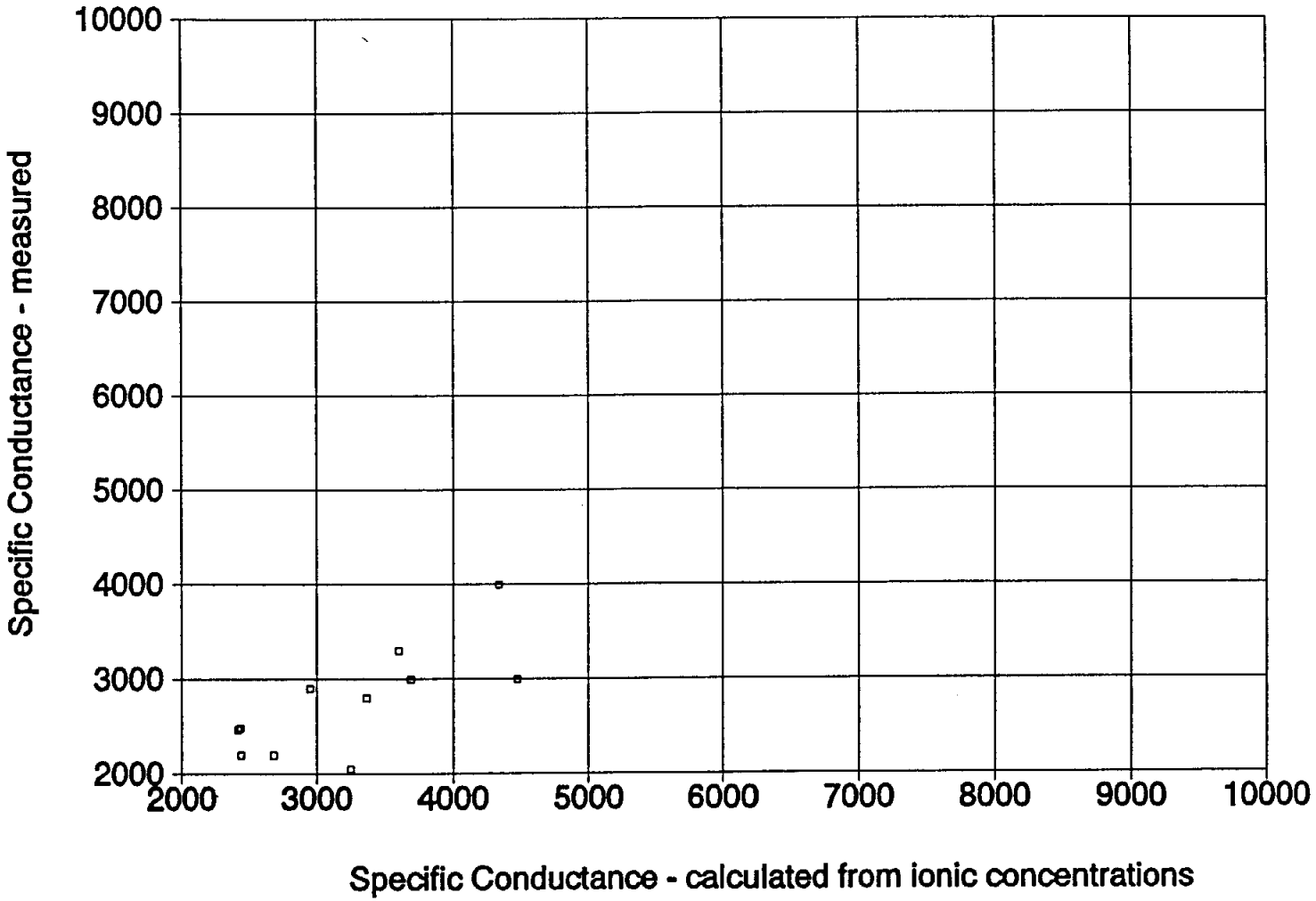

Figure 2-11. A graph of $Cw_{Measured}$ versus $Cw_{Ion\ Conc.}$ values ranging between 2,000 and 10,000 μmhos/cm. The data are from water analyses performed by Pope Testing Laboratories.

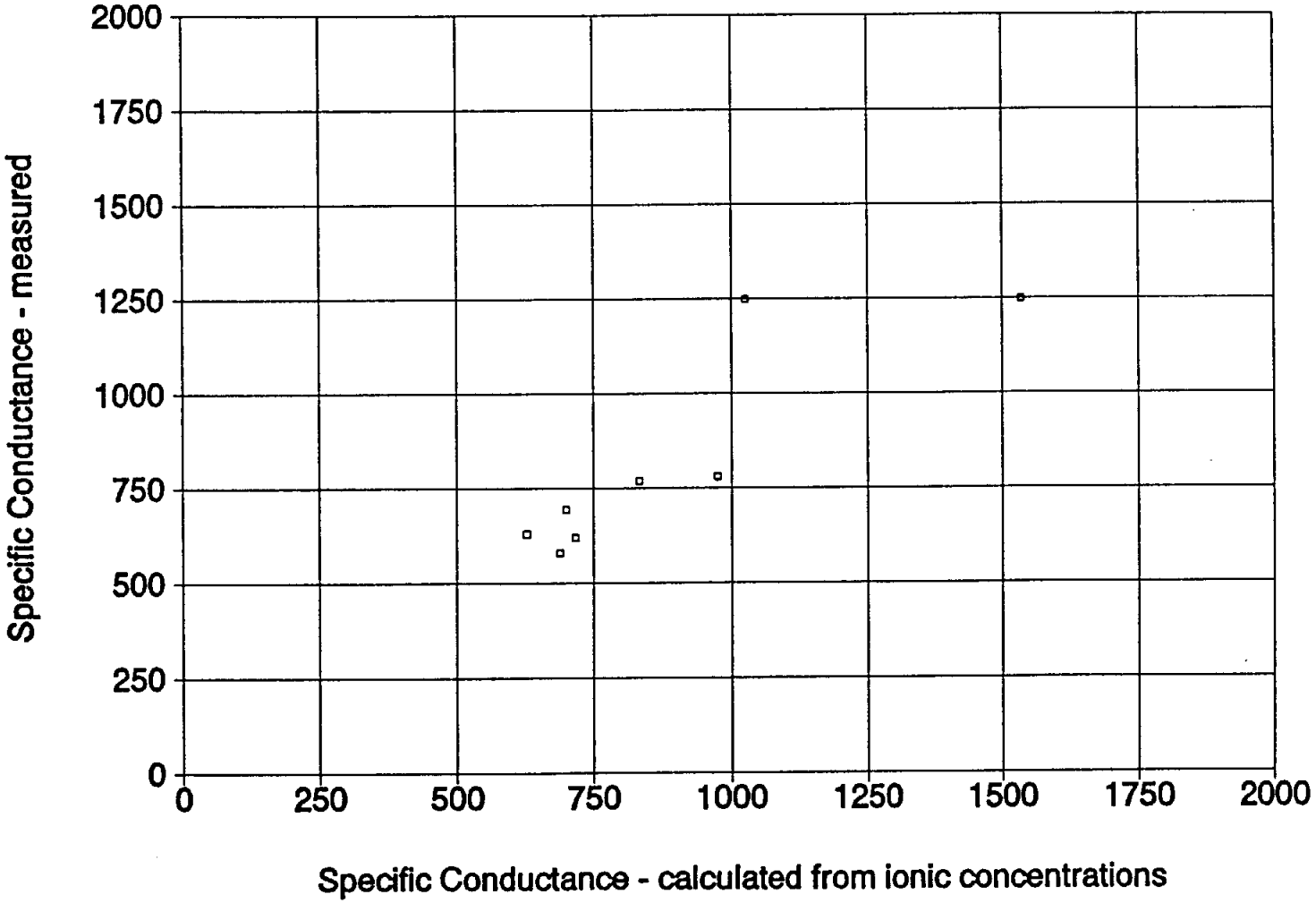

Figure 2-12. A graph of $Cw_{Measured}$ versus $Cw_{Ion\ Conc.}$ values ranging between 0 and 2,000 μmhos/cm. The data are from water analyses performed by Texas Testing Laboratories.

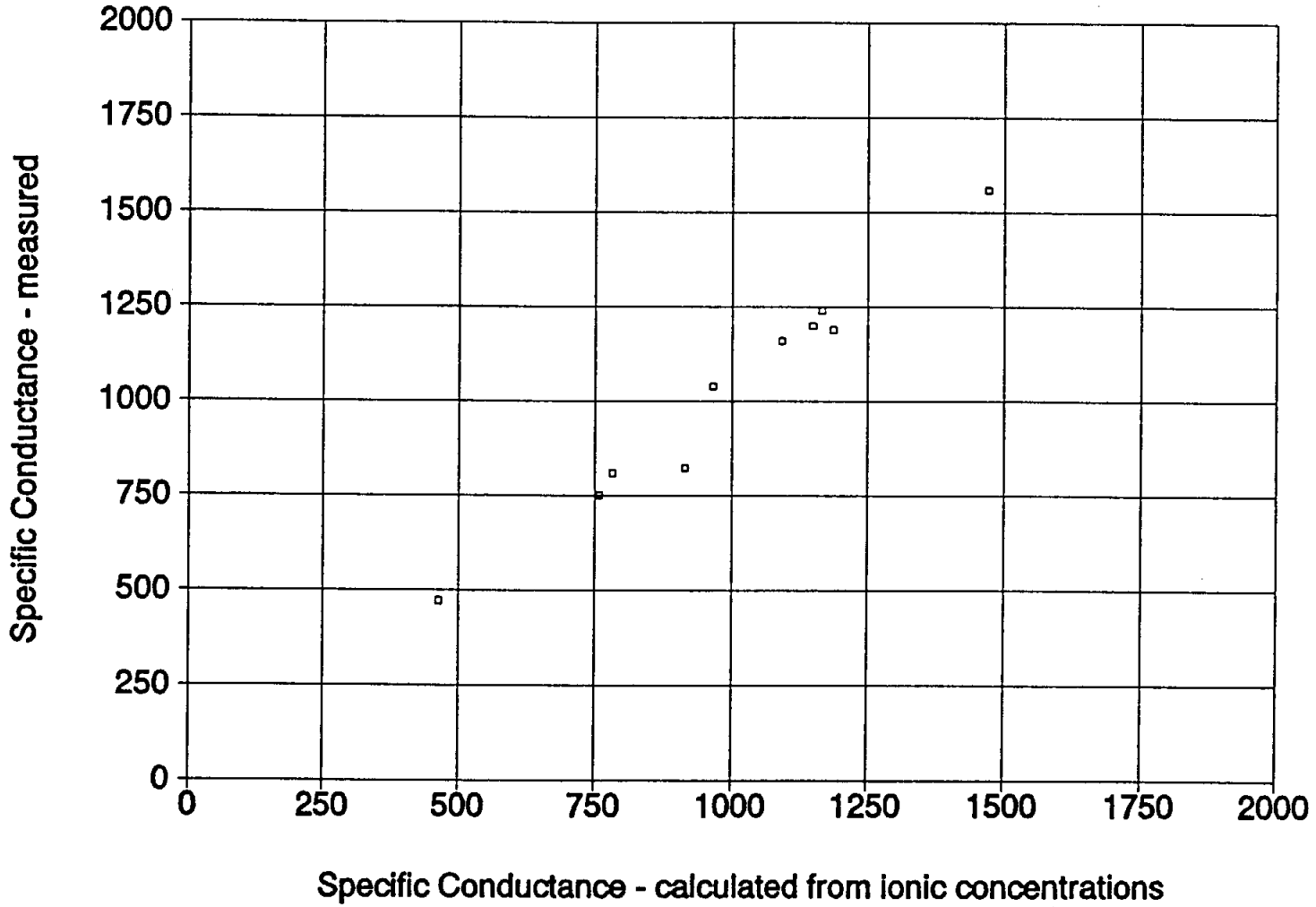

Figure 2-13. A graph of $Cw_{Measured}$ versus $Cw_{Ion\ Conc.}$ values ranging between 0 and 2,000 μmhos/cm. The data are from water analyses performed by Texas Department of Health Laboratories.

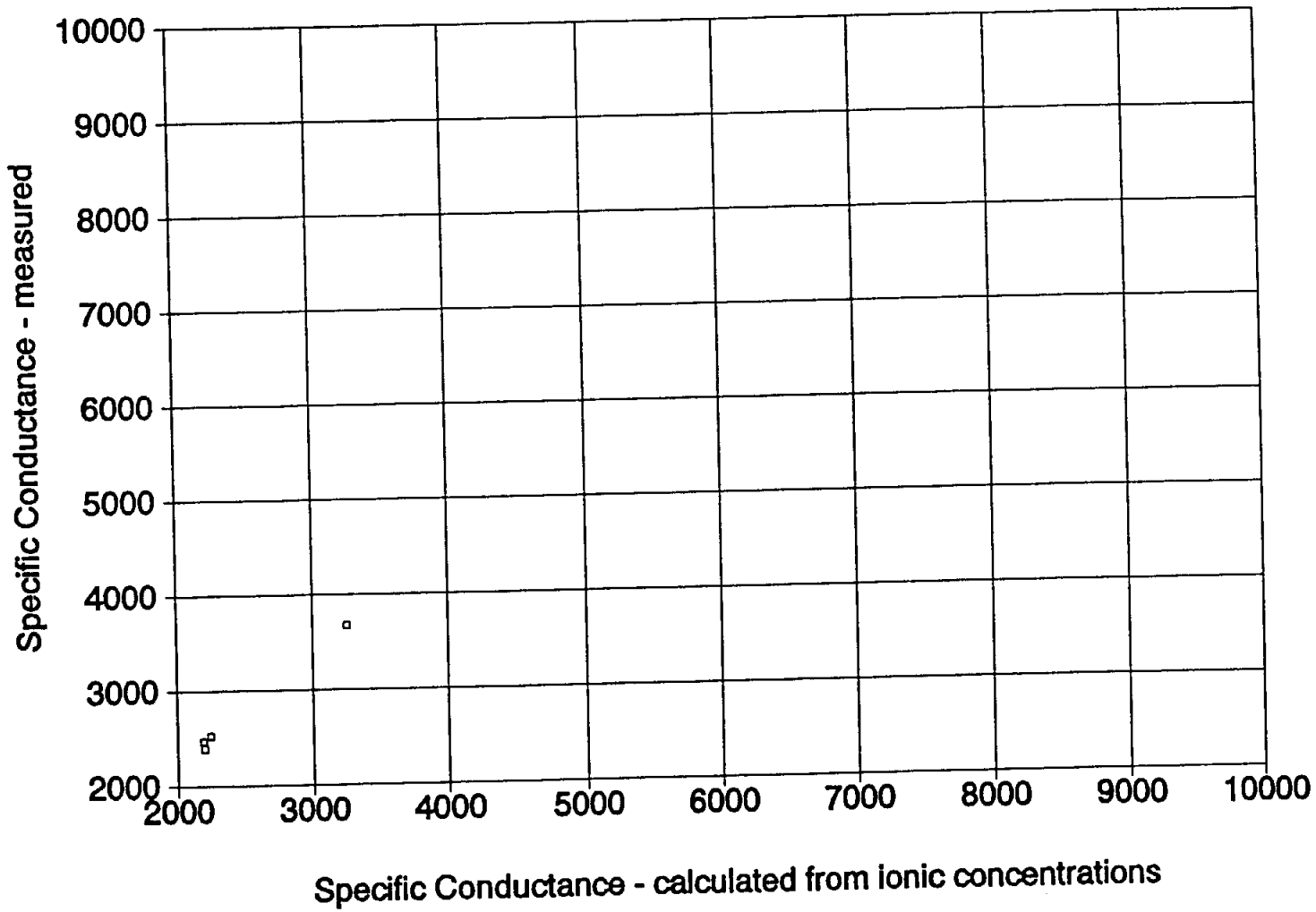

Figure 2-14. A graph of $Cw_{Measured}$ versus $Cw_{Ion\ Conc.}$ values ranging between 2,000 and 10,000 μmhos/cm. The data are from water analyses performed by Texas Department of Health Laboratories.

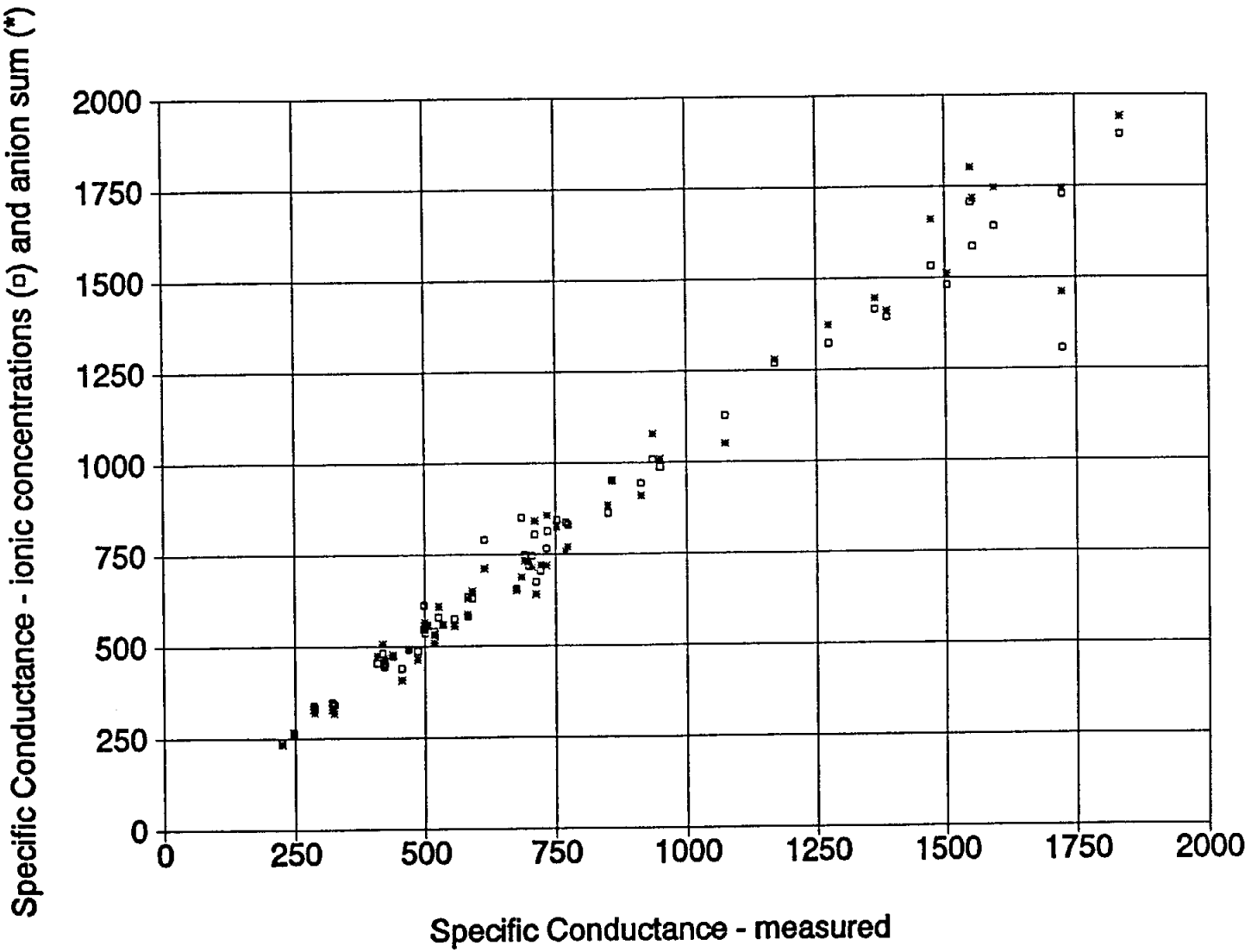

Figure 2-15. A graph of $Cw_{Measured}$ versus $Cw_{Ion\ Conc.}$ and $Cw_{Anion\ Sum}$ values ranging between 0 and 2,000 μmhos/cm. The data are from water analyses performed by Curtis Laboratories.

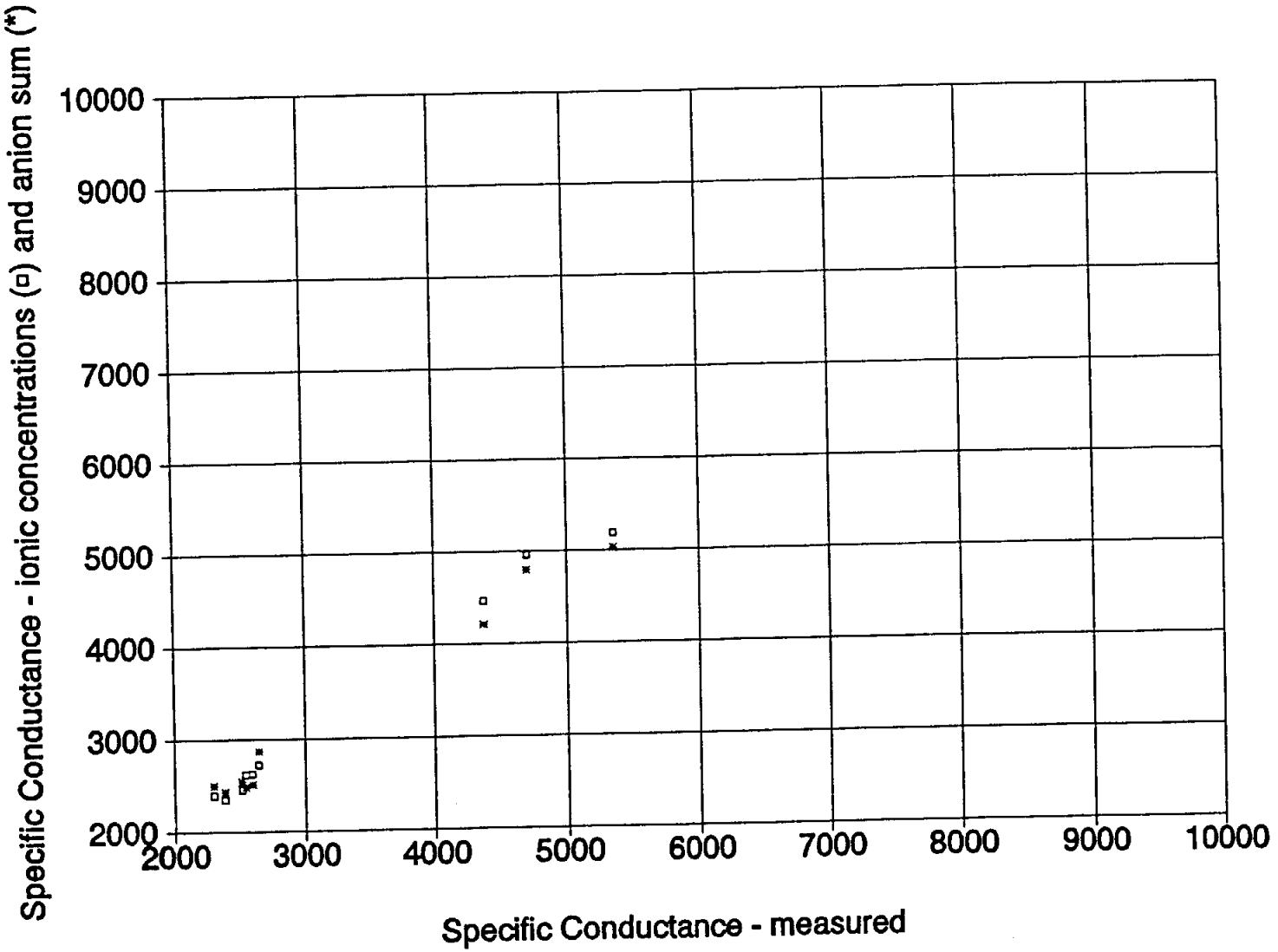

Figure 2-16. A graph of $Cw_{Measured}$ versus $Cw_{Ion\ Conc.}$ and $Cw_{Anion\ Sum}$ values ranging between 2,000 and 10,000 μmhos/cm. The data are from water analyses performed by Curtis Laboratories.

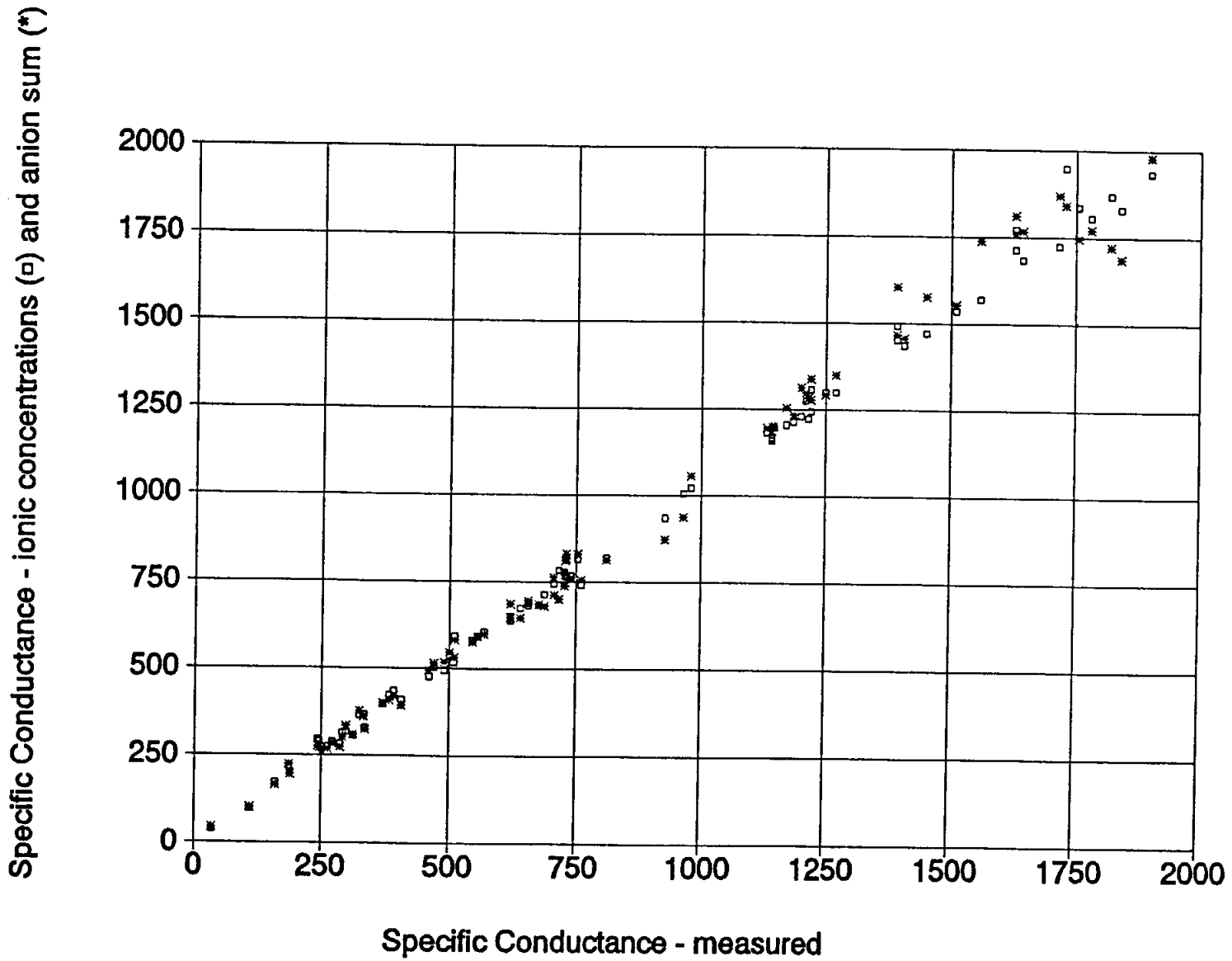

Figure 2-17. A graph of $Cw_{Measured}$ versus $Cw_{Ion\ Conc.}$ and $Cw_{Anion\ Sum}$ values ranging between 0 and 2,000 μmhos/cm. The data are from water analyses performed by Microbiology Service Laboratories.

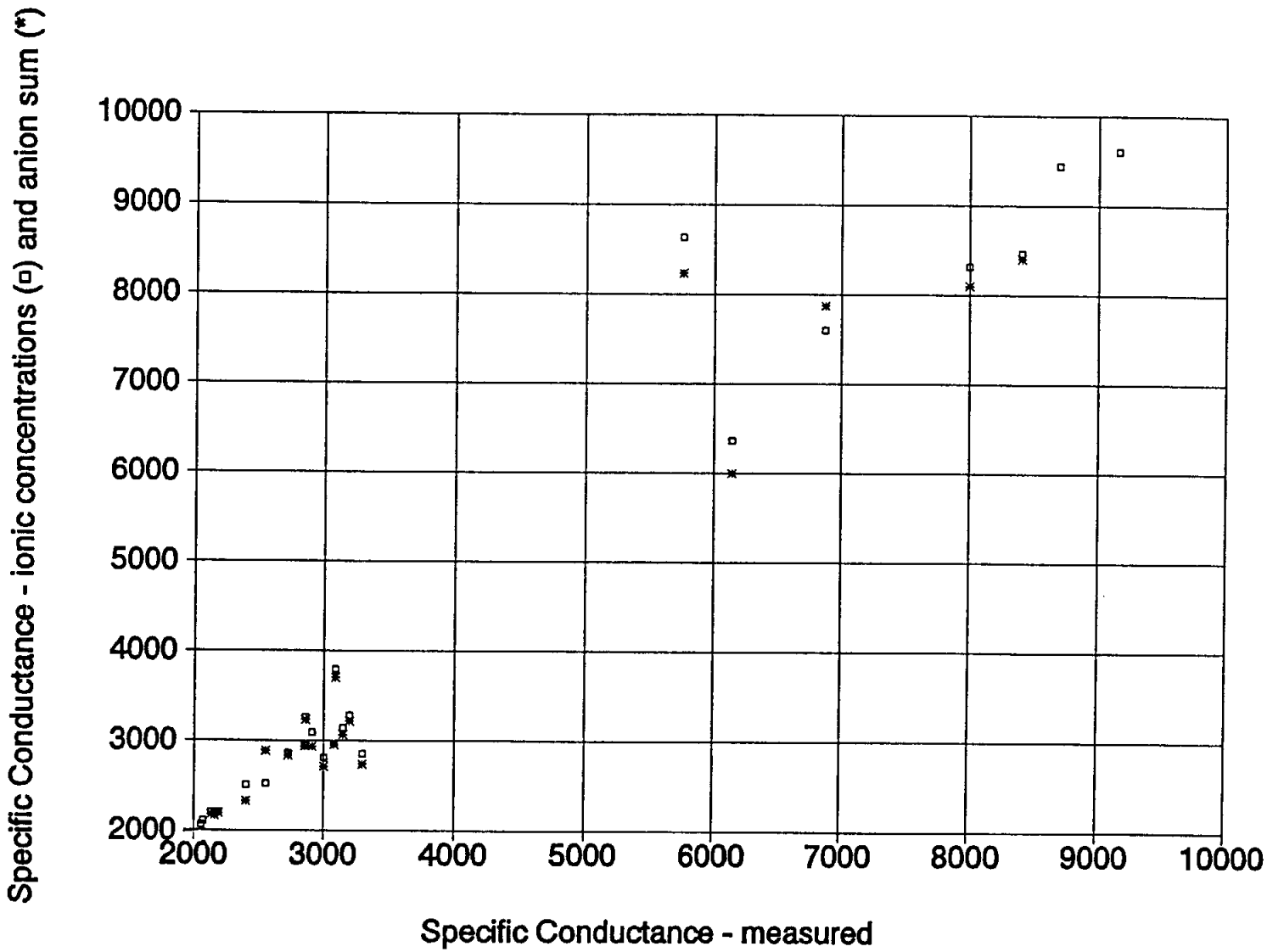

Figure 2-18. A graph of $Cw_{Measured}$ versus $Cw_{Ion\ Conc.}$ and $Cw_{Anion\ Sum}$ values ranging between 2,000 and 10,000 μmhos/cm. The data are from water analyses performed by Microbiology Service Laboratories.

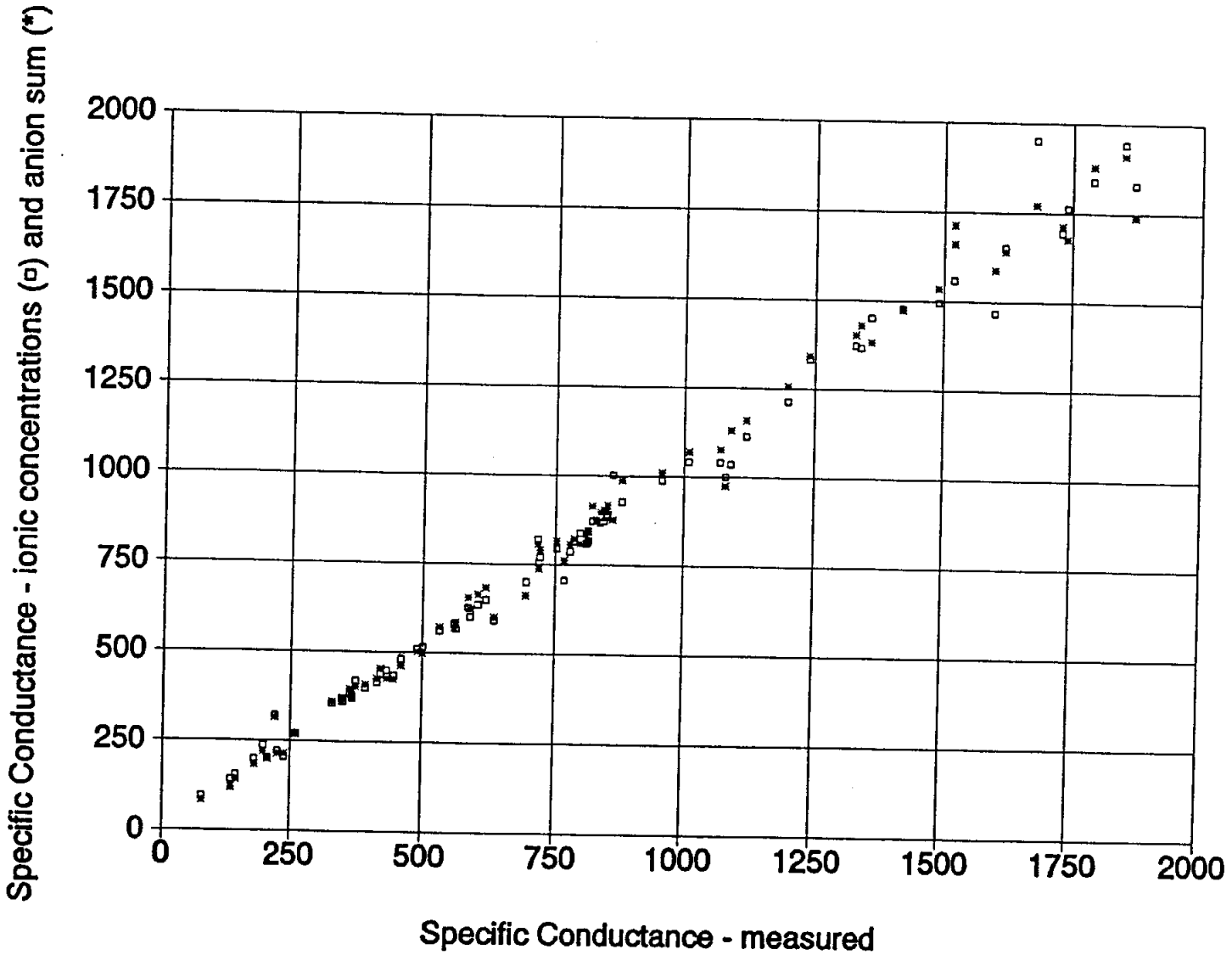

Figure 2-19. A graph of $Cw_{Measured}$ versus $Cw_{Ion\ Conc.}$ and $Cw_{Anion\ Sum}$ values ranging between 0 and 2,000 μmhos/cm. The data are from water analyses performed by Edna Wood Laboratories.

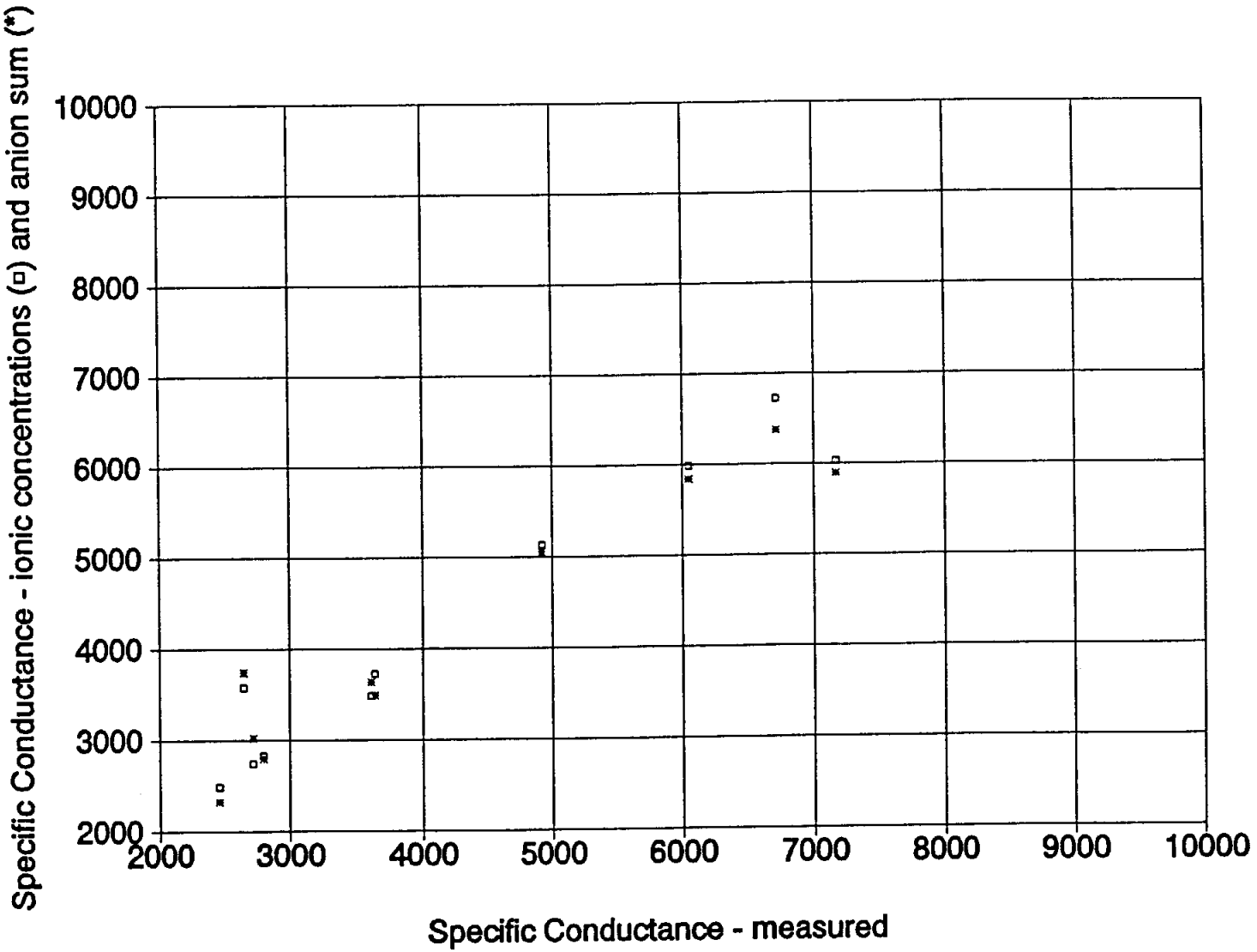

Figure 2-20. A graph of $Cw_{Measured}$ versus $Cw_{Ion\ Conc.}$ and $Cw_{Anion\ Sum}$ values ranging between 2,000 and 10,000 μmhos/cm. The data are from water analyses performed by Edna Wood Laboratories.

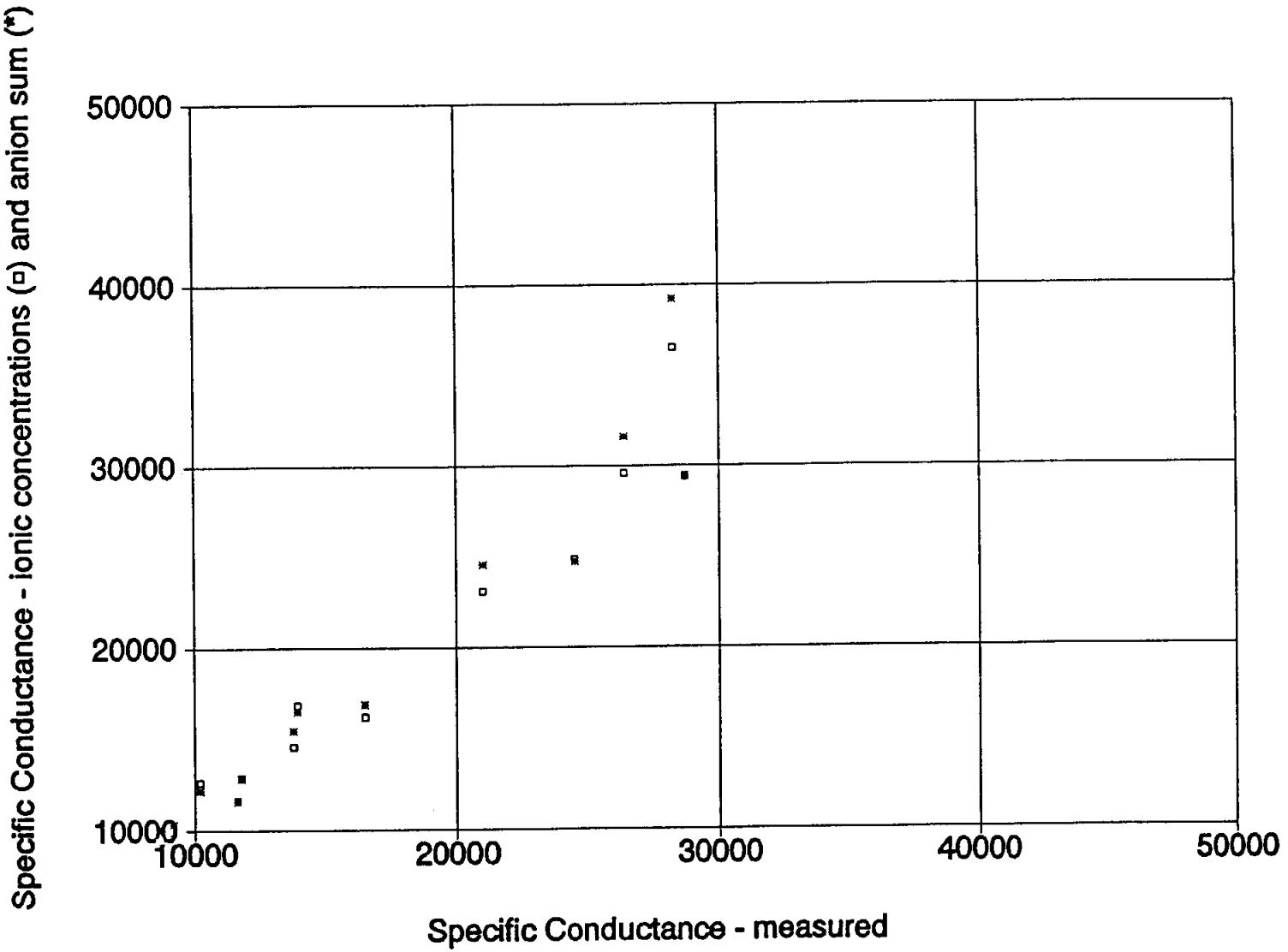

Figure 2-21. A graph of $Cw_{Measured}$ versus $Cw_{Ion\ Conc.}$ and $Cw_{Anion\ Sum}$ values ranging between 10,000 and 50,000 μmhos/cm. The data are from water analyses performed by Curtis, Microbiology Services, and Edna Wood Laboratories.

very high correlation between measured specific conductance and specific conductance calculated by ionic concentrations.

b. Table 2-5 summarizes the average percent variations for the ionic concentrations and anion sum methods.

Analysis of the data base (Figures 2-1 to 2-21 and Table 2-5) generally substantiates the conclusions drawn from the limited number of samples examined in Tables 2-1 to 2-4:

1. The accuracy of specific conductance measurements varies considerably by laboratory.

   a. A plot of measured specific conductance versus specific conductance from ionic concentrations for all six laboratories has considerable variation from a perfect correlation (Figures 2-1 to 2-3). However, separately plotting the data from each laboratory reveals considerable differences between laboratories in the quality of the correlation.
   b. Microbiology Service, Edna Wood, and Curtis have very high and consistent correlations between measured and calculated specific conductances. For waters with a specific conductance of less than 10,000 μmhos/cm the average percent variation is $\pm$3.2 to $\pm$7.7 percent, depending on the conductivity range (Table 2-5). This means that their measured conductances are apparently very accurate.
   c. Pope Testing and Texas Testing have a much lower correlation between measured and calculated specific conductance ($\pm$12.6 to $\pm$20.4 percent variation for specific conductances less than 10,000 μmhos/cm). Apparently, they do not measure conductance accurately.
   d. Texas Department of Health specific conductances less than 2000 μmhos/cm are usually within 6 percent of calculated values. Above 2000 μmhos/cm the accuracy of measured conductances decreases significantly ($\pm$10.6 percent variation).

2. Specific conductances calculated by ionic concentrations are more accurate than those calculated by anion sum. There is, however, not as much difference between the average percent variations for the data base (Table 2-5) as there is for the thirty samples in Table 2-4.

TABLE 2-5. COMPARISON OF THE ACCURACY OF SPECIFIC CONDUCTANCES CALCULATED BY THE ION CONCENTRATION AND ANION SUM METHODS

Laboratory	Cw range μmhos/cm	Number of samples	Ion concentration method Average % variation	Anion sum method Average % variation
Microbiology Service	0 - 2,000	83	5.4	6.6
	2,000 - 10,000	25	7.1	8
	10,000 - 50,000	5	13.4	16
Edna Wood	0 - 2,000	76	5.7	6
	2,000 - 10,000	10	6.6	9.2
	10,000 - 50,000	1	9.3	9.1
Curtis	0 - 2,000	59	7.7	7.7
	2,000 - 10,000	10	3.2	4.4
	10,000 - 50,000	4	12.6	13
Pope Testing	0 - 2,000	129	13.4	15
	2,000 - 10,000	13	20.4	19.1
	10,000 - 50,000	2	5.9	9.8
Texas Department of Health	0 - 2,000	10	4.4	5.9
	2,000 - 10,000	4	10.6	9
Texas Testing	0 - 2,000	9	12.6	9.8

3. The deviation between measured and computed specific conductances increases as conductivity increases.

Diluted conductance is a fourth method of determining specific conductance. The method is used when the conductivity of a water sample is beyond the range of the conductivity meter. It is a calculated, rather than measured, conductivity. Conductivity is first measured with a procedure that gives only a rough estimation of the actual value. This "measured" value is then used to determine the dilution factor. The water sample is diluted with distilled water in order to bring the conductivity down to a measurable value. The conductivity of the diluted sample is measured and then multiplied by the dilution factor to give the conductivity of the undiluted sample. Pope Testing uses this method when total dissolved solids exceeds 5000 mg/l (Pope Testing Laboratories, personal communication, 1990). The Texas Department of Health uses it routinely.

Unfortunately, diluted conductance yields values that may be grossly inaccurate (Table 2-1). Actual conductivity is less than diluted conductivity due to interionic interference. The percent of error increases as salinity increases. (The next section provides further explanation.) **Diluted conductance is not an acceptable method of measuring conductivity.**

Factors Controlling Water Conductivity

Pure water is basically nonconductive[1]. However, natural waters contain dissolved mineral matter in the form of electrically charged particles (ions)[2]. Electric current flows in water because ions move toward a current source that neutralizes them. Consequently, the current-carrying capacity or conductivity of water is a function of the movement of ions.

The movement of ions in water is primarily controlled by the concentration of the ions (total dissolved solids), the charge of each ionic species, the radius of each ionic species, the amount of interionic interference, and the water temperature. Each factor is discussed below in so far as it pertains to calculating total dissolved solids from logs. For a

---

[1] High-purity distilled or deionized water with no dissolved carbon dioxide has a conductivity of approximately 0.1 μmhos/cm. Upon reaching equilibrium with atmospheric carbon dioxide, the conductivity will be approximately 0.8 μmhos/cm (Worthington, et al., 1990).

[2] Silica, colloids, and some organic compounds are the exception. In most waters they are not electrically charged and do not contribute to conductivity (Hem, 1985).

more comprehensive discussion of these factors see Hem (1982), Miller et al. (1988), or a physical chemistry text[1].

Ionic charge and radius. The current-carrying capacity of an ion is, in part, a function of its ionic charge (valence number). Conductivity increases as ionic charge increases. However, ionic species with the same charge do not have the same current-carrying capacity. This is because each ionic species has a different radius[2]. The larger the radius of an ion, the slower it moves through water and the less it contributes to conductivity. Therefore, depending on the chemical composition of the water, two waters with identical total dissolved solids values may have significantly different conductivities! Thus, in order to accurately characterize different water types, TDS-Cw relationships must be established on a region-by-region and/or aquifer-by-aquifer basis.

Ion concentration. Ion concentration, better known as total dissolved solids, is the primary control on water conductivity. The greater the ion concentration, the greater the current-carrying capacity, and the greater the conductivity. The relationship between total dissolved solids and specific conductance is detailed in Chapter 4.

Interionic interference. As charged particles, ions in a solution interact with one another. Interionic interference decreases mobility, thus decreasing conductivity. Figure 2-22 reveals two important effects of interference on conductivity:

1. For most of the ions that commonly occur in ground waters, the rate at which conductivity increases declines as total dissolved solids increases. This is because interionic interference increases.

2. The amount of ionic interference varies according to the chemical composition of the water.

---

[1] Most of the physical chemistry and ground-water chemistry literature deals with dilute solutions. The movement of electrolytes in concentrated solutions such as saline ground waters has not been adequately studied. Moelwyn-Hughes' observation thirty years ago (1961) is still valid today: "Relatively little attention has been paid by experimentalists or theorists to the laws of conduction in concentrated solution." Fortunately, this does not adversely impact establishing accurate TDS-Cw relationships since they are empirically derived.

[2] Ions actually exist in water in a hydrated state - a layer of water molecules envelops each ion. The net effect is to increase the radius of the ion.

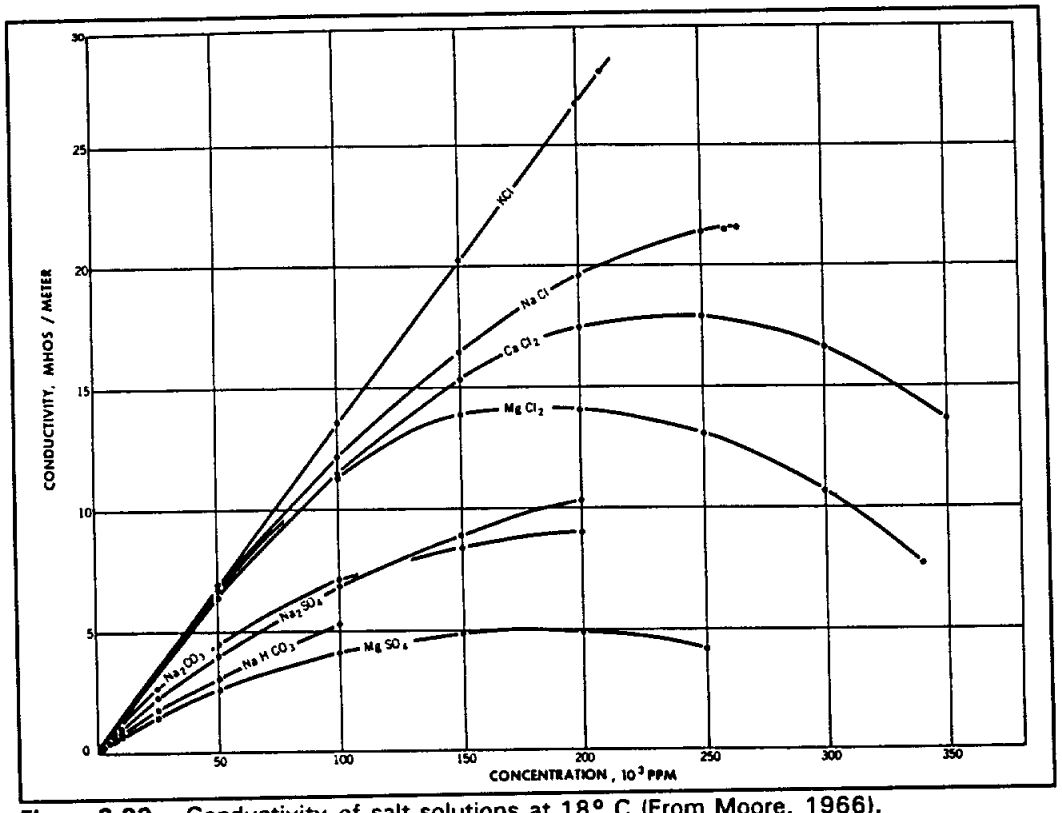

Figure 2-22. Conductivity of salt solutions at 18° C (From Moore, 1966).

a. For sodium chloride (NaCl) type waters up to 50,000 ppm TDS, the effect of interionic interference on conductivity is minimal.
b. For other types of waters, such as sodium bicarbonate ($NaHCO_3$), the effect of interionic interference on conductivity is significant at well below 50,000 ppm TDS.

Interionic interference has several important consequences for TDS-Cw relationships:

1. TDS-Cw relationships need to be established on a region-by-region and/or aquifer-by-aquifer basis in order to conform to the specific local water chemistry.

2. Errors may be introduced when extrapolating too far beyond the range of the data. When the TDS-Cw relationship for a particular water is used to calculate the total dissolved solids of a significantly more saline water, the calculated TDS will be too low.

3. Errors in calculating the TDS value of high salinity waters should be minimized by the fact that with increasing salinity most waters become predominately sodium chloride and have a similar TDS-Cw relationship.

4. Interionic interference is the reason that diluted conductivity measurements are invalid. The conductivity of a high salinity water is less than the conductivity of a diluted sample multiplied by the dilution factor. This is because the diluted sample will have little interionic interference, while the undiluted sample will have significant interference. The amount of error in diluted conductivity measurements increases as salinity increases.

Temperature. Conductivity increases as the temperature of a water sample increases. Elevating temperature increases the kinetic energy of ions and decreases water viscosity, which increases ionic movement. The effect of temperature on conductivity varies according to the ionic species.

Temperature changes can significantly alter conductivity. This is why conductivity measurements are standardized to a common temperature (25° C or 77° F). All ground-water laboratories in Texas use 77° F. The conductivity value is either measured at 77° F or converted to an equivalent conductivity at 77° F. Petroleum industry laboratories surveyed in this study use either 77° F, 75° F, or 68° F. Field measurements may be reported at sample temperature or the meter may automatically convert the measurement to 77° F.

When establishing a TDS-Cw relationship, specific conductance must be at 77° F. Also, a wireline log-derived specific conductance value must be converted from the temperature of the formation in the subsurface to 77° F before it is used in a TDS-Cw equation.

In logging literature, the Arps equation is the standard formula used to adjust water resistivity (or conductivity) for temperature changes.[1] Arps (1953) used the water resistivity (Rw) of NaCl solutions measured at varying

[1] In much of the literature, the equation is written using 6.77 instead of 7. However, 7 is easier to remember and is just as accurate given the precision with which formation temperature can be measured. Arps himself (1953) recommended rounding 6.77 to 7. Etnyre (1989, p. 56-57) has a good discussion of resistivity temperature conversion equations.

temperatures to establish an empirical relationship between water resistivity and temperature. The relationship is as follows:

$$Rw_{@T_2} = Rw_{@T_1}\left(\frac{T_1 + 7}{T_2 + 7}\right) \qquad (2\text{-}3)$$

Where:
Rw = *water resistivity*
T_1 = *temperature in °F at which Rw was measured.*
T_2 = *temperature in °F to which Rw is being converted.*
7 *is a constant when using °F. Use* 21.5 *for °C.*

Some log analysts use a simplified version of the Arps equation:

$$Rw_{@T_2} = Rw_{@T_1}\left(\frac{T_1}{T_2}\right) \qquad (2\text{-}4)$$

Resistivity is the inverse of conductivity (Cw), so when converting conductivity to another temperature equations 2-3 and 2-4 become:

$$Cw_{@T_2} = Cw_{@T_1}\left(\frac{T_2 + 7}{T_1 + 7}\right) \qquad (2\text{-}5)$$

and

$$Cw_{@T_2} = Cw_{@T_1}\left(\frac{T_2}{T_1}\right) \qquad (2\text{-}6)$$

Where:
Cw = *water conductivity*
T_1 = *temperature in °F at which Cw was measured.*
T_2 = *temperature in °F to which Cw is being converted.*
7 *is a constant when using °F. Use* 21.5 *for °C.*

The Arps equation is for NaCl type waters (i.e. most saline ground waters). Fresh and slightly to moderately saline ground waters, as well as some saline, sulfate-rich ground waters, are not NaCl type waters and may have a different relationship. In the petroleum literature Worthington et al. (1990) has issued the most recent caution: "resistivity corrections of non-NaCl brines with the Arps equation should be verified."

The need to establish temperature-conductivity relationships for different types of ground waters is mentioned in ground-water literature (Hem, 1982), but data are only available for low salinity, single salt solutions. A general rule of thumb commonly stated in the literature is that conductivity increases about 2 percent per ° C increase in temperature (Hem, 1982).

Unfortunately, conductivity corrections for non-NaCl type waters have not been published in either petroleum or ground-water literature. Moore and Kaufman (1983) have come the closest. They determined the actual temperature-conductivity relationship for five oilfield water samples. Conductivities of the waters ranged from 1,800 to 11,000 μmhos/cm at 77° F. Their paper includes only a graph of the temperature-conductivity relationships, not the raw data. Moore (personal communication, 1990) supplied the actual measurements, along with data from a sixth sample. A water analysis was only available for the sixth sample. His data are samples 1 through 6 in Table 2-6.

To document the accuracy of the Arps and the 2 percent per ° C increase in temperature equations for Texas ground waters, six water samples were selected with conductivities ranging from 1,600 to 38,000 μmhos/cm at 77° F.[1] These samples were selected because each had a complete routine water analysis, they had various conductivities, and they were available. The Austin USGS Water Resources Laboratory measured the conductivity of each sample at eight temperatures from 41° to 104° F.[2] The measurements are graphed in Figure 2-23 and listed in Table 2-7. Table

---

[1] Note: Water sample #12 from the Petrolero Corp. #1-3 is not the same water sample used in Tables 2-2 to 2-4, although both samples are from the same well. The first sample was spilled; an additional sample was obtained from the well, but the conductivity is higher (38,364 vs. 33,832 μmhos/cm).

[2] Measurements were taken with a new Beckman BB1 dip cell. The cell constant of 1.000 @ 25° C was verified with a NBS Traceable 1,000 μs Y.S.I. conductivity standard. The instrument uses a General Radio 1656 CGRL impedance bridge. Temperature was controlled by a Forma Scientific water bath to an accuracy of ±0.1° C and monitored with a Guild Line digital thermometer to an accuracy of ±0.05° C.

2-6 lists only the measurements that are within the temperature range normally of interest to ground-water studies (less than 125° F).

Based on the data compiled in Table 2-6 and Figure 2-23, the following conclusions are made about published temperature-conductivity relationships:

1. For the entire data base, the 2 percent per ° C equation has the smallest maximum variations from measured values (±7 percent). The Arps values reach 9 percent variation and the simplifed Arps values reach 14 percent. However, the variation is less than ±5 percent for most of the values from all three equations. This is within the acceptable accuracy tolerance of conductivity measurements.

2. No one equation consistently yields more accurate values.

   a. For Moore and Kaufman's samples, the simplified Arps equation clearly is the least accurate. The 2 percent per ° C equation is generally more accurate than the Arps relationship.
   b. For the Texas samples, however, the simplified Arps equation generally has the highest accuracy and the 2 percent per ° C equation usually has the lowest.
   c. The equations are such that the simplifed Arps always has the largest value, the 2 percent per ° C is the lowest, and the Arps value is in the middle. However, any of the three values may be the most accurate.

3. Since the trend of the values is not consistent between the two data sets, the relationship should be determined for some additional Texas waters of various types and chemical compositions.

4. In the absence of ~~any~~ further data, any of the three equations apparently will give acceptable temperature-corrected conductivity measurements for Texas ground waters (within ±5 to ±7 percent of the actual value). However, the 2 percent per ° C equation is less likely to yield extreme values.

TABLE 2-6. COMPARISON OF THE ACCURACY AT WHICH THREE DIFFERENT EQUATIONS CORRECT SPECIFIC CONDUCTANCE FOR TEMPERATURE CHANGES

Sample #[1]	Temp °F	Temp °C	$Cw_{measured}$	$Cw_{calculated}$ from 2%/°C	% variation[3]	$Cw_{calculated}$ from Arps equation[2]	% variation[3]	$Cw_{calculated}$ from simplified equation[2]	% variation[3]
1 - oilfield water	77	25	1,815						
	100	38	2,278	2,287	0.4	2,313	1.5	2,358	3.5
	120	49	2,786	2,686	-3.6	2,747	-1.4	2,825	1.4
2 - oilfield water	77	25	2,208						
	100	38	2,732	2,782	1.8	2,814	3	2,865	4.9
	120	49	3,311	3,268	-1.3	3,341	0.9	3,497	5.6
3 - oilfield water	65	18	2,381						
	100	38	3,333	3,333	0	3,542	6.3	3,663	10
	125	52	4,000	4,000	0	4,372	9	4,587	14.7
4 - oilfield water	72	22	5,988						
	112	44	9,009	8,623	-4.3	9,029	0.22	9,346	3.7
	125	52	10,000	9,581	-4.2	10,017	0.17	10,417	4.2
5 - oilfield water	67	19	9,524						
	104	40	13,158	13,524	2.8	13,784	4.8	14,286	8.6
	120	49	15,152	15,238	0.6	16,367	8	17,065	12.6
6 - oilfield water	77	25	73,529						
	100	38	89,286	92,647	3.8	93,717	5	95,493	7
	120	49	102,040	108,823	6.6	111,272	9	114,591	12.3
7 - BRC 58-35-721 Travis Co. 398'	77	25	1,227						
	104	40	1,654	1,595	-3.6	1,622	-2	1,705	3.1
8 - Petrolero Corp. #4-3 McMullen Co. 4030'	77	25	1,610						
	104	40	2,034	2,093	2.9	2,129	4.7	2,175	6.9
9 - Quintana #C-9 McMullen Co. 3845'	77	25	4,008						
	104	40	5,510	5,210	-5.4	5,298	-3.9	5,411	-1.8
10 - Skinner & Newman #A-11 McMullen Co. 4634'	77	25	7,580						
	104	40	10,230	9,854	-3.7	10,023	-2	10,240	0.1
11 - Skinner & Newman #C-10 McMullen Co. 4660'	77	25	7,460						
	104	40	10,390	9,698	-6.7	9,864	-5.1	10,078	3
12 - Petrolero Corp. #1-3 McMullen Co. 5533'	77	25	38,364						
	104	40	52,715	49,873	-5.4	50,729	-3.8	51,830	-1.7

[1] Data for samples 1-6 supplied by Vic Moore. Samples 1-5 were used in Moore and Kaufman (1983). The water analyses for Samples 7-12 are in Table 2-2. Note: Sample #12 is slightly different than the samples used in Table 2-2. However, both samples are from the same well.

[2] For each water analysis, the $Cw_{measured}$ at the lowest temperature was used to calculate Cw for each of the other temperatures.

[3] Percent variation from $Cw_{measured}$.

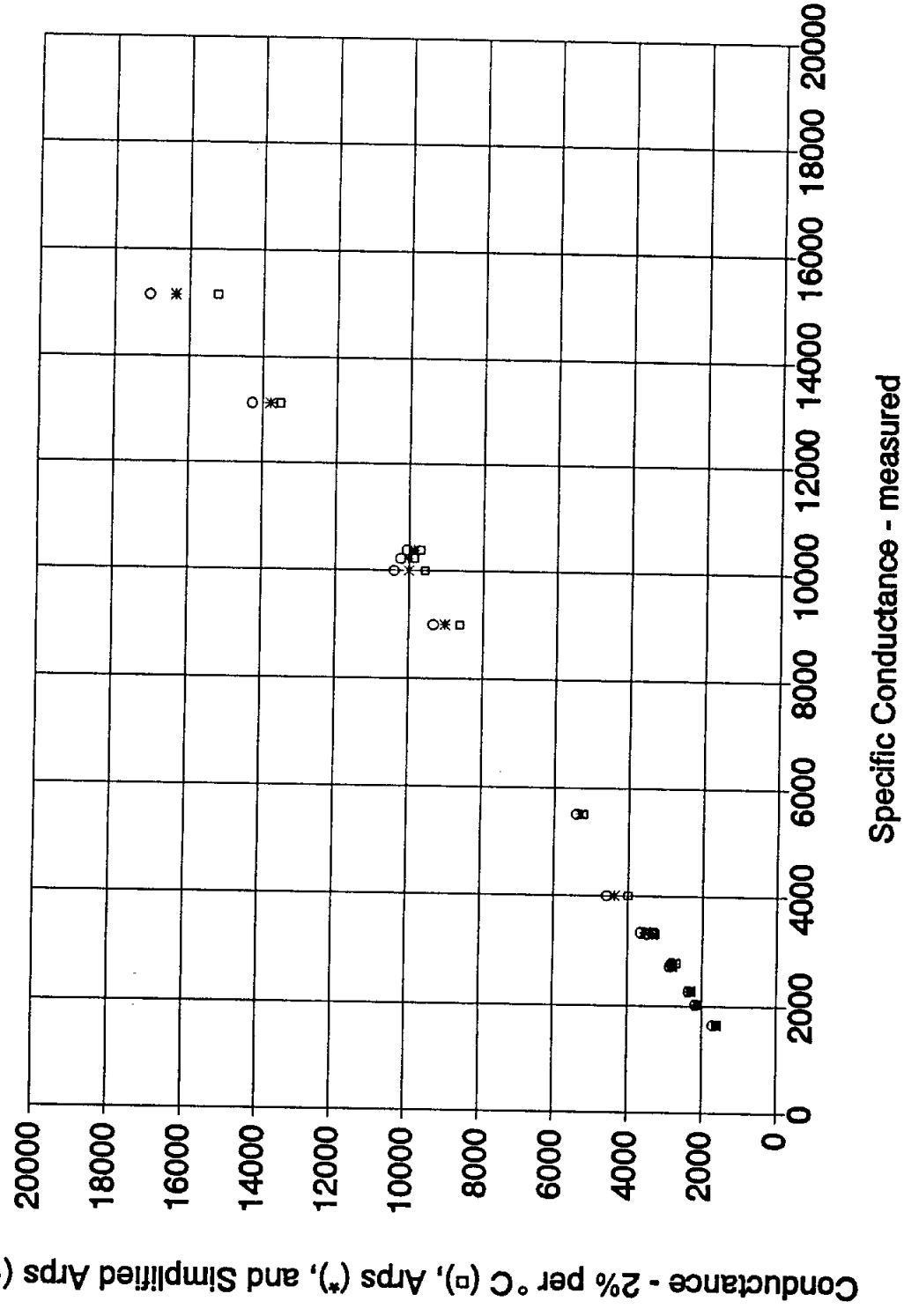

Figure 2-23. A comparison of the accuracy at which three different equations correct specific conductance for temperature changes.

TABLE 2-7. MEASURED SPECIFIC CONDUCTANCES AT VARIOUS TEMPERATURES

Temp ° F	Measured Specific Conductances					
	BRC 58-35-721 Travis Co. 398'	Petrolero #4-3 McMullen Co. 4030'	Quintana #C-9 McMullen Co. 3845'	Skinner & Newman #A-11 McMullen Co. 4634'	Skinner & Newman #C-10 McMullen Co. 4660'	Petrolero #1-3 McMullen Co. 5533'
41	768	-----	2,594	4,592	4,663	25,467
50	882	1,229	2,982	5,296	5,256	28,604
59	997	1,393	3,362	5,794	5,931	32,243
68	1,099	1,554	3,760	6,810	6,633	35,654
77	1,227	1,610	4,005	7,580	7,460	38,364
86	1,353	1,791	4,490	8,425	8,170	43,873
95	1,501	1,823	4,970	9,360	9,330	48,048
104	1,654	2,034	5,510	10,230	10,390	52,715

TOTAL DISSOLVED SOLIDS

Chapter 3

Establishing a valid TDS-Cw relationship also requires a consistent definition of total dissolved solids and a water analysis with an accurate total dissolved solids measurement. This chapter contains a discussion of the various terms used to describe total dissolved solids and the techniques used to calculate the measurement.

Units of Measurement

Describing the amount of dissolved solids in water can be a confusing task. Through the years a number of units of measurement have been used (see Hem, 1985 for a detailed discussion). Three units of measurement, which are all equivalent for fresh and slightly to moderately saline waters, are commonly used today: parts per million by weight (ppm), milligrams per liter (mg/l) and the new SI unit, kilograms per cubic meter (kg/m^3). Laboratories in Texas use mg/l or ppm (Table 3-1). This report uses mg/l and ppm interchangeably.

Strictly speaking, mg/l and ppm are not equivalent at high temperatures and concentrations above 7,000 mg/l (Hem, 1985), since a liter of water no longer weighs exactly 1 kilogram. Practically speaking, however, the difference is so slight for fresh and slightly to moderately saline waters as to be well within the accuracy limitations of logging techniques. For brines and very saline waters, however, the distinction between ppm and mg/l is significant and the terms should not be used interchangeably. For example, a water having a TDS of 50,000 mg/l would contain 50 g of dissolved solids in a liter and would weigh 1.05 g. In terms of ppm its TDS would be 50,000/1.05 or 47,600 ppm.

A fourth unit, not equivalent to the other three, is grains per gallon (1 grain/gal = 17.12 mg/l or 1 mg/l = 0.058 grain/gal). This unit of measure is rarely used.

Chemists commonly express dissolved solids in milligram equivalents per liter (meq/l or meq) or equivalents per million. These units are equivalent. Technically the term equivalents per million is used when the water analysis is recorded as parts per million. Milligram equivalents per liter is used when the analysis is in milligrams per liter (Hem, 1985). This fifth unit of measurement is used to

check the anion-cation balance of a water analysis. It is a quick, efficient means of checking the accuracy and/or completeness of a water analysis. Since all waters are electrochemically neutral, the sum of the anions in meq/l and the sum of the cations in meq/l should be equal. (See Appendix I, **GUIDELINES FOR VERIFYING THE ACCURACY OF WATER ANALYSES,** for an explanation of anion-cation balances.) The Texas Department of Health and some oilfield laboratories report both mg/l and meq/l.

TABLE 3-1. TDS NOMENCLATURE AND UNITS OF MEASUREMENT USED BY THE MAJOR TEXAS WATER LABORATORIES

Laboratory	Nomenclature	Unit of Measurement
Texas Water Development Board (TWDB)	dissolved solids	mg/l
United States Geological Survey (USGS)	dissolved solids sum	mg/l
Pope Testing Laboratories	dissolved residue calculated	ppm
Curtis Laboratories*	total solids	ppm
Texas Testing Laboratories*	total dissolved solids	mg/l
Microbiology Service Laboratories (now Edna Wood)*	total dissolved solids calculated	ppm
Edna Wood Laboratories	total dissolved solids calculated	ppm
Texas Department of Health (TDH)	total dissolved solids calculated	mg/l

*lab no longer in business

Nomenclature

In ground-water and petroleum logging literature the amount of dissolved solids in water is referred to as total dissolved solids (TDS), dissolved solids, or salinity[1]. Salinity expressed as ppm is commonly used in petroleum logging literature. The terms total dissolved solids and dissolved solids, expressed as mg/l, are used by the ground-water industry. Water laboratories in Texas use several variations of the two terms as shown in Table 3-1.

Total dissolved solids and dissolved solids are not synonymous terms. Total dissolved solids is a measurement of **all** the dissolved solids in a

[1] In some fields of science salinity and TDS are not synonymous terms. APHA "Standard Methods" (1985) defines salinity as "total solids in water after all carbonates have been converted to oxides, all bromide and iodide have been replaced by chloride, and all organic matter has been oxidized" and indicates this definition is used in oceanography (Hem, personal communication, 1990).

specific water sample. Dissolved solids is the sum of all the chemical constituents that were analyzed in a specific water sample. Since routine water analyses test for only major constituents, the argument is made that the term dissolved solids, rather than total dissolved solids, is the more accurate terminology. Nevertheless, the terms are used interchangeably by many people, including this author.

While, technically speaking, total dissolved solids and dissolved solids are not equivalent terms, practically speaking they can be used synonymously for a "complete" routine water analysis[1]. This is especially true as far as log analysis is concerned because:

1. A "complete" routine water analysis will come very close to determining the total amount of dissolved solids in a water sample. The analysis will test for silica (SiO_2), calcium (Ca^{++}), magnesium (Mg^{++}), sodium (Na^{+}), chloride (Cl^{-}), bicarbonate (HCO_3^{-}), sulfate (SO_4^{--}), and carbonate (CO_3^{--}). Generally a few other constituents such as fluoride (F^{-}), nitrate (NO_3^{-}), potassium (K^{+}), manganese (Mn^{++}), iron (Fe^{++}), and aluminum (Al^{+++}) will also be included. For normal ground waters (those that do not have excessive concentrations of organics, nitrate, sulfate, or suspended matter) this will cover nearly all the natural constituents that occur in concentrations of 1 mg/l or more (Hem, 1985, p. 54). Any other ions present will make an insignificant contribution to the dissolved solid content and specific conductance of the water[2].

2. The amount of natural constituents not analyzed for in a "complete" routine water analysis of a normal water will be so small (less than 1 mg/l for each constituent) as to be well within the accuracy limitations of logging techniques.

---

[1] See Davis (1988) for an excellent editorial on the need for "complete" routine water analyses.

[2] Hem (1985, p. 164) points out that waters having dissolved-solids concentrations over 1000 mg/l tend to have large concentrations of a few constituents. He has a thorough discussion of over forty naturally occurring ground-water constituents.

Measurement Techniques

A matter of important concern is the formula used to calculate total dissolved solids. Two methods have been used: the sum of the measured dissolved constituents, and residue on evaporation, commonly labeled dissolved residue at a specific temperature.

Until the advent of modern analytical equipment, total dissolved solids was determined by evaporating a known amount of water and then weighing the residue (called residue on evaporation). The method works well except for one shortcoming- bicarbonate is lost during evaporation. HCO_3^- is converted to CO_3^{--}, CO_2, and H_2O with 50.8 percent of the HCO_3^- driven off as CO_2 and H_2O vapor and 49.2 percent remaining as CO_3^{--}. For waters high in bicarbonate, and many in Texas are, residue on evaporation yields a TDS value that is too low by hundreds of mg/l.

With the advent of modern analytical equipment, most laboratories abandoned residue on evaporation. Today, all the laboratories listed in Table 3-1 that are still in business use various analytical techniques to measure each ionic species. The TDS they report is the sum of the measured dissolved constituents.

Since modern techniques measure 100 percent of the bicarbonate in a sample, the sum of the measured dissolved constituents will not equal residue on evaporation, unless an adjustment is made to the bicarbonate value. With proper adjustment to the bicarbonate value, the two techniques give the same TDS. The problem centers on which way to adjust the bicarbonate value- leave it at 100 percent or use only 49.2 percent? Standard procedure in the ground-water industry is to use only 49.2 percent, thus convert[illegible] sum of the measured dissolved constituents to the equival[illegible]ue on evaporation value. The formula for this co[illegible]tten two ways (using concentrations in mg/l) as

$$tal\ of\ ions + SiO_2 - \left(0.508 \times HCO_3^-\right) \qquad (3\text{-}1)$$

or

$$TDS = \left(0.492 \times HCO_3^-\right) + SiO_2 + all\ other\ ions \qquad (3\text{-}2)$$

The other option is to include 100 percent of the bicarbonate (HCO_3^-) value. In this case the formula in mg/l is as follows:

$$TDS = total\ of\ ions + SiO_2 \qquad (3\text{-}3)$$

The Texas Water Development Board, Texas Department of Health, United States Geological Survey, Environmental Protection Agency, and Texas Testing Laboratories include 49.2 percent of the bicarbonate value. Edna Wood, Pope Testing, Curtis, and oilfield laboratories include 100 percent. Not all laboratory reports specify which amount of bicarbonate is included in the total dissolved solids value.

Total dissolved solids should include 100 percent of the bicarbonate value. This is more accurate than using 49.2 percent because:

1. The total dissolved solids value will include the actual amount of bicarbonate ions in the water (100 percent). Reporting 49.2 percent of the bicarbonate ions is simply an archaic carry-over from the days before modern analytical equipment.

2. Water conductivity is a function of all the dissolved ions, including 100 percent of the bicarbonate ions.

3. Water conductivity is one of the primary controls on resistivity and induction log responses. Consequently, the log responses are affected by and reflect the 100 percent bicarbonate concentration.

4. Many ground waters in Texas are high in bicarbonate, and 100 percent bicarbonate will more accurately reflect the geochemistry of the waters.

Accuracy

A routine water analysis of a normal ground water will produce a TDS value within ±5 percent of the actual TDS value (Hem, 1985, p. 163). The accuracy can be verified by an anion-cation balance, a comparison with residue on evaporation, or a TDS-Cw relationship (see Appendix I, **GUIDELINES FOR VERIFYING THE ACCURACY OF WATER ANALYSES**). Anion-cation balances and residue on evaporation are the preferred methods. One or the other should be included in every water analysis. The TDS-Cw

relationship should only be used when the relationship has been established by utilizing water analyses in the vicinity of the sample in question. The United States Geological Survey and Texas Department of Health use anion-cation balance. Edna Wood and some Curtis water analyses use residue on evaporation. Pope, Texas Testing, and some Curtis analyses do not include an anion-cation balance or a residue on evaporation.

TDS-Cw RELATIONSHIPS

Chapter 4

Total dissolved solids cannot be calculated directly from wireline logs. It is estimated by entering a log-derived water conductivity value into a previously determined TDS-Cw relationship. Consequently, no matter how good the log data and how accurate water conductivity, a correct TDS-Cw relationship is critical to TDS calculations.

This chapter reviews the construction and utilization of TDS-Cw graphs. Also included is an explanation of the procedures used to construct TDS-Cw graphs from the Texas Water Development Board Ground-Water Data Base.

TDS-Cw graphs are to be constructed according to the following guidelines established in Chapters 2 and 3:

1. Water conductivity is controlled by ion concentration (TDS), the charge of each ionic species, the radius of each ionic species, the amount of interionic interference, and the water temperature.

2. Water conductivity (Cw) is primarily a function of TDS, which is why Cw is the best parameter for estimating TDS.

3. Water conductivity is, in part, a function of the charge and radius of the ions in the water and the amount of interionic interference. Two waters with identical TDS values but different chemical compositions can have significantly different conductivities! Thus in order to accurately characterize different types of water, TDS-Cw relationships must be established on a region-by-region and/or aquifer-by-aquifer basis.

4. Water conductivity is a function of all the ions in solution, including 100 percent of the bicarbonate ions. TDS values should include 100 percent of the bicarbonate value, not 49.2 percent.

5. The accuracy of conductivity measurements varies widely among laboratories (see Table 2-1).

6. Diluted conductivity is not an acceptable conductivity measurement. A conductivity value calculated from the ionic concentrations should be used instead.

7. Conductivity calculated from ionic concentrations ($Cw_{Ion\ Conc.}$) is a good quality control check on the accuracy of measured conductivity. It can also be used when a water analysis does not include a measured conductivity. The accuracy of $Cw_{Ion\ Conc.}$ values is as follows:

   a. $Cw_{Ion\ Conc.}$ varies by ± 5 percent or less from $Cw_{Measured}$ for conductivities up to about 35,000 μmhos/cm.
   b. Above 35,000 μmhos/cm, $Cw_{Ion\ Conc.}$ varies from ± 6 to ± 11 percent from $Cw_{Measured}$.
   c. $Cw_{Ion\ Conc.}$ normally exceeds $Cw_{Measured}$.

8. As ground waters become more saline, the amount of interionic interference increases and the slope of the TDS-Cw relationship tapers off. Consequently, extrapolating too far beyond the range of the TDS-Cw data will give TDS values that are too low.

CONSTRUCTION OF TDS-Cw GRAPHS

Acquiring the Data

Water analyses are available from a number of different sources. The ground-water industry is the source for ~~the majority of~~ fresh to moderately saline water analyses and a few very saline analyses. Almost all of the data will be complete, routine water analyses. The petroleum industry provides most of the very saline water analyses and a few fresh to moderately saline water analyses which are usually incomplete. Sources for water analyses are as follows:

1. **Texas Natural Resources Information System (TNRIS) of the Texas Water Development Board (TWDB), Ground-Water Data Base.** This is a computerized data base which contains routine water analyses collected by the Texas Water Development Board. It is the largest data base in Texas for fresh to moderately saline water analyses. A few of the analyses are of saline waters. Analyses can be retrieved by county, aquifer, state well number, and latitude-

longitude from the TNRIS by contacting their office in Austin. Locations of the wells having such analyses can be found in various TWDB files in Austin. This TNRIS data retrieval system does not provide the convenience of readily identifying and locating the wells and analyses by well name or well owner. A fee is charged to retrieve such analyses from the TNRIS files (Bob Bluntzer, personal communication, 1991).

2. **The Texas Water Commission, Central Records, Ground-Water Technical Files.** A part of these files have the hard copies of the analyses in the TNRIS Ground Water Data Base. Such analyses are provided in a subfile titled "Located Well Data" which has the analyses and other information on the related well filed by county and then by state well number in numerical order. Another part of these files contains hard copies of some water analyses (conducted by commercial laboratories) that were submitted by water well drillers with their Water Well Reports as required by the Texas Water Well Drillers Board. Such analyses are provided in subfiles titled "Drillers Logs Plotted or Unplotted" and are filed with the related Water Well Reports which are filed by county and then by partial state well number in numerical order. Locations of the wells having such analyses can be found in various TWDB reports (see Item 3. below) and/or on base maps available in TWDB files in Austin. This filing system and related maps do not provide the convenience of readily identifying and locating the wells and analyses by well name or well owner. A fee is charged for copying such data (Bob Bluntzer, personal communication, 1991).

3. **Texas Water Development Board Publications.**

   a. **Texas Water Development Board Report 157, Volume 2, <u>Chemical Analysis of Saline Waters</u>.** This volume is a catalogue of saline water analyses by county and depth. Most entries include TDS, major cations, major anions, and geological formation (water-bearing unit). Unfortunately, there is no key to the well numbers, and water resistivity (Rw) is not listed for most entries. Rw is only listed when the cations and anions are missing from the analysis. Another drawback is that the source of the water sample is not given.

b. **Texas Water Development Board Report 157, Volume 1,** A Survey of the Subsurface Saline Water of Texas. This volume contains water salinity maps for various aquifers.

c. **Various Texas Water Development Board Ground-Water Reports.** These reports contain complete, routine water analyses. The well, well owner and in some cases the well name or number can be identified for each analysis. These reports cover a county or a group of counties and can be obtained from the TWDB or from the Texas Water Commission (TWC) for a nominal fee. Those reports which are out-of-print can be readily examined and used through most large city and university libraries throughout the state. The TWC library in Austin also has a complete inventory of these reports (Bob Bluntzer, personal communication, 1991). Those analyses which are for wells given state well numbers in these reports are also retrievable from the TNRIS (see Item 1. above).

4. **Computer data base.** This study compiled a computer data base of approximately 770 fresh to saline water analyses. The data base was gathered from major water well drilling contractors and ground-water consulting firms. A complete, routine water analysis is included for most of the entries.

5. **Water well drilling contractors.** Most drilling contractors keep a file on every well that they drill. A water analysis is usually included in the file, especially if the well was a public water supply well. ~~The majority~~ most of their analyses will be fresh to slightly saline waters. However, public access to the data is usually limited.

6. **Ground-water consulting firms.** These firms have a limited number of water analyses. However, the data may be proprietary.

7. **Petroleum industry.** Various geological, engineering, and logging societies have compiled Rw (water resistivity) catalogues. A minority of the entries will be fresh to moderately saline waters. Analyses usually consist of Rw values at specified temperatures; sometimes TDS is included. The credibility of oilfield water analyses is directly related to the source of the water sample. Producing wells are less likely to be contaminated with drilling mud filtrate. Therefore, they provide more reliable samples than drill

stem tests, wireline formation testers, and samples from workover operations.

8. **Other sources of analyses.** Other analyses which are usually of fresh to slightly saline ground waters are available to the public from the files of the U.S. Geological Survey (District Office in Austin and subdistrict offices in Houston, San Antonio, and El Paso); the Texas Department of Health, Division of Water Hygiene in Austin (analyses of ground waters from public supply wells, including cities and rural public water systems); the Austin and regional offices of the Texas Railroad Commission; and on a very limited basis, from the files of the Texas Water Commission, Surface Casing Section and perhaps other sections of the Commission in Austin (Bob Bluntzer, personal communication, 1991).

Preparing the Data

TDS-Cw graphs must be constructed from an accurate data base. The data should be selected and processed according to the following guidelines:

1. All Cw values must be in μmhos/cm at 25° C (77° F).

2. For Cw's measured at temperatures other than 25° C, a conversion factor to compute an equivalent Cw at 25° C must be used. Temperature-Cw relationships vary according to the chemical composition of the water. No one has ever quantified the relationships for the various types of ground waters. Most workers just use the temperature-Cw relationship of NaCl water (Equations 2-4 or 2-6). This will result in very little error when dealing with a laboratory measured Cw, because the temperature will be very close to 25° C. However, it may be necessary to measure Cw at varying temperatures on a representative water sample and compute the relationship in order to make the proper conversion from downhole temperatures to 25° C.

3. If possible use Cw's that have been measured with a calibrated conductivity meter.

4. Do not use diluted conductivity. Instead, calculate a conductivity from the ionic concentrations. Most of the water analyses in

TWDB publications and the Ground-Water Data Base are Texas Department of Health diluted conductivities.

a. Since 1988 both field conductivities and diluted conductivities are in the Ground-Water Data Base. Prior to 1988 the TWDB did not routinely measure field conductivity, so only a few of the water analyses have both conductivities (Bob Bluntzer, personal communication, 1991).
b. Water analyses from laboratories other than the Texas Department of Health will not be diluted conductivities. These analyses are scattered throughout the data base (Bob Bluntzer, personal communication, 1991).

5. If possible, the Cw value should be verified by computing specific conductance from either the ion concentrations or the sum of the anions in meq/l.

6. TDS values that include 100 percent of the bicarbonate value should be used.

7. It is immaterial as to whether or not the silica content is included in the TDS values. Silica content is part of routine water analyses and is included in the TDS calculation. Theoretically, it should be subtracted from TDS before comparing TDS and Cw, because silica does not contribute to the conductivity of most waters (Hem, 1985). But, practically speaking, silica occurs in such small amounts (1 to 30 mg/l) in most ground waters that whether or not it is included in the TDS value will not alter the TDS-Cw relationship.

8. Graphs should be as "site specific" as possible. Since the TDS-Cw relationship varies as the chemical composition of the water varies, it is more accurate to construct a graph for a particular water type rather than to utilize a few all-purpose graphs. If data are available, a graph should be constructed for the particular aquifer and/or geographic area under study.

Plotting the Data

TDS and Cw data can be plotted on arithmetic, semi-logarithmic, or logarithmic (log-log) scales. It is usually plotted on an arithmetic scale

(Jones and Buford, 1951; Desai and Moore, 1969; Brown, 1971; Hem, 1982; Kwader, 1986) or a logarithmic scale (Vonhof, 1966; Emerson and Haines, 1974; MacCary, 1980; Fogg and Blanchard, 1986). Turcan (1962, 1966) used a semi-logarithmic scale.

There is no single "correct" scale to use when plotting the data. One's choice of scales is governed by personal preference, as well as by the nature of the data set. The following guidelines assist in choosing whether to use an arithmetic or a logarithmic scale:

1. **Logarithmic scales accommodate a wider range of data.** Arithmetic plots work fine when the data have a limited range (e.g. less than 2000 mg/l TDS). However, it is difficult to plot a wide range of values on an arithmetic scale and have acceptable resolution of the data points. Logarithmic scales do a better job in such cases.

2. **For TDS-Cw graphs, logarithmic scales transform a curvilinear trend to a linear trend.** This is necessary in order to apply straight-line fitting routines to the data set.

3. **Changing scales alters the appearance of the data, not the values.** Data plotted on logarithmic scales looks different than data plotted on arithmetic scales (see Figures 4-1 and 4-2). This can be misleading when comparing data plotted both ways. The differences are as follows:

   a. Many data sets that plot as curves on arithmetic scales become straight lines on logarithmic scales.
   b. Scatter of the data appears to be less with a logarithmic plot.

   Both of these effects are because a logarithmic graph is actually plotting the logarithms of the TDS and Cw values rather than the arithmetic values. However, neither scale is inherently better.

4. **Changing scales does alter the position of the fitted straight line.** If a data set has much scatter, the line that best fits the logarithmically transformed data will be lower (i.e. the TDS value will be lower for a given Cw value) than the best-fit line for the same data plotted on an arithmetic (untransformed) scale (see

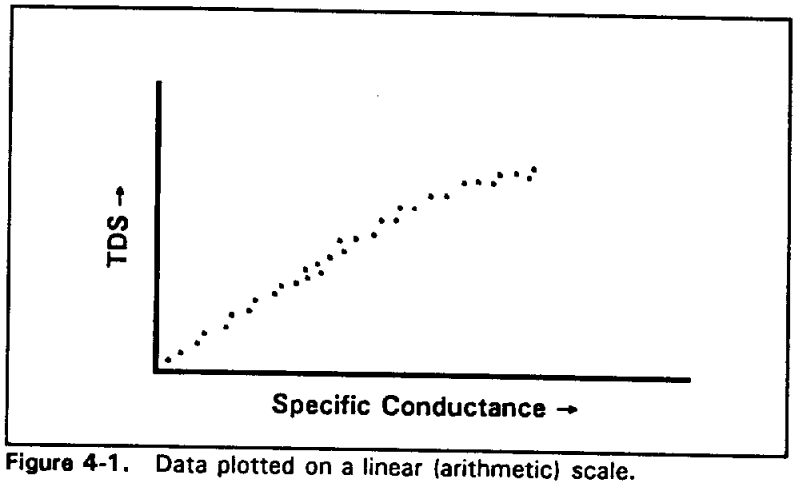

Figure 4-1. Data plotted on a linear (arithmetic) scale.

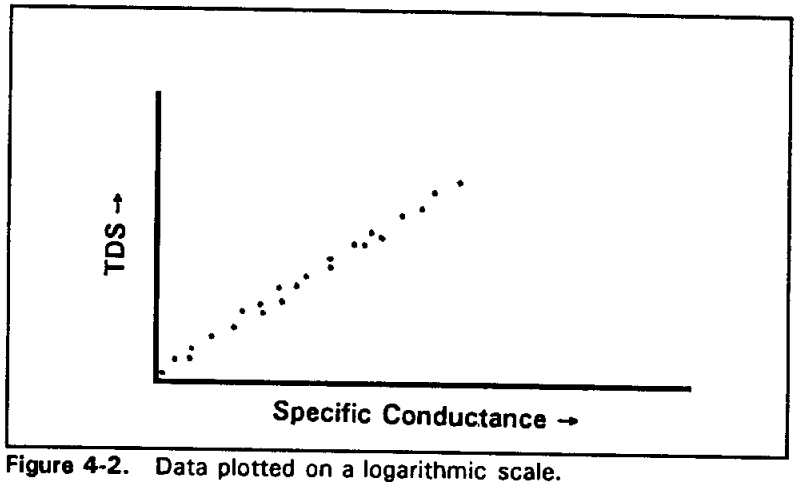

Figure 4-2. Data plotted on a logarithmic scale.

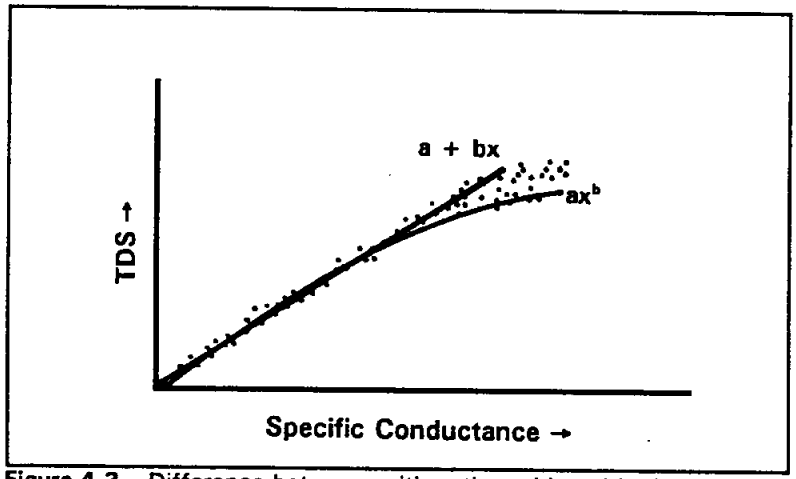

Figure 4-3. Difference between arithmetic and logarithmic curve fits when plotted on arithmetic scales.

Figure 4-3). An explanation for this is given in Appendix II, **GUIDELINES FOR SELECTING AND UTILIZING LINE-FITTING ROUTINES**, step 6. However, if the scatter is small, as is the case with most TDS-Cw plots, the two lines will nearly be the same.

Either variable can be assigned to the Y-axis (vertical axis). This manual plots Cw on the X-axis (horizontal axis). The choice depends on the line-fitting routine that is used. APPENDIX II, **GUIDELINES FOR SELECTING AND UTILIZING LINE-FITTING ROUTINES**, step 2 discusses line-fitting routines.

INTERPRETATION OF TDS-Cw GRAPHS

The chief purpose of a TDS-Cw graph is to predict TDS, given a wireline log-derived Cw value. Having plotted accurate and appropriate data, all that remains is to establish the relationship between the two variables. This can be done by visual examination of the data or by establishing an equation (see below) that relates TDS to Cw. The latter procedure is more common.

Plots of TDS vs. Cw generally show a very high correlation between the two variables. Scatter in the data is attributable to a combination of two factors:

1. **Errors in TDS and/or Cw measurements.** Errors in Cw are generally larger than errors in TDS (Chapter 2). Cw errors produce scatter along the X-axis. Errors in TDS cause scatter along the Y-axis.

2. **Variations in chemical composition of the waters.** This produces scatter along both the X and Y axes.

Since scatter exists in most graphs, it is necessary to employ a curve-fitting routine to calculate the most accurate curve fit. Appendix II, **GUIDELINES FOR SELECTING AND UTILIZING LINE-FITTING ROUTINES**, provides the rationale for the curve-fitting procedure outlined below.

Choosing Between a Linear and a Curvilinear Fit

The first step in interpretation is to decide between a linear and a curvilinear fit. For most graphs the bulk of the analyses will cluster below

Cw values of a few thousand μmhos/cm. In this region the data plots as a straight line and is accurately characterized by the following linear equation:

$$TDS = a + bCw \qquad \textbf{(4-1)}$$

Where:
a is the Y-axis intercept for the line when Cw = 0.
b is the slope of the line - the number of units that TDS changes for each one unit change in Cw.

Data becomes sparse at higher conductivities. A plot of the data starts to curve and the fit is now curvilinear. The equation of the line must be a power law as follows:

$$TDS = aCw^{b} \qquad \textbf{(4-2)}$$

Where:
a is a proportionality constant. It is the log *of a in* (4-1).
b is an exponent in the nonlinear relationship.

Most ground-water literature (e.g. Hem, 1985; Driscoll, 1986) deals with fresh water and therefore uses a straight-line equation. In actuality, what is used is a simplified version of a straight-line equation. The constant a is dropped from equation (4-1) since it has a value close to zero. The equation becomes as follows:

$$TDS = bCw \qquad \textbf{(4-3)}$$

Normally, b ranges from 0.55 to 0.75 when TDS includes 49.2 percent of the bicarbonate value. The **TDS-Specific Conductance Relationship** section in Appendix I enumerates the possible values of b.

Turcan (1966) used an exponent instead of a multiplier with Cw:

$$TDS = Cw^{b} \qquad \textbf{(4-4)}$$

Where:
b = 0.93 *for major aquifers in Louisiana.*

Once the data starts to curve, equation (4-4) fits better than equation (4-1) or (4-3), but not as well as equation (4-2). The problem with equation (4-4) is that a, which is the Y intercept, is always 1. When b is 0, Cw or x is 1. The origin is therefore always defined as (1,1) and one end of every line is (1,1). This significantly leverages the data (Etnyre, personal communication, 1990). Figures 4-4 and 4-5 demonstrate the differences between the line fit of equation (4-4) and (4-2). The differences are small in the main body of the two data sets, but they are large in the fringes (called the tails).

The following guidelines should be utilized to choose between a straight-line and a curvilinear fit:

1. To characterize fresh water, delete the high conductivity analyses, regress the fresh water data, and use equation (4-1) or (4-3). As long as the relationship is linear, and it normally will be, the data set can be plotted on an arithmetic scale.

2. Equation 4-2 is used to characterize either the entire range of conductivity values or just the high values. The data should be plotted on a logarithmic scale both for convenience and in order to apply straight-line fitting routines.

3. Another option is to divide the data set into a linear and a curvilinear group. The appropriate fit is then used for each group, rather than using only a power law.

Choosing the Best Line-Fitting Routine

The second step in interpretation is to choose the best line-fit for the data set. There is no single best procedure. Eight straight-line fitting routines are common in scientific studies: "eyeballing", averages, ordinary least squares, inverse least squares, weighted least squares, robust methods (including least absolute deviation), least normal squares, and reduced major axis (Troutman and Williams, 1987).

Fortunately, most TDS-Cw plots have a very high correlation coefficient. This means that if one is only concerned with characterizing the main body of the data set, it makes no difference which line-fitting routine is used. However, ordinary least squares is most commonly used.

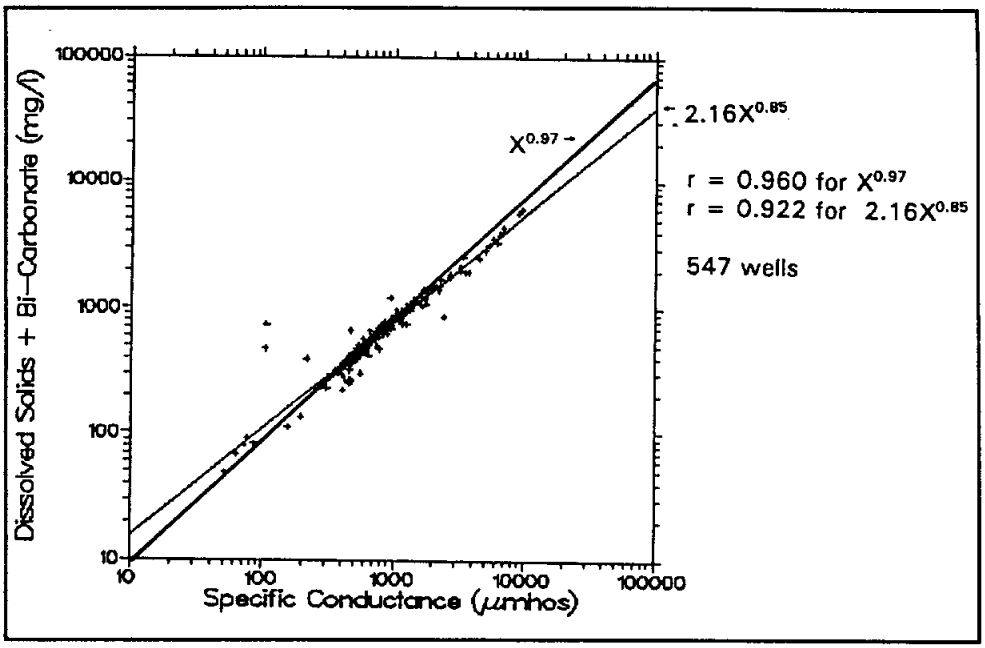

Figure 4-4. Comparison of the line fits generated by equations 4-2 and 4-4. Equation 4-2 gives the more accurate line fit. Dissolved solids includes 100 percent of the bicarbonate value. Most of the specific conductance values are diluted conductance. The plot is all the Harris County water analyses in the Texas Water Development Board Ground-Water Data Base.

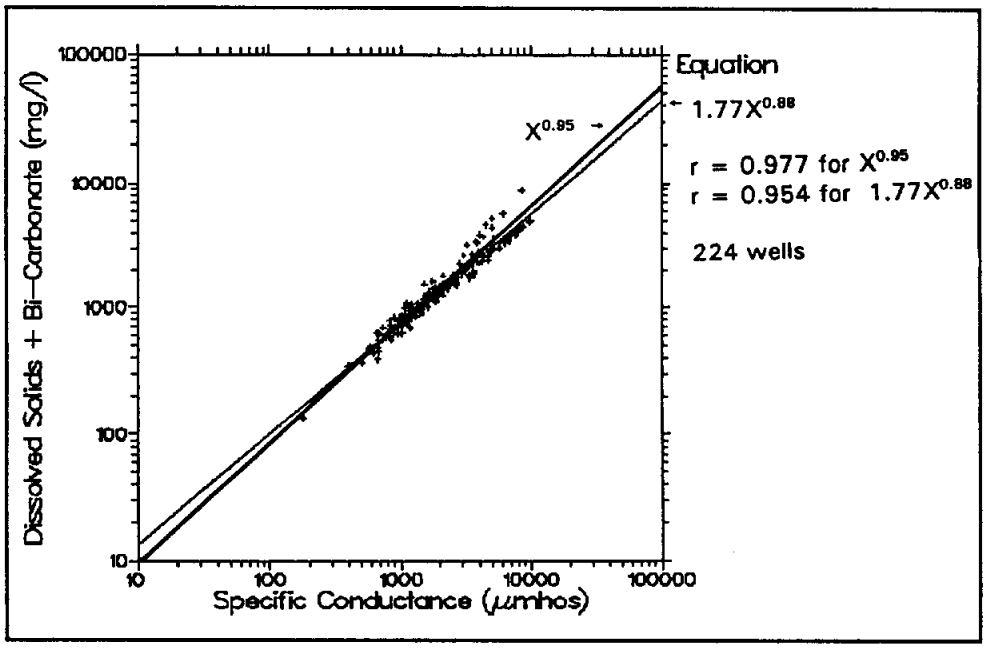

Figure 4-5. Comparison of the line fits generated by equations 4-2 and 4-4. Equation 4-2 gives the more accurate line fit. The plot is all the Jack County water analyses. The criteria used to construct Figures 4-4 and 4-5 are listed on page 73.

All eight routines give similar equations and all the equations are reversible. Also, it makes no difference which variable is plotted on the Y-axis. The only consideration, as mentioned above, is whether or not a curvilinear fit is needed.

In order to characterize saline waters, one must focus on the high-conductivity tail of the graph. Here it does make a difference which line-fitting routine is used, even when the correlation coefficient is very high. Scatter in the data is likely to occur in both the X and Y directions due to measurement errors and variations in water compositions. Therefore, the best tactic is to use a line-fitting routine that splits the deviations equally between X and Y, rather than favoring one variable. Doing this also helps to mitigate the weighting factor that a logarithmic transformation adds to a line fit. The choice is between reduced major axis and least normal squares. Reduced major axis is preferred because the equation can tolerate scale changes. Both procedures will give a similar line and both lines are reversible.

If the correlation coefficient is not high or if there are problems with the data set, it may be necessary to use a particular line-fitting routine. In the rare instance when this is so, refer to Appendix II, **GUIDELINES FOR SELECTING AND UTILIZING LINE-FITTING ROUTINES**, for assistance.

PROCEDURES APPLIED TO THE TEXAS WATER DEVELOPMENT BOARD TDS-Cw GRAPHS

To illustrate the correct procedure for constructing TDS-Cw graphs, 45 graphs from twelve aquifers were plotted. The graphs are in Volume II, Section 4, **TDS-Cw GRAPHS.** The data is from the Texas Water Development Board Ground-Water Data Base, December, 1991. The data was processed according to the following procedures:

1. Only one water analysis per well was plotted, the earliest analysis having both TDS and Cw.

2. Silica was not included in the TDS calculation.

3. Each aquifer (or portion of an aquifer) was graphed three ways. The preferred method is b., while a. and c. are alternate methods. Figures 4-6 to 4-8 are examples of the three types of graphs.

a. Calculated Conductivity vs. TDS (using 49.2 % bicarbonate)
b. Calculated Conductivity vs. TDS
c. Diluted Conductivity vs. TDS

4. TDS was recalculated to include 100 percent of the bicarbonate value for the two graphs labeled TDS. For the third graph TDS includes 49.2 percent of the bicarbonate value and is so labeled.

5. Specific conductance is at 25° C. There is no way to tell if Cw was measured at 25° C or corrected to 25° C. Most of the analyses are laboratory measurements, so they were probably measured at a temperature very close to 25° C.

6. Specific conductance was recalculated from the ionic concentrations for the two graphs labeled Calculated Conductivity. For the third graph specific conductance is as reported on the water analysis. The vast majority of them are diluted conductances and therefore the graph is labeled Diluted Conductivity.

7. The data were plotted on three-cycle log-log paper.

8. Cw is on the X-axis and TDS is on the Y-axis.

9. The lines were fitted by reduced major axis.

10. The equation of the straight line was transformed to a power law

11. A correlation coefficient was calculated for each

Table 4-1 compares the TDS-Cw relationships an coefficients for each of the three different types of grap coefficients are very high for all three (0.999 to 0.947). constructed with diluted conductivity have the lowest co coefficients, while there is little difference between the ot

Table 4-2 was compiled to illustrate the differences among the three TDS-Cw relationships. It demonstrates the differences in TDS values computed from each graph for a constant Cw value (50,000 μmhos/cm). No consistent pattern is evident. The TDS values differ by as much as 24,308 mg/l for a particular aquifer and range from 19,921 mg/l to 62,170 mg/l for all the aquifers.

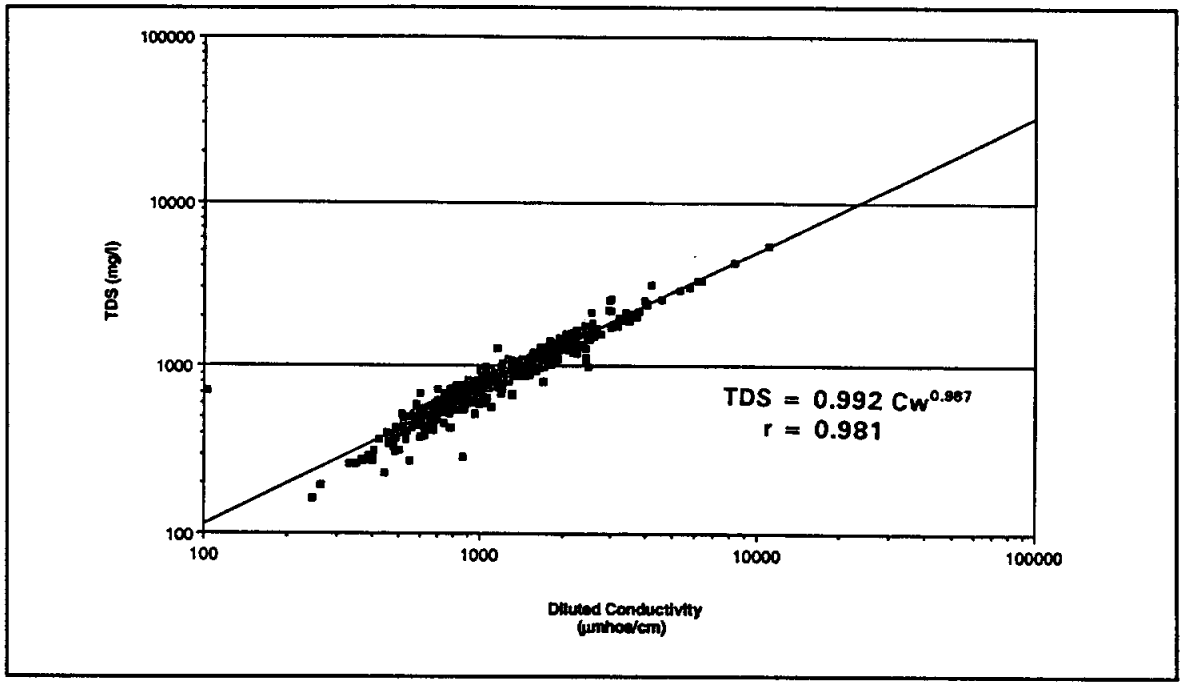

Figure 4-6. Graph of Diluted Conductivity vs. TDS for the Edwards and Associated Limestones Aquifer.

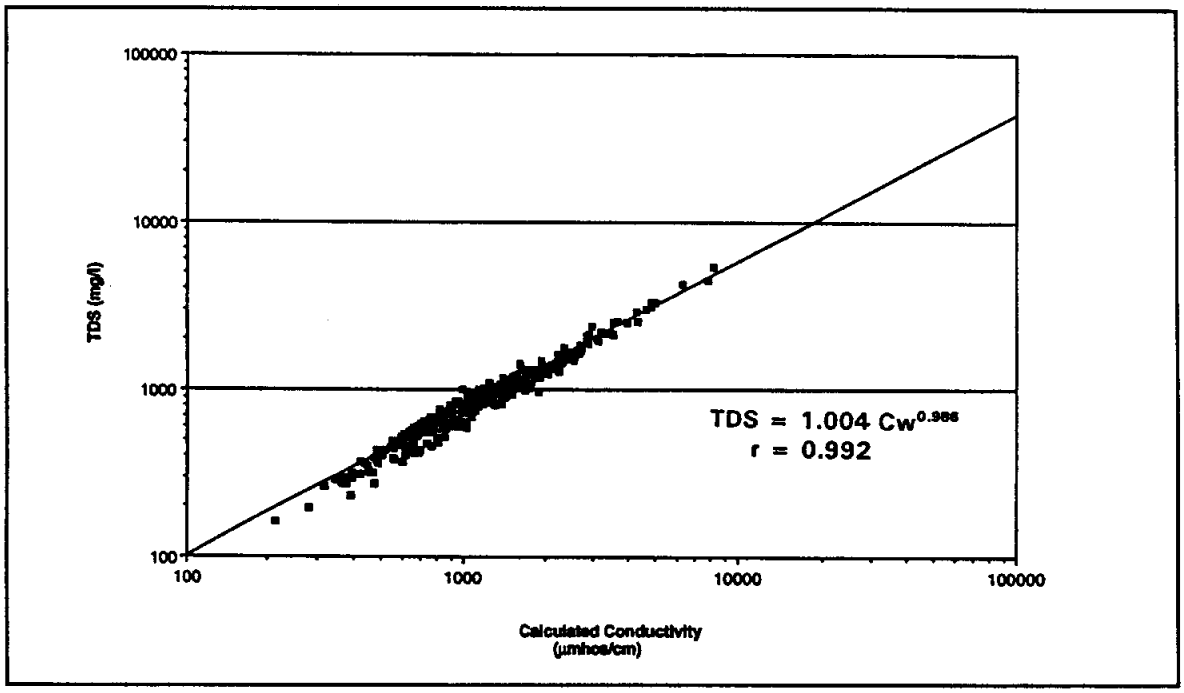

Figure 4-7. Graph of Calculated Conductivity vs. TDS for the Edwards and Associated Limestones Aquifer.

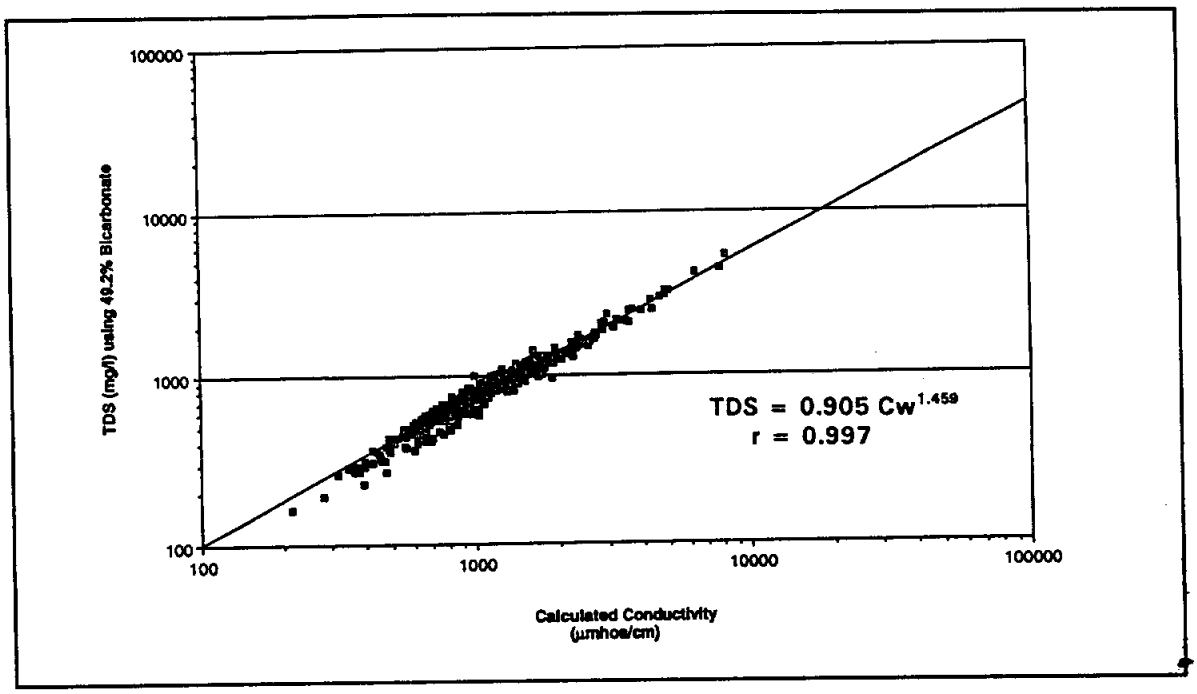

Figure 4-8. Graph of Calculated Conductivity vs. TDS (using 49.2 % bicarbonate) for the Edwards and Associated Limestones Aquifer.

TABLE 4-1. COMPARISON OF TDS-Cw RELATIONSHIPS COMPUTED FROM THREE DIFFERENT DATA SETS

Aquifer	Calculated Conductivity (using 49% bicarbonate) Graph		Calculated Conductivity Graph		Diluted Conductivity Graph	
	TDS (mg/l) =	r	TDS (mg/l) =	r	TDS (mg/l) =	r
Eastern Carrizo-Wilcox	$0.699Cw^{1.011}$	0.983	$0.699Cw^{1.011}$	0.983	$0.906Cw^{0.973}$	0.963
Central Carrizo-Wilcox	$0.383Cw^{1.063}$	0.999	$0.426Cw^{1.099}$	0.994	$0.495Cw^{1.073}$	0.992
Western Carrizo-Wilcox	$0.398Cw^{1.051}$	0.996	$0.654Cw^{1.013}$	0.988	$0.793Cw^{0.993}$	0.956
Cenozoic Pecos Alluvium	$0.386Cw^{1.677}$	0.998	$0.744Cw^{0.987}$	0.997	$0.629Cw^{1.006}$	0.968
Northern Chicot	$0.501Cw^{1.014}$	0.998	$0.780Cw^{0.994}$	0.995	$2.250Cw^{0.840}$	0.993
Central Chicot	$0.443Cw^{1.031}$	0.998	$1.283Cw^{0.922}$	0.991	$1.876Cw^{0.958}$	0.981
Edwards and Associated Limestones	$0.905Cw^{1.459}$	0.997	$1.004Cw^{0.996}$	0.992	$0.992Cw^{0.987}$	0.981
Ellenburger	$0.353Cw^{1.066}$	0.974	$1.942Cw^{0.871}$	0.987	$1.564Cw^{0.892}$	0.972
Evangeline	$0.450Cw^{1.031}$	0.998	$0.780Cw^{0.994}$	0.995	$1.149Cw^{0.934}$	0.988
Hickory	$0.390Cw^{1.053}$	0.996	$0.817Cw^{0.992}$	0.991	$0.969Cw^{0.954}$	0.988
Hueco Bolson	$0.441Cw^{1.033}$	0.998	$0.986Cw^{0.937}$	0.994	$0.973Cw^{0.939}$	0.947
Jasper	$0.454Cw^{1.036}$	0.996	$0.751Cw^{1.010}$	0.994	$1.791Cw^{0.876}$	0.967
Paluxy	$0.311Cw^{1.094}$	0.998	$1.116Cw^{0.957}$	0.995	$1.30Cw^{0.928}$	0.990
Sparta	$0.461Cw^{1.027}$	0.994	$0.642Cw^{1.016}$	0.993	$0.651Cw^{1.001}$	0.985
Travis Peak and Twin Mountains	$0.438Cw^{1.036}$	0.997	$1.563Cw^{0.896}$	0.991	$1.902Cw^{0.863}$	0.976

TABLE 4-2. COMPARISON OF COMPUTED TDS VALUES WHEN Cw = 50,000 μmhos/cm FOR THREE DIFFERENT TDS-Cw GRAPHS

Aquifer	Calculated Conductivity (using 49% bicarbonate) Graph Calculated TDS in mg/l	Calculated Conductivity Graph Calculated TDS in mg/l	Diluted Conductivity Graph Calculated TDS in mg/l
Eastern Carrizo-Wilcox	39,367	39,367	33,824
Central Carrizo-Wilcox	37,862	62,170	54,526
Western Carrizo-Wilcox	34,554	37,639	36,758
Cenozoic Pecos Alluvium	29,292,740	32,319	33,559
Northern Chicot	29,147	36,549	19,921
Central Chicot	30,977	27,585	20,401
Edwards and Associated Limestones	6,493,006	43,144	43,092
Ellenburger	36,048	24,047	
Evangeline	31,467	36,549	
Hickory	34,600	37,463	
Hueco Bolson	31,512	24,935	
Jasper	33,511	41,841	
Paluxy	42,997	35,041	
Sparta	30,870	38,167	
Travis Peak and Twin Mountains	32,330	25,365	

Dr. Collier - Please review the circled numbers above. The last sentence on page 74 conflicts with them as standards. (Possibly it's the text that needs a qualifier rather than a change in the table?)

AN INTRODUCTION TO BOREHOLE GEOPHYSICAL LOGGING

Chapter 5

Borehole geophysics is the science of measuring and analyzing various physical properties of the formations encountered in a borehole by means of wireline logging tools. Synonymous terms are **wireline logging** and **petrophysics**. **Well logging** and **logging** are the terms commonly used.

The logging tools produce a **well log** or **log**. A well log is a paper-strip graph of borehole depth versus a measured physical property of the formations. The term **log** is used to refer to both the logging tool and the recorded curves. The process of making a log is called **running** a log. Professionals who analyze logs are **log analysts**.

Technically, the terms **log, well log, logging,** and **well logging** also apply to other types of formation evaluation such as mud logs and sample logs. However, among log analysts and in this text the terms are restricted to borehole geophysical logs.

Both open and cased holes are logged. If possible, logging is done in open holes because many tools will not work in cased holes. Cased hole logs are increasingly used to evaluate formations, but they have historically been run to evaluate well construction (casing integrity, quality of a gravel pack, etc.), to measure well productivity (flow rate, etc.), and to correlate openhole logs.

Table 5-1 lists openhole logging tools according to purpose. Notations are also included in the table as to which tools work in cased holes.

Uses of logs

Wireline logs provide a wide range of information for ground-water studies. The data can be used for aquifer identification and characterization and for designing well tests, screen placement, and cement volume. It also provides the ground-truth for surface geophysical studies. For regional studies this same database is used in ground-water modeling. Logs are also used for stratigraphic correlation, mapping the lateral and vertical thickness of aquifers and confining beds, and determining depositional facies. The data available from logs include:

1. Aquifer properties

   depth
   thickness
   mineralogy
   porosity
   water quality (TDS, conductivity, hardness)
   radioactivity
   temperature
   bulk density
   rock strength parameters
   permeability variations
   fractures
   depositional facies
   moisture content in the vadose zone
   confining beds

2. Borehole characteristics

   diameter (including washouts and constrictions)
   volume
   static water level
   fluid flow (direction and velocity)

3. Stratigraphy

   lateral and vertical extent of aquifers and confining beds
   depositional facies

Although this study concentrates on techniques for determining water quality from logs (Chapter 14), techniques for characterizing the physical properties of formations are also covered (Chapters 8 to 13).

Some formation properties can be measured by other methods (e.g. cores, cuttings, packer tests), but wireline logging is the best and/or most cost effective method of acquiring these data. It has the additional advantages of being immediately available at the wellsite, providing a continuous record of the borehole, and being repeatable.

Equipment

Logging is accomplished by lowering a measuring device (called a **tool, sonde,** or **probe**) by means of a cable (**wireline**) into a borehole. A winch is used to raise and lower the tool. Measurements are transmitted up the cable to surface recording equipment (Figure 5-1).

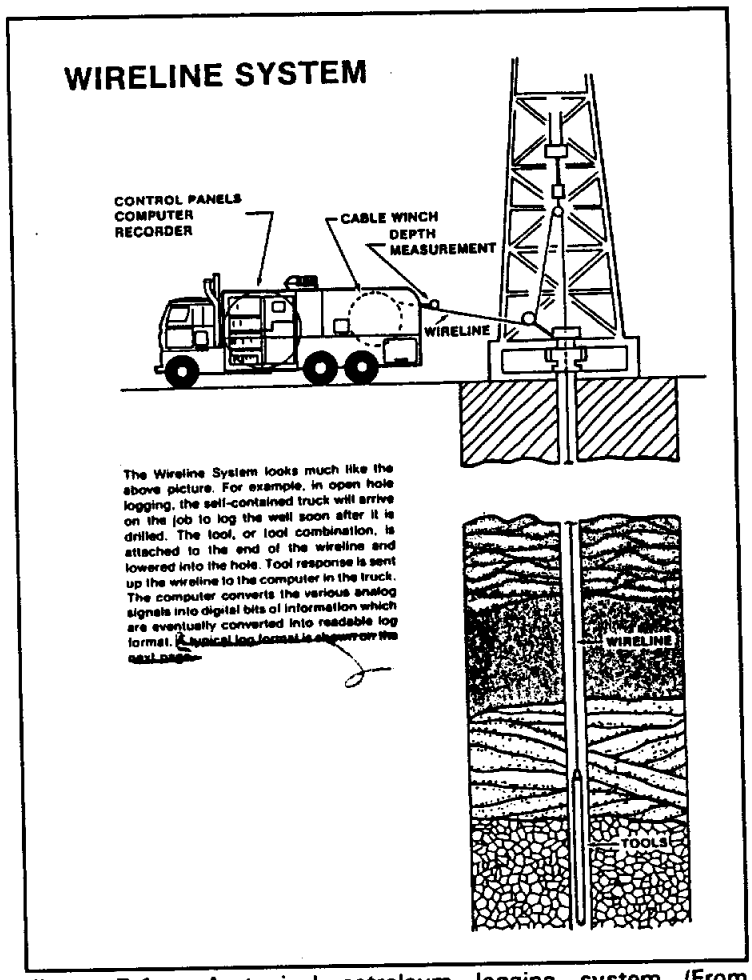

Figure 5-1. A typical petroleum logging system (From Gearhart, 1981).

The probe is usually housed in a water-proof steel housing. It consists of numerous electrical components for powering the instrument, processing the measurements, and transmitting the signals up the cable. The probe also contains some type of sensor(s): electrodes, transducers, radioactivity detector(s), etc. Most tools also have an emitter of some type (radioactive source, electrodes, etc.). Table 5-2 groups common openhole tools according to the physical property utilized in the measurement.

Most petroleum-type tools are built so that it is possible to run various combinations of tools at one time. This decreases the number of logging runs, thus saving rig time. Many slimhole tools are multi-parameter tools, but the measuring devices are usually built into a single probe that cannot be run in combination with other probes.

The cable is used to lower the tool in and pull it out of the borehole and to transmit the data to the surface recording equipment. Petroleum logging companies generally use a seven conductor cable, which allows

TABLE 5-2. OPENHOLE TOOLS GROUPED ACCORDING TO THE PHYSICAL PROPERTY UTILIZED IN THE MEASUREMENT

INDUCED
Electrical
Single-Point Resistance
Normal
Lateral
Focused electrode
Microlog
Induction
Fluid Resistivity
Dipmeter
Dielectric
Formation Microscanner
Radioactive
Density (Gamma-Gamma)
Neutron
Geochemical
Acoustic
Sonic
Borehole Televiewer
Nuclear Magnetic Resonance
MECHANICAL
Caliper
Flowmeter
Borehole Deviation
Video C-

several parameters to be transmitted at once. Slimhole cable is either single or multi-conductor. Single conductor cable limits the number of parameters that can be transmitted at once, thus restricting the number of measurements that can be built into a tool. Digital telemetry techniques and optical fiber cables are overcoming these limitations.

The surface unit includes the winch, power supply, processing system, and recording equipment. Conventional logging systems transmit the data uphole in either analog or digital form and record the data on magnetic tapes or floppy disks and on paper. Slimhole systems are also beginning to use digital signals, but most still transmit analog signals. With slimhole analog equipment the data are not stored; it can only be recorded on paper. In order to store the data the system must be outfitted with analog-to-digital converters. Many slimhole analog systems are retroactively outfitted with a converter. Conventional analog logging systems all utilize analog-to-digital converters.

Conventional Versus Slimhole Logging Systems

Petroleum logging systems are mounted on large customized trucks. The probes are usually 3⅜ to 6 inches in diameter. Individual probes are a few feet to 20+ feet in length. Probes can be run individually or in combinations. Tool combinations can reach 100 feet in length. In this text

these tools are referred to as **conventional tools**. They are routinely run in water wells, but they are specifically designed for petroleum wells. Most water wells in Texas have been logged with conventional tools.

Slimhole systems are much smaller, ranging from portable, backpackable units to units that are mounted in a standard size panel van. Midsized units are portable, but may require two people to move. Slimhole tools are less than 2 inches in diameter (Table 5-3). Individual probes are generally 4 to 8 feet in length. Sonic and guard tools are longer (11 to 20 feet). Many probes make several measurements (e.g. a gamma ray, SP, single-point resistance, neutron probe). Multi-measurement tools may reach 12 feet in length. Slimhole tools are generally used in the mining and environmental industries. In Texas slimhole tools are mainly used by government agencies, a few drilling contractors who own logging equipment, and mining companies. A few small logging companies in Texas run slimhole equipment.

There is another group of slimhole logging tools that are 2 to 3 inches in diameter. They are manufactured by the same firms that make the less than 2 inch diameter tools (Table 5-3). The oilfield logging companies also manufacture a few tools in this size range (e.g. Schlumberger's 2⅝ inch induction tool). The oilfield logging companies consider 2 to 3 inch diameter probes to be slimhole tools, while the ground-water/environmental industry generally defines slimhole as less than 2 inches in diameter. In this study **slimhole** is reserved for tools less than 2 inches in diameter.

A variety of slimhole and 2 to 3 inch diameter probes are available today (Table 5-3). However, there are limited selections of induction, microresistivity, and focused resistivity tools. There is a critical need for more of these tools. All types of porosity tools are available, but many of the density and neutron tools are count rate devices which cannot be converted to accurate porosity values. Considerable improvement needs to be made in the area of slimhole density and neutron tools.

Analog versus digital logging systems

This section is an abstract of the chapter, "Analog and Digital Systems," in Hallenburg's (1984) logging textbook.

TABLE 5-3. PRESENTLY AVAILABLE OPENHOLE SLIMHOLE LOGGING TOOLS

	Comprobe	Century	Robertson	Oyo Geospace	Keck	IFG	Auslog	Mineral Logging System	BPB	Mt. Sopris	Geonics
SP	x	x	x	x	x	x	x	x		x	
Gamma Ray	x	x	x	x	x	x	x	x	x	x	x
Spectral Gamma Ray		x[1]	x[1]			x				x	
Single-Point	x	x	x		x	x	x			x	
8" & 32" Normal	x						x			x	
16" & 64" Normal	x	x[1]	x	x		x[2]	x	x		x	
48" Normal						x	x				
Lateral[3]		x[1]	x	x				x		x	
Induction	x[1]	x	x								x
Dual Guard									x		
Guard	x[1]	x[1]	x							x	
Microlog				x			x	x[1]			
Fluid Resistivity	x	x[1]	x	x			x	x		x	
Caliper	x	x[1]	x[1]	x	x			x	x		
3-Arm Caliper	x	x	x				x	x		x	
4-Arm Caliper	x		x[1]				x	x			
Density[4]	x[1]	x[1]	x	x			x	x	x	x[1]	
4-pi Density	x	x						x	x	x	
Neutron[4]	x	x	x	x			x	x	x	x	
Sonic	x[1]	x[1]	x[1]					x[1]	x[1]	x	
Full Wave Sonic	x[1]		x[1]	x						x	
Temperature	x	x	x	x	x	x	x	x	x	x	
Deviation Survey		x	x	x		x			x	x[1]	
Flow Meter	x	x	x	x			x	x		x	
Dipmeter			x[1]						x[1]	x[1]	
Fluid Sampler	x						x	x		x	

[1]2 to 3 inch diameter tool.
[2]16" Normal, but no 64" Normal.
[3]Spacing varies from 40 inches to 18 feet.
[4]Tool may be count rate only or calibrated to calculate porosity and it may be uncompensated or compensated.

Analog logging systems utilize electrical signals for data transmission and processing. The signals correspond in an obvious way (or are **analogous** to) the parameter being measured. The signal at any place in the system is the analog of the parameter being measured. For example:

* A gamma ray tool emits an electrical analog pulse for each photon created by a gamma ray in the detector.

* Neutron response is often a direct pulse rate output that is directly proportional to the neutron flux rate at the neutron detector.

Data transmission from the logging probes to the surface instrumentation is in analog form. A surface module converts the analog signal to a standard measurement which is recorded on a chart recorder. The analog signal is not stored.

Although time consuming, the analog curve can be digitized utilizing a digitizing table. Considerable progress is being made in designing quicker and less expensive methods of digitizing logs.

Digital systems convert the tool response into a coded signal in the tool. The data is sent up the wireline cable, processed at the surface in a digital form, and stored in a digital form.

Hybrid systems (analog-to-digital converters) are analog systems with digitizing networks at the surface. An electronics module is needed for each tool. Once the data are digitized, they can be stored and computer-processed.

Table 5-4 compares the advantages and disadvantages of digital and analog systems. Hybrid systems have some of the advantages and disadvantages of each system.

All logging systems were originally analog. Today, nearly all conventional systems are hybrid, while many slimhole systems are still analog. Most manufacturers are going to digital systems. Analog to digital converters are available for existing analog systems.

The big advantage of digital data is that it can be directly computer processed. A number of very sophisticated log analysis software programs

TABLE 5-4. COMPARISON OF ANALOG AND DIGITAL LOGGING SYSTEMS

ANALOG SYSTEM

Advantages

Simple in concept.

Few components and easy to fix.

Relatively inexpensive.

The signal can be examined anywhere in the system and related to the log response.

Disadvantages

Requires considerable care and precision in building, maintaining, and using.

Components change gradually with time, temperature, pressure, or moisture. Thus the output changes and the tool is out of calibration.

Continuous signals require dedicated channels. This limits the number of tools that can be run on a single pass.

Only real time processing. Therefore, it can only average on the basis of past time.

Data not usually stored.

Scale changes require the log to be rerun.

No computer processing.

High logging speeds distort the curves.

DIGITAL SYSTEM

Advantages

Simple surface system. Little electronics savvy required to run the equipment.

Malfunctions usually produce an unintelligible signal, so failures are evident.

Simultaneous data transmission of all measurements permits multi-measurement probes. This reduces the number of logging runs.

Can use averaging systems other than time.

Data stored and easily retrieved.

Rerun recorded data at any scale.

Computer processing possible (smoothing, filtering, environmental corrections).

Takes care of many routine duties or forces the operator to do so.

Disadvantages

Complex circuitry.

Very difficult to repair in the field.

Relatively expensive.

Signal must be decoded before it can be examined.

Digital tools not compatible with analog systems and vice versa.

(Abstracted from Hallenburg, 1984.)

are now available for the PC[1]. Although they are designed for petroleum logging, the better programs have the flexibility of being tailored for groundwater applications.

Computer log analysis has the advantages of speed, accuracy, and convenience. Log presentations can be easily and quickly changed, data can be rapidly and easily corrected, and interpretation techniques can be quickly and easily applied. There is, however, a danger to this type of log analysis. The log analyst may be tempted to blindly let the logging program make the decisions as to input parameters, which environmental corrections are necessary, and how to analyze the data. This leads to a false sense of security regarding the accuracy of the interpretation. It is an inescapable fact that precise calculations based on incorrect input parameters and invalid analytical technique are precisely wrong.

History

Borehole geophysics is a fairly young science. Although its roots can be traced back as far as Lord Kelvin in 1869 (Hallenburg, 1984), well logging was developed by Conrad Schlumberger, Marcel Schlumberger, and H.G. Doll in the 1920's. They adapted the surface geophysical technique of point-by-point electrical resistivity measurements to a borehole.

The technology was developed for the petroleum industry. By 1929 oil wells in the U.S. were being logged (Frank, 1986), and within a few years water wells were also being logged. The earliest log of a water well found in this study was a 1938 Schlumberger log of a well in Houston, Texas.

Table 5-5 is a brief summary of the development of openhole well logging technology. The table includes the major areas of emphasis in each decade and the dates that tools were introduced. Some of the dates are approximate since some tools were developed years before they were commercially available and other tools were reintroduced following an unsuccessful earlier phase.

The history of well logging revolves around the petroleum industry. The petroleum logging companies have paid little attention to the groundwater industry. Their decision is simply a matter of economics; ground-

[1] The annual August/September issue of **Geobyte** carries a PC log analysis software directory.

TABLE 5-5. A HISTORY OF OPENHOLE WIRELINE LOGGING

A superscript number refers to the year in which a tool first appeared.
Much of this material was abstracted from Hilchie (1990).

1869 Lord Kelvin ran a temperature tool in a water well.

1913 A single-point resistance tool was run in a well.

1920's Fluid resistivity and temperature tools were being run.

1927 Schlumberger brothers log the first oil well with a lateral-type tool. The technique is called "electrical coring."

1930's **Qualitative log analysis (primarily correlation).**

SP[31]
Short normal[32]
Long normal[34]
Continuous temperature[35]
Sidewall coring[36]
Caliper[36]
Single-point resistance[38]
Gamma ray[39]

1940's **Quantitative analysis starts.**
Gus Archie[42] relates porosity and formation water resistivity to formation resistivity and water saturation.
Hubert Guyod[44] explains how to determine resistivity from the lateral and normal curves.
H.G. Doll[48] and M.R.J. Wyllie[48] publish on the SP curve.

Count rate neutron[41]
Induction[46]
Flowmeter[47]
Resistivity dipmeter[47]
Slimhole ground-water tools[47]
Microlog[48]

1950's **Crossplot techniques; Induction replaces lateral and normal.**

Focused tools[50]
Sonic[57]

1960's **Improved instrumentation and porosity tools.**

Density[60]
Silicon transistors[60] permit combination tools.
Cement bond log[61]
Compensated density[62]
Sidewall neutron[62]
Dual induction[63]
Compensated sonic[63]
Pulsed neutron[63]
Formation tester[65]
Borehole gravimeter[66]

TABLE 5-5 (continued). A HISTORY OF OPENHOLE WIRELINE LOGGING

1970's Computers at the wellsite and digital tools.

Combination logging systems[71]
Spectral natural gamma ray[71]
Compensated neutron[72]
Dual laterolog[72]
Carbon/oxygen[73]
Dielectric[75]
Photoelectric curve[79]

1980's Digital tools; Personal computer log analysis software; Emphasis on quality control; Stress on geological information; New cased hole tools.

Formation Microscanner[85]
Slimhole induction[86]
Borehole televiewer[87]

1990's Personal computer log analysis software; Nuclear magnetic resonance.

water logging is just not a lucrative enough market to attract their research and development dollars. However, this apathy is beginning to be mitigated because of increased environmental concerns about and by the petroleum industry.

Ground-water slimhole logging started in 1947 when Hubert Guyod and Walt Greer started WIDCO (Well Investment Development Co.). They logged water wells using SP and single-point resistance tools which they manufactured (Hilchie, 1990).

In more recent years other companies started manufacturing slimhole tools. The principal market was the ground-water and mining industries. During the past decade environmental and engineering firms started using slimhole logs more frequently.

Interest in borehole geophysics continues to increase in the 1990's among ground-water/environmental professionals, but few of them are competent in log analysis. Unfortunately, this means that too often too little attention is given to running the proper logging suite, checking the quality of the logs, and interpreting the results.

Another problem that has hampered advances in slimhole/ground-water logging is the lack of capital for research and development. Petroleum logging has benefitted from the economic incentives provided by exploring more efficiently for hydrocarbons. Oil companies, as well as logging companies, have expended considerable sums of money researching and developing logging technology. Ground-water logging technology has historically fed off the scraps from the petroleum table. This situation has improved a little in recent years. Interest in environmental studies has spurred increased expenditures in ground-water/environmental logging research by both the government and industry.

Familiarity with the history of well logging technology explains the status of ground-water logging today. A historical perspective is also important when doing ground-water studies in Texas, where petroleum and ground-water logs date back to the early days of logging. Ground-water professionals will routinely have to use these old logs with their cryptic terminology and curve shapes. A passing familiarity with the tools will make one's work much easier and much more accurate.

Those using slimhole logging tools in their ground-water/environmental studies today must of necessity be familiar with the history of well logging. Slimhole logging technology has been somewhat frozen in time. Many of the most popular logs today (single-point resistance, short normal, long normal, count rate density, and count rate neutron) were abandoned by the petroleum logging industry in the 1950's. In petroleum logging literature, which is 95 percent of all logging literature, these tools are usually given a cursory discussion. Specialized logging literature that deals with old, obsolete tools is the main source of information. These references are discussed in Chapters 8 and 9 and in the **Logging literature** section of this chapter.

Several histories of well logging have been published. Hilchie (1990) is the latest work. He sketches the histories of the early logging companies in the U.S. and the development of logging technology worldwide. Segesman (1980) published a 50-year historical review of well logging. Johnson (1962) chronicled the history of logging through 1960. Snyder and Fleming (1985) reviewed well logging developments from 1960 to 1985. Allaud and Martin (1977) traced the development of the Schlumberger organization and explained many logging techniques.

Logging companies

A number of logging companies have come and merged through the years. Table 5-6 traces the history of the major petroleum logging companies. All of these companies have operated in Texas and most of them have been headquartered in the state. Most of the logs in petroleum and ground-water well files will be Schlumberger logs, but the other companies pop up occasionally.

Today the three major petroleum logging companies are Schlumberger, Halliburton Logging Services, and Atlas Wireline. All three are headquartered in Houston and have offices throughout the state. They manufacture and run their own tools. They do not sell tools to other logging companies.

There are also a number of independent petroleum logging contractors throughout the state, most of whom have a single office. They are simply logging contractors. They neither manufacture nor develop logging tools. A few petroleum logging companies have branch offices around the state and a couple of them also manufacture logging tools which they sell to other service companies.

All petroleum logging companies will log water wells. However, they bring to the job their petroleum-type logging assumptions (see the **Petroleum versus ground-water logging** section). This often means that tool selection, log presentation, and log interpretation are not the best available options.

There are also a few independent logging companies that specialize in water wells. Tejas is the major one in Texas. Hundreds of water wells in north central and northeast Texas were logged by Tejas. Some of these companies utilize only slimhole tools; some of them run slimhole and conventional tools and log both ground-water and petroleum wells. A few drilling contractors, government agencies, and environmental firms also have slimhole logging equipment.

Slimhole tools are manufactured by several companies (Table 5-7). Most tools now being run in Texas are from Mineral Logging Systems (MLS), Comprobe, Century, and Mt. Sopris. Century is the only slimhole manufacturer operating in Texas that is also a logging contractor. Halliburton is the only major petroleum logging company that is also a slimhole manufacturer by virtue of the fact that they own MLS.

TABLE 5-6. A HISTORY OF THE MAJOR LOGGING COMPANIES

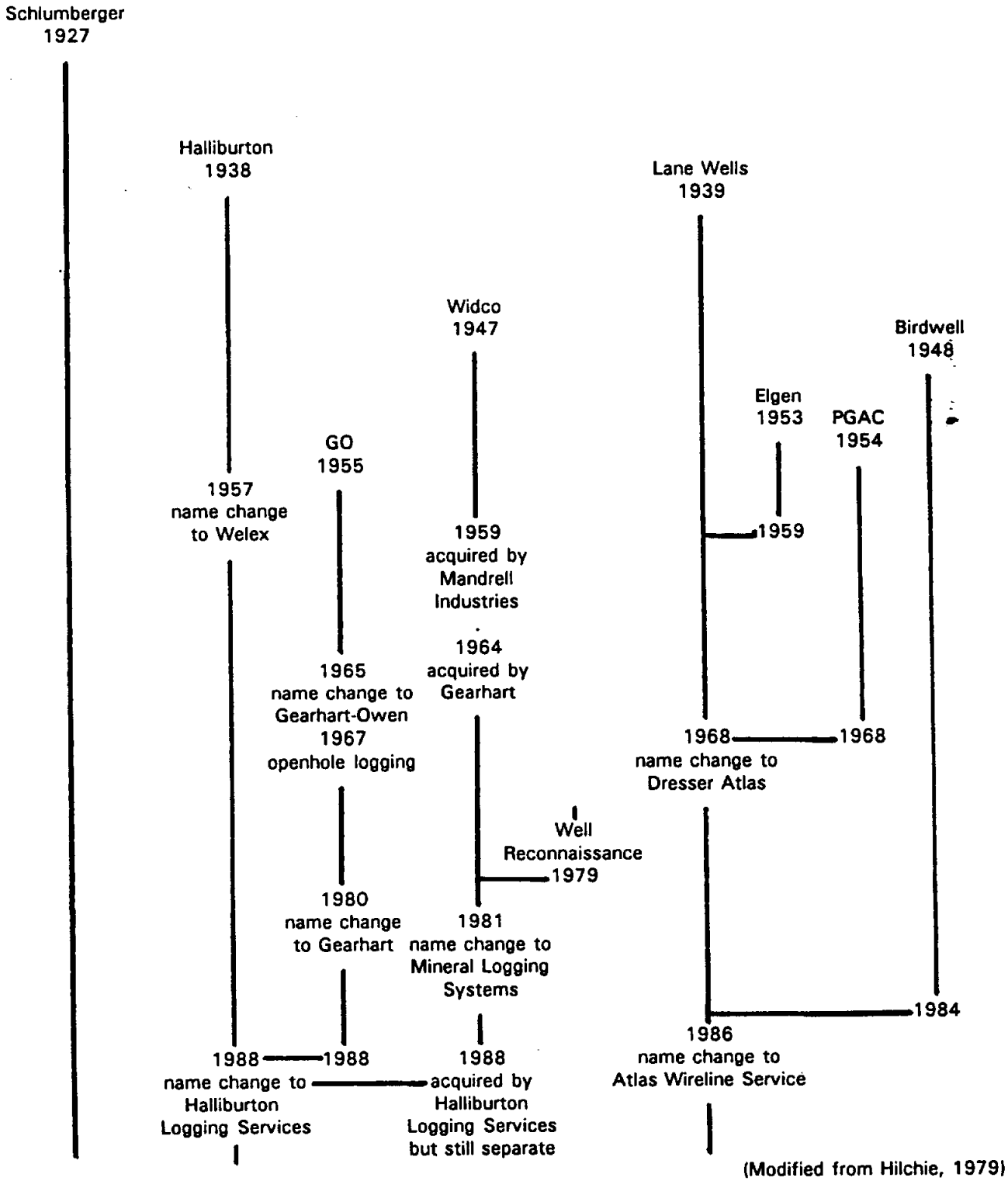

(Modified from Hilchie, 1979)

TABLE 5-7. PRINCIPLE MANUFACTURERS OF SLIMHOLE LOGGING EQUIPMENT

Century Geophysical Corp. 7517 East Pine Tulsa, OK 74115 (918) 838-9811	Comprobe 9632 Crowley Rd. Ft. Worth, TX 76134 (817) 293-7333
Geonics Limited 1745 Meyerside Drive Mississauga, Ontario L5T 1C6 Canada (416) 670-9204	Hunter/Keck Geophysical Instruments 1099 W. Grand River Williamston, MI 48819 (517) 655-4391
IFG Corp. 18 Bram Court, #5 Brampton, Ontario Canada L6W 3R6 (416) 451-5228	Mesa Scientific Inc. Box 1129 Delta, CO 81416 (303) 874-8881
Mineral Logging Systems Box 40498 Ft. Worth, TX 76140 (817) 293-1777	Mount Sopris Instrument Co. 17301 West Colfax Ave. Suite 255 Golden, CO 80401 (303) 279-3211
Oyo Geospace 7334 N. Gessner Road Houston, TX 77040 (713) 939-9700	Robertson Geologging Limited Deganwy, Conwy. Gwynedd, LL31 9PX United Kingdom Phone: 0492 582323
Auslog 83 Jijaws St. Sumner Park 4074 Brisbane, Queensland Australia	

Logging literature

An extensive body of logging literature is available. During the past decade the number of logging books increased substantially. Several of these books are excellent references. For those who do not want to delve into the primary sources, these books provide a good summary of logging technology.

Appendix V is a bibliography of logging books. Order information is provided for those books published by specialty publishing companies.

The primary journals for borehole geophysical papers are **The Log Analyst** and various Society of Petroleum Engineers publications. **The Log Analyst** is published by the Society of Professional Well Log Analysts (SPWLA) which is the professional organization of the science. SPWLA also publishes the transactions of its annual symposium. Some pertinent articles are also published in **Geophysics**.

The vast ~~majority~~ preponderance of logging literature deals with petroleum applications. Keys (1988) and Repsold (1989) have published the only books on ground-water logging. Hallenburg (1984) has a book on mineral and engineering well logging, and the Society of Exploration Geophysics has a three volume set, **Geotechnical and Environmental Geophysics**, edited by Ward (1990) which includes a few papers on borehole geophysical techniques.

Journal articles on ground-water/environmental logging are similarly scarce. Occasionally an article is included in an SPWLA publication. The Minerals and Geotechnical Logging Society, a chapter-at-large of SPWLA, has a bi-annual symposium with proceedings that usually include a few papers on ground-water applications. The Society of Engineering and Mineral Exploration Geophysicists has an annual symposium with proceedings that occasionally have a ground-water/environmental logging paper. Today, the best source of papers is National Ground Water Association (NGWA) publications: **Ground Water, Ground Water Monitoring Review**, and the proceedings of the annual Outdoor Action Conference on Aquifer Restoration, Ground Water Monitoring and Geophysical Methods.

Chapter 1 has a list of the best ground-water logging articles. The November-December issue of **The Log Analyst** includes an annual bibliography of logging literature that includes a ground-water applications section. The first instillations of this bibliography covered 1975 to 1985 and selected important papers published prior to 1975 (Prensky, 1987). The University of Tulsa (1985) published a logging bibliography covering 1965 to 1984.

Logging literature is replete with abbreviations. Symbols are used for almost all logging terms, and every company has its own tool names and abbreviations. Symbols and abbreviations are defined when they are first

in this report,

used in the text and periodically throughout subsequent chapters. Appendix IV is a glossary of symbols used in this text.

Petroleum versus ground-water logging

Logging literature should be read with the realization that most of it is based on several suppositions that are usually valid for petroleum logging, but are usually **not** valid for ground-water logging. Table 5-8 summarizes the differences between petroleum and ground-water logging. The first three differences are discussed in Chapter 14.

Ground-water logging approached from a petroleum-logging perspective has several pitfalls. Tool selection and log presentation will not be the best available options, and water quality calcuations will have serious errors.

Despite all the research that has been conducted on borehole geophysical techniques, there are still many types of formations that are difficult to analyze. In fact, the only type of formation that present borehole geophysical models and tools do an adequate job of characterizing is shale-free sandstones with intergranular porosity and carbonates that have sodium chloride formation water. Figure 5-2 graphically illustrates this point. Although Figure 5-2 is referring specifically to petroleum logging, it also applies to ground-water logging.

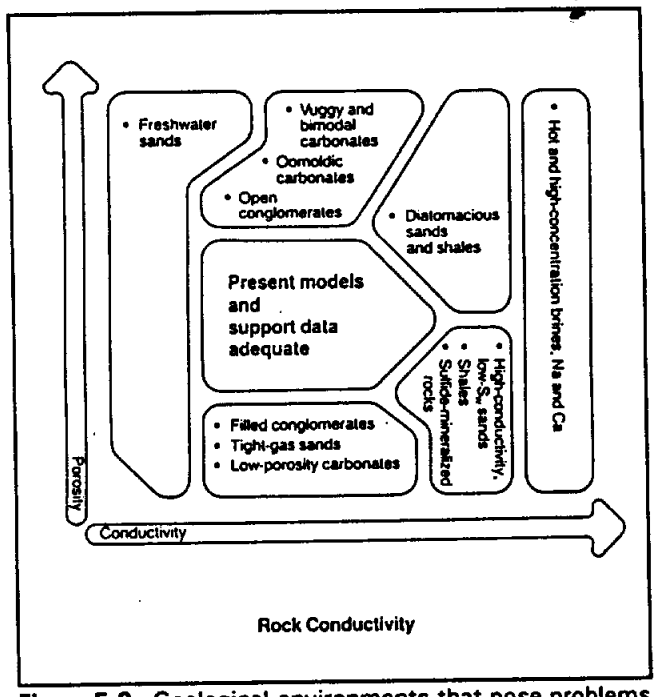

Figure 5-2. Geological environments that pose problems for log interpretation (From Schlumberger, after PSI Research Proposal, no date).

Log presentations

Petroleum logging companies use a standard API (American Petroleum Institute) log format. Some ground-water/environmental logging companies also follow this format, while the rest use a wide variety of presentations. This section describes the API format.

TABLE 5-8. DIFFERENCES BETWEEN PETROLEUM AND GROUND-WATER LOGGING

Petroleum Logging	Ground-Water Logging
Surface conductance negligible	Surface conductance significant
Sodium chloride formation water	Formation water with significant quantities of calcium and magnesium
Monovalent ions	Divalent ions
Two or three fluids in the pores (formation water, oil, gas)	Only water in the pores
8 to 10 inch diameter borehole	Borehole diameters vary considerably Environmental wells are often 2 to 3 inches; water supply wells are often 12 inches or larger
Formations are 100% saturated with water (or hydrocarbons)	Environmental logging is sometimes concerned with the vadose zone
Normally openhole	Environmental logging sometimes has to be done in cased holes

Header. The header contains information used to identify the well and interpret the log. It should always be examined carefully prior to analyzing the log. An API format header contains the following information (Figure 5-3):

1. Logging service company
2. Types of curves on the log

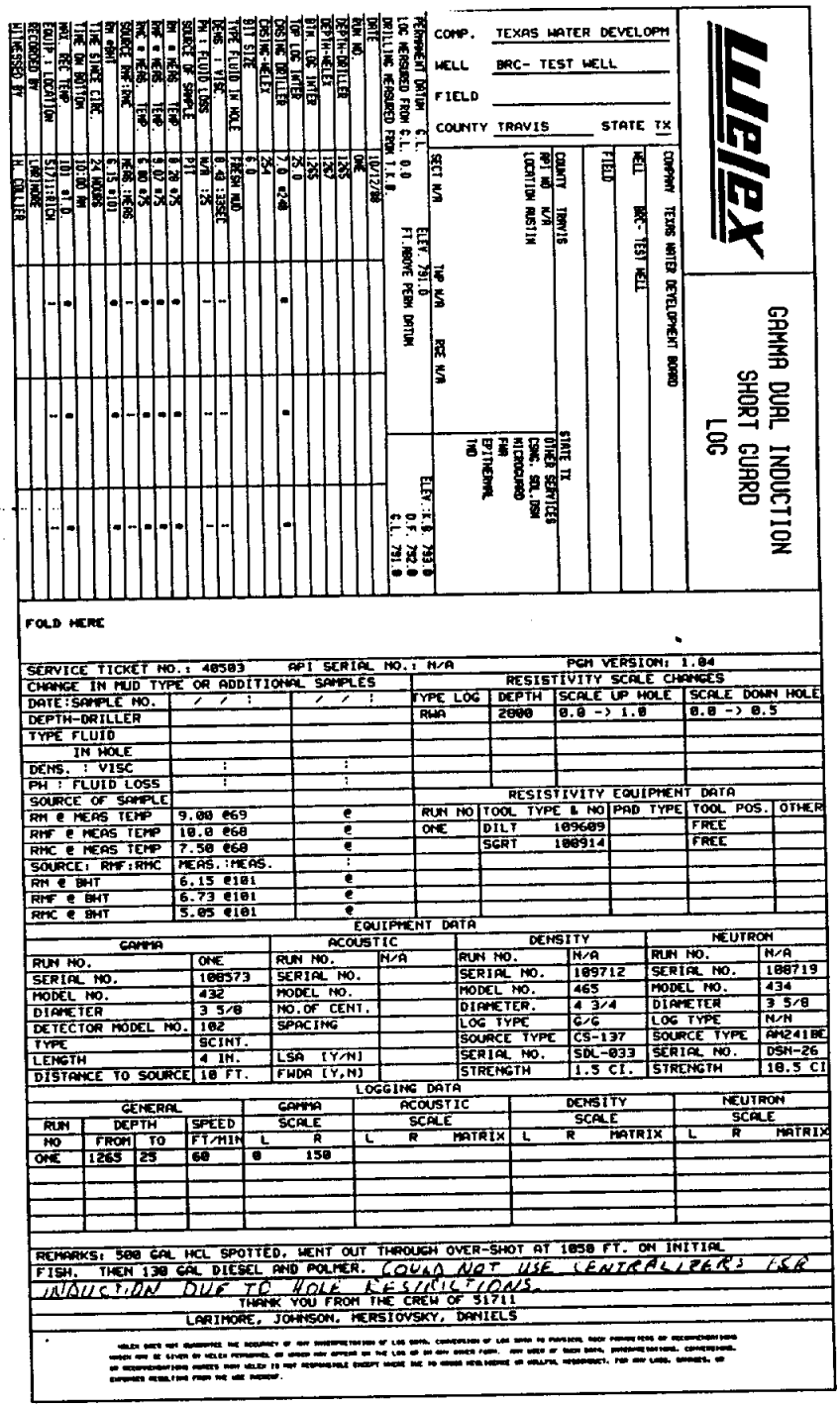

GAMMA DUAL INDUCTION
SHORT GUARD
LOG

COMP. TEXAS WATER DEVELOPM
WELL BRC- TEST WELL
FIELD
COUNTY TRAVIS STATE TX

COMPANY TEXAS WATER DEVELOPMENT BOARD
WELL BRC- TEST WELL
FIELD
COUNTY TRAVIS STATE TX
API NO N/A
LOCATION AUSTIN
OTHER SERVICES
CSNG. SDL. DSN
MICROGUARD
FAR
EPITHERMAL
TMD

SEC N/A TWP N/A RGE N/A
ELEV.: K.B. 793.0
D.F. 792.0
G.L. 781.0

PERMANENT DATUM G.L.
LOG MEASURED FROM G.L. 0.0 FT. ABOVE PERM DATUM
DRILLING MEASURED FROM T.K.B.

DATE	10/12/88
RUN NO.	ONE
DEPTH-DRILLER	1265
DEPTH-WELLS	1265
BTM. LOG INTER.	1263
TOP LOG INTER.	25.0
CASING-DRILLER	7.0 @248
CASING-WELLS	254
BIT SIZE	6.0
TYPE FLUID IN HOLE	FRESH MUD
DENS. : VISC.	8.40 :35SEC
PH : FLUID LOSS	N/A :N/C
SOURCE OF SAMPLE	PIT
RM @ MEAS. TEMP.	9.00 @69
RMF @ MEAS. TEMP.	10.0 @68
RMC @ MEAS. TEMP.	7.50 @68
SOURCE: RMF/RMC	MEAS./MEAS.
RM @ BHT	6.15 @101
TIME SINCE CIRC.	24 HOURS
TIME ON BOTTOM	10:00 AM
MAX. REC. TEMP.	101 @ TD
EQUIP. LOCATION	SOUTHSIDE
RECORDED BY	LARIMORE
WITNESSED BY	M. COLLIER

FOLD HERE

SERVICE TICKET NO.: 40503 API SERIAL NO.: N/A PGM VERSION: 1.04

CHANGE IN MUD TYPE OR ADDITIONAL SAMPLES

DATE:SAMPLE NO.	/ / :	/ / :
DEPTH-DRILLER		
TYPE FLUID IN HOLE		
DENS. : VISC	:	:
PH : FLUID LOSS	:	:
SOURCE OF SAMPLE		
RM @ MEAS TEMP	9.00 @69	@
RMF @ MEAS TEMP	10.0 @68	@
RMC @ MEAS TEMP	7.50 @68	@
SOURCE: RMF:RMC	MEAS.:MEAS.	:
RM @ BHT	6.15 @101	@
RMF @ BHT	6.73 @101	@
RMC @ BHT	5.05 @101	@

RESISTIVITY SCALE CHANGES

TYPE LOG	DEPTH	SCALE UP HOLE	SCALE DOWN HOLE
RWA	2000	0.0 -> 1.0	0.0 -> 0.5

RESISTIVITY EQUIPMENT DATA

RUN NO	TOOL TYPE & NO	PAD TYPE	TOOL POS.	OTHER
ONE	DILT 109689		FREE	
	SGRT 108914		FREE	

EQUIPMENT DATA

GAMMA		ACOUSTIC		DENSITY		NEUTRON	
RUN NO.	ONE	RUN NO.	N/A	RUN NO.	N/A	RUN NO.	N/A
SERIAL NO.	108573	SERIAL NO.		SERIAL NO.	109712	SERIAL NO.	108719
MODEL NO.	432	MODEL NO.		MODEL NO.	465	MODEL NO.	434
DIAMETER	3 5/8	NO.OF CENT.		DIAMETER.	4 3/4	DIAMETER	3 5/8
DETECTOR MODEL NO.	102	SPACING		LOG TYPE	G/G	LOG TYPE	N/N
TYPE	SCINT.			SOURCE TYPE	CS-137	SOURCE TYPE	AM241BE
LENGTH	4 IN.	LSA [Y/N]		SERIAL NO.	SDL-033	SERIAL NO.	DSN-26
DISTANCE TO SOURCE	10 FT.	FWDA [Y,N]		STRENGTH	1.5 CI.	STRENGTH	10.5 CI

LOGGING DATA

GENERAL				GAMMA SCALE		ACOUSTIC SCALE			DENSITY SCALE			NEUTRON SCALE		
RUN NO	DEPTH FROM	DEPTH TO	SPEED FT/MIN	L	R	L	R	MATRIX	L	R	MATRIX	L	R	MATRIX
ONE	1265	25	60	0	150									

REMARKS: 500 GAL HCL SPOTTED, WENT OUT THROUGH OVER-SHOT AT 1050 FT. ON INITIAL FISH. THEN 130 GAL DIESEL AND POLMER. COULD NOT USE CENTRALIZERS FOR INDUCTION DUE TO HOLE RESTRICTIONS.

THANK YOU FROM THE CREW OF 51711
LARIMORE, JOHNSON, MERSIOVSKY, DANIELS

WELEX DOES NOT GUARANTEE THE ACCURACY OF ANY INTERPRETATIONS OF LOG DATA, CONVERSION OF LOG DATA TO PHYSICAL ROCK PROPERTIES OR RECOMMENDATIONS WHICH MAY BE GIVEN BY WELEX PERSONNEL OR WHICH MAY APPEAR ON THE LOG OR ON ANY OTHER FORM. ANY USER OF SUCH DATA, INTERPRETATIONS, CONCLUSIONS, OR RECOMMENDATIONS AGREES THAT WELEX IS NOT RESPONSIBLE EXCEPT WHERE DUE TO GROSS NEGLIGENCE OR WILLFUL MISCONDUCT, FOR ANY LOSS, DAMAGES, OR EXPENSES RESULTING FROM THE USE THEREOF.

Figure 5-3. Typical API format log header.

3. Specific well information

    a. Company that operates the well
    b. Well name
    c. Oil field in which the well is located
    d. Location
    e. API serial number
    f. Elevation of the ground level (G.L.), drill floor (D.F.), and kelly bushing (K.B.)
    g. Date that the logs were run
    h. Depth of the well as measured by the driller and the logger
    i. Interval logged
    j. Casing diameter and depth
    k. Bit size
    l. Drilling mud properties (fluid type, density, viscosity, pH, fluid loss)
    m. Mud resistivity, mud filtrate resistivity, mudcake resistivity
    n. Temperature of the sample at the time of the resistivity measurements
    o. Source of the mud sample
    p. Method used to determine mud filtrate and mudcake resistivities
    q. Bottom hole temperature
    r. Time that logging started
    s. Time that mud circulation ceased

4. Other logs ran in the borehole by this service company

5. Equipment information

    a. Truck serial number
    b. Office that supplied the logging truck
    c. Tool serial numbers

6. Personnel information

    a. Logging engineer
    b. Representative of the company operating the well

7. Remarks section for describing any unusual logging conditions or log processing

Slimhole logs may deviate considerably from the API format. They sometimes contain additional information, but too often they leave out some of the information listed above (Figure 5-4).

Log curves. The main body of the log contains the log curves which are graphs of the physical parameter measured by the tool versus depth. The API format log consists of three tracks with a depth column dividing tracks 2 and 3 from track 1 (Figure 5-5). The log is 8.25 inches wide. Each track is 2.5 inches wide and the depth column is 0.75 inches wide. Slimhole logs may not be presented in API format (Figure 5-6), therefore, some of the following comments may not apply. Inconsistency in log format is the rule for many slimhole logs.

SOUTHWEST FLORIDA WATER MANAGEMENT DISTRICT

GEOPHYSICAL WELL LOG

PROJECT NO. PCO210

WELL NAME Romp DV-1 (DOVER ELEMENTARY) DATE 3/22/00
COUNTY HILLSBOROUGH BASIN HILLSBOROUGH (13) LATITUDE 275926
LOCATION W 1/2 SW 1/4 NE 1/4, S 4 T 29S R 21E LONGITUDE 821234
WELL DEPTH (1) 503 (2) 779' CASING RECORD 12" @ 36' ; @ ; @ ;
DEPTH LOGGED (1) 500 (2) 495 TOP OR START OF LOG (1) 30' (2) 779' above/(below) LSD
ELEVATION 112 ft. above NGVD WATER LEVEL 51 ft. above/(below) LSD 61 ft (above)/below NGVD
LOG TYPE GAMMA - GAMMA OPERATOR G. KINSMAN

LOGS AVAILABLE
- ☑ CALIPER
- ☑ ELECTRIC (SP,R)
- ☑ LONG-SHORT NORMAL (16"-64") + LATERAL
- ☑ FLUID CONDUCTIVITY (RESISTIVITY)
- ☑ TEMPERATURE
- ☑ NATURAL GAMMA
- ☑ GAMMA-GAMMA
- ☑ NEUTRON
- ☐ FLOW METER

INSTRUMENT SETTINGS:
___ mv ___ ohms 1K rate
9.14 pos 5.63 sens .8 time constant
___ variable span

LOGGED ☑ UP ☐ DOWN LOGGING SPEED 25'/min

QW SAMPLE:

	DEPTH	CONDUCTIVITY	TEMP
①			
②			
③			
④			

COMMENTS: _____

Figure 5-4. Example of a slimhole log header.

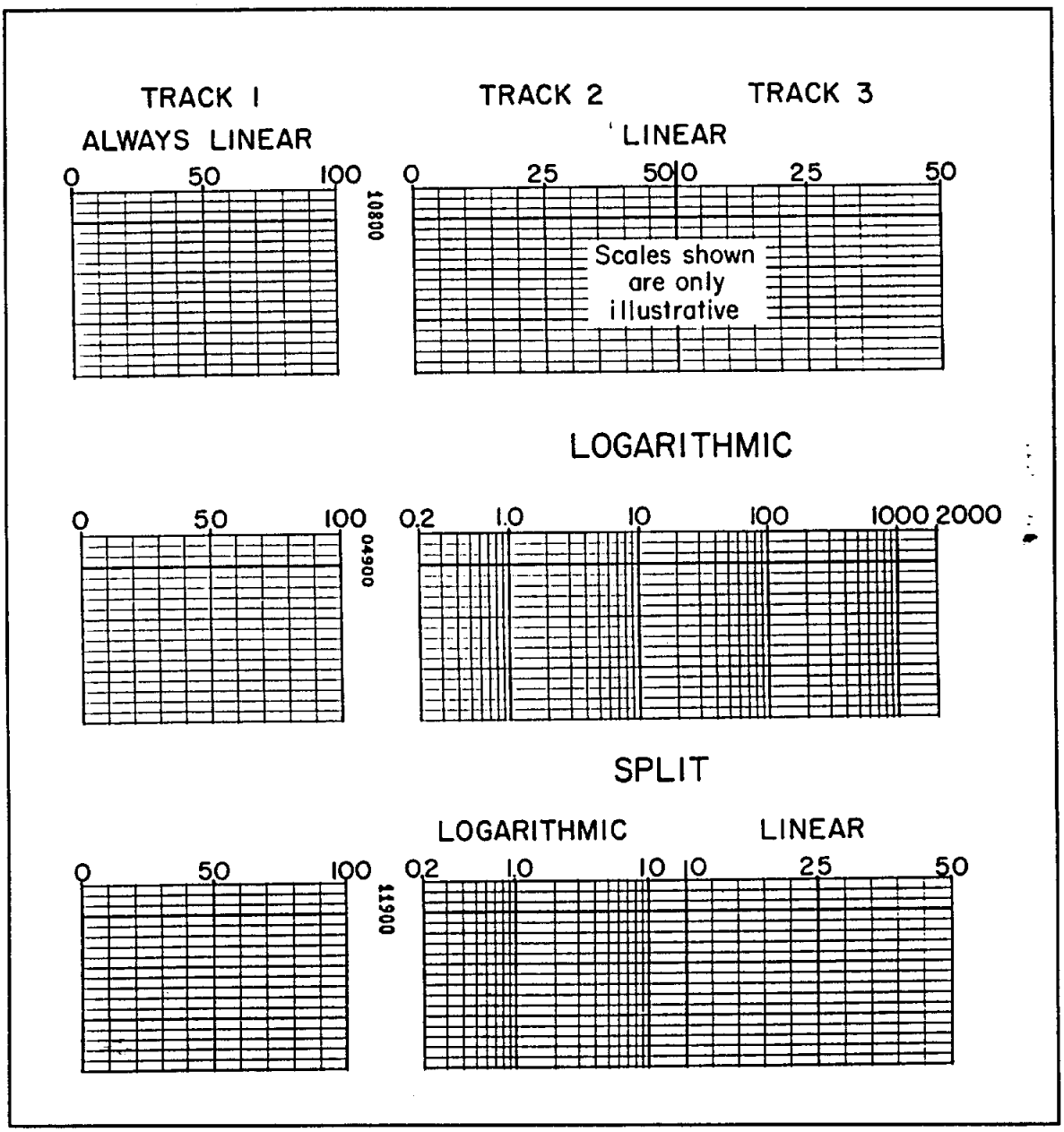

Figure 5-5. Examples of horizontal log scales. The logs are shown at a reduced size (From Schlumberger, no date).

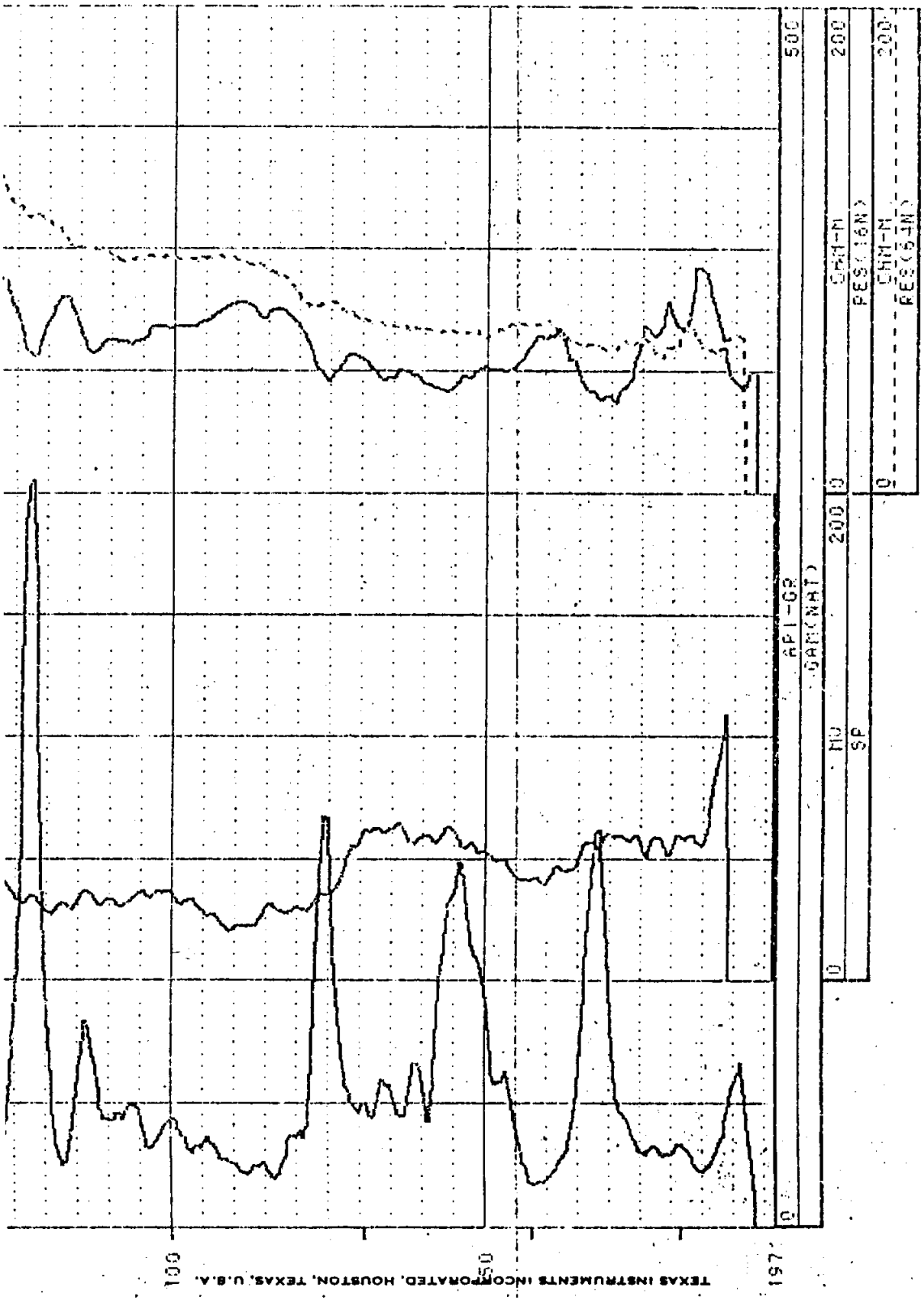

Figure 5-6. An example of a slimhole log format that does not conform to API standards.

The vertical scale is a depth scale. It is always linear and usually scaled in either 1, 2, or 5 inches per 100 feet of borehole depth, thus the logs are referred to as 1, 2, and 5 inch logs. The 1 and 2 inch scales are divided into 10 foot intervals with heavy horizontal lines every 50 feet (Figures 5-7 and 5-8), and depths are recorded every 100 feet in the depth column. The 5 inch log is scaled in two-foot increments with dark lines every 10 feet and darker lines at 50 and 100-foot intervals (Figure 5-9), and depths are recorded at 50 and 100-foot intervals.

The 1 and 2-inch scales are called correlation scales, since geologists find them a convenient scale for doing well-to-well correlations. The 5-inch scale is for detailed log analysis. With digital data, logs can easily be reproduced at any scale. Environmental logs are often expanded to greater than 5 inch scales.

A log may contain 1, 2, and 5-inch scales or any combination of the three. Logs reproduced for sale by commercial vendors have been reduced 50 percent, which means that the 5-inch scale becomes a 2.5-inch scale.

The outside border of modern conventional logs, no matter what the depth scale, has breaks that represent one-minute intervals. The number of feet between one-minute intervals indicates the logging speed (Figure 5-8).

Horizontal scales may be linear or logarithmic (Figure 5-5). Track 1 is always linear, while tracks 2 and 3 may be either (Figures 5-9 and 5-10). Track 1 is reserved for certain curves such as the SP, gamma ray, and caliper. Porosity and resistivity curves are always in tracks 2 and/or 3. Different curves may be plotted in tracks 2 and 3 (Figures 5-7, 5-8, and 5-11) or the curves may be scaled across both tracks (Figures 5-9 and 5-10). Only resistivity curves use a logarithmic scale and it is most commonly used on the 5-inch scale.

At the top and bottom of the curves are headings that identify the log curves and list the scales (Figure 5-9). Back-up or wrap-around scales are used when the log value exceeds the maximum scale value. The curve wraps around to the side of the track opposite where it went off scale and starts again at a new scale. The back-up scale should be included in the curve scale, but such is not always the case (see the gamma ray curve in Figure 5-9). Sometimes a curve in track 2 or 3 will continue off scale into the other track without wrapping around. Even though the other track is not

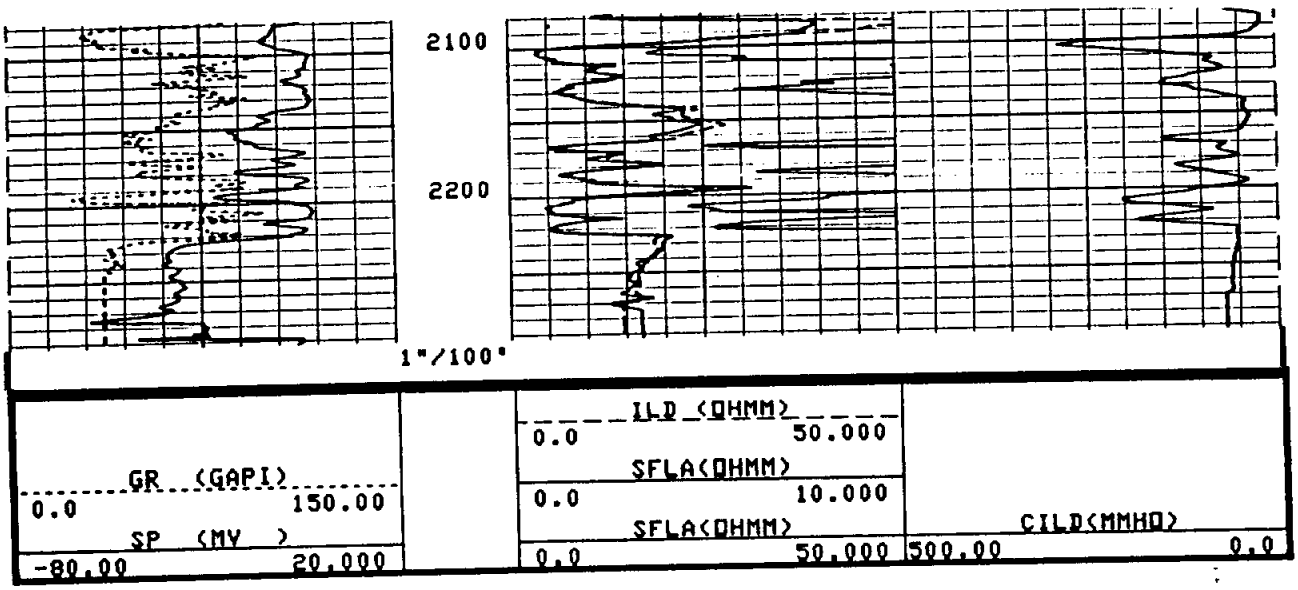

Figure 5-7. A 1 inch per 100 feet depth scale with linear curve scales. The log has been reduced in size to fit this page.

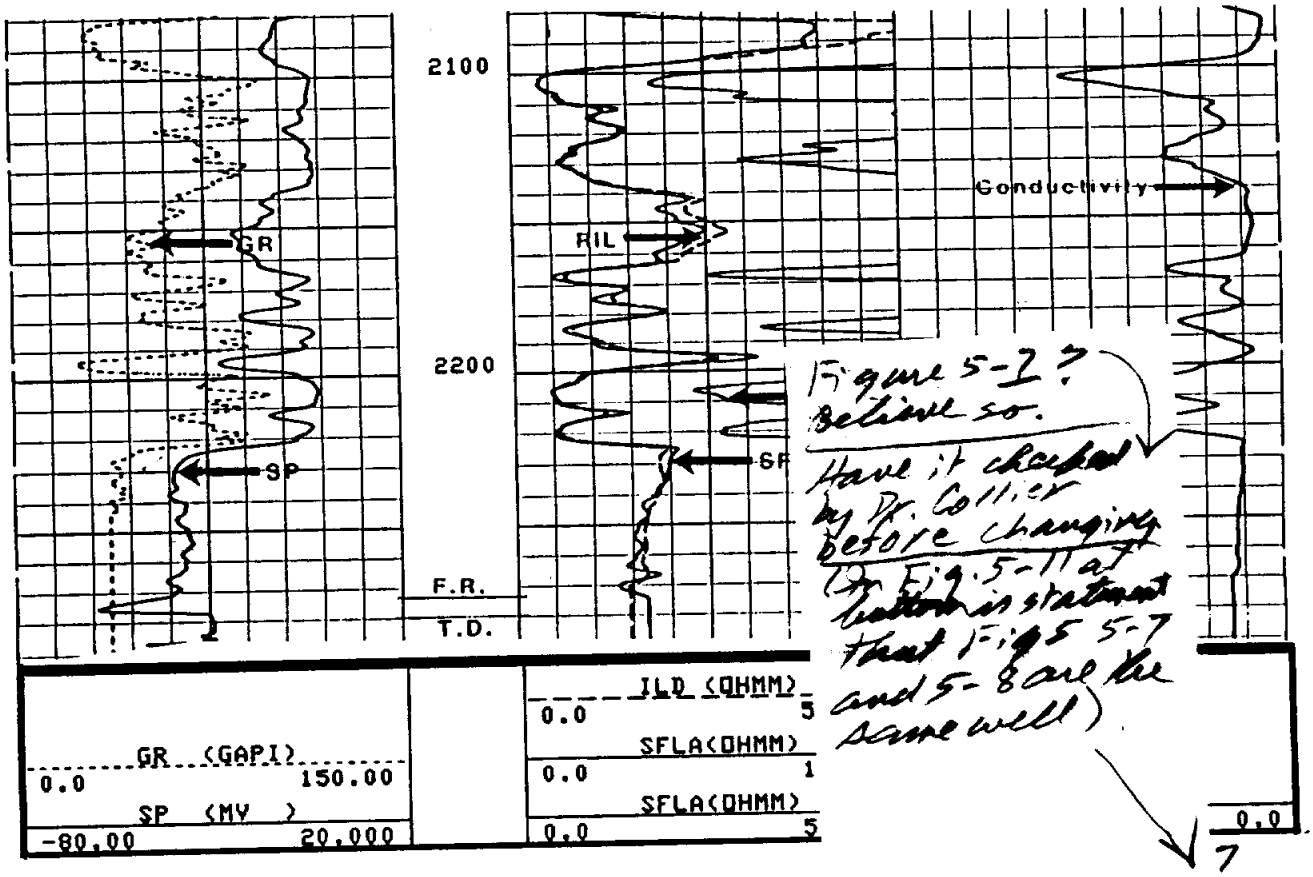

Figure 5-8. A 2 inch per 100 feet depth scale with linear curve scales. It is the same log as Figure 5-8. Track 2 contains an averaged SFL curve and an amplified averaged SFL curve. The amplified curve is of no value, it just clutters the log. The left border of Track 1 and the right border of Track 3 have breaks that indicate the logging speed. A break represents one minute. The log has been reduced in size to fit this page.

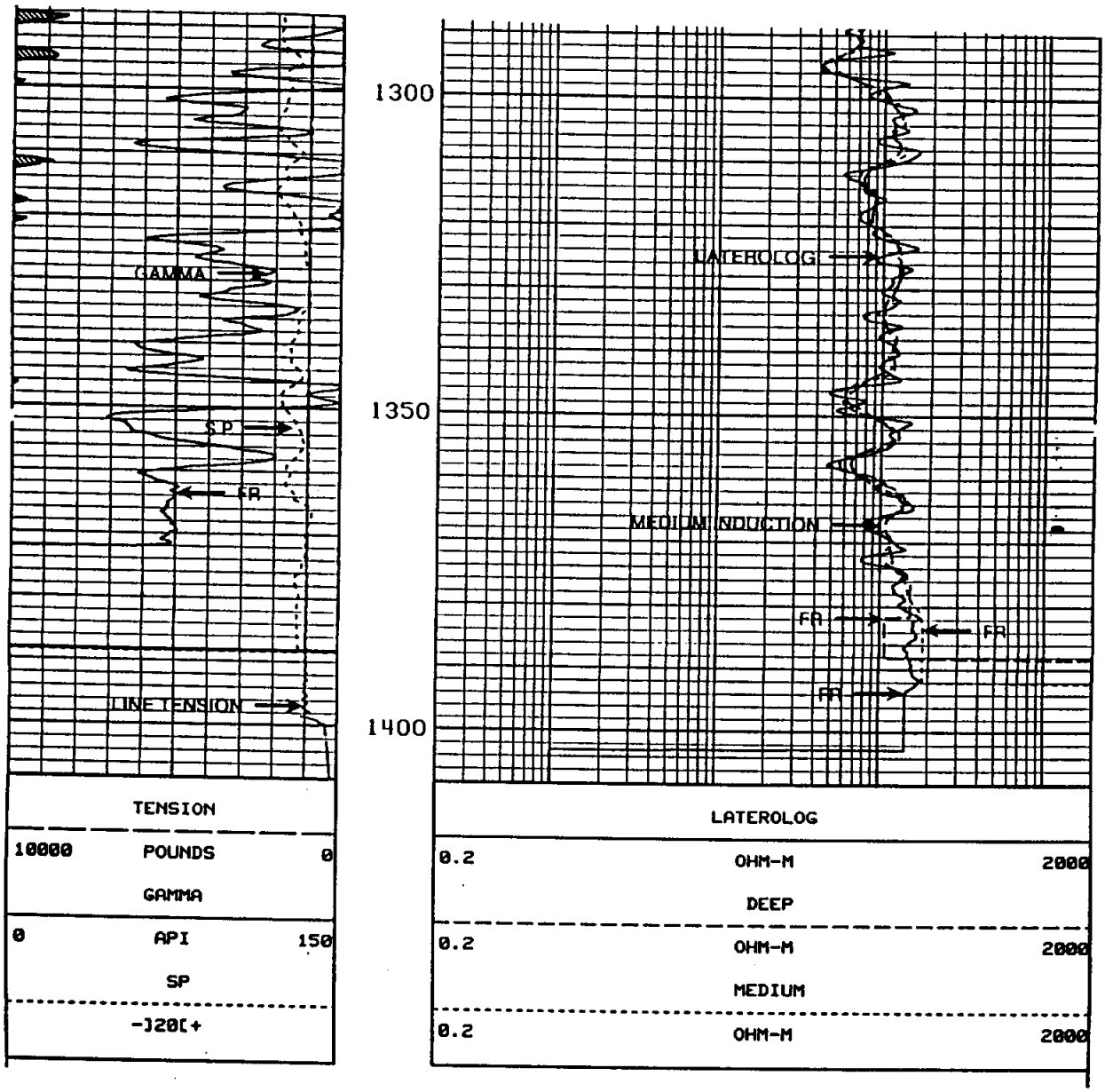

Figure 5-9. A 5 inch per 100 feet depth scale with logarithmic resistivity curves in tracks 2 and 3. FR denotes the first reading of each curve. The gamma ray curve goes off scale at 1312 feet and wraps around to start over again on the left side of track 1. The wrap-around scale for the gamma ray curve should be in the curve scale but it was left off. The log has been reduced in size to fit the page. For further details on this log see Figure 5-10.

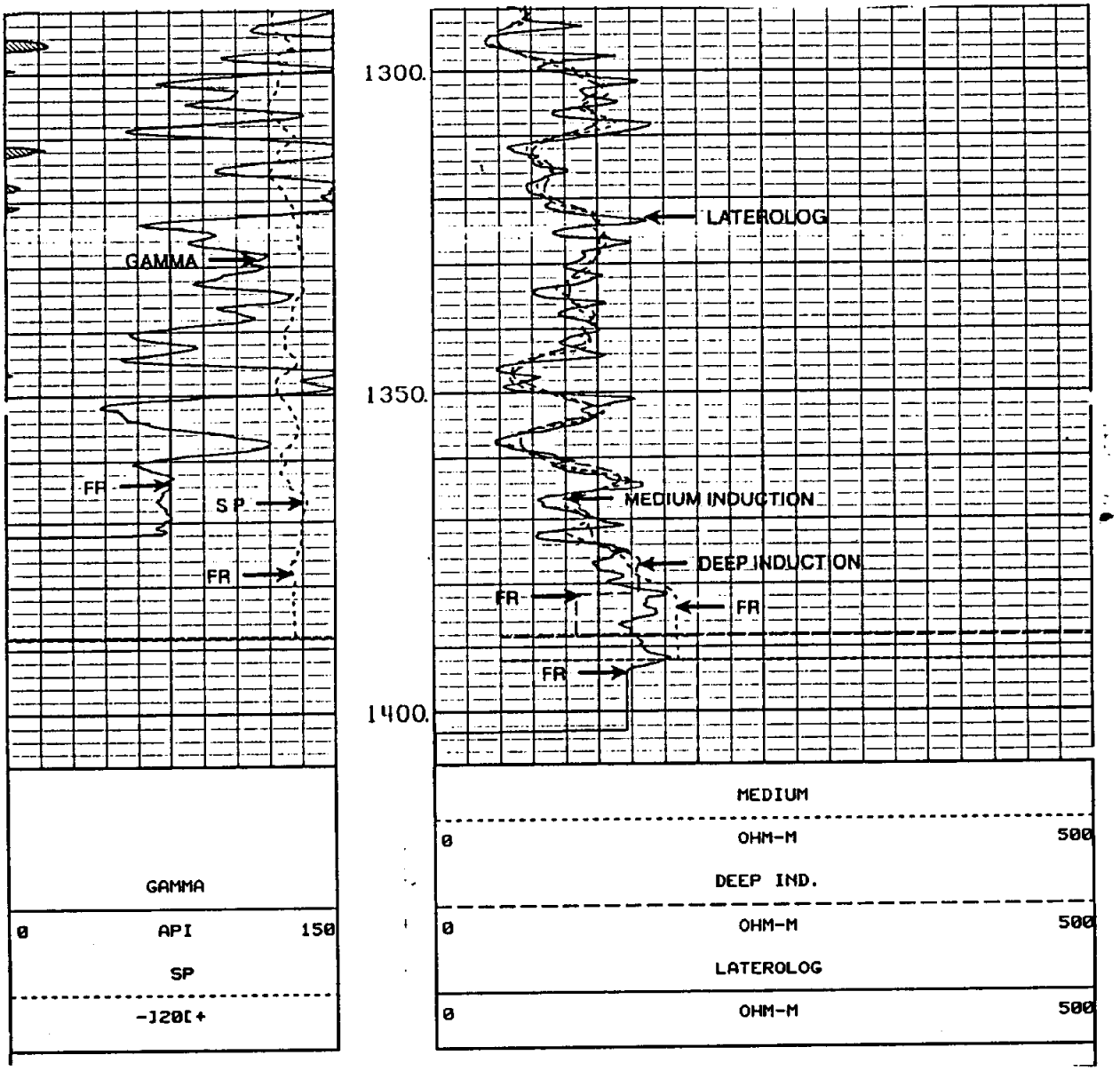

Figure 5-10. A 5 inch per 100 feet depth scale with linear resistivity curves in Tracks 2 and 3. This is the same log as Figure 5-9. The log is the Hickory Sandstone Member of the Riley Formation. The well is the Texas Water Development Board, Brady Test Hole #1, McCulloch County, Texas (state well number 42-62-909). The log has been reduced in size to fit the page.

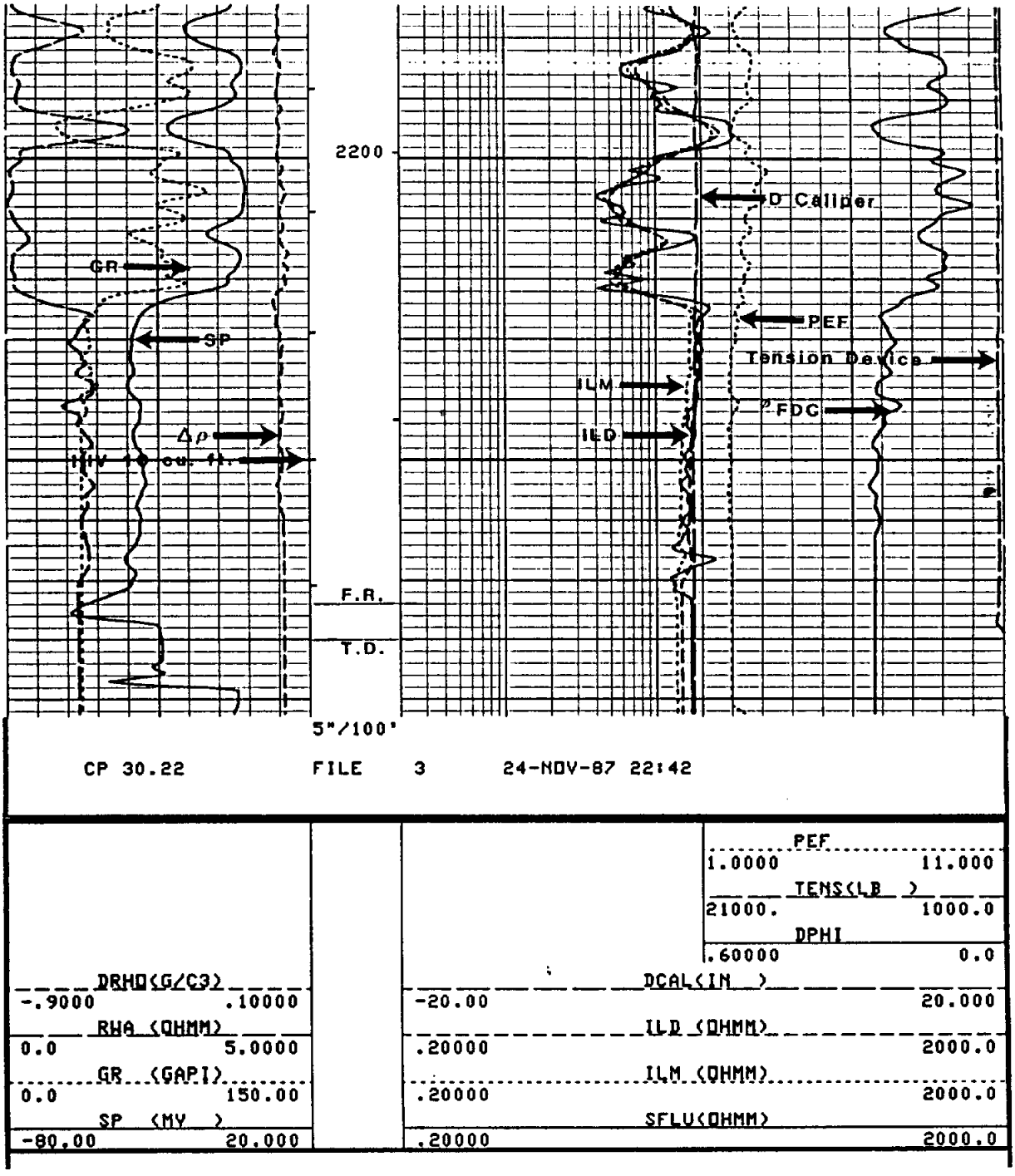

Figure 5-11. A 5 inch per 100 feet depth scale with logarithmic resistivity curves in track 2 and linear porosity curves in track 3. This is the same well as Figures 5-7 and 5-8. The log has been reduced in size to fit the page.

scaled for this curve, the curve is still scaled in the same unit of measurement.

Sometimes logs are misscaled. A knowledge of typical log values in a local area will aid one in identifying mislabeled curves. For example, mislabeled resistivity curves can be spotted by looking at the resistivity values of the shales to see if they agree with other wells.

Log curves are solid, dashed, or dotted lines. If three resistivity curves are plotted in the same track, the shallowest investigating resistivity curve is a solid line, the medium reading resistivity curve is short dashes, and the deep reading curve is long, heavy dashes (Figure 5-9). If two resistivity curves are plotted together, the shallow curve is solid and the deeper reading curve is dashed (Figure 5-7). When plotted together, the density porosity is a solid line and the neutron porosity is a dashed line. These conventions are often not followed on ground-water/environmental logs which makes for confusing, inconsistent log presentations.

At the bottom of modern conventional logs the notation **FR** (first reading) is found on each log curve (Figure 5-9). This denotes the first depth in the well bore above T.D. (total depth) at which a particular tool makes a measurement. Long tool combinations mean that some measurements will start 20 to 30 feet off bottom. Even though a curve continues to T.D. it is meaningless below the FR point and should not be used in log calculations. Unfortunately, FR is not printed on all logs so it is necessary to look closely at the nature of the curve within 30 feet of T.D. With a little practice one can spot the first reading. Some curves will be flat below FR, while radioactivity tools will have a limited amount of "squiggles" (Figure 5-9).

On modern conventional logs a tension curve is recorded somewhere on the log (Figure 5-9). It records the tension on the cable and identifies intervals where the tool pulled tight. When the tool sticks, it continues to make measurements, the cable stretches, and the log depths continue to change. The tension curve allows one to spot these intervals. With combination tools this interval will not be at the same log depth for every curve.

During the reproduction of old electric logs track 3 was often cut off (Figure 5-12). In Texas track 3 contains the long normal curve or the lateral. Valuable unrecoverable information was lost with this practice.

The common practice with petroleum logs is to plot certain curves together at the same scales. Resistivity curves are plotted together and so are porosity curves, especially density and neutron curves. Gamma ray and SP curves are plotted in the same track. This allows for useful comparisons that yield additional information about lithology and mud filtrate invasion. Unfortunately, this is not standard practice for groundwater/environmental logs. Valuable information is lost as a result.

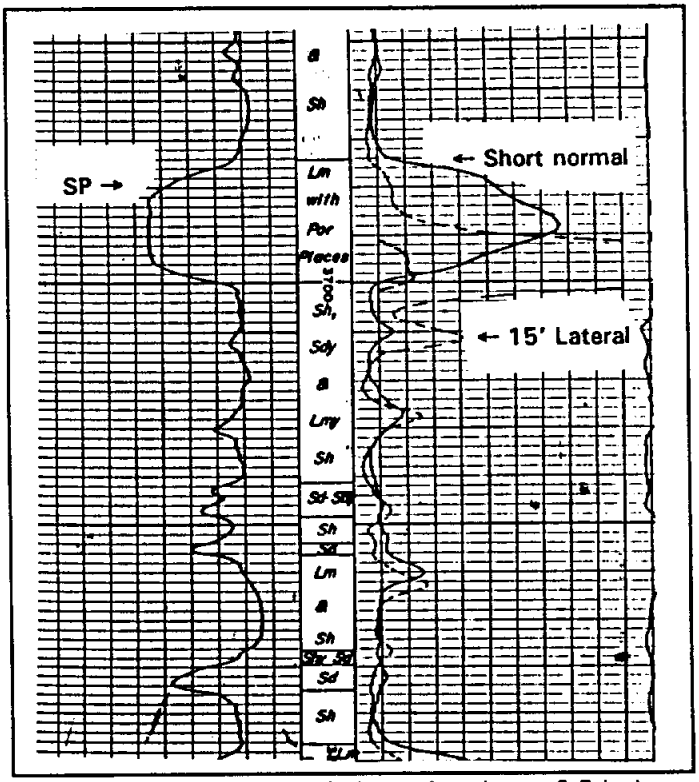

Figure 5-12. An old electric log reduced to a 2.5 inch per 100 feet depth scale. Most of Track 3 was cut off and the long normal curve is barely visible.

Log tail. The bottom of the log contains a repeat section of 200 to 300 feet. Comparison of this section with the main pass allows one to judge the repeatability of the tools which helps in determining how well the tools were working. Radioactive measurements will show some slight variations, but other tools should repeat very closely.

Before and after survey calibrations will also be at the bottom of the log (Figure 5-13). They document that the tool was working properly both before and after the logging run. Calibration records are not easy to read. The particular logging company's literature must be consulted.

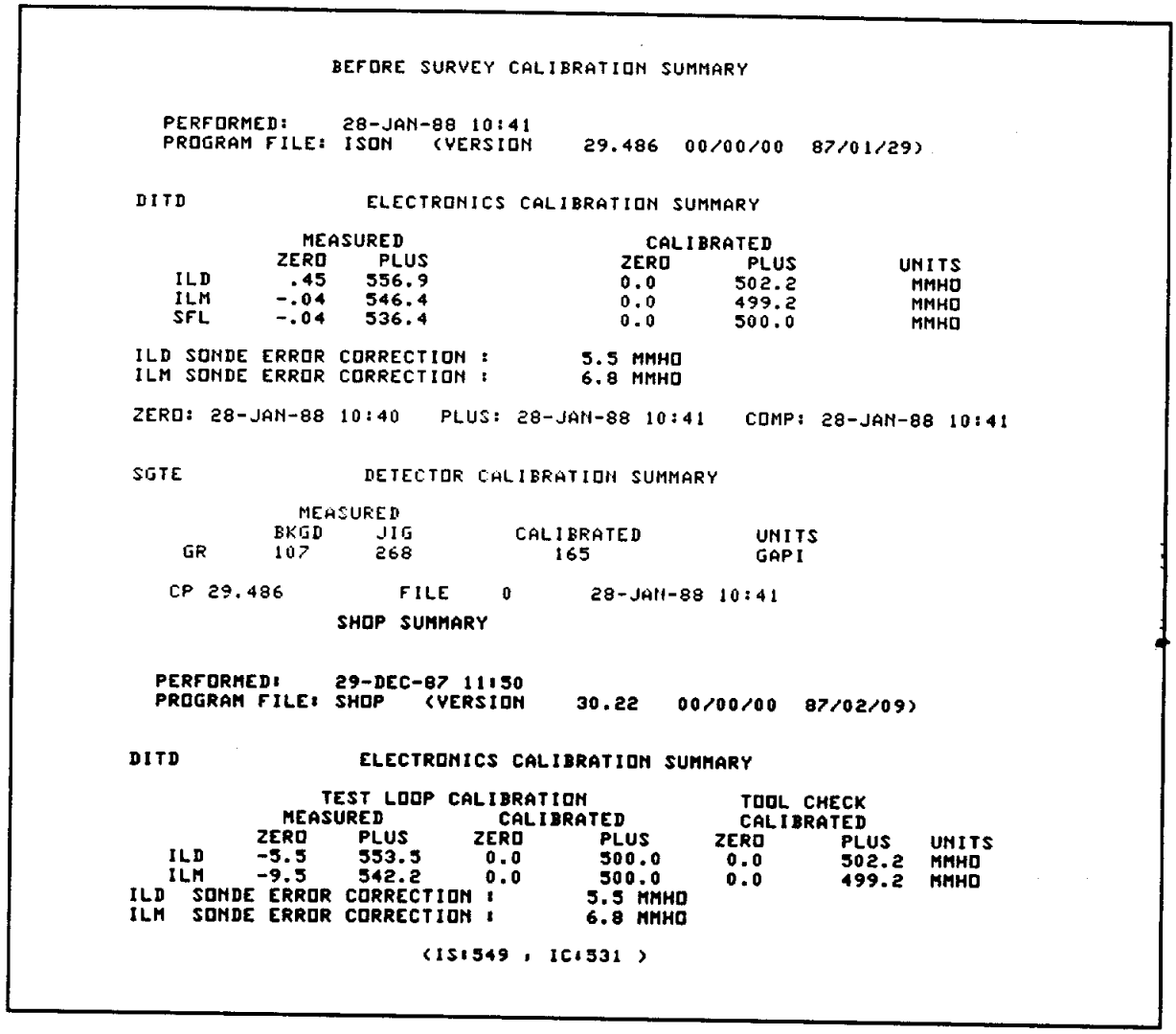

BEFORE SURVEY CALIBRATION SUMMARY

PERFORMED: 28-JAN-88 10:41
PROGRAM FILE: ISON (VERSION 29.486 00/00/00 87/01/29)

DITD ELECTRONICS CALIBRATION SUMMARY

	MEASURED ZERO	MEASURED PLUS	CALIBRATED ZERO	CALIBRATED PLUS	UNITS
ILD	.45	556.9	0.0	502.2	MMHO
ILM	-.04	546.4	0.0	499.2	MMHO
SFL	-.04	536.4	0.0	500.0	MMHO

ILD SONDE ERROR CORRECTION : 5.5 MMHO
ILM SONDE ERROR CORRECTION : 6.8 MMHO

ZERO: 28-JAN-88 10:40 PLUS: 28-JAN-88 10:41 COMP: 28-JAN-88 10:41

SGTE DETECTOR CALIBRATION SUMMARY

	MEASURED BKGD	MEASURED JIG	CALIBRATED	UNITS
GR	107	268	165	GAPI

CP 29.486 FILE 0 28-JAN-88 10:41

SHOP SUMMARY

PERFORMED: 29-DEC-87 11:50
PROGRAM FILE: SHOP (VERSION 30.22 00/00/00 87/02/09)

DITD ELECTRONICS CALIBRATION SUMMARY

	TEST LOOP CALIBRATION MEASURED ZERO	MEASURED PLUS	CALIBRATED ZERO	CALIBRATED PLUS	TOOL CHECK CALIBRATED ZERO	CALIBRATED PLUS	UNITS
ILD	-5.5	553.5	0.0	500.0	0.0	502.2	MMHO
ILM	-9.5	542.2	0.0	500.0	0.0	499.2	MMHO

ILD SONDE ERROR CORRECTION : 5.5 MMHO
ILM SONDE ERROR CORRECTION : 6.8 MMHO

(IS:549 , IC:531)

Figure 5-13. Before and after survey calibrations for the Dual Induction and gamma ray tools.

THE BOREHOLE ENVIRONMENT AND ITS EFFECTS ON LOG RESPONSES

Chapter 6

The function of most logging tools is to measure the physical properties of the formations penetrated by a borehole and then use the measurements to calculate various hydrogeological properties (e.g. porosity and water quality). These calculated properties will be correct only if the logging tools measure the physical properties of undisturbed, unaltered rocks. Obviously, this is never the case since the rocks have to be disturbed (i.e. drilled) in order to be logged. In addition to analyzing the formations, logging tools are also responding to some degree to the type and volume of borehole fluid, mudcake, and mud filtrate. The only recourse is to measure the formations in their altered state and then compensate the log responses for the effects of the borehole environment. Such compensation requires a thorough knowledge of the borehole environment.

This chapter discusses four characteristics of the borehole that can significantly affect log responses: drilling method, borehole diameter, borehole fluid, and drilling fluid invasion[1]. The following discussion is an introduction to the subject and provides some general guidelines on the use of borehole environmental correction factors. Hallenburg (1984) and Jorden and Campbell (1984) have more comprehensive treatments of the subject. For guidelines as to when correction factors should be applied to particular tools see Chapters 8 through 13.

The major petroleum-oriented commercial logging companies have published chart books containing environmental correction curves for their tools (Figure 6-1 is an example). Charts, called departure curves, are available to correct for the effects of borehole diameter, borehole fluid, mudcake thickness, and filtrate invasion. Unfortunately, correction charts exist for very few of the slimhole tools.

---

[1] Temperature and drilling mud column pressure will affect logging tools if conditions are extreme enough. However, conventional logging tools are more than adequate for ground-water environments. They are designed for pressures up to 20,000 psi and temperatures to about 400° F (Rider, 1986). Most slimhole tools are designed for much less harsh conditions. The slimhole tool manufacturer's specs should be consulted before logging holes over a few thousand feet deep and more than 200° F. Specialized logging equipment is available for geothermal wells (Vaneruso and Coquat, 1979; Itoh, et al., 1980; SPWLA, 1982).

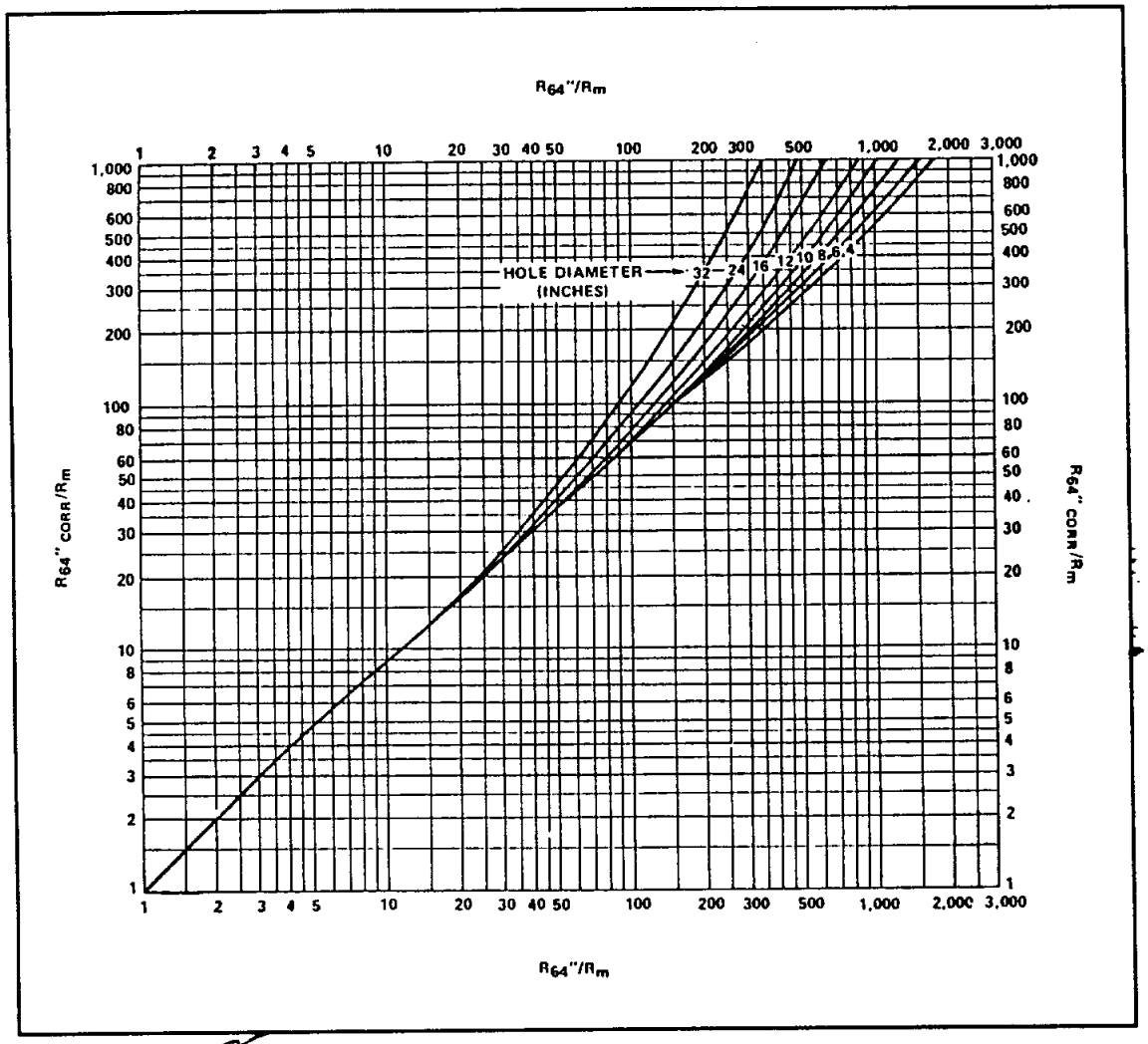

Figure 6-1. An example of an environmental correction chart. This chart corrects the 64 inch normal log for the effects of mud resistivity (Rm) and borehole diameter. Rm must be at formation temperature (From SPWLA, 1979, after Schlumberger, no date).

Before exerting a lot of effort on borehole environmental corrections consider the goal of the log analysis and decide whether or not environmental corrections are necessary. Corrections are not required for qualitative log analysis (e.g. correlation, identifying depositional facies, picking bed boundaries, identifying simple lithologies, etc.). In fact, they are not always needed for quantitative log analysis because oftentimes the corrections do not improve the accuracy enough to make them worth the time and trouble. However, the only way to know this is to have an accurate characterization of the borehole and to understand how each logging tool is affected by the borehole environment. For quantitative analysis (porosity, water quality, etc.) of critical zones in a particular well, environmental corrections are quite

often necessary. For a regional study in which hydrogeological trends are being delineated from a large number of wells, applying environmental corrections to the entire data base may not be expedient and/or result in a significant improvement in the data. Just comparing offsetting wells may be sufficient to spot the anomalous log values that require environmental corrections.

This chapter provides a ground-water investigator with the knowledge that will allow an intelligent decision as to whether or not a log needs borehole environmental corrections.

Drilling Method

Accurate log responses are largely dependent on choosing the correct drilling method and then properly implementing that method. This section concentrates on the effects of different drilling methods on logging tools.[1]

Most water and petroleum wells are drilled with the mud-rotary method, and most logging tools are designed to operate in a borehole filled with drilling mud. The most significant influences of the mud-rotary method on logging responses are the presence of drilling fluid in the borehole and mud filtrate in the formations. Both topics are covered in subsequent sections of this chapter.

A few wells are drilled by air-rotary and cable-tool methods. These drilling methods do not introduce significant amounts of drilling fluids into the borehole and the formations. These drilling methods could be considered an advantage over mud-rotary drilling. The severe drawback to this "advantage" is that most logging tools do not operate in an air-filled hole (gamma ray, induction, and caliper are the exceptions). Induction, neutron, and density tools will operate in an air-filled hole, but air-rotary drilling dries out the rock adjacent to the borehole, which affects the log responses.

The drilling methods discussed so far have little effect on the physical properties of the formations penetrated by the borehole.[2] The same cannot be said for augering, which is a method frequently used to drill shallow

---

[1] Driscoll (1986) and Shuter and Teasdale (1989) are excellent references on ground-water drilling methods.

[2] The effects of drilling-induced mechanical stresses are not important to the routine log analysis of aquifers in sedimentary rocks.

ground-water monitoring test holes in unconsolidated sediment. Augered holes normally have to be cased prior to logging. The unconsolidated sediment usually slumps around the casing creating an altered zone up to several inches thick. Many logging tools such as resistivity and SP cannot measure through casing. Some tools such as the density and neutron probes can measure through casing, but the accuracy of the measurements is very questionable. Density and neutron tools have a depth of investigation of only a few inches, so they may only be measuring the altered zone or a void behind the casing. Except for the induction and maybe the gamma ray tool, accurate log responses are almost impossible to obtain in augered holes that have been cased.

Improper drilling methods affect the borehole environment by producing washouts and crooked holes. Washouts are the more common problem and are discussed in detail in the **Borehole Diameter** section. Although crooked holes can create serious logging problems (e.g. stuck probes), this seldom happens in water wells. Drillers of large-capacity water wells keep borehole deviations to a minimum in order to comply with strict drilling specifications. Crooked holes have to be compensated for during the logging process by using standoffs, centralizers, and compensated tools.

Borehole Diameter

Conventional logging tools are designed to give their most accurate readings in a 7 ⅞ to 8 inch diameter hole. Slimhole tools are designed for maximum accuracy in considerably smaller holes (2 to 4 inches). When the borehole becomes significantly larger or smaller than the optimum diameter, a correction factor needs to be applied to most logging tool responses.

Enlarged boreholes are the result of the bit size being considerably larger than the logging tool or washouts developing in a normal diameter hole. Decreases in hole diameter are created by clay squeezing into the borehole (mud rings) and by rock shifts in fractured, rubble, and boulder-gravel zones.

For tools that are centralized in the borehole (sonic, gamma ray, SP, and mandrel resistivity probes) and for those that stand off from the borehole wall (induction), anomalous responses may be due to an increase in borehole diameter. The volume of fluid around the logging tool increases as the hole diameter increases; consequently the tool responds more and more to the borehole fluid and less and less to the rock. Above a certain hole

diameter, the tool will be responding only to the borehole fluid. A borehole less than the optimum diameter will also affect the log values of centralized tools.

For tools that are eccentralized against the borehole wall (neutron and pad devices such as microresistivity, density, and high frequency dielectric tools), pad contact is lost when the borehole is rugose (wrinkled) or elongate, when the bit size is larger or smaller than the optimum diameter,[1] and when the borehole is washed out (Figure 6-2). This introduces an error into the log response and necessitates an environmental correction.

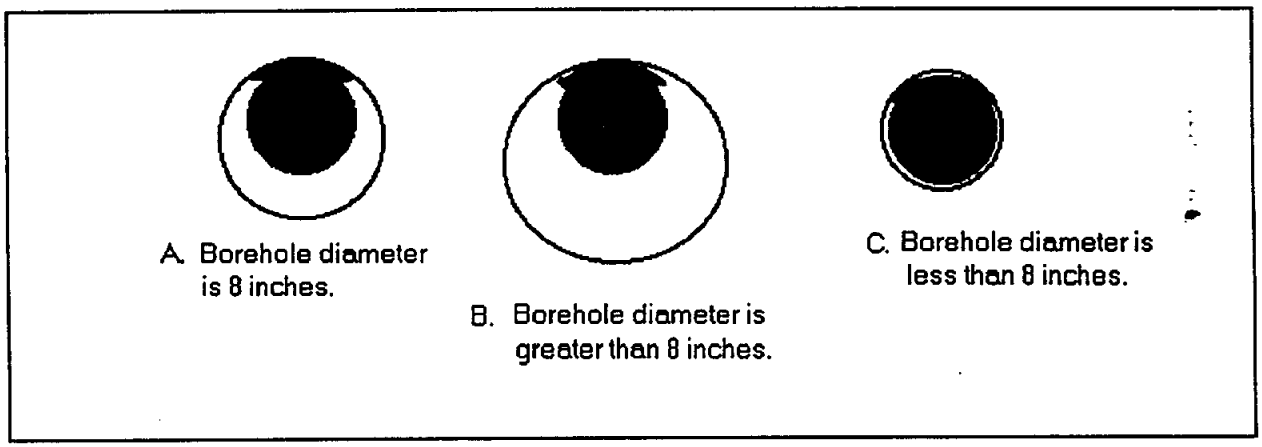

Figure 6-2. How a conventional eccentered tool fits in boreholes of various diameters.
a. Logging tools are designed to fit an 8 inch hole giving the optimum tool response.
b. and c. Pad contact is lost in holes larger or smaller than 8 inches, producing an error in the log response.

Holes in excess of about 6 inches produce significant errors in tool response for slimhole tools, and those over 10 inches significantly affect conventional tools. The chart books for conventional tools routinely have corrections for boreholes up to 16 inches, and for some tools corrections are available for up to 24 inch diameter holes. Modified tool designs and new modeling techniques have made it possible to obtain accurate log values in holes as large as 24 inches (Kienitz, et al., 1986). Clenchy (1985) and Kienitz, et al. (1986) are two good case studies of log responses in large diameter holes.

---

[1] Special positioning devices can be used on pad-type tools if borehole elongation is severe. Unfortunately, only calipers with four or more arms will characterize the borehole shape and they are not part of normal logging suites.

The fact that borehole-diameter corrections are necessary for decreases as well as increases in hole size is often overlooked. However, corrections for borehole enlargements are more frequently needed because washouts and large diameter holes are more common than decreases in hole size. Borehole enlargements also tend to be of a more severe nature since there is no upper limit on hole size, while the minimum hole diameter for safe logging is usually not much smaller than the bit size.

The following guidelines should be followed ~~before~~ drilling ~~and~~/or analyzing a well:

Before a test hole is drilled

1. The hole diameter should be compatible with the size of the logging probes or vice versa. Each logging tool has a maximum as well as a minimum hole diameter requirement.

   a. The minimum hole diameter for safe passage of conventional logging tools is 5 to 6 inches. Most slimhole tools will fit into a 2 inch hole, but some require 3 inches.
   b. For hole diameters greater than 6 inches, conventional logging tools are preferred over slimhole tools.
   c. An 8 inch diameter hole is ideal for conventional tools.
   d. For hole diameters greater than 12 inches, conventional logging tools that have been modified for large boreholes should be used. Such equipment is not commonly available, so arrangements must be made with the logging company well in advance of logging.
   e. If accurate logs are critical to the evaluation of a very large diameter borehole, it may be advantageous to first drill and log a smaller diameter pilot test hole.

During the drilling

1. The use of proper drilling tools and practices, and particularly, a good quality mud and mud monitoring program will control washouts.

During the logging

1. A caliper log should always be run. It is the only way to measure the borehole diameter and it is critical for interpreting other logging curves.

2. Porosity tools should be compensated. Compensated tools will correct for a few inches of washout.

3. In very large diameter boreholes (more than 16 inches for conventional tools and more than 8 inches for slimhole tools), logging probes that are normally centralized in the hole may need to be eccentralized.

4. Very large diameter holes require tools that have a deeper, lateral depth of investigation; namely, a long spaced sonic rather than a normal sonic, density and neutron tools with higher count rates, and the deeper reading resistivity tools.

After the logging

1. The bit size(s) should be determined by looking at the log heading. If the bit size is much larger than 10 inches, a correction factor will significantly improve gamma ray, induction, and mandrel resistivity values. A combined borehole diameter/Rm correction is the first environmental correction that should be applied to mandrel resistivity and induction values.

2. Anomalous log responses may be the result of unconfirmable washouts. If a caliper log is not available, there may be hints on the log header as to the borehole conditions:

   a. The time required to drill the well should be determined. An unusually long time may have produced a very rugose hole. The logging date is on the header. The spud date is not. It has to be obtained from the well file for ground-water wells and from a completion card for petroleum tests. Also, the shallower the formation in the well bore, the longer it has been exposed to the drilling environment relative to the rest of the borehole, and the greater the amount of washout.

b. The mud program should be examined. A poor quality mud program is likely to increase the amount of washout in unconsolidated sands and in shales (See Appendix III, **TECHNIQUES TO EVALUATE THE QUALITY OF DRILLING MUD**). Ground-water wells, which are often drilled with poor quality mud and are usually in semi-consolidated or unconsolidated formations, are particularly susceptible to this problem.
c. If the log is from an oil or gas well, shallow ground-water aquifers may be severely washed out because drillers typically do not mud up while drilling the upper portion of the hole. Unfortunately, the depth at which the driller muds up is not noted on the heading.

3. If a caliper log is available, it should be used to determine if any borehole-diameter corrections for washouts are required.

   a. Much of the borehole may be washed out, but if the aquifers are consolidated rocks the washouts are usually restricted to the shales and corrections are not necessary.
   b. Aquifers in unconsolidated or semi-consolidated sand may wash out, necessitating borehole-diameter corrections.
   c. The caliper log should be scanned for any aquifer-quality formations for which the borehole diameter is more than an inch larger than the bit size. Borehole-diameter corrections should be made on a zone or two to see if they significantly change the log value.
   d. Caliper tools vary greatly in resolution (see Chapter 11). A thin zone (less than 2 feet wide) that shows slight enlargement in borehole diameter (as little as 1 inch) on many caliper logs may represent an actual enlargement of several inches that will greatly affect porosity tools.
   e. Logging tools vary in their sensitivity to borehole enlargements. A correction factor may not improve the accuracy of the log response enough to be worth the time and effort.

Borehole Fluid

Borehole fluid is drilling mud in the case of mud-rotary drilling and formation water or air in the case of air-rotary, cable-tool, and auger drilling.

In the logging literature the term refers to water or drilling mud; air and foam are not included.[1] The same convention is followed in this text.

Water in the borehole is essential to mud-rotary drilling and unavoidable for any drilling process once a significant water-bearing formation is penetrated. Most boreholes (ground-water and petroleum) are drilled with the mud-rotary method, and most test holes drilled by other methods penetrate water-bearing rock, so logging is almost always done in a liquid-filled hole. In fact, most logging tools are designed for liquid-filled holes; some tools do not work in air-filled holes and others are very difficult to interpret (Table 6-1).

A borehole filled with drilling mud and/or water is a mixed blessing for resistivity tools. They cannot function without a conductive borehole fluid and yet, at the same time, its presence can significantly alter the resistivity values. (For pad type tools it is the resistivity of the mudcake, rather than the resistivity of the mud, that affects the tool. Mudcake is discussed in the next section.) The severity of the influence is a function of the contrast between the resistivity of the formation and the resistivity of the borehole fluid (R_m) at formation temperature (see Table 6-1). Remember, it makes no difference whether the borehole fluid is water, native mud, bentonite mud, or any other type of mud. The determining factor for environmental corrections is simply the resistivity of the fluid (R_m). R_m departure curves are available for each induction and mandrel-type resistivity tool. The same chart corrects for borehole diameter. R_m and hole diameter corrections are intimately linked, since resistivity tools are affected by both the amount of mud and the resistivity of the mud. R_m/borehole correction charts are discussed in detail in Chapters 8 and 9.

The density of the borehole fluid influences the gamma ray response; the denser the mud the lower the gamma ray count (see Figure 10-5). Mud salinity affects neutron tools (see Chapter 13). Correction charts are available for these borehole fluid effects.

Borehole fluid is so closely linked to the **Drilling Fluid Invasion** section that guidelines for selecting and characterizing borehole fluids are deferred to the next section.

[1] In fact, it is rare that the borehole fluid is drilling mud.

TABLE 6-1. THE EFFECT OF BOREHOLE FLUIDS[1] ON LOG RESPONSE

Logging Tool	Borehole Fluid Required for Logging		The Effect of Drilling Mud or Water on the Log Response	
	Drilling mud or water	Air, foam, drilling mud or water	High R_a/R_m ratio[2]	Low R_a/R_m ratio[2]
SP	✓		--	--
Gamma Ray		✓	--	--
Single Point	✓		R_a too low	--
Short Normal	✓		R_a too low	--
Long Normal	✓		R_a too high	--
Lateral	✓		R_a too high	--
Latero or Guard	✓		R_a a little high	R_a a little high
Microlog	✓		--	--
Microguard or Microlatero	✓		--	R_a too high
Fluid Resistivity	✓		--	--
Induction		✓	--	--
Density (Gamma Gamma)	✓[3]		--	--
Neutron	✓[3]		--	--
Sonic (Acoustic)	✓		--	--
Caliper		✓	--	--
Temperature		✓	--	--
Flow meter	✓		--	--

1 Borehole fluids are defined as water, normal water well drilling mud, and normal fresh water oilfield drilling mud (i.e. no barite, KCl, oil-based mud, salt mud, etc.).

2 R_a is apparent resistivity - the resistivity value recorded by the logging tool. R_m is mud resistivity - in this case it denotes the resistivity of whatever fluid is in the borehole. In the case of microguard and microlatero tools, R_m is actually the resistivity of the mudcake (R_{mc}).

3 Can be run in air-filled holes but porosity calculations are very questionable if the pores are not 100% filled with water.

Drilling Fluid Invasion

Most boreholes (ground-water and petroleum) are drilled with mud. Drilling mud is a mixture of either natural clay or a clay additive and locally available water from surface sources and/or water-bearing rocks encountered by the borehole. The clay additive is bentonite, a sodium type montmorillonite clay.[1] Often in water well drilling no bentonite is added; the clay component is simply formation clays liberated by the drilling process. This is referred to as native or natural mud. Approximately 50 percent of the wells examined in this study were drilled with native mud (see the Mud Type column in the **WATER-QUALITY DATA BASE,** Section 1, Volume 2).

The hydrostatic pressure (head) exerted by the mud column is normally higher than the hydrostatic pressure (head) of water in the formation. This overbalanced condition forces mud to infiltrate porous, permeable rocks. As the bit enters the rock, a surge of whole mud invades the pores. As drilling continues, the rock acts as a filter. The solid constituents (clay additive and ground-up rock) filter out on the borehole wall forming a mudcake and the water in the mud (mud filtrate) invades the rock displacing the formation water. Accordingly, the invasion process should be considered in two parts: an impregnation phase during the surge (or spurt) loss and an infiltration phase during the mudcake building process.

Impregnation

Impregnation occurs only during the surge phase. Mud moves into the pores until they are plugged by bridging of the particles. The whole process lasts only a few minutes (Beeson and Wright, 1952) and the average depth of mud impregnation is only a few inches (Jorden and Campbell, 1984). The amount of impregnation is controlled by the permeability of the rock, mud quality, and the pressure differential between the mud column and the formation water.

The higher the permeability, the larger the pore throat diameter, the easier it is for mud solids to move through the pores, and the greater the amount of impregnation. Ground-water aquifers with high permeabilities are particularly susceptible to impregnation. Since permeability cannot be

---

[1] Oilfield drilling mud sometimes contains special additives such as barite, KCl, and oil. These additives seriously effect certain log responses. They are not commonly used and therefore are not discussed in this text.

changed, the only way to minimize impregnation is to control the size distribution of particles in the mud. The best mud is one that has a broad range of particle sizes larger than clay. To achieve such a mud, drilling contractors should refrain from using desilters (Jorden and Campbell, 1984).

Vuggy-cavernous carbonate aquifers and highly fractured aquifers have extremely large pore diameters and are even more susceptible to impregnation. For these rocks the best way to counteract impregnation is to switch to reverse air-rotary drilling. This drilling method has proven very successful in the Edwards Aquifer (John Hoyt, personal communication, 1990) and in the Florida Peninsula (Tony Gilboy, personal communication, 1990).

The greater the pressure differential between the mud at the bit face and the formation water, the greater the amount of impregnation (Glenn, et al., 1957). A high differential pressure can be created by either excessive mud weight or excessive pump pressure. Thus both shallow and deep water wells are susceptible to impregnation. The remedy is to keep the mud weight down below 9.5 lb_m/gal_m and keep the pump pressure from getting too high.

Impregnation can affect log responses. For instance, impregnation may decrease resistivity log values. However, in water wells the effects will probably be minimal. The important consequence of impregnation is the possibility of an irreversible decrease in permeability. Glenn and Slusser (1957) documented this phenomenon. Although some investigators do not consider impregnation to be significant, Jorden and Campbell (1984) warn that "if conditions during drilling favor impregnation, formation damage can be expected."

Infiltration

After impregnation, the mudcake starts to build and mud filtrate invades the rock. Infiltration continues until an impermeable mudcake forms. For good quality mud the whole process takes only minutes to hours. Eventually, filtrate invasion and mudcake formation ceases and the borehole looks like Figure 6-3. After the borehole is created, mud fills the hole, mudcake coats porous and permeable formations, formation water has been replaced by mud filtrate near the borehole in the flushed zone, and between the flushed zone and the uninvaded zone mud filtrate is mixed with formation water in the transition zone. The flushed and transition zones are often referred to collectively as the invaded zone.

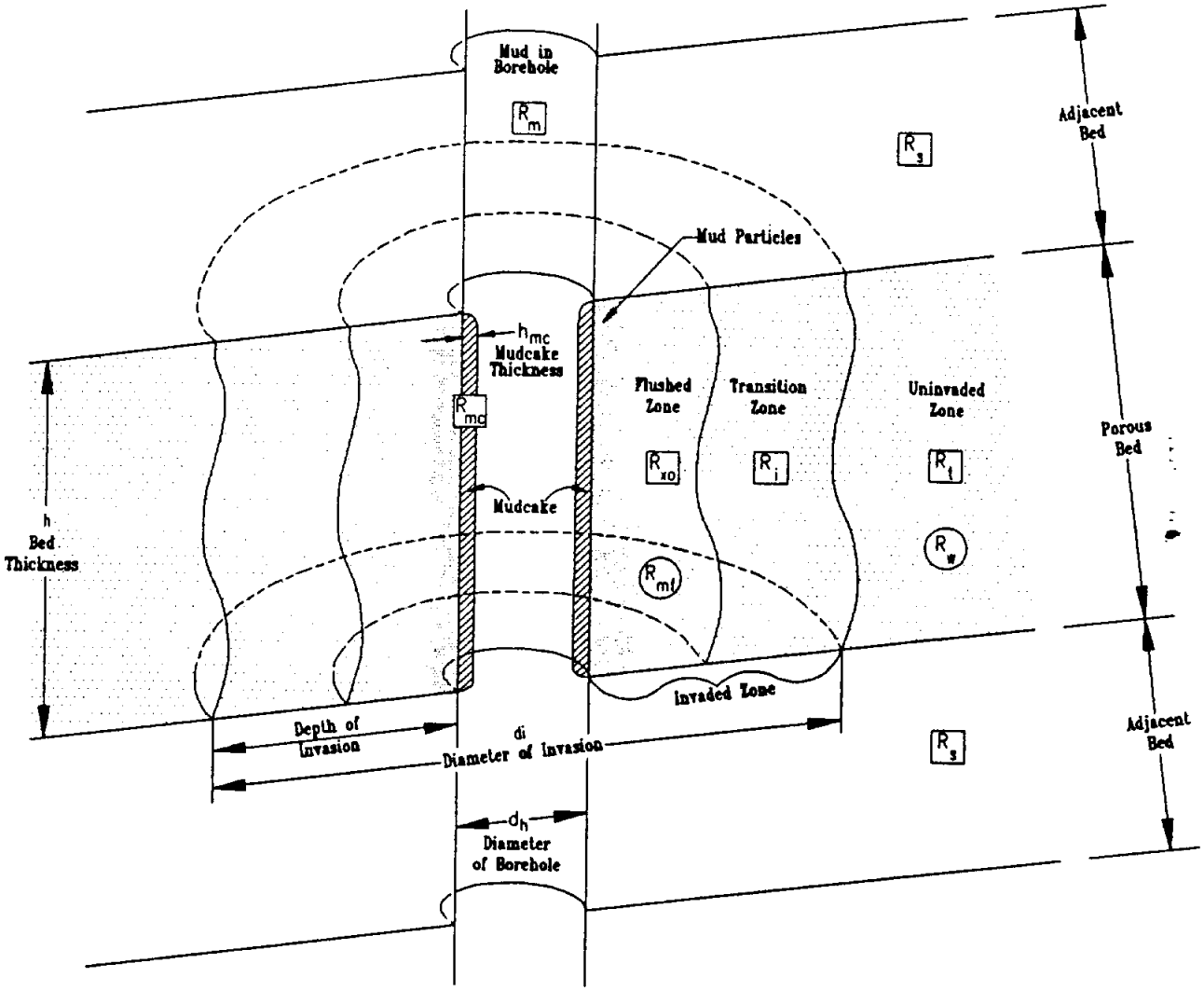

EXPLANATION

□ Resistivity of the zone

○ Resistivity of the water in the zone

Figure 6-3. Generalized invasion profile of a porous formation with nomenclature and abbreviations (Modified from Frank, 1986, after Schlumberger, no date).

The width of the invaded zone is referred to as either the depth or the diameter of invasion (Figure 6-3). The relationship between the two is

$$\textit{depth of invasion} = \frac{\textit{diameter of invasion} - \textit{borehole diameter}}{2} \quad (6\text{-}1)$$

The depth of invasion is a function of the porosity and permeability of the rock, the quality of the drilling mud, and the drilling history. ~~These same factors plus the quality of the drilling mud control the mudcake thickness.~~

Mudcake thickness is generally less than 3/ invasion varies from less than one foot uch as 10 to 15 feet in low porosity form ed zone is at least a few inches wide.

Mudcake thickness is not invasion is. If all other factors remain cc re differential, volume of mud filtra shallower the depth of invasion to be the opposite of what it should be because as porosity increases, a smaller t contain a given volume of mud filtrate. Ex uggy carbonates and highly fractured r rocks, mudcake formation is extremely c onnected

TABLE 6-2. RULES OF THUMB FOR ESTIMATION OF THE DIAMETER OF INVASION FROM POROSITY

Porosity	Diameter of Invasion
> 20%	2d
15 - 20%	3d
10 - 15%	5d
5 - 10%	10d

d = borehole diameter From Pirson (1963).

openings which afford considerable invasion and at times lost circulation of the mud system. This condition is most frequently encountered in Texas in the Edwards aquifer and other carbonate aquifers.

Pirson (1963) provided rules of thumb for estimating the diameter of invasion (Table 6-2). His guidelines are for oilfield test wells, which may or may not be equivalent to ground-water wells. However, at least they provide some guidance when considering the effect of porosity on the depth of invasion.

Very low permeability formations (shales and impermeable carbonates and sandstones) have no filtrate invasion and no mudcake. Very high permeability rocks (vuggy-cavernous carbonates and highly fractured formations) may have deep mud invasion and no mudcake. For rocks in between the two extremes, if all other factors remain constant, the filtration rate is almost the same irrespective of the permeability (Jorden and Campbell, 1984). This means that there is no correlation between either the mud filtrate volume or the thickness of the mudcake and permeability. For these rocks the other factors listed above control the depth of invasion.[1]

The quality of the drilling mud controls the mudcake thickness and has an influence on the depth of invasion. Native mud, mud with a high mud weight, and mud with a high waterloss form abnormally thick mudcakes and have deep depths of invasion.

The drilling history principally influences the depth of invasion. The more the bit is tripped, the more the mudcake is knocked off and replaced, and the deeper the invasion. Often the driller does not mud up until a certain depth is reached, which means that formations above this depth will probably have deeper invasion. Time is a third factor. The longer that drilling mud is exposed to a formation, the greater the depth of invasion and the thicker the mudcake (Jorden and Campbell, 1984).

Mudcake affects pad-type logging tools. The pad of a microresistivity tool rides on the mudcake as the tool is pulled up the well bore. Therefore, the tool can require a significant correction for both mudcake resistivity (R_{mc}) and mudcake thickness (see Figure 9-10). R_{mc} must be at formation

---

[1] Porosity is one of the main controls on depth of invasion and since for many rocks permeability is directly proportional to porosity, there does end up being a correlation between permeability and depth of invasion. As with porosity, as permeability increases the depth of invasion decreases.

temperature. The corrections are discussed in detail in Chapter 9. The sidewall neutron tool also requires a significant correction. Compensated neutron and density tools are automatically compensated for mudcake thickness.

Filtrate invasion affects only the resistivity and induction tools if the pores are 100 percent saturated with water. (If the pores are air-filled, filtrate invasion will also affect the density ~~of the~~ tools.) If the mud filtrate resistivity (R_{mf}) and the formation water resistivity (R_w) are different, filtrate invasion will alter the resistivity of the rock in the flushed and transition zones. The resistivity of the flushed zone (R_{xo}) is a function of the mud filtrate resistivity. The resistivity of the transition zone (R_i) is influenced by both the mud filtrate and the formation water. The influences of the mud filtrate decrease laterally through the transition zone until uninvaded rock (R_t) is reached.

If the filtrate invasion is deep and if R_{mf} does not equal R_w, the deep reading resistivity curve will be significantly affected and a correction factor will be needed. The only way to determine invasion depth is to establish the invasion profile by running a series of resistivity or induction tools with differing depths of investigation (see Figures 9-19 and 9-20). Three resistivity tools are best; one to read the flushed zone, one for the transition, and a deep reading curve to reach what may or may not be the uninvaded zone. If invasion is deep, departure curves are used to correct the deep reading curve.

Corrections to the deep reading resistivity curve for filtrate invasion are normally not needed or not practical in ground-water log analysis:

1. Most ground-water aquifers have high porosity, which favors shallow invasion.

2. Some logs only have two resistivity curves. Without a third curve it is impossible to determine the depth of invasion.

    a. Many small-scale, old petroleum logs only have short and long normal curves. The lateral curve was often cut off during reproduction of the original 2 and 5 inch scale log to a smaller scale. The only way to recover the curve is to track down an original 5 inch scale copy.

b. Some recent ground-water logs only have the shallow and the deep reading curves. A medium reading curve was recorded, but it was left off the log at the customer's request. This is done so that the log will conform to the format of older logs that the customer is accustomed to using.
c. Many slimhole logging suites only have the short and long normal curves. (These logs may include the single point resistance curve, but it cannot be used for modeling invasion.)

Chapters 8 and 9 contain additional information on making filtrate invasion corrections. Hilchie (1979) has a good discussion on the procedure for correcting normal and lateral curves. Several sets of departure curves have been published for these tools, but Guyod and Pranglin (1959) have the best and most accurate. However, all of these curves are complicated and their use is fraught with a number of difficulties. Correcting latero, guard, and induction tools is much easier. The techniques are discussed in a number of logging texts.

The resistivity contrast between mud filtrate and formation water also influences the depth of investigation of some resistivity tools. Chapters 8 and 9 contain further details on this subject.

Drilling Fluid Guidelines

To minimize and evaluate the effects of borehole fluid, filtrate invasion, and mudcake on logging tools, the following guidelines should be utilized:

Before a test hole is drilled

1. Design a logging program that takes into account the type of fluid in the borehole, or vice versa. Remember that most logging tools require a liquid-filled hole.

2. Design a logging program that takes into account the expected mudcake thickness and depth of invasion.

   a. A microlog tool requires mudcake. It will not work in an air-rotary, auger, or cable-tool hole even if it is filled with fluid.
   b. Moderate to low porosity aquifers will have deep invasion. In order to determine the depth of invasion and make corrections to the deep reading curve, three resistivity curves should be included in the logging program.

3. A good quality mud program must be designed that is appropriate for the drilling conditions (see Appendix III for details). The mud properties should be specified in the drilling contract. The following generalized ranges for each property may need to be adjusted according to local hydrogeological conditions:

   a. Mud weight: less than 9 to 9.5 lb_s/gal.
   b. Viscosity: 32 to 38 sec_s/qt.
   c. Filtercake thickness: less than $^3/_{32}$ inch.
   d. Filtrate loss: 12 to 15 cc.
   e. Sand content: less than 2 percent by volume.
   f. pH: 8 to 9.5.
   g. Specify the frequency of the tests.

During the drilling

1. A good quality mud should be maintained (see 3. above and Appendix III).

2. The mud properties should be measured on a regular basis: mud weight, viscosity, filtercake thickness, filtrate loss, sand content, pH, resistivity, and temperature of the mud at the time of the resistivity measurement.

3. The sample should be taken from the flowline before the mud has traveled through any surface equipment.

4. Any significant changes to the mud system should be documented.

5. The mud circulation system should be well designed.

   a. The mudpit design should maximize settling time.
   b. The mud pump suction should be kept off the bottom of the mud pit.
   c. A shale shaker should be used.
   d. If necessary, desander cones should be used.
   e. The pump pressure should not get too high.

6. Good drilling practices should be maintained.

During the logging

1. The hole should be logged as soon as possible after T.D. is reached. This will minimize the effects of invasion. On rare occasions it may be desirable to log the hole as soon as a particular zone is drilled, then drill and log the rest of the hole.

2. The type of fluid in the hole, density, viscosity, pH, and fluid loss (filtrate loss) should be recorded on the log header.

3. The logging company should measure the resistivities of the drilling mud (R_m), mud filtrate (R_{mf}) and mudcake (R_{mc}). If the borehole fluid is water, all that can be measured is R_m.

   a. A circulated sample of the borehole fluid should be used. A mud pit sample should be used only as a last resort.
   b. R_{mf} and R_{mc} should be measured rather than calculated.
   c. The temperatures of the mud and the filtrate at the time of the resistivity measurements should be recorded.
   d. The data should be recorded on the log header.

4. The logging company should run maximum recording thermometers on every logging run. The highest temperature is used for bottom hole temperature. This will allow the geothermal gradient of the borehole to be calculated, from which the temperature at any depth in the hole can be determined. Chapter 14 discusses the calculations. Formation temperature can also be obtained from a temperature log. Environmental corrections for R_m and R_{mc} must be made at formation temperature.

5. Any major changes in mud properties during the drilling of the hole should be recorded in the remarks section on the log header.

6. A caliper should always be run. It can be used to determine mudcake thickness if the hole is in gauge.

7. Porosity tools should always be compensated. Compensated tools correct for the influence of mudcake.

8. Three resistivity curves (not counting the single point resistance) should be run in order to determine the depth of invasion.

After the logging

1. The log heading should be examined for information on the borehole fluid. The fluid type, density, fluid loss, mud resistivity, temperature of the mud resistivity measurement, and bottom hole temperature are especially useful for log analysis.

2. A combined R_m/borehole size correction is the first environmental correction that should be applied to mandrel-type resistivity and induction logs. R_m must be converted to formation temperature before making the correction. Equation 2-4 is used to make the conversion.

3. Mud resistivities also can be obtained from a mud log. If a microlog was run, a mud log may have been made. A mud log is a recording of the microlog curves as the collapsed tool is lowered down the borehole. Certain sections of the curve will record mud resistivity.

    a. Spiky intervals are where the tool was bumping against the borehole. The resistivity value is a mixture of the mud and borehole resistivities.
    b. A flat section over several feet is probably recording mud resistivity. Shale sections are the best candidates for good R_m values, since shales often wash out and washouts make it easier for the tool to avoid any borehole influence.
    c. The mud log R_m can be compared with the R_m on the log header.
    d. Old logs of the Trinity aquifer in north and central Texas often include a microlog and a mud log.

4. It must be determined whether or not any of the curves need corrections for mudcake thickness. The vast majority of the time no corrections will be needed.

    a. Compensated porosity tools automatically factor out the effect of mudcake.
    b. Sidewall neutron tools require a correction for mudcake.
    c. Microresistivity tools require mudcake thickness and R_{mc} corrections, but only if quantitative log analysis is being conducted on a formation (e.g. Resistivity Ratio Method for

calculating water conductivity). R_{mc} must be converted to formation temperature before making the correction.

5. If a caliper was run, it is used to determine mudcake thickness on zones of interest. The mudcake thickness is **½(bit size - borehole diameter)**. For a caliper on a conventional density tool the mudcake thickness is **bit size - borehole diameter.** If a formation has mudcake, no correlation exists between thickness of the mudcake and porosity or permeability.

6. There are several ~~different~~ kinds of calipers and they vary in their ability to measure mudcake thickness (Chapter 11).

   a. Finger-type caliper arms have small contact areas that will slice through the mudcake and thus not record it. High-resolution calipers fall into this category.
   b. Pad-type tools have a larger contact area and a lower contact pressure. They generally override the mudcake and therefore give a better measurement of mudcake thickness. Among the pad devices, density calipers are less sensitive to mudcake because the tool has greater contact pressure and it has a skid to cut through the mud.
   c. The ability of bowspring calipers to detect mudcake depends on their design.
   d. The ability of common openhole calipers to detect mudcake, in order of increasing sensitivity, is density, sonic, microlog, and 3 or 4 arm finger-type caliper.

7. If a caliper was not run, the log heading should be examined for information on the mud quality. The data can be used to make an educated estimate as to mudcake thickness. For a critical zone, the corrections for mudcake thicknesses from ¼ to 1 inch can be calculated in order to determine the range of possible correct values.

8. It must be decided whether or not the deep reading resistivity curve requires a correction for filtrate invasion. In ground-water log analysis such a correction ~~to the deep reading resistivity curve for filtrate invasion~~ is usually not needed or not practical.

   a. High porosity formations (more than 15 to 25 percent):

i. The depth of invasion is usually shallow, so the deep reading curve is little affected by filtrate and reads R_t.
ii. The long normal curve will read R_t for these formations if the bed is over 20 feet thick.
iii. Most ground-water aquifers will be high porosity formations.

b. Low to moderate porosity formations (less than 15 to 20 percent):

i. The depth of invasion is moderate to deep and filtrate significantly affects the deep reading curve.
ii. Invasion corrections should only be made when the resistivity values are being used to determine water quality.
iii. Few ground-water aquifers are low to moderate porosity formations.

9. Three resistivity curves (not counting a single point resistance) are required to make a correction for moderate to deep filtrate invasion. Environmental corrections for borehole size, R_m, bed thickness, and the resistivity of adjacent beds have to be made first. Chapters 8 and 9 discuss these corrections in detail.

a. With Dual Induction-SFL, dual guard-R_{xo}, and dual laterolog-R_{xo} suites, both the diameter of invasion and R_t can be calculated.
b. For old electric logs (short normal, long normal, and lateral) the accuracy of invasion corrections is very questionable because:

i. The lateral curve is severely affected by bed thickness. A bed must be at least 40 feet thick before any confidence can be placed in the resistivity value.
ii. The diameter of invasion, which the log analyst can only estimate, is used to select the proper departure curve. Therefore, the correction will be only as accurate as the estimation of invasion diameter.

10. As long as R_{mf} and R_w are different, it is possible to visually estimate the depth of invasion. This gives a good approximation of the influence of filtrate on the deep reading curve (Figure 6-4).

11. If R_{mf} and R_w are similar there will be no invasion profile no matter what the depth of filtrate invasion. The resistivity curves will

stack no matter what the depth of invasion. In such cases the resistivity logs offer no supporting evidence as to whether water samples obtained by packer tests or wireline sampling devices are actually the formation water.

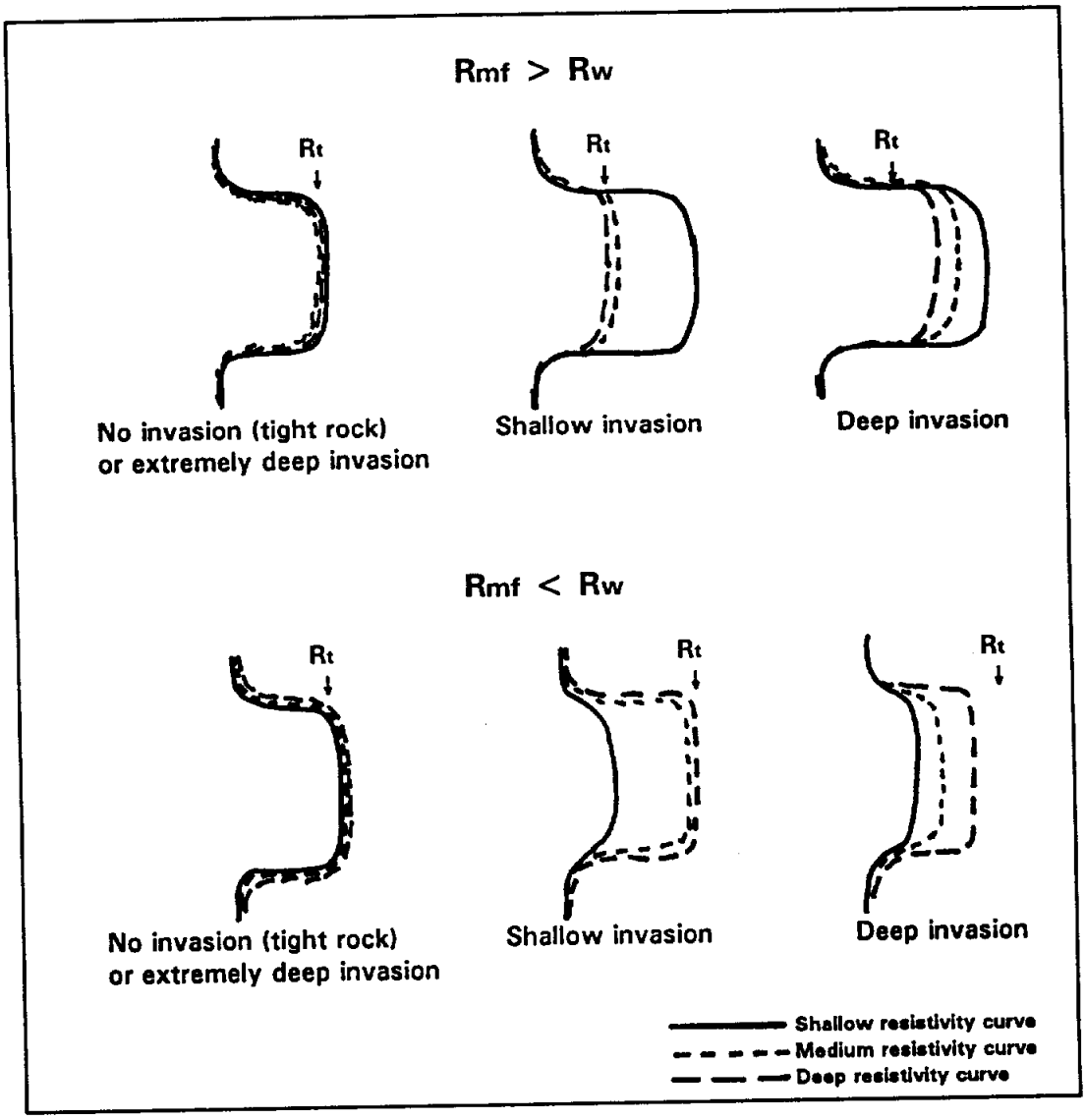

Figure 6-4. Generalized invasion profiles for estimating the depth of invasion and the effect of filtrate on the deep reading resistivity curve. The log patterns represent curves that already have been corrected for all other influences (e.g. R_m, bed thickness, and tool design).

TOOL DESIGN AND ITS EFFECTS ON LOG RESPONSES

Chapter 7

This chapter discusses, in general terms, the effect of tool design on depth of investigation and vertical resolution. For information regarding a specific tool, consult Chapters 8 through 13, a good reference work such as Serra (1984) or Helander (1983), or the tool manufacturer's technical literature.

In addition to being affected by the borehole environment, log responses are also significantly influenced by the tool design. Of particular importance is the configuration and/or spacing of the sensor(s), since it controls the depth of investigation and vertical resolution of the logging tool. Both qualitative and quantitative log analysis require an understanding of how the sensor design affects log curves.

There are basically three types of sensors:

Single sensors. Some logging devices have a single sensor (e.g. an electrode in the case of the SP and the single-point resistance tools, and a sodium iodide crystal in most gamma ray tools). Theoretically (i.e. in a homogenous formation with no borehole), the tool measures a spherical volume of rock with the sensor at the center. In reality the shape of the volume is a function of the borehole environment.

Emitter-receiver sensors. Many tools use an emitter or source (e.g. current electrodes and radioactive source) and a single detector (e.g. measuring electrode, receiver coil, and radioactivity detector). Resistivity, induction, and uncompensated neutron and density (gamma-gamma) tools are in this category, along with slimhole "compensated" neutron and density tools that do nothing more than display the near and far count rates as separate curves. The height of the volume of rock measured by the tool is approximately the emitter-receiver spacing.

Dual detector sensors. Compensated sonic, neutron, and density (gamma-gamma) tools use the difference between the two detector readings to calculate a formation property. The spacing between the

two detectors is approximately the height of the volume of rock investigated by the tool.

Remember, logging tools (at least common ones) do not take point measurements. At any instance in time the sensors are measuring a finite volume of formation and borehole around the sensors. Therefore, any point on a log curve is an **average** value. The shape and dimensions of the volume represented by this value are largely determined by the sensor configuration.

The guiding principle in this discussion is that depth of investigation and vertical resolution are mutually exclusive (Figure 7-1). A small emitter-to-receiver spacing allows a tool to resolve very thin beds but the depth of investigation is very shallow. A longer spacing gives a greater depth of investigation at the expense of the vertical resolution.

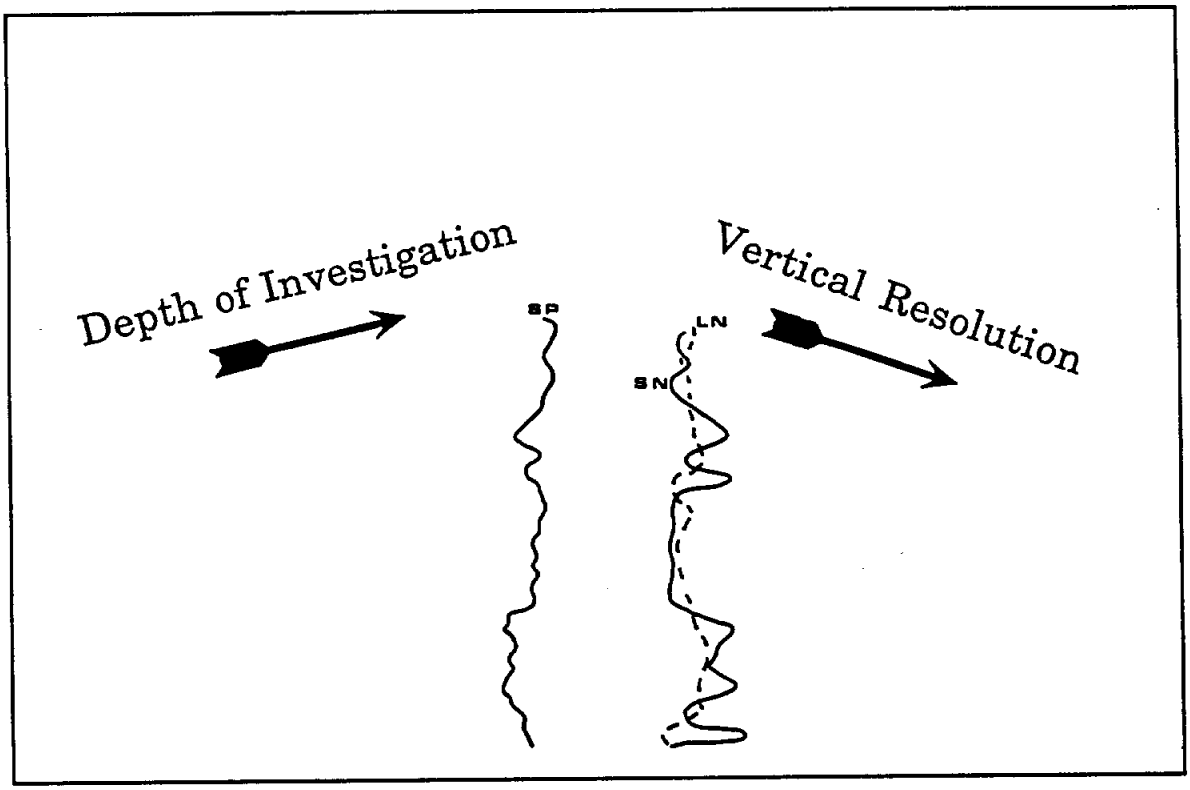

Figure 7-1. As the depth of investigation of a logging tool increases, the vertical resolution decreases. The 16" short normal (SN) and the 64" long normal (LN) curves serve as an excellent illustration of this point. The long normal curve has a much deeper depth of investigation, but its vertical resolution is much poorer. It does not recognize the thin resistive beds discernible on the short normal curve.

Depth of Investigation

As stated in the introduction, logging tools take volumetric rather than point measurements. This means that just as they do not take point measurements vertically in the borehole, neither do they take discrete measurements at a certain distance **x** horizontally into the formation. The contribution of the formation to the log signal increases in a cumulative manner, as illustrated in Figure 7-2. Any point on a logging curve, therefore, represents an "average" value that has both a horizontal component (depth of investigation) and a vertical component (vertical resolution).

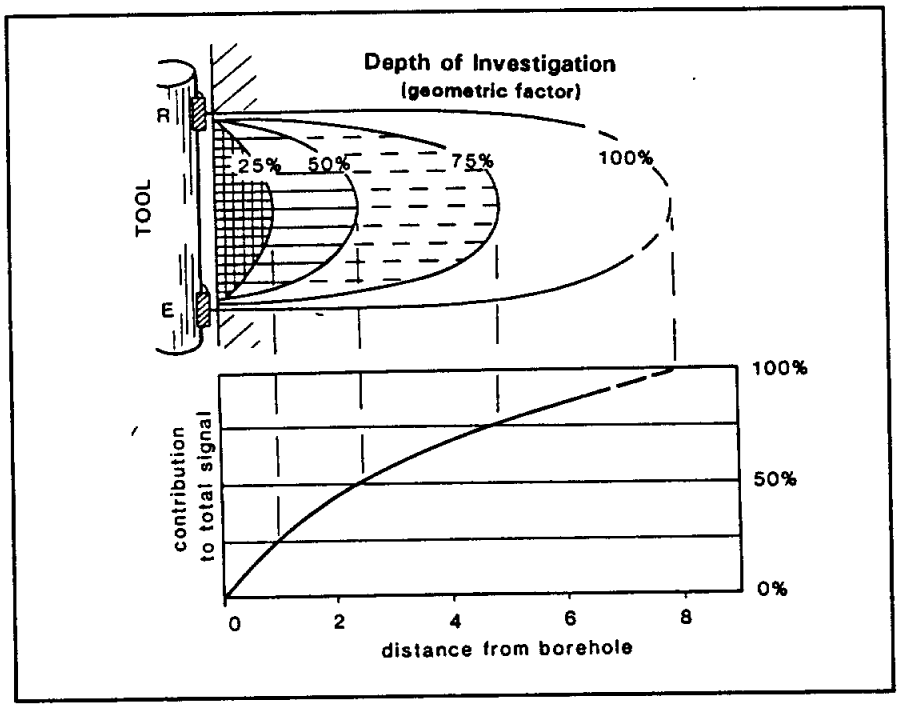

Figure 7-2. This figure illustrates what is meant by the terms depth of investigation and geometric factor. The contribution of the formation to the log signal increases in a cumulative manner away from the logging tool (Modified from Rider, 1986).

Depth of investigation is the width of the zone from the logging tool horizontally into the formation that provides ~~the majority~~ most of the log response. The width of this zone is governed by the geometric factor (G) of the tool, which is a measurement of how the contribution of the formation to the log signal increases with increasing distance into the formation (Figure 7-2). At a given depth into a formation, G designates the percent of the log response that is generated by the interval between the probe and the given depth. Geometric (G) or pseudogeometric (J) factor charts can be constructed for all

logging tools (Figure 7-3).[1] For nuclear tools the depth of investigation is customarily defined as G = 0.9 and for resistivity tools it is G = 0.5 (Tittman, 1986). For resistivity tools a G of 0.8, on the average, corresponds to a depth twice the depth of G = 0.5 (Dewan, 1983). In this report, as in most introductory logging literature, the term depth of investigation is used instead of geometric factor.

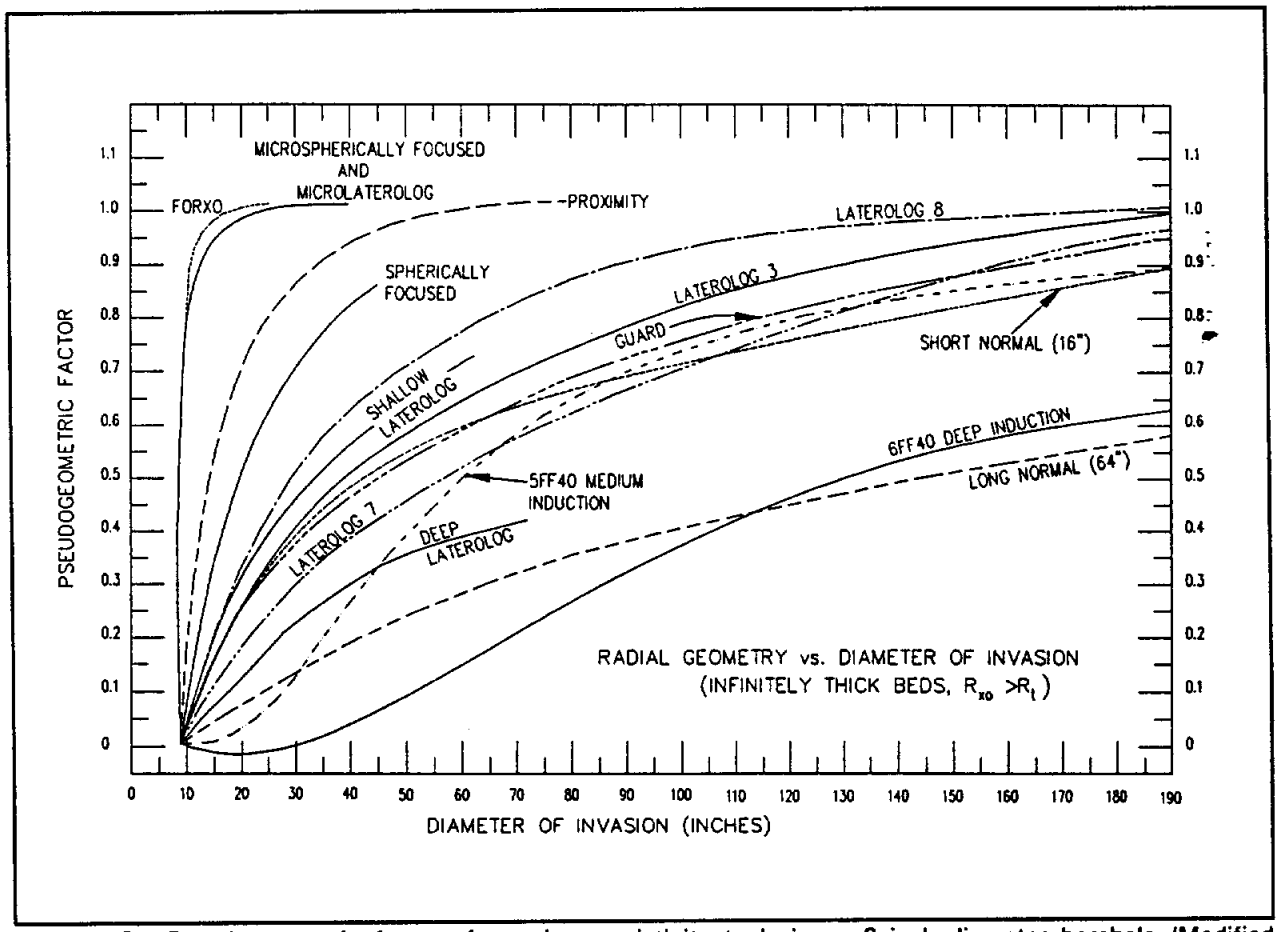

Figure 7-3. Pseudogeometric factors for various resistivity tools in an 8 inch diameter borehole (Modified from Helander, 1983).

The depth of investigation of a logging tool is a function of the following:

---

[1] Technically, the induction log is the only tool for which the concept of geometric factor is reasonably rigorous (Schlumberger, 1989). The charts for other tools (such as Figure 7-3) are actually pseudo-geometrical factors, since the geometric factor changes as borehole conditions change. For resistivity tools a chart is valid for only one set of conditions - there are no all-purpose charts (Schlumberger, 1989). Nonetheless, such charts are instructive for comparative evaluation of different tools.

1. The emitter-receiver spacing.

2. The type of measurement being made.

3. The nature of the formation.

4. The nature of the borehole fluid.

The principal limit on depth of investigation is the emitter-receiver spacing: the longer the spacing, the greater the depth of investigation (see Table 7-1). For some logging tools the nature of the logging measurement itself also determines the depth of investigation (Rider, 1986). For instance, the depth of investigation for nuclear tools is in large part determined by the penetration rate of the nuclear particle.

The nature of the formation (whether or not it is susceptible to penetration by the particles emitted by the tool) also has a significant influence on the depth of investigation. For instance, the depth of investigation of neutron tools will decrease as porosity increases (Figure 7-4).

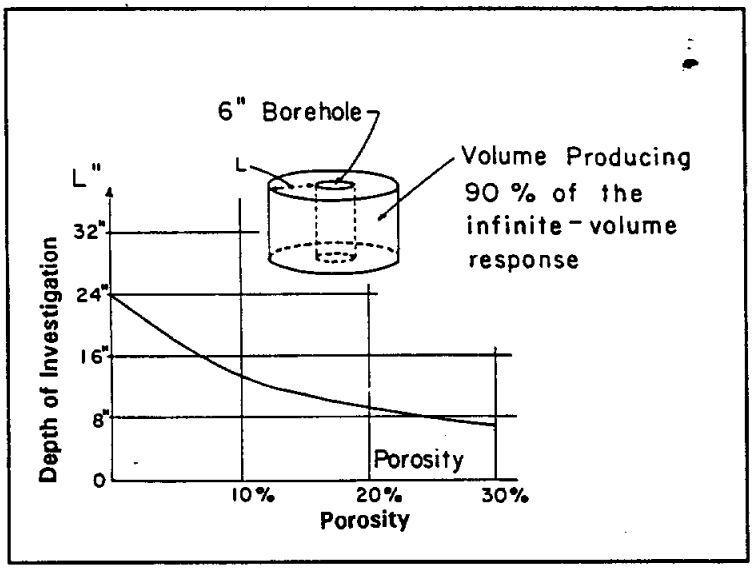

Figure 7-4. Depth of investigation of neutrons as a function of porosity (Modified from Schlumberger, 1958).

The depth of investigation of unfocused resistivity tools can be greatly reduced by excessively saline borehole fluids (salt muds). The mud short circuits the current path. Most of the current stays in the borehole rather than traveling into the formation.

Logging tools, especially resistivity tools, are classified according to their depth of investigation. The four catergories are micro, shallow, medium, and deep reading tools. Micro-reading tools investigate less than a few inches into the formation. Many of these are pad-type tools (microlog,

TABLE 7-1. EFFECTS OF TOOL GEOMETRY ON COMMON OPENHOLE LOGS

Logging Tool	Emitter to Receiver Spacing	Minimum vertical resolution	Minimum bed thickness for true log values under ideal conditions	Approximate depth of investigation	Percent of circumference of 8 ¾ inch borehole surveyed
	inches	inches	inches	inches	
CALIPERS					
3-Arm Bow Spring Recorded with:					
Induction Electric		18		0	25%
Compensated Sonic		18		0	25%
1-Arm					
Compensated Density		6		0	6%
Sidewall Epithermal Neutron		6		0	6%
2-Arm					
Proximity-Microlog		12		0	36%
Microlaterolog		12		0	36%
4-Arm					
4-Arm Dual Caliper		1		0	4%
High Resolution					
4-Arm Diplog		12		0	50%
SP		12		0	100%
GAMMA RAY		24		6	100%
SINGLE POINT RESISTANCE	2-3	2-3	–	6	100%
RESISTIVITY					
16" Normal	16	24	60	32	100%
64" Normal	64	96	240	128	100%
18' 8" Lateral	224	240	448	224	100%
Dual Induction					
SFL	12	12	12	40	100%
Medium Induction	40	48	48	70	100%
Deep Induction	40	48	48	120	100%
Laterolog 3	12	12	24		
Laterolog 7	32	32	30	120	
Laterolog 8	14	14	24		
Dual Laterolog					
Shallow Laterolog	24	24	30	30	100%
Deep Laterolog	24	24	30	120	100%
Microlog					
Micro Inverse	1	2		1	7%
Micro Normal	2	4		2	7%
Proximity Log	1	12	4	10	7%
Microlaterolog	1	4	4	4	7%
POROSITY					
Sidewall Sonic		6		0 to 4	4%
Compensated Sonic	12-36	12-36	24	0 to 4	100%
Compensated Density	18	18	24	4	12%
Compensated Neutron	24	24	24	8	30%

This table provides average values. Values may vary depending upon the particular brand of logging equipment and the specific borehole conditions. (Modified from McCoy, et al., 1980)

microlaterolog, microspherically focused, and density)[1]. However, a few are mandrel-type tools (single-point resistance, neutron, sonic, gamma ray, SP, and the 4π density)[2]. For the common openhole logs, shallow, medium, and deep investigating devices are all mandrel-type resistivity tools. Shallow tools investigate only a foot or two, medium tools read approximately 2 to 6 feet, and deep resistivity tools measure 6 to 20 feet into the formation. Borehole conditions and the porosity of the rock (see Chapter 6) determine the actual depth of investigation in a given situation. Table 7-1 lists the approximate depths of investigation for common openhole tools under ideal circumstances.

Depth of investigation is mainly of concern in regard to resistivity tools, since the log value will be significantly altered depending on how much of the invaded zone the tool is responding to. Deep investigating tools usually read the resistivity of the uninvaded zone. Micro-resistivity tools read the mudcake and/or the flushed zone. Shallow reading tools measure the invaded zone, and medium reading tools measure the invaded or uninvaded zone (Figure 8-3). Chapters 6, 8, and 9 discuss how resistivity tools with varying depths of investigation are used to characterize the invaded zone.

When designing a logging program or evaluating a log curve, depth of investigation must be kept in mind when considering the effect of the borehole environment on a log response. This relates back to several of the points made in Chapter 6, **THE BOREHOLE ENVIRONMENT AND ITS EFFECTS ON LOG RESPONSES**. Also, the depth of investigation of a particular logging tool is not a single value. It varies according to the nature of the formations and the borehole conditions. Depth of investigation is important in ground-water and environmental logging for the following reasons:

1. Micro-reading tools (microresistivity, density, neutron, sonic, gamma ray, and single-point resistance) will not be recording true rock properties if:

    a. The drilling method (e.g. augering) has disturbed the formations for a few inches away from the borehole.

---

[1] Pad-type tools have the sensors mounted in a pad that must be pressed against the borehole wall. (For further details see Chapter 9).

[2] Mandrel-type tools consist of a probe that stands away from the borehole wall. (For further details see Chapters 8 through 13.)

b. The formation is washed out. Instead of recording rock properties, the tools will record a combination of rock and borehole fluid properties. Pad-type tools are adversely affected when the washout is of such a nature that pad contact with the formation is lost. The single-point resistance which is a micro-resistivity tool, will be adversely affected when the washout is greater than a few inches.
c. The mudcake is too thick. This will adversely affect microresistivity and uncompensated porosity tools. The log response will include too large a contribution from the mudcake.

Such conditions will yield porosity calculations that are too high and specific conductances calculated by the Resistivity Ratio method that are either too high or too low.

2. For specific conductance calculations that utilize R_t and/or R_{xo}, it is very important to make sure that the depth of investigation of the resistivity tools for a particular set of borehole conditions is such that the tools actually read R_t and/or R_{xo}.

3. In extremely large boreholes, mandrel-type tools with micro or shallow depths of investigation may record little more than the properties of the borehole fluid.

Vertical Resolution

The vertical resolution of a logging tool determines how well the tool delineates bed boundaries and how accurately it measures a particular physical property of a bed. Vertical resolution depends on several factors:

1. The emitter-receiver spacing.

2. The type of measurement being made.

3. The contrast between adjacent beds.

4. Auxiliary tool responses.

5. Time constant and logging speed.

The emitter-receiver spacing, which is itself governed by the type of measurement the tool makes, is the main control on vertical resolution. These two factors control the volume of formation that the tool investigates. At any point on the log, the tool is measuring a volume of rock with a vertical dimension equal to the emitter-receiver spacing.

A logging tool will make a true measurement and delineate bed boundaries only if the bed is thicker than the emitter-receiver spacing. A bed that is thinner that the emitter-receiver spacing may be to some degree identifiable on the log, but the true log value will be unattainable. The bed will only contribute some percent **x** of the log response. The thinner the bed, the smaller the contribution, until the bed disappears (Figure 7-5).

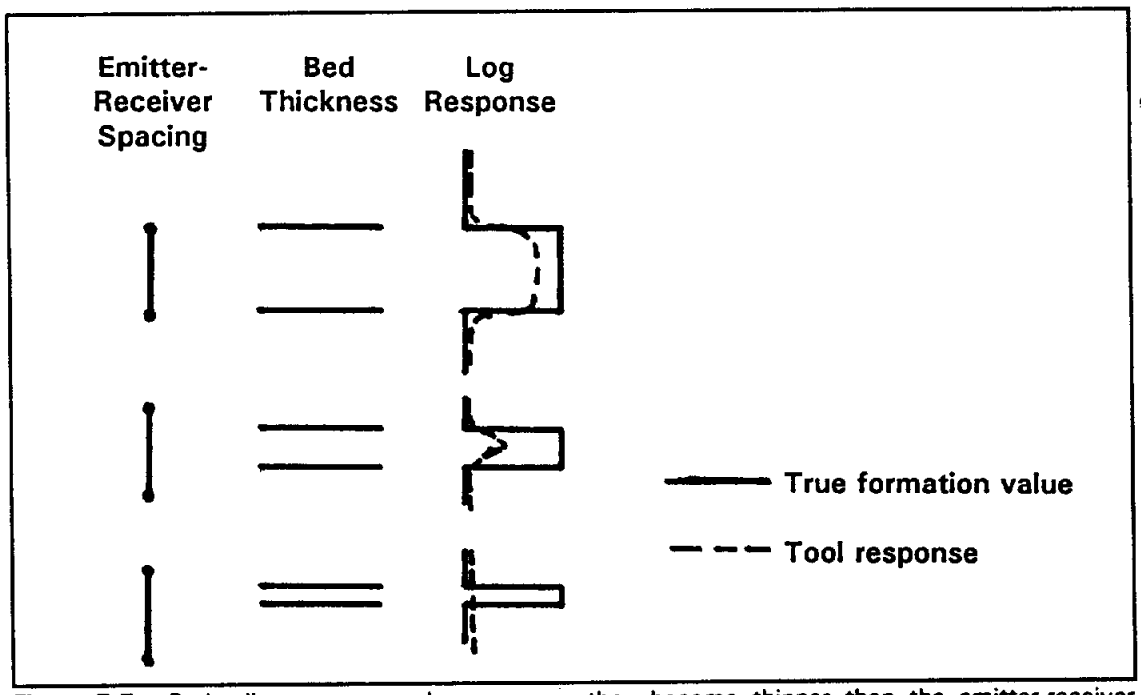

Figure 7-5. Beds disappear on a log curve as they become thinner than the emitter-receiver spacing.

Table 7-1 lists the emitter-receiver spacing, minimum vertical resolution, and minimum bed thickness for true log values under ideal conditions for common openhole tools. The values are averages.

The emitter-receiver spacing also determines the sharpness of bed boundaries. The smaller the spacing, the sharper the bed boundary (Figure 7-6).

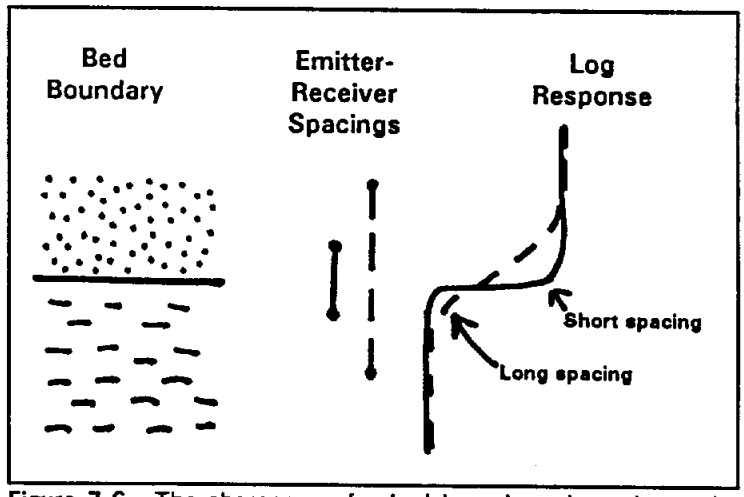

Figure 7-6. The sharpness of a bed boundary depends on the emitter-receiver spacing.

The effect of bed thickness[1] on vertical resolution was largely covered in the previous paragraphs on emitter-transmitter spacing. The thinner the bed, the harder it is for a logging tool to delineate the bed and measure a particular physical property of the bed. As a bed becomes thinner, its log response takes on more and more the characteristics of the adjacent beds. Hartmann (1975) quantified how the vertical resolution of different logging tools varies according to the contrast in bed thickness between adjacent beds. Figures 7-7 to 7-9 illustrate the effect of bed thickness on the vertical resolution of resistivity tools. Departure curve corrections for bed thickness are discussed in Chapters 8 and 9.

Resistivity tools are sensitive to the resistivity contrast between adjacent beds, as well as being sensitive to the contrast in bed thicknesses. The resistivity contrast affects both the resistivity readings and the vertical resolution of the curves. The greater the contrast the poorer the vertical resolution and the greater the effect on resistivity values. Departure curves are available to correct for the effects of adjacent beds. The same chart corrects for bed thickness. Bed thickness and adjacent bed corrections are closely linked, since resistivity tools are affected by both the resistivity and the amount of an adjacent bed that a tool averages in with a particular measurment. Bed thickness/adjacent bed correction charts are discussed in Chapters 8 and 9. Figure 7-10 illustrates how the vertical resolution of a laterolog varies according to the resistivity contrast between adjacent beds.

---

[1] The abbreviation for bed thickness is h, but in the literature prior to the 1960's e was used.

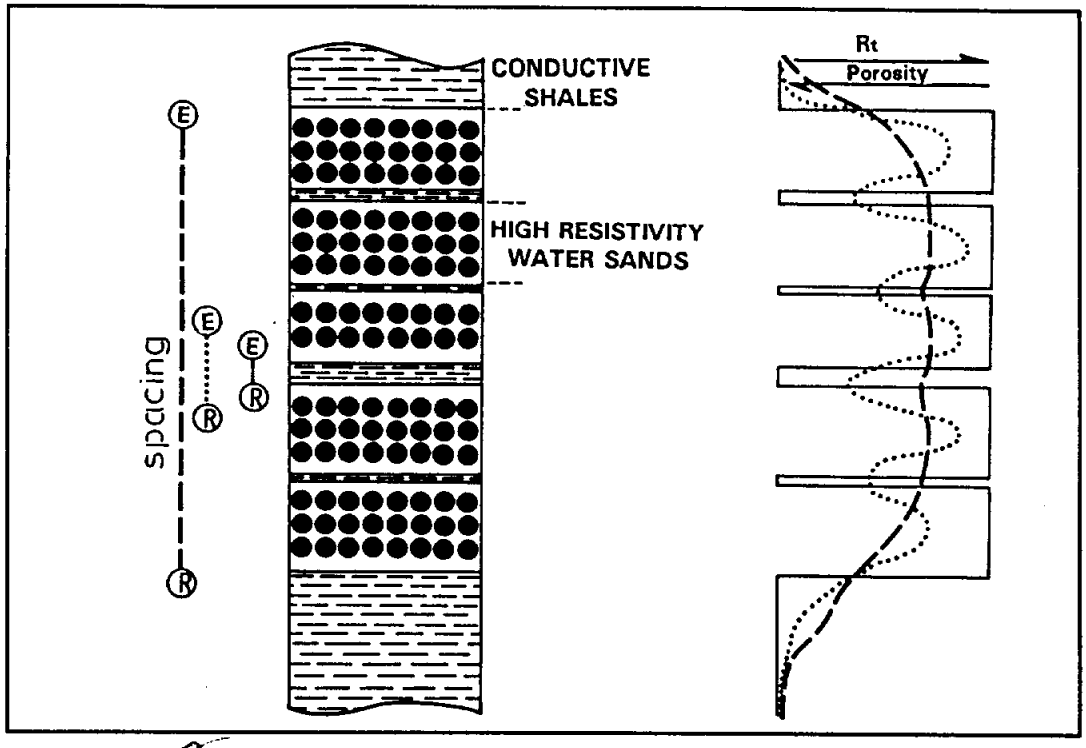

Figure 7-7. The effect of bed thickness and emitter-receiver spacing on resistivity log responses in a sandstone with thin interbedded shales. Long spaced tools give very little indication of the thin shale bed (Modified from Hartmann, 1975).

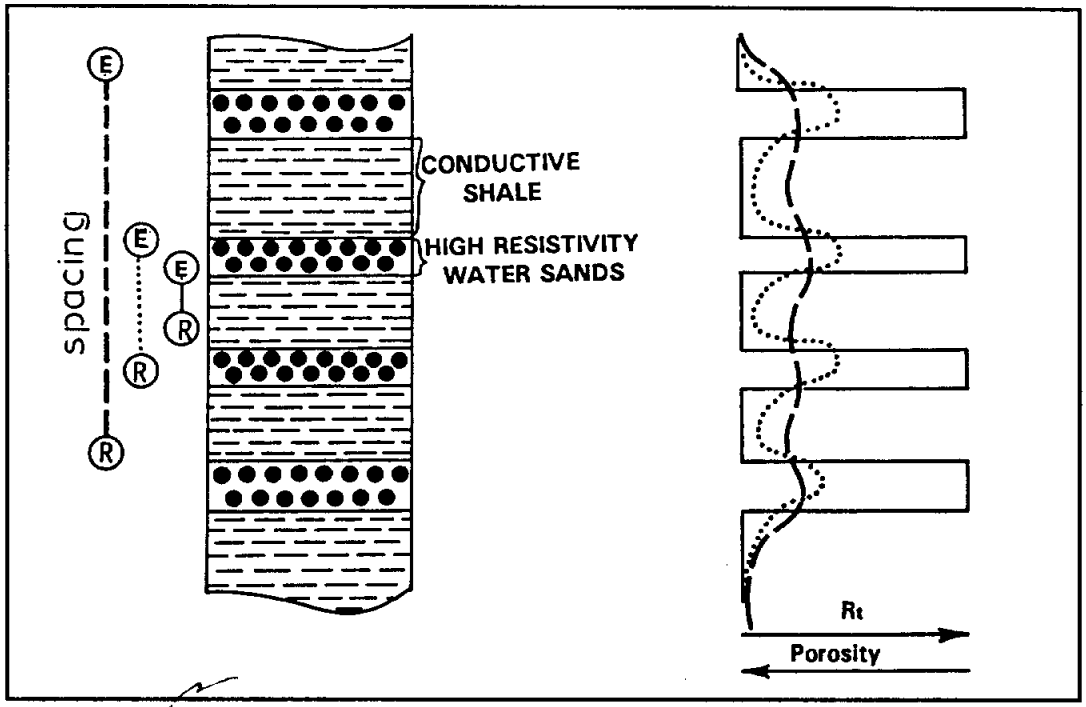

Figure 7-8. The effect of bed thickness and emitter-receiver spacing on resistivity log responses in a shale with thin interbedded sandstones. Long spaced tools give very little indication of the thin sandstone beds (Modified from Hartmann, 1975).

Hartmann

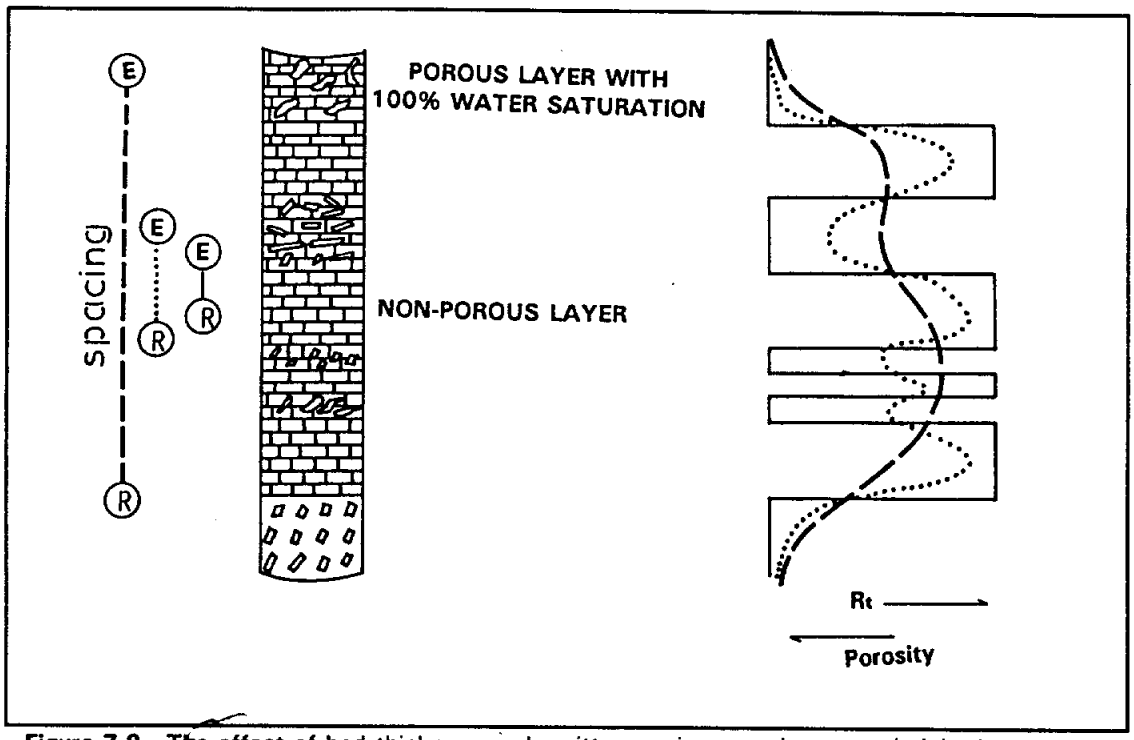

Figure 7-9. The effect of bed thickness and emitter-receiver spacing on resistivity log responses in a carbonate with alternating porous and nonporous intervals. Many of the porous intervals are very hard to identify with the long spaced tool (Modified from Hartmann, 1975).

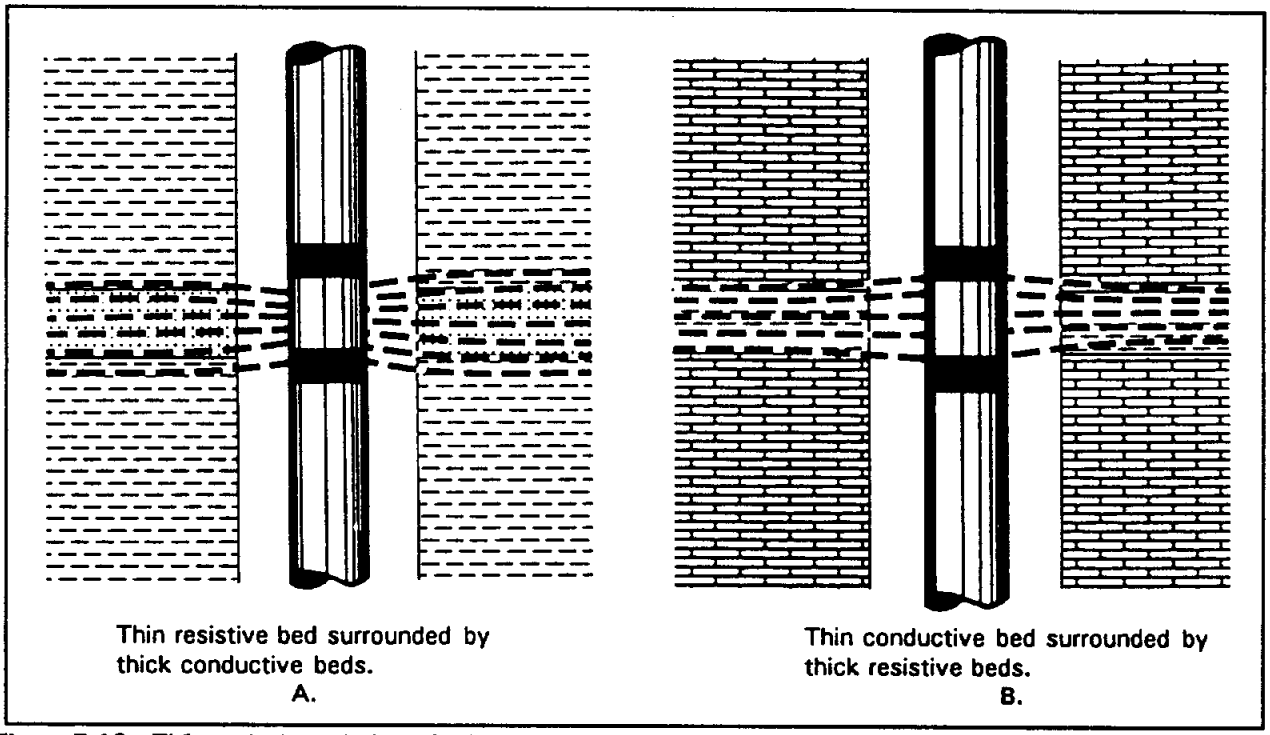

Figure 7-10. The vertical resolution of a laterolog varies according to the resistivity contrast between the beds. A. could be a sandstone with fresh to slightly saline water surrounded by shale. B. could be a porous carbonate with water of any salinity surrounded by very low porosity carbonate (From Dresser Atlas, 1982).

Auxiliary tool responses, which are a product of tool design, alter log values and distort or hide bed thickness. They are common to normal and lateral curves (see Chapter 8 for further elaboration).

Time constant and logging speed only affect the nuclear tools. Nuclear reactions are random by nature, so it is necessary to accumulate counts over a span of time (called the **time constant**) and then use the mean as the log value (Serra, 1984). The time constant needs to be chosen according to the count-rate level of the formations and the particular tool design (type of detector, strength of the nuclear source, etc.). The logging speed is adjusted so that the tool moves 1 foot in one time constant period (see Table 7-2). The faster the tool moves, the poorer the vertical resolution and the less accurate the log values (Figure 7-11).

TABLE 7-2. RECOMMENDED MAXIMUM LOGGING SPEEDS

Logging tool	Maximum logging speed[1] (ft/min)
SP	100+
Induction	100+
Sonic	70
Laterolog	50+
Microlaterolog	20
Neutron	30
GR	20
Density	15

[1]These are generalized speeds. The actual value varies with specific tool design.

The logging speed is noted on modern conventional logs by a break in the vertical grid-lines at the left and right edges of the log (Figure 7-8). Every break represents one minute of logging time. Slimhole logs and old conventional logs do not have this notation. Some slimhole tools note the logging speed on the log heading, but there is no way to be sure this was the actual speed.

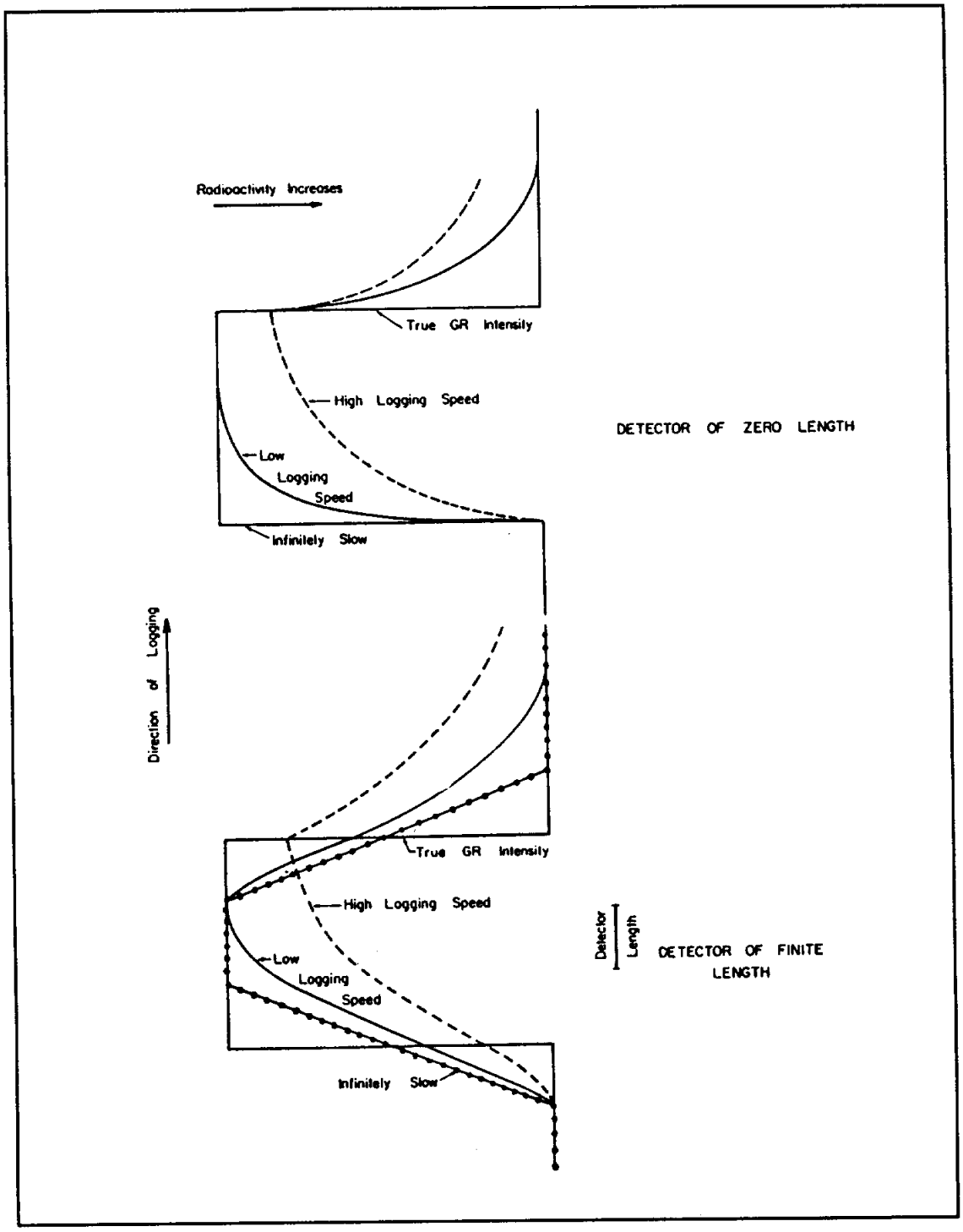

Figure 7-11. Effect of detector length and speed of logging on the vertical resolution of the gamma ray curve. A detector of zero length illustrates how increasing the logging speed distorts vertical resolution. For a detector of finite length distortion is due to detector length and movement during the time constant (From Pirson, 1963).

Different types and different brands of logging tools vary in vertical resolution due to differences in emitter-receiver spacing and other aspects of tool design. The following conditions explain the differences observed when comparing different logging curves:

1. Measurements made by different brands of the same logging tool will not be identical (although they should be very close). Figure 7-12 illustrates this principle with two sonic tools. The conventional compensated sonic is in good agreement with the slimhole sonic. The differences are largely due to variations in tool design.

2. Measurements made by different types of resistivity tools do not agree, even when there is no invasion (which occurs when there is no porosity or when formation water is the only fluid in the borehole). Figure 7-13 demonstrates this. There is no invasion in the formation so the three curves, each with a different depth of investigation, should read the same. They do not, however, due to differences in vertical resolution. The shorter the emitter-receiver spacing, the smaller the volume of rock measured for any particular point on the log, the sharper the bed boundary, and the more accurate the resistivity value. The "invasion profile" seen in the thin beds (e.g. 776 feet, 856 feet, 875 feet, etc.) is simply an artifact of the varying vertical resolutions. It is not caused by a horizontal resistivity gradient in the formation water due to mud filtrate invasion.

3. Count-rate gamma ray curves (most slimhole tools) may appear to have better vertical resolution than curves scaled in API units (conventional logs). Statistical variations in the gamma ray count, which have no relationship to vertical resolution, give count-rate curves their spiky appearance. When the counts are standardized to API units, the statistical variations may also be filtered out resulting in a curve that is smoother. Figure 7-14 illustrates this.

Vertical resolution is not critical for the log analysis of ground-water aquifers that have very high specific capacities (e.g. highly porous carbonates such as the Edwards and thick, massive sandstones like the Carizzo-Wilcox). It is critical, however, in sandstone aquifers which have interbedded shale or tightly cemented zones (Trinity and north central Texas Paleozoic aquifers), aquifers that produce mainly from fractures, and

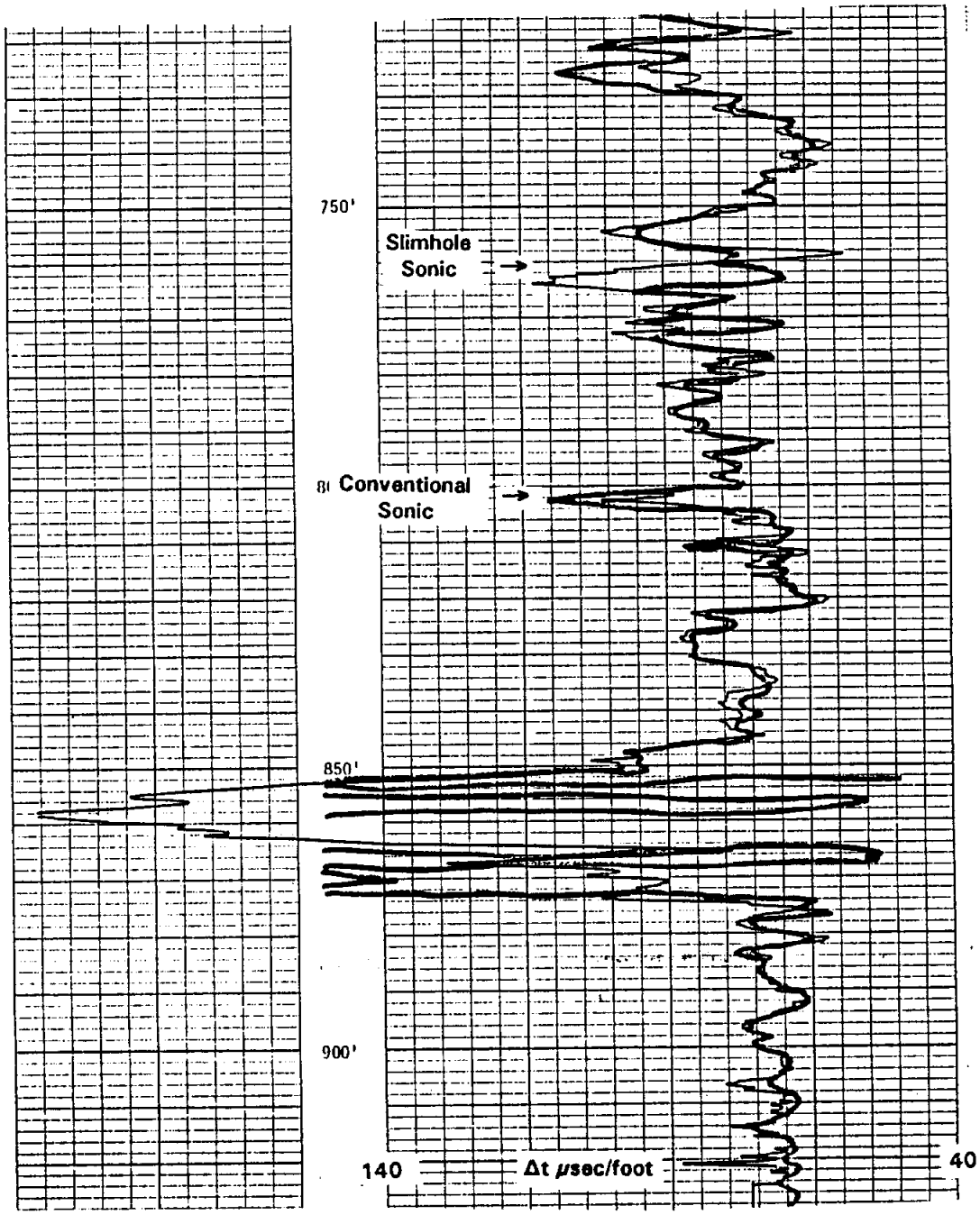

Figure 7-12. A comparison of the vertical resolution of a slimhole and a conventional sonic tool. The two are in good agreement. The differences are largely due to variations in tool design. This well is in the Edwards Aquifer, New Braunfels, Texas. The well is the Edwards Underground Water District, A-1 (state well number 68-23-616). The bit size is 7 ⅞ inches. The borehole fluid is formation water.

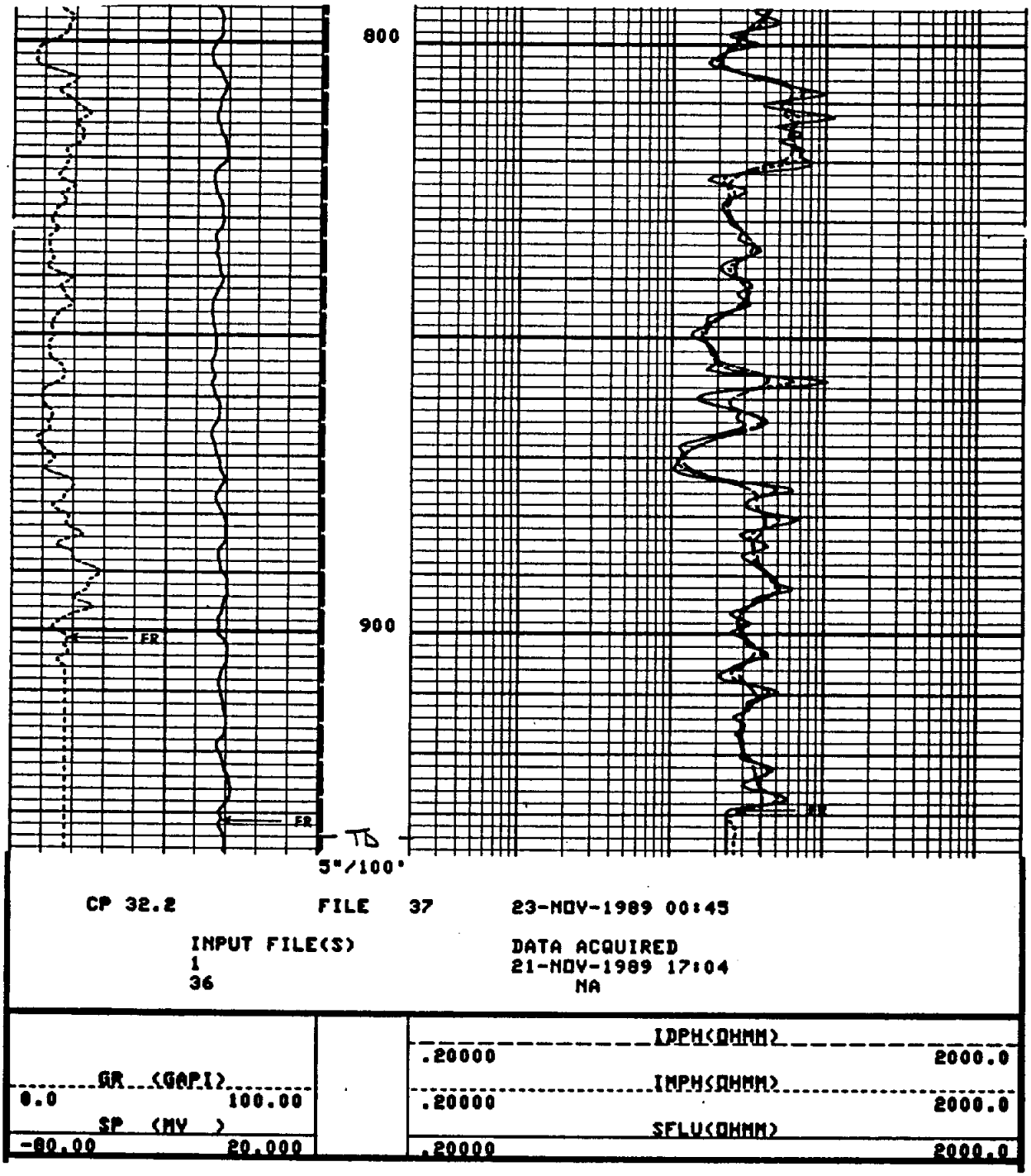

Figure 7-13. The effect of vertical resolution on resistivity curves. There is no invasion in the formation (the well was drilled reverse air-rotary). The curves do not overlay in thin beds becasue each tool has a different vertical resolution. The SP is flat because the borehole fluid is the same as the formation water. IDPH = Phasor Deep Induction, IMPH = Phasor Medium Induction, SFLU = Unaveraged Spherically Focused Log. This well is in the Edwards Aquifer, New Braunfels, Texas. The well is the Edwards Underground Water District, A-1 (state well number 68-23-616). The bit size is 7⅞ inches. The borehole fluid is formation water.

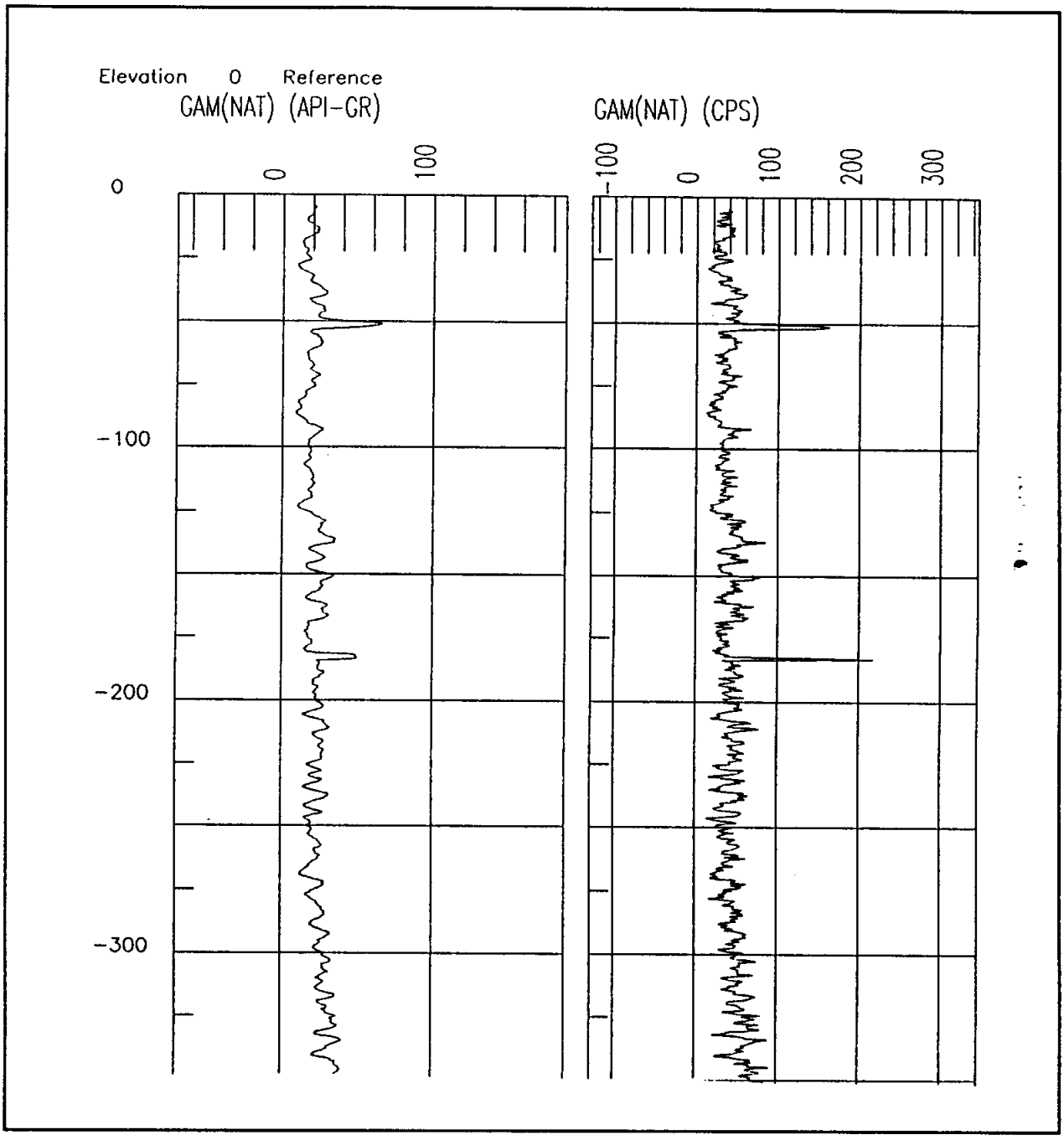

Figure 7-14. The difference in appearance of a gamma ray curve scaled in API units versus the same curve scaled in count rates. The well is in the Ellenburger Group, McCullouch County, Texas. The well is the TWDB, Brady Test Hole #2 (state well number 42-62-910). The bit size is 7⅞ inches. R_m is 14 ohm-meters and R_{mf} is 9.5 ohm-meters at formation temperature (73° F). Mud density is 10.2 lb/gal. Figure 8-14 is also from this interval.

carbonate aquifers that have interbedded porous and tight zones (Ellenburger). Figure 7-15 illustrates how the excellent vertical resolution of the microlog is invaluable in determining the net feet of sand and screen depth in this Trinity well.

Vertical resolution is also important for any type of detailed geological analysis of an aquifer such as is required in environmental and geotechnical site assessments. Good vertical resolution is essential to identifying vertical permeability barriers. It is also very helpful in characterizing depositional facies and in identifying some diagenetic products (e.g. cemented zones).

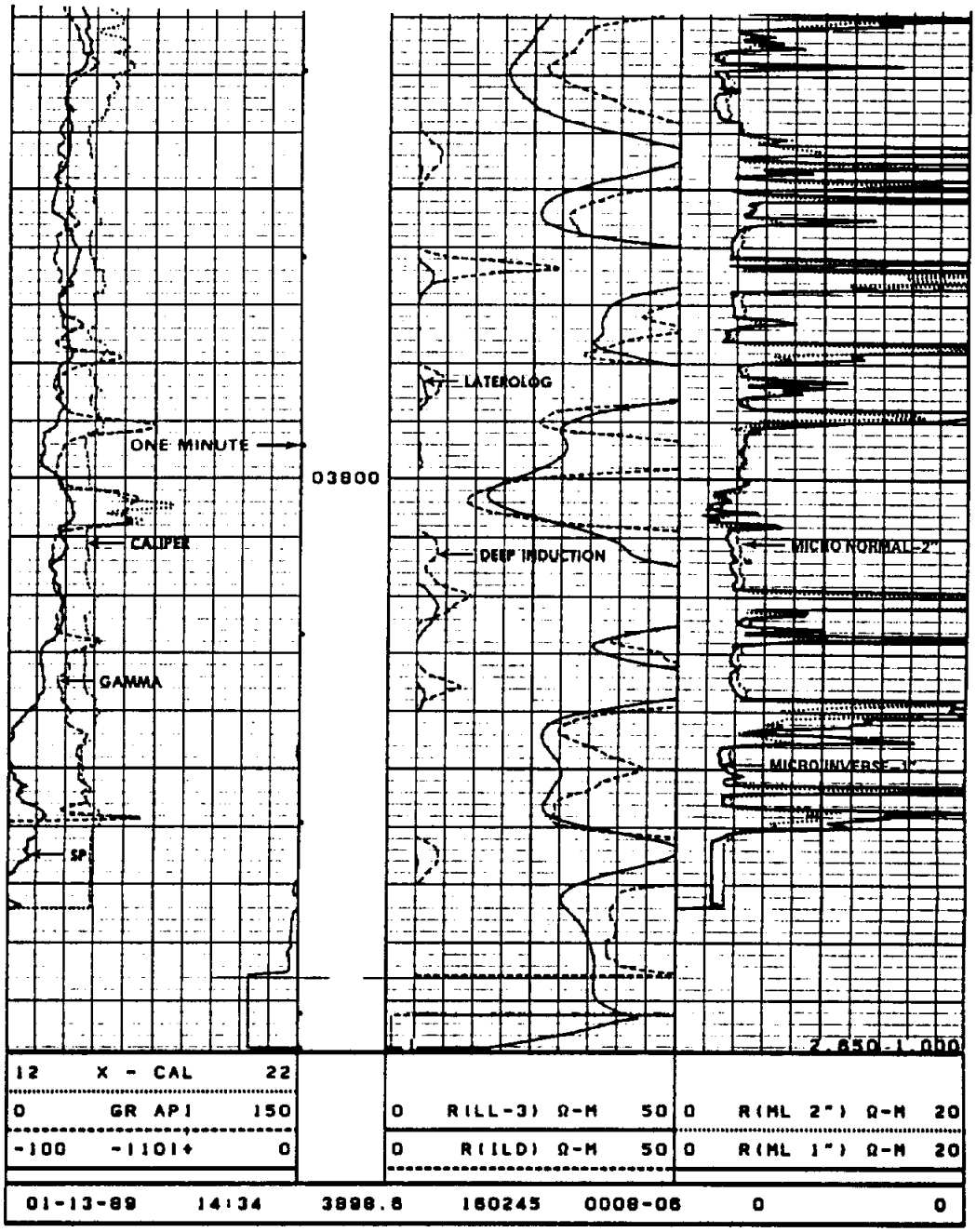

Figure 7-15. The microlog (Track 3) has vertical resolution of a few inches and is an excellent tool for delineating porous/permeable streaks in aquifers with alternating porous and nonporous intervals. This log is the Trinity Aquifer. The caliper log shows mudcake buildup on porous-permeable zones (borehole diameter is less than 14.75 inches). The well is the J.L. Myers, Tri-County Water Supply Corp. #5, Falls County, Texas. The bit size is 14.75 inches. R_m is 1.8 ohm-meters and R_{mf} is 1.1 ohm-meters at formation temperature (122° F).

NONFOCUSED RESISTIVITY TOOLS

Chapter 8

Resistivity logs are a standard component of both ground-water and petroleum openhole logging programs. In many ground-water and hazardous waste studies, they are one of the few logs run. In such cases resistivity curves are the principal borehole geophysical source of geological and hydrogeological data. The curves can be used to correlate stratigraphy, identify lithology, estimate texture, and identify depositional facies. Quantitatively, resistivity data can be used to calculate water quality (total dissolved solids content and hardness), permeability (hydraulic conductivity), and porosity (Alger and Harrison, 1988; Taylor, et al., 1988; Chapter 14, **TECHNIQUES FOR CALCULATING Cw FROM LOGS**).

The induction tool is the only resistivity tool that works in cased holes and it only works in nonmetallic casing. Several companies are currently working on resistivity tools that will work in metallic casing.

A variety of resistivity tools is available (Table 8-1). Resistivity tools can be divided into two types: electrode and induction. Electrode tools are what are properly known as resistivity tools. Electrode tools can be further divided as to whether or not the current is focused and whether the electrodes are embedded in a mandrel (cylindrical probe housing) or in a pad that attaches to the probe. Pad tools are pressed against the borehole wall, while mandrel tools dangle centralized or eccentered in the well bore.

Selecting the proper tool is critical, because they vary widely in tool design, curve response, and application. Failure to run the proper tools and lack of environmental corrections are mistakes that will nullify or, at best, significantly reduce the value of the log data.

This chapter and Chapter 9 review resistivity tools. Tool theory, curve response, environmental corrections and applications to ground-water investigations are discussed for each tool.

TABLE 8-1. CLASSIFICATION OF RESISTIVITY TOOLS

ELECTRODE

Nonfocused

Mandrel
- Single-point
- Normal
- Lateral
- Limestone lateral

Pad (Microelectrode)
- Microlog

Focused

Mandrel
- Guard
- Point-electrode
- Shallow investigating
- Spherically focused
- Dual focusing

Pad (Microelectrode)
- Microlaterolog
- Proximity
- Microspherically focused

INDUCTION
- Dual Induction
- Phasor Induction
- Array Induction
- Slimhole Induction

RESISTIVITY

Resistivity is the specific electrical resistance of a given volume of material to the flow of an electrical current through the substance. The unit of measurement is ohm-meter^2 per meter, which is commonly abbreviated to ohm-meter or simply ohm-m. In conversation it is often further abbreviated to ohm. The symbol for ohm is Ω. Another way to determine this same physical property is to measure the ability of a substance to conduct an

electrical current. This is called conductivity and it is the reciprocal of resistivity. It is measured in mhos per meter (ohm spelled backwards). To avoid decimal points, log analysts usually express conductivity in millimhos per meter (mmhos/m). Most log analysts convert conductivity measurements to resistivity units. The relationship between resistivity and conductivity is as follows:

$$Resistivity\ (ohm\text{-}m) = \frac{1{,}000}{Conductivity\ (mmhos/m)} \qquad (8\text{-}1)$$

Under ideal conditions (i.e. no borehole and no filtrate invasion) the resistivity of the formation (R_t) is a function of the amount of water present (porosity), the resistivity of the formation water (R_w), and the geometry of the pores. A fourth factor, which is usually inconsequential, is the resistivity of the rock.

Resistivity of the Rock. Most rocks are infinitely resistive so only water in the pores conducts electricity (Figure 8-1). However, a few minerals such as glauconite, pyrite, graphite, and galena conduct electricity and have low resistivities. Clay minerals and shales have low resistivities because of their cation exchange capacity (CEC). Ions that are loosely attached to the surface of the clay platelets move under the influence of an electrical potential and conduct an electric current.

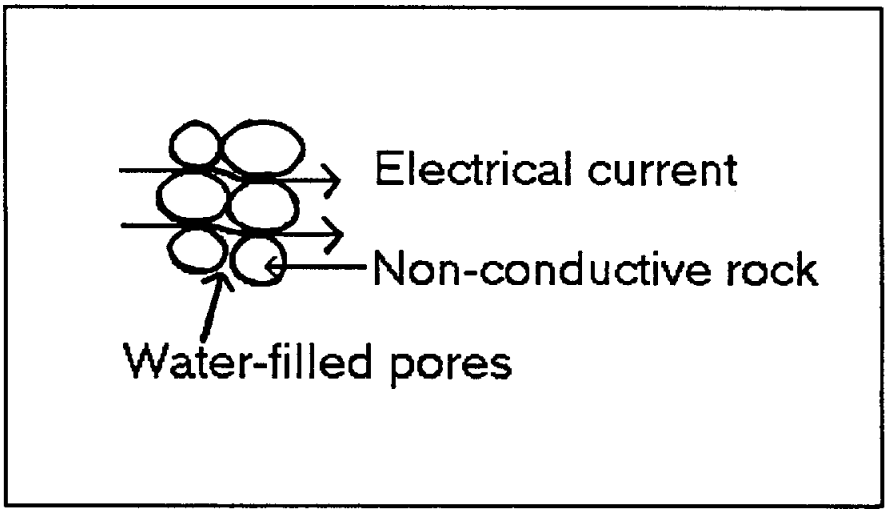

Figure 8-1. Only the formation water conducts an electrical current in normal rocks. This figure depicts the homogenous, intergranular pore system common to sandstones and also present in a few carbonates.

Amount of water present (porosity). Since the rocks in most ground-water aquifers are infinitely resistive, the resistivity of the formation (Rt) is in large part determined by the amount of water in the formation. Porosity, in turn, controls the amount of water. As porosity increases, resistivity decreases. The relationship between porosity and Rt has been quantified by log analysts. The relationship is discussed in Chapter 14.

The percent of the pores filled with water will also influence Rt. If air or hydrocarbons partially fill the pores, the amount of water is reduced and the resistivity is increased. Neither condition is common in ground-water aquifers, so these exceptions are not considered in this discussion.

Geometry of the pores. The more heterogeneous and tortuous the pore geometry, the harder it is for current to flow through the rock and the higher the resistivity. Sandstones normally have intergranular, homogenous pore structures (Figure 8-1), while carbonates often have more heterogenous and tortuous pore paths (Figure 8-2). Thus sandstones normally have lower resistivities than carbonates. Sandstones usually have more porosity than carbonates, which also contributes to the lower resistivities of sandstones.

The relationship between Rt and pore geometry has also been quantified. Chapter 14 discusses the relationship.

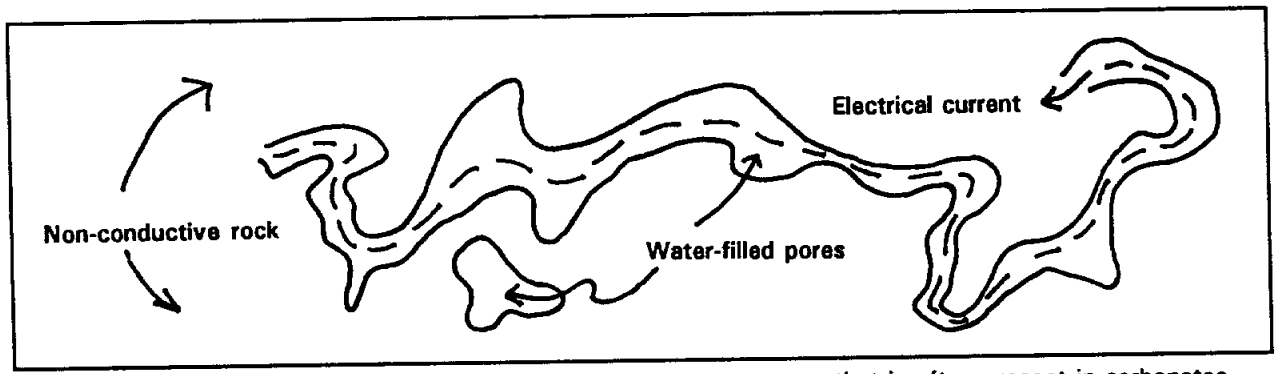

Figure 8-2. This figure depicts the heterogenous, tortuous pore system that is often present in carbonates. The formation water still conducts all of the electrical current, but the route the current follows is longer and therefore resistivity is higher than in an intergranular pore system.

Resistivity of the formation water. Rt is, in large part, determined by the resistivity of the formation water (Rw), which is a function of the total dissolved solids in the water. Dissolved solids are in an ionic state. Under the influence of an electrical field, the ions move and conduct an electrical

current through the water (see Chapter 2). As the total dissolved solids content (often called salinity) of the water increases, the resistivity decreases.

Formation resistivities vary from 0.1 to 2000$^+$ ohm-meters. As a general rule, very low porosity formations with fresh to very saline waters will have R_t's ranging from hundreds to thousands of ohm-meters. High porosity, shale-free, sand and carbonate aquifers with fresh water will have R_t's in the tens to 100$^+$ ohm-meter range. High porosity sands and carbonates with very saline water will have R_t's from 0.1 to 10$^+$ ohm-meters. The presence of clay minerals can significantly reduce R_t.

THE ENVIRONMENT OF RESISTIVITY MEASUREMENTS

As was pointed out in Chapter 6, **THE BOREHOLE ENVIRONMENT AND ITS EFFECTS ON LOG RESPONSES**, resistivity measurements are never made under ideal conditions. R_t measurements are always affected to some degree by the borehole environment: borehole size (d_h), bed thickness (h; e in older literature), mud resistivity (R_m), resistivity of adjacent (also called shoulder or side) beds (R_s), mud filtrate resistivity (R_{mf}), and depth of mud filtrate invasion (Figure 6-3). R_t is also affected by tool design (Chapter 7). The uncorrected resistivity recorded on the log is actually an apparent resistivity (R_a). R_a is a composite of R_t, R_m, R_s, R_{mf}, and tool design. R_a may equal R_t only after environmental corrections (departure curves) are applied to the log.

Environmental corrections for mandrel resistivity and induction tools group into three categories:

Borehole corrections. This correction compensates for the effect of borehole size and R_m on R_a.

Bed thickness and adjacent bed corrections. This correction compensates for the effect of R_s and bed thickness on R_a.

Invasion correction. This correction compensates for the effect of depth of invasion and R_{mf} on R_a.

Corrections must always be made in the same order: borehole, bed thickness and adjacent bed, invasion. All three corrections do not have to be applied in every case. Pad-type tools only require a correction for R_{mc}.

Departure curves are discussed for each resistivity tool. Corrections for R_m and R_{mc} must be at the temperature of the formation being analyzed. The equation used to calculate formation temperature is discussed in Volume II, Section 3, explanation 3. Equation 2-4 is then used to convert R_m and R_{mc} to formation temperature.

A problem with all departure curves is they have to be constructed for specific conditions such as no invasion, thick beds, centered tool, 8 inch borehole. The conditions upon which a chart is based are seldom the same as those in a particular borehole. However, they are the best available method of correcting for the effects of the borehole environment.

Choice of a resistivity logging suite should be based on the compatibility of tool and borehole conditions. Myriad combinations of borehole influences mean that no single resistivity tool is applicable to all situations. Furthermore, varying depths of mud filtrate invasion mean that a single deep reading curve may or may not be unduly influenced by R_{mf}. Three resistivity curves of varying depths of investigation are necessary to insure that the deep resistivity curve is reading R_t. There are a plethora of resistivity tools, each with a different depth of investigation (Figure 8-3).

The effect of mud filtrate invasion on R_t measurements is discussed in detail in Chapter 6. In high porosity formations invasion is usually very shallow and mud filtrate has minimal effect on the deep investigating tools. In fact, invasion may be so shallow that microelectrode tools are affected by R_t. Two resistivity curves (shallow and deep) may be adequate to determine R_t. But the only way to be certain that the deep curve has not been overly influenced by R_{mf} is to run a third curve with a medium depth of investigation. In low and moderate porosity formations three resistivity curves are necessary.

As was pointed out in Chapter 7, depth of investigation and vertical resolution for a particular resistivity tool varies according to borehole conditions and the nature of the formation. Even though in this chapter specific values are assigned for each tool, the numbers are average values that are valid only for ideal conditions. The actual values may be considerably smaller.

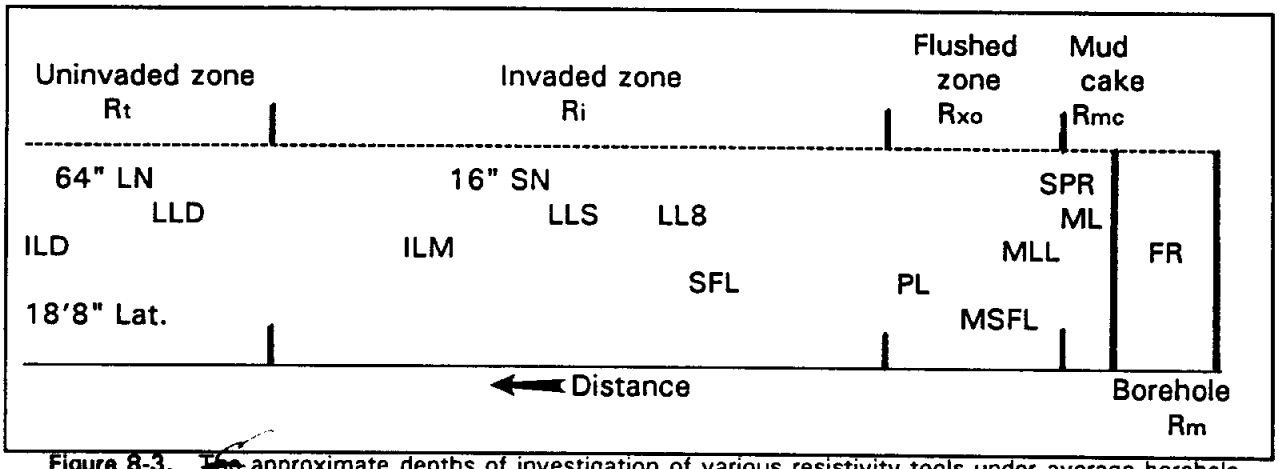

Figure 8-3. The approximate depths of investigation of various resistivity tools under average borehole conditions (Modified from Rider, 1986).

FR	Fluid resistivity	LLS	Shallow laterolog
SPR	Single-point resistance	16" SN	16" Short normal
ML	Microlog	ILM	Medium induction log
MLL	Microlaterolog	LLD	Deep laterolog
MSFL	Microspherically focused log	64" LN	64" Long normal
PL	Proximity log	ILD	Deep induction log
SFL	Spherically focused log	18'8" Lat.	18'8" Lateral
LL8	Laterolog 8		

RESISTIVITY VERSUS INDUCTION TOOLS

There is a fundamental difference between resistivity and induction tools. Resistivity tools measure resistivity. The tools use electrodes to send a current into a formation and to measure the ease with which it flows through the rock. Induction tools measure conductivity. The tools use coils to induce an electric current in a formation and to measure the amount of the current.

Petroleum logging service companies use the term induction tool and display the measurements in resistivity units. The tool uses Equation 8-1 to convert the conductivity measurements to resistivity units. Some ground-water slimhole induction tools are called conductivity tools. The logs are scaled in conductivity units (millisiemens per meter or mS/m, which is the International System of units). Millisiemens per meter are equivalent to millimhos per meter. Some ground-water log analysts prefer the term conductivity rather than induction. This study uses induction.

In most logging literature it is common practice to include induction tools under the term resistivity tools because both types of tools record

resistivity. A distinction between the two becomes important and is made when discussing tool theory and operation. For instance, resistivity tools require a conductive fluid in the borehole in order to operate; induction tools do not. In Table 8-1 all the electrode tools, except for a few laterologs, are resistivity tools.

NONFOCUSED MANDREL ELECTRODE TOOLS

From the inception of wireline logging in 1927 until about 1950, the only tools available for measuring formation resistivity were nonfocused electrode devices (also called conventional resistivity logs or E logs). The three types of tools in this category are single-point, normal, and lateral.

In the 1950's nonfocused electrode tools were replaced by focused electrode and induction tools in the petroleum industry. Nonfocused tools were abandoned because the tools have a serious problem - the current direction is not controlled. Consequently the current takes the path of least resistance, preferring very conductive mud and conductive side beds over the resistive beds opposite the current electrode (Figure 8-4). As the resistivity contrast (R_t/R_s and R_t/R_m) increases, so does the difficulty of obtaining an accurate resistivity value. Both nonfocused and focused centralized electrode tools work best when R_m is 3 to 5 times R_w (Frank, 1986).

An additional limitation, shared with all other electrode tools, is that nonfocused mandrel electrode tools require a conductive borehole fluid. It will not work in oil-based muds, air-filled holes, or foam-filled holes.

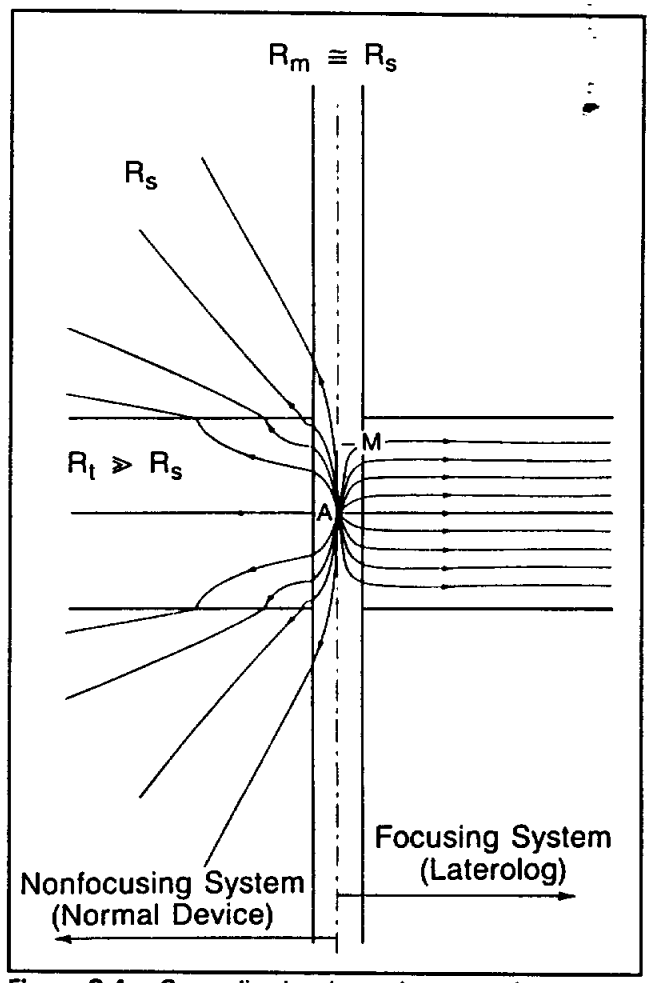

Figure 8-4. Generalized schematic comparing current distribution in a resistive bed opposite a nonfocused and a focused tool (From Frank, 1986).

The nonfocused nature of these tools has important consequences for designing the proper ground-water logging suite. In ground-water environments with high R_t/R_m values, nonfocused electrode tools are not the best resistivity tools to run. When they are run, the log values often require significant corrections in order to have R_t's that are accurate enough to be used to calculate log-derived hydrogeological parameters.

All three types of nonfocused tools continue to be used routinely in the ground-water industry. Their popularity is probably due, in large part, to the fact that very few other types of slimhole resistivity and induction tools are available.

The log files of petroleum and ground-water firms are full of pre-1960 vintage normal and lateral logs. A regional ground-water study anywhere in Texas will include a high percentage of these logs, so ground-water log analysts need to be familiar with them.

Because these tools are considered antiquated by the petroleum logging industry, there are few reference books available. The best reference is Hilchie (1979). Other good references include SPWLA (1979) and Frank (1986).

Single-Point Resistance

Single-point resistance tools are also known as single-point, point-resistance, or single-electrode tools. The tool was rarely used in the petroleum industry. For a limited time, Halliburton and Lane Wells used the single-point as a substitute for the short normal (Hilchie, 1979). Only slimhole single-points are available today. They are used extensively in ground water, coal, uranium, and environmental site assessment logging.

Tool theory. The single-point is the simplest type of "resistivity" tool. The tool actually measures resistance rather than resistivity. Resistance is a function of both resistivity and the geometry of the material being measured. The relationship between resistance and resistivity can be illustrated in terms of a copper wire. The wire has a specific electrical resistance for a given volume, meter^2 per meter, which is its resistivity. It is an inherent physical property of the wire which does not change in value. The resistance of the wire to the flow of an electrical current is a function of both its inherent resistivity and the length of the wire (geometry of the material). Resistance changes as the geometry of the wire changes. A long wire has a high

resistance while a short wire has a very low resistance.

There are two types of tools: conventional and differential. The conventional single-point system consists of a surface and a downhole electrode (Figure 8-5). The differential system has both electrodes downhole; the return electrode is the probe housing (Figure 8-6).

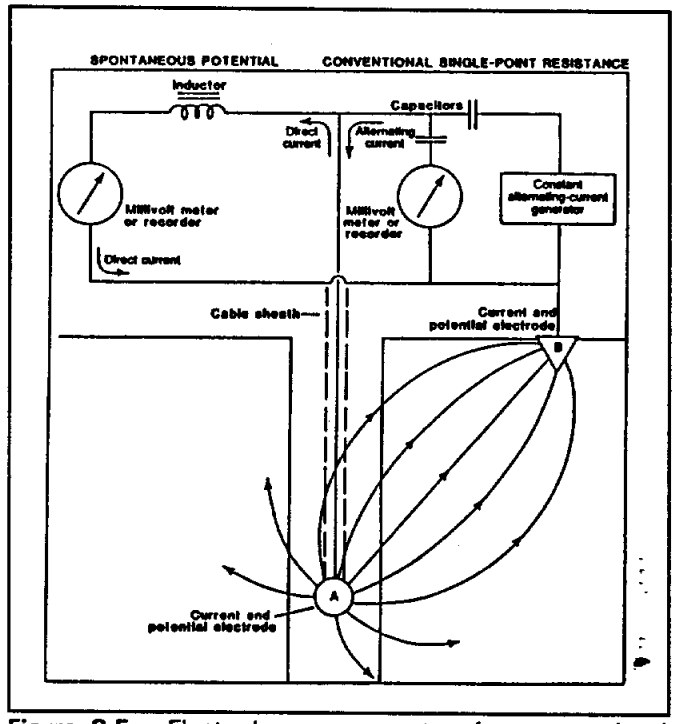

Figure 8-5. Electrode arrangements of a conventional single-point and SP tool (From Keys, 1988).

In the conventional single-point system, AC current travels down electrode A, moves radially throughout the surrounding mud and rock, and returns to the ground electrode, B (Figure 8-5). In the differential system the current flows from electrode A around an insulated section of the tool to the probe housing which serves as the B electrode (Figure 8-6). Both tools measure the potential difference between the two electrodes in volts. The potential difference between A and B is inversely proportional to resistance, thus allowing resistance to be measured.

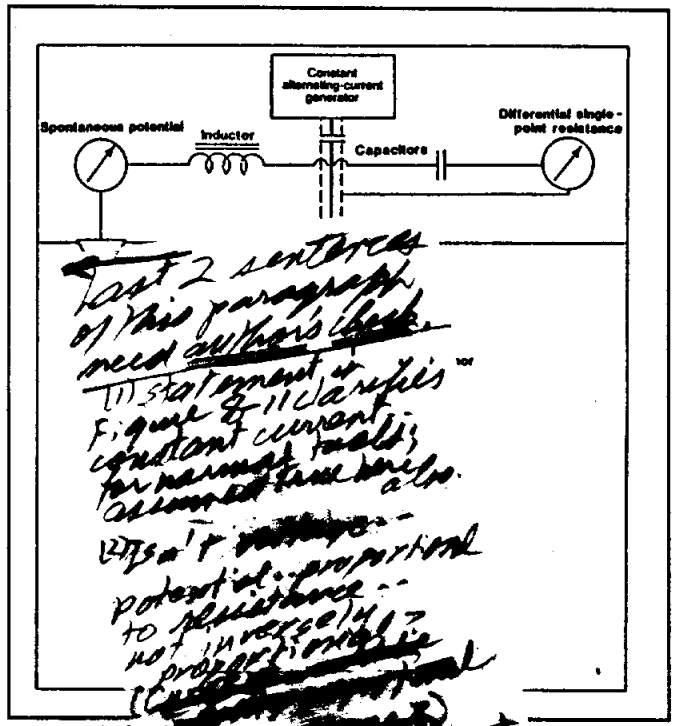

Figure 8-6 ... differential single-point ...

The A electrode serves as both a current and a potential-sensing electrode. This gives the tool a very short electrode length and a very shallow depth of investigation. The length of the electrode (2 to 3 inches) determines the depth of investigation and the vertical resolution. The ... or 50

percent of the signal is twice the electrode length (Hilchie, 1979). The vertical resolution is equal to or greater than the electrode length. The differential single-point has better vertical resolution than the conventional tool (Keys, 1988).

Not much literature exists on the single point. Guyod (1944) has an excellent discussion of the tool. Keys (1988) gives a detailed discussion of the tool theory for both the conventional and the differential single-point systems.

Log presentation. Both conventional and differential tools measure the resistance in ohms of the material lying between the two electrodes. The log curve is a solid line and is scaled in ohms per inch (Keys, 1988). It is possible to convert resistance to resistivity if the electrode dimensions are known (Keys and MacCary, 1971, p. 32-34; Hallenburg, 1984). However, borehole environmental corrections are often so severe that quantitative resistivity values are very inaccurate.

Interpretation. The single-point has a few strengths and several weaknesses.

Strengths.

1. The electrode configuration gives excellent thin bed resolution (2 to 3 inches, depending on the length of the electrode). See Figures 8-7 and 8-8.

2. The tool is able to detect fluid-filled fractures. However, for serious fracture identification, tools such as the borehole televiewer, full waveform sonic, and formation microscanner should be used.

3. The curve is symmetrical. The tool configuration eliminates distorted curve shapes such as are common to normal and lateral curves.

4. Measurements can be made to the bottom of the borehole and right up to either metallic casing or fluid level (Guyod, 1944).

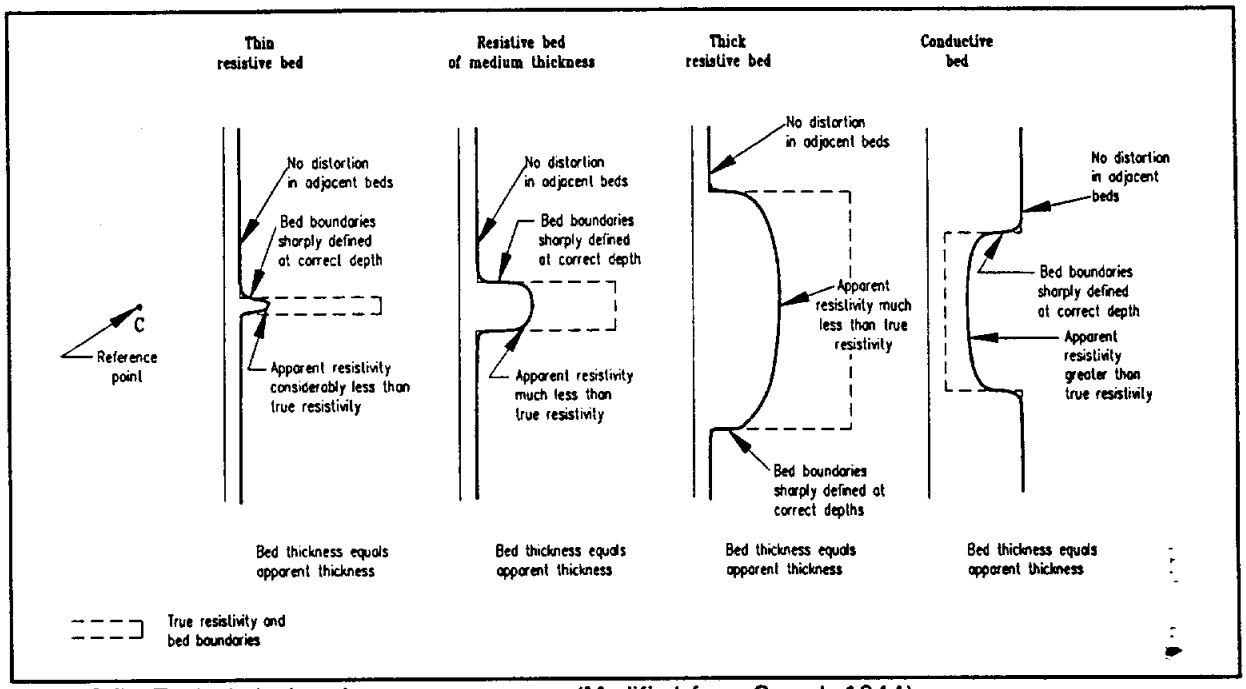

Figure 8-7. Typical single-point curve responses (Modified from Guyod, 1944).

Weaknesses.

1. The shallow depth of investigation means that the current path is dominated by the borehole fluid and borehole diameter. The tool is adversely affected by large boreholes and high Rxo/Rm values (Figure 8-9). Hallenburg (1984) and Guyod (1944) have published the only single-point borehole correction charts that this author has located. Hallenburg (1984) points out that correction charts have not been verified for single-point tools.

   a. For boreholes much larger than 5 inches, the tool is primarily measuring the resistance of the borehole fluid.
   b. When the flushed zone resistivity is greater than the borehole fluid resistivity (Rxo/Rm greater than 1), which is usually the case in ground-water aquifers, the tool measures far less than true resistivity.

2. The severity of the borehole effect, plus the nonlinear curve response, means that no confidence can be placed in the resistance values. The curve is strictly qualitative, showing nothing more than relative changes in resistivity.

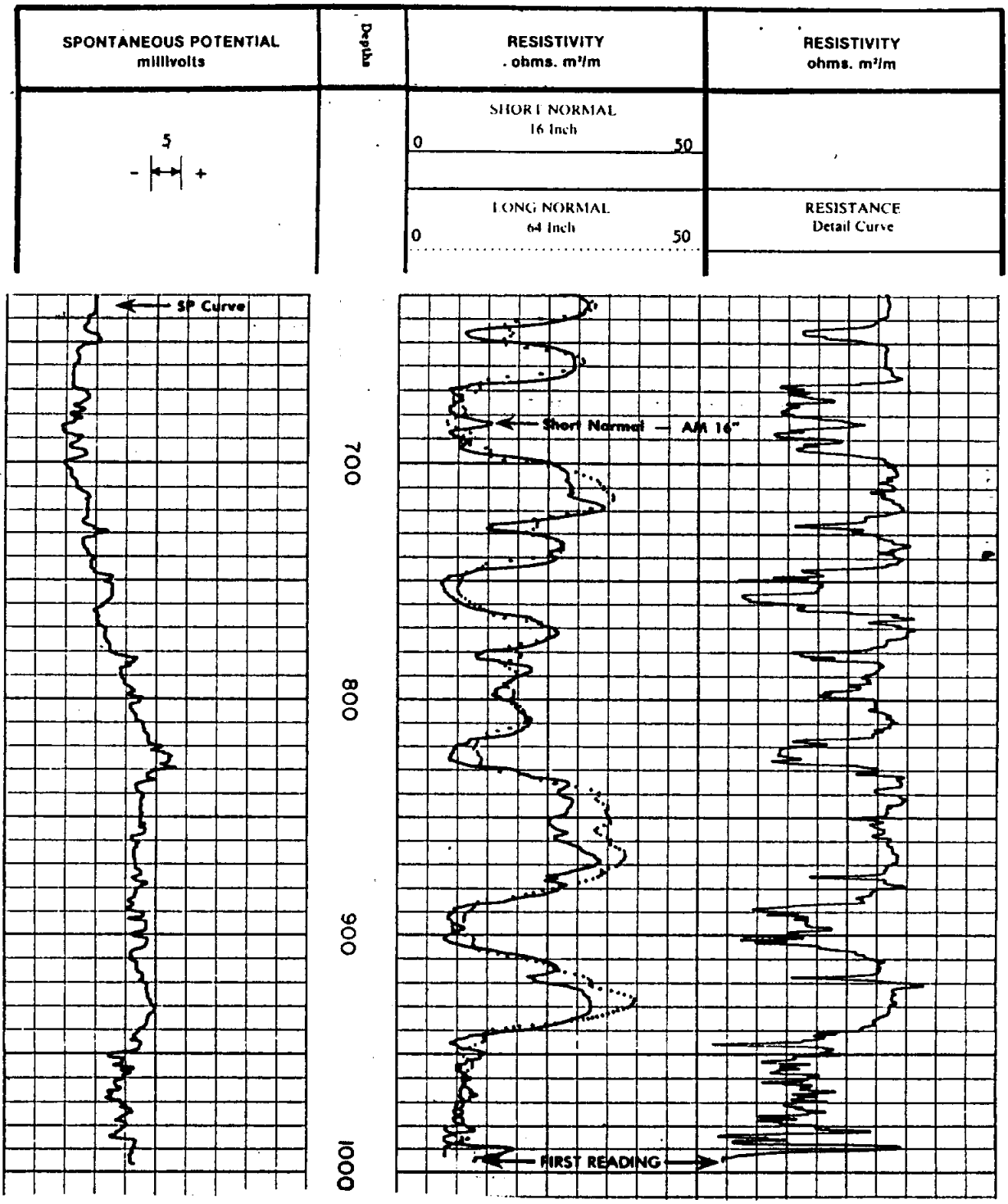

Figure 8-8. Comparison of a single-point resistance curve with short and long normal curves. The single-point curve has better bed boundary definition than the normal curves, even though the bit size is 27.5 inches. The borehole fluid is water and Rm is 18.5 ohm-meters at 75° F. Rm is very close to the resistivity of the formations (20 to 35 ohm-meters) which explains why the single-point has such good resolution in a large borehole. A bottom hole temperature was not available. The log is a sand-shale sequence in Kern County, California.

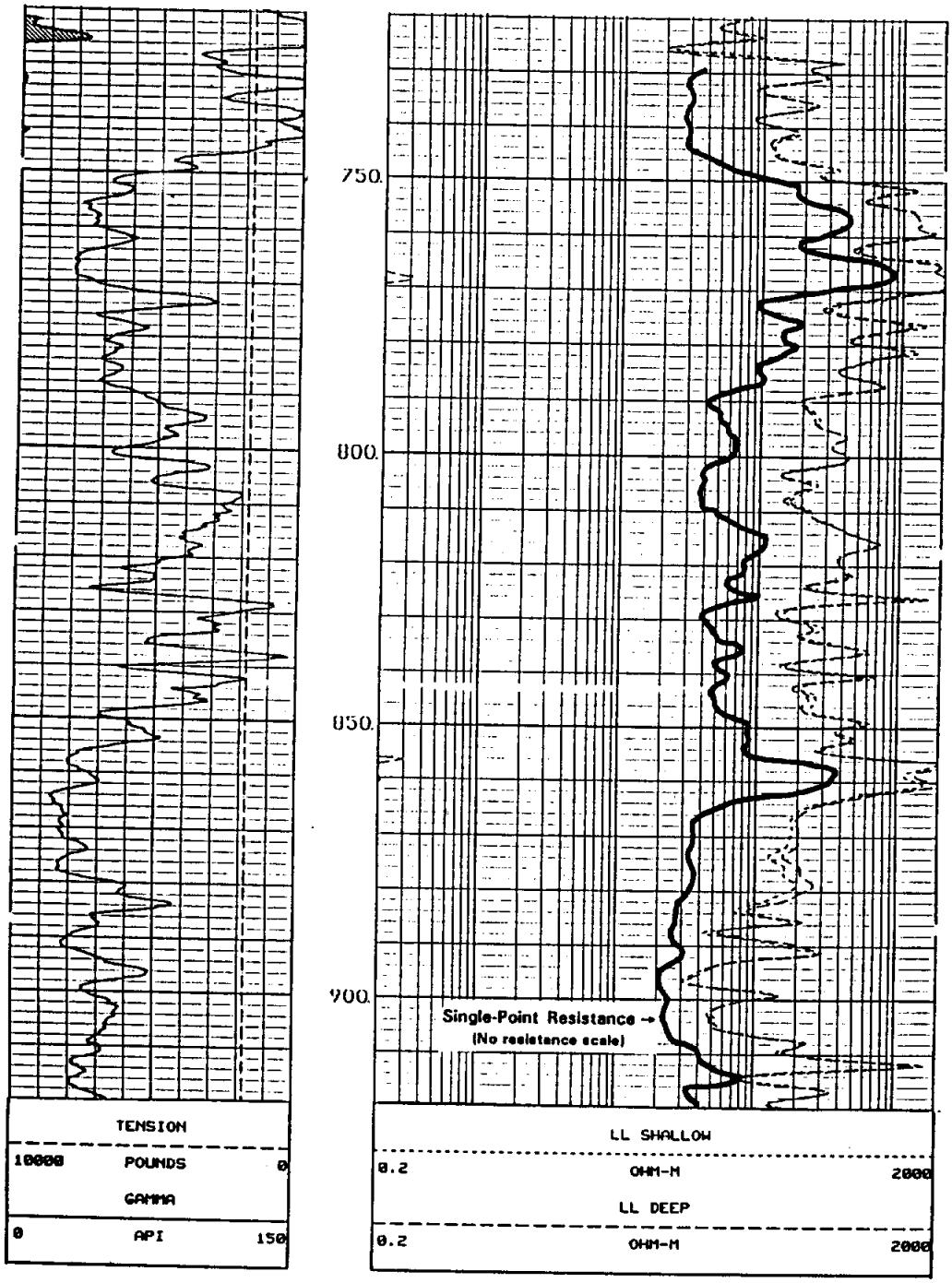

Figure 8-10. Comparison of a single-point resistance curve with a dual laterolog. The single point curve was drafted onto the dual laterolog. The dual laterolog has better vertical resolution, plus the resistivity values can be used quantitatively. Borehole size is 6 inches. Borehole fluid is water and R_m is 17.3 ohm-meters at formation temperature (77° F). The formations are the Morgan Creek Limestone and the Welge Sandstone (below 864 feet) in McCulloch County, Texas. The well is the TWDB, Brady Test Hole #1 (state well number 42-62-909).

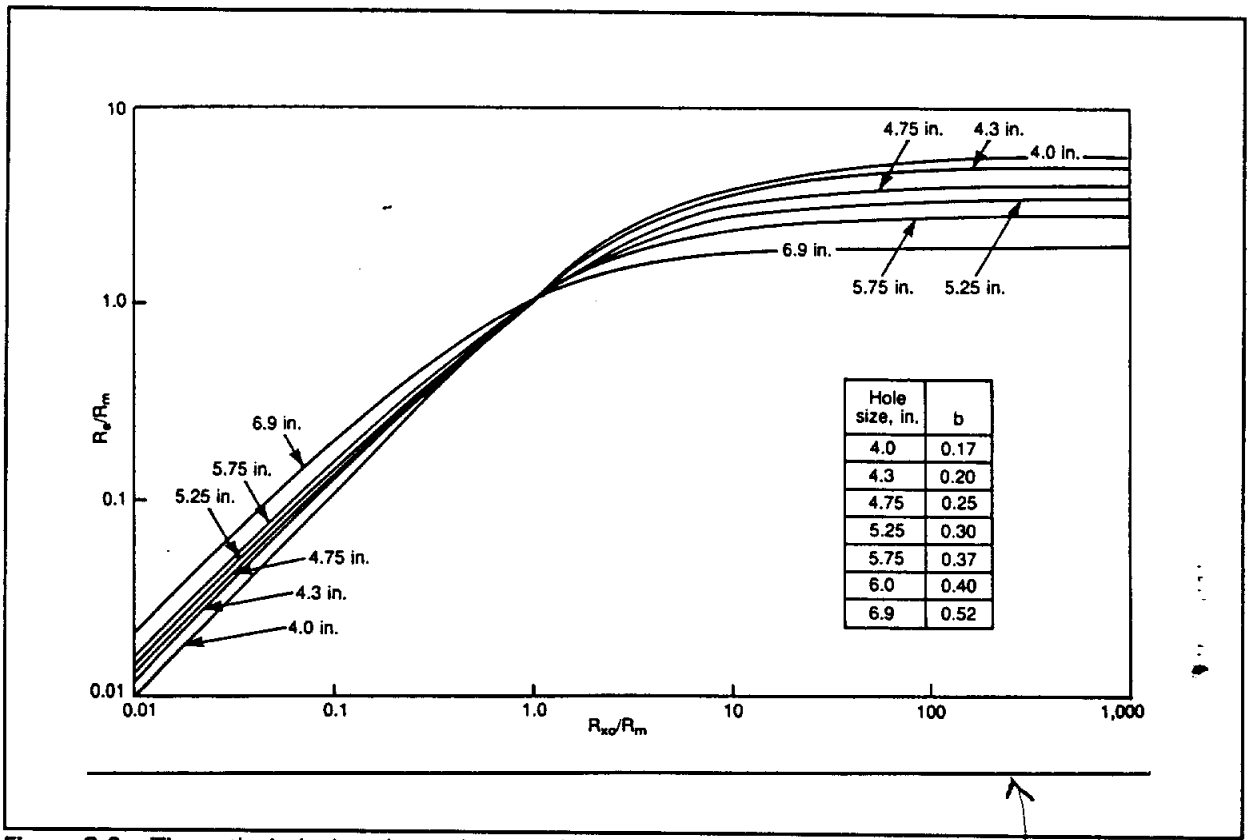

Figure 8-9. Theoretical single-point resistance departure curve corrections for Rm and hole size. Rm must be at formation temperature (From Hallenburg, 1984).

(? un-needed line ?)

3. As with all nonfocused electrode tools, the single-point is adversely affected by any type of stray electrical currents (e.g. grounding problems, powerlines, etc.).

Recommended use. In view of its limitation the single-point should never be the primary resistivity log. Other resistivity tools can distinguish bed boundaries just as well as the single-point, plus give accurate resistivity values (Figure 8-10).

Normal

The normal tool was introduced in 1931. Normal curves were an integral part of every resistivity logging suite until the 1950's when they were replaced by induction and laterolog tools. Today they are the mainstay of ground-water and environmental slimhole resistivity logging suites. In fact, slimhole logging companies are the only ones still running the tools.

There are no trade names for the normal tool. The logging suite consisting of a short normal, long normal, lateral, and SP was variously called an Electrical Survey (ES), an Electric Log (EL) or an E log.

Ground-water log analysts today must be familiar with the log response of normal tools because:

1. Petroleum and ground-water log files are full of pre-1960 normal logs. A ground-water study of any area in Texas will include a sizeable percentage of these logs.

2. Some water wells in Texas are still being logged with normal tools.

Tool theory. The normal tool is also called the two-electrode tool. In practice, three electrodes are downhole as illustrated in Figure 8-11. The N electrode is the bare cable armor. Between N and the normal device, a distance of 10 to 20 feet, the cable is wrapped with insulating tape. The electrodes can be arranged so that N is on the surface, which makes the tool a true two-electrode tool.

The tool measures the voltage (V_{mea}) between electrodes M and N. R_a is calculated from the equation $K(V_{mea}/I) = R_a$. K is a constant which is dependent on the electrode configuration. I is the survey current. For a more detailed discussion of tool theory see Helander (1983) or Jorden and Campbell (1986), which also has a chart supplement (sections 6.4.1 to 6.5.1) detailing resistivity tool specifications.

The position of the N electrode determines how close to fluid level and to metallic casing the tool can log. If N is on the surface, the tool can log right up to either. If, however, N is the cable armor, the tool can only log to within an AN spacing of either.

Through the years the electrode spacing (initially designated as AM∞, but standardized as AM) has ranged from 8" to 84". Halliburton's 18 inch spacing was designated as 2Z 18". Many slimhole tools offer four spacings (8", 16", 32", and 64"). Only two of the spacings can be run at one time. The most popular AM spacings are a 16" short normal for R_i and a 64" long normal for R_t.

Depth of investigation increases as the electrode spacing increases. For normal tools the depth of investigation in isotropic, homogenous formations is equal to or less than 2AM. This means that a short normal will have good vertical resolution, but the tradeoff is a shallow depth of investigation which makes for a significant R_{xo} influence on the curve.

However, the ability to measure R_{xo} is desirable when attempting to calculate R_w by means of a resistivity ratio method. In unconsolidated formation of low to moderate porosity (less than 20 percent), invasion may be deep enough for the short normal to measure R_{xo}.

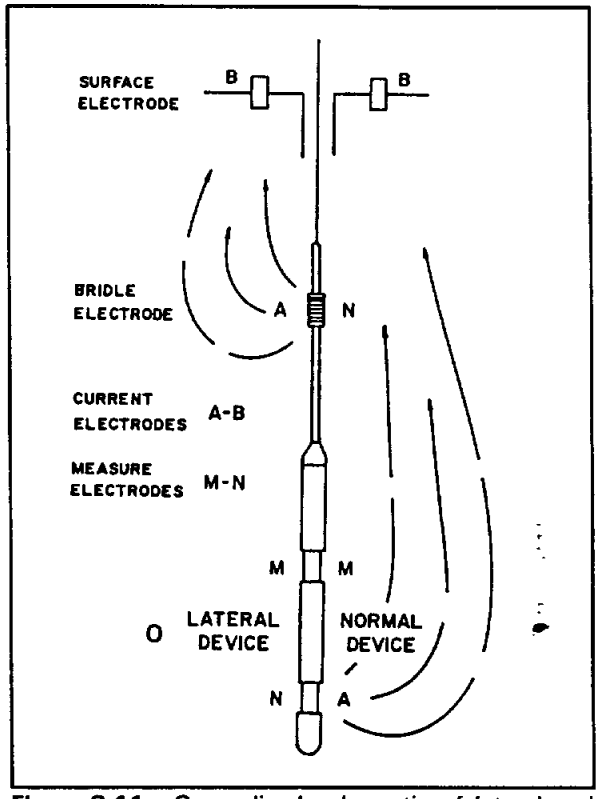

Figure 8-11. Generalized schematic of lateral and normal tools. A constant survey current flows from electrode A to electrode B (From Labo, 1986).

Log presentation. The curves are presented in either track 2 (Figure 8-8) or tracks 2 and 3 (Figure 8-20). The short normal is always a solid curve. The long normal is usually dashed. However, some slimhole logs also have the long normal as a solid line.

Environmental corrections. Borehole size, mud resistivity, bed resistivity, bed thickness, mud filtrate invasion, and resistivity of adjacent beds all adversely affect the curves. Resistivity values will usually be correct only after environmental corrections (called departure curves) are applied to the log. Environmental correction curves were never constructed for any of the slimhole normal and lateral tools. However, Guyod's research with analog models indicated that correction charts for conventional size tools are also valid for slimhole tools (1957, p. 1-5). Departure curves for normal tools will work for any brand of tool.

Eccentricity of the tool in the borehole, mudcake thickness, and mud weight have no effect on the curve (Pirson, 1963).

Borehole corrections. The definition and sharpness of the curves decreases as hole size increases and as mud resistivity decreases. Corrections for borehole size and Ra/Rm values should be routinely applied (Figures 8-12 and 8-13). Rm must be converted to formation temperature before using the chart. Ra is $R_{16"}$ in Figure 8-12 and $R_{64"}$ in Figure 8-13. Either the $^{R16"}/_{Rm}$ or the $^{R64"}/_{Rm}$ value is entered into the chart and at the intersection with the appropriate hole diameter the $R_{16"corr}/Rm$ or the $R_{64"corr}/Rm$ value is read. This value multiplied by Rm equals Rt.

Several pertinent facts about normal curve responses can be gleaned from these two charts:

1. Resistivity decreases as borehole diameter increases.

2. The short normal is more adversely affected by borehole diameter than is the long normal.

3. Long normal curves require corrections when $R_{64"}/Rm$ is greater than 20. Ra is greater than Rt in these cases.

4. Short normal curves in 8 to 10 inch boreholes require corrections when $R_{64"}/Rm$ is greater than 50. Ra is less than Rt in these instances.

5. As formation resistivity increases, the long normal starts reading higher than the short normal. As resistivity increases, the separation increases (Figure 8-14).

Bed thickness and adjacent bed corrections. Beds thinner than 1.5AM cannot be corrected. Beds thicker than 4AM (5 feet for the 16" short normal and 20 feet for the 64" long normal) require no correction. For beds between 1.5AM and 4AM correction charts are available but are seldom used (Hilchie, 1979). Corrected values are of dubious accuracy because the charts apply to specific borehole conditions such as hole diameter, Rm, Rs, etc. Suffice it to say that Ra is less than Rt in resistive beds (beds with a higher resistivity than the adjacent beds), while in conductive beds (beds with a lower resistivity than the adjacent beds) Ra is greater than Rt.

Invasion corrections. Departure curves are available to correct for the influence of mud filtrate invasion. Guyod and Pranglin (1959) published the best set of departure curves. Hilchie (1979) discusses the Lane Wells

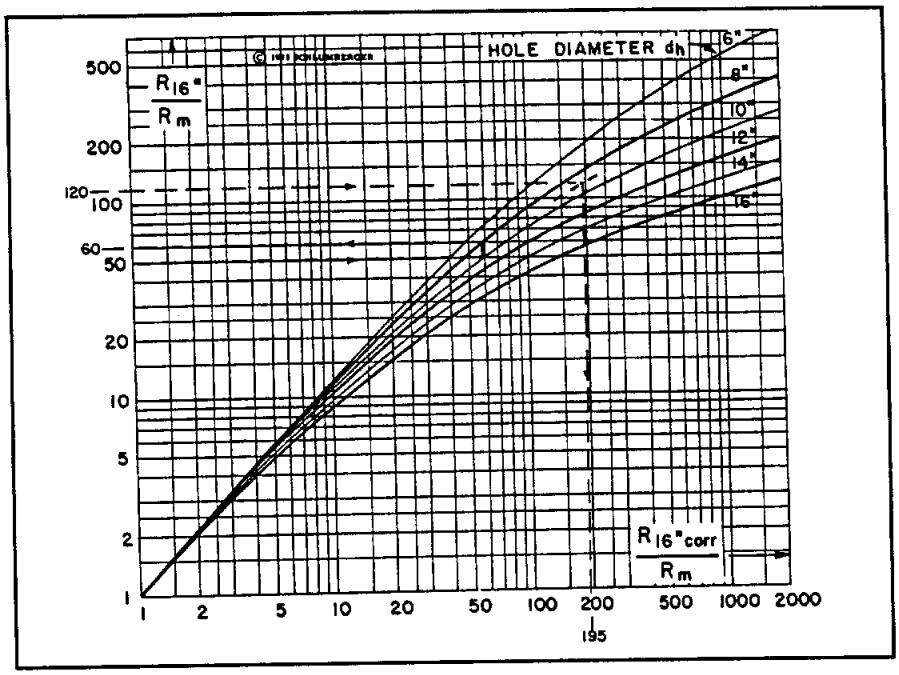

Figure 8-12. Borehole size and Rm corrections for the Schlumberger 16" normal. The chart is applicable to relatively thick formations of moderate to high resistivity. Rm must be at formation temperature (From SPWLA, 1979, after Schlumberger, no date).

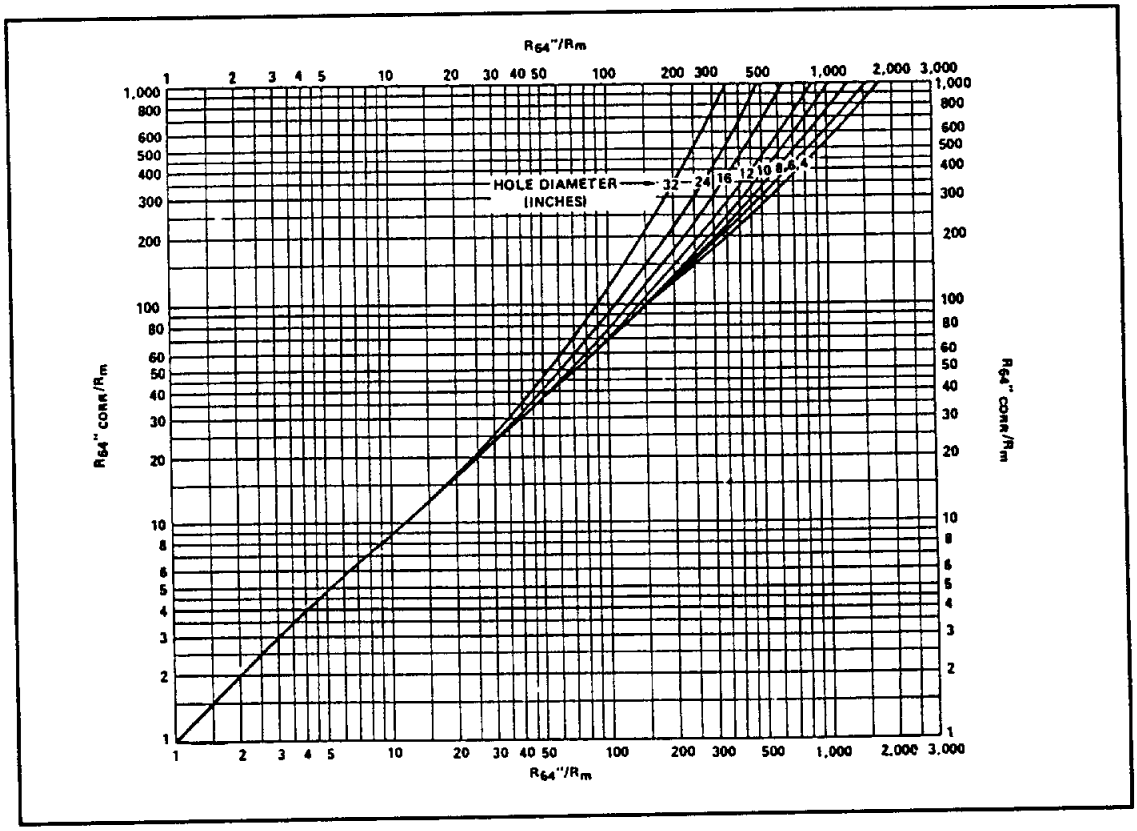

Figure 8-13. Borehole size and Rm corrections for the Schlumberger 64" normal. The chart assumes thick beds and full or no invasion. Rm must be at formation temperature (From SPWLA, 1979, after Schlumberger, no date).

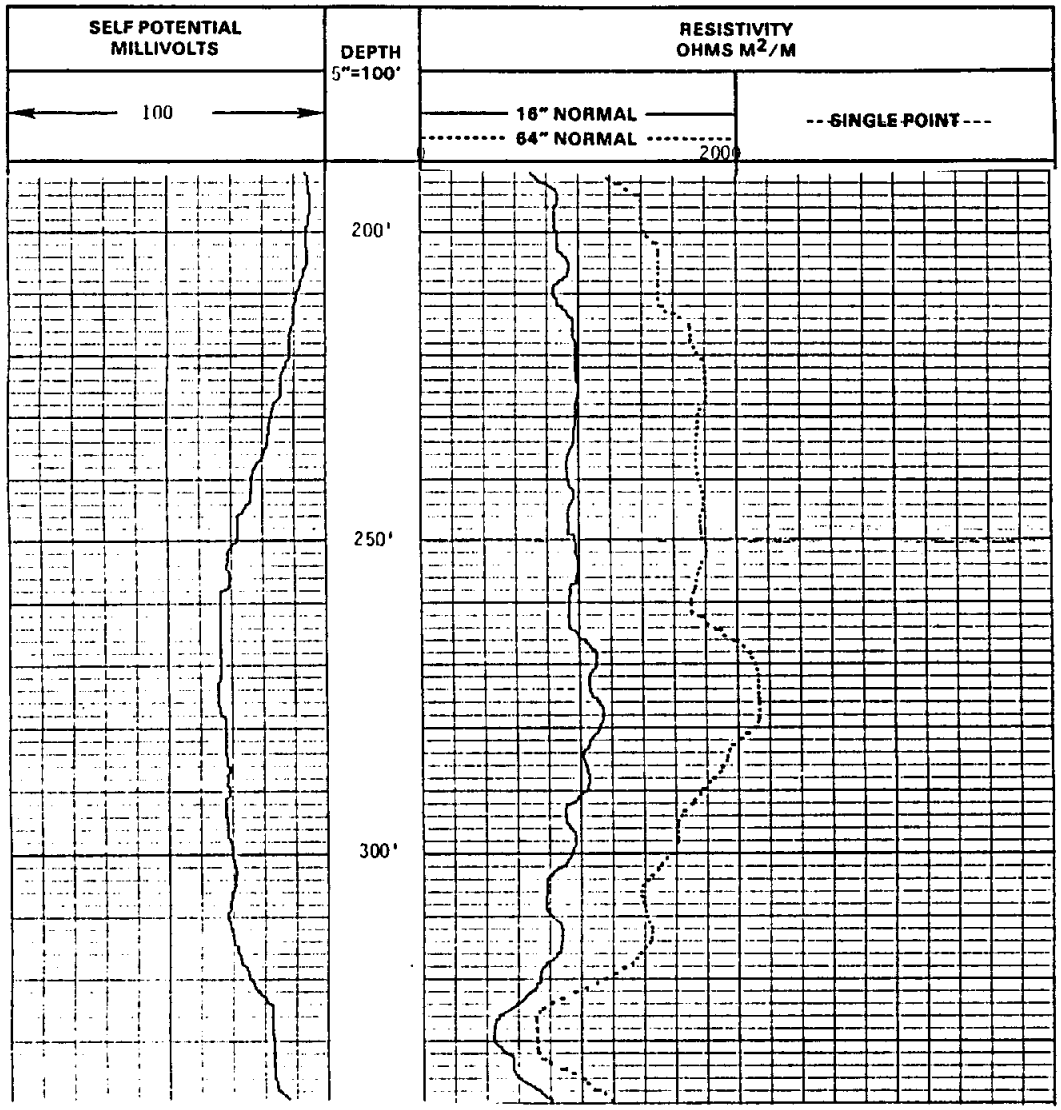

Figure 8-14. The separation between the short and long normal curves is due to the behavior of nonfocused current in a borehole with highly resistive formations (high R_a/R_m ratios). The separation has nothing to do with an invasion profile. Indeed there is very little invasion in this rock. Porosity is 1% to 3% and R_t is 1000+ ohm-meters (as obtained from other logs). The SP curve just wanders, since the carbonate is highly resistive and contains few shale beds. This log is the Ellenburger Limestone in McCulloch County, Texas. The well is the TWDB Brady Test Hole #2 (state well number 42-62-910). Bit size is 7⅞ inches. R_m is 23.4 ohm-meters at 44° F and R_{mf} is 15.8 ohm-meters at 45° F. Figure 7-[illegible] is also from this interval.

The short and long normal curves will read very similar after corrections for borehole size and R_a/R_m are applied. As an example, the interval from 220 feet to 230 feet corrects as follows:

1. The R_m of 23.4 ohm-meters at 44° F is adjusted to formation temperature (73° F) using equation (2-4). 23.4 ohm-meters x $^{44}/_{73}$ = 14 ohm-meters
2. Figure 8-12 is used to correct the short normal curve. Using $R_{16"}$ = 1000 ohm-meters and R_m = 14 ohm-meters, $R_{16"}/R_m$ = 71 and $R_{16"}$-corr/R_m = 75. $R_{16"}$-corr is 1050 ohm-meters.
3. Figure 8-13 is used to correct the long normal. Using $R_{64"}$ = 1800 ohm-meters and R_m = 14 ohm-meters, $R_{64"}/R_m$ = 129 and $R_{64"}$-corr/R_m = 90. $R_{64"}$-corr is 1260 ohm-meters.
4. The short and long normal curves now agree much better: 1050 ohm-meters and 1260 ohm-meters respectively.

curves and is a good reference on invasion corrections. Despite their availability, departure curves are not worth using because:

1. High porosity ground-water aquifers will normally have shallow invasion and thus do not require corrections.

2. Low porosity formations will have deeper invasion that may require corrections, but these formations will usually have thinner beds and/or alternating porous and nonporous intervals. Curve shapes become very distorted in these environments. It is very difficult to derive an accurate resistivity value to use in a departure curve.

3. Three resistivity curves (short normal, long normal, and lateral) are required in order to make the correction. Often only two curves are available. A single-point resistance curve cannot be used as one of the three curves.

4. The charts are not simple to use.

The following guidelines are an alternative to using departure curves:

1. The long normal or the lateral curve is used as Rt in high porosity formations. If both curves are available, they should be compared.

2. The lateral is used as a quick approximation of Rt in low and moderate porosity formations.

3. Hilchie (1979) suggests using the following empirical relationship to calculate Rt:

$$Rt \approx \frac{R_{64''} \times R_{64''}}{R_{16''}} \qquad (8\text{-}2)$$

Electrode spacing. The ratio of the AM spacing to bed thickness has considerable effect on curve response, especially for resistive beds. (This is one of the auxiliary tool responses mentioned in Chapter 7 in the **Vertical Resolution** section.) Figures 8-15 and 8-16 illustrate the curve responses for resistive and conductive beds of varying thicknesses. Resistive beds are by definition beds that have a higher Rt than the adjacent or shoulder beds. Conductive beds have a lower Rt than adjacent beds. Figure 8-17 illustrates the curve response in highly resistive formations.

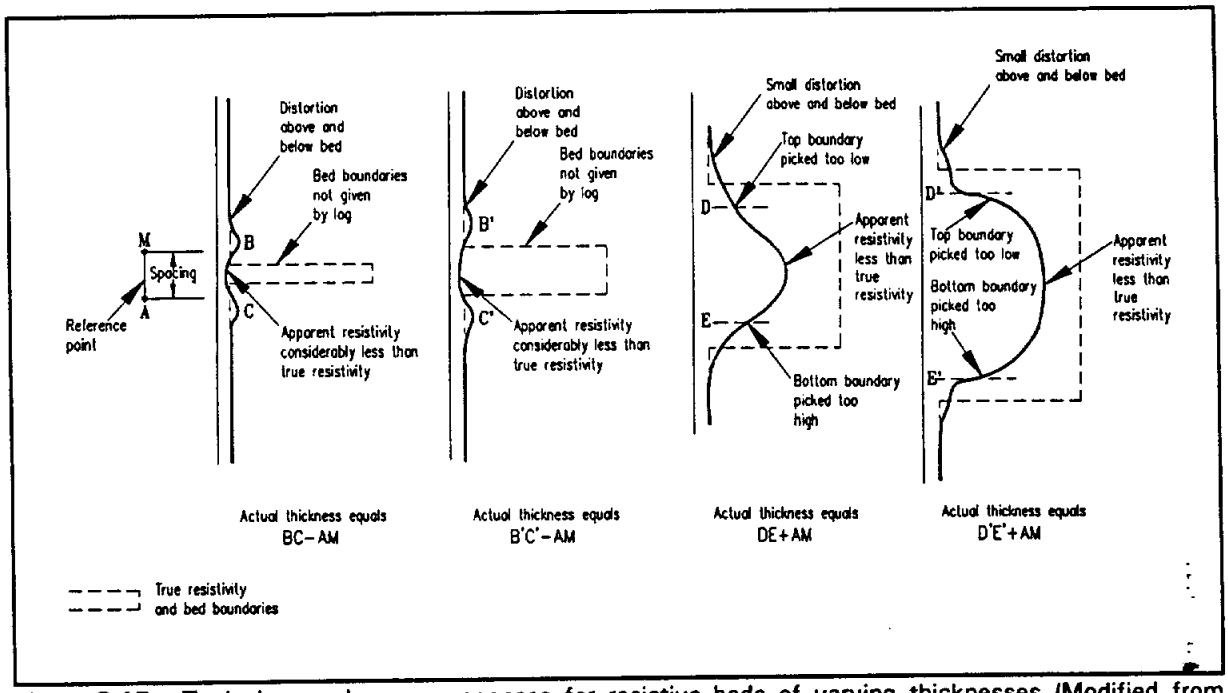

Figure 8-15. Typical normal curve responses for resistive beds of varying thicknesses (Modified from Guyod, 1944).

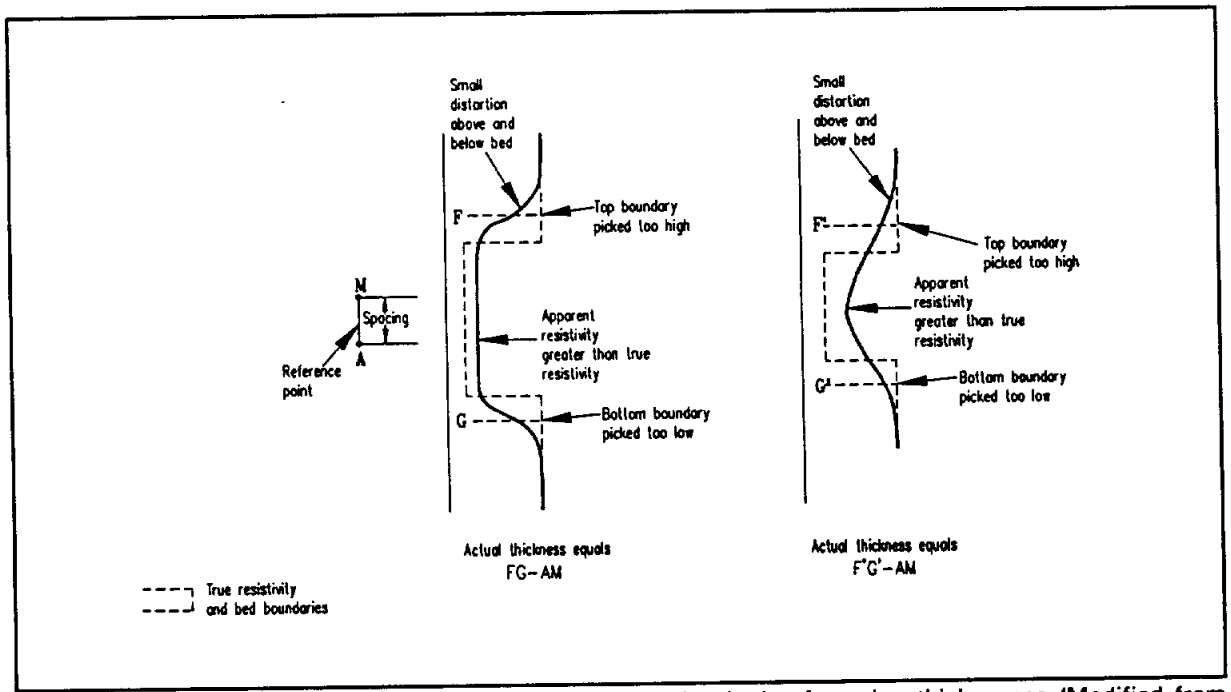

Figure 8-16. Typical normal curve responses for conductive beds of varying thicknesses (Modified from Guyod, 1944).

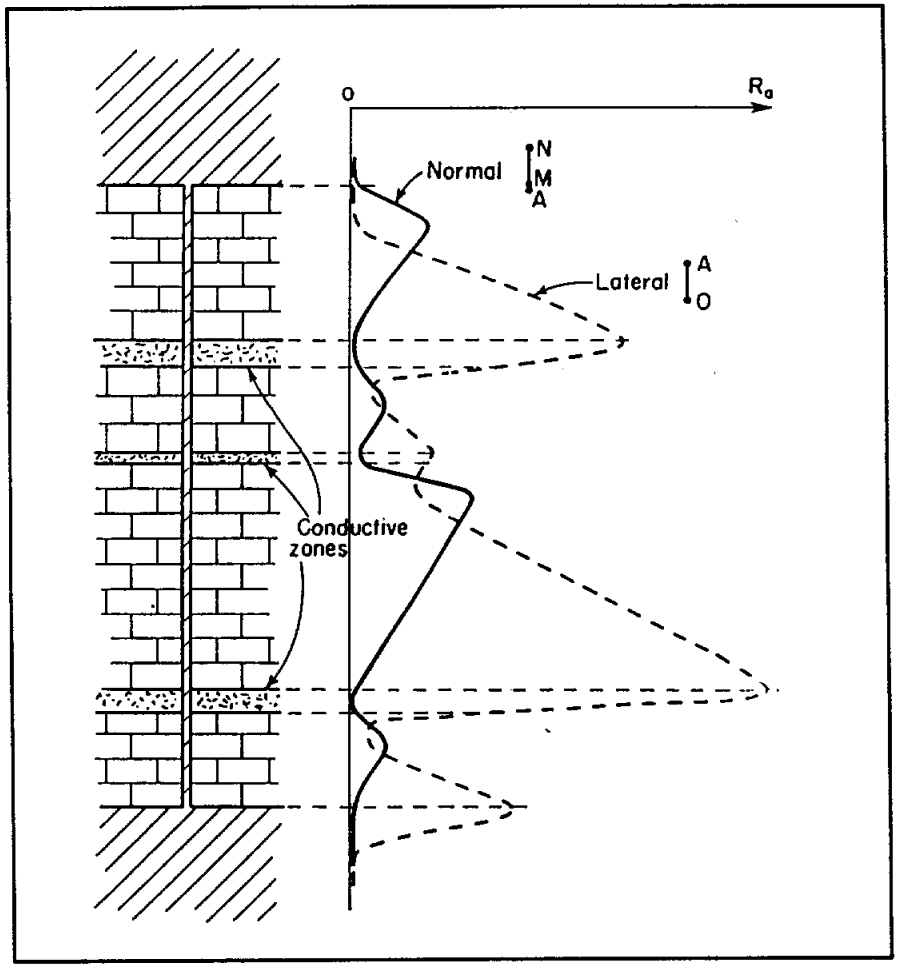

Figure 8-17. Normal and lateral curves take on asymmetrical triangular curve shapes in highly resistive formations. AMN and AO are the electrode spacings (From Schlumberger, 1949).

Interpretation:

Normal curves should be interpreted according to the following guidelines:

1. Resistivity values are picked at the point of maximum deflection.

2. Normal curves are symmetrical in resistive beds that have less than about 200 ohm-meters (Douglas Hilchie, personal communication, 1986) and in conductive beds.

3. Bed boundaries are not sharp because the tool is averaging a sample volume equal to the diameter of the AM spacing.

4. Resistive beds appear thinner than they are by an AM spacing (½AM spacing at the top and ½AM spacing at the bottom). Refer to Figure 8-15.

5. For resistive beds, the accuracy of R_a varies with bed thickness. Refer to Figure 8-15.

   a. Beds thicker than 4AM record the true resistivity value.
   b. For beds between 4AM and 1.5AM in thickness, as bed thickness decreases, so does the resistivity value.
   c. Beds thinner than 1.5AM "disappear" and appear to be conductive beds. Horns appear above and below the bed.

6. Conductive beds appear thicker than they are by an AM spacing (½AM spacing at the top and ½AM spacing at the bottom). Refer to Figure 8-16.

7. The thinner a conductive bed is, the higher the log resistivity. However, it always appears as a conductive bed no matter how thin it becomes. Refer to Figure 8-16.

8. Above about 200 ohm-meters (Hilchie, personal communication, 1986) resistive beds take on asymmetrical triangular curve shapes. Refer to Figure 8-17. The peak is displaced upward toward an adjacent conductive bed. It occurs a distance of AN below the upper resistive bed boundary. The curve is asymmetrical because the tool has three electrodes downhole. If two electrodes are used downhole, the curve maintains a symmetrical shape at high resistivities (Schlumberger, 1987).

9. In a low resistivity formation at the bottom of the hole, the curve will read too high and in a high resistivity formation at the bottom of the hole it will read too low (Pirson, 1963).

10. In thinly bedded sequences of varying resistivities (e.g. sand-shale or porous-nonporous carbonate sequences) the adjacent beds begin to influence each other's log values and greatly complicate the curve shapes. In order to interpret these curve shapes, Guyod (1958) did extensive modeling of normal curve shapes using analog models. His report is not easy to obtain because few copies were printed and it was only published as an in-house

report. However, Hilchie (1979) has included a brief summary of Guyod's analog models that is detailed enough for most work.

Recommended use. The following guidelines outline when to run normal tools:

1. In high porosity, fresh ground-water environments with beds thicker than 20 feet and in high to moderate porosity, saline aquifers with beds thicker than 20 feet, normal curves work well (Figures 8-18 and 8-19). The values will not require a correction for bed thickness and the 64" normal will read Rt. However, a R_a/R_m correction may be necessary for the fresh water formations.

2. In low porosity formations with fresh or saline water and in moderate porosity formations with fresh water, R_a/R_m values are high. The logs require a large borehole correction. Invasion may be deep, in which case the 64" normal will not record Rt.

3. For beds much thinner than 20 feet, focused tools (induction, guard, and latero) will give much more accurate resistivity values (Figures 8-20 and 8-21).

4. Normal curves are not the best resistivity tools for detailed lithological characterization of formations.

    a. They do not do a good job of detailing thin, impermeable streaks such as shale beds and tightly cemented intervals in sandstones.
    b. Neither do they do a good job of delineating thin porous and nonporous intervals in carbonates (Figures 8-20 and 8-21).

5. If the N electrode is the cable armor, the tool cannot log closer than the AN spacing to fluid level or metallic casing.

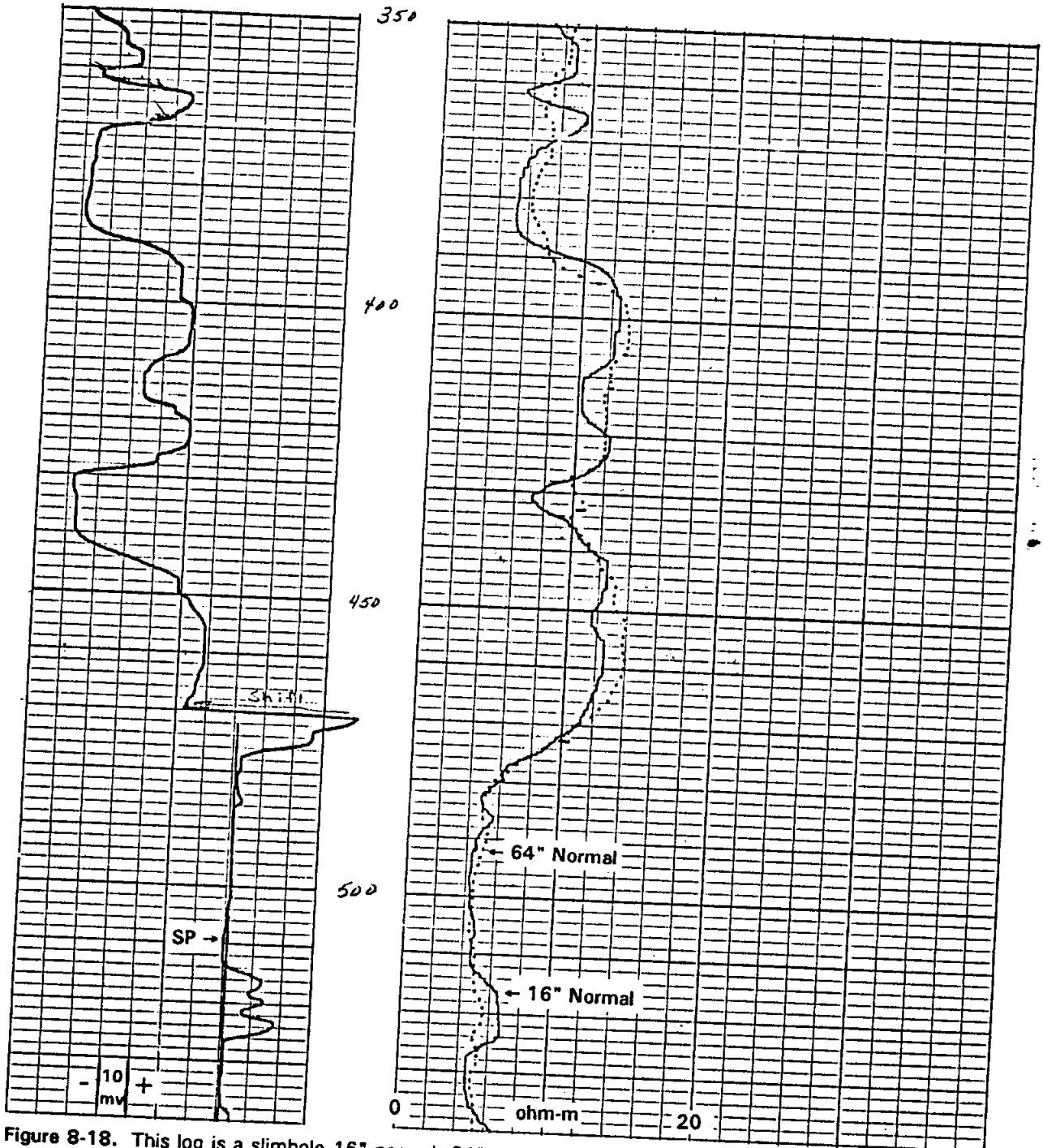

Figure 8-18. This log is a slimhole 16" normal, 64" normal, and SP. A comparison with the deep induction-guard curves ran in the same borehole (Figure 8-19) confirms that normal curves work well in high porosity formations thicker than 20 feet. The 64" normal agrees very well with the deep induction even without borehole corrections to either curve. The 16" normal, with its deeper depth of investigation, reads higher than the guard. Another explanation for the difference is that the amount and depth of mud filtrate invasion has changed between logging runs. (The normal curves were run while the well was being drilled, 13 days before the induction log.) See Figures 8-19 and 12-7 for further details on this well.

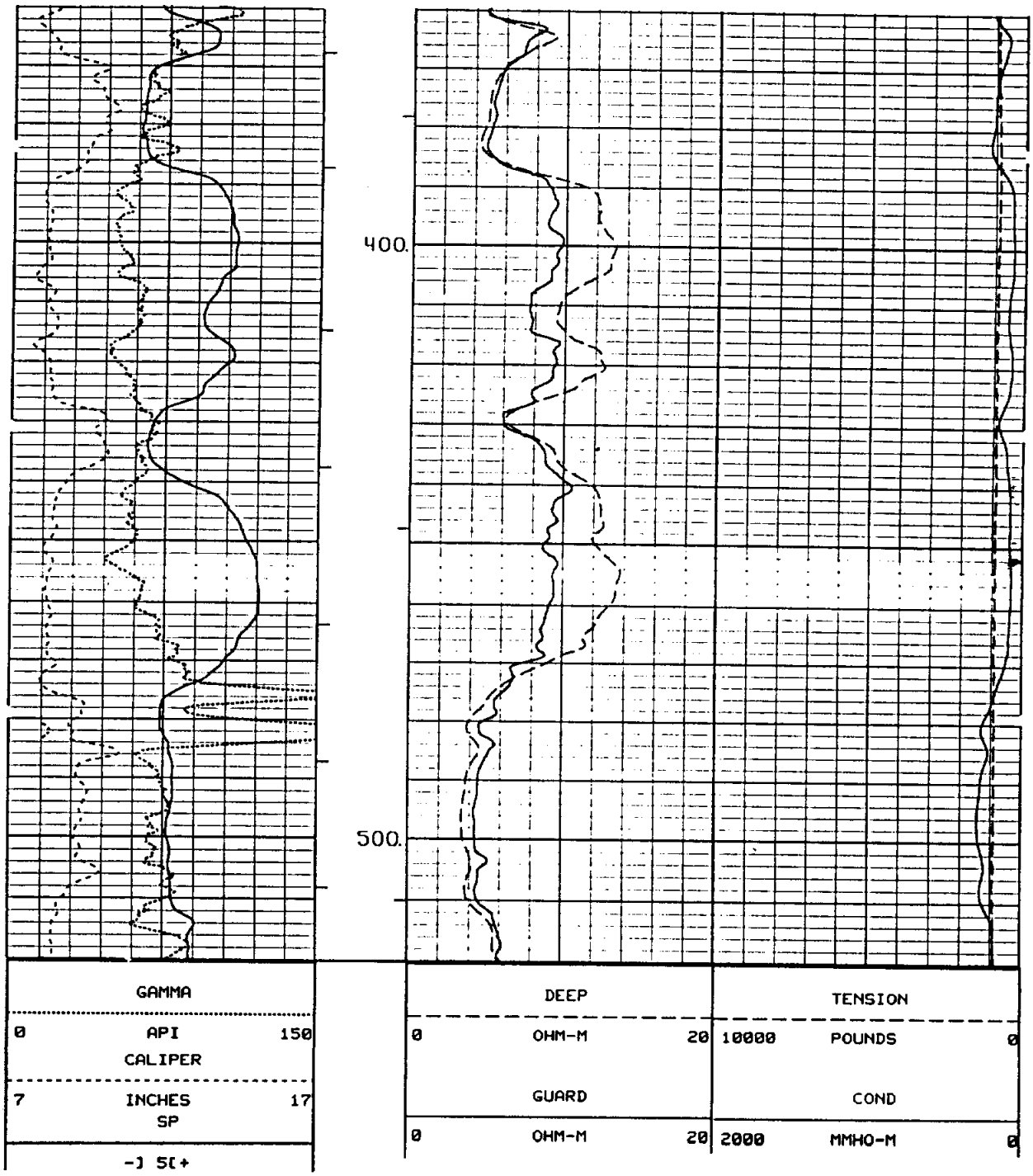

Figure 8-19. This log is a conventional deep induction, guard, SP, and gamma ray. It was run in the same borehole as the log in Figure 8-18. The guard curve has better vertical resolution than the deep induction and both curves have better resolution than the normal curves in Figure 8-18. Porosity in these sands is 30 to 36 percent. The lithology is a sand-shale sequence in Cameron County, Texas. The well is the TWDB-PUB Test Well Site F (state well number 88-59-410). Borehole size is 8.5 inches. Borehole fluid is bentonite based drilling mud with an R_m of 2.1 ohm-meters at formation temperature (89° F).

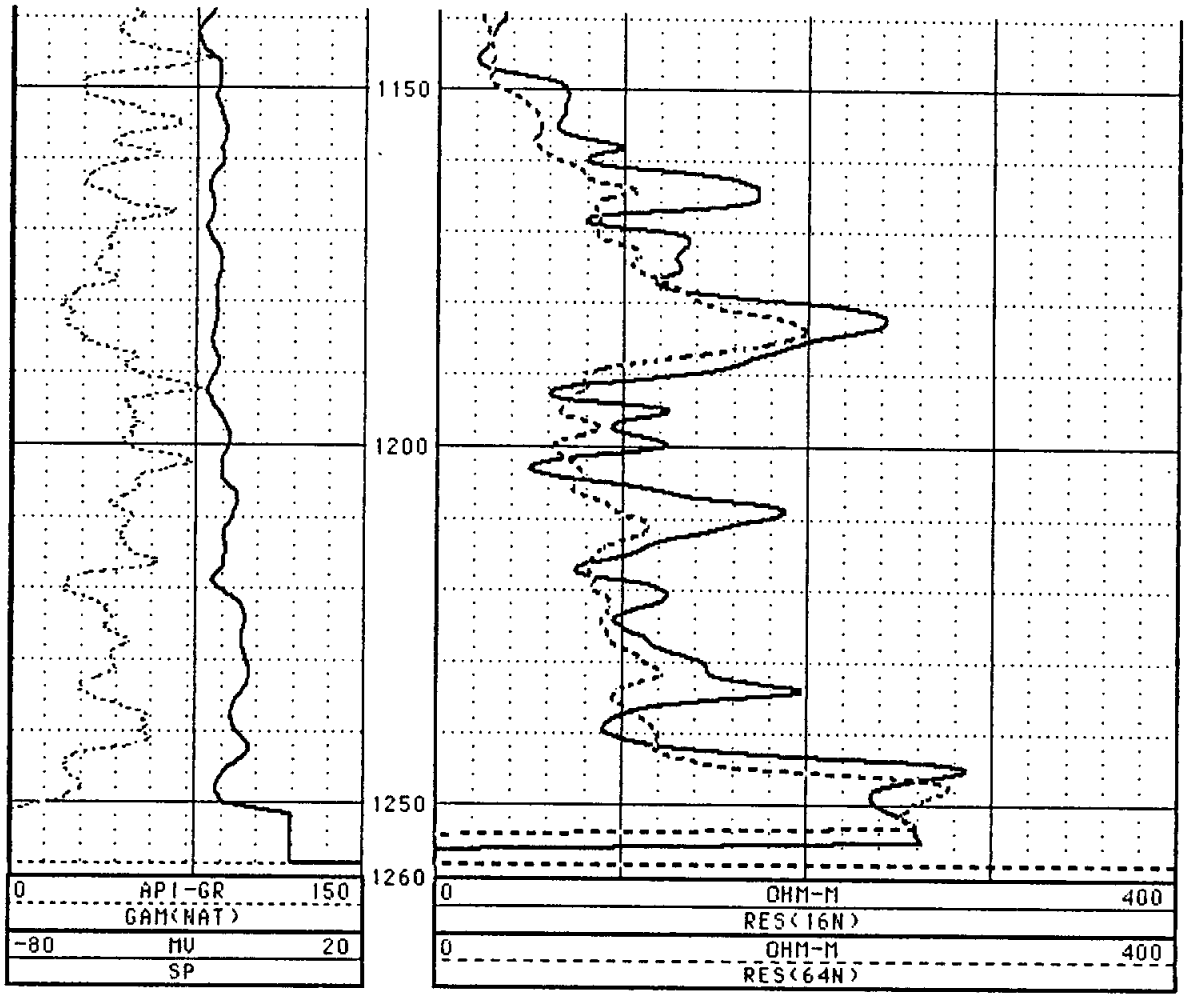

Figure 8-20. This log illustrates several of the problems inherent in interpreting normal curves:

1. Resistive beds appear thinner than they are by an AM spacing. The long normal curve between 1180 and 1190 feet shows the bed to be thinner than it actually is by about 5 feet, which is the AM spacing (64"). The short normal curve with a smaller AM spacing (16") is closer to the actual bed thickness.
2. Resistive beds thinner than the AM spacing disappear. This is especially evident on the long normal at a number of depths (1158 feet, 1195 feet, 1200 feet, and 1220 feet).
3. Thin conductive beds have resistivities that are too high. This is why the long normal reads higher than the short normal from 1237 to 1242 feet.

This slimhole log should be compared with laterologs from the same hole (Figure 8-21). The lithology is predominately limestone with thin shale beds. Porosity ranges from 9 to 15 percent. The log is the Cow Creek Limestone Member of the Pearsall Formation, Trinity Group, Travis County, Texas. The well is the TWDB, Balcones Research Center Test Well (state well number 58-35-721). Borehole size is 6 inches. Borehole fluid is water with an R_m of 4.5 ohm-meters and an R_{mf} of 4.1 ohm-meters at formation temperature (101° F).

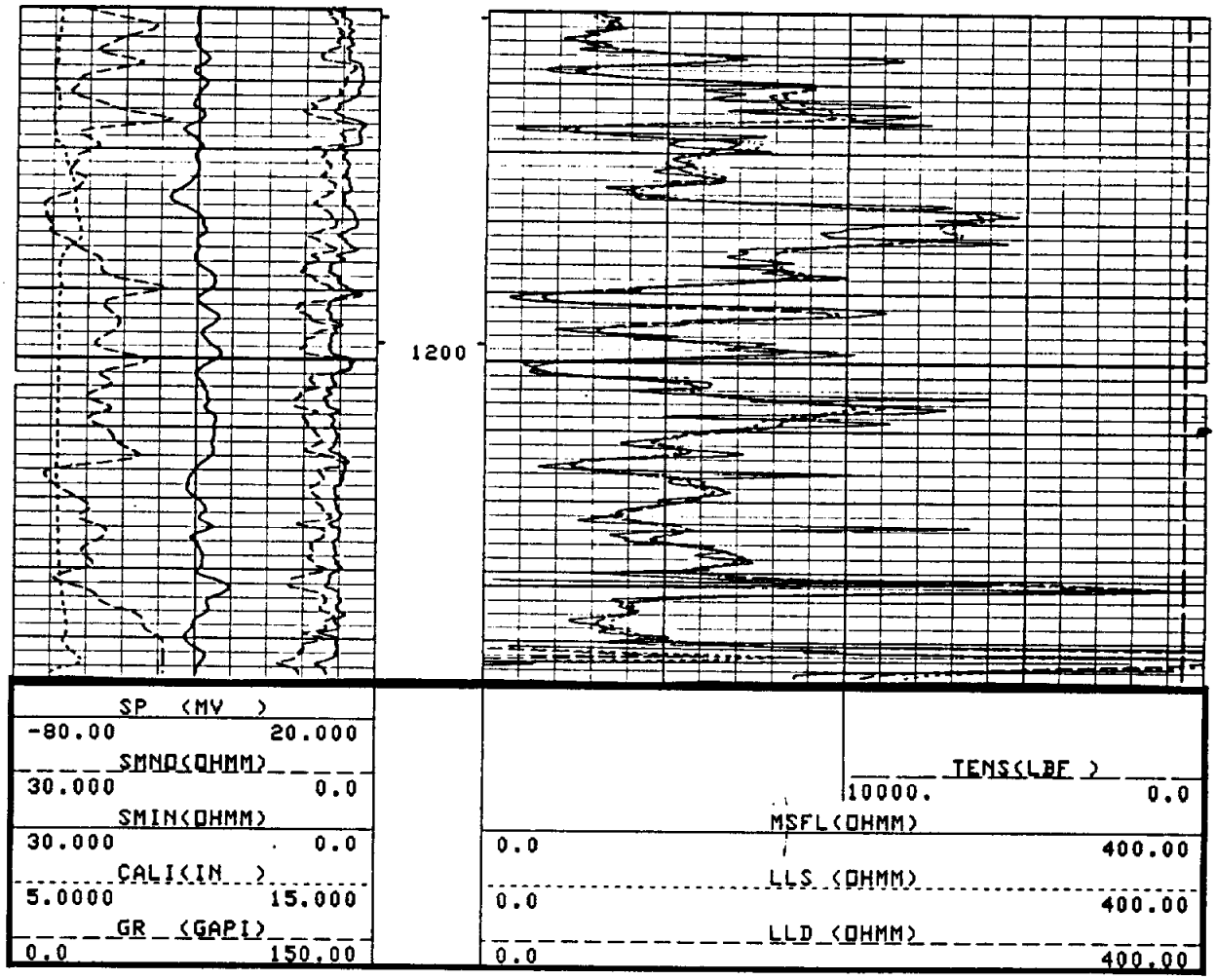

Figure 8-21. The resistivity curves are a deep laterolog (LLD), shallow laterolog (LLS), and a microspherically focused log (MSFL). A comparison of these curves with the normal curves in Figure 8-20 demonstrates the superior vertical resolution of the laterolog and the even better resolution of the MSFL tool. The SMNO and SMIN curves in Track 1 is a microlog. "S" is Schlumberger's designation for a particular model of microlog. The caliper curve shows the hole to have only one washout (1170 to 1184 feet). The intervals with high gamma ray counts such as at 1190 feet are shaly zones. Note that these ~~curves~~ are two feet ~~high to~~ the curves in Figure 8-20. For further information on this well see Figure 8-20.

Lateral

The first log ever run was a lateral or three-electrode curve (Hilchie, 1979). Until the 1950's, resistivity logging suites were a combination of lateral and normal curves. Today a 6 foot slimhole lateral is run by a few ground-water logging companies. The tool has no trade name.

Even though the lateral tool is seldom run today in Texas, ground-water log analysts still need to be familiar with lateral log responses. Petroleum and ground-water log files are full of pre-1960 lateral logs. A ground-water study anywhere in Texas will include a sizable percentage of these logs.

Tool theory. Tool theory is summarized in Figure 8-11. The electrode spacing (AO) ranges from 5 to 24 feet, but 18'8" became the predominate spacing in the petroleum industry. Halliburton designated their electrode spacing 3iZ.

Depth of investigation equals the electrode spacing. A long tool spacing gives the lateral the greatest depth of investigation of any nonfocused electrode tool. The tool usually measures Rt.

Log presentation. The standard oilfield presentation in Texas was a solid lateral curve in track 3. The presentation varied in other parts of the country.

Environmental corrections. Eccentricity of the tool in the borehole, mudcake thickness, and mud weight have no effect on the curve (Pirson, 1963). Departure curves are available for bed thickness, adjacent bed effects, borehole size, Ra/Rm, and invasion. Published departure curves can be used for any brand of tool.

Borehole corrections. The definition and sharpness of the curve decreases as hole size increases and as mud resistivity decreases. Borehole effects become significant when Ra/Rm is greater than 20 (Figure 8-22). Ra is greater than Rt in these cases. Ra is $R_{18'8"}$ in Figure 8-22. Rm must be converted to formation temperature before using the chart. Enter the chart with the $R_{18'8"}$/Rm value, move horizontally to the hole diameter, and then move vertically to read $R_{18'8"corr}$/Rm. This value times Rm equals Rt.

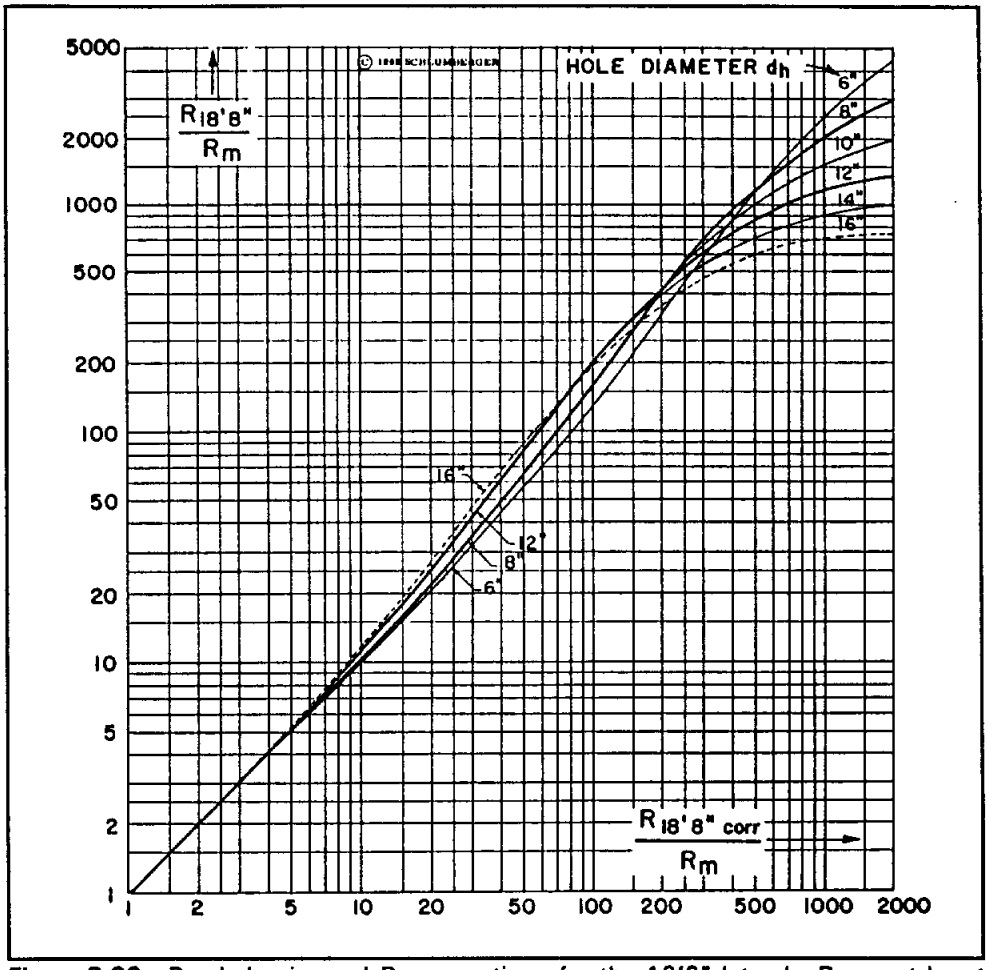

Figure 8-22. Borehole size and Rm corrections for the 18'8" lateral. Rm must be at formation temperature (SPWLA, 1979, after Schlumberger).

Bed thickness and adjacent bed corrections. Bed thickness effects become significant when bed thickness is less than twice the tool spacing (Jorden and Campbell, 1986). This correction is seldom made.

Invasion corrections. Departure charts are available but are seldom used. (See this same section under normal tools for further explanation).

Electrode configuration. The effect of the electrode configuration makes the curve very difficult to interpret. Figures 8-23 and 8-24 illustrate the curve responses for resistive and conductive beds of varying thicknesses.

Interpretation.

The following guidelines should be used to ~~determine~~ interpret lateral curves:

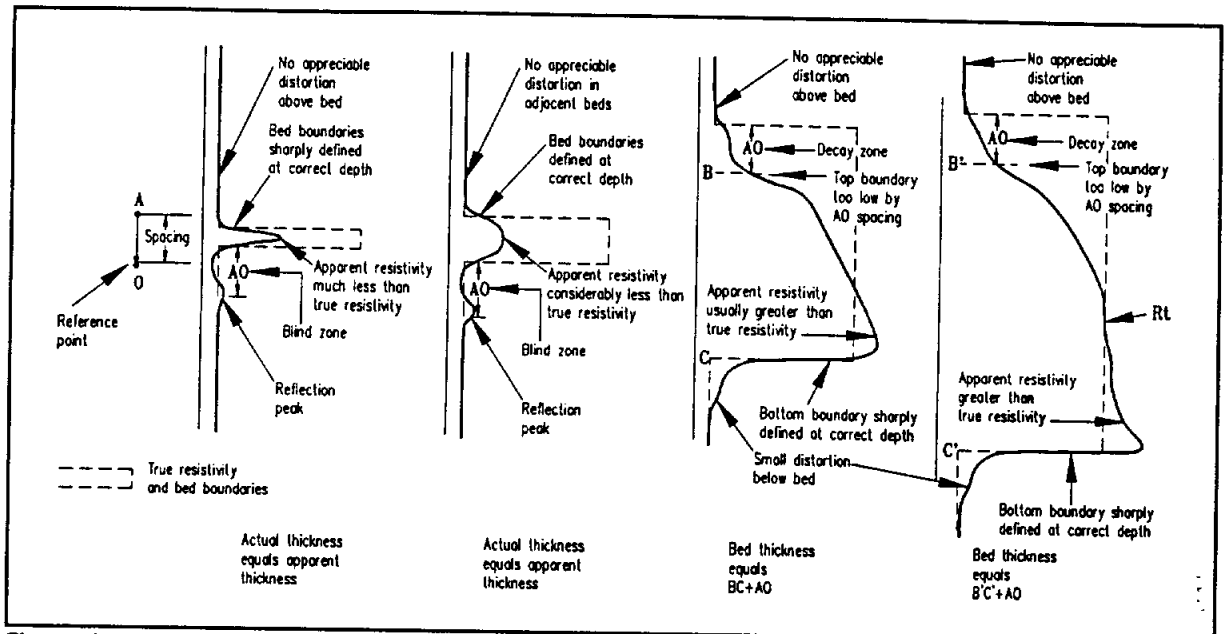

Figure 8-23. Typical lateral curve responses for resistive beds of varying thicknesses (Modified from Guyod, 1944).

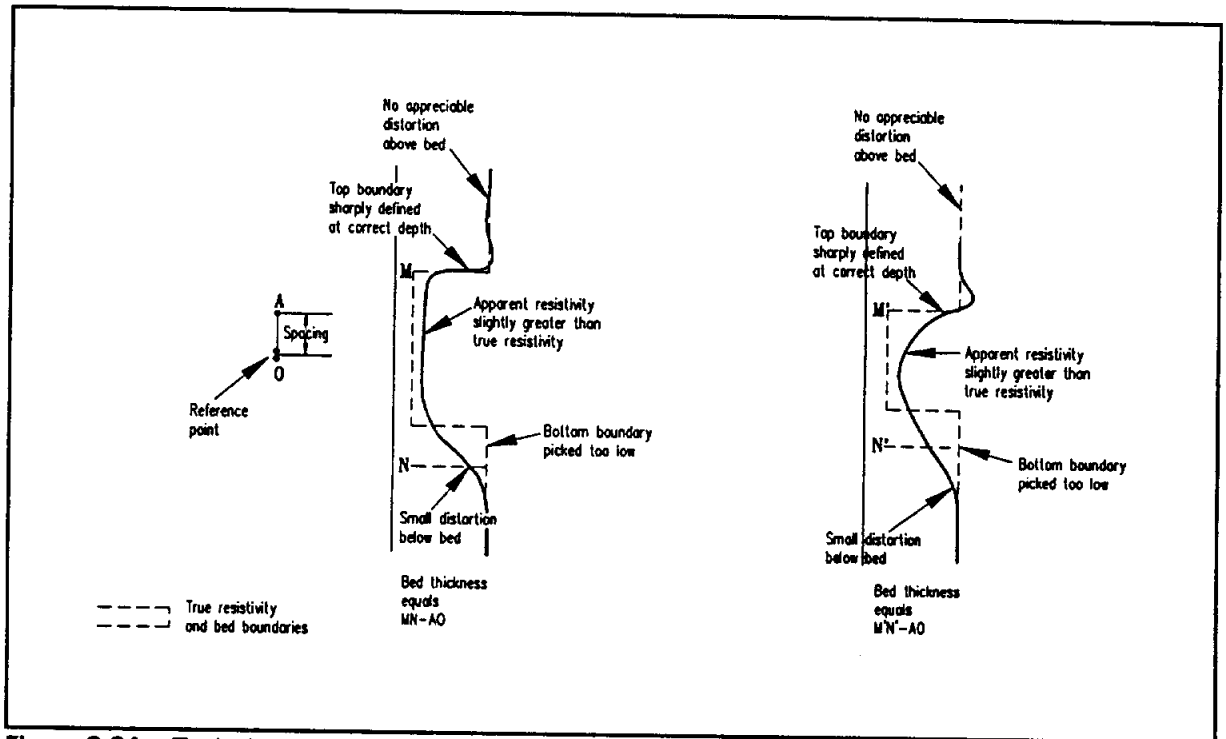

Figure 8-24. Typical lateral curves for conductive beds of varying thicknesses (Modified from Guyod, 1944).

1. All lateral curves are asymmetrical (Figures 8-23 and 8-24).

2. Resistive beds, no matter how thin, always appear to be resistive (Figures 8-23 and 8-24).

3. In thick resistive beds only one spot on the curve is R_a and the location of that point varies with bed thickness (Figures 8-25 and 8-26). The rest of the curve is an artifact of the electrode configuration (Figure 8-23).

    a. A decay zone with a very low resistivity is present at the top of the bed. It has a length equal to AO.
    b. The base of the bed has too high a resistivity.
    c. A "low resistivity" notch is sometimes present at the upper bed boundary.
    d. The lower bed boundary is sharp and is correctly defined by the curve.
    e. Below the base of the bed it takes an AO spacing for the curve to return to the value of the adjacent bed.

4. Resistive beds thinner than the AO spacing have the following characteristics (Figure 8-23):

    a. R_a is much less than R_t.
    b. Both bed boundaries are sharply defined at the correct depths.
    c. A reflection peak consisting of an increase in resistivity is present at an AO spacing below the base of the bed.
    d. Between the base of the bed and the reflection zone is a blind zone. The curve shape of the blind zone always appears to be a conductive bed, but it in no way reflects the true resistivity of this interval. The zone may be conductive or resistive, there is no way to tell from the lateral curve. However, the normal curves will reveal the resistivity of the zone.

5. Conductive beds are easier to interpret (Figure 8-24).

    a. The upper bed boundary is sharply defined by the curve at the correct depth. A "high resistivity" notch is also present at the bed boundary.
    b. The lower bed boundary is harder to define. The curve gradually trails off to the value of the adjacent bed.

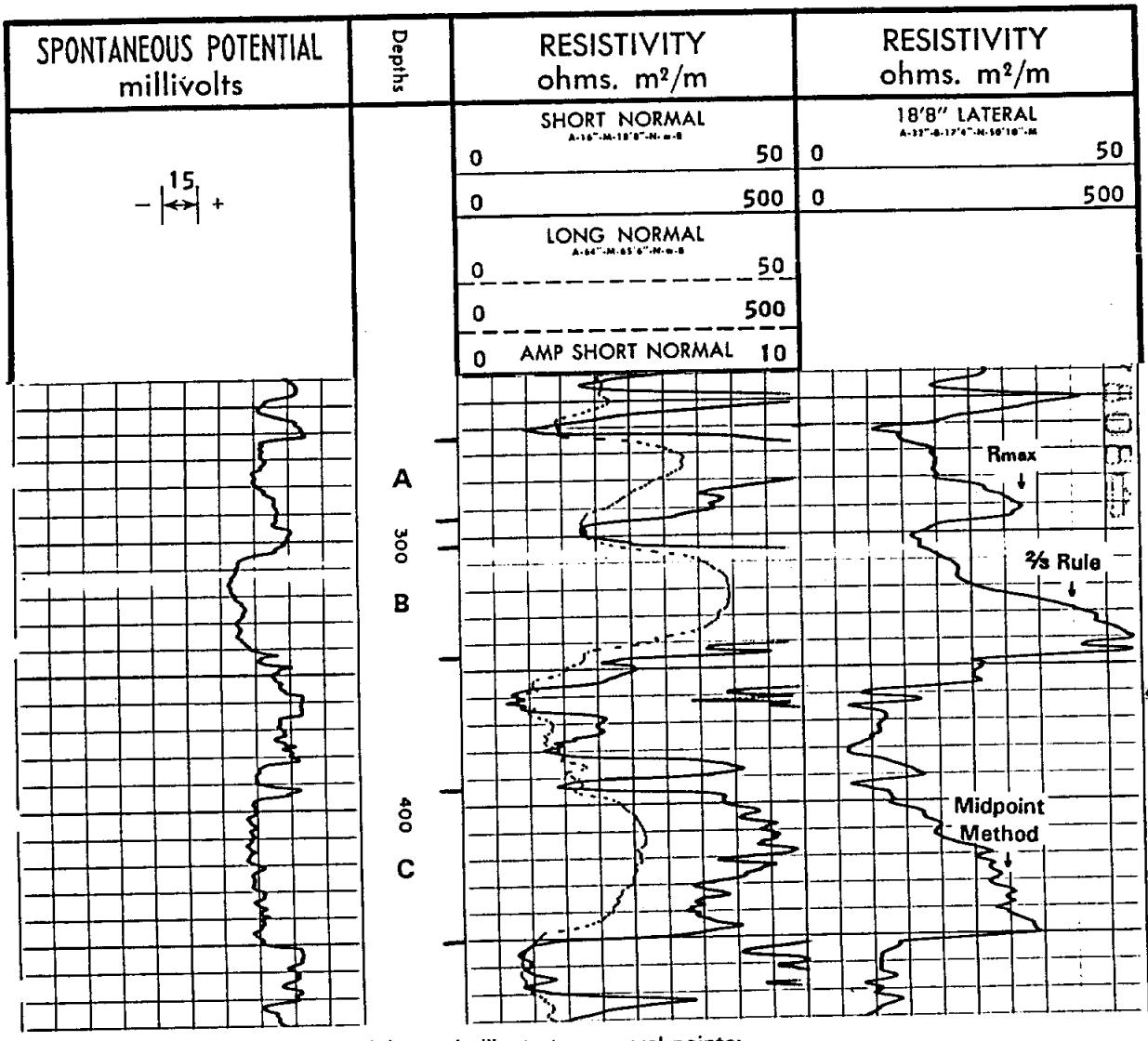

Figure 8-25. This suite of resistivity tools illustrates several points:

1. Resistive beds, no matter how thin, remain resistive on the lateral curve while on the long normal beds thinner than 5 feet disappear (look at 250 feet and 382-90 feet). In many respects the lateral has better resolution than the long normal, but not as good as the short normal.
2. Zones A, B, and C illustrate how to pick R_a from the lateral curve for beds of varying thicknesses as detailed in Figure 8-26. Bed A is 33 ohm-meters, bed B is 40 ohm-meters and bed C is 27 ohm-meters. For each zone only one spot on the curve is R_a. The 18'8" decay zone at the top of each bed bears no resemblance to R_a.
3. In zones A, B, and C the lateral and long normal curves read identical R_a's. This indicates that mud filtrate invasion is shallow and that both curves are reading R_t. One would expect this to be the case in high porosity sandstones such as these.
4. In Zone C the short normal shows thin shale laminations in the sandstone. The long normal gives no hint of their presence, but both the SP and the lateral confirm their presence.

The curve going off scale in Track 2 is an amplified short normal, which is a short normal curve with an expanded scale (in this case 0 to 10 ohm-meters rather than 0 to 50 ohm-meters). The lithology is alternating sands and shales. The hole size is 6¾ inches. The borehole fluid is native mud. R_m is 10 ohm-meters at 87°F. A bottom hole temperature was not available. The well is the Layne Texas, Gum Springs Water Supply Corp. Area Test #6-66 in Harrison County, Texas.

Midpoint Method. Use for beds thicker than 2AO (40 feet for an 18'8" tool). Locate the point midway between the top and bottom of the bed. Move an AO spacing below the midpoint and use the resistivity value at this point as R_s.

⅔ Rule. Use for beds between 2AO and 1.5AO in thickness (about 40 feet to 28 feet for an 18'8" tool). Go down an AO spacing from the top of the bed. From this point move two-thirds of the distance toward the peak value at the base of the bed and read R_s. Note: If the bed has a backup curve, the scale changes for the backup curve. Therefore, two-thirds of the distance no longer corresponds to two-thirds of the difference between the two resistivity values. Use two-thirds of the difference as R_s.

R_{max}. Use for beds between 1.5AO and 1AO in thickness (about 28 feet to 18 feet for an 18'8" tool). Take the peak value for R_s.

Thin beds. Use for beds less than 1AO in thickness (less than 18 feet for an 18'8" tool). The equation shown ~~above~~ gives an approximation of R_s. R_s is usually at least 4 times R_{max} (Hilchie, personal communication, 1986).

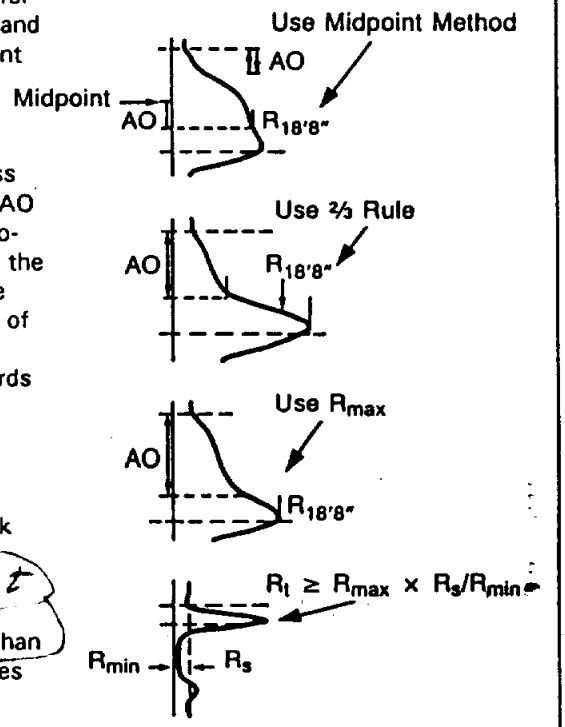

Figure 8-26. Guidelines for picking the lateral resis of varying thicknesses when the surrounding beds are homogenous. The Rt. AO is 18' 8". R_s is the resistivity of the side bed (Modified from Schl

c. As the bed thickness decreases, ity value increases but the curve continues to read close to Rt.
d. Use the lowest value in the lower half of the bed as the resistivity of the bed.

6. In a low resistivity formation at the bottom of the hole the curve will read too low and in a high resistivity formation at the bottom of the borehole it will read too high (Pirson, 1963).

7. Resistive adjacent beds greatly influence the log response and can make the log all but impossible to read. Hilchie (1979) and Guyod (1958) are good references for explanations of the complex curve shapes that can be generated by the tool.

Recommended use. The following guidelines can be used to determine when to run a lateral tool.

1. Lateral curves are so difficult to interpret that they should not be a part of modern slimhole logging suites.

2. In massive sandstones (thicker than 2AO) the curve will yield a good Rt value.

3. In thin interbedded sandstones such as the Trinity and Paleozoic aquifers and in carbonate aquifers such as the Edwards the curve is very difficult to interpret because the curve responses interfere with one another.

Limestone lateral

The limestone lateral is a double lateral tool. It was designed to detect porous intervals in massive carbonates. Most of the logs were run in West Texas between 1945 and 1956. Its popularity declined after the introduction of the microlog (Frank, 1986).

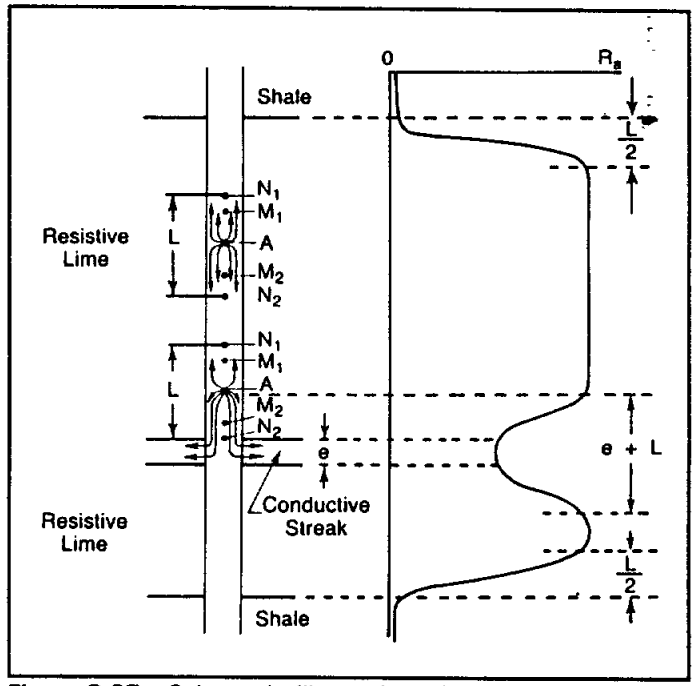

Figure 8-27. Schematic illustration of the limestone lateral curve shapes of a very low porosity zone and a porous (conductive) zone (From Frank, 1986).

The curve is symmetrical (Figure 8-27). In a zone with very low porosity, Ra is a function of borehole size and Rm. Ra remains constant until the tool is opposite a conductive (porous) zone. Resistivity decreases in a conductive bed. On the log the height of the conductive bed is the bed thickness plus the length of the electrode array (L in Figure 8-27). The electrode array was usually 32 inches (a few were 37½ inches). In a conductive bed the tool measures Ri.

Figure 8-28 is an example log. The limestone lateral was recorded in Track 2 along with a 10 inch normal. A 19 foot lateral is in Track 3.

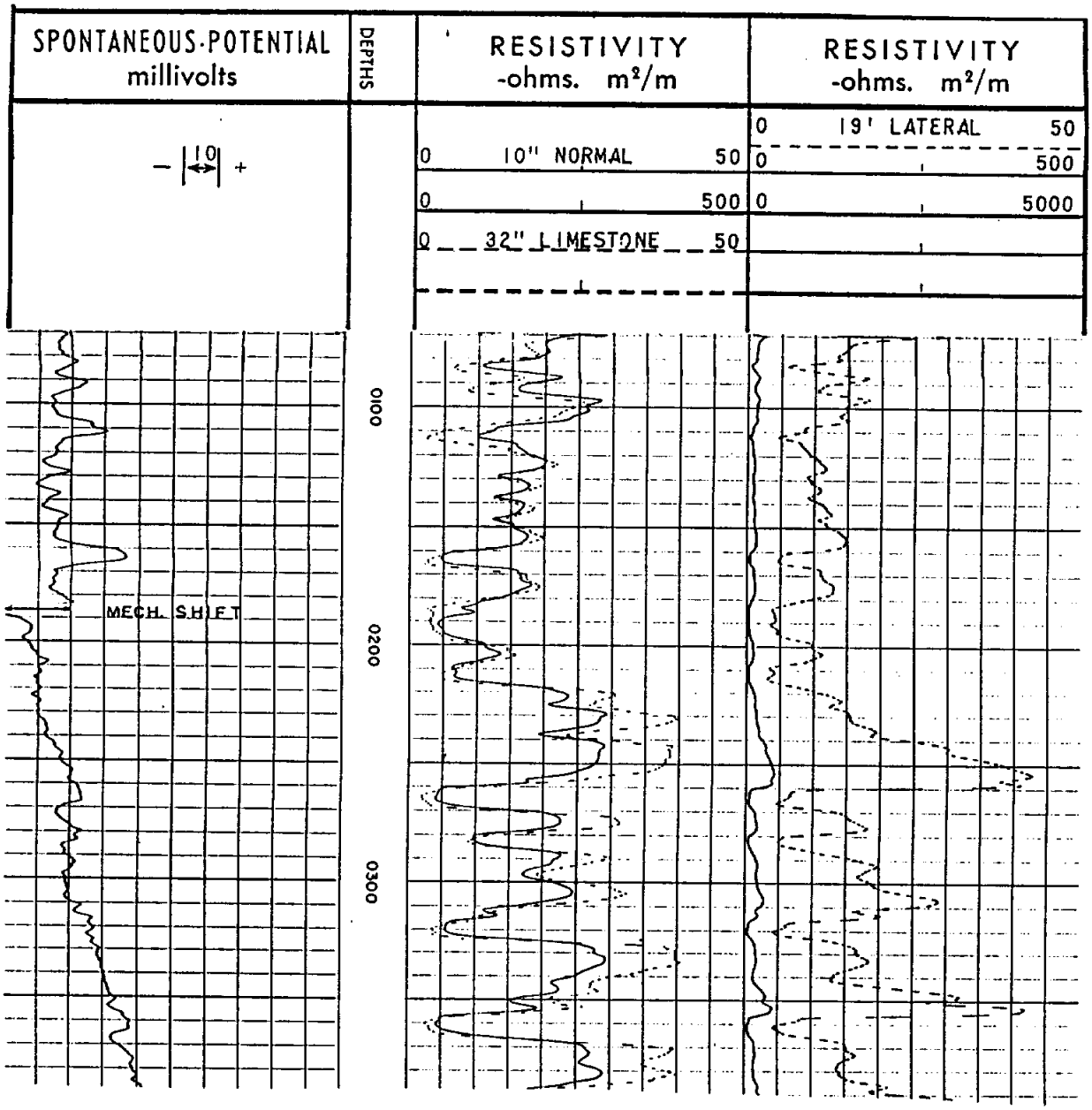

Figure 8-28. An example of a limestone lateral log in a water well. The formations are not low porosity, so the limestone and 10 inch normal curves are very similar. The well is the Layne Texas, Phelps Dodge #4, El Paso County, Texas. Bit size is 7⅞ inches. R_m is 6.6 ohm-meters at 76° F. Bottom hole temperature was not recorded.

An approximate porosity can be calculated with the limestone lateral. Hilchie (1979) explains the porosity calculations.

NONFOCUSED PAD MICROELECTRODE TOOLS

The nonfocused microelectrode tool, commonly called the microlog, was introduced in 1948. Microlog is Schlumberger's commercial name that has become a generic name. Today the tool is also called a Minilog (Atlas Wireline). In the past it was also referred to as a Contact log, Permalog, Micro-contact log, and Micro-survey log.

In many areas of Texas the tool is still used extensively by petroleum logging companies. It is occasionally run in water wells, most commonly in the Trinity aquifer. Slimhole micrologs are rare. Micrologs are very abundant in petroleum log files from the 1950's. Usage tapered off in the 1960's with the introduction of modern porosity tools. Old ground-water log files, especially Trinity wells occasionally contain a microlog.

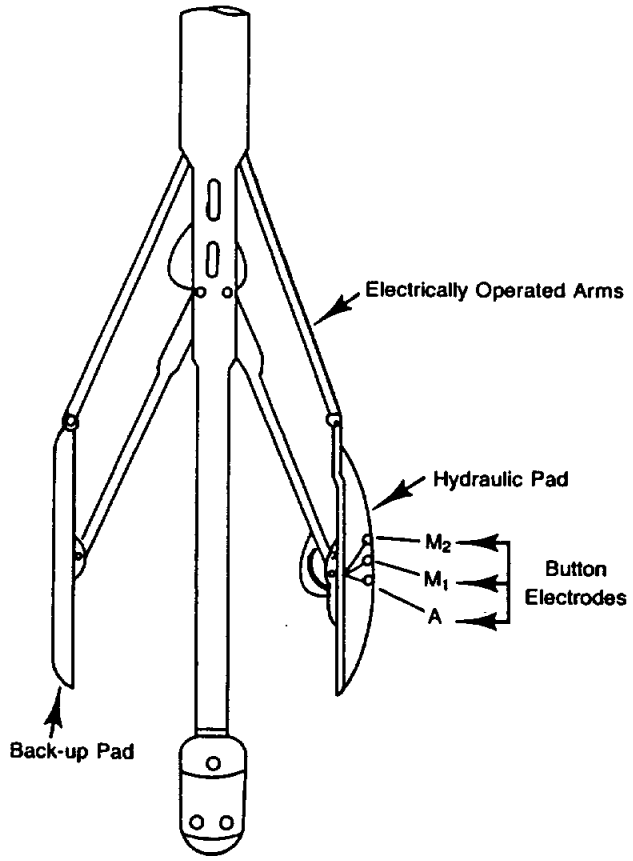

Figure 8-29. Schematic diagram of a microlog (Helander, 1983).

Tool theory. The microlog tool consists of three dime-size electrodes imbedded 1 inch apart in a rubber pad (Figure 8-29). The original hard rubber pad (Type D) was replaced by a hydraulic pad (Type H). The rubber pad shields the electrodes from the short-circuiting action of the drilling mud. The pad is pressed against the borehole by means of two arms

(Figure 8-29) which at the same time make a caliper measurement. The caliper measures the borehole diameter with an accuracy of ⅛ inch (Schlumberger, 1958). Up until about 1956 the arms were actually bowsprings. The bowspring was not flexible enough and so the caliper measurement was too optimistic (Douglas Hilchie, personal communication, 1986).

The tool can only be run coming up the hole. The pad overrides the mudcake and makes two resistivity measurements (Figure 8-30): a 2 inch normal measurement (2" Micronormal) between electrodes A and M_2 (Figure 8-29) and a 1 inch by 1 inch lateral type measurement (1" × 1" or 1½" Microinverse) from electrodes A to midway between M_1 and M_2 (Figure 8-29). The micronormal has a deeper depth of investigation than the Microinverse (about 4 inches verses 1.5 inches). The vertical resolution of each curve is a few inches (Schlumberger, 1958).

Log presentation. Figure 8-30 is a typical microlog. The micronormal (dashed ~~curve~~) and microinverse (solid ~~curve~~) curves are scaled in ohm-meters. The scales are usually limited to resistivities less than 20 times the mud resistivity (Rm). In petroleum wells, which usually have Rm's less than a few ohm-meters, 20 times Rm is usually the maximum microlog resistivity encountered in porous, permeable zones. Generally the resistivities of permeable zones are only a few times Rm (Schlumberger, 1958). This is why petroleum micrologs are usually scaled 0 to 20 or 0 to 40 ohm-meters. The same ratio holds true for fresh to moderately saline water wells. However, the scale may have to exceed 0 to 40 ohm-meters because Rm is usually greater than a few ohm-meters.

Track 1 usually contains a caliper and SP curves (Figure 8-30). The caliper is labeled a microcaliper by Schlumberger. The earliest micrologs did not have a caliper. If the SP curve is from the electric log a dashed curve is used. A line representing the bit size is often present.

On most old micrologs permeable zones were flagged in the depth column (Figure 8-30). Different symbols were used to denote good; good but broken; and poor permeability. The term "porosity" was used, but a more accurate term is permeability. These notations, which are interpretations of the curves, were drafted onto the log. On many modern logs positive separation is automatically shaded (Figure 7-15).

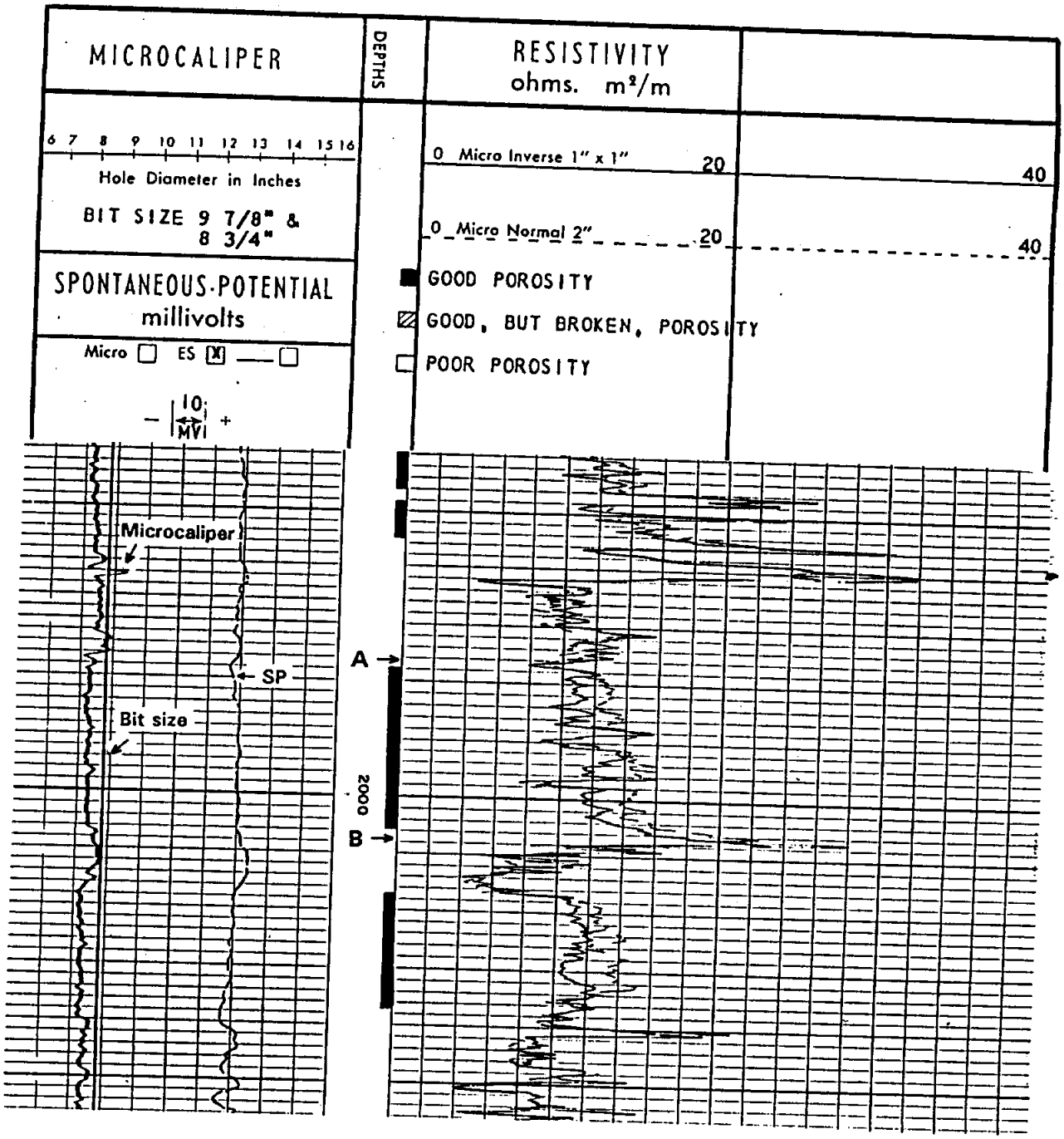

Figure 8-30. Example of a 1950's vintage Schlumberger microlog. Positive separation (micronormal resistivity greater than microinverse resistivity) denotes mudcake, which is an indication of permeability. Permeable zones (called porosity on old micrologs) are flagged in the depth column. Positive separation occurs at 1976-78 feet (A) but the microcaliper and SP curves indicate that the interval is an impermeable shale. Positive separation at 2007-08 feet (B) does not indicate permeability because the microlog resistivities are too high. The well is the Layne Texas, Chance Vought #3-A, Dallas County, Texas. R_m is 4 ohm-meters at formation temperature (90° F). The log is part of the Trinity aquifer. Figure 8-34 is also from this well.

Interpretation. If mudcake is present on the borehole wall, the micronormal (dashed curve) usually reads higher than the microinverse (solid curve). This is called "positive" separation (Figures 8-30 and 8-31). Positive separation occurs because the microinverse measures primarily the resistivity of the mudcake (R_{mc}), while the micronormal measures primarily the more resistive flushed zone (R_{xo}). Mudcake is usually limited to porous, permeable zones, so positive separation is a means of identifying permeable zones.

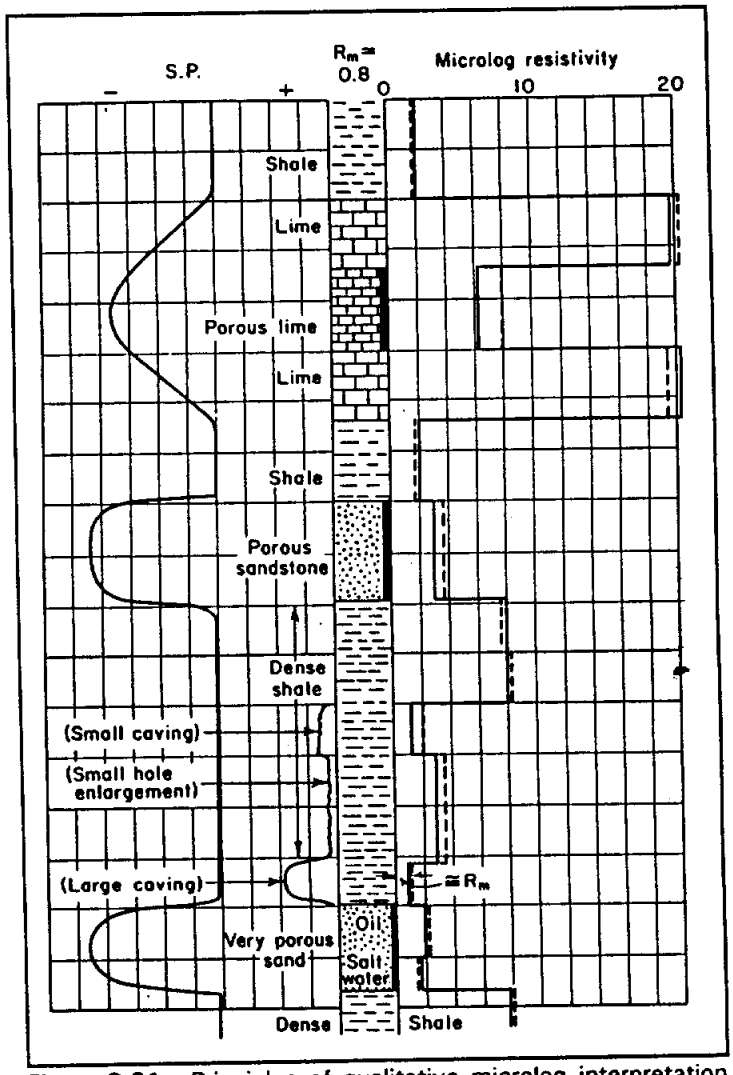

Figure 8-31. Principles of qualitative microlog interpretation (Pirson, 1963, after Schlumberger).

Impermeable zones such as shales and very low porosity carbonates do not develop a mudcake. Opposite a formation with no mudcake either the microlog curves have no separation or the micronormal reads lower than the microinverse, which is called "negative" separation (Figure 8-31). Negative separation is common in homogenous formations with no mudcake because a small negative separation is built into the tool response (Jorden and Campbell, 1986). It will also occur when R_m is greater than the resistivity of the shale, which often occurs in water wells.

Shales sometimes have slight positive separation (Schlumberger, 1958). In such cases the shale is recognizable by the fact that it has a lower microlog resistivity than either permeable sandstones or carbonates with positive separation. Shales have much lower microlog resistivities than impermeable carbonates and impermeable streaks in sandstones.

In impermeable zones with no mudcake, microlog resistivities are lower than Rt. This occurs because: (1) current leaks around the pad and (2) borehole rugosity allows mud to be present between the pad and the formation (Jorden and Campbell, 1986).

Many people interpret the microlog too casually. Microlog interpretation is not always straightforward. Positive separation does not always imply permeability and negative or no separation does not always mean impermeable. Micrologs should be interpreted according to the following guidelines:

1. Positive separation denotes only the presence or absence of mudcake and, by inference, permeability. It says nothing qualitative or quantitative about the permeability. Neither the amount of positive separation nor the microlog resistivity values have any correlation with the amount of permeability in a zone. Neither can they be used to compare the permeabilities of different zones (Figure 8-32).

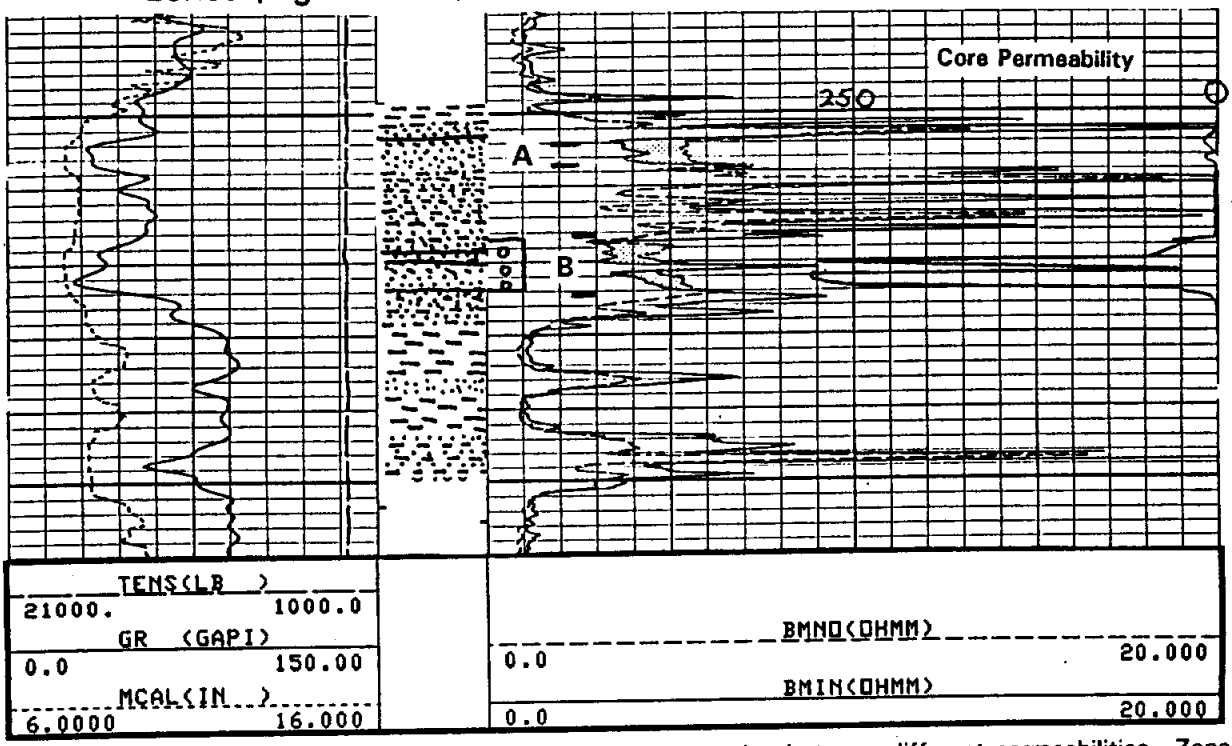

Figure 8-32. Two intervals with similar positive microlog separation but very different permeabilities. Zone A has core permeabilities from 2.5 md to 10 md. Zone B, which has a microlog character similar to Zone A, has permeabilities ranging from 20 md to 342 md, with three feet having 245 to 340 md. The core permeabilities are plotted in Track 3. A lithologic description of the core is in the depth column. The letter "B" on the scale refers to a particular version of Schlumberger's microlog. The log is an oil well in the Paluxy sandstone in East Texas. The well is producing from Zone B. The bit size is 7⅞ inches. R_m is 1.13 ohm-meters and R_{mf} is 1 ohm-meter at formation temperature (167° F).

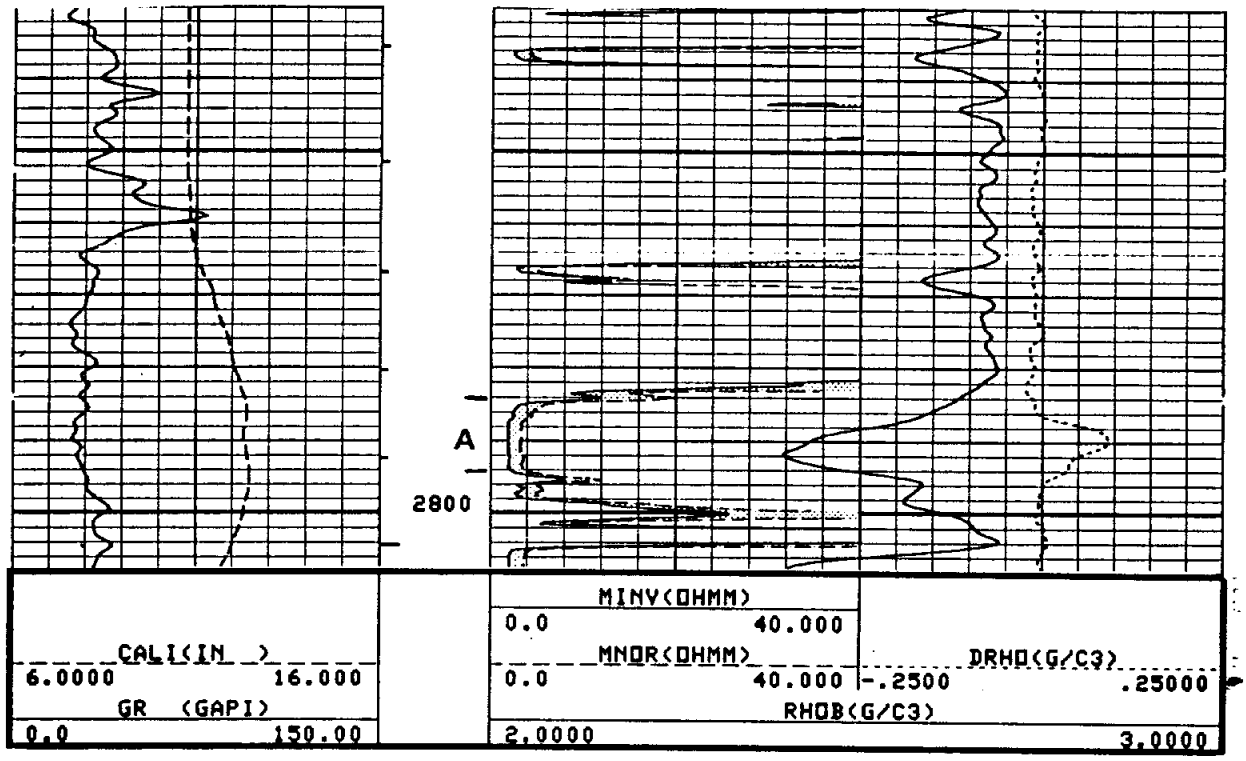

Figure 8-33. Positive microlog separation when the permeability is less than 1 md. Zone A has core permeabilities less than 1 md and half the zone has 0.1 to 0.2 md. The borehole enlargement is large enough for the microlog to maintain good pad contact, so the curves are not affected by the borehole enlargements. The well is a Pennsylvanian Canyon limestone in North Texas. Hydrocarbons are present in the pores. Core porosities reach 17 percent. Permeabilities are low because the pores have developed an isolated, biomoldic pore system. Bit size is 7⅞ inches. R_m is 1.75 ohm-meters and R_{mf} is 1.3 ohm-meters at formation temperature (93° F).

2. Positive separation can occur when the permeability is as low as 0.1 md (Figure 8-33). Therefore, the microlog must be used with caution to calculate the net feet of permeable rock and to estimate the specific capacity of a well. Look for hints of low permeability on the SP and gamma ray curves. Additional logging tools (porosity logs, repeat formation testers, and sidewall coring devices), as well as pump tests, will provide further information about permeability (hydraulic conductivity) and specific capacity.

3. Positive separation occurs opposite washouts when the microinverse reads the resistivity of the mud and the micronormal reads the resistivity of the formation. This may lead to an interpretation error if it is an impermeable zone that has washed out. Fortunately, shales are the only impermeable rocks that routinely wash out. To identify positive separation as a shale look

for borehole enlargement on the caliper curve (Figure 8-30, point A). Also examine the SP and/or gamma ray to determine if the zone is a shale.

4. If a washout is large enough, the curves will have no separation. Both the microinverse and the micronormal will read the resistivity of the mud. The washout may be in impermeable shale or in permeable rocks such as ~~semi~~/or unconsolidated, high porosity sandstones and vuggy or fractured carbonates. The caliper curve and the fact that the microlog curves read a resistivity equal or close to R_m are used to identify such washouts. The SP and gamma ray curves are then used to determine whether or not the washout is shale.

5. Opposite permeable zones that have mudcake and positive separation the caliper will often, but not always, show borehole diameters less than bit size. In high porosity, ~~semi~~ to unconsolidated sandstones, the borehole may wash out slightly. Even though mudcake is present, the hole diameter will remain greater than bit size.

6. Impermeable sandstones, carbonates, and dense shales with microlog resistivities greater than 20 times R_m may occasionally have spiky positive separation (Figures 8-31 and 8-30, point B). This may be ignored. It is usually due to poor fit of the pad against the formation (Hilchie, 1979).

7. The microlog does not work well if the mudcake is thick enough to hold the pad off the borehole wall or i n. In such instances there will be very li Most salt muds and low-solids, low water mudcakes.

8. The microlog cannot be used to identify permeable zones if the borehole fluid does not form a mudcake.

9. The microlog may not show positive separation if the mudcake has been disturbed considerably by previous logging runs, pump tests, etc.

10. Normal microlog interpretation is predicated on the assumption that neither curve reads beyond the flushed zone and that R_{xo} is greater than R_{mc}. If the depth of filtrate invasion is less than 4 inches, the micronormal curve will be influenced by R_t and this assumption breaks down. A highly permeable zone may have positive, negative, or no separation. The type of separation depends on the resistivity contrast between R_t and the R_{mc} and R_{xo} values. Several conditions can create invasion of less than 4 inches:

    a. Very high porosity sandstones such as Gulf Coast and Carrizo-Wilcox aquifers.
    b. Low-water-loss muds (not usually the case in water wells or in the upper portions of petroleum test wells which is where slight to moderately saline waters occur).
    c. Near T.D. where there has been less time for invasion (possible in water wells).

Recommended use. The microlog was initially designed to determine porosity and R_{xo}. In fact, on old micrologs positive separation was labeled porosity (Figure 8-30). Charts are available for calculating porosity from micrologs. Hilchie (1979) and Helander (1983) have detailed explanations of the calculations. Charts from different service companies are not interchangeable because they are empirically constructed to fit a particular tool design (Pirson, 1963). Unfortunately, the microlog does not do a good job of calculating either porosity or R_{xo}. The calculations work best when:

1. The value of R_{xo}/R_{mc} is less than about 15, which generally corresponds to a porosity greater than 15 percent.

2. The mudcake thickness is less than ½ inch.

3. Depth of invasion is greater than 4 inches (Schlumberger, 1989).

Very seldom today is the microlog used to calculate either porosity or R_{xo}. Density, neutron, and sonic tools are used to calculate porosity, and focused pad microelectrode resistivity tools are used to measure R_{xo}. These tools are not available in old log files. Even though the microlog is about the only method of calculating porosity and R_{xo} from old logs, the technique is not recommended because calculated values will not be consistent, little

confidence can be placed in the values, ~~therefore~~ and there is no way to check the accuracy of the calculations.

The microlog is best used to determine the presence of mudcake and as an indicator of permeability. If used in conjunction with the SP, gamma ray, ~~and~~/or caliper, the microlog does a good job delineating permeable zones. In ground-water studies the microlog is a quick, visual means of calculating the net feet of permeable rock and of making an inference about the specific capacity of a well. It is especially useful in sandstones with alternating permeable and highly cemented zones such as the Trinity aquifer (Figure 7-15) and in carbonates with sporadic permeable zones. It is excellent for delineating thin shale laminations in sandstones. The excellent vertical resolution of the microlog means that it is about the best curve for picking bed boundaries. Conventional micrologs work in 6 to 20 inch boreholes.

The microlog also can be used to make a mud log (Figure 8-34). A mud log is made by recording the microinverse and micronormal curves with the arms in a retracted position as the tool is run to the bottom of the hole. The electrodes have such shallow depths of investigation that in washouts and caves they only read R_m and the two curves will overlay (Figure 8-34, at 1350 feet). When the curves are spiky and the micronormal reads higher than the microinverse, the curves are being influenced by the resistivity of the mudcake ~~and~~/or the formation (Figure 8-34, Zone C). The mud log provides a good check on the accuracy of the R_m measured at the surface and recorded on the log heading. But the two R_m's have to be measured at the same temperature before a valid comparison can be made. Equation 2-4 is used to adjust one of the R_m's to the temperature of the other.

A mud log should be made whenever a microlog is run. However, the logging service company will not make a mud log unless asked to do so. There is no additional charge for the mud log.

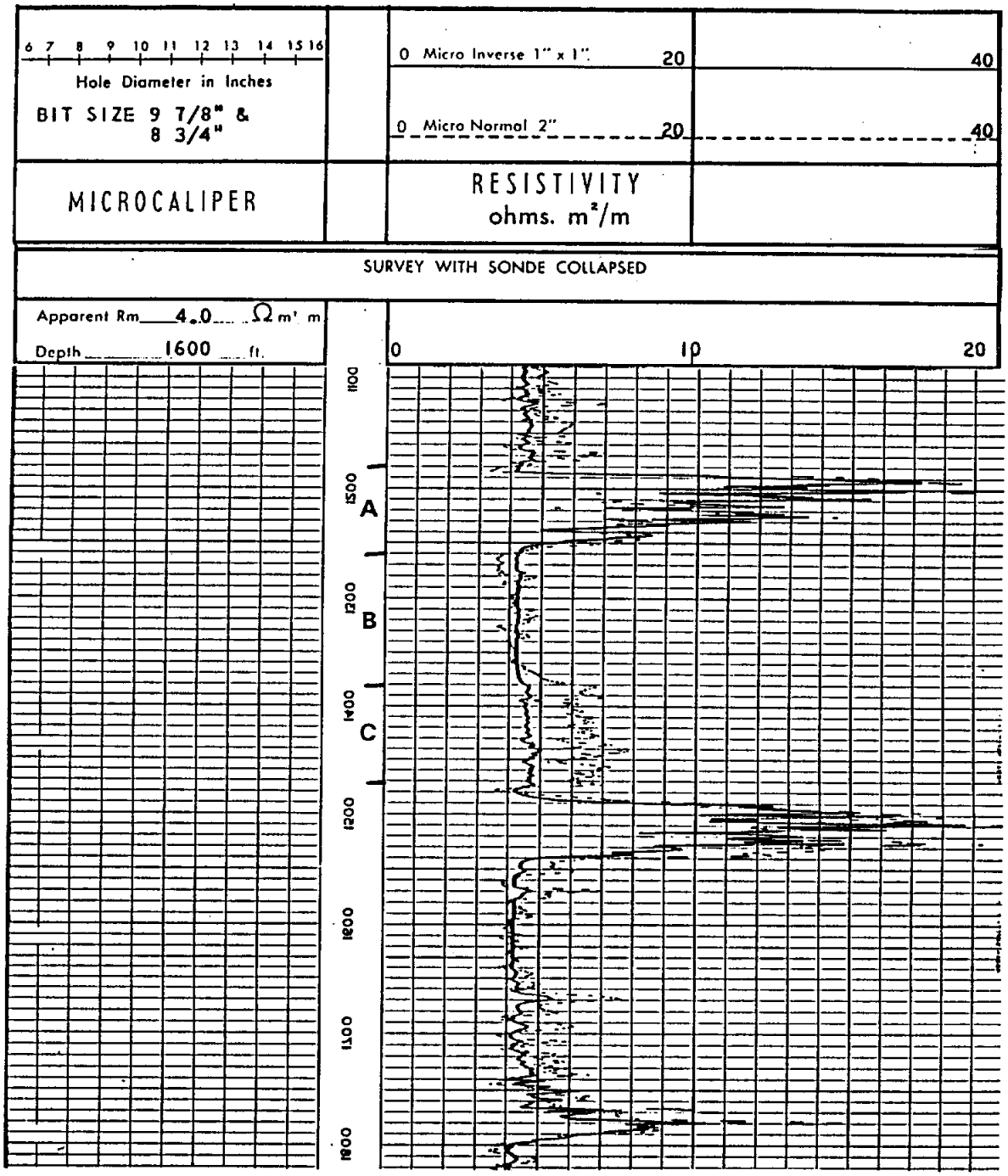

Figure 8-34. Example of a 1950's vintage Schlumberger mud log. Rm decreases down the borehole. At 1800 feet Rm is about 4 ohm-meters, which agrees with the resistivity of the mud pit sample. At Zone A the electrodes are against the borehole wall and both curves are responding to the formation resistivity. At Zone B the Microinverse is reading Rm and the Micronormal is reading Rm plus a little formation resistivity. At 1350 feet the curves overlay because the interval is washed out (as seen on the microcaliper on another part of the log). At Zone C both curves are reading a combination of mud and formation resistivities. Figure 8-30 is from the same well.

FOCUSED ELECTRODE AND INDUCTION TOOLS

Chapter 9

Focused electrode tools gained widespread usage in the petroleum industry during the 1950's. The tools were developed in response to the need for a resistivity tool that could handle very conductive muds (salt muds), thin beds, and highly resistive formations. Curve response is vastly improved over nonfocused tools (Figures 8-10, 8-20, 8-21, and 9-1).

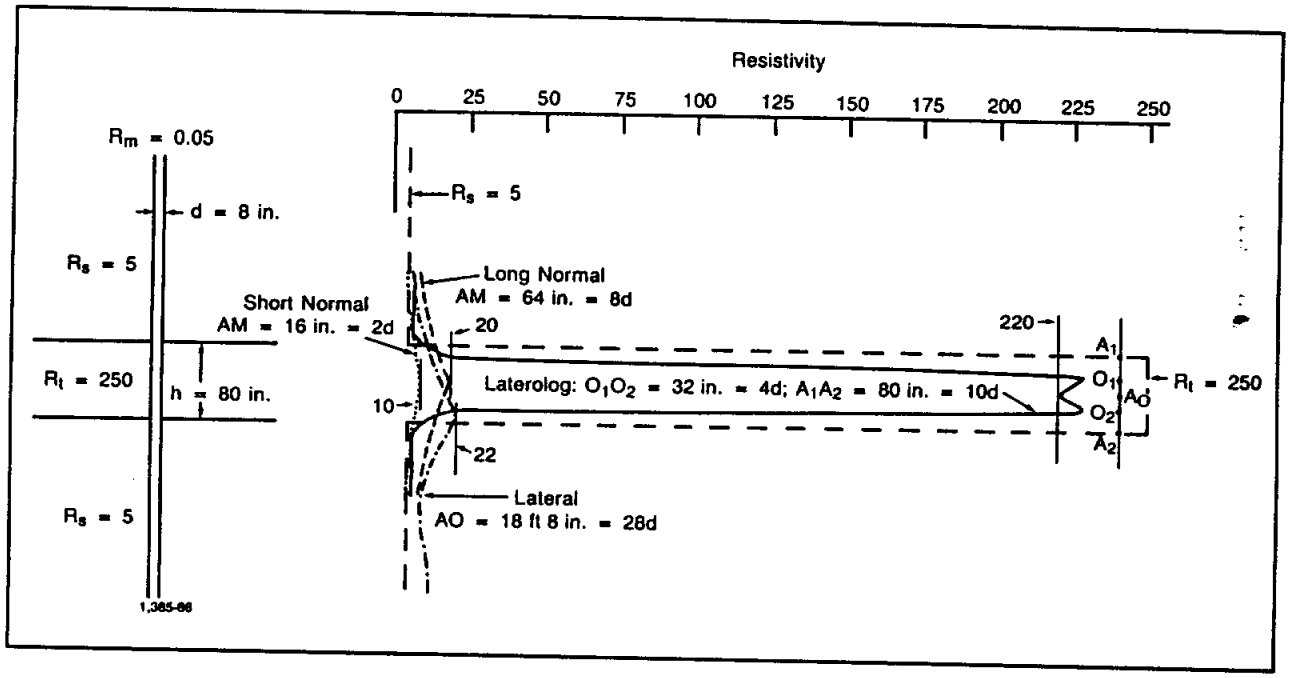

Figure 9-1. Comparison of log responses of nonfocused (short normal, long normal, and lateral) and focused tools opposite a thin, noninvaded bed with very salty mud (From Schlumberger, 1989).

These tools are still used by the petroleum industry. They are readily available only in West Texas where salt muds and high resistivity formations are common[1]. The tools have been used sparingly by the ground-water industry. However, with sufficient notification, a logging company will ship a tool to any part of the state. A few slimhole tools are available; most are single curve guard tools.

---

[1] This statement is slightly misleading. The Dual Induction log, which is run throughout Texas, utilizes a focused electrode tool as the shallow reading resistivity device.

FOCUSED MANDREL ELECTRODE TOOLS

There have been various types of focused electrode tools used through the years. This section reviews the salient features of the different types of tools and documents their application to ground-water studies.

Focused electrode tools control the current path by the use of auxiliary current electrodes above and below the primary current electrode. Two types of tools are available, the guard-focusing device and the point-electrode system.

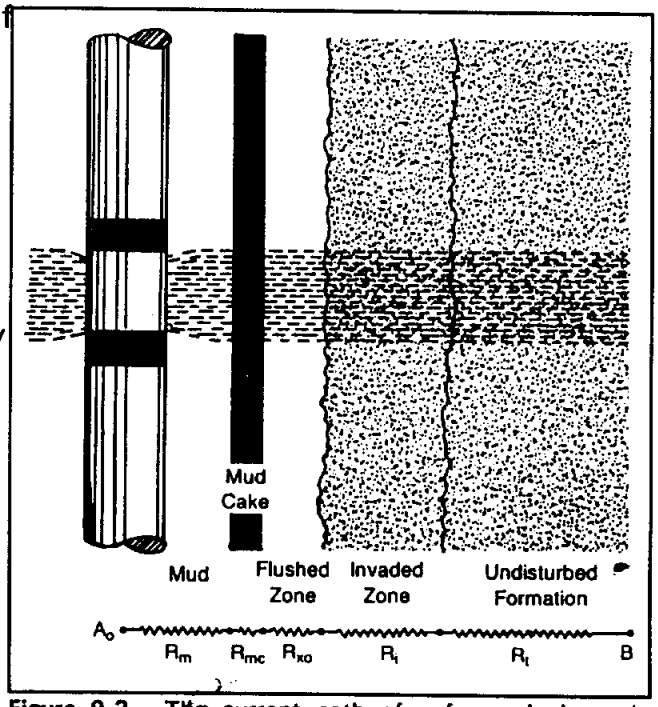

Figure 9-2. The current path of a focused electrode tool. All the resistivities from A_o to B contribute to Ra (From Dresser Atlas, 1982).

The current path for focused electrode tools is a series circuit. The Ra value measured by the tool is a combination of all the resistivities between the probe and its depth of investigation. For deep reading tools this means Rm, Rmc, Rxo, Ri, and Rt (Figure 9-2). As long as Rm is less than Rw, Rxo and Ri will be less than Rt and will not significantly contribute to Ra. A shallow depth of invasion also means that Rxo and Ri have little effect on Ra. This makes the tool ideal for many ground-water wells, since the borehole environment usually satisfies these conditions.

The Laterolog 7, Laterolog 3, deep Guard tools, and the deep laterolog of the Dual Laterolog tool measure Rt. The Laterolog 8 and the Spherically Focused Log measure Ri. The number in the name refers to the number of electrodes. The tools will not work in cased holes.

Guard

Commercial names are Guard (Halliburton Logging Service), Focused Log (Atlas Wireline), and Schlumberger's Laterolog 3 (LL3) which is obsolete. Three different types of guard tools exist: resistivity, conductivity, and multiple measuring devices. See Jorden and Campbell (1986) for details on tool theory. These tools are available on a limited basis today. Figure 9-3

has a schematic of the electrode configuration of the LL3. The guard electrodes A_1 and A'_1 are each 5 to 6 feet long. The guard electrodes force current from A_o to flow into the formation as a horizontal sheet with the same height as A_o (12 inches). The depth of investigation is equal to the point at which the current starts to flare, about three times the length of one guard electrode (Helander, 1983). The longer the guard, the greater the depth of investigation (Pirson, 1963). Guard tools measure Rt.

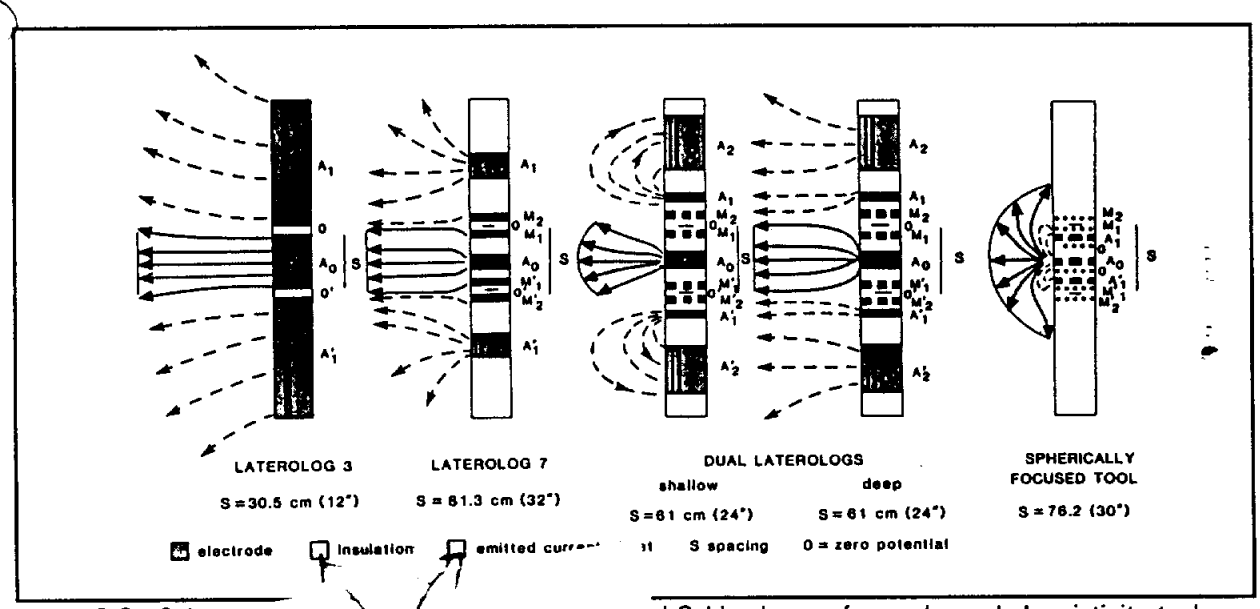

Figure 9-3. Schemati al Schlumberger focused mandrel resistivity tools. A = electrode, M = 1986).

Point-Electrode

The point-ele y known as the Laterolog 7 (LL7) is obsolete. Some point-electrode as the shallow laterolog. The curr point electrodes (Figure 9-3). The LL7 has seven electrode... M_1, M_2, M'_1, and M'_2 are potential measuring electrodes. Current to electrodes A_1 and A'_1 is adjusted so as to maintain a focused current beam from A_o. The O to O' spacing (32 inches) is the current height and vertical resolution. The bed appears thinner than it actually is by an OO' spacing (Figure 9-3). The depth of investigation is somewhat greater than A_1 A'_1 which is 80 inches. Point-electrode tools measure Rt.

Shallow Investigating

Various shallow investigating focused tools have been run through the years in combination with the induction log (Table 9-1). The devices are either guard or point-electrode tools. Shorter guard lengths or electrode spacings give shallower depths of investigation (Ri). The LL8 has a vertical resolution of 14 inches and a depth of investigation of about 30 inches (Schlumberger, 1989). See Jorden and Campbell's (1986) Chart 6.28 for specifications on the various tools.

TABLE 9-1. SHALLOW INVESTIGATING FOCUSED TOOLS THAT HAVE BEEN USED WITH THE DUAL INDUCTION

Logging Company	Tool Name
Atlas Wireline (Dresser Atlas)	Focused Log
Halliburton Logging Services	Guard Log
Gearhart	Laterolog
Welex	Guard Log
Schlumberger	Laterolog 8 (LL8)*
	Spherically Focused (SFL)

* obsolete

The Spherically Focused Log (SFL) replaced the 16" short normal and the LL8 as the shallow investigating tool on Schlumberger's Dual Induction Log. The SFL does not focus the current into horizontal beams as guard and point-electrode tools do. Instead the tool uses auxiliary currents to create essentially spherical equipotential shells around the current electrode (Figure 9-2). The SFL measures conductivity which is converted to resistivity values. Schlumberger (1989) has more details on tool theory.

The SFL is better than the LL8 or 16" short normal at measuring Ri because the electrode configuration reduces borehole effects, bed thickness effects, and depth of investigation (Jorden and Campbell, 1986). The depth of investigation is about 20 inches. The tool is accurate over a high range of R_{SFL}/Rm values, but boreholes greater than 10 inches or less than 7 inches in diameter require some correction (Figure 9-4). No correction is required for bed thickness. The vertical resolution is about 1 foot. The SFL curve is

often averaged over a 3 foot interval to reduce its detail to that of the induction curves (Dewan, 1983).

Dual Focusing Electrode

Dual focusing electrode tools are known as Dual Laterologs (DLL) or Dual Guard Logs (Figures 8-10 and 8-21). Every major logging company now runs a Dual Laterolog. (Welex had a Dual Guard Log). This is the focused centralized electrode tool presently being used by the petroleum industry. Both the deep (LLD) and the shallow (LLS) use the same electrodes. Different focusing changes the depth of investigation so that the tool measures Ri and Rt. Jorden and Campbell's (1986) Chart 6.30 summarizes tool specifications.

Current beam thickness and vertical resolution (2 feet) is the same for both curves (Schlumberger, 1989). The LLD has a deeper depth of investigation than previous laterologs (LL7 and LL3). The DLL has a range of 0.2 to 40,000 ohm-meters, which is much wider than previous laterolog tools (Schlumberger, 1989).

One drawback to using the tool in some water wells is the length of the tool. The probe is 28 feet and the bridle attached to the top of the probe is 40 to 80 feet long. The bridle has to be in fluid for the tool to work, so the tool cannot measure closer than to within 68 to 128 feet of the water level.

Log presentation. The dual laterolog is presented as a logarithmic scale across tracks 2 and 3. The deep laterolog curve is long dashes and the shallow curve is short dashes or a solid line. An Rxo curve is often included as a solid curve (Figure 8-21).

Environmental corrections. Departure curves are available for several tools, but only the point-electrode tool has been evaluated extensively for composite effects of borehole, bed thickness and invasion (Jorden and Campbell, 1986). Due to variations in tool design, departure curves are only valid for one particular brand of tool. Slimhole tools do not have departure curves. Environmental corrections must always be made in this order- borehole, bed thickness, invasion. The LLD is not significantly affected by eccentering the tool, while the LLS is greatly affected.

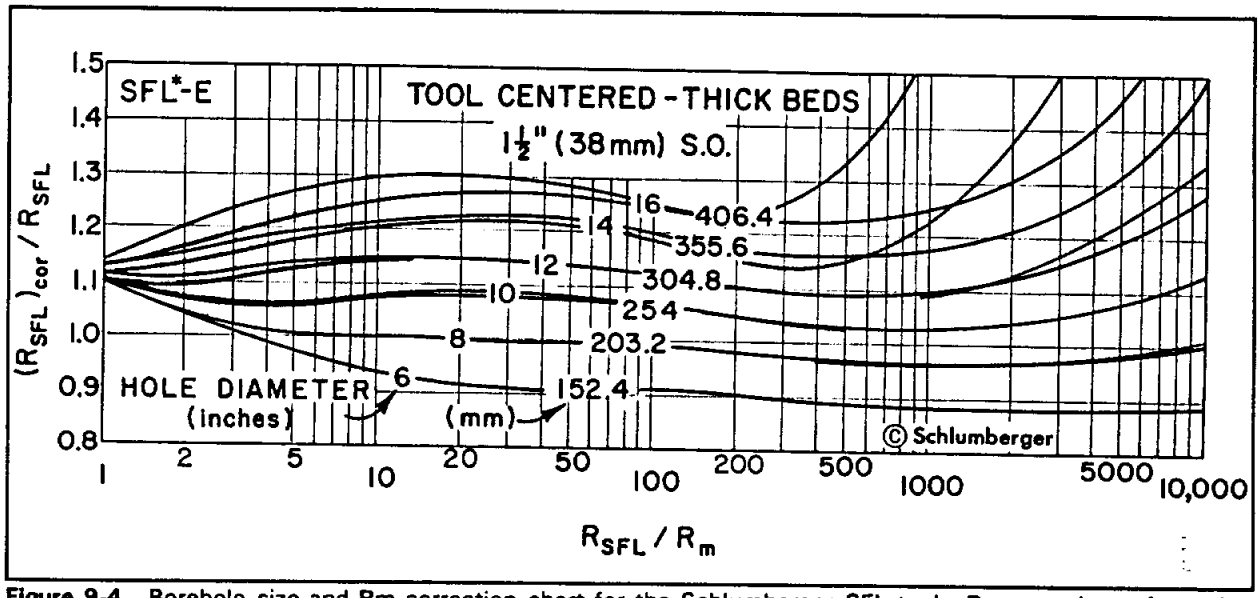

Figure 9-4. Borehole size and Rm correction chart for the Schlumberger SFL tool. Rm must be at formation temperature. S.O. is standoff (From Schlumberger, 1979).

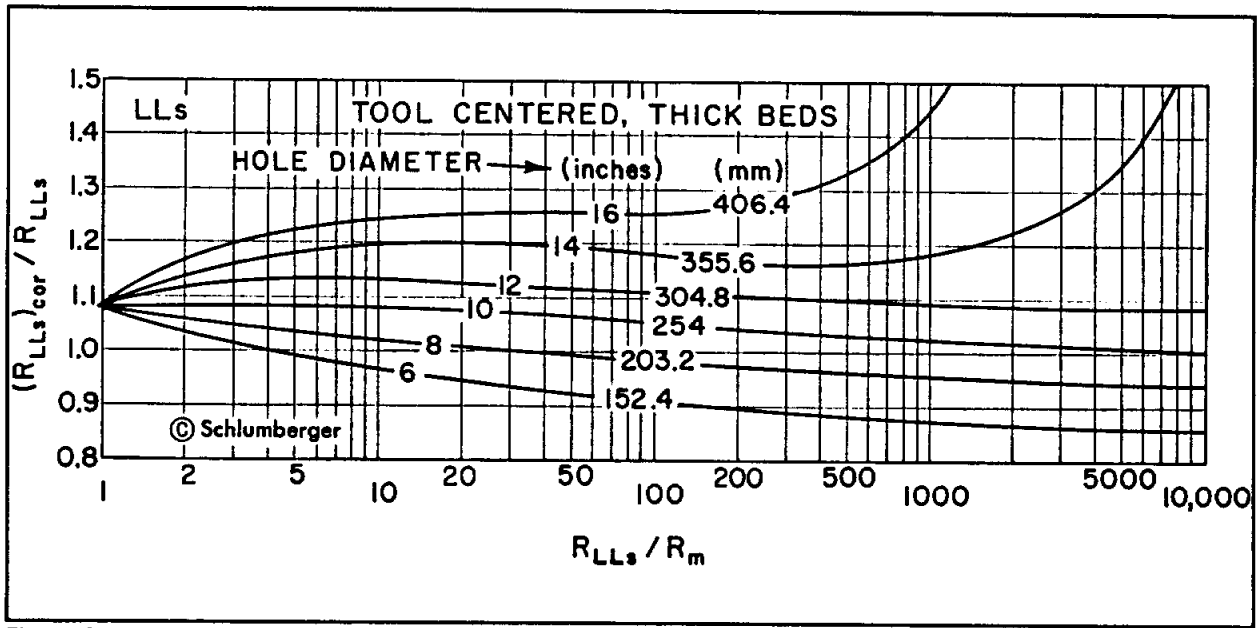

Figure 9-5. Borehole size and Rm correction chart for the Schlumberger LLD (Version DLS-B). Rm must be at formation temperature (From Schlumberger, 1979).

Borehole corrections. Very little correction to the LLD is required for high Rt/Rm values and 8 to16 inch boreholes (Figure 9-5). Generally the corrections are less than for other resistivity and induction tools. Rm must be adjusted to formation temperature before using the chart.

The LLS requires more correction, but it is not used for Rt when the LLD is functioning. Borehole correction charts are available for the various types of conventional focused electrode tools.

Bed thickness and adjacent bed corrections. Correction charts are available for idealized conditions (infinitely thick shoulder beds and no invasion). Figures 9-6 and 9-7 are correction charts for one particular generation of LLD and LLS tools. The charts (Figures 9-6 and 9-7) reveal the following characteristics of the Dual Laterolog:

1. If the adjacent beds are more resistive than the bed of interest, Ra is too high (bottom half of each chart). The phenomenon is

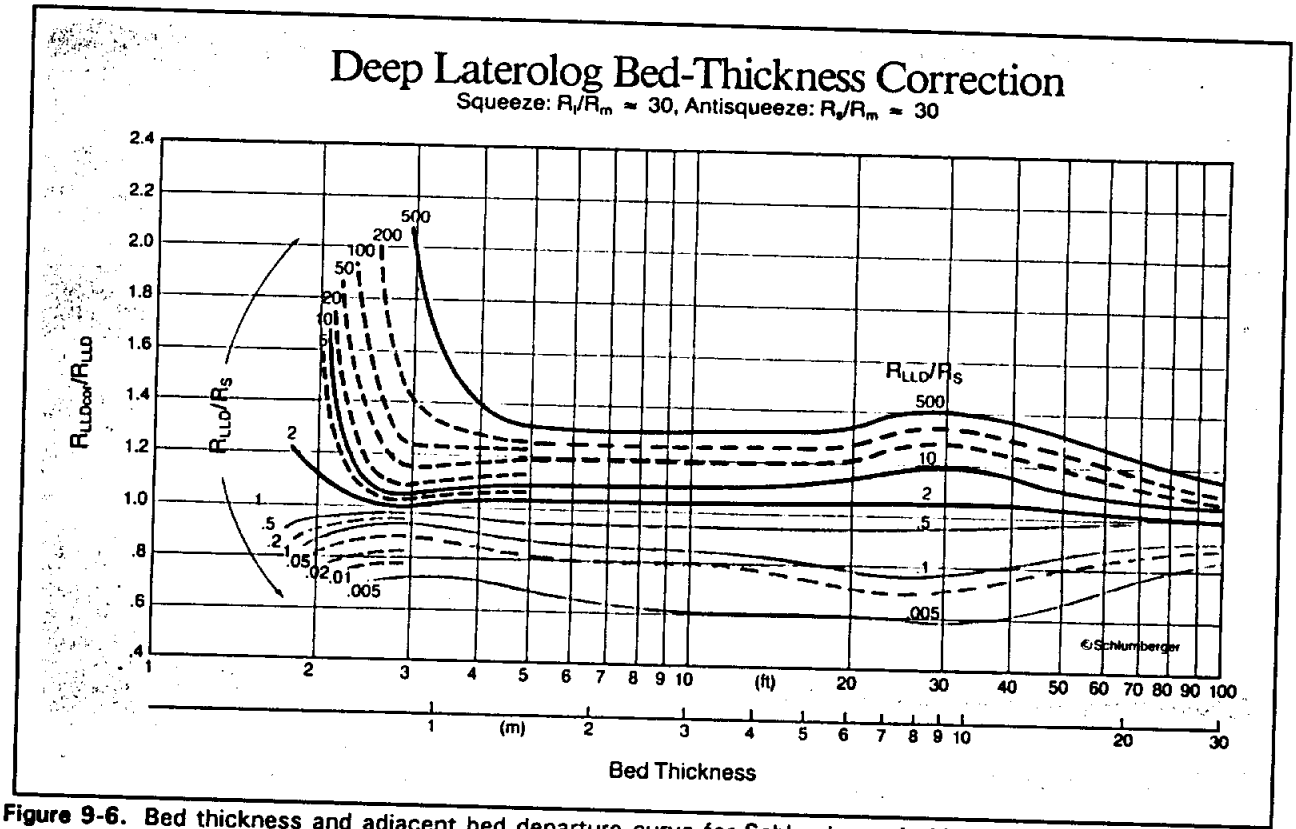

Figure 9-6. Bed thickness and adjacent bed departure curve for Schlumberger's LLD (Version DLS-D/E). The chart assumes no invasion, semi-infinite adjacent beds, and an 8 inch borehole (From Schlumberger, 1989).

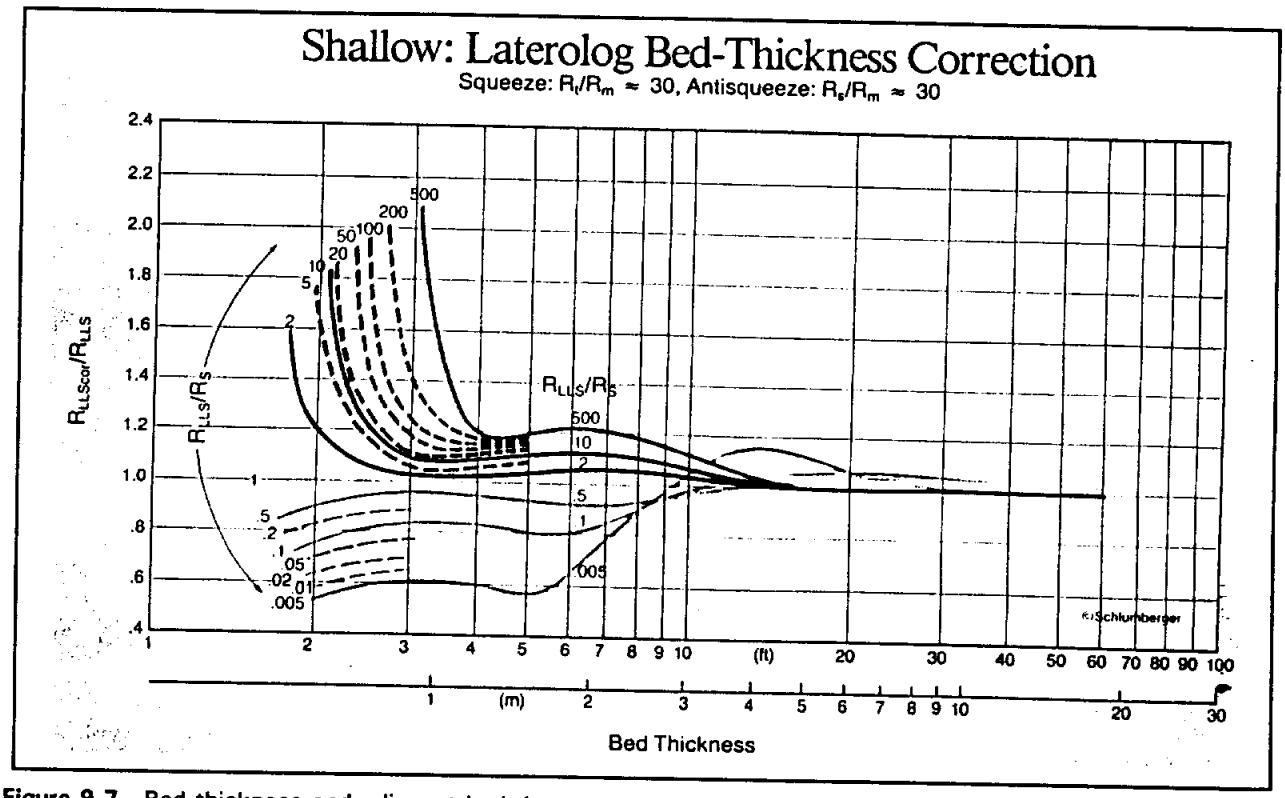

Figure 9-7. Bed thickness and adjacent bed departure curve for Schlumberger's LLS (Version DLS-D/E). The chart assumes no invasion, semi-infinite adjacent beds, and an 8 inch borehole (From Schlumberger, 1989).

referred to as "squeeze". But above a bed thickness of 10 feet the effect reverses for the LLS tool and the bed of interest appears to be slightly less resistive than it actually is.

2. If the adjacent beds are less resistive than the bed of interest, R_a is too low (top half of each chart). The phenomenon is called "antisqueeze". The LLS is hardly affected if the bed is thicker than ~~twenty~~ feet.

3. The LLD is much more affected than the LLS.

4. Beds 2 feet thick can be accurately measured.

5. Both tools have the same vertical resolution.

However, these corrections are seldom used because idealized conditions are seldom encountered in a borehole. The corrections, if made, are much less than would be required for induction tools.

Invasion corrections. Invasion effects on the LLD or the deep Guard will usually be small in high porosity ground-water environments. Invasion corrections are not needed in such cases. In moderate to low porosity formations invasion corrections should be made (Hilchie, 1982). Invasion corrections require three curves, either a DLL-MSFL (Schlumberger), DLL-MLL (Atlas Wireline) or Dual Guard-FoRxo (Halliburton). The chart book of the company that logged the well must be consulted for invasion correction charts.

Recommended use. Focused mandrel electrode tools are excellent for many ground-water environments and should be used more often. They are the best tools to use when Rt is greater than 100 ohm-meters, Rt/Rm is high, Rt/Rs is high, Rmf/Rw is less than 3 (Figure 9-8) and good vertical resolution is needed. One or more of these conditions is met in most water wells.

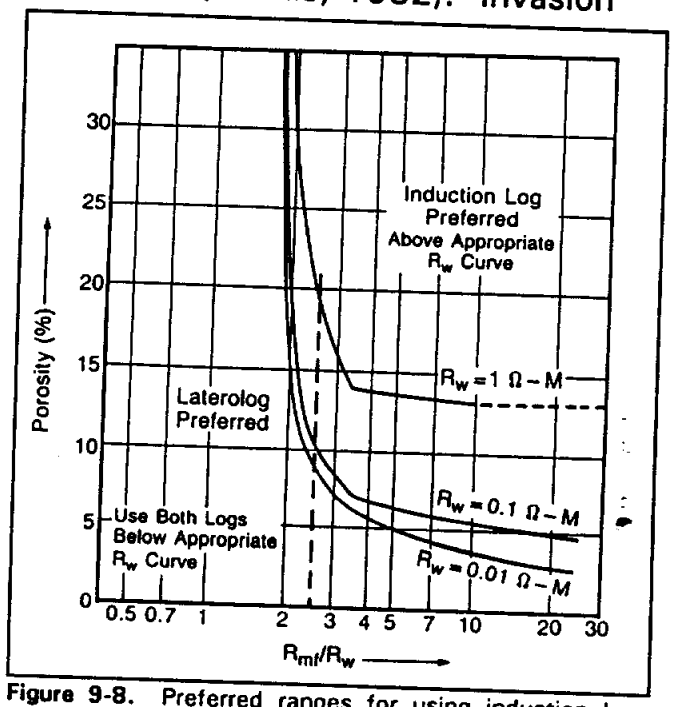

Figure 9-8. Preferred ranges for using induction logs and laterologs under normal borehole conditions (From Schlumberger, 1989).

FOCUSED PAD MICROELECTRODE TOOLS

Focused microelectrode tools are used to measure Rxo. In fact, they are commonly called Rxo tools. The tool was developed to overcome the problem of high Rxo/Rmc values, which affects the nonfocused pad tool (microlog). The Microlaterolog (MLL) was the first focused pad tool. Schlumberger and Dresser Atlas added the Proximity Log (PL), which Schlumberger replaced with the Microspherically Focused Log (MSFL). Welex ran a FoRxoLog, but Halliburton now runs a Microspherically Focused Log.

Tool theory. All the tools have a closely spaced focusing electrode arrangement mounted on an insulated pad (Figure 9-9). The tools are basically pad-mounted, microversions of the focused centralized electrode

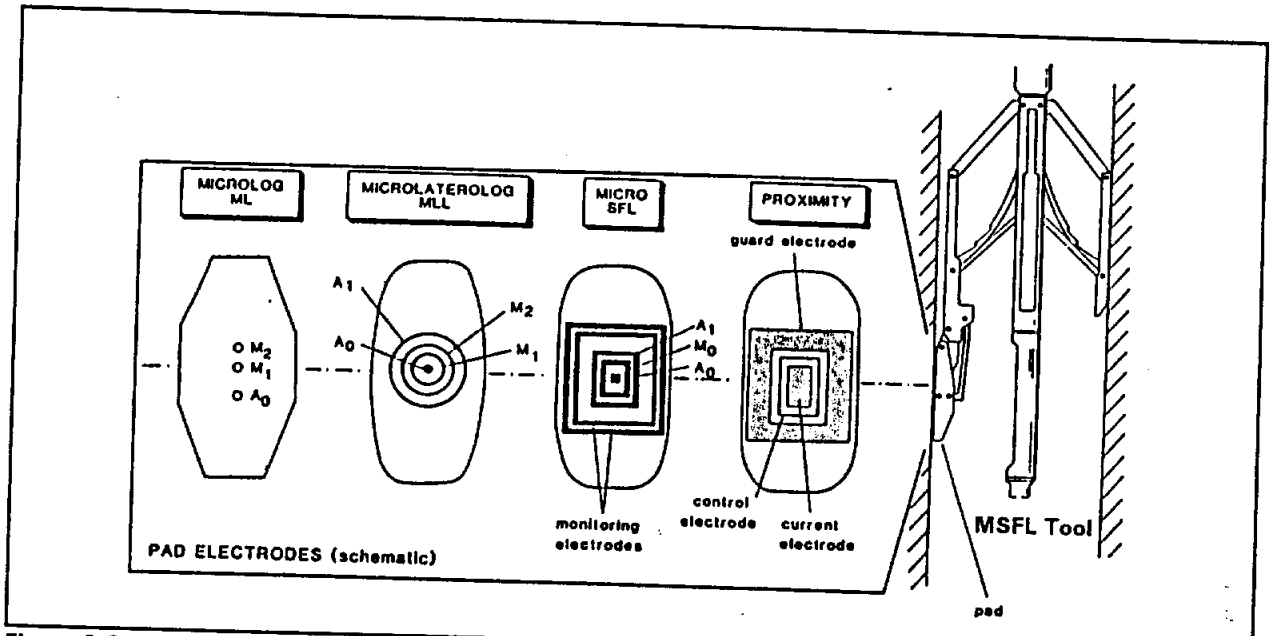

Figure 9-9. Schematic electrode configuration of focused pad microelectrode tools. A and M are electrodes (From Rider, 1986).

tools. The MLL and Proximity tools are similar in design, while the MSFL design is somewhat different (see the SFL section).

The MLL tool was replaced in fresh muds because mudcake thickness greater than ⅜ ~~of an~~ inch significantly affects the resistivity values. Its replacement, the Proximity Log, has a deeper depth of investigation, which means that the mudcake influence is less (negligible if mudcake thickness is less than ¾ ~~of an~~ inch). The greater depth of investigation, however, means that for the Proximity Log to read R_{xo} requires deeper invasion (a radius of about 20 inches). Invasion is not this deep in most high porosity formations, so the curve is influenced by R_i and/or R_t. The MSFL was developed to better deal with the problems experienced by the MLL and the Proximity tools. It has a shallower depth of investigation (about 2 to 3 inches) than either the MLL (3 to 4 inches) or the Proximity (6 to 20 inches). Also, it tolerates thick mudcake better than the MLL (little correction for less than ¾ ~~of an~~ inch).

The vertical resolution of the Proximity tool is 6 inches to 12 inches. The MSFL and the MLL tools have a vertical resolution of a few inches.

Environmental corrections. Mudcake corrections and R_{xo}/R_{mc} correction charts are available for each R_{xo} tool. Figure 9-10 is a correction chart for an early MSFL tool. In ground-water environments where invasion

is sufficiently deep and mudcake thickness is normal, the MLL and the MSFL will still require an important environmental correction. R_{mc} must be adjusted to formation temperature before using the chart. R_{xo}/R_{mc} values are usually less than 15, which causes the log values to read considerably higher than R_{xo}. Figure 9-11 is an example of an MSFL curve before and after corrections for the R_{xo}/R_{mc} value. The Proximity Log does not require this correction.

Recommended use. R_{xo} values are essential to determining water quality by the resistivity ratio method. The MSFL, with corrections for R_{MSFL}/R_{mc}, is the best log for measuring R_{xo}. It should be run in more ground-water studies.

A mud log can be made with an MLL or an MSFL tool. The resistivity value in washouts (identified from the caliper) is R_m. R_m values are harder to establish than with a microlog mud log, which has two curves to compare. The logging service company will not make a mud log unless asked to do so. There is no additional charge for the mud log.

A synthetic microlog can be made from the MSFL data by the logging engineer. The quality of the log varies according to the borehole conditions. The logging company should provide assistance with interpreting the curve.

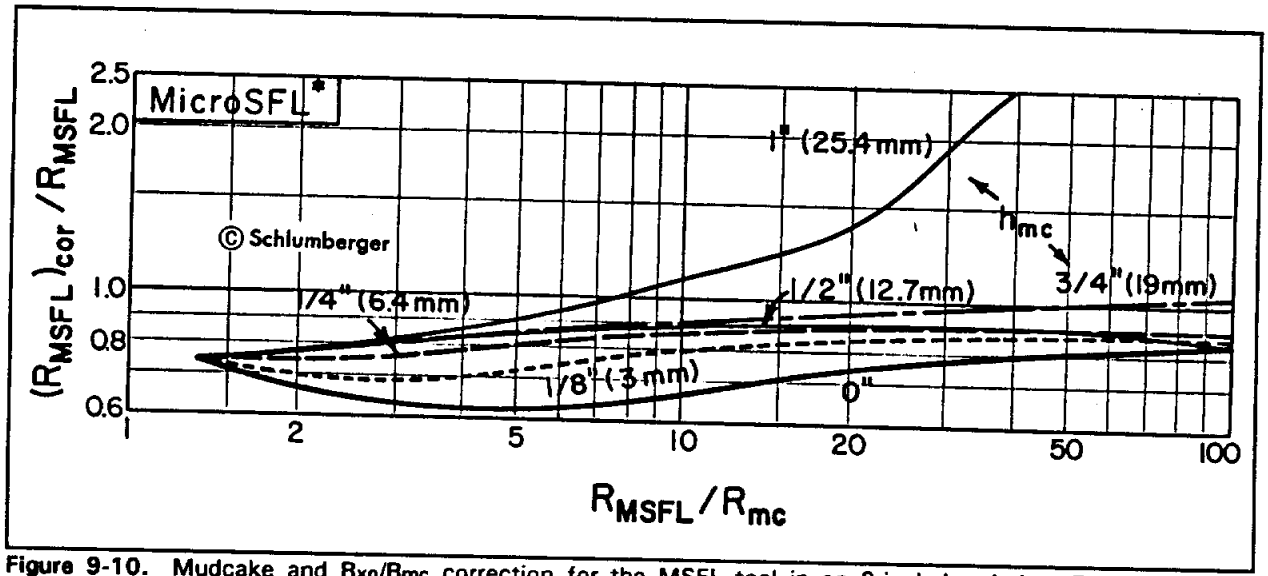

Figure 9-10. Mudcake and R_{xo}/R_{mc} correction for the MSFL tool in an 8-inch borehole. R_{mc} must be at formation temperature (From Schlumberger, 1979).

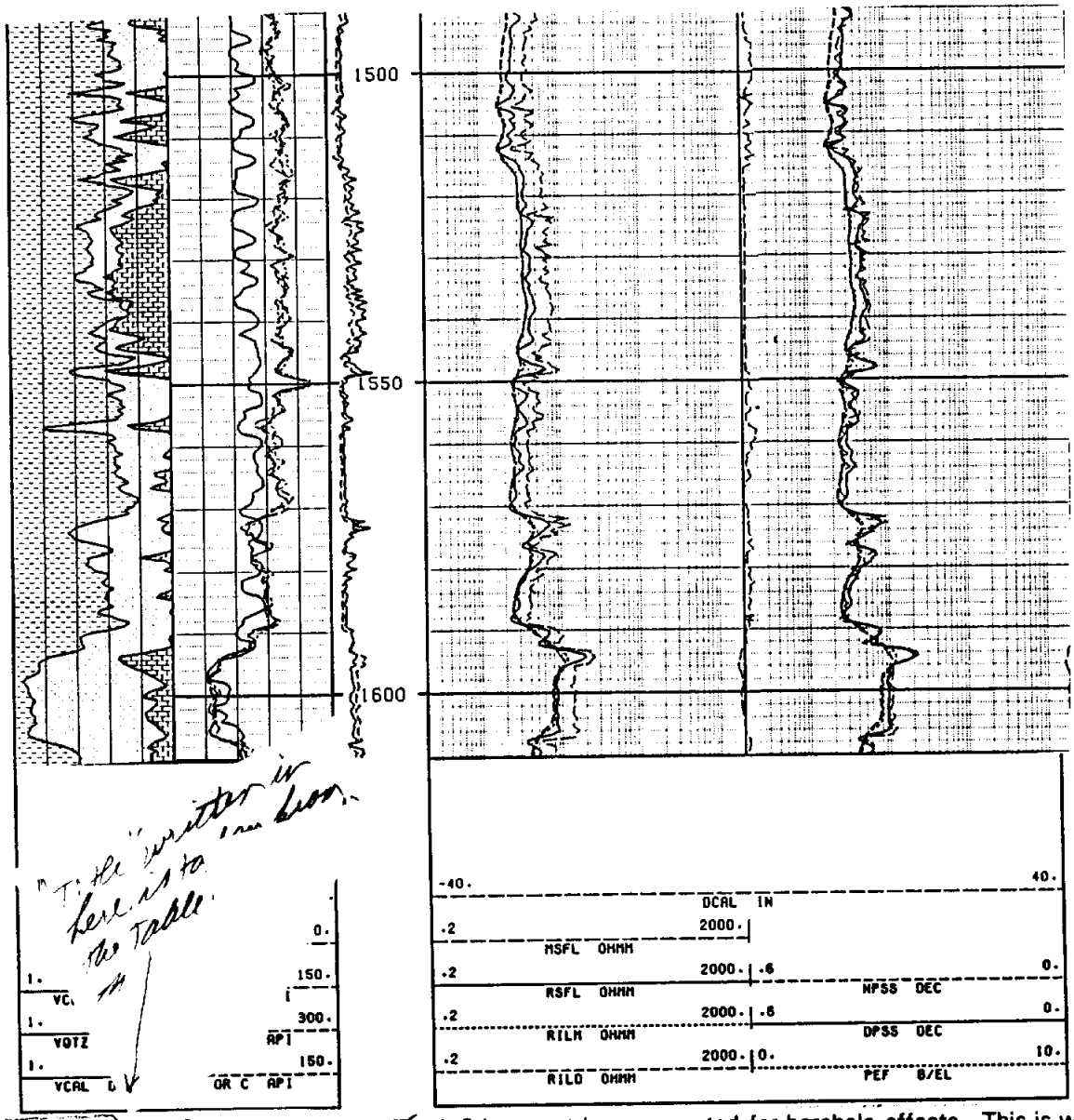

Figure 9-11. The ~~resistivity~~ curves in Track 2 have not been corrected ~~for borehole effects~~. This is why the MSFL is consistently reading about 30 percent too high. The error is noticeable because the difference between the MSFL and the other resistivity curves is very consistent and in the shales (1490 to 1550 feet) the MSFL does not agree with the other resistivity curves. The SFL reads higher in the shales than the ILD and the ILM curves, which overlay, because the laminated nature of this shale increases the SFL values. The curves in Track 3 have been corrected for borehole effects. An R_{xo}/R_{mc} correction was applied to the MSFL (Figure 9-10). Track 1 has a lithology log with the volumes of clay (VCL), quartz, (VQTZ), and calcite (VCAL) graphed. The lithologies were calculated by cross plotting the porosity and gamma ray logs. Also in Track 1 are SP and gamma ray curves. The SP curve has serious problems. It does not correlate very well with the other curves because a sine-wave pattern with a 6 foot wavelength is imposed on the curve. A microlog is in the depth column. The only positive separation is the sandstone at 1594 to 1608 feet. The shales are not clean, as indicated by the spiky nature of all the curves and the slightly elevated resistivity values. The sandstones are calcareous, as indicated by the lithology plot. The differential caliper (DCAL) in Tracks 2 and 3 shows the borehole to have few washouts. Mudcake is present across the sandstone at 1594 to 1607 feet. The log is the Woodbine Sandstone. The well is the J.L. Myers, Bristol Water Supply #2, Ellis County, Texas. Bit size is 12¼ inches. At formation temperature (95° F) R_m is 2.6 ohm-meters, R_{mf} is 2.9 ohm-meters and R_{mc} is 2.2 ohm-meters.

INDUCTION

Induction tools were introduced in the 1950's. The tool was developed for boreholes with nonconductive fluids (oil-based mud, air, or foam). It is the only resistivity tool that will work in nonconductive borehole fluid and in nonmetallic casing. (No resistivity tool works in steel casing.) Today in the petroleum industry it is the most commonly run resistivity log. It is the resistivity log of choice for boreholes with low to medium resistivity formations and muds that are more resistive than the formation waters. Slimhole tools are available, but are not commonly used in the ground-water industry.

The induction tool has been part of several different tool combinations through the years. Petroleum and ground-water well files are filled with these logs and any ground-water log analysts should have some familiarity with them. Schlumberger ran most of them, so their terminology is emphasized in this discussion.

1. Induction-electric survey (IES), induction electric log (IEL), and induction electrolog are trade names for a combination of 16 inch short normal, induction and SP. Schlumberger's induction was the 6FF40. (Six refers to the number of coils and 40 is the number of inches between the main transmitter-receiver pair). This logging suite was common in the 1960's.

2. Schlumberger's induction-SFL (ISF) had an SFL in place of the short normal, an SP, and an induction similar to the 6FF40. This tool is still available today, but the Gulf Coast is one of the few areas where it is still commonly run.

3. The Dual Induction tool was introduced in the 1960's. The tool consists of a deep induction (ILD), a medium induction (ILM), a shallow reading focused tool, and an SP. Schlumberger used an LL8 for the shallow reading focused tool. Other service companies use guard or laterolog devices (see Table 9-1). ILD and ILM are actually Schlumberger's terminology, but they are often used as generic abbreviations. 8FF34 is Schlumberger's medium induction and 6FF40 is their deep induction.

4. The DIL-SFL was introduced by Schlumberger in the mid 1970's. The SFL replaced the LL8. This is still Schlumberger's principal induction tool.

5. In the mid 1980's Schlumberger introduced the Phasor Induction SFL. The tool consists of a deep induction (IDPH), a medium induction (IMPH), an SFL, and an SP.

6. Array induction tools are being introduced by several service companies today.

7. Schlumberger's 6FF28 tool is their "slimhole" tool. It is 2⅝ inches in diameter. The induction device is a scaled-down version of the 6FF40. The tool includes a 16 inch short normal and an SP.

8. Robertson Geologging, Geonics, and Century Geophysical manufacture induction tools that are less than 2 inches in diameter.

Tool theory. Induction tools induce a current in the formation. A high-frequency alternating current in a transmitter coil creates an alternating electromagnetic field in the formation. The alternating magnetic field induces Foucault currents in the surrounding formation (Figure 9-12). These currents flow in horizontal ground loops in the formation. The currents create a magnetic field in the formation which induces a voltage in a receiver coil. The induced voltage is proportional to the formation conductivity (C), which is the reciprocal of resistivity ($R_{ohm\text{-}meters} = 1000/C_{mmhos/m}$).

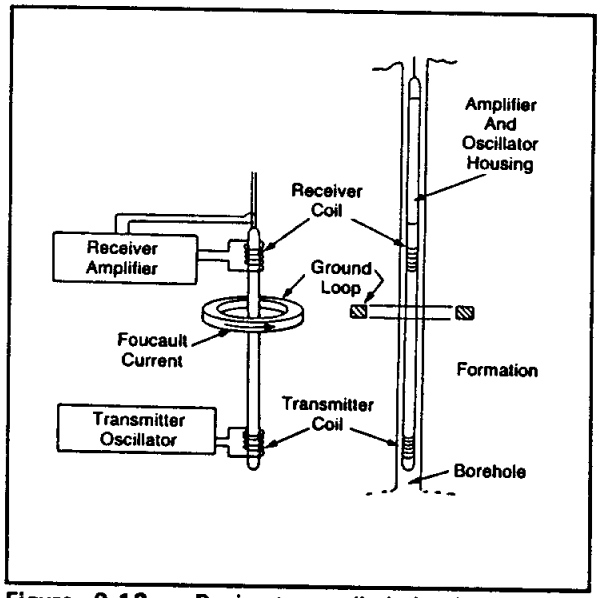

Figure 9-12. Basic two-coil induction system (From Schlumberger, 1989).

Figure 9-12 illustrates a simple unfocused two-coil system. Such a system would be significantly influenced by the borehole, the side beds, and the invaded zone. In reality induction tools are focused by employing an array of coils (Figure 9-13). The deep induction typically employs 6 coils (three transmitters and three receivers), while the medium induction uses

fewer. A few deep induction tools employ more than 6 coils. A focused tool has better vertical resolution, increased depth of investigation, minimized adjacent bed effects, and minimized borehole effects (Schlumberger, 1989).

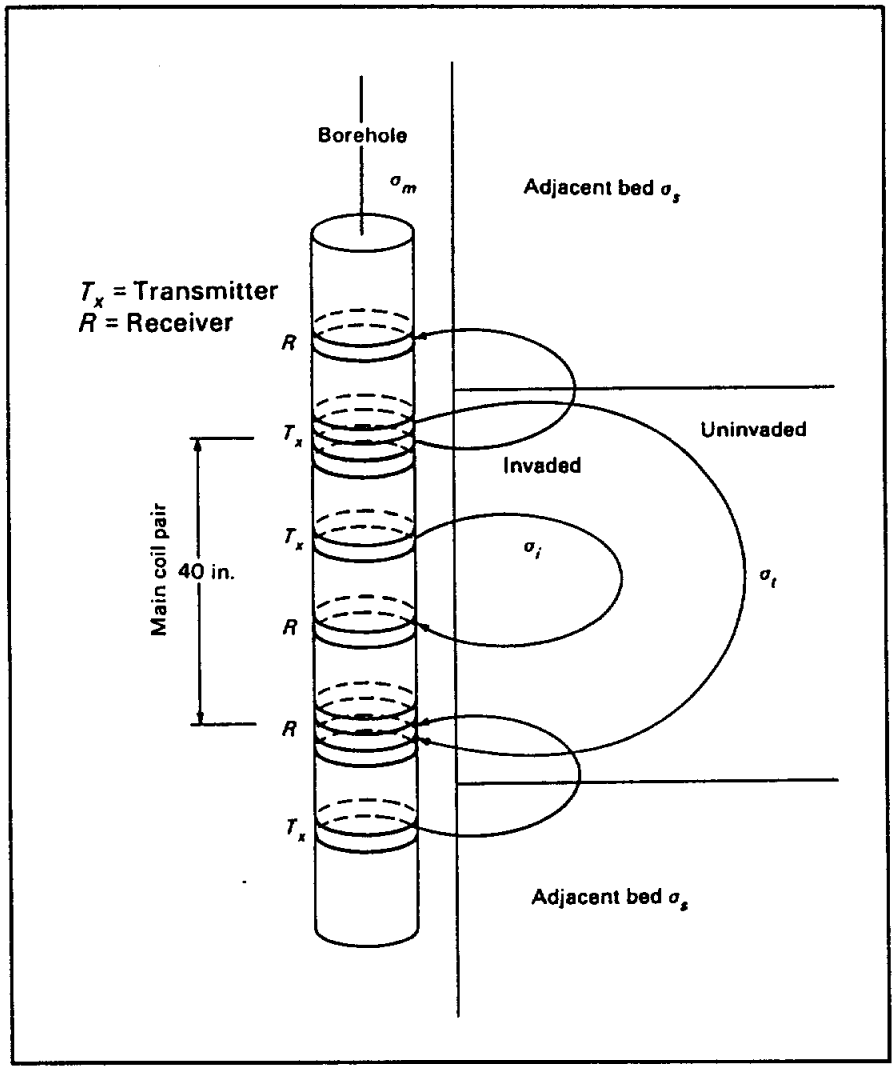

Figure 9-13. A focused induction tool uses additional transmitter and receiver coils to focus the main coil pair. This conceptual tool follows Schlumberger's 6FF40. Conductivity is σ and the subscripts are mud (m), invaded zone (i), uninvaded zone (t), and adjacent bed (s) (From Etnyre, 1989).

Vertical resolution is about 3 feet for the medium induction and 4 to 5 feet for the deep induction. Depth of investigation is greater than 5 feet for the deep induction, about 3 feet for the medium, and about 4 feet for the 6FF28 (Schlumberger, 1989).

Log presentation. Induction curves are always in tracks 2 and/or 3. The curves are displayed as resistivity. The only time that conductivity values appear on the log is on a 2 inch linear scale where the deep induction conductivity is in track 3 (Figure 9-14). The conductivity values can be used as a quality control check of the log (Figure 9-14). The deep induction curve is long dashes, the medium induction curve is short dashes, and the shallow reading curve such as the SFL or Guard is a solid line (Figure 9-15).

Environmental corrections. Departure curves are available for all the conventional tools but are not available for the Geonics and Century tools. Corrections must be applied in the proper order: borehole, bed thickness, invasion. Departure curves apply only to a particular brand of tool.

Borehole corrections. Figure 9-16 is the borehole correction chart for Schlumberger's deep and medium induction tools. This chart illustrates several important principles of borehole corrections that apply to all tools.

1. R_m's greater than 1 ohm-meter require virtually no correction to any of the tools, no matter what the hole diameter and whether or not a standoff is used. The fresher the mud, the less the correction. Air is a perfect medium for the tool. Most water well muds are fresher than 1 ohm-meter and therefore require no borehole correction.

2. As R_m decreases below 1 ohm-meter, borehole corrections can become significant depending on hole size and whether or not a standoff is used. R_m's below 1 ohm-meter will commonly be encountered in many petroleum wells.

    a. In almost all cases, for all induction tools, R_a is less than R_t.
    b. Using a standoff, which is a rubber fin device designed to keep the tool away from the borehole wall, significantly decreases the borehole correction. Also, it is difficult to get a good repeat log without a standoff (Etnyre, 1989). A 1.5 inch standoff is standard, but other sizes are available.
    c. The deep induction with a standoff requires little correction in boreholes less than 12 inches in diameter no matter what the R_m.
    d. The medium induction requires little correction in boreholes less than 9 inches in diameter no matter what the R_m. Above 9

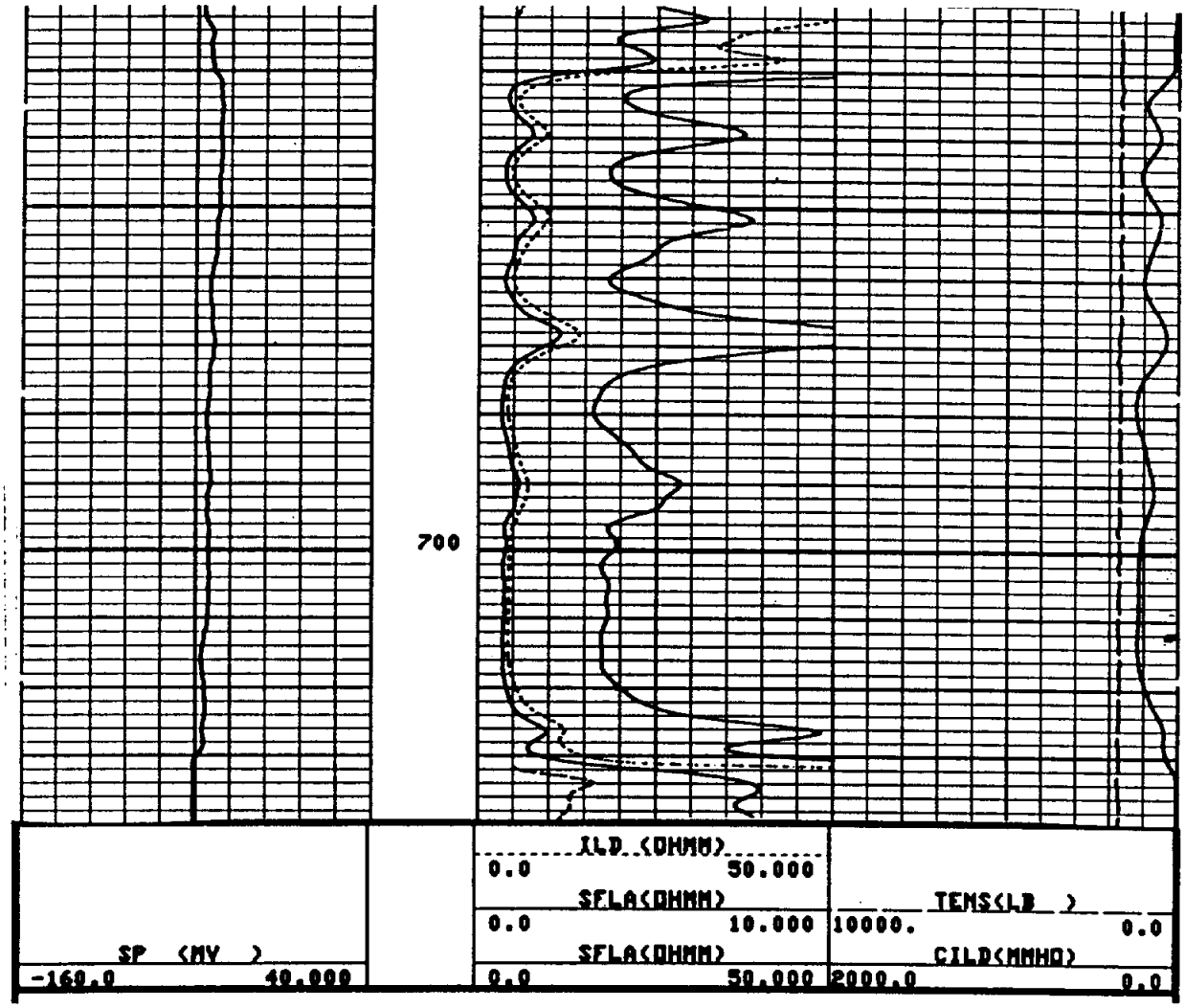

Figure 9-14. Typical log presentation of the deep induction (ILD) and shallow focused (SFLA) curves, along with the deep induction conductivity (CILD) curves. An amplified SFLA curve (0 to 10 ohm-meters) is also present. It is not needed and is just cluttering the log. The conductivity curve should be used as a quality control check of ILD. The induction curve is wrong as evidenced by:

1. The conductivity curve (C_{ILD}) reads less than 0, which is an impossibility. The tool was miscalibrated. A statistical study indicated that the C_{ILD} zero was actually -25 mmhos. This being the case, all R_{ILD} data above 40 ohm-meters (25 mmhos) was lost.
2. R_{ILD} is greater than R_{SFL} in shales, when it should be R_{ILD} is less than or equal to R_{SFL}.
3. At 730-50 feet R_{ILD} is 150 ohm-meters (6.7 millimhos) and R_{SFL} is 40 ohm-meters (25 millimhos). The two curves should be reading about the same because the bed is porous (40 percent porosity) and the flat SP indicates that R_{mf} is close to R_w. By adding a 25 millimho correction to R_{ILD}, the two curves are now close: 31 ohm-meters (32.7 millimhos) versus 40 ohm-meters (25 millimhos). R_{ILD} reads 40 ohm-meters after a bed thickness correction is applied.

The log is the Gulf Coast aquifer and the lithology is alternating sandstone and shale. The well is the Alsay, Cypress Creek U.D. #3, Harris County, Texas. Bit size is 9⅞. At formation temperature (82° F). R_m is 15.5 ohm-meters and R_{mf} is 8.2 ohm-meters.

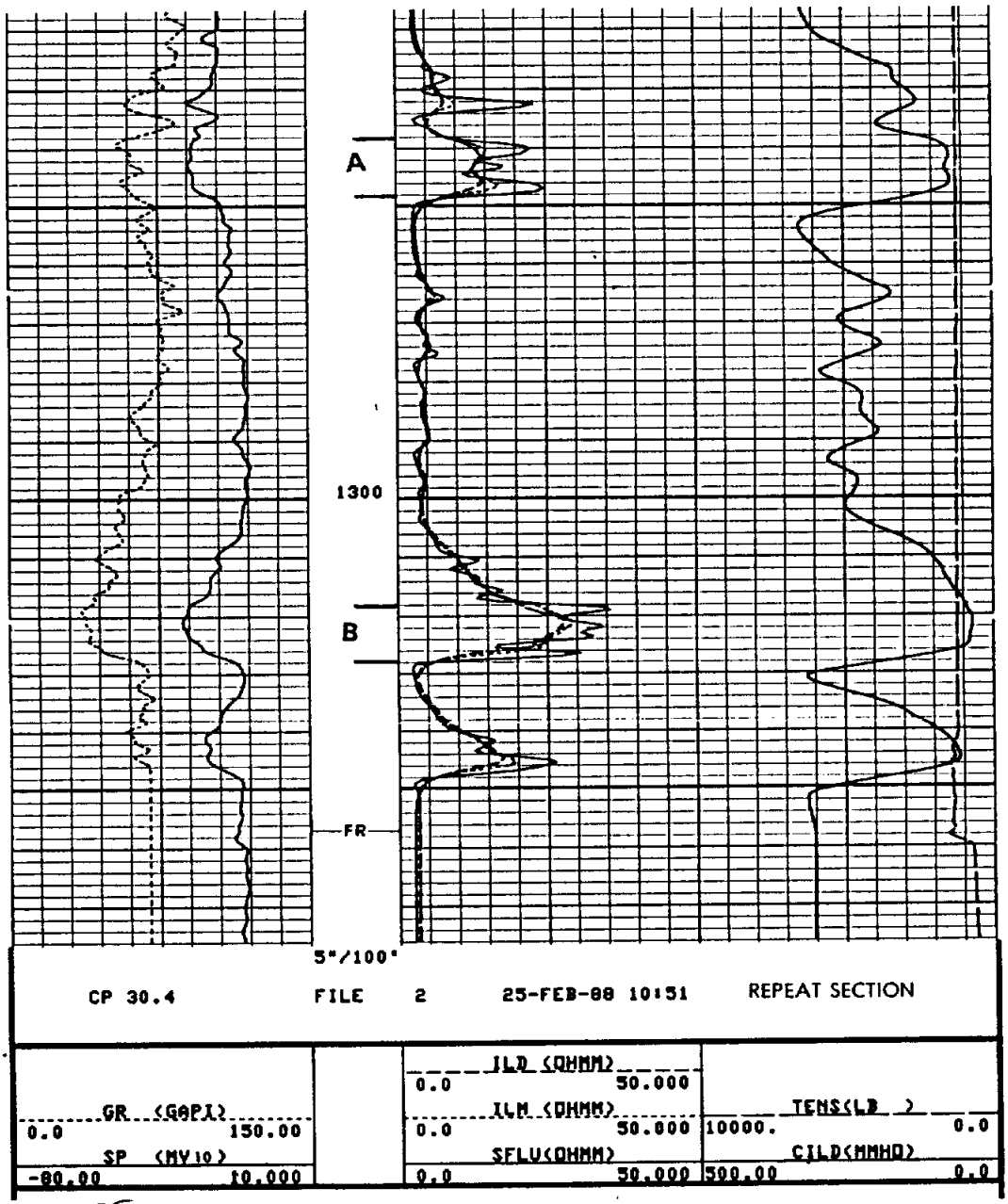

Figure 9-15. Dual Induction-SFL log on a 5-inch linear scale. The deep induction conductivity (CILD) curve is in track 3. SFLU means that the SFL is unaveraged. The SFL curve has much better vertical resolution than the induction curves. The resolution of the SFL is similar to that of the gamma ray curve. In Zones A and B the SFL reads higher than the induction curves, which read about the same. Without applying bed thickness/adjacent bed corrections these zones would be interpreted as having R_t less than R_{mf} and shallow invasion. After corrections are applied (Figures 9-17 and 9-18) the induction curves read the same as the SFL curve. Invasion is now interpreted as either being very shallow with all three curves reading R_t or R_{mf} equals R_w with any amount of invasion possible. Either scenario is possible. The log is alternating sandstones and shales of the Gulf Coast aquifer. The well is the Alsay, Kingwood B-3, Harris County, Texas. Bit size is 9⅞ inches. At formation temperature (92° F) R_m is 13.6 ohm-meters and R_{mf} is 8.4 ohm-meters.

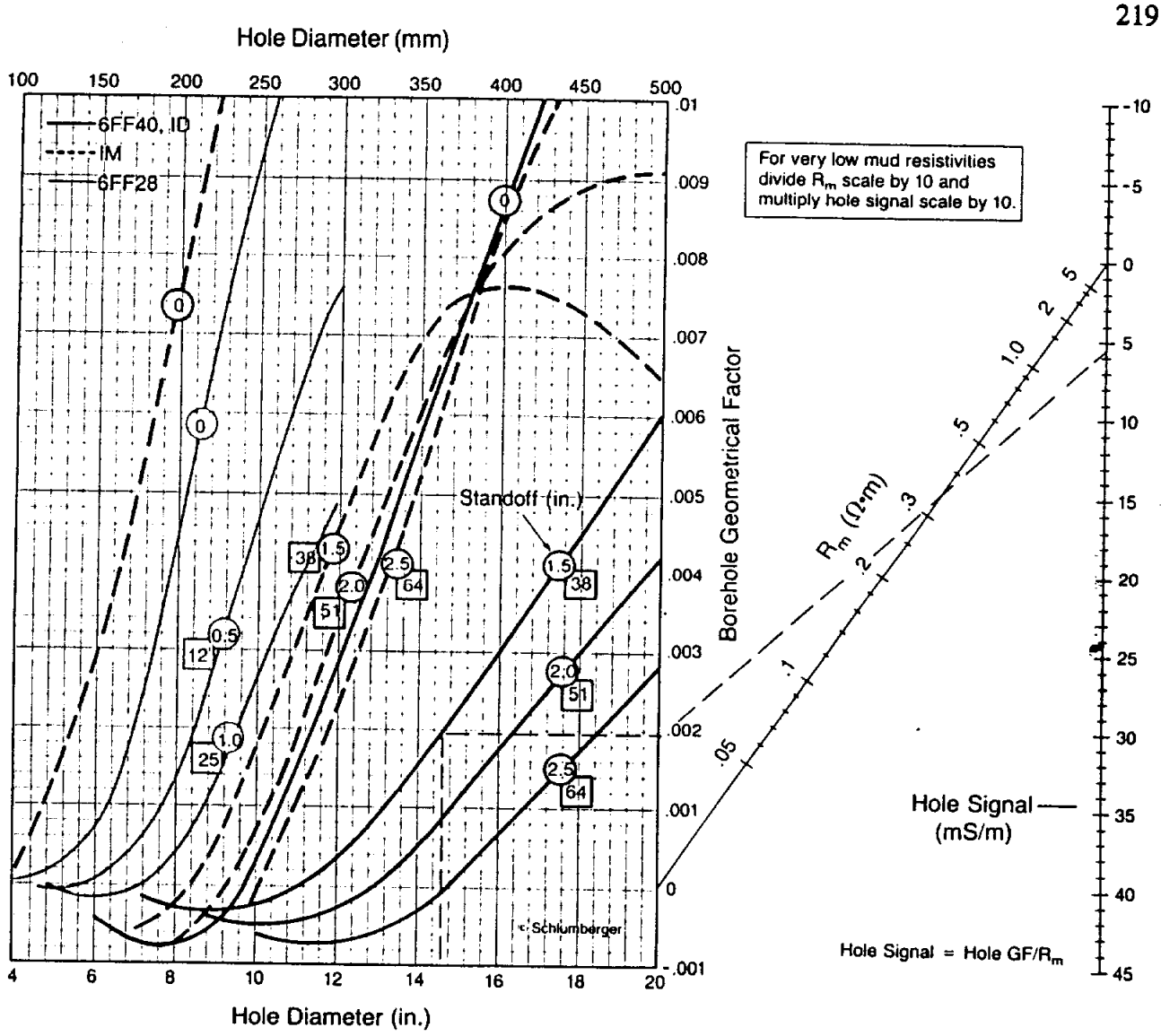

The hole-conductivity signal is to be subtracted, where necessary, from the induction log conductivity reading before other corrections are made.* This correction applies to all zones (including shoulder beds) having the same hole size and mud resistivity.

Rcor-4 gives corrections for 6FF40 or ID, IM, and 6FF28 for various wall standoffs. Dashed lines illustrate use of the chart for a 6FF40 sonde with a 1.5-in. standoff in a 14.6-in. borehole, and R_m = 0.35 Ω•m. The hole signal is found to be 5.5 mS/m. If the log reads R_t = 20 Ω•m, C_t (conductivity) = 50 mS/m. The corrected C_t is then (50 − 5.5) = 44.5 mS/m. R_t = 1000/44.5 = 22.4 Ω•m.

***CAUTION:** Some induction logs, especially in salty muds, are adjusted so that the hole signal for the nominal hole size is already subtracted out of the recorded curve. Refer to log heading.

Figure 9-16. Induction log borehole corrections for Schlumberger's tools. The size of the standoff is given in inches (circles) and in millimeters (squares) (From Schlumberger, 1989).

inches the correction is considerable and above 17 inches the amount of correction starts to decrease.

e. The medium induction requires more correction than the deep induction.

Borehole corrections assume round boreholes (Hilchie, 1982). Corrections for out-of-round boreholes are normally extremely difficult to make, if for no other reason than because three- and four-arm calipers are seldom available.

A borehole correction can be applied as the log is being run. A notation to this effect should be on the log heading. The correction will be for a particular bit size. If borehole enlargements in a zone of interest are larger than this, additional corrections will be made.

Remember that borehole corrections will not be needed as long as Rm's are greater than 1 ohm-meter, which includes almost all water wells. It also includes the shallow part of many petroleum logs where the water-bearing units have less than 50,000 ppm TDS. Drilling practices (not mudding up until the borehole is below this depth), and the lengthy amount of time this interval of the borehole is exposed, usually creates considerable borehole enlargement. However, as long as Rm is greater than 1 ohm-meter, borehole enlargements in this interval will not affect the induction tools.

Bed thickness and adjacent bed corrections. Figures 9-17 and 9-18 are Schlumberger's resistive bed departure curves for the deep and medium induction tools. Resistive beds are by definition any bed that is more resistive than its surrounding beds. The charts were constructed assuming thick, homogenous adjacent beds. The charts also assume a shoulder-bed resistivity (SBR) of 1 ohm-meter. The SBR setting, which is recorded on the log heading, is a filtering process designed to improve tool response (Etnyre, 1989). These charts illustrate several important principles of bed thickness and adjacent bed corrections of resistive beds that apply to all induction tools.

1. Ra decreases as Rs decreases. For each tool there are departure curves for Rs values of 1, 2, 4, and 10 ohm-meters. These conditions correspond to sandstones with fresh to moderately saline water surrounded by shale. They can also include formations with waters up to 50,000 ppm TDS depending on how low the porosity is.

INDUCTION LOG BED THICKNESS CORRECTION

6FF40 or ILd and 6FF28

These charts give bed thickness corrections for the 6FF40, ILd, and 6FF28 in beds thicker than 4 feet (1.2 m). A skin-effect* correction is included in these charts. Select appropriate chart for value of adjacent-bed resistivity (R_s). Enter the bed thickness and proceed upward to the proper R_{IL} curve. Read ordinate values of $(R_{IL})_{cor}$.

To use these curves for the small-diameter 6FF28, simply multiply the bed thickness by the ratio of the spacings. For a 6FF28 tool reading in a 7-ft bed, the bed thickness used to enter the chart is $40/28 \times 7 = 10$ ft.

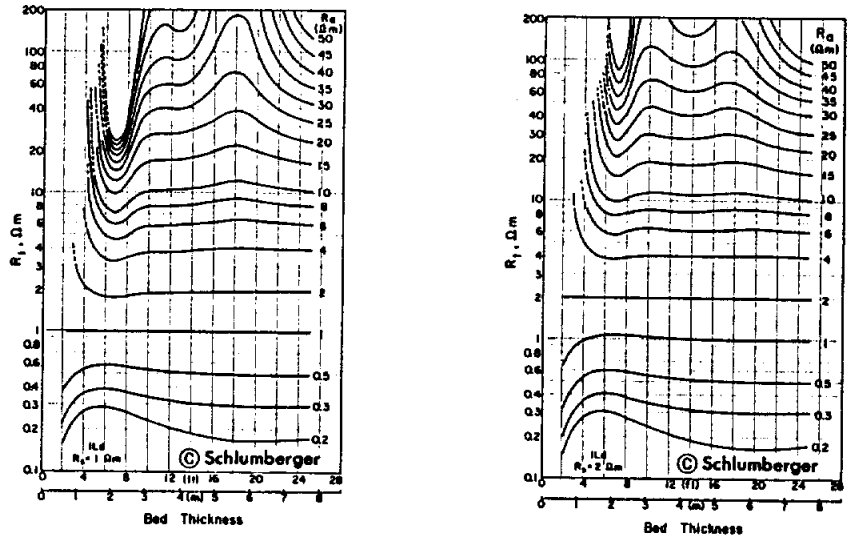

NOTE: These corrections are computed for a shoulder-bed resistivity (SBR) setting of 1 Ω·m. Refer to log heading.

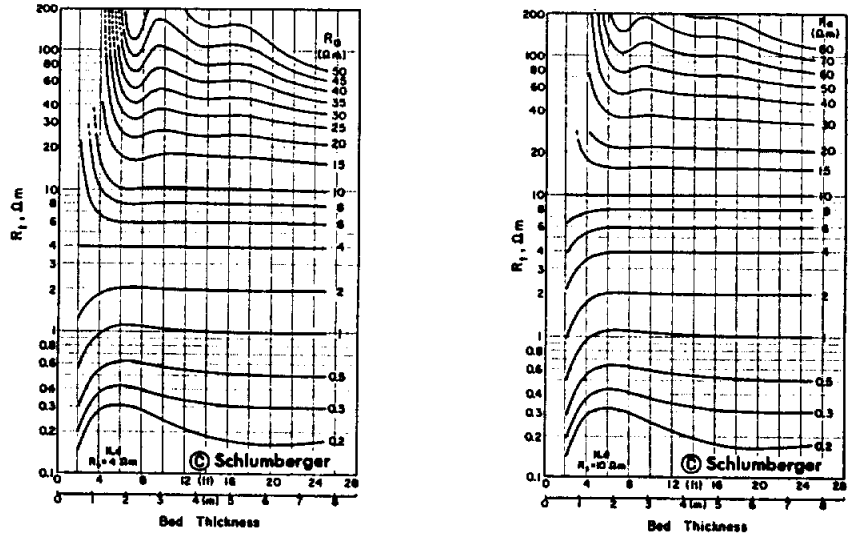

* Skin effect corrections are made automatically by Schlumberger induction tools. However, these internal corrections are necessarily based on the total conductivity signal measured by the tool, and are therefore correct only in homogeneous, anisotropic beds of considerable extent. In thin beds, adjustments are needed to the corrections made by the tool, and are included in these charts.

Figure 9-17. Schlumberger's bed thickness and adjacent bed corrections for the deep induction tool in cases of resistive beds. Charts are for R_s's of 1, 2, 4, and 10 ohm-meters (From Schlumberger, 1979).

INDUCTION LOG BED THICKNESS CORRECTION

ILm

These charts are for the ILm in beds thicker than 4 feet (1.2 m). A skin-effect* correction is included in these charts. Select appropriate chart for value of adjacent-bed resistivity (R_s). Enter the bed thickness and proceed upward to the proper R_{IL} curve. Read ordinate values of $(R_{IL})_{cor}$.

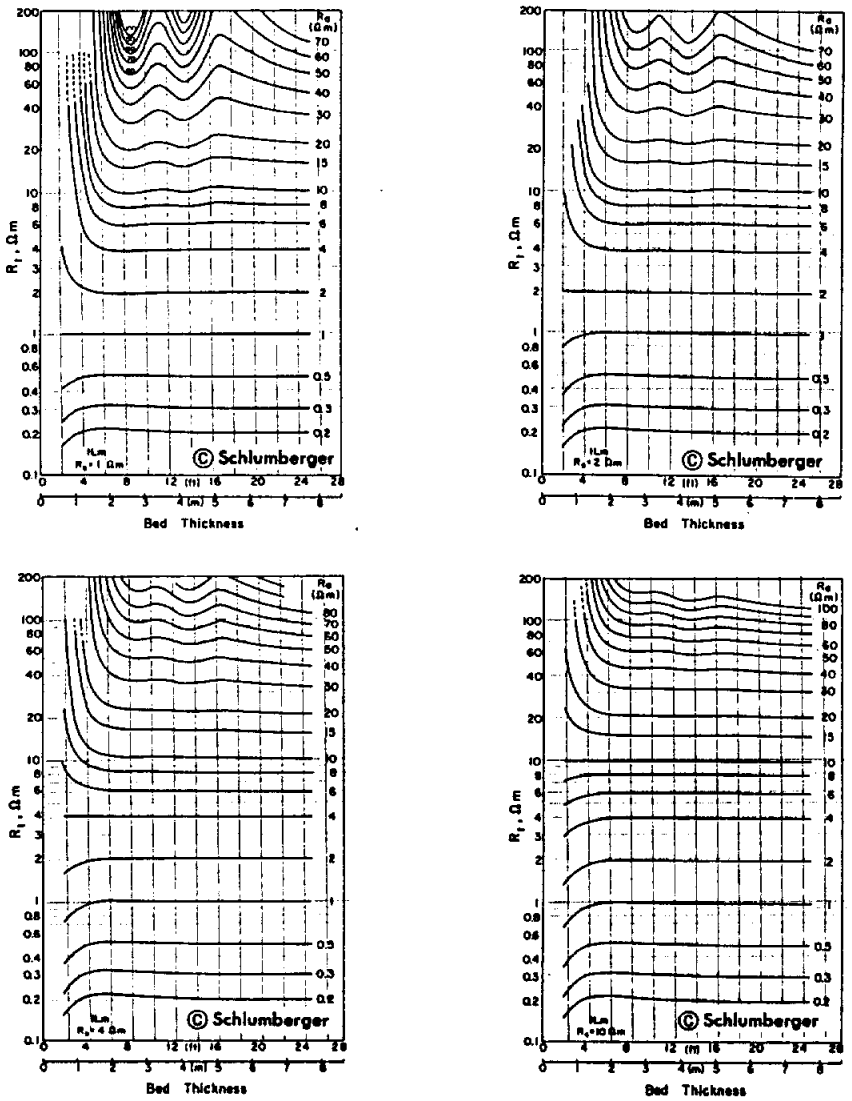

* Skin effect corrections are made automatically by Schlumberger Induction tools. However, these internal corrections are necessarily based on the total conductivity signal measured by the tool, and are therefore correct only in homogeneous, anisotropic beds of considerable extent. In thin beds, adjustments are needed to the corrections made by the tool, and are included in these charts.

Figure 9-18. Schlumberger's bed thickness and adjacent bed corrections for the medium induction tool in cases of resistive beds. Charts are for R_s's of 1, 2, 4, and 10 ohm-meters (From Schlumberger, 1979).

2. Beds less than 5 feet thick cannot be corrected to Rt.

3. The deep induction reads much lower Ra's than the medium.

4. The deep induction requires correcting for a wide range of bed thicknesses and Rs's.

   a. Ra's above 20 ohm-meters are significantly lower than Rt when Rs is less than 4 ohm-meters. For an Rs of 10 ohm-meters, Ra's above 40 ohm-meters are significantly less than Rt.
   b. Beds up to 28 feet thick read much lower than Rt.
   c. In some circumstances a thick bed may require more correction than a thin bed with the same Rt.

Bed thickness and adjacent bed corrections for resistive beds are often overlooked by log analysts. They are extremely important in ground-water log analysis. Formations with fresh to moderately saline water that are less than 30 feet thick will have an Ra that is too low (Figure 9-15). Low porosity beds less than 30 feet thick will have a pseudoinvasion profile and appear to be permeable (Figure 7-13). The deep induction will be less than the shallow reading tool, so it will appear that Rw is less than Rmf.

A bed thickness correction must always be applied before making invasion corrections. Unfortunately, the bed thickness correction cannot be made by a computer program. Some computer programs calculate invasion bed corrections. This

(might be helpful to elaborate why not, for the un-knowledgeable?)

quire any correction.
tion. This correction will
erwise nonporous
r would not require this
onductive bed correction
n.

(Somehow need to get a context setting first -- it's really a strange statement for those who don't grasp its background.)

(i.e. "reading" -- during the logging?)

(Or -- isn't the service companies don't provide it?)

are examples of invasion
ornado chart (due to its
of Rt less than Rxo
They are constructed for
a particular tool string (Figure 9-15 is for Schlumberger's DIL-SFL, DIS-EA type tool) and for a given set of borehole conditions (thick beds, 8 inch hole,

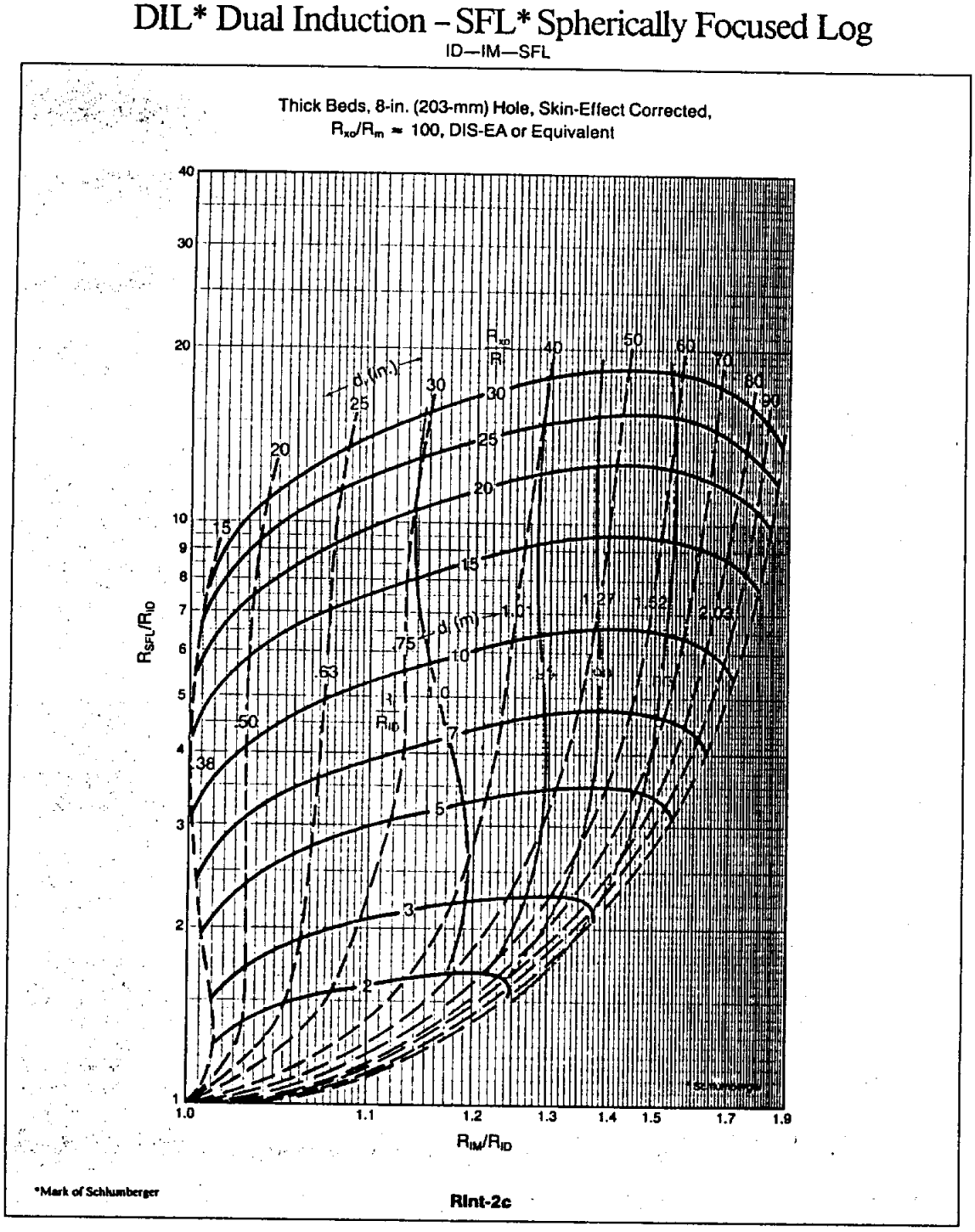

Figure 9-19. Schlumberger invasion correction chart for the DIL-SFL tool. This chart is used when R_t is less than R_i. R_{ID} is the deep induction curve, R_{IM} is the medium induction curve, and R_{SFL} is the SFL curve (Schlumberger, 1988).

and Rxo/Rm of 100 for Figure 9-19). Most tornado charts, including Figure 9-19, require the log to have been corrected for skin effect (see the following section on skin effect). Most induction logs have been corrected for skin effect and a notation to this effect should be on the heading.

Tornado charts are used to correct the deep induction tool for the effects of invasion. The chart also estimates the diameter of invasion and Rxo.

The charts should be utilized according to the following guidelines:

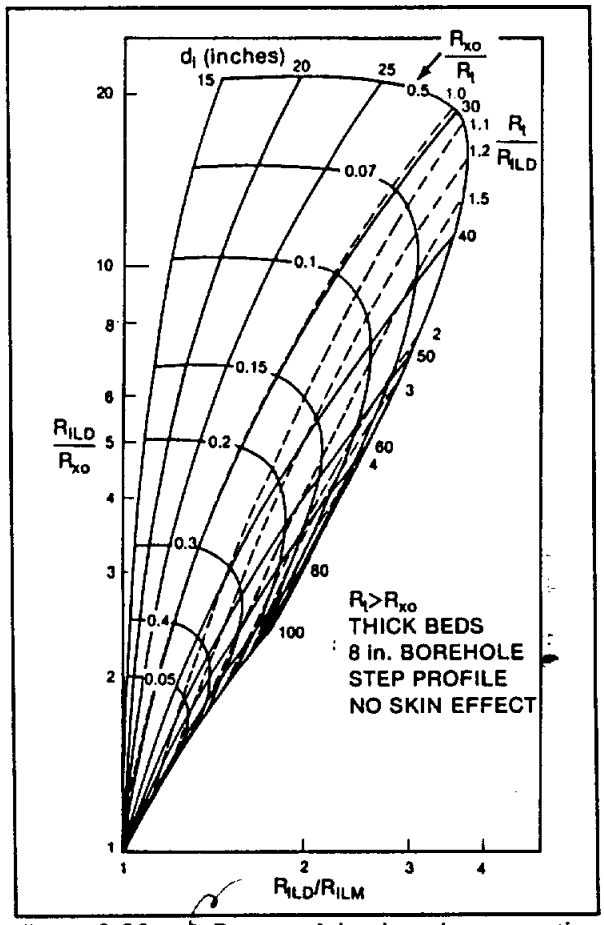

Figure 9-20. Dresser Atlas invasion correction chart for when Rt > Rxo. Uses an Rxo log, if available (From Dresser Atlas, 1982).

1. The induction log must first be corrected for borehole, bed thickness, and adjacent bed effects.

2. The appropriate invasion chart must be selected according to the service company and tool string.

3. If a skin effect is required by the chart, it is essential that a skin-effect correction was applied to the log.

4. The appropriate chart is selected according to whether Rt/Rxo is less than 1 or greater than 1. Charts for Rt greater than Rxo are not readily available. The logging company that ran the log may be able to provide a chart.

5. The R_{IM}/R_{ID} and R_{SFL}/R_{ID} values are then entered in the chart. The point at which the values intersect defines the diameter of the invasion, Rt/R_{ID}, and Rxo/Rt.

6. The value of Rt/R_{ID} multiplied by R_{ID} equals Rt.

7. The value of R_{xo}/R_t multiplied by R_t equals R_{xo}. Much credence should not be assigned to the R_{xo} value. It will not usually be accurate enough to use in the R_{xo}/R_t method of determining water quality.

Several important principles about invasion corrections can be gleaned from Figures 9-19 and 9-20:

1. If the diameter of invasion is shallow to moderate (less than 35 inches), the deep induction reads R_t. This also can be stated in terms of R_{IM}/R_{ID} being less than 1.2. This condition will usually be satisfied in high porosity sandstones such as the Gulf Coast and Carrizo-Wilcox aquifers, low water loss muds, and the part of the borehole close to T.D.

2. For diameters of invasion beyond 35 inches, the effect of invasion on R_a is a function of the contrast between R_i and R_t plus the depth of invasion.

3. As the diameter of invasion increases, the difference between the deep and medium curves increases.

4. For deep invasion when R_t is less than R_i, R_a is greater than R_t.

5. For deep invasion when R_t is greater than R_i, R_a is less than R_t.

6. For the case of R_t greater than R_i, the dual induction works within certain limitations.

    a. An R_{xo} value (MSFL, Microlaterolog, etc.) needs to replace the shallow reading value (SFL, Focused Log, Guard, etc.) on the chart. This is because a shallow reading device is overly influenced by R_t under these conditions and as depth of invasion changes the shallow reading tool will not show much change (Dresser Atlas, 1982). An independent value of R_{xo} is needed.
    b. To make a valid correction with the chart, invasion diameter should be less than 35 inches.
    c. Beyond an invasion diameter of 35 inches, the deep induction resistivity (R_a) rapidly drops lower than R_t. At an invasion diameter of 50 inches R_a is half of R_t. This change is much

more rapid than when Rt is less than Ri (Figure 9-20). When at 50 inches, Ra is only 12 percent different than Rt.

The explanation for this goes back to the theory of induction measurements. Because the invaded zone and the uninvaded zone act in parallel for the induction tool, the higher conductivity contributes more to the zone with the log value (Dresser Atlas, 1982). Therefore, the influence of invasion on the induction tool is greater if the invaded zone has a lower resistivity than the uninvaded zone, or to put it another way, if Rmf is less than Rw. When Rmf is greater than Rw, the invaded zone does not contribute as much to the conductivity signal and the deep induction is not as dramatically affected. This goes back to Figure 9-8 and explains the differences between induction and laterologs. The deep induction gives its best measurement of Rt when a resistive fluid (Rmf > Rw) occupies the invaded zone. The dominant influence on the induction will be the more conductive uninvaded zone. On the other hand, the laterolog gives its best measurement of Rt when a conductive fluid (Rmf < Rw) occupies the invaded zone. The dominant influence on the laterolog will be the more resistive uninvaded zone. The induction tool works best when Rmf/Rw is greater than 3.

If the invasion diameter is definitely less than 35 inches in the zone of interest, an invasion correction is not needed. Such cases are low water loss muds and high porosity sandstones. If the invasion diameter is possibly greater than 35 inches, an invasion correction should be done after borehole, bed thickness, and adjacent bed corrections have been made. When invasion is deep, if Rt > Ri (restated as Rw > Rmf) then Ra is less than Rt, and if Rt < Ri (restated as Rw < Rmf) then Ra is greater than Rt.

Sonde error. Even after proper calibration, the DIL has a sonde error of ±2 mmhos/m. The sonde error is due to an imbalance in the receiver circuits or to residual coupling between the transmitter and receiver coils (Dewan, 1983). For low resistivity formations the error is not significant, but for a formation above 100 ohm-meters (10 mmhos/m) the error in the resistivity value is greater than or equal to 20 percent (see Table 9-2). Low to moderate porosity fresh water formations have Rt's of more than 100 ohm-meters and can therefore not be logged accurately with induction tools.

TABLE 9-2. THE EFFECT OF A SONDE ERROR ON THE Ra OF RESISTIVE AND CONDUCTIVE BEDS

	True Conductivity ohm-meters	True Resistivity mmhos/cm	Effect of a +2 mmhos/cm error on conductivity μmhos/cm	Effect of a +2 mmhos/cm error on resistivity ohm-meters	Effect of a -2 mmhos/cm error on conductivity μmhos/cm	Effect of a -2 mmhos/cm error on resistivity ohm-meters
Resistive Bed			2	83	8	125
Conductive Bed			2	19	48	21

check -- (are the circled terms reversed?) (Appear to be)

The so[illegible] d by downhole calibration in a low porosity, high[illegible]tion. Unfortunately, such a formation will not be present in most water wells.

Skin effect. Skin effect, more properly called propagation effect, is a reduction of the conductivity signal generated in a formation due to interference between the current ground loops. It makes the formation (and therefore Rw) appear more resistive than it actually is. Skin effect increases as formation conductivity increases and as the transmitter-receiver coil spacings increase. The phenomenon is predictable and can be automatically corrected. The correction should be noted on the log heading. Skin effect only becomes significant when Rt is less than 1 ohm-meter (Schlumberger, 1989), which corresponds to a water conductivity of 60,000 μmhos/cm or greater. Therefore, skin effect is normally of no consequence to groundwater log analysis.

Interpretation. Bed boundaries are best picked in combination with other curves (Figure 9-21, Zones C and D). Usually, however, bed boundaries are more accurately picked from another curve: gamma ray, shallow focused curve, or microlog. In thin resistive or conductive beds the peaks point in the right direction, but low values are not low enough for conductive beds and for resistive beds the values are not high enough (Figure 9-21, Zones A and B). In thick beds an average value is taken for Ra (Figure 9-21, Zone C). Some intervals are best zoned into two or more resistivity values (Figure 9-21, Zone D).

In shales, induction values will be either equal to or less than the shallow reading curve. An isotropic shale makes the curve read too low.

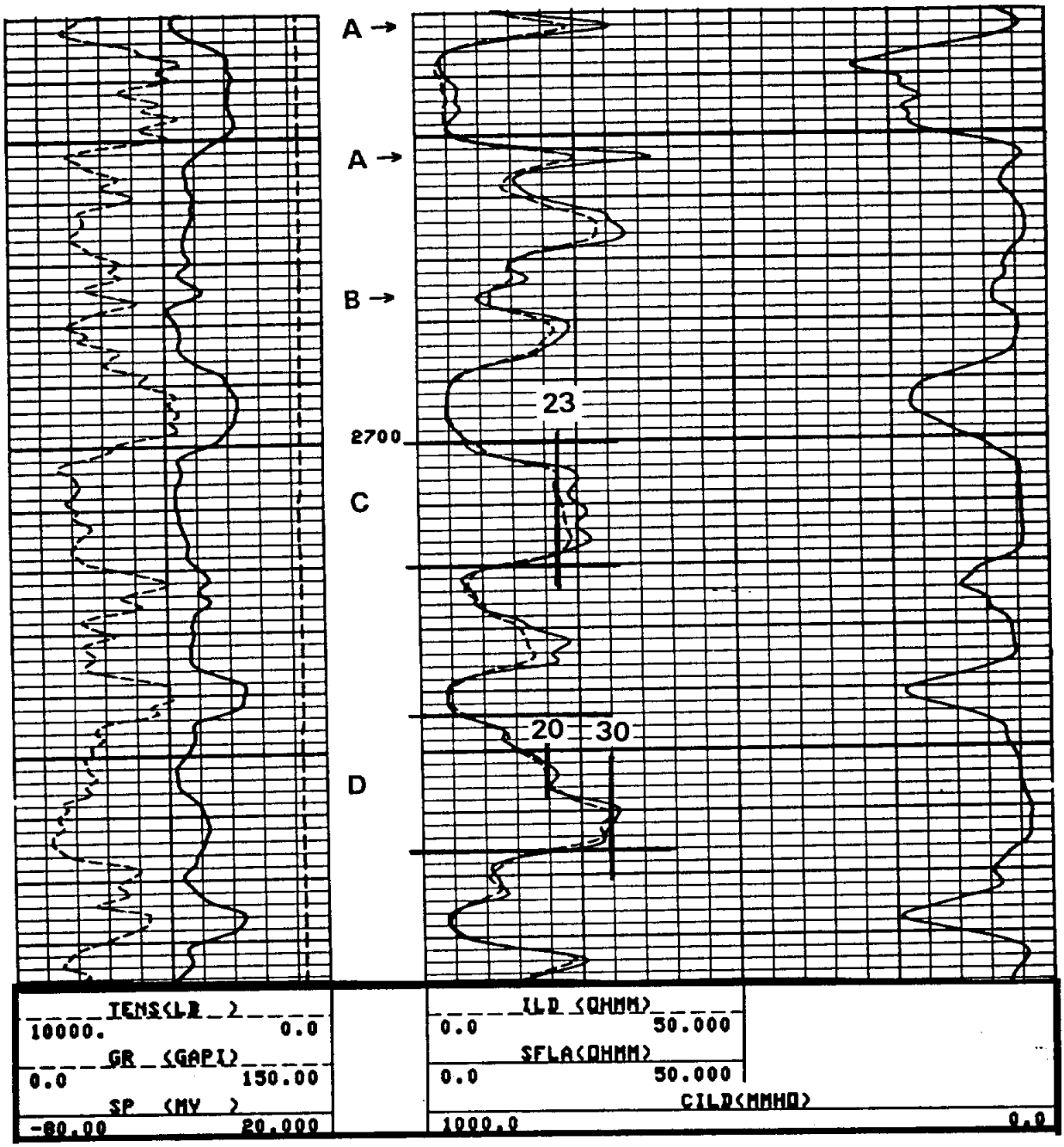

Figure 9-21. This log illustrates how to pick bed boundaries and resistivity values on an induction log. Zones A are more resistive than they appear to be on the ILD curve (as confirmed by the SFL curve). The resistivities are decreased by the conductive side beds. Zone B is a shale bed less than 2 feet thick. It shows to be conductive but due to the more resistive side beds the resistivity is not low enough. Zone C has an average value of 23 ohm-meters. Zone D is best divided into two intervals with an average value taken for each (20 ohm-meters and 30 ohm-meters). The bed boundaries for both C and D are best picked from the gamma ray curve. Only the lower boundaries match the midpoint on the resistivity curves. The SFL has been averaged (SFLA) to smooth the curve out and make it agree better with the poorer resolution of the ILD. The logging tool is a DIL-SFL. The ILM was left off at the request of the drilling contractor. The log is the Paluxy Sandstone. The well is the J.L. Myers, City of Van Alstyne #3, Grayson County, Texas. Bit size is 9¾ inches. R_m is 5.4 ohm-meters and R_{mf} is 4.3 ohm-meters at formation temperature (98° F).

It has nothing to do with invasion. This explains the separation between the shales at 370 to 384 feet and 474 to 520 feet in Figure 8-19.

The resistivity tool with the smallest emitter-receiver spacing has the best vertical resolution. The micrologs has the best vertical resolution, followed by R_{xo} tools, then shallow reading tools (SFL, Guard, short normal), laterologs, induction, and long normal. Lateral curves have good resolution, better than induction tools, as long as there is not interference from side beds (Figure 8-25).

For most logging suites the short normal or a shallow focused tool (Guard or SFL) will be the resistivity curve with the best vertical resolution. The curves can yield considerable geological information. They can be used as lithology/porosity indicators. The curves will respond to thin shale stringers and variations in porosity (Figures 8-19, 8-25, 9-15, and 9-22).

The amount of separation between the three curves is a function of the depth of invasion and the R_{mf}/R_w values. When plotted on a logarithmic scale this separation can be used to estimate the depth of invasion and R_w of porous permeable formations. As the depth of invasion increases the separation between ILM and ILD increases (Figure 6-4). This assumes that R_{mf} and R_w are not equal. If they are the same all three curves will agree no matter what the depth of invasion. If R_w is greater than R_m, R_{ILD} will be greater than $R_{shallow}$ and as the resistivity of the formation water increases in relation to R_{mf}, so will the separation between the two curves. If R_w is less than R_m, R_{ILD} will be less than $R_{shallow}$ and the separation will increase as R_m decreases. This technique is only valid if any needed borehole and bed thickness corrections have already been applied to the curves (Figure 9-15).

Recommended use. Induction tools provide accurate resistivity values if environmental corrections are first applied and if they are used in the appropriate environment (R_t is less than 100 ohm-meters and R_{mf}/R_w is greater than 3). In other environments focused electrode logs (Laterologs and Guard Logs) are the best choice. Figure 9-23 compares a deep laterolog and a deep induction. Induction logs do not require borehole corrections if R_m is greater than 1 ohm-meter. Bed thickness corrections are extremely important for resistive beds less than 30 feet thick. They should be applied routinely. Invasion corrections are only needed if the invasion diameter is greater than 35 inches. Induction tools are the only resistivity tool that will work in air-filled boreholes and in nonmetallic casing (Figure 9-24).

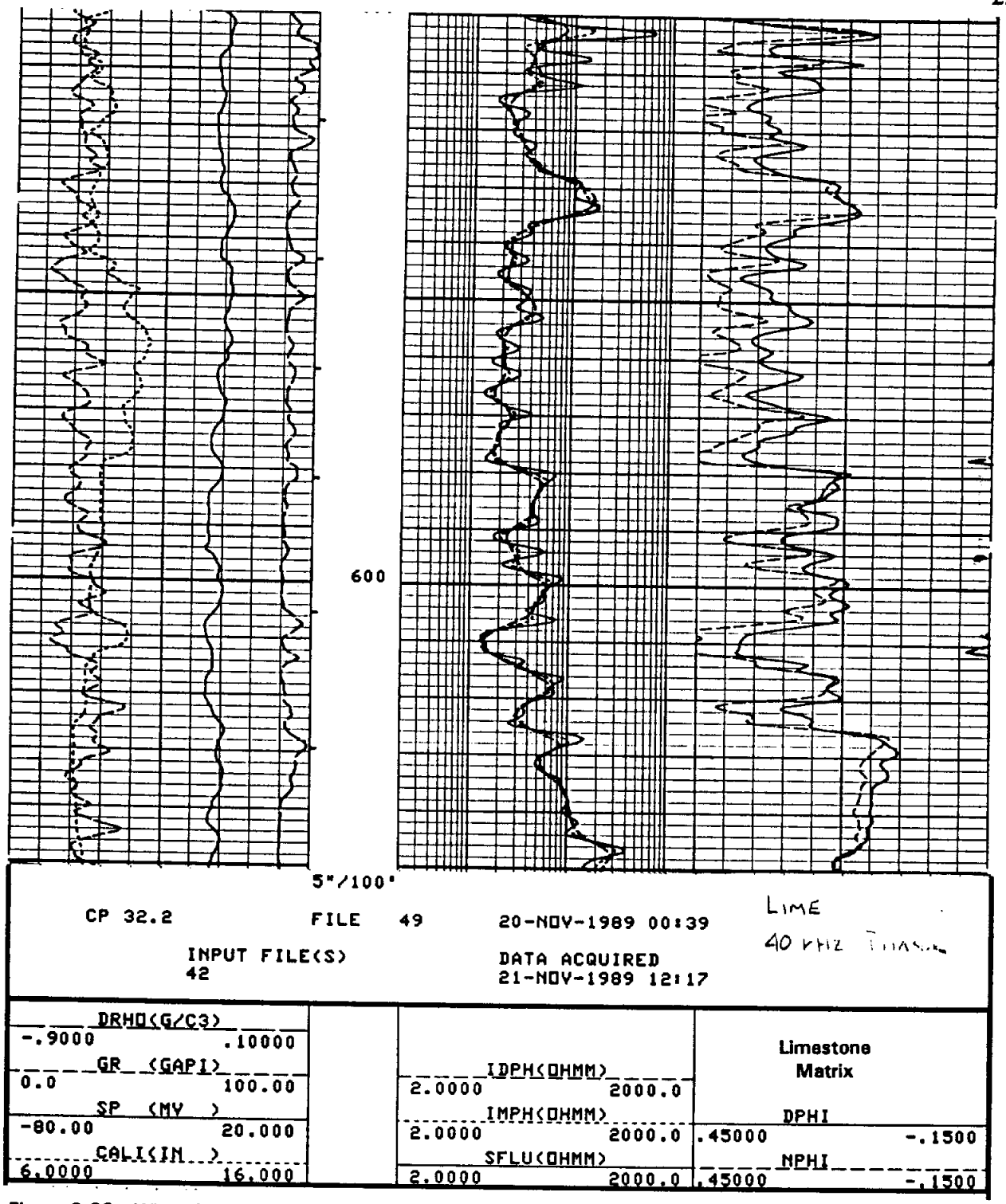

Figure 9-22. When Rw remains fairly constant over an interval, R_a is a function of porosity. The induction tool, a Phasor Induction SFL, follows very closely changes in porosity. The borehole fluid is the same as the formation water (the well was drilled reverse air-rotary), so the SP is flat. Bit size is 7⅞ inches. The log is an interval in the Edwards Aquifer. The well is the Edwards Underground Water District, B-1, New Braunfels, Texas (state well number 68-23-616). Figures 13-5, 13-8, 13-28, 13-32, and 13-33 are also from this well.

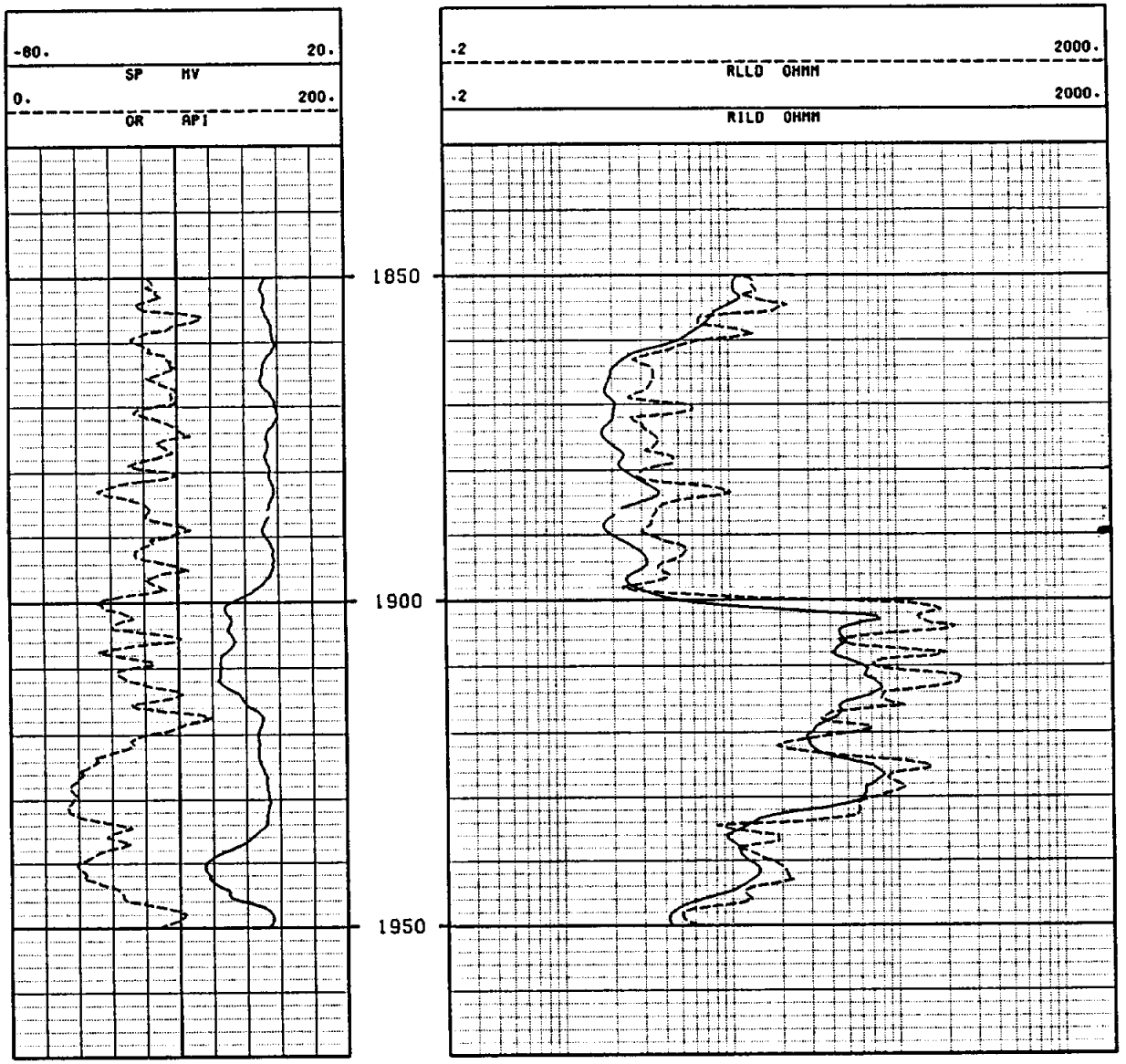

Figure 9-23. Comparison of a deep laterolog (R_{LLD}) and a deep induction (R_{ILD}). R_{LL} values are more accurate and have better bed resolution. The LL bed resolution is close to that of the gamma ray. The induction values are low by about 100 percent in thin beds because the tool is influenced by the surrounding shales. The induction curve requires extensive thin-bed corrections. Notice that the bed at 1920-34 feet is not a shale, even though it falls on the shale base line. The bed is not shale because the gamma ray values are low and the resistivity values are high. The zone has no SP deflection because it is a nonpermeable sandstone or limestone. The log is an interval in the Trinity Group. The well is the J.L. Myers, City of Van Alstyne #3, Grayson County, Texas. Bit size is 9¾ inches. At formation temperature (80° F) R_m is 6.6 ohm-meters and R_{mf} is 5.6 ohm-meters.

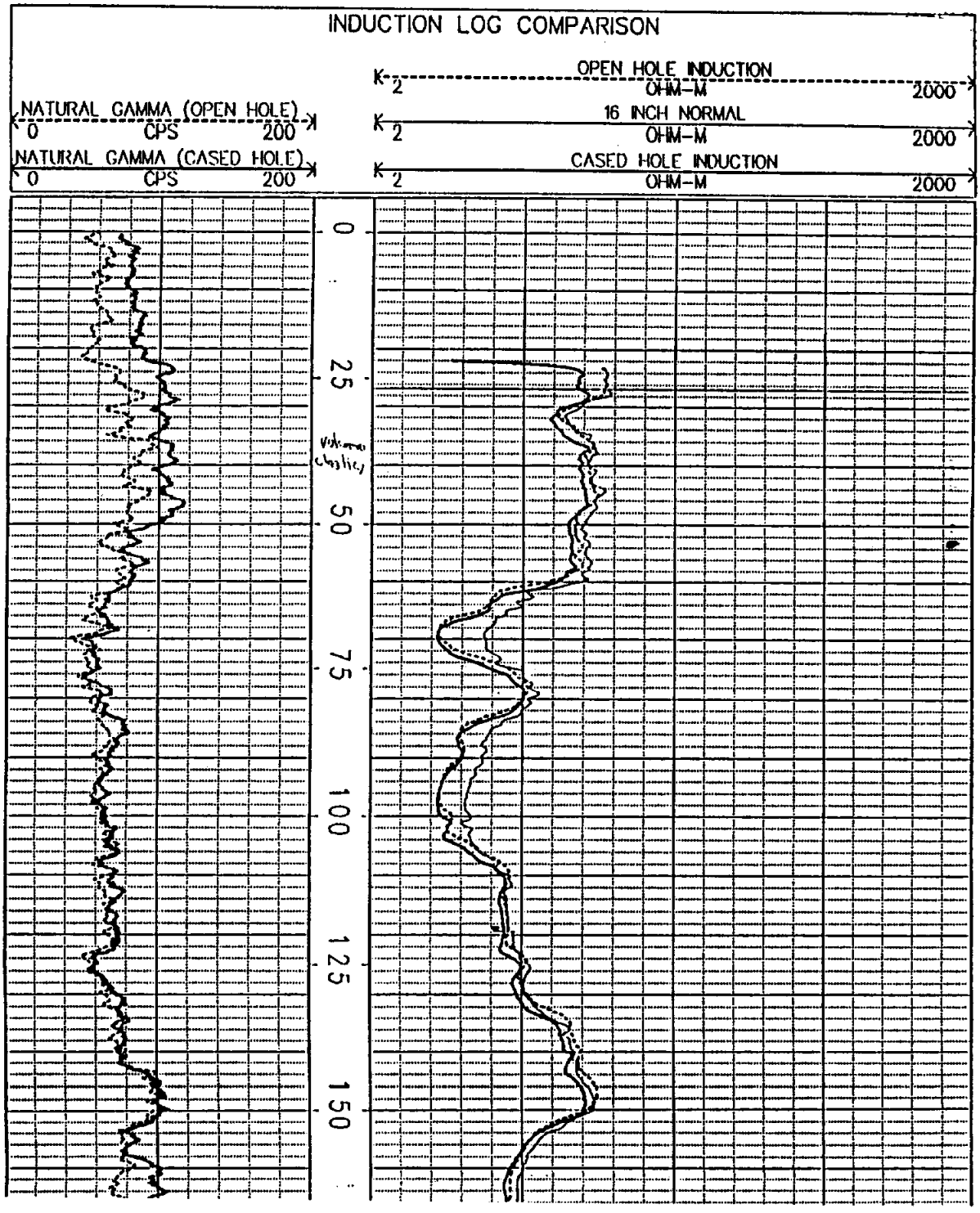

Figure 9-24. A comparison of a slimhole induction tool in a borehole (open and cased). The tool has excellent repeatability in the nonmetallic casing. The open hole diameter is 9 inches. The cased hole is 4 inch PVC and is grouted with 5 percent bentonite cement. The open and cased hole gamma rays also have excellent repeatability. The lithology is volcaniclastics. The well is in Colorado. The nature of the borehole fluid is not known.

Phasor Induction

The Phasor Induction SFL was introduced in the mid 1980's by Schlumberger. The tool makes the standard ILD and ILM (R-signals) measurements, plus a deep and a medium quadrate signal (X-signals). These four measurements are combined utilizing new advances in signal processing and electronics technology to produce an improved Dual Induction log (Schlumberger, 1989).

Most environmental corrections are done automatically by the tool. This was not possible with the DIL-SFL because of the nonlinearity of the R-signals, which were the only measurements made by the tool.

Advantages of the Phasor over the DIL include:

1. A calibration error of less than ± 1 mmho/m (versus ± 2 mmhos/m).
2. Thin bed resolution to 2 feet (versus 5 feet).
3. Most environmental corrections are automatic.
    a. Shoulder effect and thin bed resolution (not possible with the DIL)
    b. Invasion effects (not possible with the DIL)
    c. Skin effect (possible with the DIL)
    d. Borehole and cave effect (possible with the DIL)
    e. Large boreholes (DIL requires considerable correction)

Figure 7-13 is an example of a Phasor Induction. Figure 9-25 demonstrates the accuracy of the tool in a 23 inch hole.

The Phasor Induction should be used instead of the Dual Induction. It works fine in many conditions in which the Dual Laterolog is normally the preferred tool. The Phasor Induction will be the best induction tool until the Array Induction is readily available.

Slimhole tools

Only a few slimhole induction tools are available (Table 5-3). The slimhole tools are not as well focused as conventional size tools, and

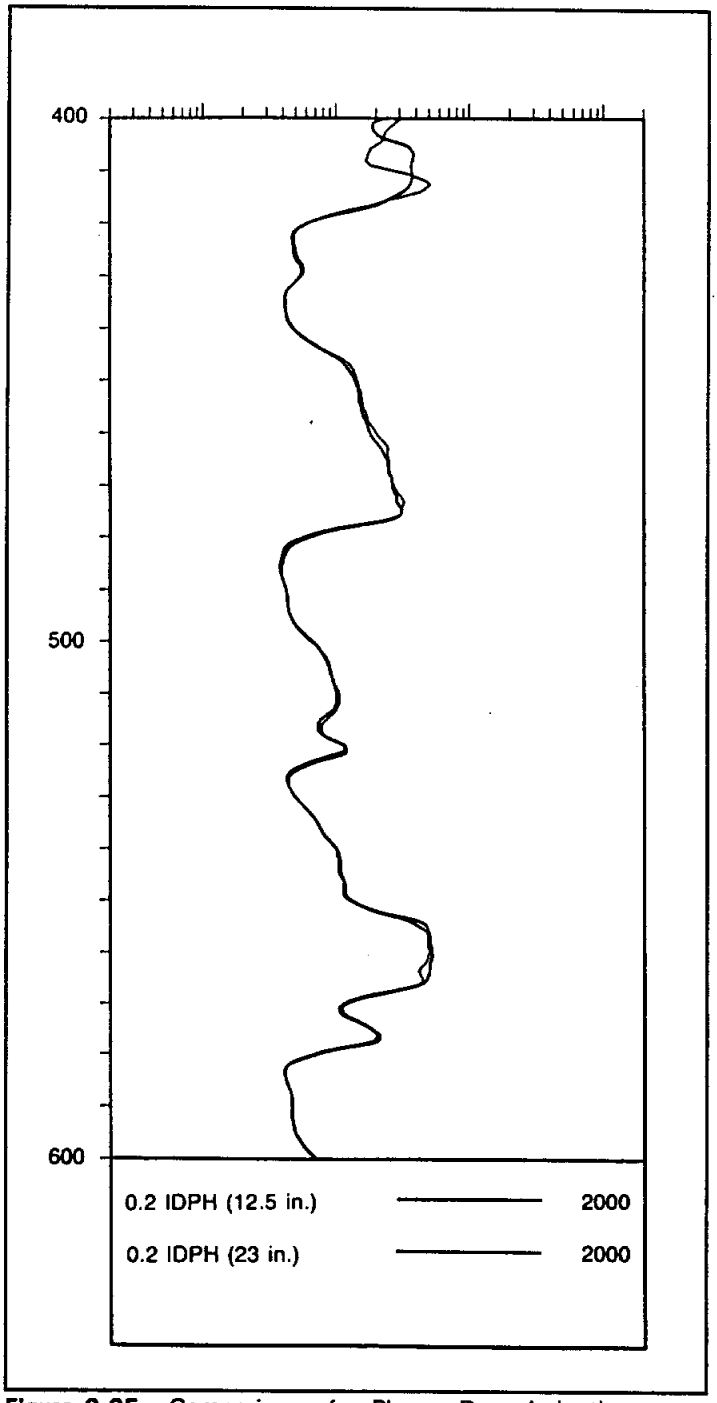

Figure 9-25. Comparison of a Phasor Deep Induction curve (IDPH) in a 12.5 inch diameter borehole that was then reemed to 23 inches (From Schlumberger, 1989).

environmental correction curves are not available. Taylor et al. (1989) is the only published evaluation of a slimhole induction tool.

Slimhole induction tools have numerous applications in groundwater/environmental studies. However, more and better tools need to be developed.

GAMMA RAY AND SPECTRAL GAMMA RAY TOOLS

Chapter 10

This chapter discusses two tools that are very useful for ground-water studies. The gamma ray should be a standard part of every ground-water logging suite. The spectral gamma ray is a specialized tool that should be run routinely in parts of the state which have problems with radioactive water.

Gamma Ray

The gamma ray tool measures the natural radioactivity of formations. The log is used to distinguish shale and clay from other rock types, to pick bed boundaries, to correlate, and to calculate shale volume in sandstones and carbonates. In this discussion shale and clay are used interchangeably.

The tool may be used in open or cased holes. It is usually run in combination with other tools. **Gamma ray** is the only name for the tool. A variety of slimhole and conventional tools are available.

The gamma ray curve correlates well with the SP curve (Figure 10-1). It is substituted for an SP curve when conditions are such that an SP curve is featureless (low porosity formations, air-filled and cased holes, and R_{mf} equal to R_w).

Tool theory. The gamma ray tool is basically just a gamma ray detector. Most conventional tools use a scintillation counter which consists of a sodium iodide crystal and a photomultiplier tube. Each gamma ray that strikes the crystal produces a light flash. The light flashes are converted to electrical pulses by the photomultiplier and multiplied into a voltage that can be counted. The tool records the number of pulses per unit of time.

Modern conventional tools and a few slimhole tools are scaled in API (American Petroleum Institute) units. An API unit is defined as $^1/_{200}$ of the response generated by a calibration standard at the University of Houston. The standard is composed of known amounts of uranium, potassium, and thorium. It was designed to have twice the gamma ray response of an average shale, which is considered to be 6 ppm (parts per million) uranium, 12 ppm thorium, and 2 percent by weight potassium (Dewan, 1983). Thus most shales measure about 100 API units.

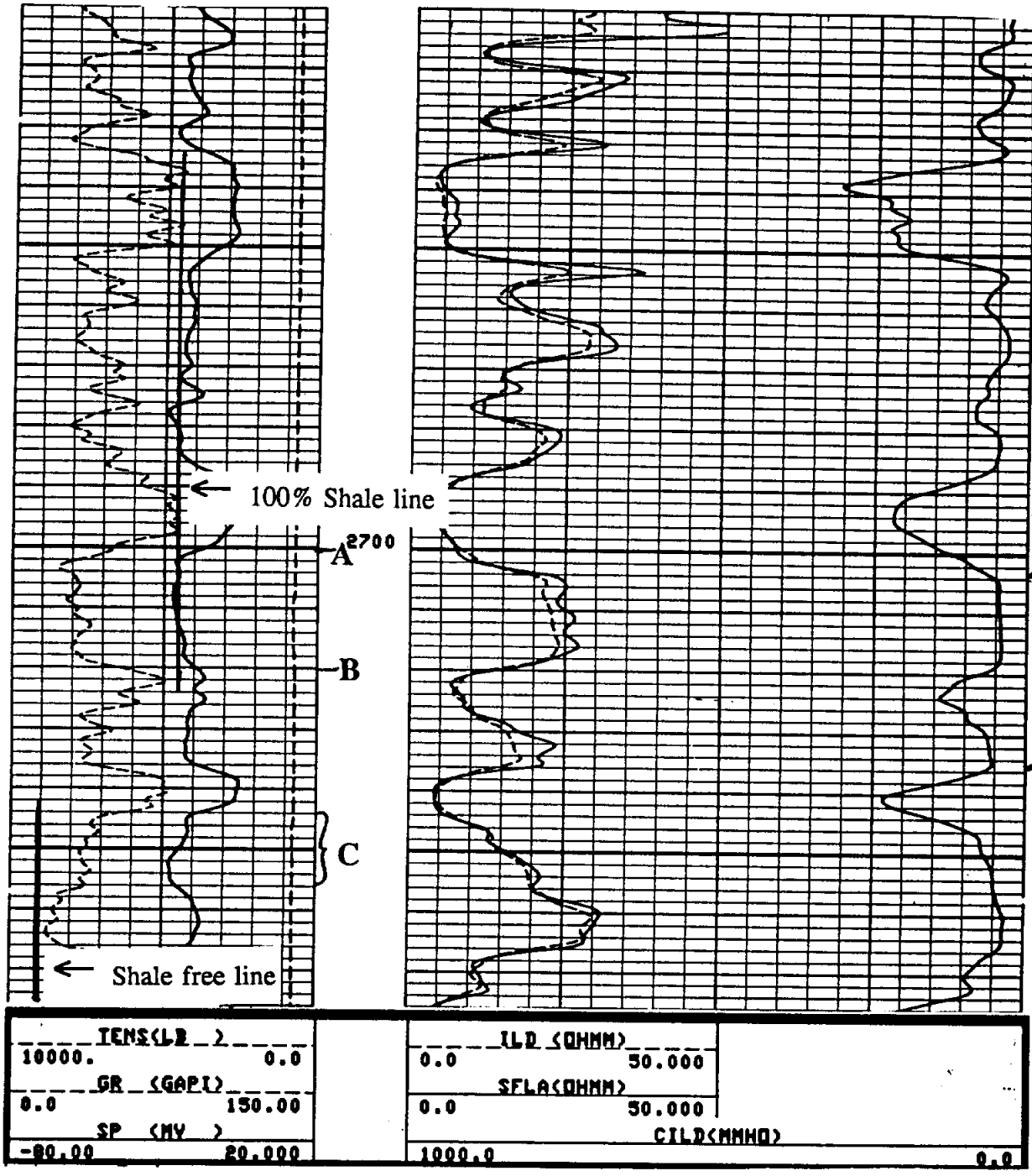

Figure 10-1. This log shows a typical gamma ray presentation. The gamma ray and SP curves are both scaled so that shale-free formations are to the left and shale content increases to the right. The SP and gamma ray curves correlate well, with the gamma ray having the best bed resolution. Bed boundaries are picked on the gamma ray curve half way between the high and low values. For example, point A at 2700 feet and point B at 2720 feet are the bed boundaries for a sandstone. The 100 percent shale line and the shale-free line have been drawn on the log. The shale content of zone C is approximately 24 percent. (The calculation is explained under the **Recommended Use** section in this chapter.) The bit size is 9⅞ inches and the mud is 9 lb/gal, fresh water bentonite. See Figure 9-21 for more information on this log.

Conventional tools prior to 1959 were scaled in different units of measurement by each service company. Hilchie (1979) gives the conversion factors for converting several service companies' logs to API units. Many slimhole tools are simply scaled in counts per second (Figure 7-14).

Prior to the late 1950's the detectors were ionization chambers and Geiger-Mueller counters. These detectors were inefficient so they were long (up to 3 feet) in order to increase the count rate. Long, inefficient detectors yielded curves with poor vertical resolution and high statistical variations (Hilchie, 1979). Also, the tools were often pulled too fast which further reduced the vertical resolution. Conventional tools and most slimhole tools switched to scintillation chambers, which have an efficiency of 50 to 60 percent versus 1 to 5 percent for the old detectors (Serra, 1984). The improved efficiency allowed the detector length to be shortened to 4 to 8 inches, thus improving the vertical resolution.

Depth of investigation and vertical resolution. The vertical resolution of gamma ray tools with scintillation counters is about 3 feet (Dewan, 1983). Vertical resolution is a function of logging speed, detector length, and time constant (see the next section). The depth of investigation, 6 to 12 inches, is a function of the penetrating power of gamma rays and the formation density. Depth of investigation increases as formation density decreases (i.e. as porosity increases). The effect of formation density on the gamma ray count is not significant for gamma ray tools. However, it is the basis of the density or gamma-gamma tool (Chapter 13).

Statistical variations and logging speed. Gamma ray emissions fluctuate greatly in a completely random manner when viewed from the time span of a few seconds. This fluctuation, called **statistical variation,** is inherent in all radioactivity measurements. It manifests itself on gamma ray curves as small fluctuations in the curve response that do not repeat on repeat passes (Figure 10-2). The fluctuation is $\pm$5 to 10 API units in shales and $\pm$2 to 4 API units in shale-free sandstones and limestones (Dewan, 1983). Major fluctuations in the log values, as well as small variations that repeat, are due to lithology variations (Figure 10-2).

Statistical variations are accentuated by the fact that only a small ~~percent~~ proportion of the gamma rays emitted by a formation strike the detector. For example, a cubic foot of shale emits about 100,000 gamma rays per second (Schlumberger, 1958). But the gamma rays travel in all directions and only a minute fraction of them (250 to 300 per second) intersect the detector

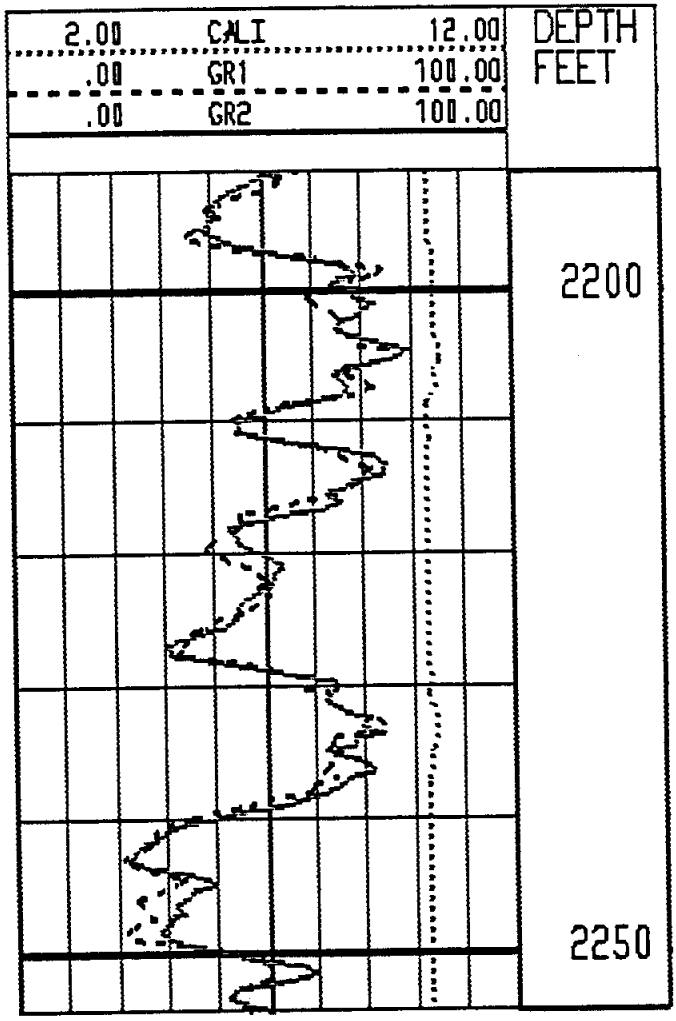

Figure 10-2. The effect of statistical variations on gamma ray curves. Both passes are the same eccentered tool pulled at 40 feet per minute. Differences are due to statistical variations. Shales are reading about 70 API units. The sandstones are shaly. Bed boundaries have excellent repeatability. The caliper shows slight washouts in two of the shales. The borehole fluid is fresh water bentonite mud. The log is the Paluxy Sandstone in Grayson County, Texas. Figures 9-21, 9-23, 10-1, 10-6 and 11-5 are from the same well.

(Dewan, 1983). Over time intervals of a few seconds such a small count rate yields statistical variations even if the detector is stationary in the borehole. The smaller the count rate the greater the percentage of statistical fluctuation (Schlumberger, 1958). Therefore, averaging the curve for a unit of time is necessary to smooth the curve and avoid a spiky, hard-to-read curve.

When viewed from a longer time span (a few minutes), gamma ray emissions are not random but rather average out to a constant value. Herein lies the problem with gamma ray measurements--it is too time consuming to make stationary measurements so measurements have to be made while the tool is moving. In order to minimize statistical variations the count rate is averaged for a unit of time (called the **time constant**). Accurate gamma ray measurements require a logging speed that is not too fast (30 to 40 feet per minute is best) and a sufficiently long time constant for the detector to receive a statistically valid sample. The longer the time constant the less the fluctuation in the count rate. Time constants are usually from 1 to 5 seconds. The proper time constant depends on the relative radioactivity of the formations. The lower the radioactivity contrast between formations the longer the time constant. For instance, shaly Gulf Coast sands require a longer time constant than clean north central Texas sandstones.

A time constant which is too long, however, rounds formation boundaries and displaces the apparent bed boundaries upward. As logging speed increases, this effect is accentuated (Figure 7-11). A balance must be maintained between logging speed and logging accuracy. Many conventional tools are run at a speed that moves the tool one foot during the time constant (Dewan, 1983). This means that the time constant is adjusted according to the logging speed. For a 2-second time constant this is 30 feet per minute. Modern computer logging systems average over a **depth interval** (typically 1 foot) which, at 30 feet per second, is equivalent to a 2 second time constant (Dewan, 1983).

If a time constant is used, it should be noted on the log heading. The logging speed is automatically recorded on modern conventional logs (see Figure 5-8).

Log presentation. The gamma ray curve is placed in Track 1 on conventional logs (Figure 10-1). It is almost always included with the porosity log and is sometimes included on the resistivity log. The curve is linear and is usually scaled from 0 to 100 API units or 0 to 150 API units, depending on the radioactivity level of the shales in the well bore. Increasing radioactivity is to the right, thus the curve mimics the SP curve.

Slimhole tools are often scaled in counts per second and there is little consistency to the log presentation. A few companies do use API units.

Interpretation. Gamma rays are high-energy electromagnetic waves that are emitted naturally from the nuclei of certain radioactive elements. They are most commonly emitted by elements of the uranium-radium series, the thorium series, and potassium-40, a radioactive isotope of potassium that occurs in association with normal potassium. These elements may either be an allogenic (primary) constituent of the rock as part of the chemical composition of the minerals or they may be an authigenic (secondary) product, which is absorbed onto the surface of the mineral. In sedimentary rocks, shales and clays, both of which are referred to as shale in this text, have by far the highest concentrations of these elements, while rocks such as sandstones and carbonates usually have very little. This means that the tool can be used to distinguish shale from nonshale and to calculate the percent of shale in nonshale formations. This is why many people refer to the gamma ray curve as a lithology log.

Figure 10-3 lists the API units of various types of sedimentary rocks. In general gypsum, anhydrite, halite, and coal have the lowest API readings. Carbonates are a little higher and sandstones still a little higher (20-30 API units). Shales or clays are much higher, around 100 API units. The radioactivity of a rock increases as the organic content increases due to the affinity between organic matter and uranium and thorium. While it is true that shales generally have much higher gamma ray counts than other sedimentary rocks, there are important exceptions. Each lithology has a range of gamma ray radioactivity rather than a discrete value. Therefore, interpretation of a gamma ray curve is not always straighforward.

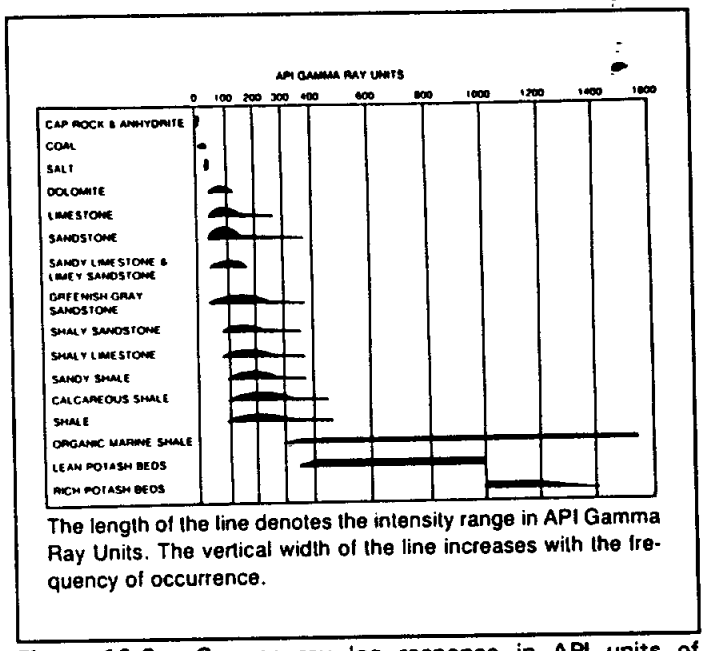

Figure 10-3. Gamma ray log response in API units of common sedimentary rocks (From Dresser Atlas, 1982).

High gamma ray counts do not always correspond to shale. Both feldspathic sandstones (arkose, granite wash) and micaceous sandstones have high gamma ray counts due to high potassium concentrations.

Glauconite, heavy minerals, volcanic ash, and uranium salts also give high gamma ray counts and can occur in both carbonates and sandstones.

Conversely, **low gamma ray counts do not always mean that a formation is shale free.** Kaolinite and chlorite are two common clay minerals that have low radioactivity levels and are indistinguishable from sandstones and carbonates (Figure 10-4). These clays are nonradioactive because they do not contain potassium and they adsorb very few uranium ions due to very low cation exchange capacities, which is the tendency of some clays to absorb cations to fill unsatisfied electrical charges. Of the common clay minerals only smectite (montmorillonite) and illite have a high API value. These two clays do have significant radioactivity because illite contains potassium and both clays have an appreciable cation exchange capacity (CEC).

Acidic and intermediate igneous rocks (those with potassium feldspar) such as granite and rhyolite and metamorphic rocks have even higher radioactivities than shales. Any formation with an appreciable amount of these rock fragments will appear to be a shale. Basic igneous rocks (e.g. basalt and gabbro) have very low radioactivities. Some evaporites, principally potash minerals, contain high potassium concentrations and are very radioactive.

The gamma ray tool works very well in cased holes (Figure 9-24). It can be accurately interpreted by following a few guidelines. Steel casing reduces the gamma ray activity by about 30 percent (Helander, 1983). PVC casing only slightly reduces the gamma ray count. Cement, which contains clay, may increase or decrease the gamma ray count depending on the radioactivity of the formation relative to the cement. Bentonite grout will significantly increase the gamma ray count. Cased holes with a few inches of a fairly uniform thickness of grout or cement will produce an overall shift in the gamma ray response, but shale/nonshale bed boundaries will still be discernible. However, the gamma ray curve will mask the formation response if the cement or the grout is abnormally thick. If the cement or the grout varies greatly in thickness up and down the well bore, the curve can be misleading.

Despite the aforementioned pitfalls, the gamma ray tool is still an excellent shale indicator. It is a very valuable logging tool.

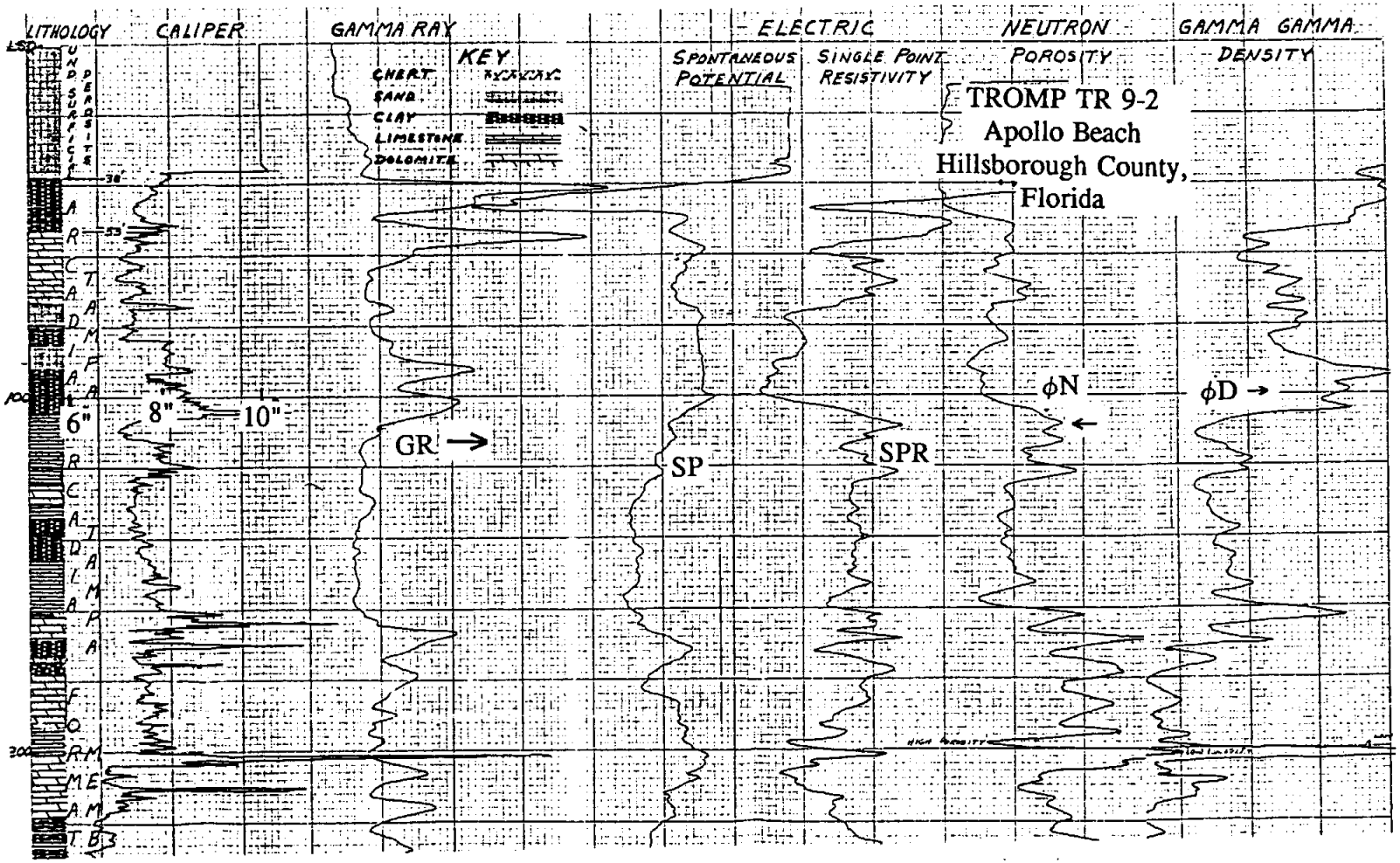

Figure 10-4. Shales with low gamma ray values occur from 46 to 50 feet and at 100 feet. The clay from 46 to 50 feet is kaolinite, which has a very low gamma ray response. The lithology column is based on core descriptions. The gamma ray, neutron, and density curves are scaled in unspecified counts per second. The logs are slimhole tools. The logs are not all on depth. The caliper, gamma ray, and SP curves correlate fairly well. Notice that the caliper is very sensitive to changes in hole size. The lithology is alternating clay, limestone, and dolomite. ϕ is the symbol for porosity; an arrow denotes the direction of increasing porosity or gamma ray activity. The well is the TROMP TR 9-2, Apollo Beach, Hillsborough County, Florida.

Bed boundaries. Bed boundaries are picked halfway between the high and low values (Figure 10-1). For a bed less than 3 feet thick, the peak is taken as the gamma ray value. For thicker beds an average value should be used in order to compensate for statistical fluctuations.

Borehole corrections. Borehole diameter, mud weight, tool position, and tool size affect the gamma ray count. Correction charts are available for conventional tools but not for slimhole tools. Good computer log analysis programs include these borehole corrections. Figure 10-5 contains correction charts for two of Schlumberger's gamma ray tools. Ideal conditions for which the conventional tool (3⅝ inch diameter) requires no corrections are an 8 inch borehole with 10 lb/gal mud and the tool eccentered. For heavier muds, larger boreholes, and centralized tools there is more gamma-ray-absorbing matter between the borehole and the tool, so the gamma ray count is reduced. Conversely, for smaller boreholes and lighter muds or air-filled boreholes, the gamma ray response is increased. A borehole correction shifts the entire curve by a fixed percent (Figure 10-6).

Ground-water wells normally have mud weights close to 10 lb/gal, thus the curve will be little affected by mud weight. Boreholes over 12 inches in diameter will have a significantly reduced count rate.

If a gamma ray tool is run in combination with a density-neutron tool, it is run eccentered. If it is run with induction or laterologs, it is usually run centered in the well bore.

Borehole corrections need to be applied only if the curve is used to calculate the percent of shale in a sandstone or carbonate. For picking bed boundaries and correlating, corrections are not necessary unless the borehole has washed out several inches. If the shales are washed out, they will have too low a gamma ray count, while if the sands are washed out the gamma ray count may be too high or too low, depending on the borehole fluid.

Oil field muds containing potassium chloride will give a high background level to the entire curve. Barite increases the mud density, which reduces the gamma ray response. These additives should be noted on the log heading.

Recommended use. The gamma ray is a very useful curve and should be included in every ground-water/environmental logging suite. Qualitatively, the curve should be used to:

English

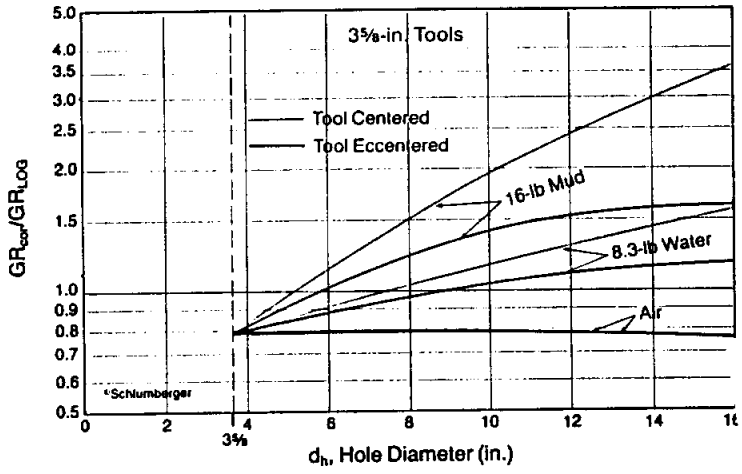

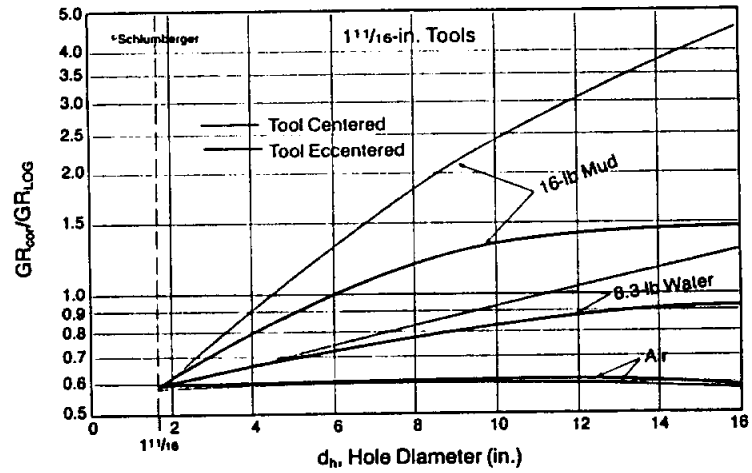

GR_{cor} is defined as the response of a 3⅛-in. tool eccentered in an 8-in. hole with 10-lb mud.

These charts are based on laboratory work which was done for the express purpose of modernizing the Por-7 chart (1973 and earlier editions).

The primary changes in these charts result from the following:

- Data taken from sodium iodide-type scintillation tools.
- "Standard Logging Condition" is defined here as the response of a 3⅛-in. tool eccentered in an 8-in. hole, with 10-lb mud in the hole. When used with metric units, Standard Logging Condition is the response of a 92-mm tool eccentered in a 203-mm hole with mud of 1.20 specific gravity.

(continued on next page)

Por-7

Figure 10-5. Hole size and mud weight corrections for Schlumberger's gamma ray tools (Schlumberger, 1989).

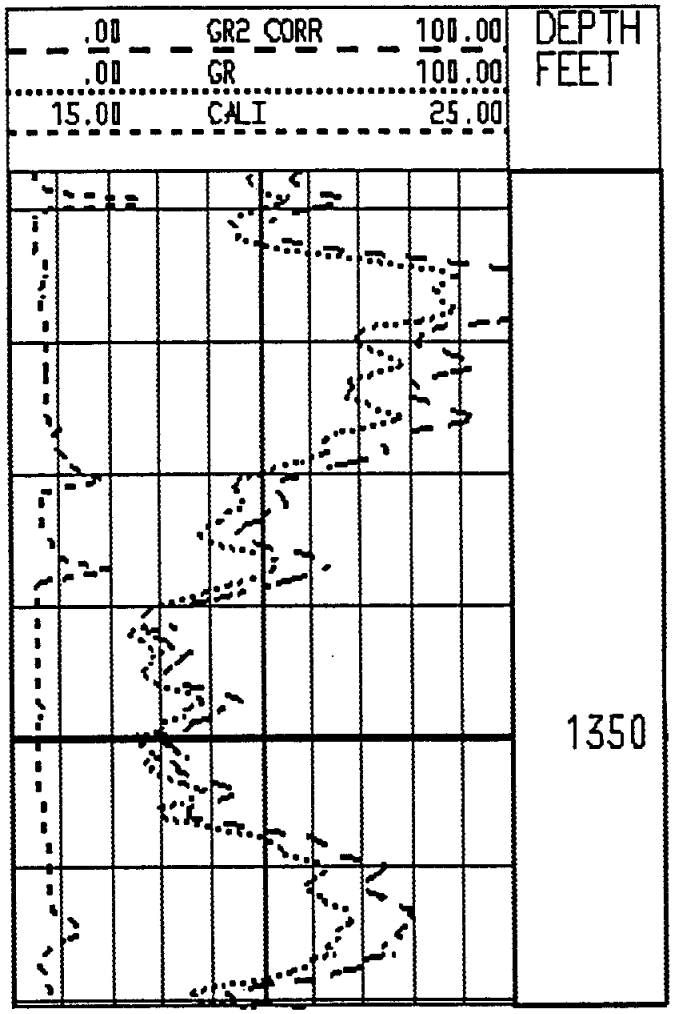

Figure 10-6. The effect of hole size and mud weight corrections on a gamma ray curve. GR2 CORR is the corrected curve. The corrected curve shape remains the same, but the entire curve is shifted. Bit size is 14.75 inches and mud weight is 9 lb/gal. The log is the Paluxy Sandstone in Grayson County, Texas. Figures 9-21, 9-23, 10-1, 10-2 and 11-5 are from the same well.

1. Pick bed boundaries between shale and nonshale formations.

2. Recognize shale laminations in sandstones and carbonates. However, shale laminations of chlorite and kaolinite will be indistinguishable from the host rock and statistical variations can be interpreted as thin shale laminations.

3. Correlate from one well to another. Shales and thin limestone stringers are especially good for correlation since they are laterally

continuous and mineralogically consistent. Sandstone gamma ray patterns, on the other hand, are a product of the depositional facies and are often laterally discontinuous. Correlation of sandstones may be difficult.

4. Correlate between openhole logs and cased hole depths.

5. Identify depositional facies.

6. Recognize unconformities. Uranium-enriched phosphates and organic matter are often associated with unconformities. The zones appear as narrow, isolated high gamma ray spikes.

7. Recognize intervals with high uranium concentrations. Such intervals, if screened, may give the water unacceptable radioactivity levels.

8. Recognize certain lithologies. Especially in a localized area, certain lithologies will have diagnostic gamma ray responses (e.g. coal and halite will be very low; arkose will be very high).

9. Estimate relative permeability in sandstones. Sandstones with shale laminations and/or clay in the pore spaces will have reduced permeability. However, remember that sandstones containing kaolinite or chlorite will appear to be clay-free.

10. For qualitative use, slimhole tools scaled in counts per second are just as good as curves scaled in API units. However, a problem develops when comparing gamma ray curves scaled in counts per second from different logging companies. Each tool has a somewhat different response due to variations in detector size and tool construction. In order to be able to compare curve responses the curves must be scaled in a common unit of measurement (API units).

Quantitatively, the gamma ray curve is used to calculate the percent of shale (clay) in sandstones. It can be scaled in either counts per second or API units (Hilchie, personal communication, 1991). The technique can be used with carbonates, but aquifer-quality carbonates have very small amounts of shale. The technique is not always accurate because some of

the assumptions used to make the calculation are not correct in all situations. The technique tends to give the upper limit of a shale volume.

Shale or clay volume (V_{Sh} or V_{Clay}) is calculated by:

1. Establishing the average gamma ray value in a 100 percent shale close to the zone of interest.

2. Establishing the average gamma ray value in a nearby shale-free formation that is the same lithology as the formation of interest.

3. Calculating the gamma ray shale index (I_{GR}).

$$I_{GR} = \frac{GR - GR_{Cl}}{GR_{Sh} - GR_{Cl}} \qquad \textbf{(10-1)}$$

Where:
I_{GR} is the gamma ray shale index.
GR is the gamma ray response in the zone of interest.
GR_{Cl} is the gamma ray response in a shale-free zone of the same lithology.
GR_{Sh} is the gamma ray response in 100 percent shale.

4. Converting I_{GR} to shale volume (V_{Sh}) using Figure 10-7. I_{GR} has been empirically correlated to the shale volume in different types of formations. Gamma ray response decreases as formation density increases: the older the formation, the greater the amount of compaction, and the denser the rock.

   a. Relationship 1 is linear and provides an upper limit to the shale content in any type of formation. The gamma ray curve can be scaled in counts per second or API units. Using this relationship the gamma ray curve can be scaled in equal increments from 0 to 100 percent.
   b. Curve 2 applies to highly consolidated Mesozoic and Paleozoic rocks.
   c. Curve 3 applies to younger, unconsolidated Tertiary rocks.

5. V_{Sh} also can be calculated from the SP curve, the density-neutron logs, or the spectral gamma ray log. V_{Sh} calculated from the

gamma ray will not be accurate if the following assumptions used in the calculation are invalid:

a. The shale (clay) in the formation of interest may not have the same mineralogy and radioactivity as the surrounding shale.
b. The assumption that shale is providing all the radioactivity in the formation of interest may be invalid.
c. The shale may not have an average radioactivity.
d. The wrong I_{GR}/V_{Sh} curve may have been used.

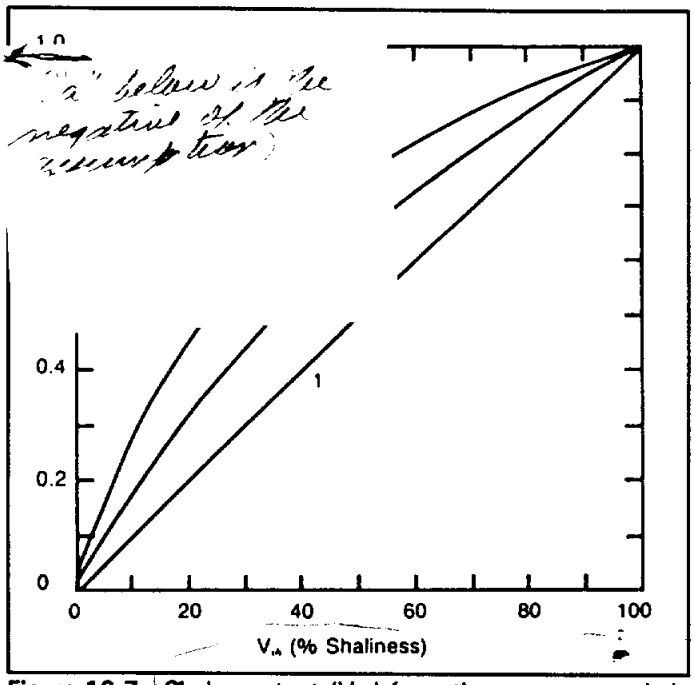

Figure 10-7. Shale content (V_{Sh}) from the gamma ray shale index (I_{GR}) (From Dresser, 1982).

In Figure 10-1 Zone C is a shaly sandstone. After establishing the 100 percent shale line and the shale free line, I_{GR} can be calculated:

$$I_{GR} = \frac{40 - 15}{85 - 15} = 0.36$$

The I_{GR} of 0.36 is input into Figure 10-7. Curve 2 is used since the rock is Mesozoic (Cretaceous Paluxy Sandstone). V_{Sh} is 24 percent.

Spectral Gamma Ray

The spectral gamma ray tool also measures the natural radioactivity of formations. In addition to measuring the total gamma ray activity, the tool measures the energy level of each gamma ray and calculates the concentrations of uranium, thorium, and potassium.

Spectral gamma ray is a generic name for the tool. Each logging company has its trade name for the tool: Spectralog or SGR (Atlas Wireline), Natural Gamma Ray Spectral Log or SGR (Gearhart), Compensated Spectral

Natural Gamma Ray or CSNG (Welex and Halliburton Logging Services), and Natural Gamma Ray Spectrometry Log or NGS (Schlumberger). A few slimhole tools are also available.

Tool theory. Uranium, thorium, and potassium-40 each emit gamma rays of different energy levels (Figure 10-8). Potassium-40 decays directly to stable argon-40 and in the process emits gamma rays of a single energy level, 1.46 Me-V (million electron volts). Uranium and thorium, on the other hand, decay through a series of daughter isotopes before transforming to stable lead isotopes. Each decay series emits gamma rays of various energy levels (Figure 10-8). By measuring the energy level of each gamma ray, the tool is able to calculate the concentrations of uranium, thorium, and potassium.

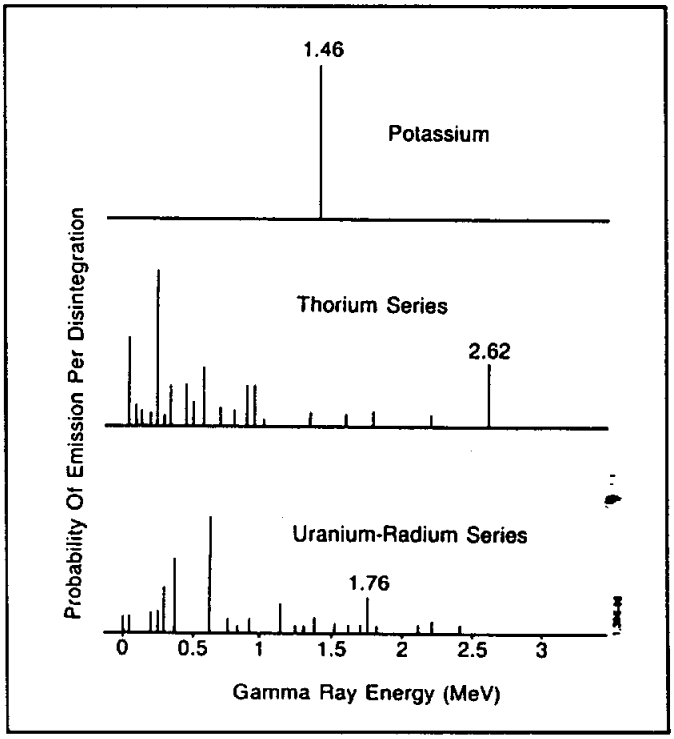

Figure 10-8. Gamma ray emission spectra of radioactive minerals. The energy level of the principal peak of each element is noted (From Schlumberger, 1989).

Separating the emission spectras of uranium, thorium, and potassium-40 is not a simple task. The gamma rays lose energy as they move from the formation to the detector (Compton scattering), resulting in a continuous spectrum of gamma ray energy levels (Figure 10-9). However, the diagnostic peaks are still visible. By combining proper instrumentation with careful filtering and analysis of the spectrum, the concentrations of the three radioactive elements can be identified. The total amounts of each element (radioactive and

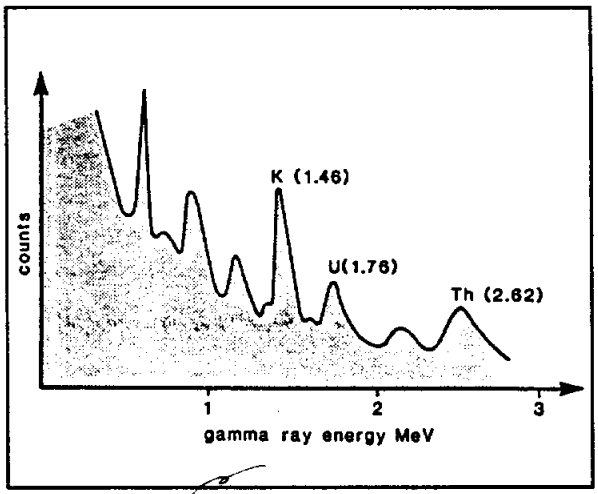

Figure 10-9. An example of a complex spectrum detected by the spectral gamma ray tool (After Hassan, et al., 1976, in Rider, 1986).

nonradioactive isotopes) can then be calculated from the known ratios of the radioactive to nonradioactive isotopes.

The spectral gamma ray tool uses a scintillation counter to detect gamma rays. The energy of the gamma rays is determined by measuring the intensity of the flashes they produce upon entering the sodium iodide crystal.

The tool is run by itself or in combination with the density-neutron log. Its depth of investigation and vertical resolution are about the same as the ordinary gamma ray. Serra (1984) has a good in-depth review of the tool.

Log presentation. Curve scales and presentations vary according to the logging service company. Figure 10-10 is a fairly typical presentation. Track 1 has both total gamma ray activity (SGR) and a gamma ray curve minus the uranium radioactivity (CGR). Tracks 2 and 3 have separate uranium, thorium, and potassium curves. The curves can also be plotted as ratios. The scales are linear and are scaled in percent for potassium and in parts per million (ppm) for uranium and thorium.

Statistical variations and logging speed. Statistical fluctuations are greater with spectral gamma ray tools because the counting rates of the channels is 3 to 10 times lower than that of the standard gamma ray tool (Dewan, 1983). This means that the time constant has to be increased to 4 to 6 seconds and the logging speed slowed to 10 to 15 feet per second.

Borehole corrections. Spectral gamma ray and ordinary gamma ray tools are affected by the same things. Correction charts for the spectral gamma ray tool, however, are not published in service company chart books. Correction charts must be obtained from the particular logging company that ran the log.

Interpretation. Quantifying the amounts of potassium, uranium, and thorium in a formation greatly increases the interpretative power of a gamma ray log, since each of the three elements is somewhat restricted to particular minerals and diagenetic environments. Therefore, shales can be identified much more accurately and certain other lithologies can also be identified.

Uranium is very soluble and usually occurs as an authigenic (secondary) mineral. As such, its occurrence is related more to specific diagenetic conditions than to a particular lithology. Since uranium is very

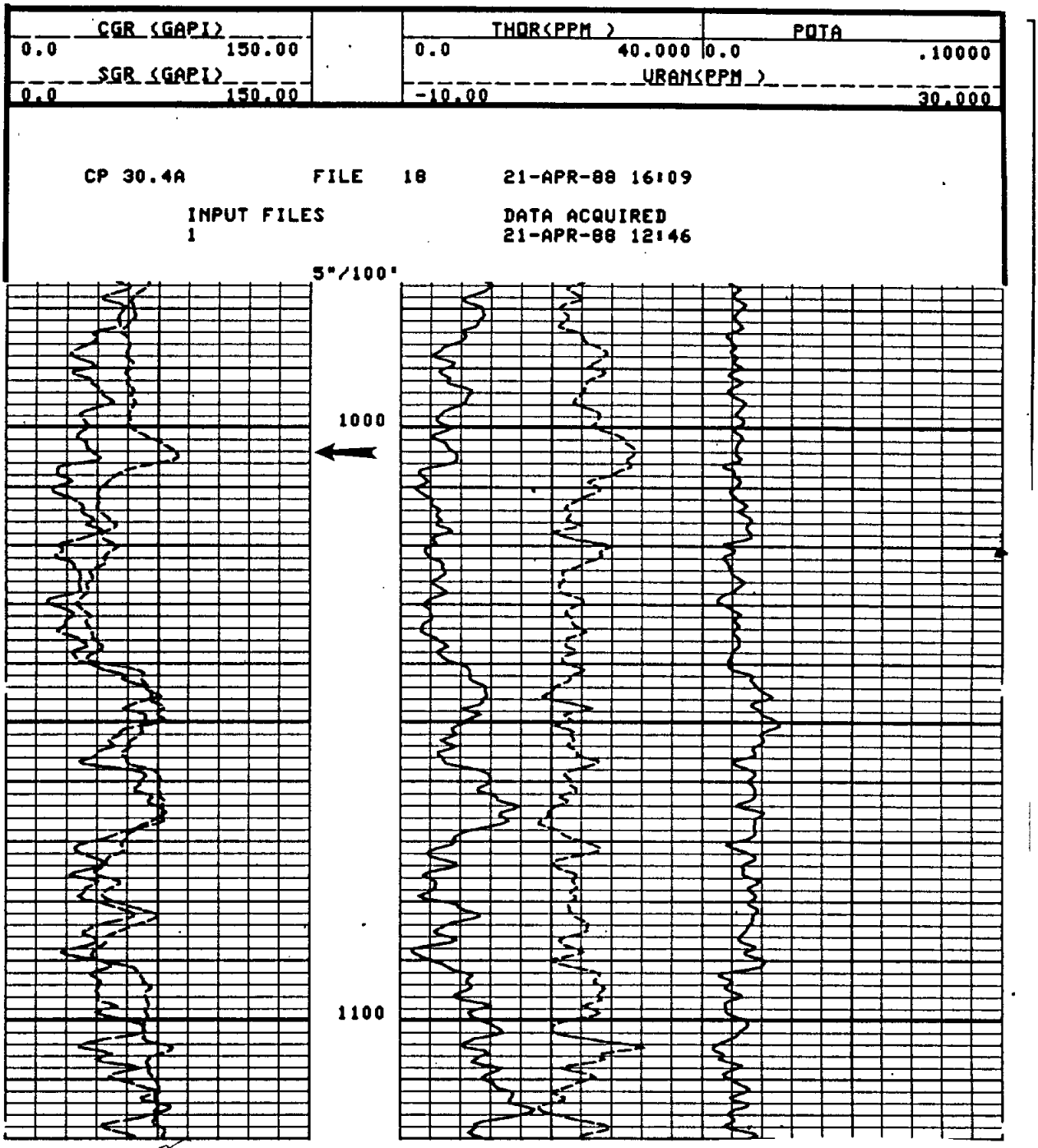

Figure 10-10. A typical spectral gamma ray log. Track 1 has both total gamma ray activity (SGR) and a gamma ray curve minus the uranium component (CGR). Tracks 2 and 3 have the individual curves. Thorium and uranium are scaled in parts per million (ppm) and potassium is scaled in weight percent. The gamma ray kick at 1004 feet (arrow) is due to uranium. The sandstone at 1006 to 1040 feet is slightly shaly. The shale below this sandstone has fairly typical radioactivities: thorium about 12 ppm, uranium 2 to 3 ppm, and potassium about 2 percent. The bit size is 9⅞ inches and the borehole fluid is a 9 lb/gal native gel. The log is an interval in the Gulf Coast Aquifer. The well is the Alsay, NW Harris County MUD 21 and 22 #2. Figures 11-1, 13-3, 13-4, and 13-9 are from the same well.

radioactive, a small amount can give any rock-type the total gamma ray count of a shale. It contributes 10 to 20 percent of the total radioactivity of average shales (Rider, 1986). Therefore, uranium concentration is a poor shale indicator. In fact, stripping the uranium response from the total gamma ray count produces a gamma ray curve that is a much better indicator of whether or not a formation is indeed shale. Uranium enriched zones are usually irregularly distributed peaks on the uranium curve (Figures 10-10 and 10-11).

Thorium is a very stable mineral. Since it has a low solubility, it concentrates in residual soils such as bauxite, in placer concentrations as heavy minerals, and in shales (Rider, 1986). It has a fairly constant concentration in most shales (about 12 ppm) even though its concentration in individual clay minerals varies. This, plus the fact that it contributes 40 to 50 percent of the total radioactivity of average shales, makes the thorium curve a very good shale indicator. However, soil horizons and heavy mineral concentrations may be misidentified as shales.

Potassium is concentrated in mica, alkali feldspars (orthoclase and microcline) and in a few evaporites (sylvite, polyhalite, and carnallite). Its concentration in clay minerals varies considerably, but in shales it is fairly consistent at about 2 percent by weight. Potassium contributes 35 to 45 percent of the total radioactivity of average shales (Rider, 1986). Thus the potassium curve is a fairly good shale indicator. It also can be used to identify arkosic sands.

When calculating shale volumes from spectral gamma ray data, the same procedure outlined in the **Gamma Ray, Recommended use** section should be used. However, instead of using the total gamma ray curve one should use either the thorium and potassium curve or the thorium curve scaled in API units.

In cased holes the lower-energy gamma rays are preferentially attenuated by the casing and cement. The curves are thus weighted toward the high energies (Serra, 1984).

Recommended use. Basically the spectral gamma ray can do everything the ordinary gamma ray tool can do, only better. Additionally, it allows the source of high gamma ray activity to be identified. This is invaluable in determining whether high gamma ray kicks are really shale. In ground-water studies it allows uranium-bearing intervals in aquifers to be

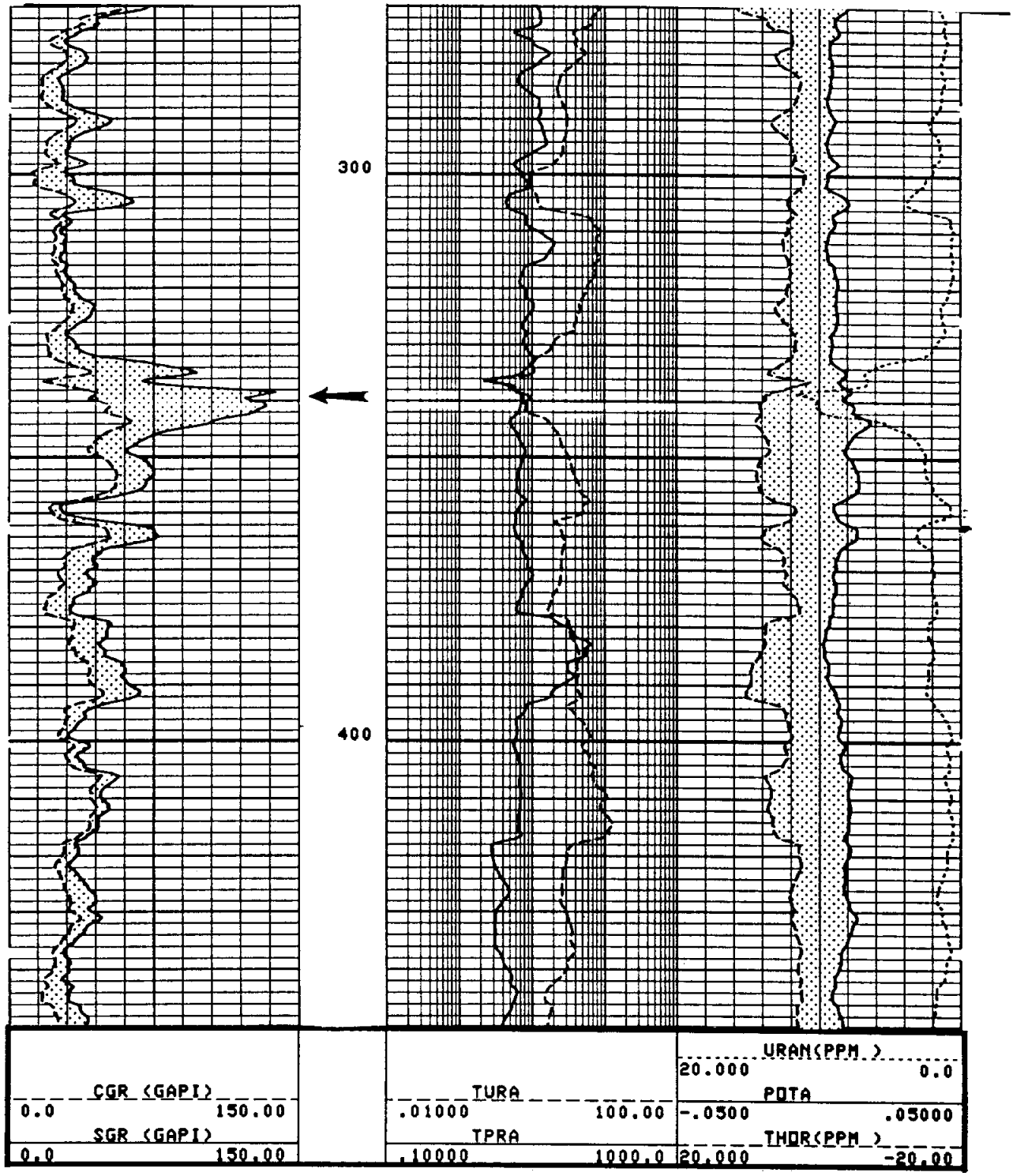

Figure 10-11. A spectral gamma ray log shows uranium to be the cause of the high gamma ray count at 340 feet (arrow). The high gamma ray count is mainly due to uranium; the zone is not nearly as shaly as it appears to be on the total gamma ray curve (SGR). The resistivity curves show a sandstone at 336-40 feet. The bit size is 9⅞ inches and the borehole fluid is 9 lb/gal native gel. The interval is part of the Gulf Coast Aquifer. The well is the Alsay, Kingwood Well B-3, Harris County, Texas.

identified. These intervals may then be cased off if the well is to be utilized as a water supply. Spectral gamma ray curves are routinely used for this purpose in Harris County. They should be used in any part of the state where water wells produce waters with high radioactivity.

Spectral gamma ray tools also can be used to decipher complex mineralogies when rock samples (cuttings and cores) are not available. Theoretically the curves may be used to identify clay mineralogies and to calculate clay volumes, but "often, the result is ambiguous . . ." (Schlumberger, 1989). This is because such interpretations utilize several generalizations about clay mineralogies. Another problem is that the concentrations of each element are the concentrations as determined by the tool, which are not the same as the concentrations in the formation. Attenuation of the gamma rays as they travel from the formation to the detector masks the actual concentrations in the formation. Spectral gamma ray interpretation techniques are still being refined.

All in all, the tool is best utilized as a qualitative indicator of shales, nonshales, and uranium-bearing intervals. Ground-water log analysts will find the tool very useful for these applications. In the rare case where mineral identification and volume are important, on should consult with specialists from the particular logging company to design the optimum spectral gamma ray logging program.

For detailed mineralogical analysis, Schlumberger's **geochemical logging tool (GLT)** may be worth running. The tool combines a spectral gamma ray tool with an aluminum activation clay tool and a gamma ray spectrometer tool. The tool directly measures aluminum, uranium, thorium, and potassium and calculates silicon, calcium, iron, sulphur, titanium, and gadolinium. From these data the mineralogical composition of the rock can be computed. Hertzog, et al. (1989) has a good discussion of the tool.

CALIPER TOOLS

Chapter 11

Caliper logs measure borehole diameter and shape. The tool is used to calculate borehole volume, make environmental corrections for borehole size and mudcake thickness, evaluate the condition of the borehole, identify porous and permeable zones, correlate, identify shale, select packer seats, and identify fractures and cavities.

A variety of conventional and slimhole calipers is available. **Caliper** is the generic name for the tool. Schlumberger used to run a bowspring caliper which they called a Section Gauge. Their Borehole Geometry Tool (BGT) is a borehole deviation tool with an X-Y caliper.

Tool theory. The physical movement of one or more arms on a logging tool is converted to a borehole diameter by means of electrical circuitry. The arms are spring loaded so that they press against the borehole wall. Caliper tools vary widely in the number and types of arms which they employ.

The principal use of one-arm calipers is as an auxiliary measurement on certain pad-type tools (density and some neutron tools). One-arm calipers are standard on conventional pad-type tools, and many slimhole pad-type tools also have them. A one-arm caliper actually has two arms, the eccentering arm and the tool body, which is pressed against the borehole wall. True two-arm calipers are used on microresistivity and high frequency dielectric tools. Three-arm, four-arm, and calipers with more than four arms are also available. The caliper arms may be rod-shaped or bowsprings. Three-arm bowspring calipers are typically standard on conventional sonic tools and on some slimhole sonic tools where their primary function is to centralize the tool in the well bore. Four-arm calipers are found on dipmeters. Some calipers with four or more arms are stand-alone tools. Slimhole calipers are as good as conventional calipers (Figure 10-4).

The tool has no depth of investigation. Vertical resolution depends on the design of the arms.

Log presentation. The caliper curve is usually placed in Track 1 on conventional logs. It is scaled in inches (Figure 11-1). A line representing

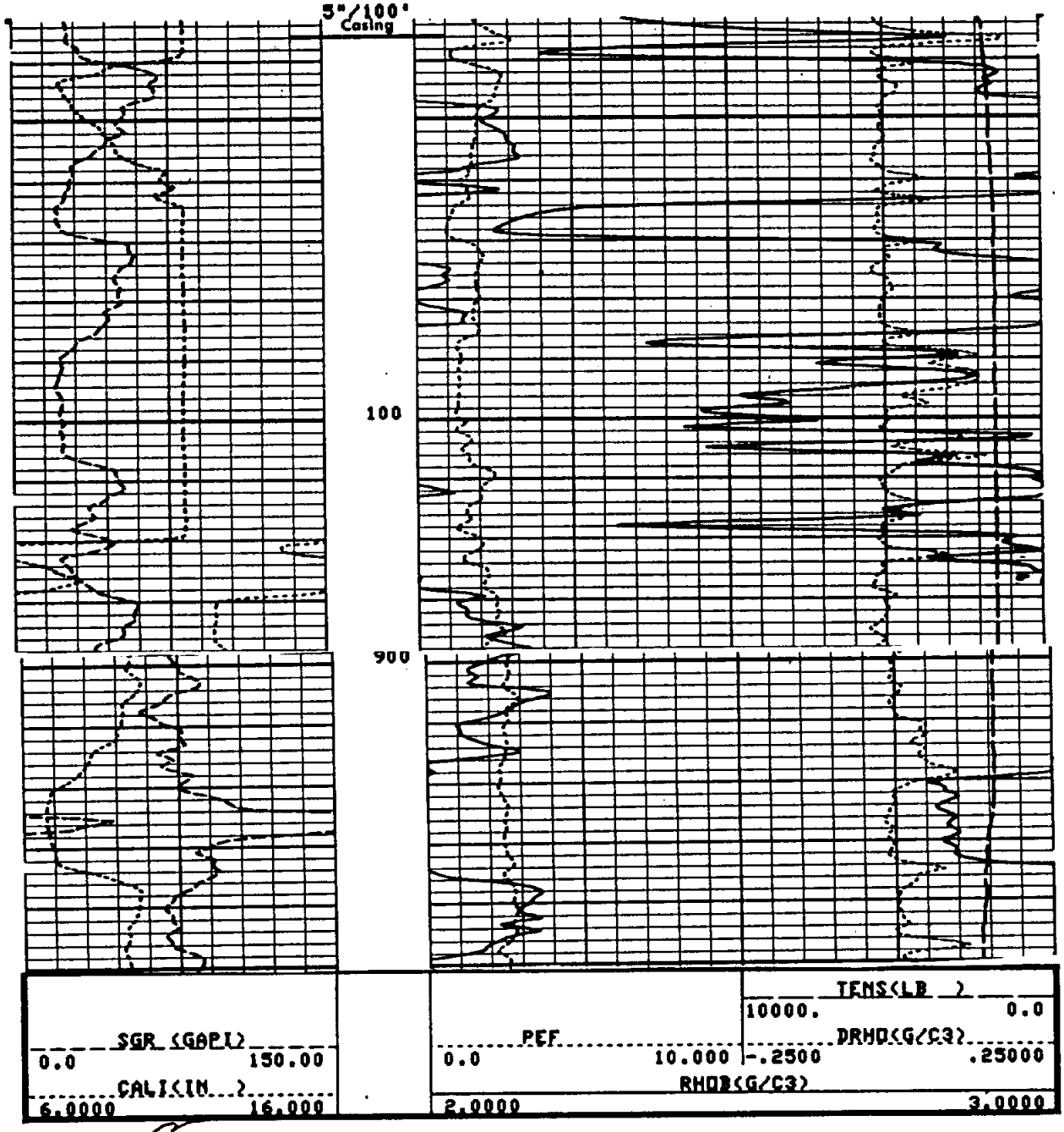

Figure 11-1. A typical conventional caliper log presentation. The caliper is a one-arm tool, the eccentering arm of a density tool. From 64 to 120 feet the hole has washed out greater than 21.5 inches. At 120 feet the curve goes off scale at 16 inches, wraps around and pegs out as a flat line up to 64 feet. The flat line at 21.5 inches is the maximum hole diameter that can be measured by this tool. Checking the caliper reading in casing is a good quality control check. However, in this well the casing is 30 inches in diameter, so the caliper response is a flat line at 21.5 inches. A quick look at the caliper may lead one to overlook that the caliper curve is on a backup scale, in which case the casing would appear to be 11.5 inches. However, the casing diameter is noted on the log heading. The hole is close to being in gauge (9⅞ inches) at the bottom of the well. However, from 910 to 925 feet a shale is squeezing into the borehole and the borehole is less than bit size. An alternate explanation is that the tool is key seated (Hilchie, personal communication, 1991). Figures 10-10, 13-3, 13-4, and 13-9 are from the same well.

bit size is sometimes added to Track 1. Slimhole caliper curves may be presented in any column.

The borehole diameter is sometimes displayed as a differential caliper (Figure 9-11). This is typically presented along the border between Tracks 2 and 3. The border represents bit size; enlargements in borehole diameter are plotted to the right as positive values, while decreases in hole size are plotted to the left as negative values. The differential caliper is also scaled in inches.

Calipers with four or more arms typically will have at least two caliper curves. They may be presented as a separate log with the calipers plotted in Tracks 2 and 3 (Figure 11-2).

Interpretation. Borehole enlargements are due to fractures, cavities, soluble rocks (e.g. salt and gypsum), and unconsolidated rocks that disintegrate and cave (Figure 11-3). Fractures usually occur in carbonates, igneous, and metamorphic rocks. Cavities occur in carbonates. In Tertiary age formations unconsolidated rocks may be shale, sand, or gravel. In Mesozoic and Paleozoic rocks usually only the shales washout.

A hole diameter less than bit size is due either to swelling, sloughing shale or to mudcake buildup on permeable formations (Figures 11-1 and 11-3). Most of the time it will be due to mudcake (Figure 7-15). A hole diameter equal to bit size (an in gauge hole) will be a low permeability, unconsolidated formation (Figure 11-3).

Calipers vary considerably in their resolution due to differences in the amount of contact area on the arm (rod or bowspring), the number of arms, and the pressure exerted by the arms. Bowspring calipers are less sensitive. Calipers with small arms and/or high pressure may cut through the mudcake, while others ride on the mudcake.

Many boreholes are noncylindrical. Figure 11-4 illustrates how different types of calipers theoretically behave in such holes. However, remember that there is no way to be sure that each caliper tool is tracking the borehole as described in the following discussions. One and two-arm calipers both tend to measure the long axis. However, they each contact the borehole wall and sense changes in diameter differently (Jorden and Campbell, 1984). Three-arm calipers generally measure only one diameter—something in between the maximum and minimum diameters. Four-arm

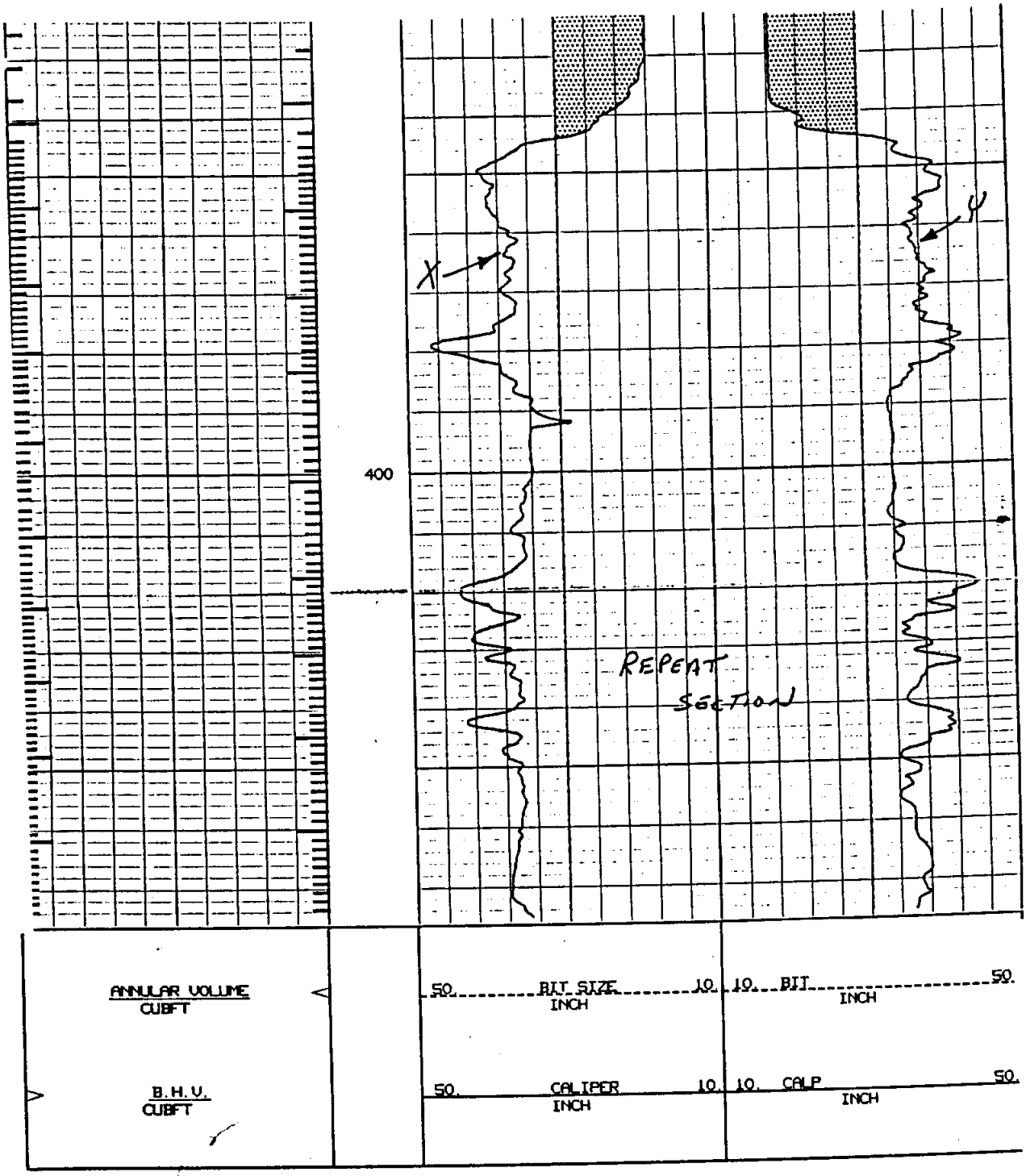

Figure 11-2. Welex X-Y caliper. The casing extends to 340 feet and its diameter is 18 inches. The hole was underreamed from 340 feet to T.D. with a 30 inch bit. Bit size is represented by a dashed line (barely visible on the 30 inch lines). The entire borehole has washouts. Two caliper measurements perpendicular to each other do a much better job of characterizing the borehole diameter. Along the left margin of Track 1 is the integrated borehole volume (B.H.V.). The annular volume for a particular casing size is noted along the right side of Track 1. Unfortunately, the casing size used in the calculation is not specified on the log. Each tic mark is one cubic foot.

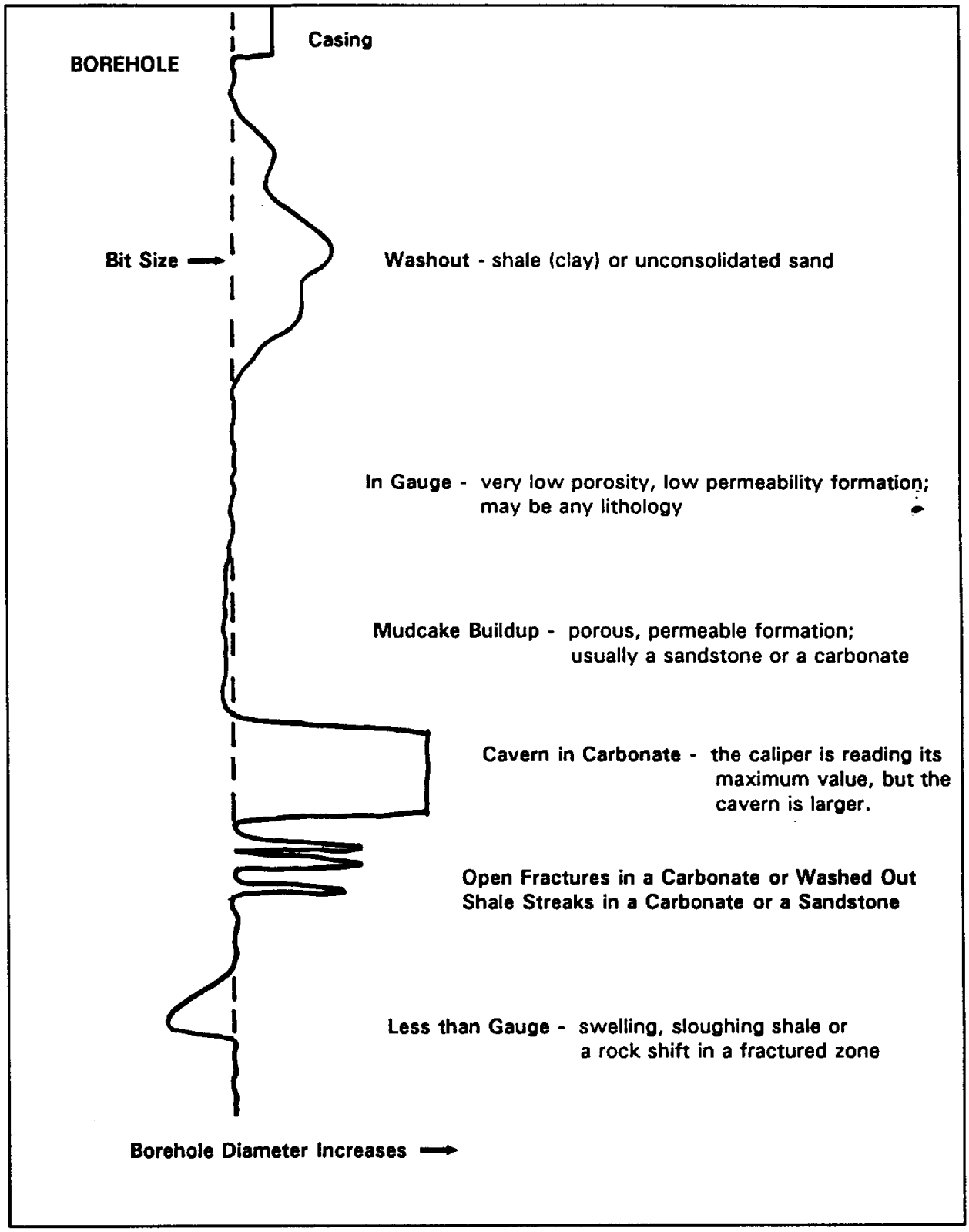

Figure 11-3. Typical caliper log responses.

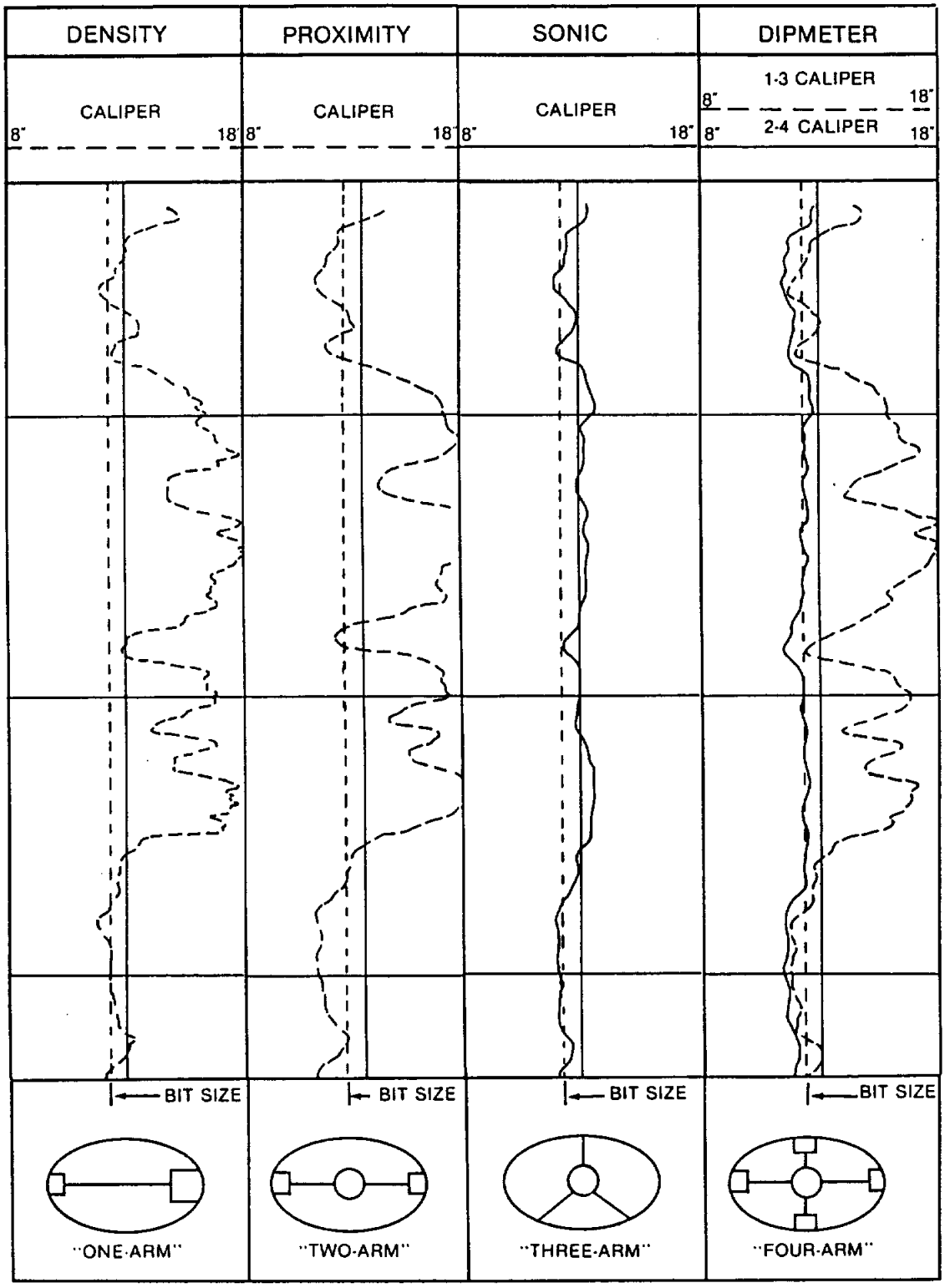

Figure 11-4. A comparison of the response of different types of calipers in the same noncylindrical borehole (From Jorden and Campbell, 1984).

calipers (sometimes called X-Y calipers) display two perpendicular measurements, generally the minimum and maximum diameters. Thus each type of caliper gives a different picture of the well bore.

Rod-type arms such as those on one-arm calipers have small contact areas and therefore generally slice through mudcake. However, the vertical resolution of the one-arm caliper is better than that of the two-arm which has a larger arm. Pad-type arms used on microresistivity tools tend to ride on the mudcake. Bowspring arms may or may not cut through the mudcake, depending on the pressure and width of the spring. One-arm calipers are usually found on density and neutron tools which have a leading edge on the sonde that cuts through the mudcake. Only the backup arm of the tool is measuring mudcake. Thus, theoretically, the caliper measures only one-half the mudcake thickness.

An additional complication is the fact that the same caliper tool will not repeat perfectly on multiple runs. The tool will not always measure the same part of the well bore on each pass (Figure 11-5).

Hilchie (1968) has an excellent, although somewhat outdated, summary on caliper tool theory and interpretation.

Recommended use. A caliper log is essential to any logging suite, since all tools are adversely affected by variations in borehole diameter. The following guidelines are recommended for utilizing caliper logs:

1. At least one caliper log should be included in every logging suite.

2. All calipers run in the borehole should be printed out on the logs. Sometimes when more than one pad-type tool is run, even though each tool has a caliper, the logging company will display only one. Each caliper varies in sensitivity and in the side of the borehole that it transverses, thus each one provides a slightly different picture of the borehole, and should be displayed.

3. Calipers should be used cautiously in formations that have a history of gravel or consolidated rubble caving into the borehole. Such debris may wedge open the caliper and stick the tool.

4. The caliper log should be utilized for the following purposes:

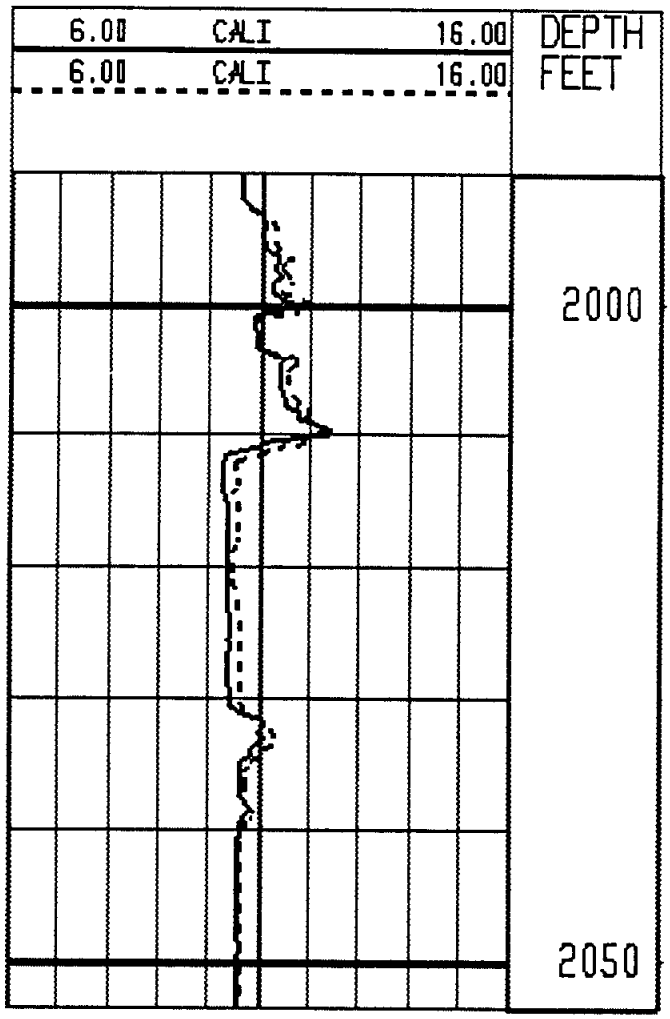

Figure 11-5. Repeat passes of the same one-arm type density caliper. The passes do not match exactly because the caliper passes over different parts of the well bore on the repeat pass. This is the same well as Figures 10-2 and 10-6.

a. **Environmental corrections of other logs.** Borehole diameter is used in correction charts for mandrel resistivity, induction, gamma ray, density, and neutron tools. Pad-type resistivity tools use mudcake thickness in their correction charts.
b. **Permeability indicator in nonshales.** Borehole diameter less than bit size indicates mudcake. However, there is no relationship between mudcake thickness and magnitude of permeability (see Chapter 8, **NONFOCUSED PAD MICRO-ELECTRODE TOOLS**). Mudcake can develop when permeability is as low as 0.1 md (Figure 8-33). Also, if an unconsolidated

sand washes out and develops a mudcake, there is no way to recognize the mudcake on the caliper curve.

c. **Borehole volume for well completion.** The volume of cement or grout to cement a given casing size can be computed. The volume of gravel needed to gravel pack a water well also can be calculated. Integrated hole volume (I.H.V.), also called borehole volume (B.H.V.), is placed in the depth column of some conventional logs (Figure 5-11) as tic marks. Each tic mark represents a given borehole volume. The hole is assumed to be circular when a single caliper curve is used to calculate borehole volume. For a two curve caliper the hole is assumed to be elliptical (Krygowski, 1991). Calipers with three or more arms provide the best calculations of borehole volume.

d. **Selection of packer seats.** Consolidated, in gauge intervals make the best packer seats.

e. **Correlation.** Some formations have diagnostic borehole diameters due to their lithology and degree of cementation. Certain formations routinely washout, while others normally remain in gauge.

f. **Lithology determination.** Shales almost always wash out (Figures 11-1 and 8-19). Sands, gravel, and carbonates that are unconsolidated also sometimes wash out.

g. **Fracture and cavern detection.** In carbonate rocks caverns are easy to detect. Open fractures may be detectable, especially with sensitive calipers. Fractured zones that cave into the well bore are also detectable.

THE SP LOG

Chapter 12

The SP was one of the first logging measurements developed, yet it is still one of the most commonly run logs. The tool measures the naturally occurring potential (voltage) in the well bore.

The SP curve is used to distinguish shale from other rock types, to pick bed boundaries, to correlate, to calculate formation water resistivity (Rw), to identify permeable zones, and to calculate shale (clay) volume in sandstones. In this chapter, the terms shale and clay are used interchangeably.

SP is the only name for the tool. SP stands for **spontaneous potential** or **self potential**. On old electric logs the curve was labeled a porosity log. An SP electrode is a standard part of conventional and slimhole resistivity logging suites and is also built into many other logging tools. All SP logs are the same and are interpreted the same way.

The measurement only works in an open hole that is filled with conductive fluid. SP currents are not measured in air-filled holes and oil-based muds. As with all logs, the measurement is normally made as the tool is pulled up the borehole.

There is often a fundamental difference between the formation waters in petroleum wells and those in water wells, which makes a difference when studying research done on the SP curve. Petroleum wells in Texas normally penetrate formations with sodium chloride (NaCl) waters that are saline and have basically one type of cation, monovalent sodium ions. Water wells, on the other hand, commonly penetrate formations containing fresh waters that have appreciable amounts of divalent calcium and magnesium cations. Calcium and magnesium ions have a larger ionic charge and have approximately ten times the ionic activity of sodium ions (Alger, 1966). This means that ion for ion, divalent ions in formation water create a larger SP deflection than monovalent ions. This difference affects some aspects of SP interpretation, principally Rw calculations.

Gondouin, et al. (1957) state that in their experience calcium and magnesium have a significant effect on the SP curve in waters with an Rw

greater than 0.3 ohm-meters at 75° F (32,500 μmhos per cm at 77° F). They also found that waters with significant concentrations of sulfate ($SO_4^=$) and bicarbonate (HCO_3^-), which includes many ground waters, behave the same as when chloride (Cl^-) is the dominant anion.

Discussions of SP interpretation in petroleum logging literature assume that the formation water is NaCl. In this chapter, explanations are given for aspects of SP analysis for which divalent ions make a difference.

Most petroleum logging literature also assumes that the formation water is more saline than the drilling fluid. However, the opposite is frequently true in water wells, which makes a significant difference in SP theory and interpretation. In this chapter the SP log is discussed in terms of both cases.

Tool theory. The name spontaneous potential aptly summarizes the nature of the SP measurement. The tool sends no current into the formation; it simply measures the natural potential (voltage) difference between an electrode moving up the borehole and a stationary reference electrode. The SP has very little depth of investigation (Figure 12-1).

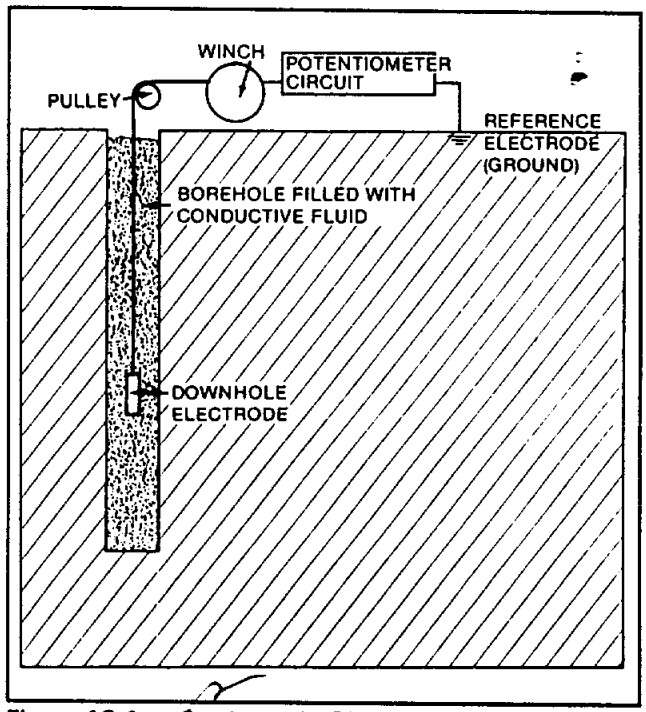

Figure 12-1. Schematic SP circuitry (Dresser Atlas, 1982).

The reference electrode, called a **fish**, is normally located on the surface, but it is sometimes placed on the logging cable. The electrodes are usually lead.

The SP current is generated by a combination of electrochemical (E_c) and electrokinetic (E_k) potentials. The electrokinetic potential is generally negligible; if present, it produces an abnormal SP. Normally the SP is a product of the electrochemical potential.

The **electrochemical potential** is a product of ions moving between the borehole fluid and the uninvaded formation water. This potential is only

generated when there is a contrast in the ionic concentrations of the two fluids. An electrochemical potential has two components: a liquid-junction potential (E_{lj}) and a shale membrane potential (E_m).

The **shale membrane potential,** or simply **membrane potential,** is created by the flow of cations across a shale bed separating a formation water and a drilling fluid of different salinities. The negatively charged clay minerals allow cations to pass through the shale while inhibiting the movement of anions. The boundary between the shale and the less saline fluid therefore becomes positively charged and the boundary with the more saline fluid develops a negative charge (Figure 12-2). This creates a potential difference across the shale.

A **liquid-junction potential,** also called a **diffusion potential,** is created because cations (Na^+, Ca^{++}, Mg^{++}) and anions (Cl^-, HCO_3^-) diffuse at different speeds between two liquids (formation water and mud filtrate) of different ionic concentrations (Figure 12-3). Cations are less mobile because they are larger and have an affinity for the slight negative charge of water molecules. For example, at 77° F (25° C) in a NaCl solution the Cl ion is approximately 1.5 times more mobile than the Na ion (Jorden and Campbell, 1986). Therefore, at the contact or **junction** between the two waters the less saline water becomes negatively charged and the more saline water becomes positively charged (Figure 12-3). This induces a current flow from the less saline to the more saline water. The intensity of the current is proportional to the salinity contrast between the fluids.

The liquid-junction potential is normally one-fifth that of the shale membrane potential. The liquid-junction potential is always smaller because both cations and anions are migrating whereas in the case of the shale membrane potential only the cations migrate. Since it is the excess of one type of ion verses the other that creates the potential, the shale membrane potential is always larger (Schlumberger, 1989).

The two potentials create polarities that are opposite. When R_{mf} is greater than R_w, the liquid-junction potential creates a negative charge opposite a permeable formation while the shale membrane creates a positive charge opposite the adjacent shale (Figure 12-4). The result is a spontaneous current flowing between the borehole fluid, the permeable formation, and the adjacent shale. The potential only changes at the bed boundary between the permeable formation and the shale. The SP electrode detects these changes in potentials in the well bore and records them as relative

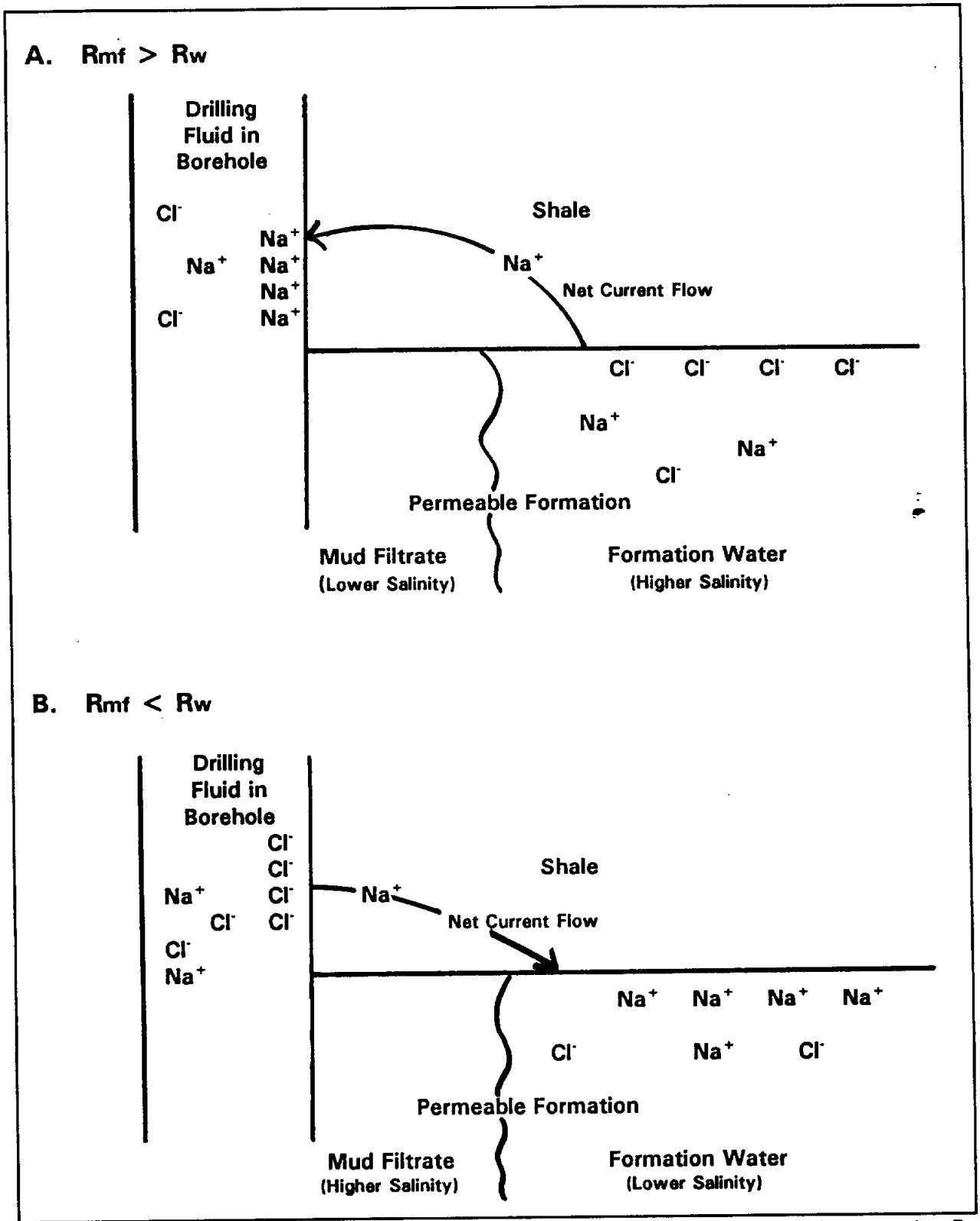

Figure 12-2. Shale membrane potential generated with a NaCl formation water, when R_{mf} is greater than R_w and when R_{mf} is less than R_w.

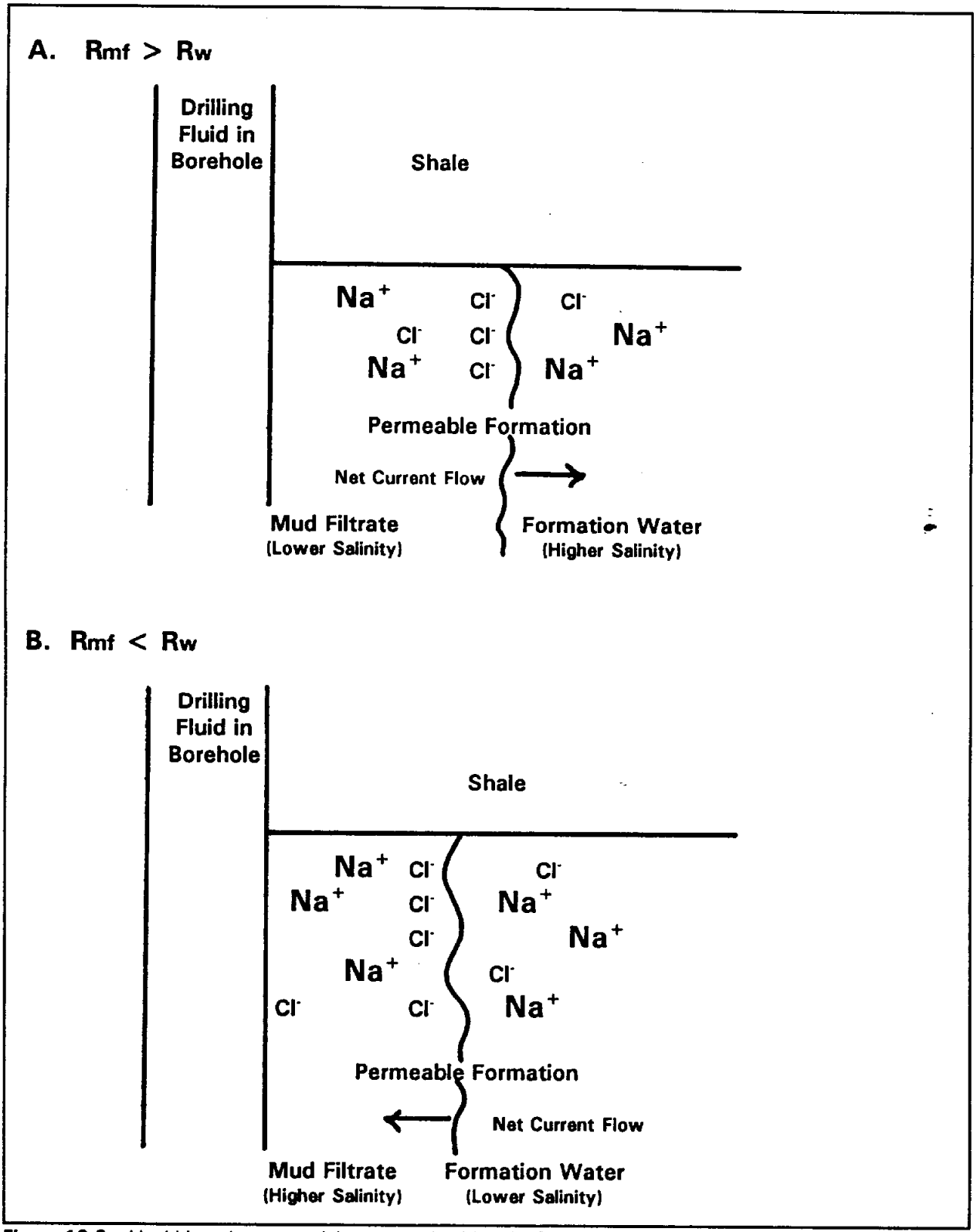

Figure 12-3. Liquid-junction potential generated with a NaCl formation water when R_{mf} is greater than R_w and when R_{mf} is less than R_w.

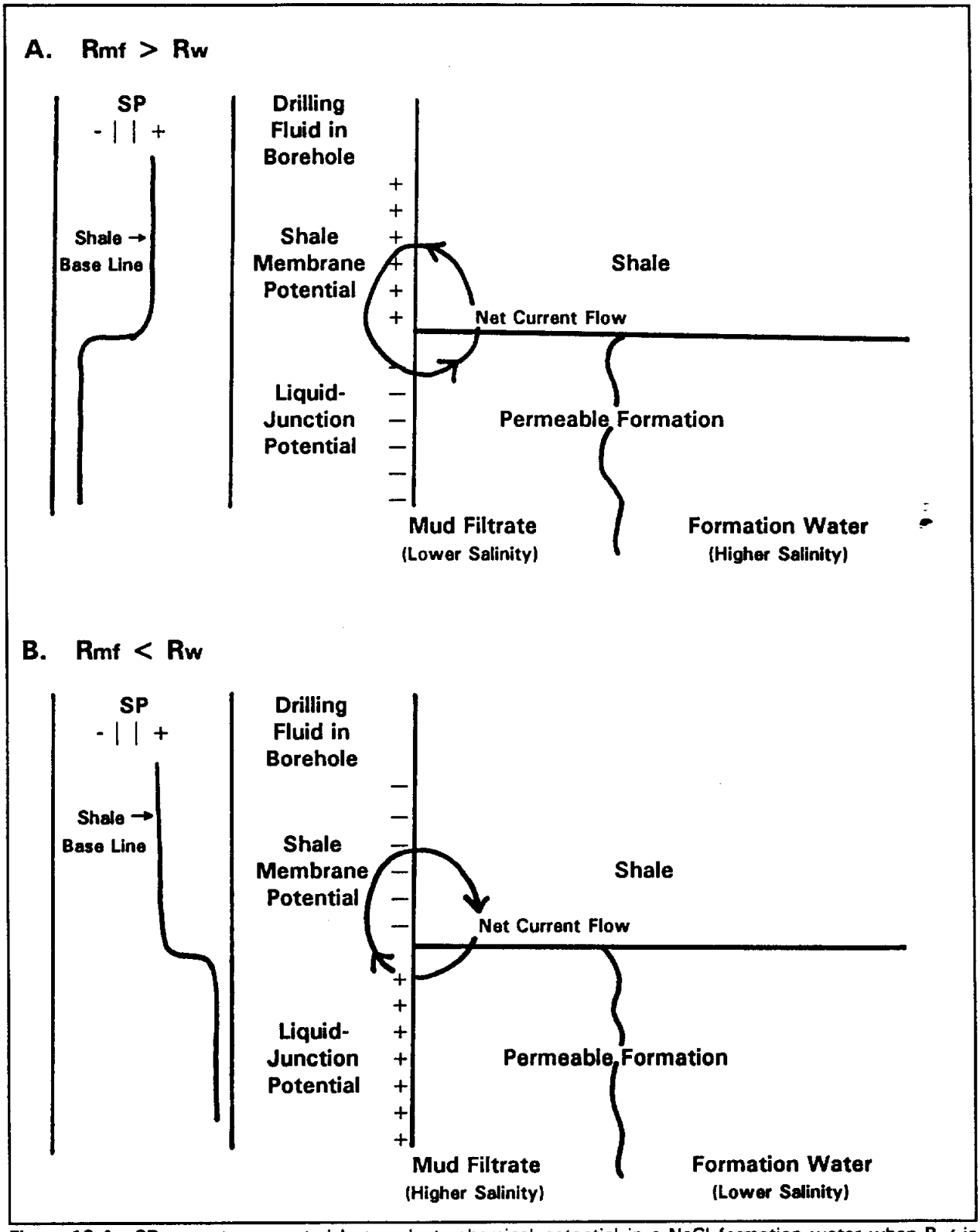

Figure 12-4. SP currents generated by an electrochemical potential in a NaCl formation water when R_{mf} is greater than R_w and when R_{mf} is less than R_w.

negative values on the SP curve. If Rmf is less than Rw, the current flows in the opposite direction, the potentials are reversed, and the SP deflection is positive (Figure 12-4). If a formation is not permeable to ionic movement, there is no current flow, no potential change at a bed boundary, and no SP deflection.

The **electrokinetic potential**, also called the **electrofiltration** or **streaming potential**, can also create an SP current. It develops when an ionic solution flows through a nonmetallic, porous medium that has at least slight permeability (enough to permit ionic movement). The moving fluid shears the ionic double layer that exists along the pore walls of most rocks (Figure 12-5). (See Chapter 14 for an explanation of the ionic double layer.) This results in a net movement of cations (a current flow) in respect to the negatively charged pore walls and creates a potential difference (Jorden and Campbell, 1986).

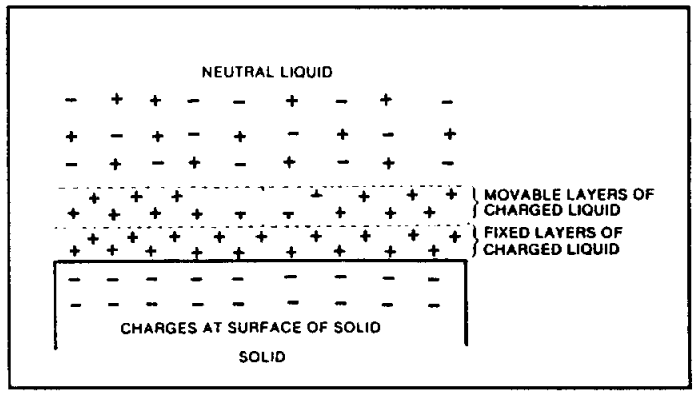

Figure 12-5. The ionic double layer produces an electrokinetic potential when the movable layer is sheared by fluid flow (Modified from Dresser Atlas, 1982).

An electrokinetic potential develops opposite a permeable formation as mud filtrate flows through the mudcake. Another electrokinetic potential is generated opposite shales if just a tiny amount of fluid flows into them. Both of these potentials contribute negative millivolts to the SP signal. Because they are similar in magnitude, the net effect on the SP deflection is the difference between the two potentials. This difference is usually minimal (Schlumberger, 1989).

The magnitude of the electrokinetic potential cannot be predicted with much accuracy. It is proportional to several factors: pressure differential between the borehole fluid and the formation water, resistivity of the moving fluid, rate of fluid movement, ~~resistivity of the moving fluid~~, and mudcake thickness. With normal borehole conditions and a good quality drilling mud, these factors are such that the electrokinetic potential is negligible. However, under certain conditions which are more prevalent in water wells than in petroleum wells, these factors can generate a large electrokinetic potential and increase the SP by tens of millivolts. Conditions favorable to large electrokinetic potentials include:

1. High resistivity drilling fluid and high resistivity formation water. A low salinity contrast between the two fluids minimizes the electrochemical potential, which in turn increases the relative contribution of the electrokinetic potential to the SP current.

2. Poor quality drilling mud (low viscosity, high filtrate loss).

3. Large pressure differential (several hundred psi) between the borehole fluid and the formation water. If drilling mud is flowing into the formation, either the drilling mud is abnormally heavy or the formation is underpressured. If formation water is flowing into the well bore, either the mud is too light or the formation is overpressured. In either case the pressure differential across the formation will probably be considerably different from the pressure differential across the adjacent shale. When this is the case, the two electrokinetic potentials are no longer balanced and the contribution of the electrokinetic potential to the SP current is enhanced (Figure 12-6).

4. Very low permeability formations (less than 5 md) that do not develop a mudcake (Serra, 1984). In this case the pressure differential is applied across the face of the formation rather than across a mudcake.

5. Relatively clay-free formations. Clay greatly reduces the electrokinetic potential (Serra, 1984).

Electrokinetic SP's may be abnormally large but at other times they are difficult to detect. Such SP's cannot be used for any quantitative calculations.

For the situations listed above, if the mud filtrate is fresh, even the very slow movement of fluid into a formation creates a large negative SP deflection. If formation water is moving into the borehole, the result can be a large positive deflection.

Oxidation-reduction (redox) reactions can create a third type of electrical potential-a **redox potential**. Many types of mineral deposits (sulfides, petroleum, uranium, coal, etc.) are accompanied and/or created by redox reactions. Surface SP measurements of redox potentials have been more commonly employed for mineral exploration than have borehole redox

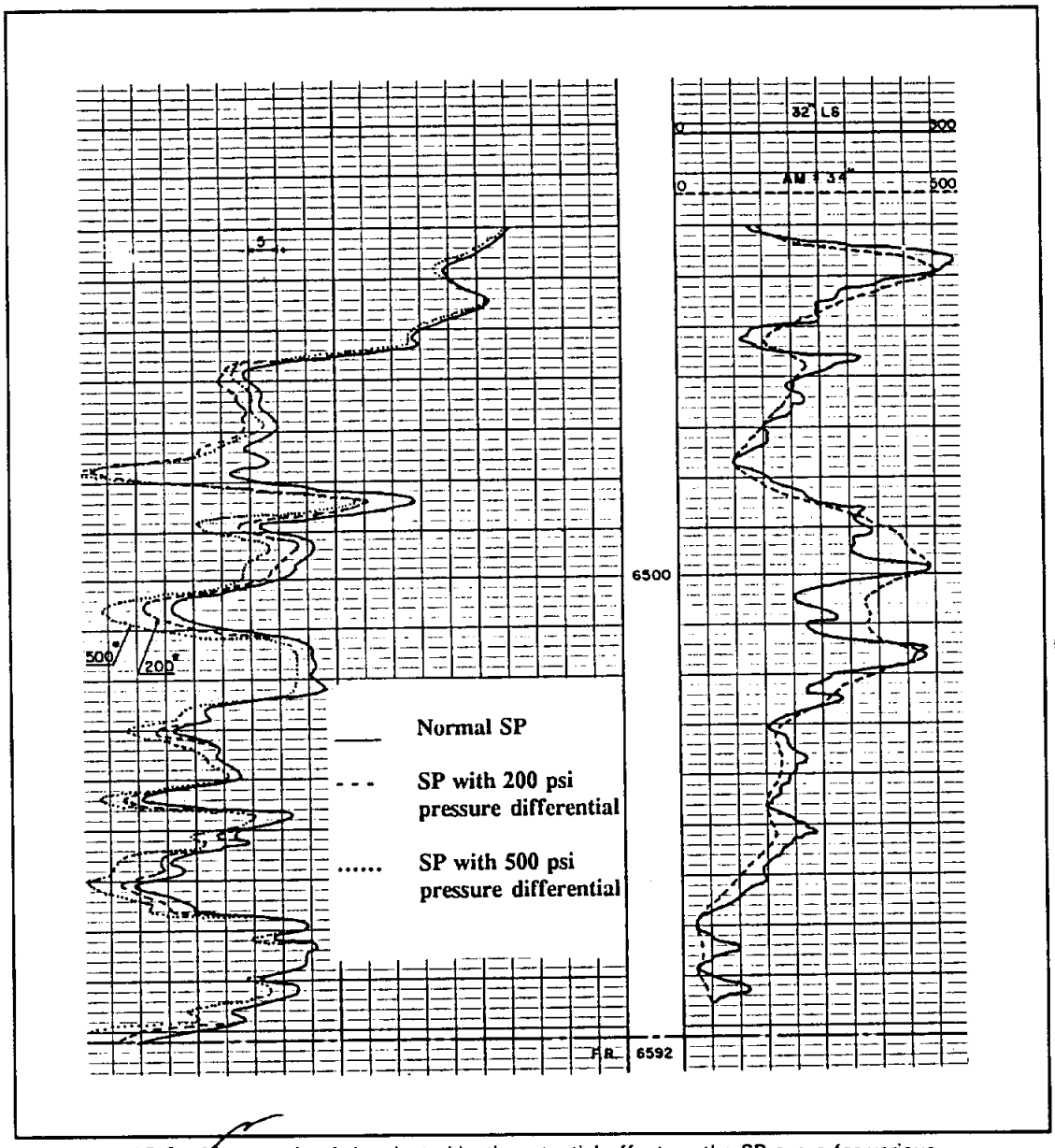

Figure 12-6. An example of the electrokinetic potential effect on the SP curve for various pressure differentials (Modified from Pirson, 1963).

potential SP measurements. Redox potentials are usually ignored by the petroleum logging industry, although Pirson (1983) is a notable exception.

Though redox potentials apply mainly to mineral exploration, they do help explain the base-line drift commonly seen on SP logs. A base-line drift to the left (negative direction) occurs when the SP electrode approaches a more oxidized zone (Hallenburg, 1984). A shift to the right (positive direction) occurs as a more reduced zone is encountered. The SP normally drifts to the left as the surface is approached since oxidation increases toward the surface. Hallenburg (1984) suggests that redox potentials may account for many of the SP anomalies that are explained by other mechanisms.

Log presentation. The SP curve is placed in Track 1 (Figure 12-7). It is almost always found on the resistivity log, and it is sometimes placed on the porosity log. The SP scale is in + or - millivolts (mv). The curve has no absolute values. Zero is defined as the SP value opposite thick shales, the **shale base line** (Figure 12-7). SP deflections to the left of the shale base line are - SP's and those to the right are +. The magnitude of these deflections is measured relative to the shale base line (Figure 12-7). Slimhole tools are scaled the same way, but the curve is not always in Track 1.

The curve is scaled with large enough millivolt units to eliminate backup curves and yet the units are kept as small as possible to maximize resolution. On petroleum logs the number of millivolts per division is normally a multiple of 5, anywhere from 5 to 20. Ground-water logs where R_{mf} and R_w are very similar and the curve is very flat may use an expanded scale such as 2 millivolts per division to enhance the resolution.

On older conventional logs and on slimhole logs the scale is designated as -|10|+, which designates the number of millivolts per each of the 10 divisions in Track 1. Modern conventional logs use a different label **(-80.00 SP (MV) 20.00)** to represent the same scale. This scale does not assign any specific value (-50 mv, -40 mv, etc.) to a particular division; all specific values are still determined in reference to the shale base line.

On conventional logs the engineer normally places the shale base line about two divisions from the right side of Track 1. As the tool is pulled up the hole the curve often drifts (Figure 12-7). To keep the curve from drifting out of Track 1 the engineer may have to shift the curve. Any manual shifts

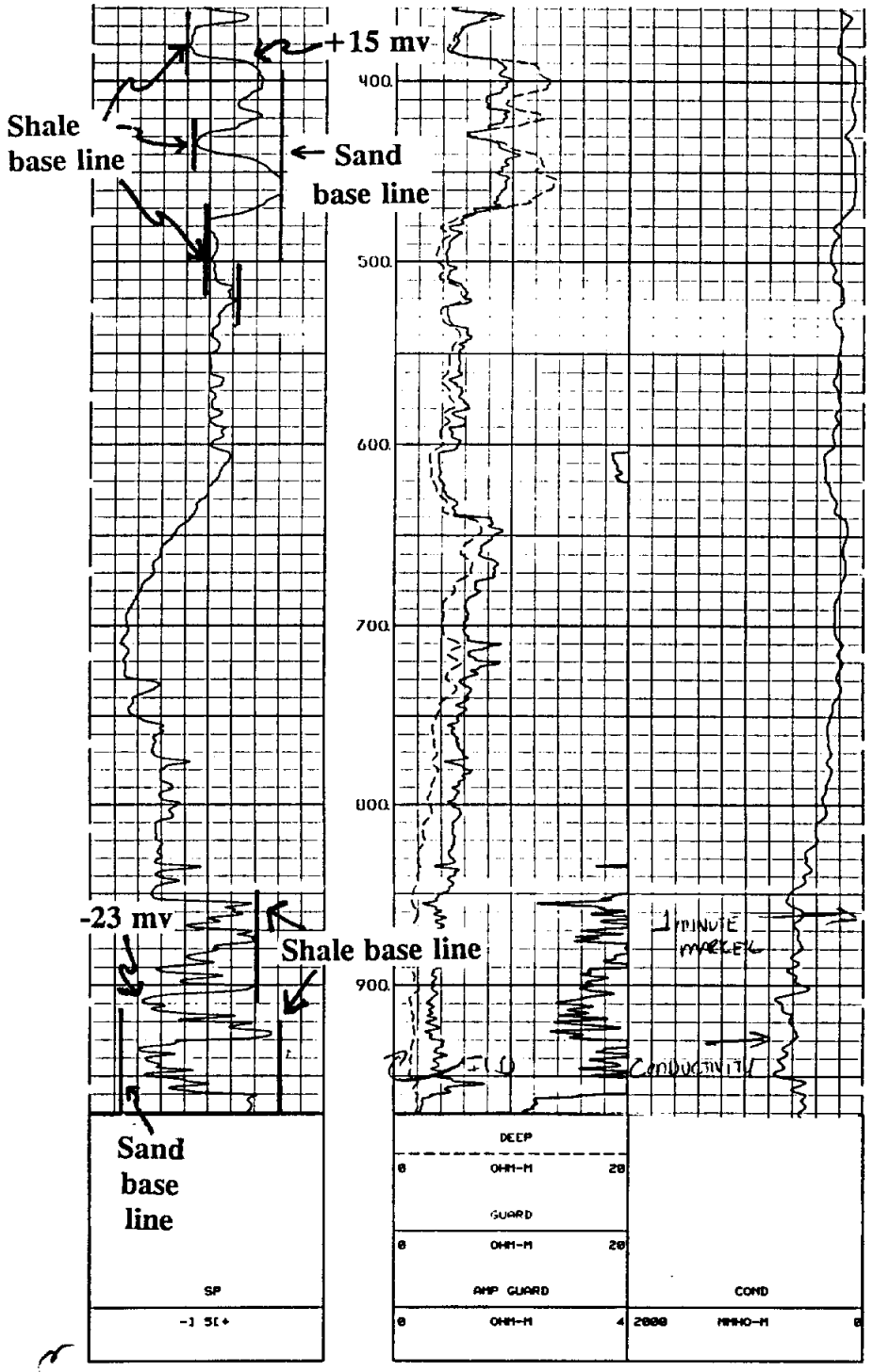

Figure 12-7. A typical SP curve presentation. The shale base line is drifting to the left as depth decreases. The abnormal SP from 690 to 610 feet may be where the logging engineer slowly moved the SP curve to the right in order to keep it from running off the left side of Track 1. An alternate explanation is that the drift is due to water salinity in the formations changing up the well bore from saline to fresh. Above 550 feet the sands have positive SP deflections because Rw is greater than Rmf (as confirmed by the deep induction curve reading higher than the shallow guard curve). Below 800 feet the sands all have negative SP deflections because Rw is now less than Rmf (as confirmed by the reversal in the resistivity curves). A positive and a negative SP value have been picked on the log. Figures 8-18 and 8-19 are also from this well.

should be done rapidly over a vertical interval of only a few feet and should be so labeled on the log (Figure 8-18). Some engineers slowly adjust ("knob") the SP during the course of a logging run. This creates havoc with quantitative SP analysis and is a poor practice. It cannot be detected on the log.

Factors affecting the SP curve. Several borehole and formation factors reduce the magnitude and vertical resolution of the SP curve and alter its shape. Qualitative, as well as quantitative, interpretation of the curve requires an understanding of these effects. The following discussion assumes that the contribution of the electrokinetic potential to the SP curve is negligible.

The maximum SP deflection that a bed will develop under ideal conditions is termed **static SP** (SSP). Only thick, shale-free, porous, permeable formations can develop static SP. All other types of formations have an SP less than static SP. This section discusses the various factors that affect the SP curve.

Salinity (resistivity) contrast between the drilling fluid and the formation water. This is the main control on the magnitude of the SP curve. The magnitude of the SP deflection is proportional to the contrast (Figure 12-8). An appreciable amount of divalent cations (usually calcium and magnesium) in the formation water acts the same as an increase in the salinity contrast.

Permeability and porosity. There is no direct relationship between the magnitude of the SP deflection and either permeability or porosity. Just a fraction of a millidarcy of permeability is sufficient to permit enough ionic movement to generate an SP current.

Formation resistivity (R_t). More precisely, the ratio of R_t to R_m affects the curve. As the ratio increases the curve becomes rounder, the deflection decreases, and the bed boundaries are less defined (Figure 12-9). Figure 12-10 can be used to quantify the amount of SP reduction. However, it is for the borehole condition where R_m equals R_s. The chart will not be accurate for other R_m/R_s values. Charts have not been constructed for other ratios.

Bed thickness. As bed thickness decreases the curve becomes rounder, the deflection decreases, and the bed boundaries are less defined (Figure 12-9). However, if R_t and R_m are equal, a bed as thin as twice the

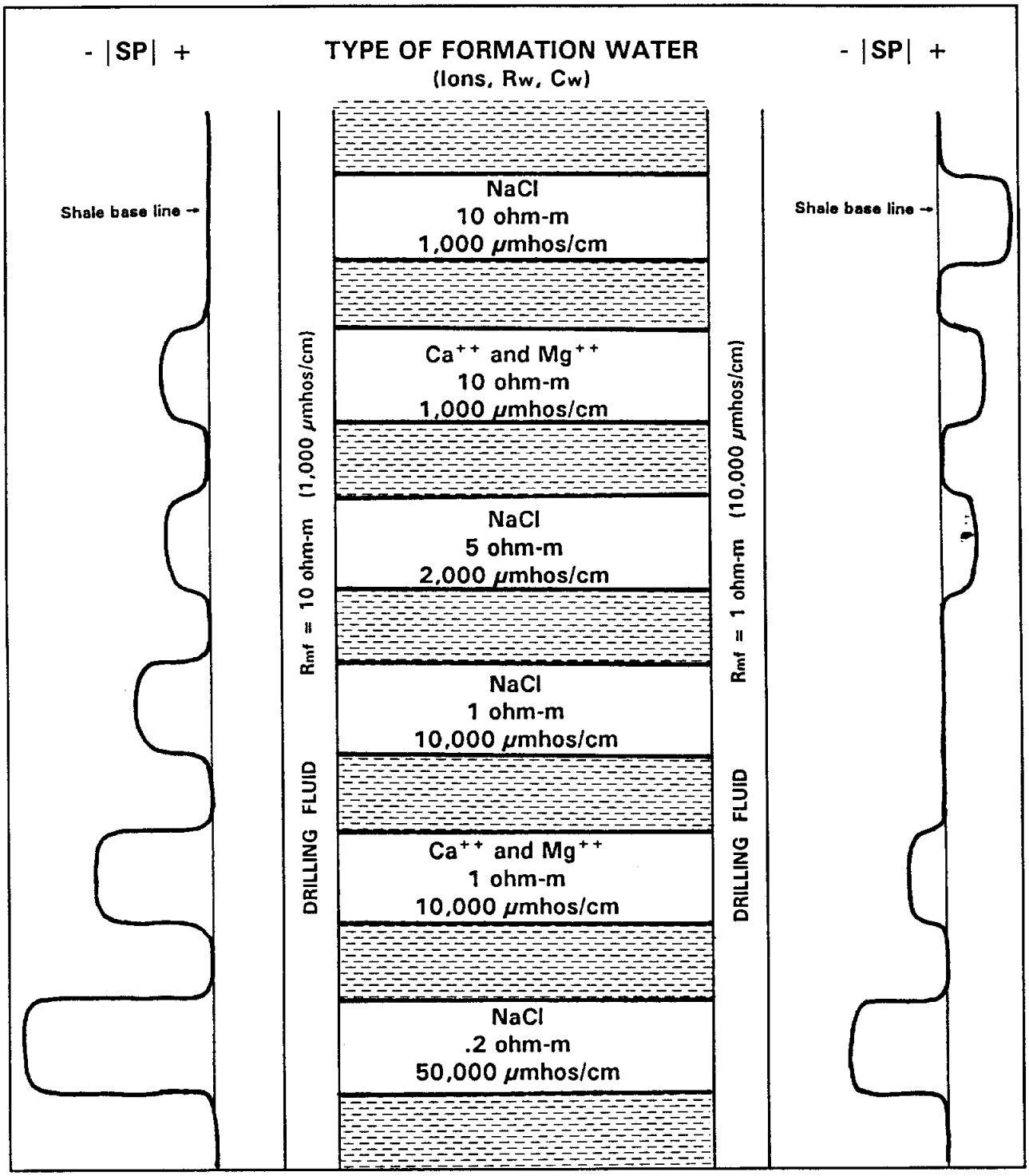

Figure 12-8. Schematic SP curves illustrating the effects of varying R_{mf}'s and R_w's on the curve deflection in porous, permeable formations.

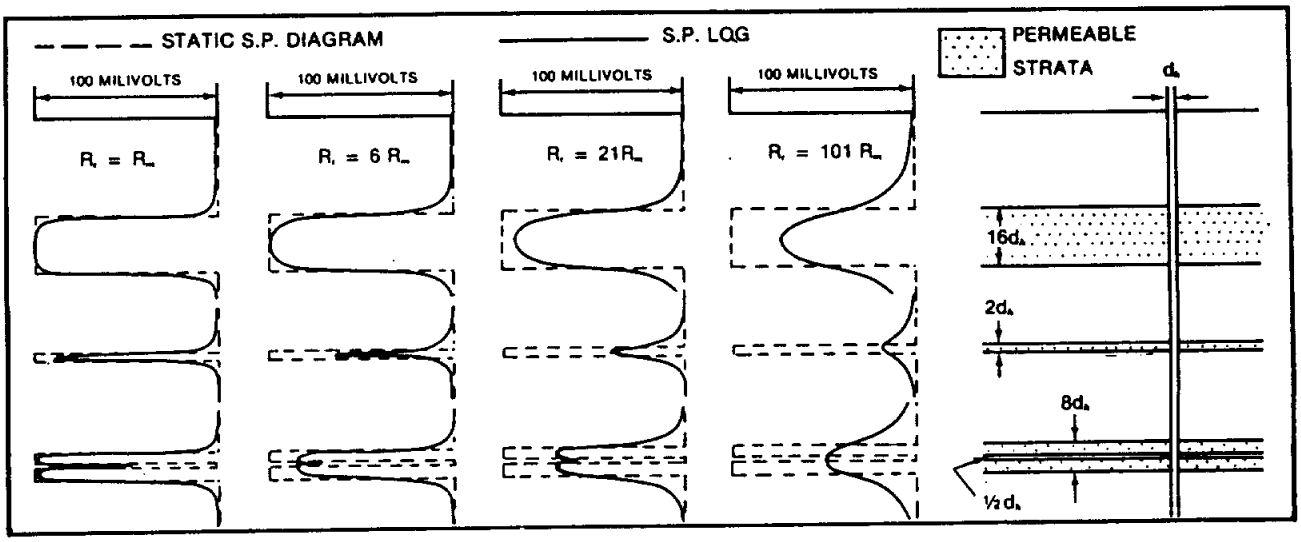

Figure 12-9. Calculated SP responses demonstrate that as the R_t/R_m ratio increases and the bed thickness decreases, the quality of the curve decreases. The responses were calculated assuming that $R_m = R_s$ (From Jorden and Campbell, 1986, after Doll, 1949).

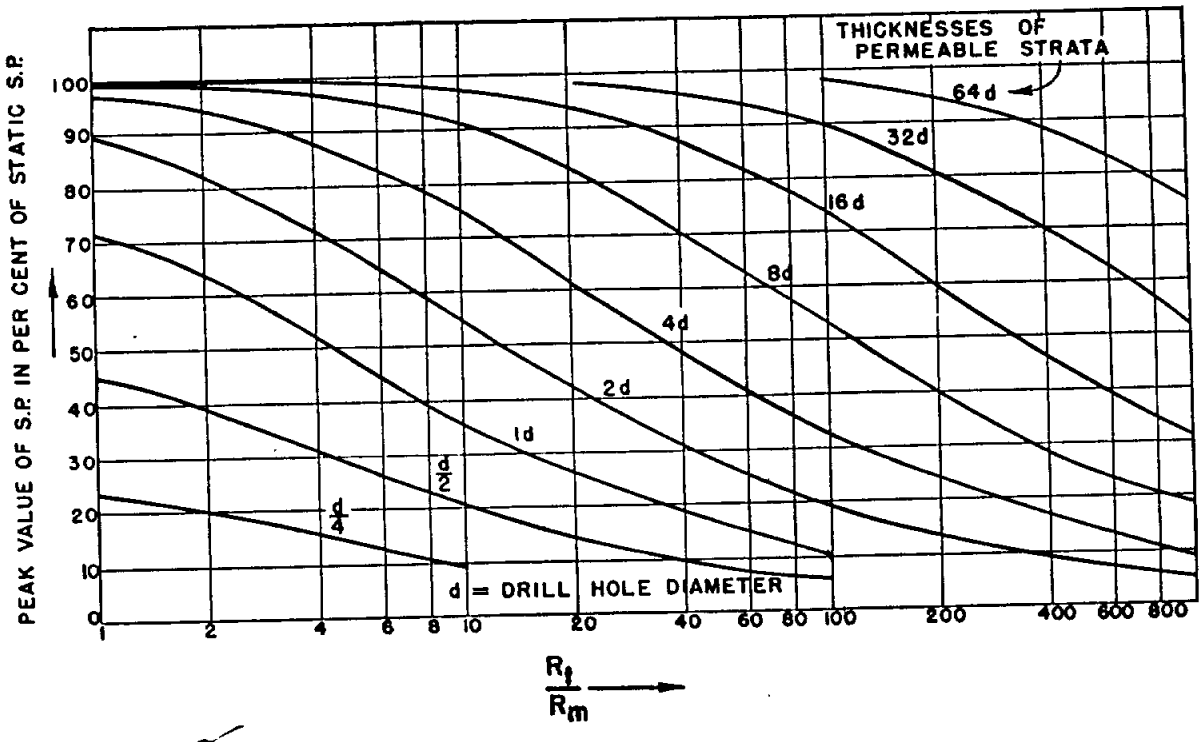

Figure 12-10. Environmental correction chart for various R_t/R_m, bed thicknesses, and borehole diameters. The chart was constructed for the case where $R_m = R_s$ (From Doll, 1949).

hole diameter will have an accurate SP value (Figure 12-9). Figure 12-10 quantifies the effect of bed thickness on the SP deflection. The chart was constructed for an Rm/Rs ratio of 1. Charts have not been constructed for other ratios.

Borehole diameter. An increase in borehole diameter has the same effect as an increase in Rt/Rm or a decrease in bed thickness: the curve becomes rounder, the deflection decreases, and the bed boundaries are less defined. Figure 12-10 quantifies the effect of borehole diameter on the SP deflection. The chart was constructed for an Rm/Rs ratio of 1. Charts have not been constructed for other ratios.

Depth of mud filtrate invasion. The larger the depth of invasion the smaller the SP deflection, the rounder the curve, and the less defined the bed boundaries (Figure 12-11). Correction charts for depth of invasion are available, but are usually not needed. In thick beds the correction factor is negligible, less than 10 percent and often less than 5 percent (Hartline course notes, no date). High porosity aquifers have limited invasion, therefore the SP curve is affected very little by invasion. There are, however, two exceptions to this rule:

1. Ultrashallow invasion will result in a reduced SP deflection (Segesman and Tixier, 1959).

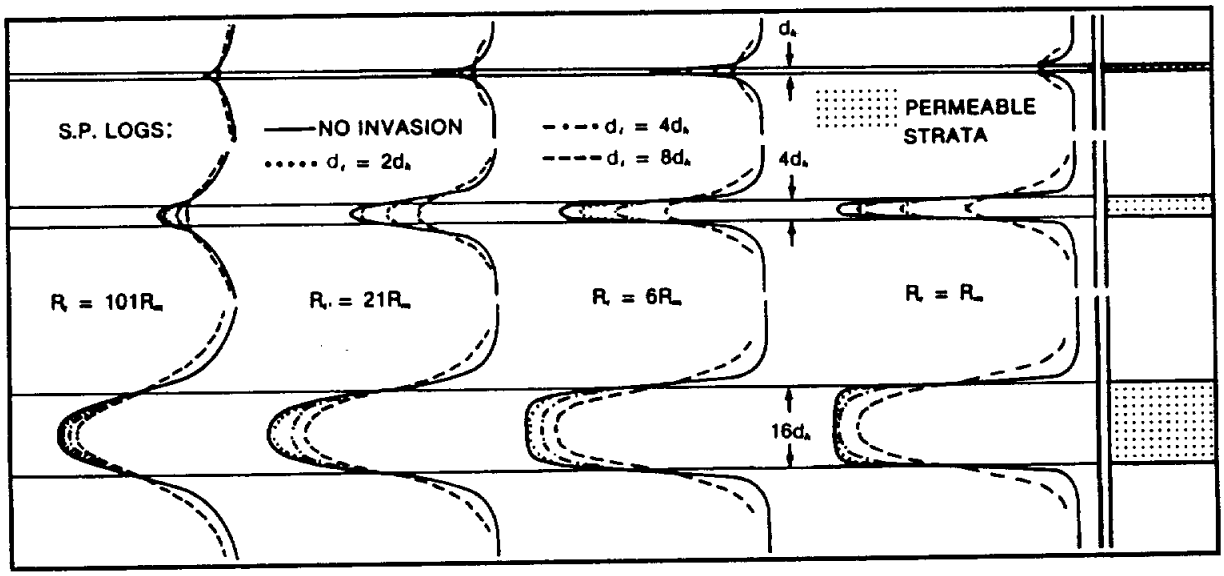

Figure 12-11. Calculated SP responses demonstrate that as the diameter of invasion increases, the quality of the curve decreases. The responses were calculated assumming that $R_t = R_s$ (From Jorden and Campbell, 1986, after Doll, 1949).

2. As the depth of invasion increases, the SP deflection increases until all formation water has been removed from the flushed zone. This can be seen on successive logging runs made before the flushed zone is fully established. After the flushed zone is established, the SP deflection does decrease as invasion increases.

Shale. Dispersed shale in a permeable formation will reduce the SP deflection by creating a shale membrane potential in the formation of opposite polarity to the liquid-junction potential in the formation (Hartline course notes, no date). The reduced SP is called **pseudostatic SP** (PSP). Hydrocarbons in a shaly reservoir rock will further reduce the SP deflection.

Formation mineralogy. Certain minerals such as pyrite and marcasite create a large negative SP deflection.

Formation temperature. As temperature increases, the amount of SP deflection increases.

Mud composition. Normal fresh water muds have no adverse effect on the curve. Most muds behave as sodium chloride fluids. Gyp-base muds and calcium chloride ($CaCl_2$) muds require corrections. They contain divalent cations which reduce the amount of negative deflection (Pirson, 1963). Oil-base muds and inverted oil emulsion muds are nonconductive and have no SP current (Pirson, 1963).

Tool eccentricity. The position of the SP electrode in the borehole has no effect (Pirson, 1963).

Instrumentation problems. Magnetization of any part of the winch will superimpose a sine wave on the SP curve (Figure 9-11). Improper grounding of the surface electrode will cause the shale base line to drift (Figure 12-12). Dry soil makes it difficult to get a good ground. If a downhole ground is used, the base line will drift appreciably as the ground approaches metallic casing (Bateman, 1985). If the tool has been repaired with a dissimilar metal, the contact of the two metals (**bimetallism**) can generate an SP current and cause the curve to drift. However, the amount of drift is small and is really only noticeable opposite highly resistive formations (Schlumberger, 1989). Any bare metal, except for other electrodes, within 7 feet of the electrode will cause problems (Hallenburg, 1984). If the electrode contacts the borehole wall, a sharp potential change occurs for a few seconds. This can be prevented by recessing the electrode in the probe

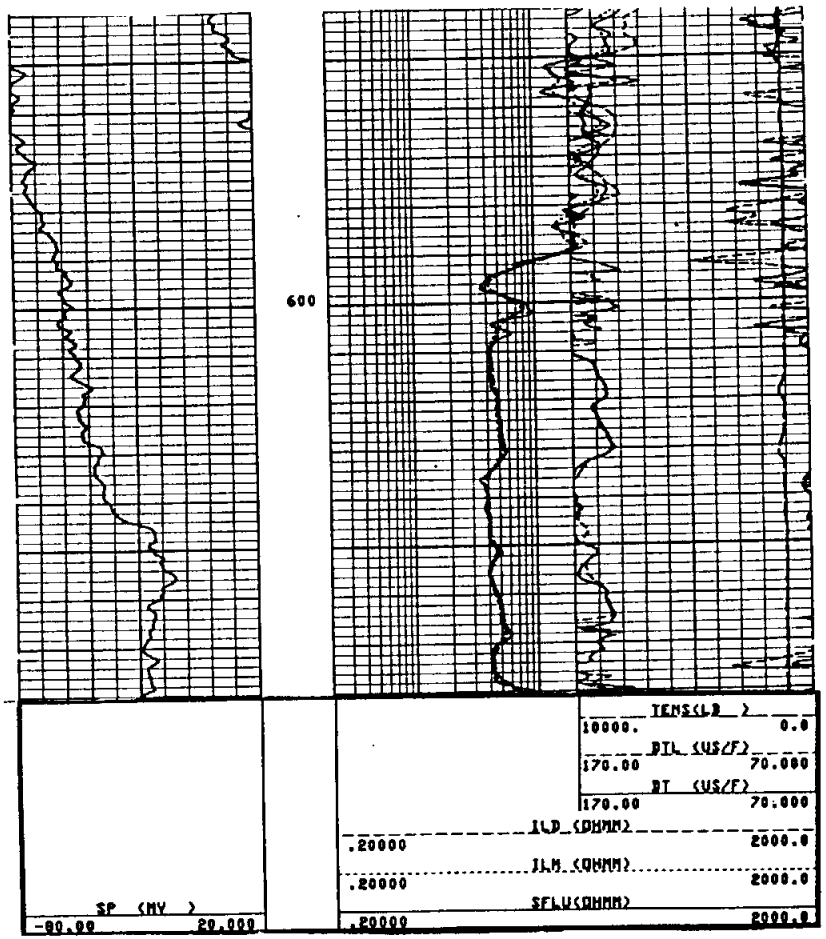

Figure 12-12a. The SP drift is caused by a poor electrical ground of the surface electrode. Tracks 2 and 3 are too cluttered, the sonic curves should be on a separate log. The sonic log has two Δt curves (a long and a short space curve), neither of which is working properly. The large rugose borehole (12¼ inches bit size and 15+ inches caliper reading) and the uncompacted, unconsolidated nature of the rock precludes accurate sonic porosities. In places, the Δt curves are reading nothing but borehole fluid (Δt 189 μs/ft). Δt peaks greater than 190 μs/ft are cycle skips.

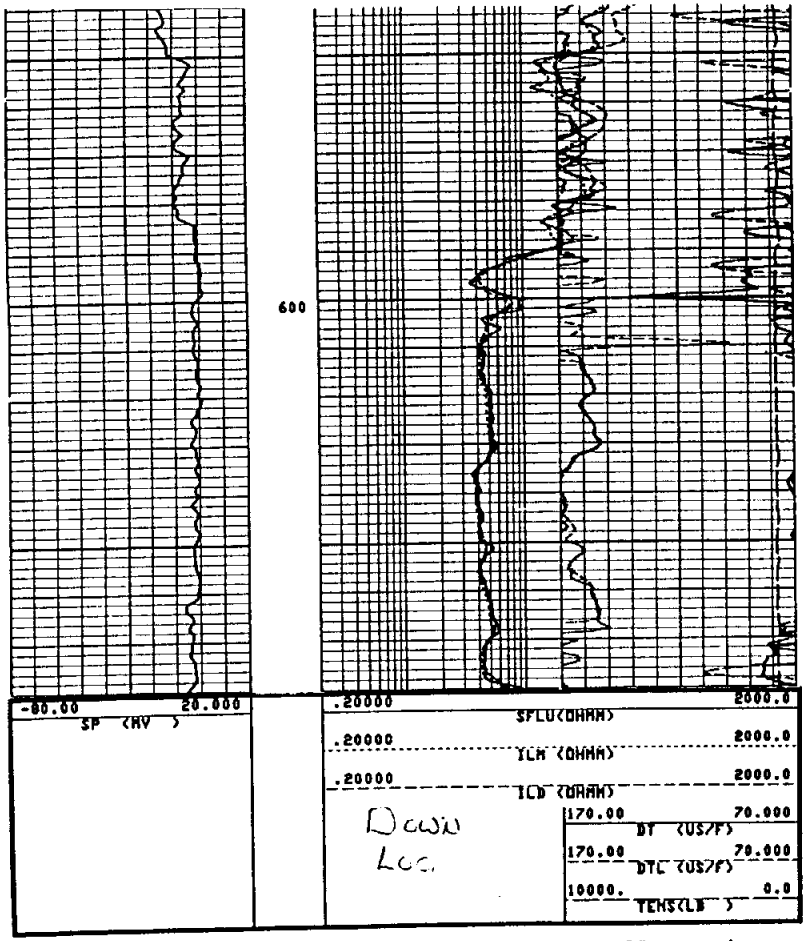

Figure 12-12b. Same log as Figure 12-12a. The SP curve is now woking properly after corrosion was removed from the surface electrode. The SP curve does not have large deflections because Rmf is very close to Rw. The log was made going into the hole. The log is the Gulf Coast Sandstone Aquifer. The well is the Layne Western, M.U.D. 275 Plant #1, Harris County, Texas. At 700 feet Rm is 9.5 ohm-meters and Rmf is 7.6 ohm-meters at 85° F.

body. The electrode can be further protected by building tape bumpers (Hallenburg, 1984). Stopping the logging run for several minutes can alsc affect the curve (Figure 12-13).

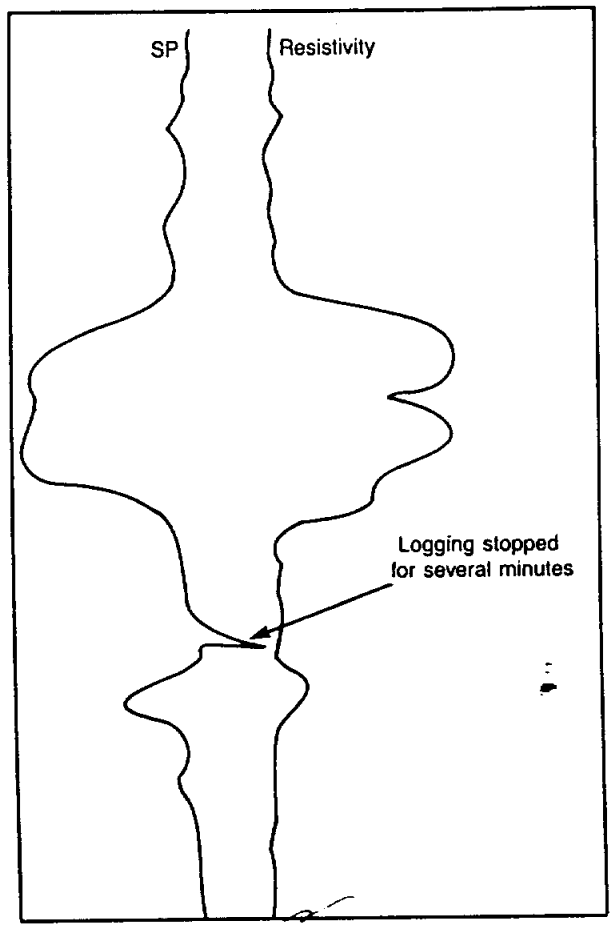

Figure 12-13. The effect of stopping the SP electrode for several minutes (From Hallenburg, 1984)..

Stray electrical currents. Nearby electrical currents such as cathodic protectors and power lines will adversely affect the curve. Redox potentials also affect the curve. In the northern latitudes the Aurora Borealis will severely affect the curve.

Interpretation. While measurement of the SP current is simple, interpretation of the curve is not. As explained in the previous section, curve response is greatly affected by formation and mud properties. However, the curve contains a wealth of information if the effects of these influences are taken into account.

Opposite shales the SP curve is a relatively straight line - the **shale base line** (Figure 12-7). Impermeable beds such as thin limestones will also have a flat line that falls along the shale base line (Figure 9-23). The position of the base line may shift with depth. This occurs when the shale is not a perfect cationic membrane (Schlumberger, 1989) and when the electrical properties of the shales change. In water wells, especially at shallow depths, the shales are often not perfect membranes.

Opposite porous, permeable formations the curve deflects from the shale base line. If the formation water is fresher than the drilling fluid (R_w greater than R_{mf}), the deflection will be to the right, a positive SP (Figures 12-7 and 12-8). The deflection will be to the left, a negative SP (Figures 12-7 and 12-8), when the formation water is more saline than the drilling fluid (R_w less than R_{mf}). When the formation water and the drilling fluid are approximately the same salinity, the curve will be flat and fall along the shale

base line (Figures 7-13, 9-14, and 12-8). Petroleum wells normally have negative SP's, while water wells may have all three types.

Waters with significant amounts of divalent ions complicate the explanations offered in the above paragraph. Such waters move the SP deflection in the negative direction, thus making the formation water appear more saline than it actually is (Figure 12-8).

In thick, shale-free, porous, permeable sandstones the deflections reach a maximum value, the **sand base line** (Figure 12-7) or **static SP** (SSP). The sand base line is used to calculate shale volume in a sandstone. The position of the sand base line in a well shifts as the ratio of R_{mf} to R_w changes.

The slope of the SP curve indicates the rate of change in potential in the borehole. Since the maximum rate of change occurs at bed boundaries, the maximum slope (called the **inflection point**) on an SP curve is the bed boundary. As disc ection, a number of factors influence the slope oundary: the ratio of R_t to R_m, bed thickness, dep hole diameter. The resistivity of the adjacent shale curve shape. The principal control on the shape of a f a permeable bed and a shale is the resistivity cont eds (R_s and R_t). Opposite the more resistive bed t more, thus "moving" the inflection point to ne lowest resistivity (Figure 12-14).

Bed boundar lt to distinguish in carbonate sequences, which k, resistive (impermeable) zones separated by thin, able carbonate or impermeable shale). The resisti current from entering or leaving the borehole opposite them (Figure 12-15). Therefore, the intensity of the SP current remains constant until it reaches a conductive bed. If the hole diameter remains constant, the potential drop will be constant opposite the resistive zone and the SP curve will be a straight sloped line (Figure 12-16). Permeable zones have a convex SP curve shape that points toward the sand line (Figure 12-16). Shales have their convex side pointing toward the shale line (Figure 12-16). It is only at a shale bed that current can return to the mud. Thick, highly resistive carbonate formations with no shale sections have an SP curve that just "wanders" (Figure 8-14).

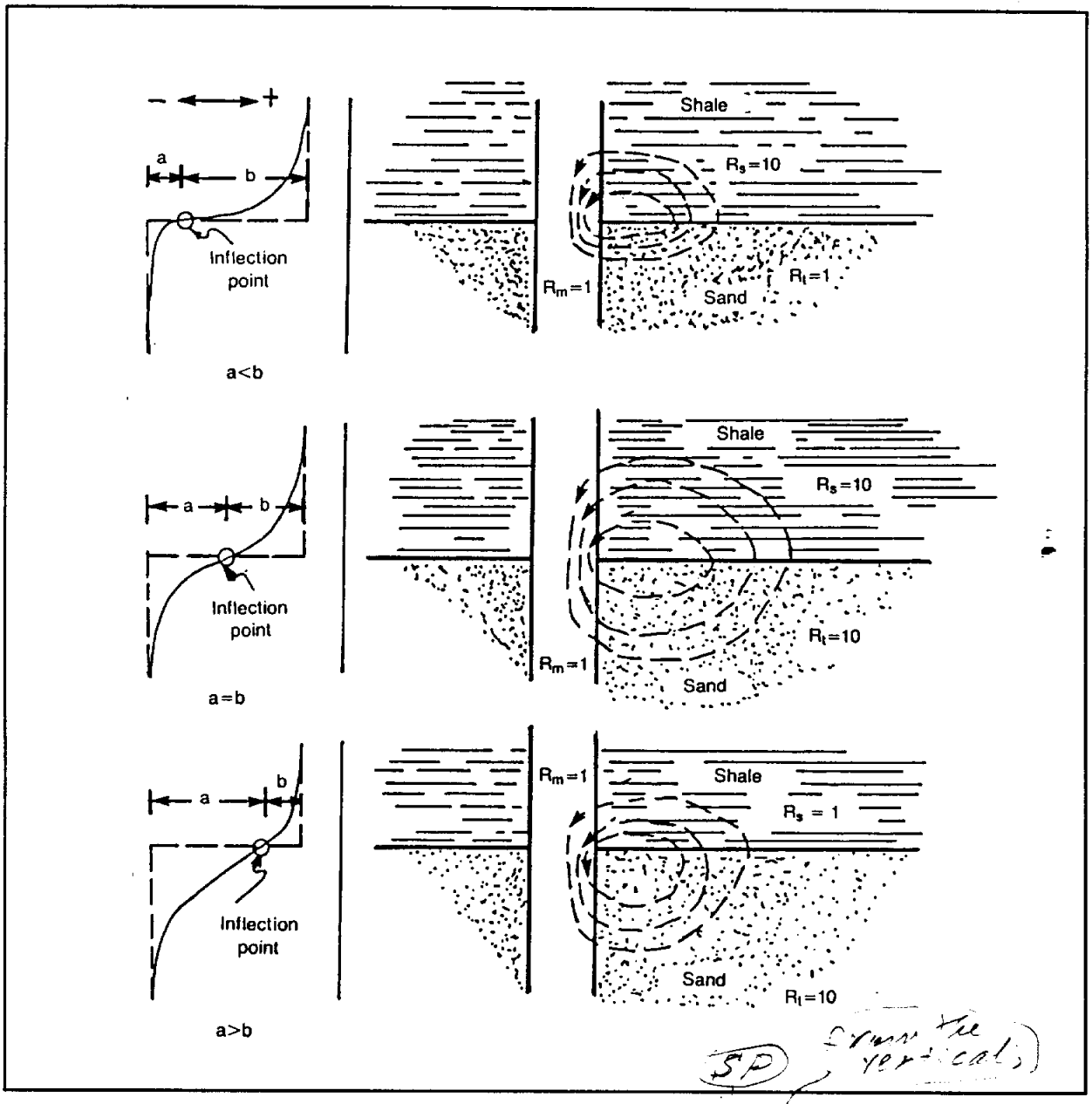

Figure 12-14. The inflection point, located at the maximum slope of the curve, defines the bed boundaries. The slope of the curve varies according to the R_t/R_s value. The inflection point "moves" toward the bed with the lower resistivity (From Helander, 1983).

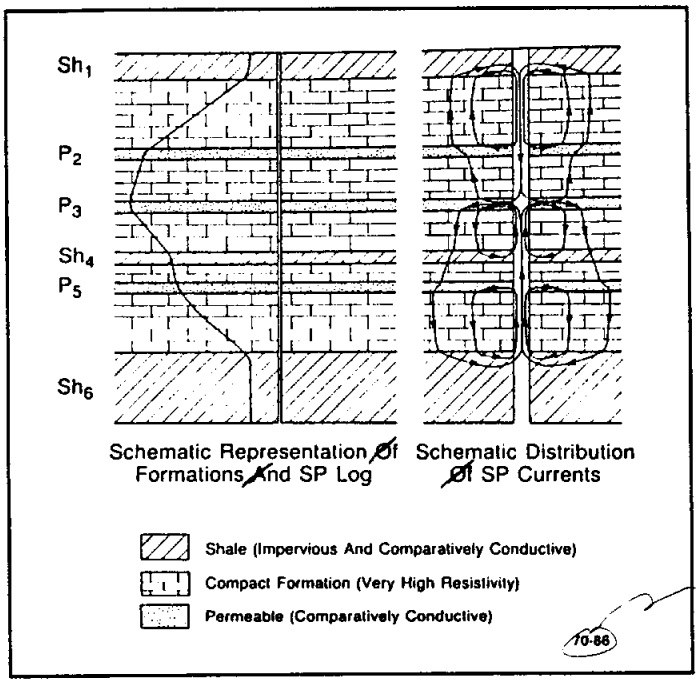

Figure 12-15. Schematic diagrams of SP current flow in very resistive formations and the resulting SP curve. **Sh** are shales and **P** are permeable beds (From Schlumberger, 1989).

Recommended use. The SP is the most universal curve in both old well files and in modern logging suites. The curve contains a wealth of information about a formation, if interpreted properly. Interpretation of the curve is more difficult in fresh to moderately saline water than it is in very saline waters.

The SP and the gamma ray curves are used for many of the same purposes: correlating, picking bed boundaries, distinguishing shale from other rock types, and calculating shale volume in sandstones. The gamma ray is the better curve for these tasks. However, it is not run in many water wells. Even when a gamma ray is included in the logging program, the SP curve should still be run since there is no extra charge for it.

The SP curve can be used for two quantitative calculations: estimating shale volume in a sandstone and calculating Rw. Both calculations assume that the electrochemical potential generates all the SP current.

Calculating shale volume. The SP curve can be used to calculate the volume of shale (V_{Sh}) in a sandstone as follows:

$$V_{Sh}\ (\%) \leq \left(\frac{SSP - PSP}{SSP}\right) \times 100 \qquad \textbf{12-1}$$

Where:

V_{Sh} (%) is the percent by volume of shale (clay) in a sandstone.
PSP is pseudostatic SP, the SP value of a shaly sandstone.
SSP is static SP, the SP value of a shale-free sandstone.

This calculation probably overestimates V_{Sh} (Rider, 1986). It is not as accurate as V_{Sh} calculated from a gamma ray curve.

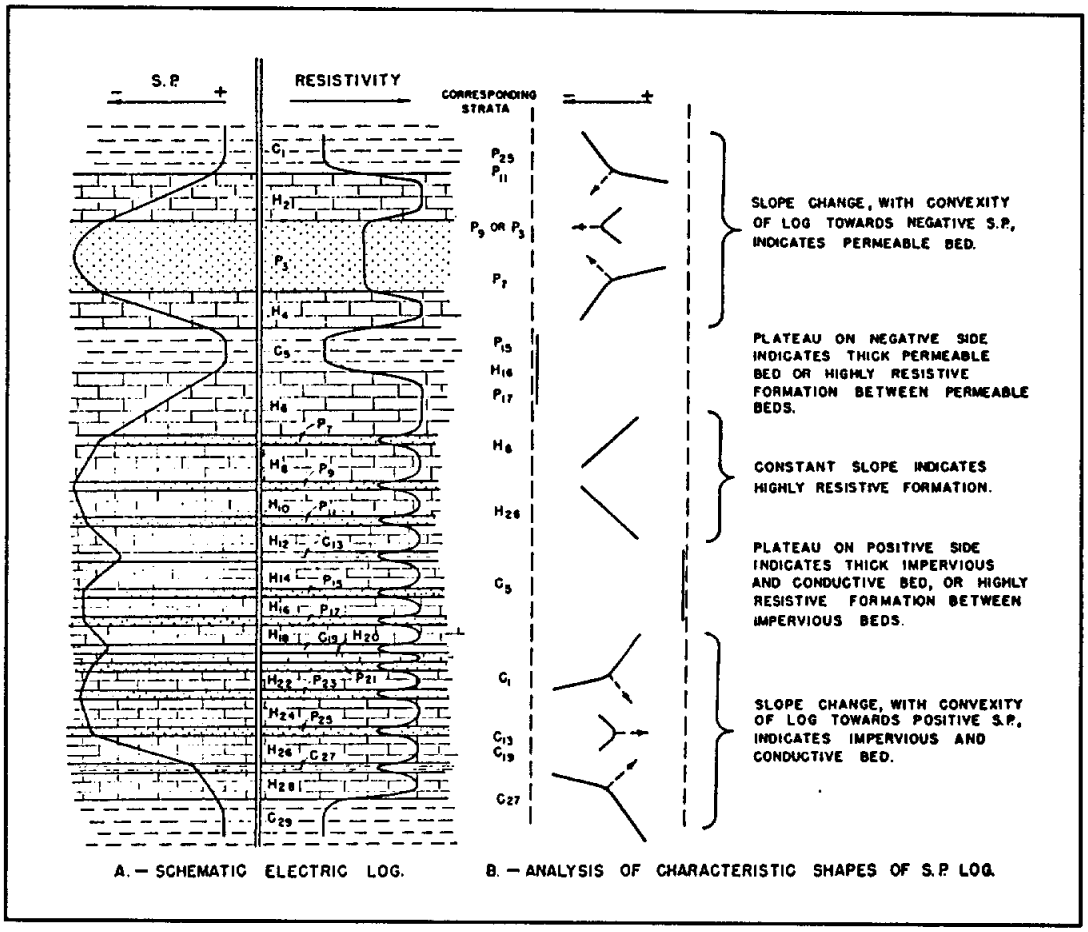

Figure 12-16. Schematic SP curve in very resistive formations and guidelines for interpreting the curve shapes (From Doll, 1949).

Calculating Rw. Rw calculations only work if the formation water is NaCl and if the formation is a thick, clean sandstone. (See Chapter 14 for a discussion of the technique.)

If the SP curve is to be used for Rw calculations, the mud properties should be kept fairly constant during drilling. Field experience has proven that when a mud system is significantly altered, it takes the SP curve a considerable length of time to reflect the properties of the new mud system (Schlumberger, 1989). This can result in a situation where the Rw calculation is using the SP response of the old mud system and the R_{mf} value of the new mud system measured just prior to logging.

POROSITY TOOLS

Chapter 13

Porosity is the fraction of a given volume of rock that is pore space. The standard abbreviation is ϕ. Porosity is a dimensionless number. It is expressed as either a percentage or as a decimal fraction. In calculations with porosity as one of the variables this distinction is very critical. Most log analysts reference porosity values as whole numbers, but use the term **porosity unit (pu)** instead of percentage. This avoids the potential confusion of referring to changes in porosity values as "percent changes". An increase in porosity from 10 percent to 20 percent is more clearly understood when it is called an increase of 10 pu, rather than saying porosity increased 10 "percent".

Porosity logs provide valuable information for ground-water studies. In addition to providing accurate porosity values, they are used to identify lithology and to calculate rock mechanical properties. They are also used in some methods for calculating water quality. Porosity logs are run in most oil and gas wells in Texas. However, they are seldom run in water wells. Only 2.2 percent of the water-well files collected for this study included a porosity log.

Three porosity tools are commonly available: density, neutron, and sonic. A fourth tool, the dielectric, can be used to calculate porosity. A nuclear magnetic resonance tool is presently being developed by the petroleum industry as a fifth porosity tool. Slimhole versions of the density, neutron, and sonic tools are available. Slimhole porosity logs, however, are not nearly as common as their conventional counterparts.

Proper interpretation of porosity logs is predicated on four principles:

1. **No logging tool measures porosity.** "Porosity" logs measure rock and fluid property, which is then used to calculate porosity. Porosity values are correct only when the log analyst uses the appropriate porosity equation and the correct constants.

2. **All porosity tools are affected by lithology.** Porosity values are correct only when the correct lithology constant is used in the porosity equation. Each porosity tool has a significantly different response to each of the common sedimentary rock types.

3. **Tool measurements are adversely affected by borehole enlargements, mudcake, and tool tilt.** All porosity tools investigate, at most, only a few inches into the formation. This makes them very susceptible to the influence of borehole enlargements (washouts, caverns, etc.), mudcake, and tool tilt. Compensated tools, developed to overcome these problems, provide more accurate porosities than uncompensated tools.

4. **Porosity tools must be properly calibrated.** Unfortunately, slimhole tools are often not calibrated.

Density (Gamma-Gamma)

The density or gamma-gamma tool is an excellent porosity tool. It is also used to pick bed boundaries. In conjunction with other porosity tools it can be used to determine lithology. It is used in conjunction with the sonic log to calculate acoustic impedance for synthetic seismic traces and to calculate formation mechanical properties such as Poisson's ratio and Young's modulus. While it is predominately an openhole tool, research is being conducted into methods of obtaining quantitative data through metallic casing (Jacobson and Fu, 1990). Density tools are used to detect voids in gravel packs in cased holes. Attempts have been made to evaluate the distribution of bentonite grout behind PVC casing utilizing slimhole density tools (Yearsley, et al., 1991).

In some parts of the country the tool cannot be run in openhole water wells. The concern is that the radioactive source would create very localized radioactive contamination if the tool should become stuck in the borehole.

The most common name for modern conventional tools is Compensated Density (CDL). Atlas Wireline uses the name Compensated Densilog (CDL); Schlumberger calls their tool the Compensated Formation Density (FDC). Slimhole tools are called either density or gamma-gamma and the term compensated is added when appropriate.

Tool theory. Conventional and some slimhole density tools utilize a source which emits medium-energy gamma rays (Cobalt 60 or Cesium 137) and which is mounted in a shielded sidewall skid. The skid is pressed against the borehole wall by means of an eccentering arm that also functions as a caliper (Figure 13-1). The pressure of the eccentering arm, plus the plow-shaped design of the leading edge of the skid, usually allows the skid

to cut through the mudcake.

The tool design creates collimated (focused) gamma rays that pass into the formation. As the gamma rays pass through the formation several reactions take place. Compton scattering is the only reaction of consequence to most density tools. It occurs when gamma rays lose energy and change direction due to collisions with electrons in the rock and fluid.

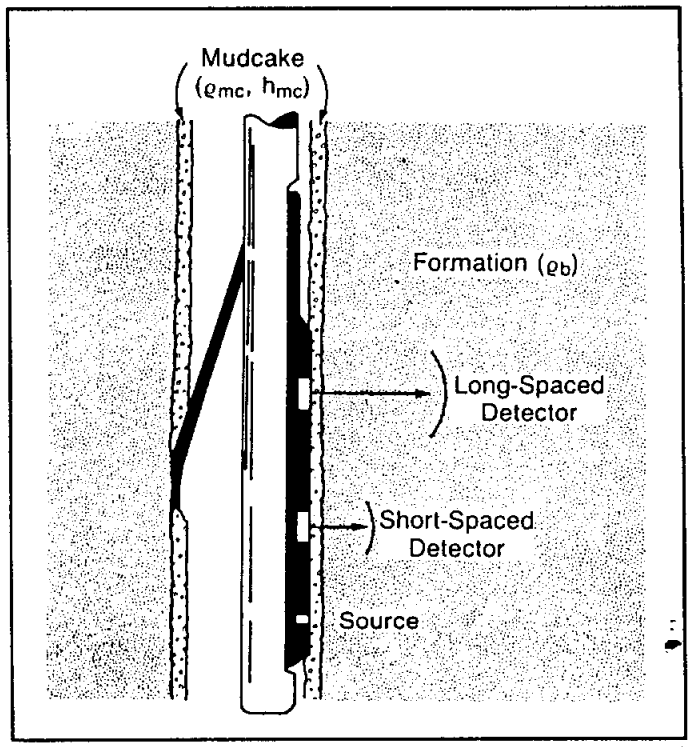

Figure 13-1. Schematic drawing of a compensated density tool (From Schlumberger, 1989, modified from Wahl, et al., 1964).

Density tools measure the attenuation of gamma rays between the source and one or two detectors. The detectors emit an electrical pulse for each gamma ray that is intercepted. The count rate varies by a factor of 5 to 10 for common sedimentary rocks (Dewan, 1983). The detectors are shielded in such a way that they respond only to the gamma rays undergoing Compton scattering. Such shielding makes the count rate a function of the electron density.

The gamma ray count measured by the detector(s) is inversely proportional to the electron density (ϱ_e) of the formation. Electron density, in turn, is proportional to the bulk density (ϱ_b) of the formation. For common sedimentary rocks the ratio of ϱ_e to ϱ_b varies very little. This means that it is a relatively easy, accurate, and straightforward process to convert the gamma ray count to bulk density. Conventional and some slimhole density tools output bulk density as the "raw" data curve.

There is considerable variation in the design of slimhole density tools. Some tools are compensated (dual detectors), but many are single detector. The single detector tools include omnidirectional, mandrel tools as well as sidewall tools. Omnidirectional density tools are commonly called 4-pi density tools. The name alludes to the fact that the tool investigates a spherical area, the volume of which is $4\Pi r^3/3$. The Greek letter Π is pi. The

tool may or may not be centralized. Uses include gravel pack evaluation and delineation of thin beds in coal sequences (personal communication, Lynn Gray Breaux, 1991).

Calibration. Proper calibration of the tool is critical for accurate bulk density and porosity values. One should always discuss calibration procedures with the tool manufacturer or the service company.

It is impossible to calculate accurate bulk density and porosity values with most slimhole density tools because of either the tool design or the lack of tool calibration. Hallenburg (1984) has aptly stated the case for proper calibration of the tool:

> **Literally, no quantitative use of a density system is possible without calibrations. With them the results are precise, and the possibilities are endless.**

Conventional density tools are calibrated to fresh-water saturated limestones. For all other lithologies the log-measured bulk density value will be at least slightly different than the actual bulk density. Figure 13-2 quantifies these differences for various lithologies. The figure shows that for water-fillled sandstones and dolomites the differences are inconsequential, but for some lithologies not usually of interest to ground-water studies (salt, coal, etc.) the differences are significant.

Depth of investigation and vertical resolution. Depth of investigation is only a few inches, with ~~five~~ inches a good average value. Experimental results using a 35 percent porosity sandstone saturated with fresh water reveal that 90 percent of the gamma ray response from a Schlumberger compensated density tool originates from within ~~five~~ inches of the tool (Sherman and Locke, 1975). Depth of investigation increases by a few inches as bulk density decreases (which occurs when either porosity increases or matrix density decreases), and it decreases by a similar amount as bulk density increases.

This shallow depth of investigation makes the tool response very susceptible to the influence of borehole conditions such as excessive hole rugosity and thick mudcake. Porosity values are too high when such conditions exist. Drilling methods (such as augering) that disturb the formation for just a few inches away from the well bore will adversely affect the ability of the tool to measure true bulk density.

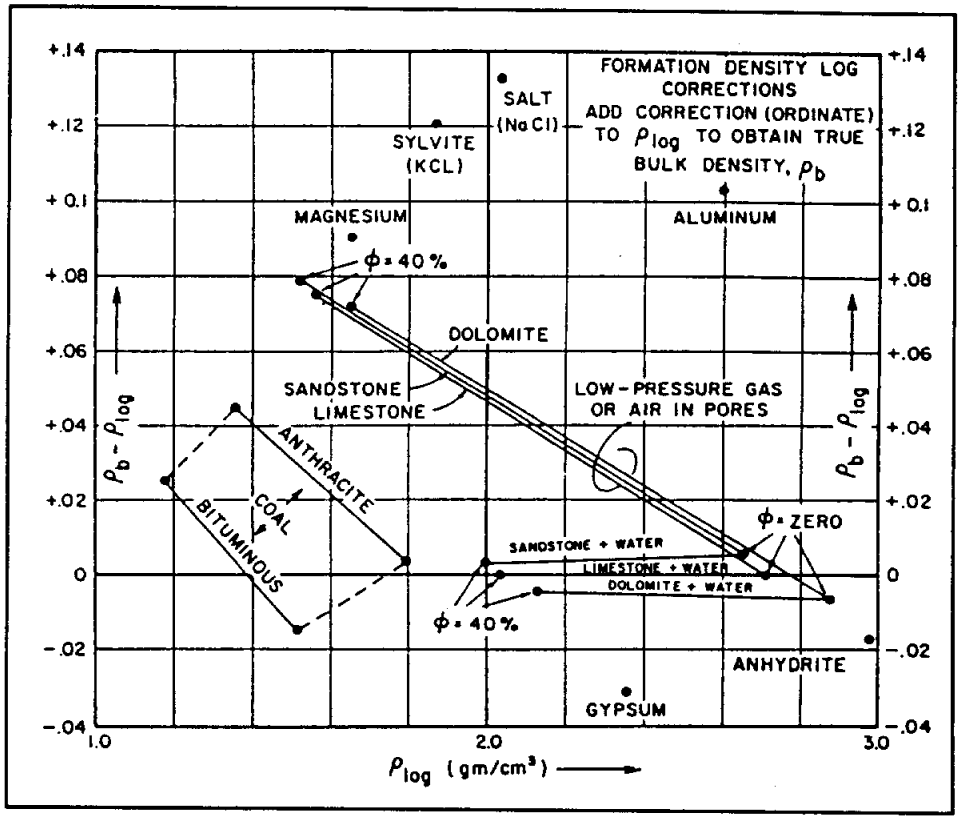

Figure 13-2. Corrections to be applied to apparent bulk density, ϱ_{log}, in order to derive true density, ϱ_b (From Serra, 1984, after Tittman and Wahl, 1965).

Vertical resolution of conventional tools is about 3 feet at average logging speeds (30 feet per minute). Slowing the logging speed to about 15 feet per minute improves the statistics, thus increasing the vertical resolution to 1.5 feet. Schlumberger offers a high resolution density log with a vertical resolution of 0.5 feet (Figure 13-3a). The improved resolution of this tool is accomplished by combining a slower logging speed and an increased sampling rate with a different processing technique.

Vertical resolution is also a function of the source-to-detector(s) or the detector-to-detector spacing. The smaller the spacing the better the vertical resolution. While the spacing varies somewhat for each brand of density tool, average values are 16 inches for single detector conventional tools and 10 inches between detectors for compensated conventional tools (Serra, 1984). Slimhole tools usually have spacings that are a few inches smaller. Good vertical resolution makes the density log useful for determining bed boundaries.

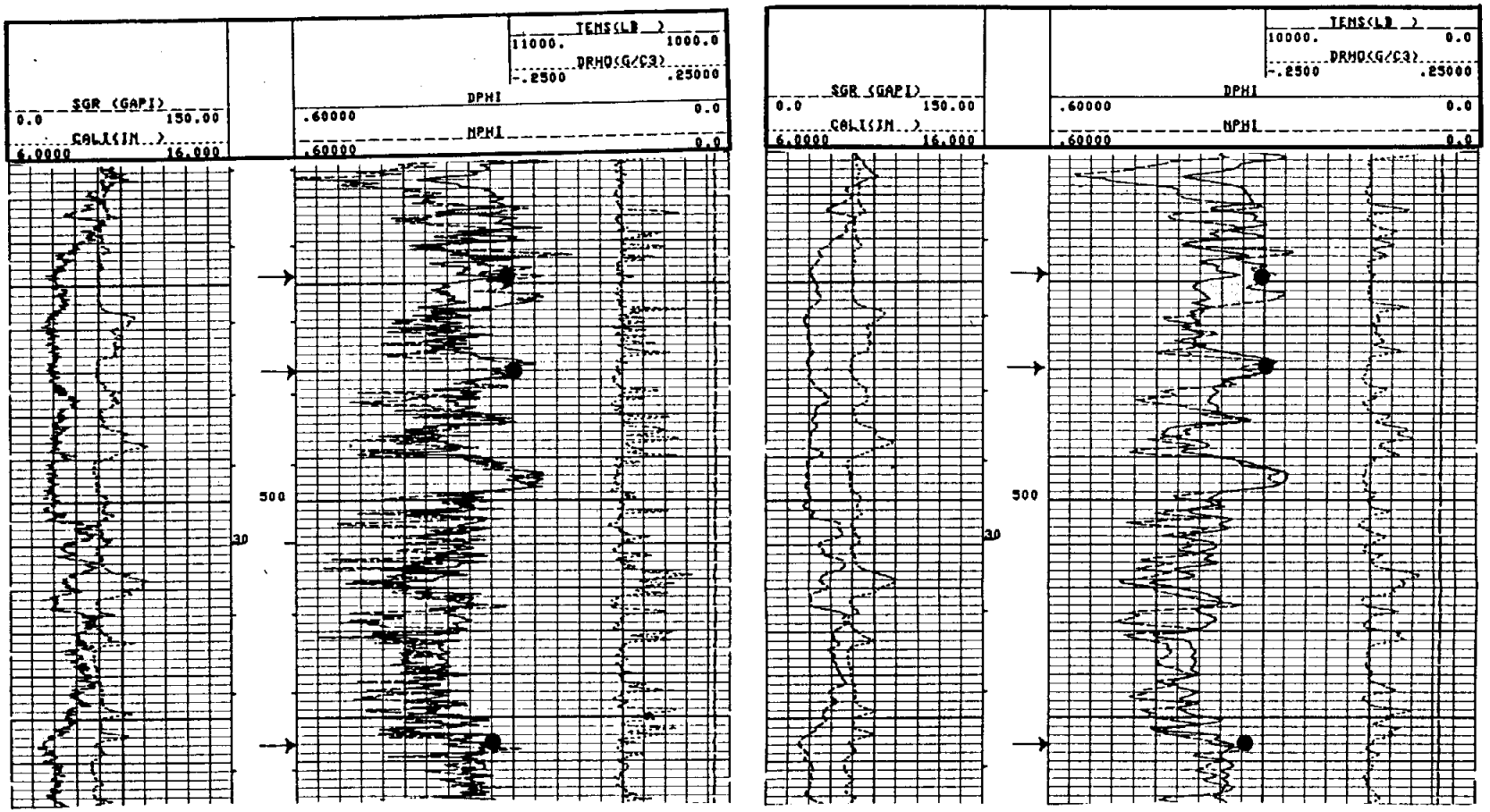

Figure 13-3 a & b. Comparison of high resolution (1.2 inch sampling rate) compensated density-neutron logs (13-3a) and normal density-neutron logs (13-3b). The high resolution pass has better vertical resolution. These logs illustrate the standard log presentation for conventional density and neutron porosity curves. In addition to the two porosity curves, the logs contain gamma ray (SGR), caliper (CALI), tension (TENS), and bulk density correction (DRHO) curves. Both porosity curves are plotted on a sandstone matrix. In shaly sandstones and shales neutron porosity (NPHI) reads greater than density porosity (DPHI). The curves overlay in shale-free sandstones. Zones in which density porosity reads greater than the neutron are due to either gas in the pores or mineralogical variations. Percussion sidewall cores were taken at the depths indicated by the arrows. Core porosities (plotted on the log) agree within 3 pu of the log porosities. Horizontal air permeabilities were 2565 md at 470 feet and 6541 md at 556 feet. See Figure 13-30 for a photomicrograph of a sidewall core. The negative DRHO corrections are due to the tool being miscalibrated. Positive corrections are due to washouts. The bit size is 9 ⅞ inches and the borehole fluid is 9 lb/gal, native gel. The log is the Gulf Coast Aquifer. The well is the Alsay, NW Harris County MUD 21 and 22 #2, Harris County, Texas. Figures 10-10, 11-1, 13-4, and 13-9 provide additional data on this well.

Statistical variations and logging speed. Due to statistical variations in the gamma ray count a time constant is necessary to smooth the measurement. In most formations a time constant of 2 seconds and a logging speed of 30 feet per minute is recommended. In low porosity formations the count rate is much lower, so a larger time constant (4 seconds) and a slower logging speed should be used to improve the resolution and the accuracy of the measurement (Etnyre, 1989). The time constant should be recorded on the heading. Time constants are discussed in more detail in Chapters 7 and 10.

Repeat passes are run to assist in determining the quality of the data. They will not be identical due to statistical variations in the gamma ray count rate. The standard deviation between repeat runs should be about 0.04 g/cm^3 for high bulk densities and about 0.02 g/cm^3 for low bulk densities (Dewan, 1983). Formations with irregularly distributed porosity (e.g. vuggy carbonates and fractured zones) and borehole walls with irregularly distributed enlargements have greater variations between repeat passes. This is because collimated density tools investigate only about 12 percent of the borehole on any given pass (Table 7-1). Subsequent passes may measure a different portion of the borehole. However, in a slightly deviated hole the sonde has a tendency to ride on the downhill side, thus increasing the likelihood of the same portion of the borehole being investigated on repeat passes. This is more likely to occur with heavier conventional tools than it is with lighter slimhole tools.

Log presentation. Density logs vary considerably in their presentation. They may consist of one to seven curves, but the common format is five curves: bulk density, porosity, correction, caliper, and tension.

Conventional and some slimhole density tools record bulk density as the "raw" data curve (Figure 13-4), but some logs include count rate curves. The bulk density curve is labeled RHOB on the header, which is computer keyboard phonetics for ϱ_b. The unit of measurement is grams per cubic centimeter (g/cm^3). The curve is usually placed across Tracks 2 and 3 with a linear scale of 2.0 g/cm^3 to 3.0 g/cm^3. This scale covers the range of values occurring in common sedimentary rocks with less than 46 percent porosity.

The output of many slimhole tools is simply the count rate of each detector scaled in counts per second (Figure 13-5). For many of these logs no further processing is or can be done to the data.

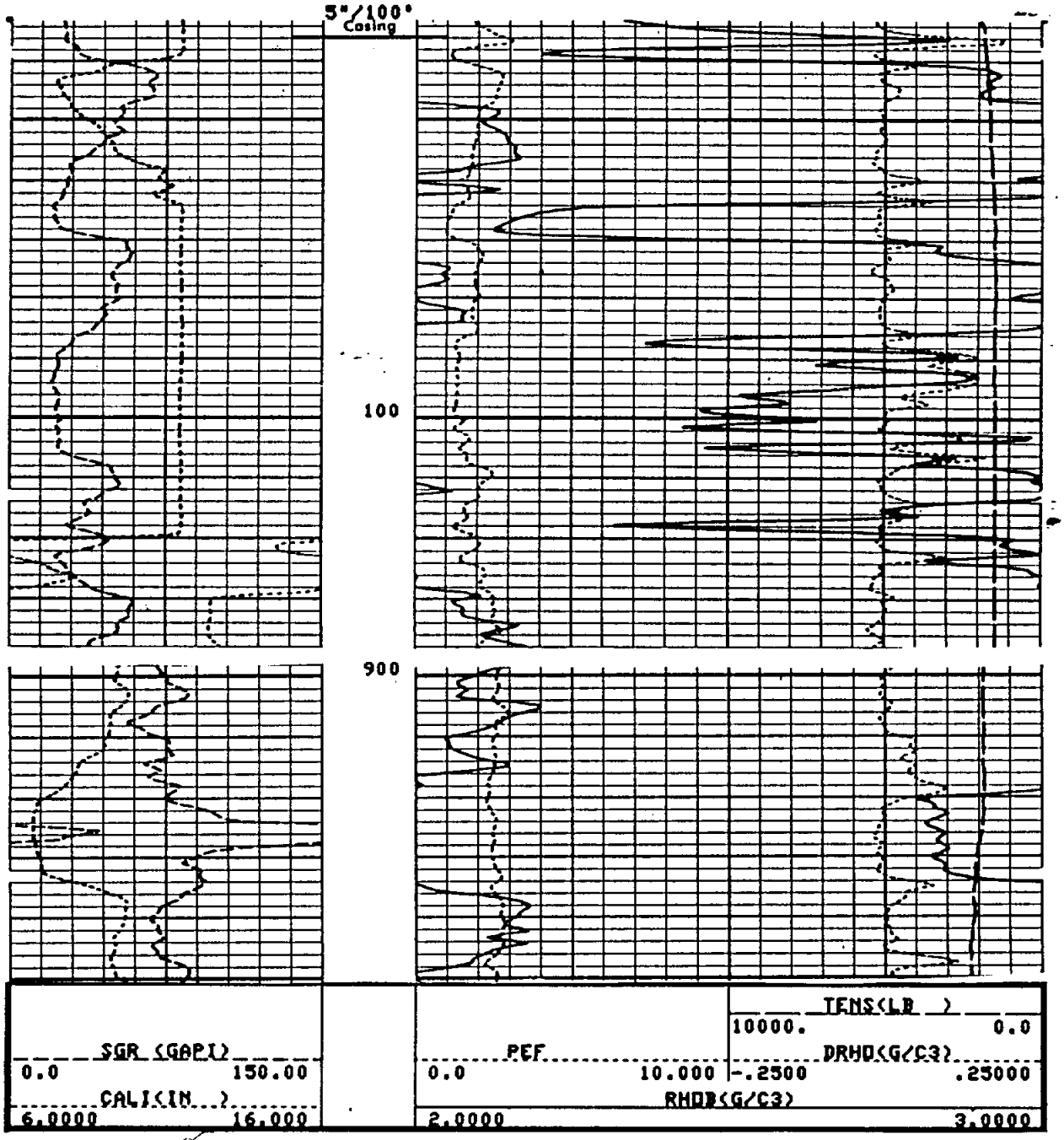

Figure 13-4. ~~The~~ typical format for a conventional compensated density log. (The example is actually a lithologic density log). Track 1 contains total gamma ray (SGR) and caliper curves. Track 2 contains a photoelectric factor (PEF) curve which is only found on a lithologic density log. As is standard practice, the unit of measurement of the PEF curve is not noted. Track 3 contains the tension (TENS) and $\Delta\varrho$ (DRHO) curves. The ϱ_b curve plots across Tracks 2 and 3. In the large washout from 64 to 120 feet the ϱ_b curve is predomionately reading the bulk density of the mud. The washout is so large that the $\Delta\varrho$ curve makes no correction. Figure 11-1 discusses the caliper curve of these zones. Figures 10-10, 13-3, and 13-9 provide additional data on this well.

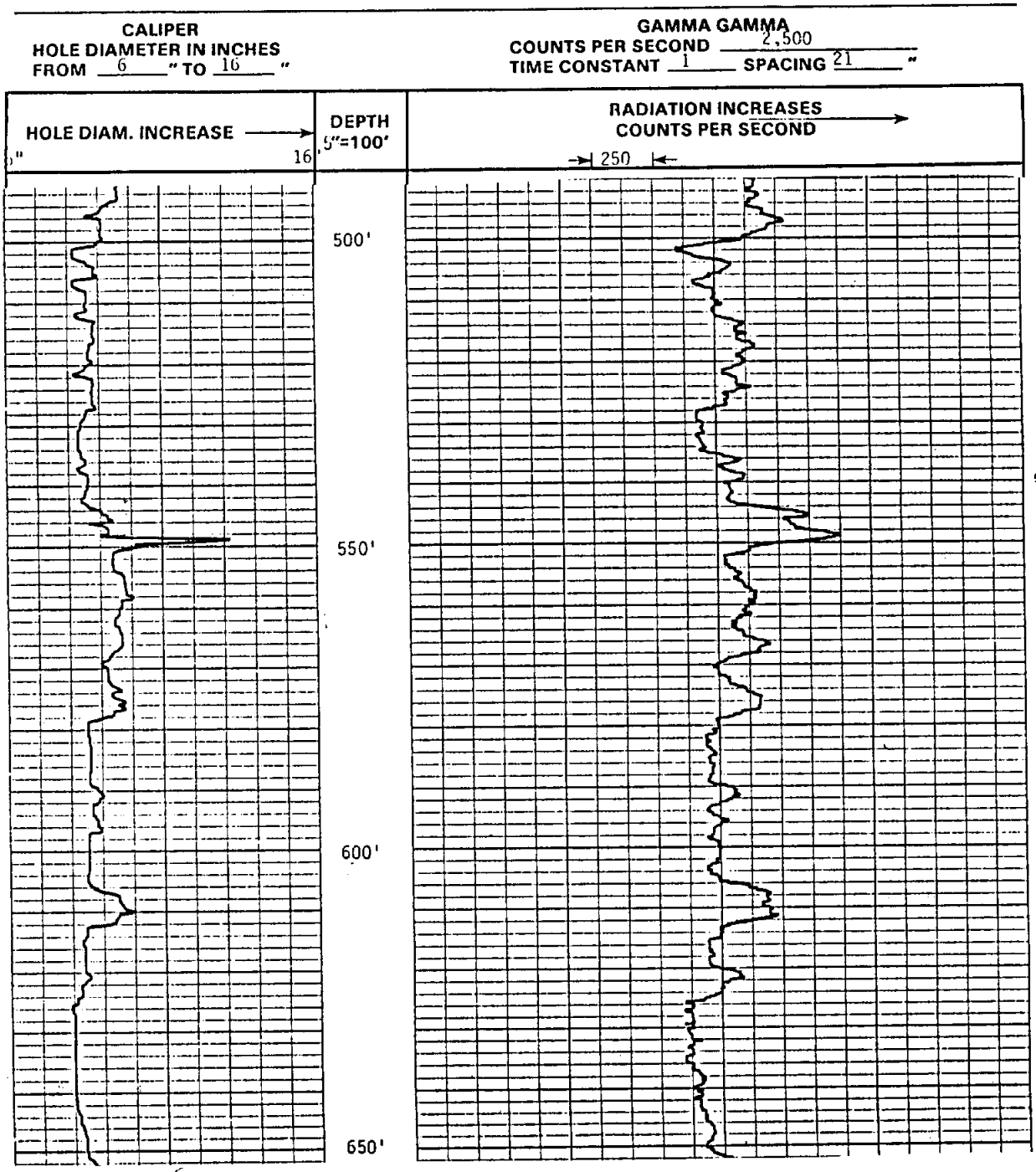

Figure 13-5. A typical slimhole density (gamma gamma) log presentation. Gamma ray count increases to the right, which means that porosity increases to the right. On conventional porosity logs porosity increases to the left. Figure 9-22 contains a conventional density log of this well. The count rate curve shows general trends in porosity, but is not as sensitive as the conventional log. It is hard to correlate the two logs. The slimhole caliper is more sensitive that the conventional caliper.

Compensated density tools correct the bulk density curve for the presence of mudcake not removed by the leading edge of the sonde and for washouts and borehole rugosity by comparing the differences in the count rates of the two detectors by means of an experimentally derived "spine-and-ribs" plot. The correction is automatically added to the bulk density curve, making it in actuality a corrected bulk density curve. The amount of correction is documented on the log as a separate curve labeled **Δρ (DRHO)**. The curve is usually placed in Track 3 with a scale of -0.25 g/cm^3 to 0.25 g/cm^3 (Figure 13-4).

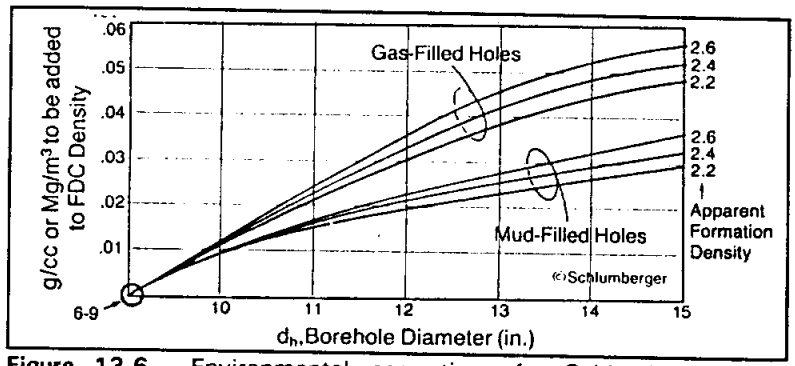

Figure 13-6. Environmental corrections for Schlumberger FDC. (From Schlumberger, 1989, after Wahl, et al., 1964).

A caliper curve is standard on most density logs. The backup arm of the sonde makes the caliper measurement. The curve is usually placed in Track 1 (Figure 13-4). It serves as another good quality-control indicator of the bulk density curve.

A porosity curve, if included, is usually placed in Tracks 2 and 3 (Figure 13-3). The values are expressed as decimal fractions. The curve is variously scaled. In sandstone provinces 0.6 to 0.0 is common. In boreholes with both sandstones and carbonates 0.45 to -0.15 is common. Porosity calculations and negative porosity values are explained in the following **Interpretation** section. The lithology on which the curve is calculated is noted on the log.

Modern conventional density logs include a tension curve. It is usually recorded in Tracks 1 or 3 (Figure 13-4). It is another quality control curve, because zones that pull tight will have erroneous log responses. The tension curve is discussed further in Chapter 5.

A gamma ray tool is usually run in conjunction with the density. The curve is recorded in Track 1 (Figures 13-3 and 13-4). In the oilfield the neutron porosity tool is commonly run in combination with the density.

Borehole corrections. Compensated density tools correct, up to a point, for the effect of mudcake, borehole rugosity, and washouts. Hole diameters of less than 10 inches do not require borehole corrections (Figure 13-6). Holes as large as 15 inches require a correction of only 3 pu, which for high porosity aquifers is a relatively small fraction of the actual porosity. Single detector tools cannot correct for any of these conditions.

Scanning the $\Delta\varrho$ curve gives a good indication of the accuracy of the bulk density values. Negative corrections should only occur when the drilling mud contains barite. Consistent negative corrections when the mud system has no barite are an indication of a malfunctioning tool (Figures 13-3 and 13-4). Positive corrections of up to 0.15 g/cm^3 can be accurately made by the spine-and-ribs plot. Larger corrections are probably insufficient and so the accuracy of the corresponding bulk density value is suspect (Dewan, 1983). Many log analysts, however, maintain that a correction of over 0.05 g/cm^3 makes the accuracy of the corresponding bulk density value questionable (Etnyre, 1989). The absence of a correction, however, does not always insure that the bulk density value is accurately measuring formation density. Large borehole enlargements may have very small $\Delta\varrho$ corrections. These enlargements appear as low-density spikes on the bulk density curve and are often detectable on the caliper curve (Figure 13-4).

Bulk density can be accurately measured in air-filled boreholes if proper corrections are made to the data (Figure 13-6). A different spine-and-ribs plot must be used (Schlumberger, 1989). In air-filled holes the density log can tolerate much less rugosity than in liquid-filled holes because of the greater density contrast between the two fluids. If the pores within the depth of investigation of the tool are filled with air, an additional correction will be necessary. Since air stops fewer gamma rays than drilling mud or water, the bulk density will be lower (i.e. log porosity will read higher) than in a liquid-filled hole. The difference increases as porosity increases, reaching 0.08 g/cm^3 (5 porosity units) at 40 percent porosity (Figure 13-2). By making this correction to the bulk density curve, porosity is still calculated using a fluid density of 1.0 g/cm^3.

Interpretation. The main purpose of density logs is to calculate porosity. The bulk density of a formation is primarily a function of porosity and secondarily a function of rock and pore fluid density. The mathematical expression of this relationship is as follows:

$$\varrho_b = \phi\varrho_f + (1-\phi)\varrho_m \qquad \textbf{(13-1)}$$

Where:

ϕ = *porosity*

ϱ_b = *bulk density in g/cm*^{3}

ϱ_f = *pore fluid density in g/cm*^{3}

ϱ_m = *matrix (grain) density of the rock in g/cm*^{3}

The equation can be rearranged to solve for porosity:

$$\phi = \frac{\varrho_{ma} - \varrho_b}{\varrho_{ma} - \varrho_f} \qquad \textbf{(13-2)}$$

Figure 13-7 is a graphical solution of Equation 13-2. It works for any any brand of density log.

The density tool provides only the ϱ_b value. The log analyst must provide ϱ_{ma} and ϱ_f. These values should always be recorded on the log header when a porosity curve is included . Table 13-1 contains ϱ_{ma} and ϱ_f values for common minerals and fluids. Service company chart books contain more detailed lists. Hallenburg (1984) has a very extensive list.

In ground-water studies the fluid density is seldom in question. The ρ_b of fresh water (1.0 g/cm^3) is used for the entire borehole. In a borehole with several lithologies, however, matrix density may vary from formation to formation. Accepted practice is to plot the porosity curve on a limestone matrix (2.71 g/cm^3). Porosities of other lithologies are mentally corrected as the log analyst scans the curve (Figure 13-8). Depending on the porosity of the formation, 2 to 3 pu are subtracted from the porosity value of sandstones and 4 to 6 pu are added to dolomite porosities (Figure 13-8). Negative density porosities can occur when the wrong ϱ_{ma} is used in the porosity calculation (e.g. when a dolomite with less than 9 percent porosity is calculated on a limestone matrix).

If the lithology of a formation is not known, a crossplot of density porosity and neutron or sonic porosity will identify the lithology and correct the porosity value. Crossplots utilizing the density log are discussed in the **Porosity Crossplots** section of this chapter.

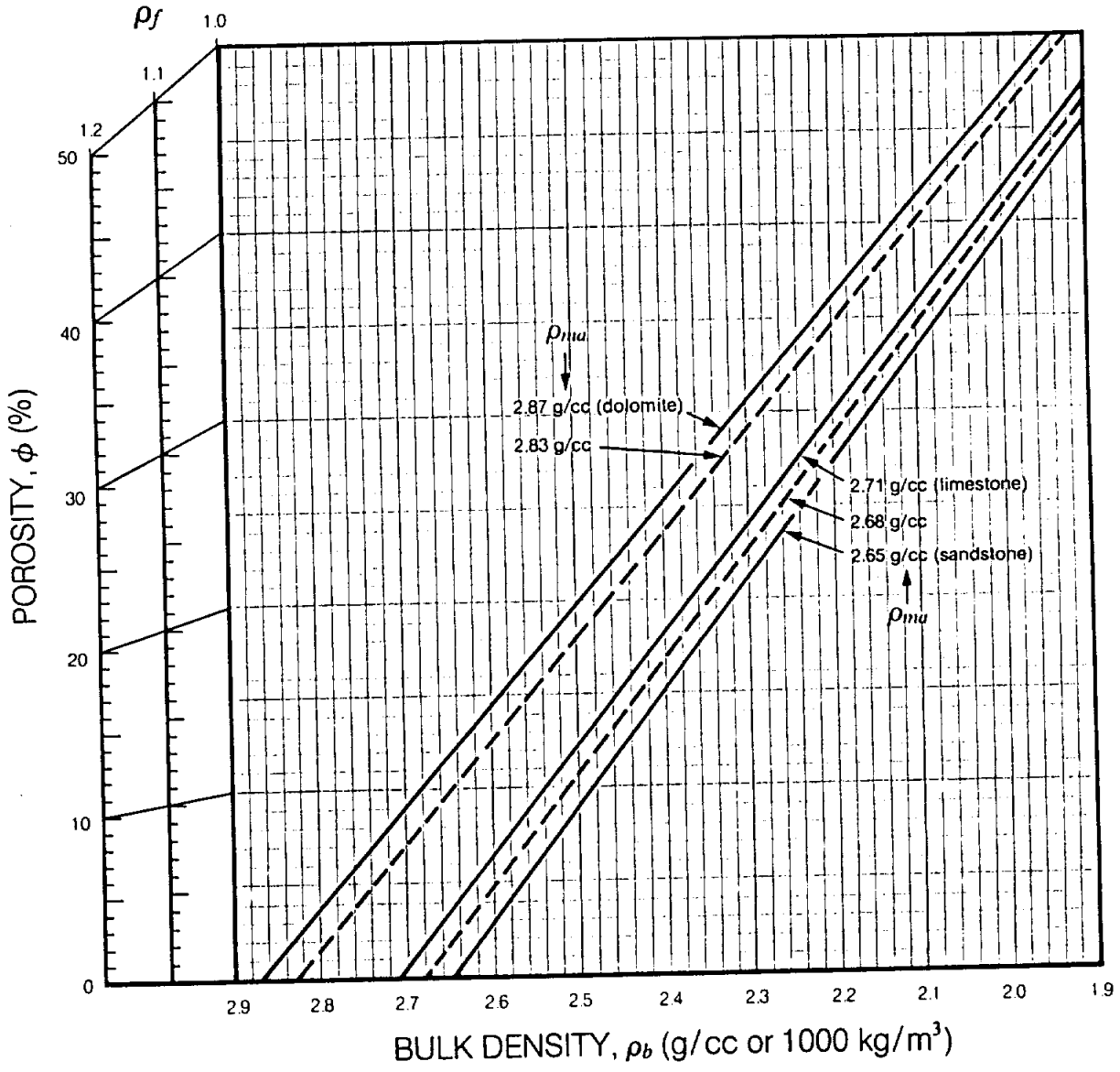

Figure 13-7. Graphical solution for calculating porosity from bulk density (Equation 13-2). Fluid density is ρ_f and matrix density is ρ_{ma}. This chart can be used for any brand of density log (From Welex, 1985).

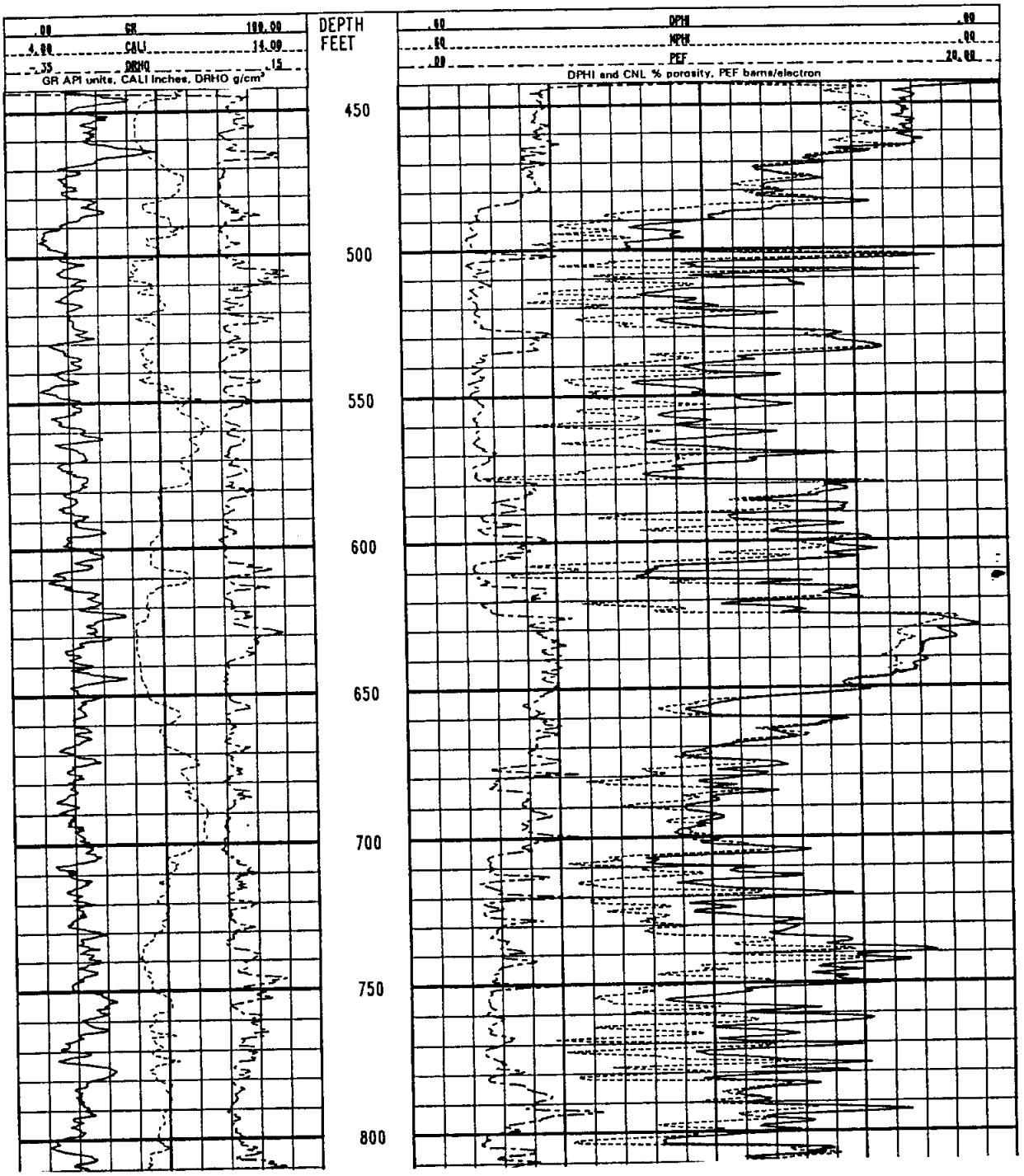

Figure 13-8. Determining lithology from a density-neutron log. Both porosity curves are calculated on a limestone matrix, so when the formation is limestone the curves will overlay (e.g. 528 to 536 feet). If the formation is shaly, the neutron curve will read a few porosity units higher than the density (e.g. 625 to 646 feet). In dolomites the neutron reads about 9 porosity units higher than the density (e.g. 720 to 734 feet). The PEF curve and thin section petrography confirm these interpretations. The log is the Edwards Aquifer. An ρ_f of 1.0 g/cm^3 was used to calculate density porosity. Figures 9-22, 13-5, 13-28, 13-32, and 13-33 provide additional information on this well.

TABLE 13-1. ϱ_{ma}, ϱ_f, AND Pe VALUES OF COMMON MINERALS AND FLUIDS

Mineral/Fluid	ϱ_{ma} or ϱ_f	Pe
Gas (CH_4)	0.0009	0.095
Oil	0.85- 1.1	0.12
Fresh Water	1.0	0.36
Saline Water (100,000 ppm NaCl)	1.05	0.73
Coals	1.2- 1.7	0.2 or less
Quartz	2.65	1.8
Kaolinite	2.4	1.8
Montmorillonite	2.1	2.0
Potassium Feldspar	2.5	2.9
Dolomite	2.87	3.1
Average Shale	2.65	3.4
Illite	2.5	3.45
Gypsum	2.35	4.0
Anhydrite	3.0	5.06
Calcite (Limestone)	2.71	5.08
Chlorite	2.76	6.3
Glauconite	2.54	6.4
Ankerite	2.9	9.3
Limonite	3.6	13.0
Iron Oxides	4.3- 5.2	19 - 22
Sulfides	3.9- 5	17 and up

(Modified from Schlumberger, 1988 and 1989.)

The density log is the best porosity log for shaly sands because it is less affected by shale then are other porosity tools (Figure 13-9). It gives more accurate porosity values than the other tools because the densities of most shales (2.2 g/cm^3 to 2.65 g/cm^3) are close to that of quartz (2.65 g/cm^3).

Density logs that just contain count rates can only be used as a qualitative indicator of porosity changes. The count rate is a logarithmic function of porosity (Etnyre, 1989).

Lithologic density. The lithologic density tool is an improved and expanded version of the compensation density. In addition to measuring bulk density, the tool measures the **photoelectric absorption index (Pe, PE,** or **PEF)** of the formation. Photoelectric absorption, also called the photoelectric effect, is primarily a function of lithology. This means that the log can be used to identify lithology as well as porosity, thus making the lithologic

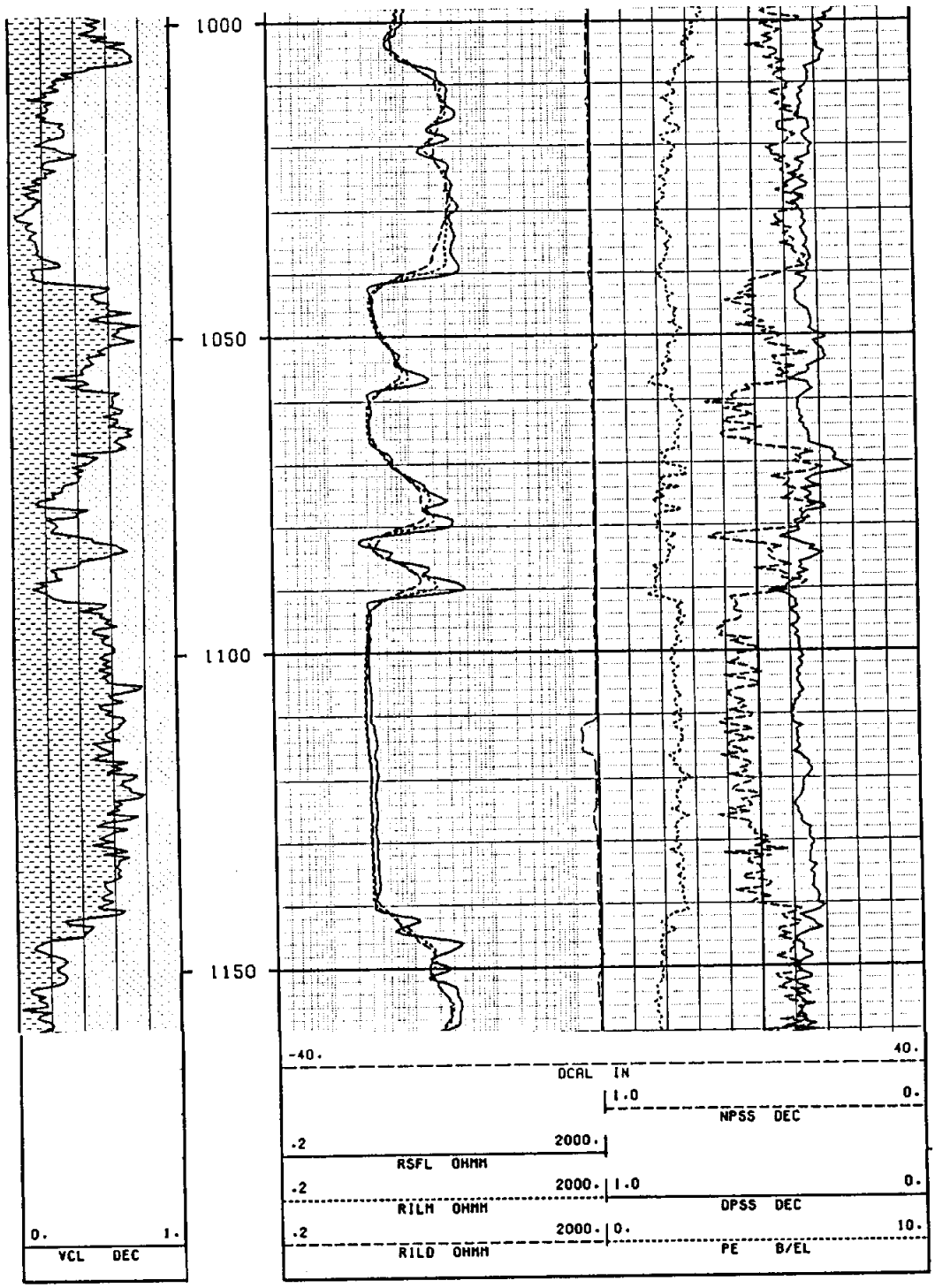

Figure 13-9. Identification of shaly sandstones and shales from density (DP) and neutron (NP) logs. Both curves are calculated on a sandstone matrix (SS) in decimal fractions (DEC), so when the formation is shale-free sandstone the curves overlay. In shaly zones the neutron reads higher than the density, with the density porosity being more accurate. The Pe curve reads 1.8 in sandstones and 1.8 to 2.5 in shaly zones. Dual Induction curves are in Track 2. The lithology column in Track 1 is calculated from the log data. VCL is volume of clay in decimal fractions (DEC). The log is the Gulf Coast Aquifer. Figures 10-10, 11-1, 13-3, and 13-4 provide additional information on this well.

density log self-interpreting. Addition of the Pe curve makes it an excellent, stand-alone porosity/lithology tool.

At the present time only the major logging companies have Pe curves. Trade names are Litho-Density (LDT) for Schlumberger, Spectral Density Log (SDL) for Halliburton, and Compensated Z-Densilog (ZDL) for Atlas Wireline.

Except for the Pe curve, the log presentation is identical to that of a compensated density log. The unit of measurement (barns per electron) is seldom used. The curve is usually placed in Track 2 or 3 (Figures 13-4 and 13-8). Modifications to the conventional density tool design have yielded higher count rates for the lithologic density tool, resulting in lower statistical variations and better repeatability of the measurments (Schlumberger, 1989). Statistical fluctuations are one-half that of a compensated density tool (Dewan, 1983). Vertical resolution is also better than that of compensated tools, due to a shorter source-to-detector spacing.

Whereas other density tools only detect gamma rays affected by Compton scattering, lithologic density tools measure gamma rays affected by both Compton scattering and photoelectric absorption. Some tools use the near detector only for measuring gamma rays affected by Compton scatter, while other tools also measure photoelectric absorption. The far detector measures gamma rays affected by both Compton scatter and photoelectric absorption.

Photoelectric absorption occurs when a gamma ray collides with a nucleus and is absorbed. The rate at which the reaction occurs increases as the energy level of the gamma rays decreases. The rate is also a function of the type of atoms in the formation. The photoelectric absorption index of an atom increases exponentially with increasing atomic number (Z). This means that pore fluids (water and gas) have much lower Pe values than rocks (Table 13-1). Consequently, the Pe value of a formation is relatively independent of porosity and can be used to identify lithology.

Although Pe values are relatively independent of porosity, they do decrease slightly as porosity increases (Figure 13-10). Thus high porosity formations have lower Pe values than published values such as those in Table 13-1. This is important in ground-water logging, because aquifers usually have higher porosities than the formations encountered in petroleum logging. The Pe values for high porosity formations would possibly be attributed to a mixture of lithologies by log analysts used to working with

lower porosity petroleum-bearing formations.

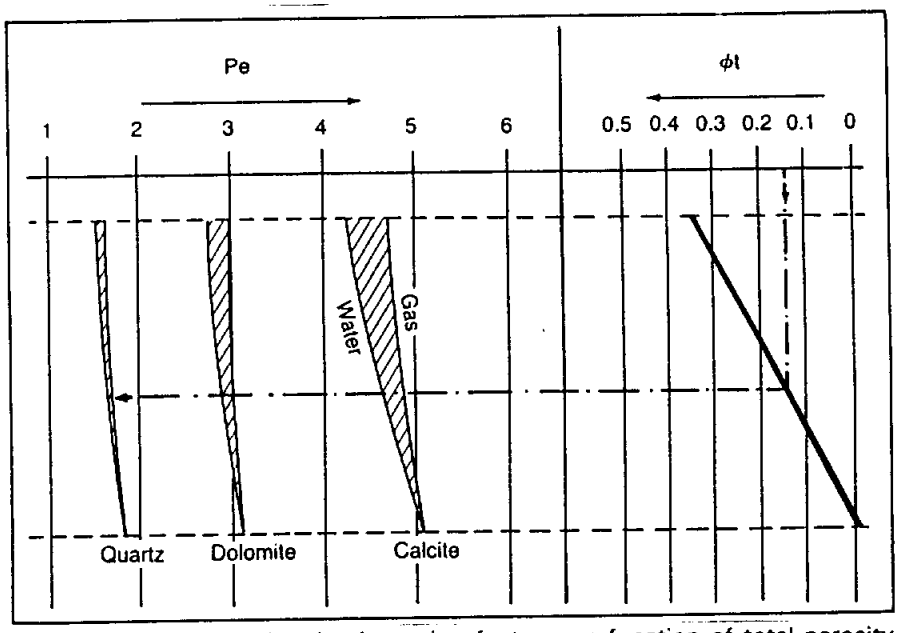

Figure 13-10. Photoelectric absorption factor as a function of total porosity (ϕt) and fluid type (From Dewan, 1983, after Gardner and Dumanoir, 1980).

Neutron

The neutron tool is used to calculate porosity and pick bed boundaries. It can also be used to delineate water-saturated zones. In conjunction with another porosity tool, usually the density, it can be used to determine lithology. In combination with the density it can be used to identify gas-saturated zones below the water table. Certain neutron tools can be used in air-filled holes and in cased holes.

In some parts of the country the tool cannot be run in openhole water wells. The concern is that the radioactive source would create very localized radioactive contamination if the tool should become stuck or lost in the borehole.

Most service companies call their modern, coventional tool a Compensated Neutron. However, each company uses a different abbreviation for the tool: Schlumberger (CNL), Atlas Wireline (CN), and Gearhart (CNS). Halliburton calls ~~their~~ tool a Dual Spaced Neutron (DSN). Sidewall neutron tools are called Sidewall Epithermal Neutron Log (SWN) by Atlas Wireline, Sidewall Neutron Log (SNL) by Gearhart, Sidewall Neutron (SWN) by Welex and Halliburton, and Sidewall Neutron Log (SNP) by Schlumberger. Several other names have been used for other brands and types of conventional tools. Slimhole tools with one detector are called neutron-neutron or neutron tools; two detector tools are called compensated neutron tools.

Several types of specialized neutron tools are also available, including pulsed neutron decay logs (neutron lifetime and thermal decay time logs) and neutron activation logs. Most of these are cased hole tools and have seldom been used in ground-water studies. Schlumberger (1989b) has a good discussion of these tools. Keys (1988) also discusses them.

Various types of neutron tools are also used to measure moisture content in the vadose zone. Soil moisture probes utilize a neutron source to measure moisture content in the soil horizon. Neutron porosity tools are sometimes utilized in open holes to detect perched water tables.

Tool theory. Neutrons are electrically neutral particles with the mass of a hydrogen atom. Naturally occurring free neutrons are very rare in most formations. All neutron tools measure the response of a formation to bombardment from a neutron source in the tool.

High velocity, high energy (about 4 Mev) neutrons are emitted by a radioactive source in the tool. During the brief life span of a neutron (a few milliseconds), it passes through three energy levels that are of interest to neutron logging (Figure 13-11). As neutrons travel through the borehole and formation they undergo elastic collisions with nuclei, continuously changing direction and losing energy. The final stage of the slowing down process is an energy level called the **epithermal** state. As collisions continue, neutrons reach the **thermal** equilibrium energy state of atoms in the formations. While in the thermal state neutrons travel about, neither gaining nor losing energy. The final state is reached when a thermal neutron collides with a nucleus, resulting in the absorption of the neutron and the emission of a **capture gamma ray(s).**

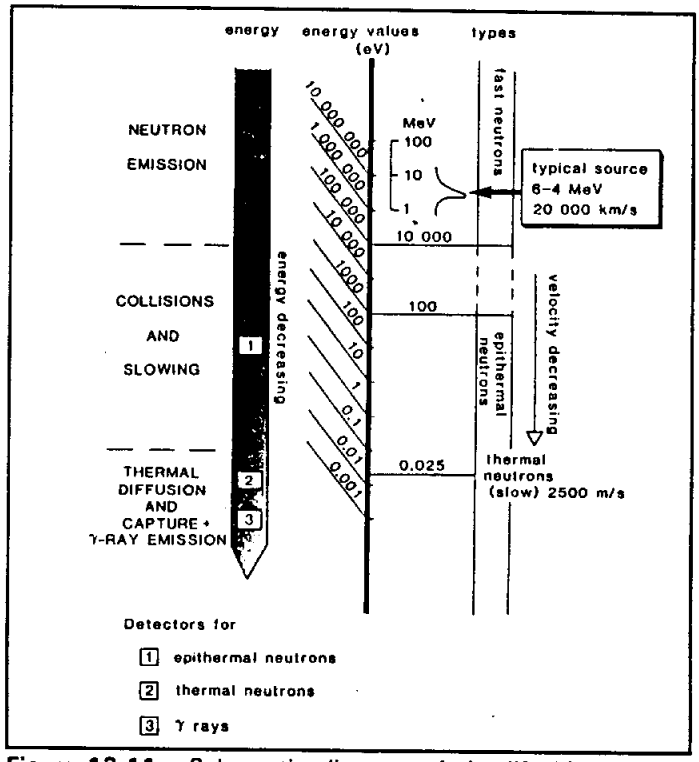

Figure 13-11. Schematic diagram of the life history of a neutron, showing energy levels and detector types (From Rider, 1986).

The ability of a nucleus to reduce the energy level of a neutron is measured in terms of its elastic interaction and thermal capture cross sections (Serra, 1984). Elastic interaction cross section is the ability of a nucleus to slow a neutron. It is a function of the size of the nucleus and the speed of the neutron. The closer the two particles are in size, the greater the amount of energy lost per collision and the greater the elastic interaction cross section. A hydrogen nucleus is approximately the same size as a neutron, giving it by far the highest elastic interaction cross section (Table 13-2). The average energy loss per collision between neutrons and hydrogen is 50 percent (Serra, 1984), with neutrons reaching a thermal state after only 18 collisions. No other element commonly occurring in aquifer-quality rocks has anywhere near the elastic interaction cross section of hydrogen.

Thermal capture cross section is the ability of a nucleus to capture a neutron. The factors governing the thermal capture cross section of an element are not well understood. Elements with a high thermal capture cross section have a low elastic interaction cross section. Chlorine has one to two orders of magnitude higher thermal capture cross section values than any other element commonly occurring in aquifer-quality rocks (Table 13-2). A few elements such as boron, cadmium, and gadolinium have extremely high cross sections, but these elements do not normally occur in sufficient ~~enough~~ concentrations in aquifer-quality rocks to affect neutron tool response. However, they are concentrated enough in some shales, igneous rocks, and metamorphic rocks to affect the neutron log.

A measurement of the neutron (or capture gamma ray) count rate by a detector located some distance from the source normally correlates to the hydrogen concentration of a formation. Since in most aquifer-quality rocks hydrogen only occurs in pore-filling fluids (water and hydrocarbons), the neutron count rate can be related to porosity.

Neutron tool design. All neutron tools utilize the same basic design, a neutron source and one or two detectors. Most tools employ a chemical source that is a mixture of beryllium and a radioisotope. The source provides a continuous emission of neutrons. Considerable variation exists in the type of detector(s) used. Detectors are available to measure epithermal neutrons, thermal neutrons, and capture gamma rays.

TABLE 13-2. ELASTIC INTERACTION AND THERMAL CAPTURE CROSS SECTIONS OF 2 MeV NEUTRONS.

Mineral	Abundance ppm	Cross Section		Collisions to 0.025 eV
		Thermal Capture	Elastic Interaction	
Hydrogen	1,400	0.30	20.0	18
Beryllium	----	0.01	6.1	87
Boron	----	700.00	3.0	105
Carbon	320	0.00	4.8	115
Nitrogen	----	1.88	10.0	130
Oxygen	466,000	0.00	4.1	150
Sodium	28,300	0.51	3.5	215
Magnesium	20,900	0.40	3.6	227
Aluminum	81,000	0.23	1.5	251
Silicon	277,000	0.13	1.7	261
Sulfur	520	0.53	1.5	297
Chlorine	314	31.60	10.0	329
Potassium	25,900	2.20	1.5	362
Calcium	36,300	0.43	9.5	371
Iron	50,000	2.50	11.0	514
Cadmium	----	2,500.00	5.3	1028

(From Bateman, 1985.)

The count rate registered by all types of neutron detectors responds primarily to the hydrogen concentration of the formation. All detectors respond the same way to hydrogen: neutron count rate decreases as hydrogen concentration increases. However, all detectors do not respond the same to elements with high thermal capture cross sections (chlorine, boron, gadolinium, etc.). Epithermal count rates are not affected nearly as much as are thermal and capture gamma ray count rates. This difference in tool response is very important for proper neutron log interpretation.

Neutron tools which measure capture gamma rays have a count rate that is a function of both the thermal capture and the elastic interaction cross section. Consequently, these tools are very sensitive to changes in chlorine concentration (i.e. TDS) and trace element (boron, gadolinium, etc.) concentrations as well as changes in porosity. This makes calculating porosity very difficult (Bateman, 1985). Very few neutron tools today measure capture gamma rays.

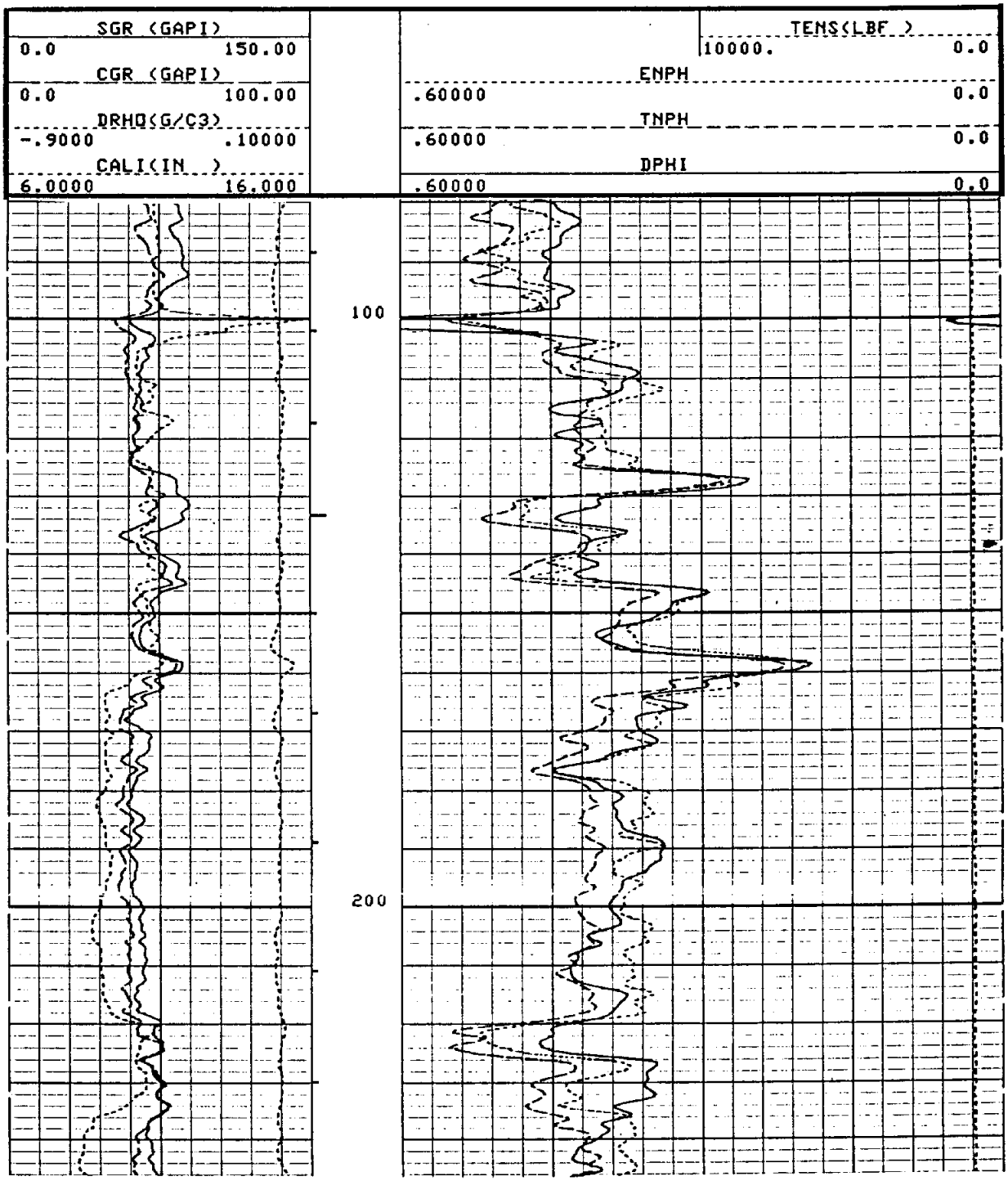

Figure 13-12. Schlumberger's CNT-G neutron log illustrates the differences between an epithermal neutron porosity curve (ENPH) and a thermal neutron curve (TNPH). The ENPH curve reads closer to density porosity (DPHI) because it is not as affected by thermal absorbers as is the TNPH curve. The porosity curves were calculated on a sandstone matrix. The well is the TWDB-PUB Test Well Site F, Cameron County, Texas (state well number 88-59-411). Borehole size is 8.5 inches. Borehole fluid is bentonite based drilling mud with an Rm of 2.2 ohm-meters at 100° F. This well is a direct offset to the well in Figures 8-18 and 8-19.

controlling the depth. As hydrogen content increases, depth of investigation decreases.

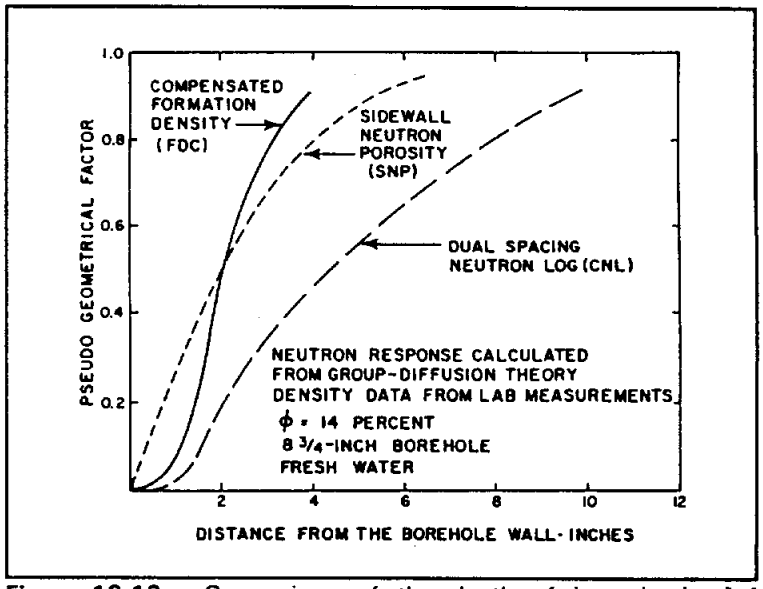

Figure 13-13. Comparison of the depth of investigation of Schlumberger neutron and density tools (From Truman, et al., 1972).

Several factors determine hydrogen content (porosity, borehole rugosity, and mineralogy), but porosity is the chief control. As water-filled porosity increases, depth of investigation decreases from 24 inches to just a few inches (Figure 7-4). Formations with minerals that contain significant quantities of hydrogen or other elements with high thermal capture cross sections will also reduce the depth of investigation. In water-filled boreholes, rugosity and cavities increase hydrogen content and decrease depth of investigation, while in air-filled holes the depth of investigation is slightly increased for the same hole conditions.

Vertical resolution is a function of the source-to-detector or detector-to-detector spacing and the logging speed. As the spacing and/or the logging speed increases, the vertical resolution decreases. If the tool is stationary in the well bore, the vertical resolution equals the spacing (about 10 to 15 inches). At a logging speed of 30 feet per minute, the vertical resolution is 3 feet. Schlumberger has enhanced processing that, combined with a slower logging speed, improves the vertical resolution to 12 inches (Figure 13-3).

Statistical variations and logging speed. As with all other radioactive logging tools, statistical variations in the count rate(s) necessitate a time constant to smooth the logs. Time constants vary from 2 to 4 seconds. The time constant should be recorded on the heading. In high porosity formations and in cased holes the count rate is much lower, so a larger time constant and a slower logging speed is used to improve the vertical resolution and the accuracy of the count rate. Statistical fluctuations average about 1 pu for very low porosity formations and about 3 pu for high

porosity rocks (Dewan, 1983). Further discussion of time constants is found in Chapters 7 and 10.

Log presentation. Neutron logs have a simple format. Modern conventional logs consist of only a porosity curve. A few slimhole logs present a porosity curve and some of them also include count-rate curves. Most slimhole log presentations, however, consist solely of a count rate curve(s).

The porosity curve is usually placed across tracks 2 and 3 (Figure 13-3). The values are expressed in decimal fractions. The scale depends on the range of anticipated porosity values. In sandstone provinces 0.6 to 0.0 is common. In mixed sandstone and carbonate provinces 0.45 to -0.15 is common when a density curve is included. Negative porosity values usually only occur on density curves (see the **Interpretation** section under **Density** for an explanation). The lithology on which the curve is calculated is noted on the log.

Count rate curves are usually placed in tracks 2 and 3. Count rates are usually expressed in counts per second. However, old conventional logs used a number of other units of measurement including environmental units, API units, and standard units (Hilchie, 1979).

Borehole corrections. A number of factors can affect the neutron tool response: borehole size, amount of standoff, mudcake thickness, salinity of the borehole fluid, mud weight, temperature, and pressure. Compensated tools correct for a certain amount of borehole effect. Nondirectional tools with single sources are more affected by the borehole environment than are other neutron tools. Except for mudcake and rugosity, sidewall tools are not as affected by the borehole environment as are compensated tools.

Borehole corrections are not available for nondirectional, single-source tools. Some sidewall neutron curves are automatically corrected for most borehole effects. Borehole correction charts are available for conventional compensated tools. Correction charts are tool and service company specific. If a caliper is available, the compensated neutron curve can be automatically corrected for borehole size. In ground-water wells borehole size is normally the only correction that ever needs to be applied to any neutron tool. Borehole size corrections are not available for slimhole tools. However, applying all the available borehole corrections normally changes porosity by only 1 to 2 porosity units.

In air-filled holes neutron count rate increases as hole diameter increases. This gives borehole enlargements the appearance of a decrease in porosity, which is opposite the response seen in liquid-filled holes.

Cased hole correction charts are available for casing and cement thickness. Casing and cement both reduce the neutron count rate (i.e. increase the porosity values). The magnitude of the effect depends on the position of the casing in the well bore and the relative size of the casing and borehole. As hole size increases, eccentered casing can cause significant errors. Polyvinylchloride (PVC) casing contains a significant amount of chlorine, and some fiberglass casing contains boron. In both cases the count rate will be significantly reduced, thus increasing the porosity values.

Calibration. Proper calibration of neutron tools is critical for accurate porosity values. Neutron tools must be periodically recalibrated because the neutron output of the source changes with time. The rate of change and thus the frequency of recalibraton depends on the half-life of the source.

Major logging companies routinely calibrate their tools. However, many slimhole tools are seldom, if ever, calibrated. As with any logging tool, calibration procedures should be clearly documented by both the tool manufacturer and the service company.

Proper calibration of neutron tools is not complete until the neutron count rate has been quantified in terms of porosity units. This is accomplished by running the tool in a test pit such as the one at the University of Houston. All modern conventional and a few slimhole tools are calibrated by this method. Modern conventional tools output a porosity curve on the log (see the **Log presentation** section). Slimhole tools that have been calibrated in porosity units may output a porosity curve, or a chart may be available to convert count rates to porosity units. Most slimhole tools, however, have never been calibrated for porosity.

It is possible to calibrate a single detector tool in terms of porosity units. The relationship between count rate and porosity is as follows:

$$CR = C + D\log\phi \qquad \textbf{(13-3)}$$

C and D are parameters that are a function of the tool design and borehole environment (Etnyre, 1989). For single-detector thermal neutron

Where:

CR = neutron count rate, which can be in any unit of measurement
C = intercept of the linear trend of CR at ϕ = 100 percent
D = Slope of the linear trend
ϕ = porosity units

tools, a plot of CR versus ϕ on semi-log paper will plot as an S curve (Figure 13-14). The usable area of the curve is the linear portion (usually from 2 pu to between 20 and 30 pu). Measurements of low porosities (less than 2 pu) become questionable because high count rates saturate the detector. At high porosities (above 20 to 30 pu) the measurements are questionable because the count rate is so low that statistical fluctuations become a high percentage of the count.

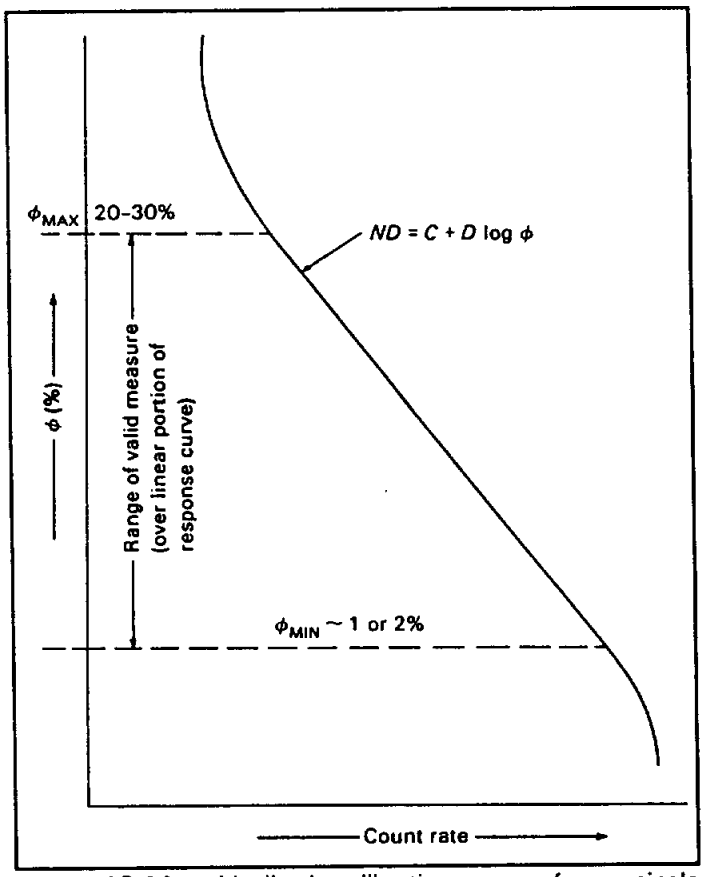

Figure 13-14. Idealized calibration curve for a single detector neutron curve (From Etnyre, 1989).

Figure 13-15 illustrates how the count rate of a single detector tool is converted to porosity units. The procedure is as follows:

1. The tool must be run in a borehole for which accurate porosity values are available.

   a. The borehole should be in gauge.

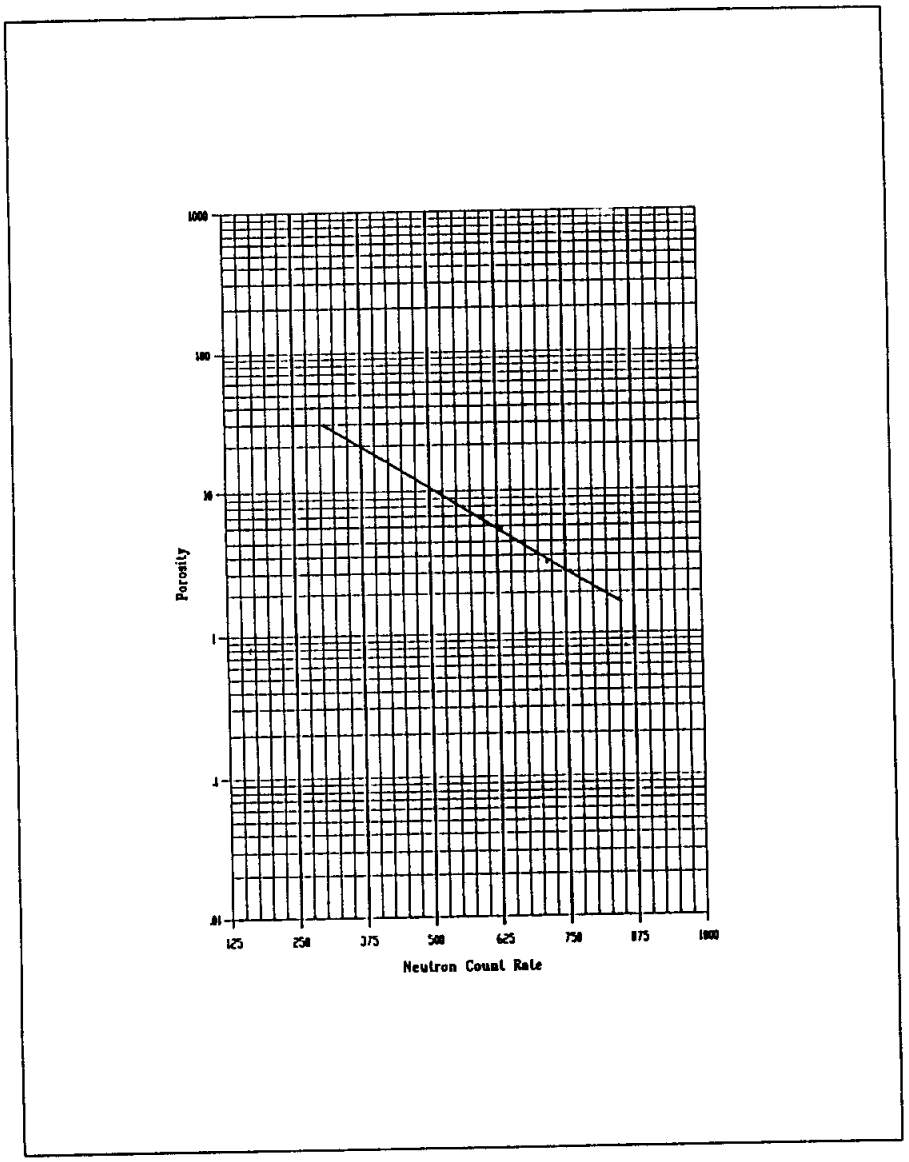

Figure 13-15. Calibration of a single-detector neutron tool. Count rates from the neutron tool are plotted against density-neutron crossplotted porosity values. The lithology is limestone. The limestone in this well had a limited range of porosity values. Figures 7-14 and 8-14 provide additional data on this well. The data used in the plot are as follows:

Depth feet	Neutron Count Rate counts/second	Density-Neutron Porosity
170-176	630	6.0
240-245	650	5.0
208	720	3.5
270-280	767	3.0
520-530	860	<1.0

b. Accurate porosities from either core analyses or conventional porosity logs must be available.

2. The data is plotted on semi-log graph paper.
   a. Porosity values must be from a single lithology.
   b. Porosity values are plotted on the logarithmic axis.
   c. Count rates are plotted on the linear axis.
   d. A linear fit is applied to the data. The equation of the line will be in the form of Equation 13-3.
   e. A separate linear fit must be calculated for each lithology.

3. The count rates can now be converted to porosity units. Porosity can be determined either by plotting count rates on the graph or by solving the equation of the line.

In the absence of accurate porosity values, a neutron count rate can be calibrated in porosity units for a particular borehole by the two-point method. This method yields at best semi-quantitative values. The count rates for two points, a shale and a very low porosity zone (normally a carbonate), are plotted on semi-log graph paper (Figure 13-16). A quicker version of this technique is to pick the two points on the log and then mark the intervening values with a two-cycle logarithmic scale (Figure 13-17). Porosity is assumed to be about 40 percent for the shale and 1 to 3 percent for the dense zone. The equation of this line will be equation 13-3.

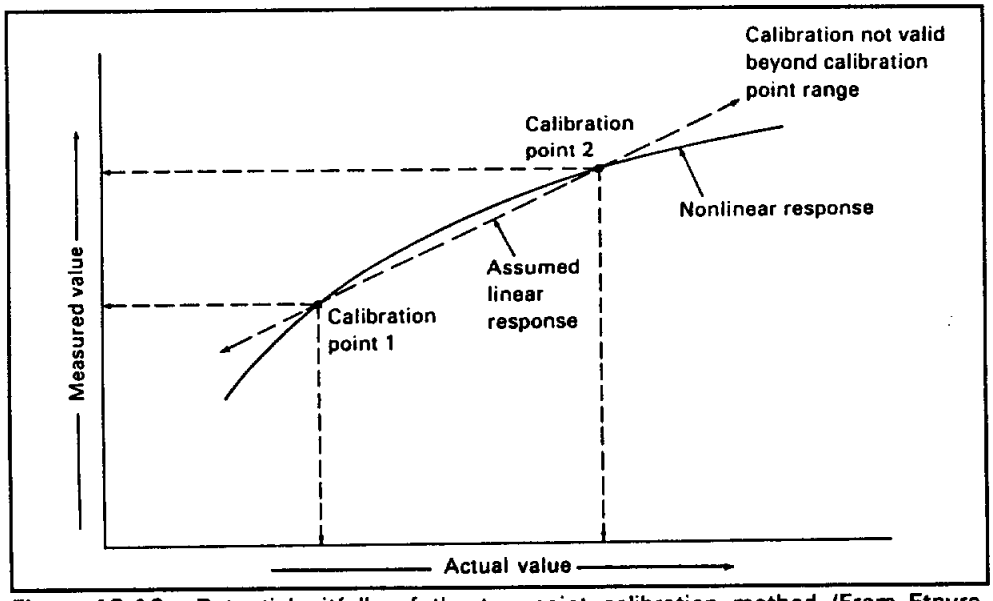

Figure 13-16. Potential pitfalls of the two-point calibration method (From Etnyre, 1989).

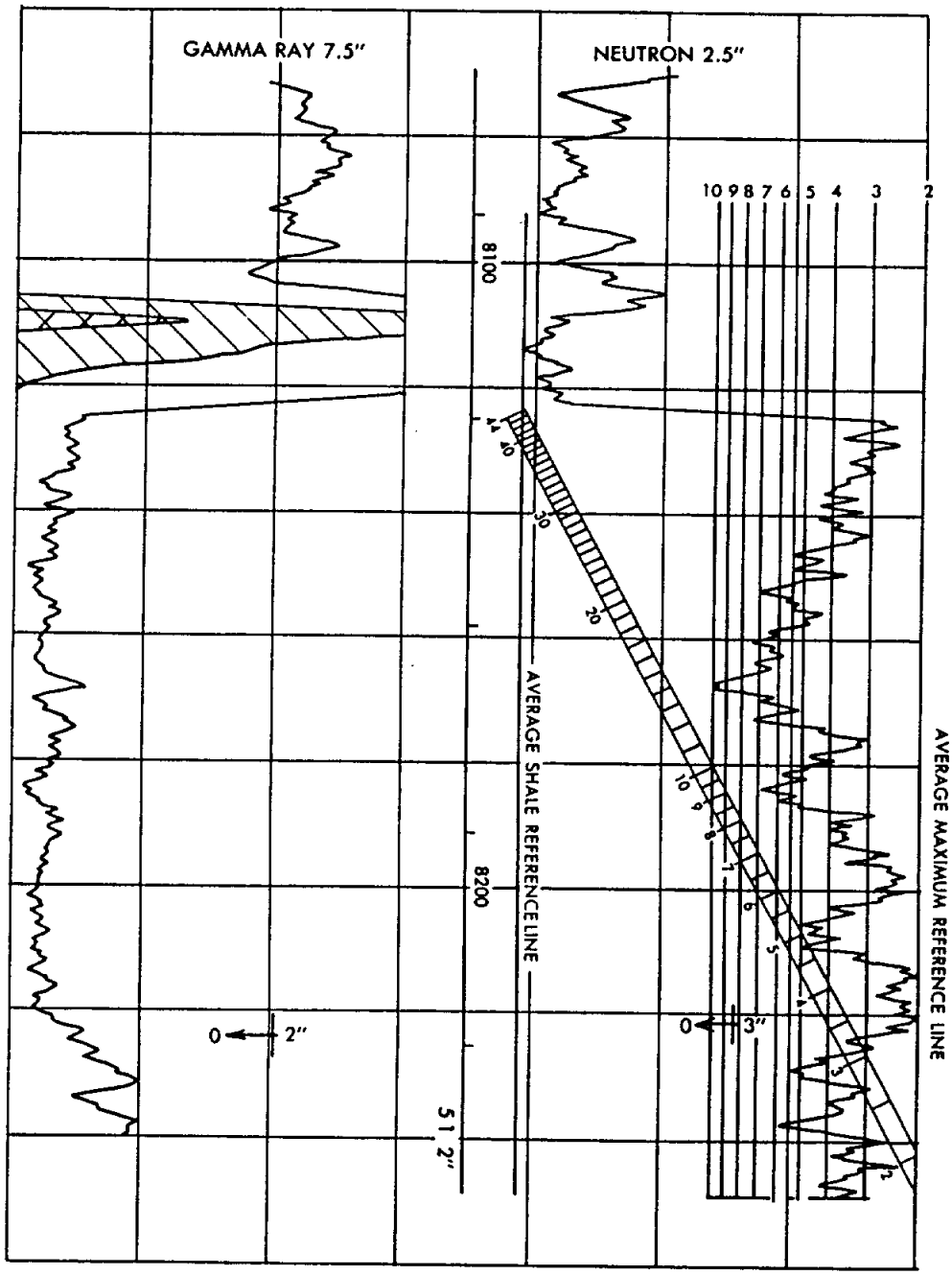

Figure 13-17. Two-point calibration of a neutron log by overlaying a two-cycle logarithmic scale between a shale and a dense carbonate (From Pirson, 1963).

The two-point calibration technique has two significant drawbacks:

1. It will not work in many ground-water environments because usually there is no low porosity zone in the well bore.

2. It assumes that the relationship between the two points is linear. As illustrated by Figure 13-16, the relationship may not be linear or it may only be linear in the area between the two points.

Interpretation. Neutron porosity values, as with all log-derived porosities, require a certain amount of interpretation. Since the neutron curve is subject to substantial lithology effects, it is normally run in conjunction with a density tool. Accurate porosities are obtained by comparing the two logs.

Accurate neutron porosity values are based on two assumptions:

1. **All water in a formation occurs as free pore-water.** Water occurring as water of crystallization, such as is present in gypsum, and bound water in clays will make the log porosity values too high.

2. **The neutron count rate is responding only to hydrogen atoms.** Thermal neutron absorbers make the porosities read too high. Epithermal neutron tools provide more accurate porosity values when thermal absorbers are present.

Neutron porosity curves are lithology dependent. The curve is, by convention, calculated on a limestone matrix when both clastics and limestones are present in a well. However, the curve can also be run on a sandstone or a dolomite matrix. In sand-shale sequences a sandstone matrix is used. When a formation of interest has a lithology other than that of the matrix used to compute the neutron porosity curve, a chart such as Figure 13-18 is used to determine the true porosity. Such charts are tool and service company specific.

In Figure 13-18 the SNP lithology corrections apply only to tools run in liquid-filled holes. In air-filled holes the lithology effect is negligible and porosity values are the same for all three lithologies (Schlumberger, 1989). Lithology corrections for the DNL log also use Figure 13-18. The epithermal curve uses the SNP response and the thermal curve the CNL response.

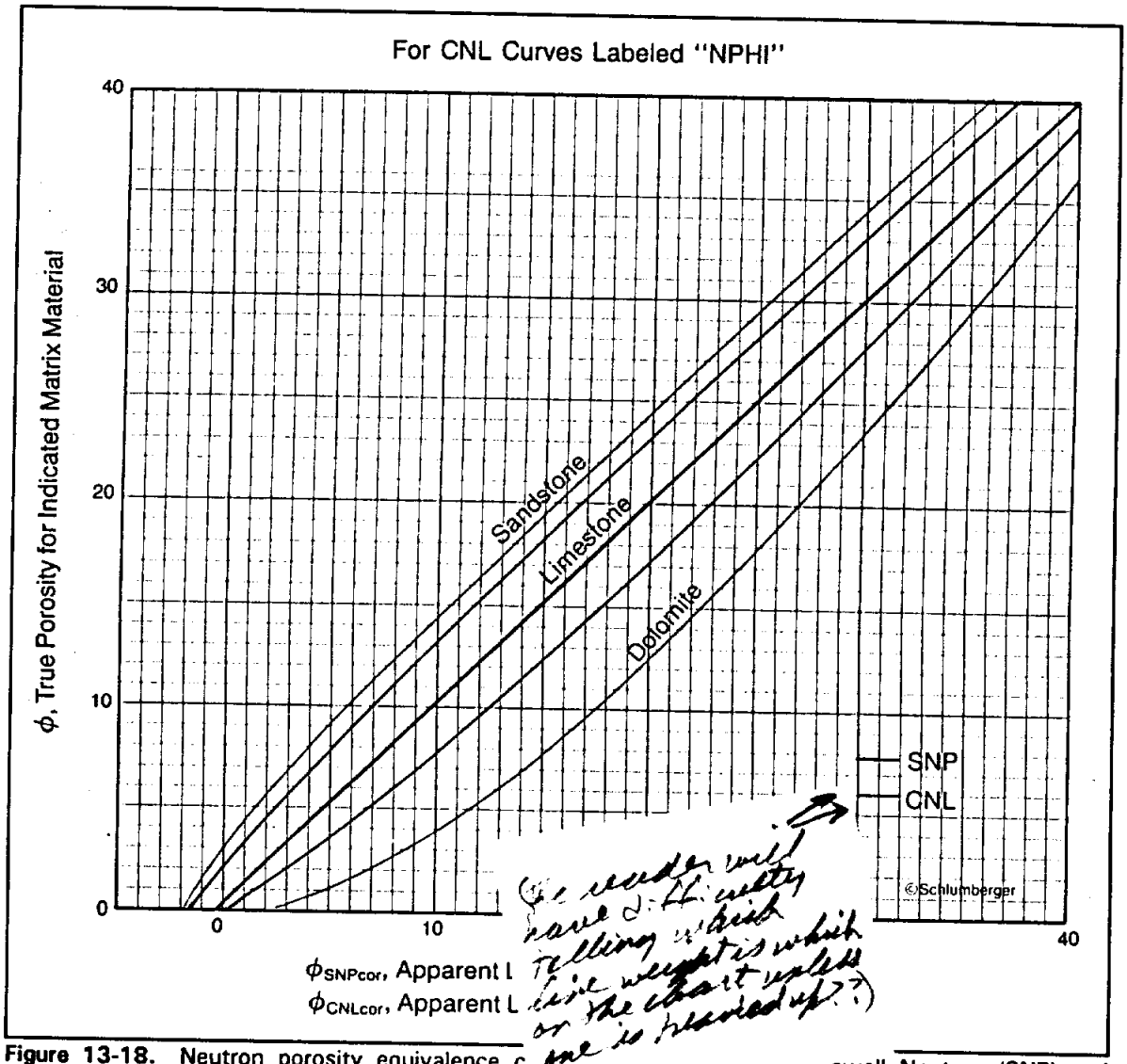

Figure 13-18. Neutron porosity equivalence c ... Sidewall Neutron (SNP) and Compensated Neutron (CNL) tools (From Schlum ...).

Proper interpretation of neutron porosities requires an understanding of tool theory, tool construction, and borehole corrections. Additional details on neutron log interpretation are scattered thoughout the previous parts of this section. Cased hole neutron curves are discussed briefly in the Borehole corrections section. Schlumberger (1989b) has a good review of cased hole neutron logs.

Sonic (Acoustic)

The sonic tool is used to calculate porosity, pick bed boundaries, and identify abnormally pressured formations. In conjunction with another porosity tool, it can be used to determine lithology. In conjunction with the density tool it is used to create synthetic seismograms and to calculate rock mechanical properties such as Poisson's ratio and Young's modulus.

Specialized sonic tools have been developed to identify fractures (Variable Density Log), evaluate cement bond quality (Cement Bond Log), and image the borehole (Borehole Televiewer). Research is presently underway to develop methods to calculate permeability from the sonic . Efforts are underway to develop accurate cased hole sonic porosity tools, but presently the tool works much better in open holes. Normal sonic tools only operate in liquid-filled holes.

The sonic was the first porosity tool. Popular in the 1950's, it has been supplanted in oilfield logging by the density-neutron combination. In ground-water/environmental investigations, however, it is more widely utilized. This is probably due in large part to the ease and safety (no radioactive source) with which it can be operated.

Modern conventional tools carry a variety of names: Borehole Compensated Acoustic (AC) for Atlas Wireline, Borehole Compensated Sonic (BCS) for Gearhart, Compensated Acoustic Velocity (CAV) for Welex and Halliburton, and Borehole Compensated Sonic Log (BHC) for Schlumberger. Each company also has a Long Spaced Sonic and a Full Wave Sonic, as well as various other specialized sonic tools. Jorden and Campbell (1986) contains succinct summaries of the different types of sonic tools. Slimhole sonic tools are available and a few are compensated. Slimhole full wave sonic tools are also available.

Tool theory. Ordinary sonic tools utilize a transmitter(s) and receivers to measure the velocity of sound in a formation. The transmitter generates 10 to 60 times a second a high frequency (20 to 40 kilohertz) sound wave that travels out in all directions through the tool, borehole fluid, and formation. This sound wave actually consists of several different types of waves: compression (P, pressure, or longitudinal), shear (S or transverse), Rayleigh, and Stonely. Under normal conditions, the first component of the wave to arrive at a receiver is that part of the compression wave which struck the borehole wall at the critical angle and traveled vertically through

the formation (Figure 13-19). This is the only wave of interest to ordinary sonic tools and it is the wave used to calculate porosity. Other sonic tools record the amplitude, attenuation, travel time, and/or frequency of the various components of the wave train.

The sonic tool measures the time it takes a sound wave to travel from the transmitter to each receiver. The difference between the two values, divided by the receiver spacing, is the time it takes for the compression

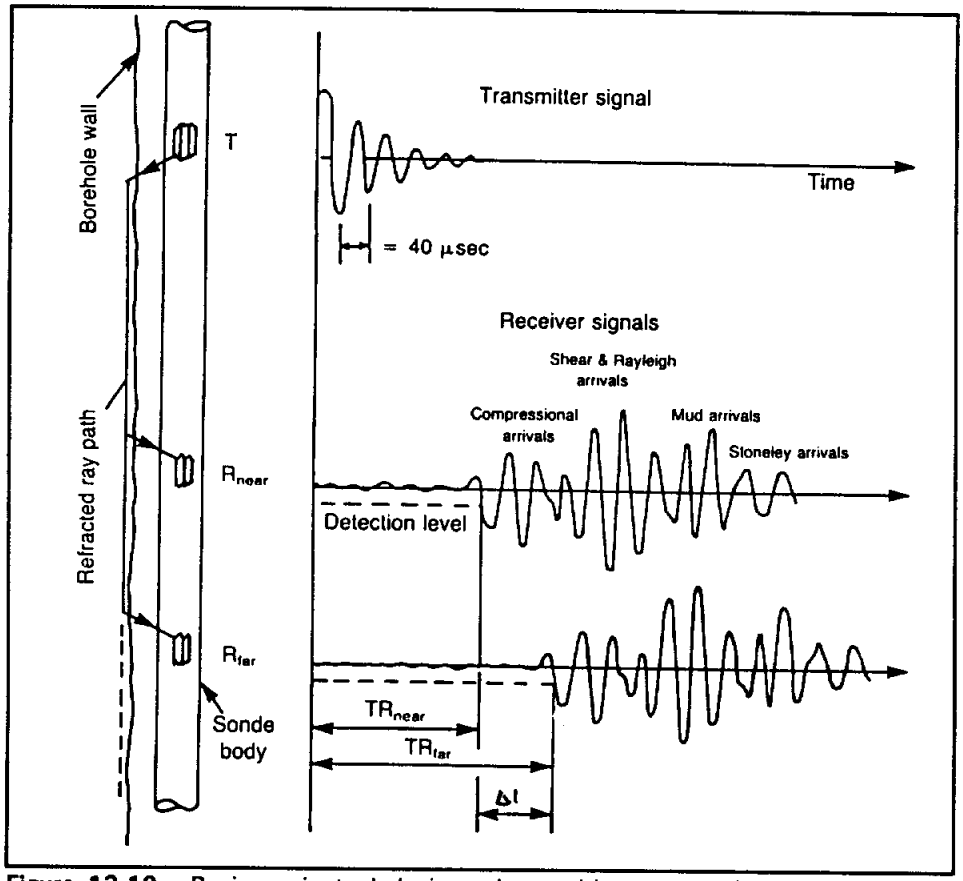

Figure 13-19. Basic sonic tool design, along with an acoustic wavetrain. The compression wave activates the receivers (Modified from Dewan, 1983).

wave to travel 1 foot in the formation. This calculation assumes that the distance from the borehole wall to each receiver is the same. The only way to be assured of this is to compensate the tool.

Tool design. Modern conventional tools and some slimhole tools are compensated. The standard design used to be a double array of one

transmitter and two receivers inverted to each other (Figure 13-20). Averaging the two measurements factors out errors in calculating sonic velocity due to washouts and tilted tools. Today some sonic tools are compensated by other methods, but the result is the same. In severe washouts compensated sonic measurements are less affected than are other porosity tools.

Most modern tools use piezoelectric ceramic crystals as the transmitting transducers. Electric current is used to physically deform the crystal, thus producing a sound wave. The receivers are also transducers, except in this case they convert acoustic energy to electrical energy.

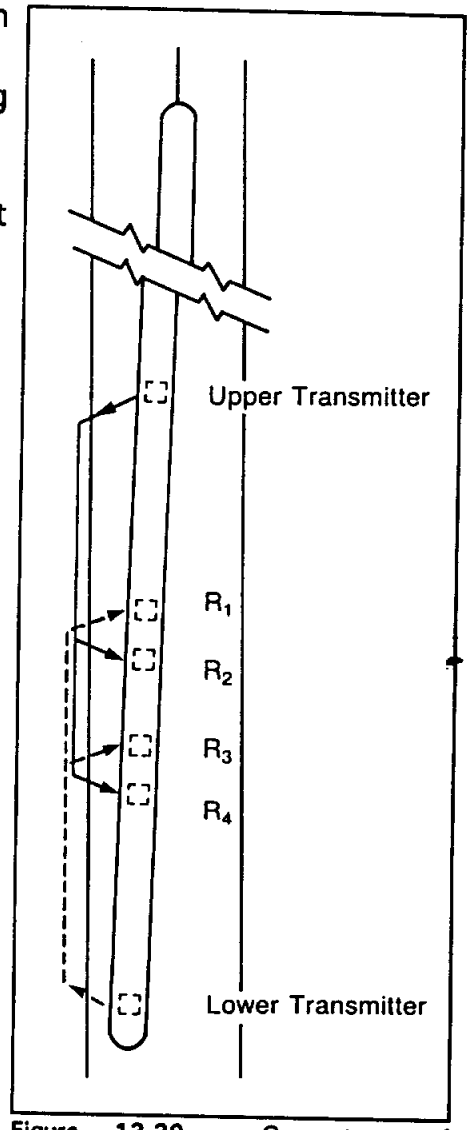

Figure 13-20. One type of compensated sonic tool (From Schlumberger, 1989).

Typically the distance between the transmitter and the near receiver is 3 feet, but it can be up to 10 feet. The distance between the two receivers is normally 2 feet, but spacings of 1 to 3 feet are used. The tool is constructed in such a way as to attenuate the sound wave traveling the length of the tool. Slots in the steel housing or a rubber insert in the housing are commonly used to accomplish this.

Jorden and Campbell (1986) list the specifications of conventional sonic tools. Their book contains one of the best available discussions of sonic logging. Included is a detailed discussion of single-transmitter/dual-receiver tools, which is a common type of slimhole tool.

Sonic tools perform best when centralized in the borehole. One of the centralizers is also utilized as a caliper. The centralizers are normally bow springs, which means that the caliper measurement is not very sensitive. (Chapter 11 discusses calipers in detail.)

Calibration. There is very little in the way of calibrations to be done to the tool. A good quality-control check on the tool is to measure its response

in uncemented steel casing. It should be 57 μsec/ft. However, upon entering casing the travel time may not immediately jump to this value. The engineer may first need to adjust for the drastic change in signal amplitude created by going from open to cased hole (Dewan,1983).

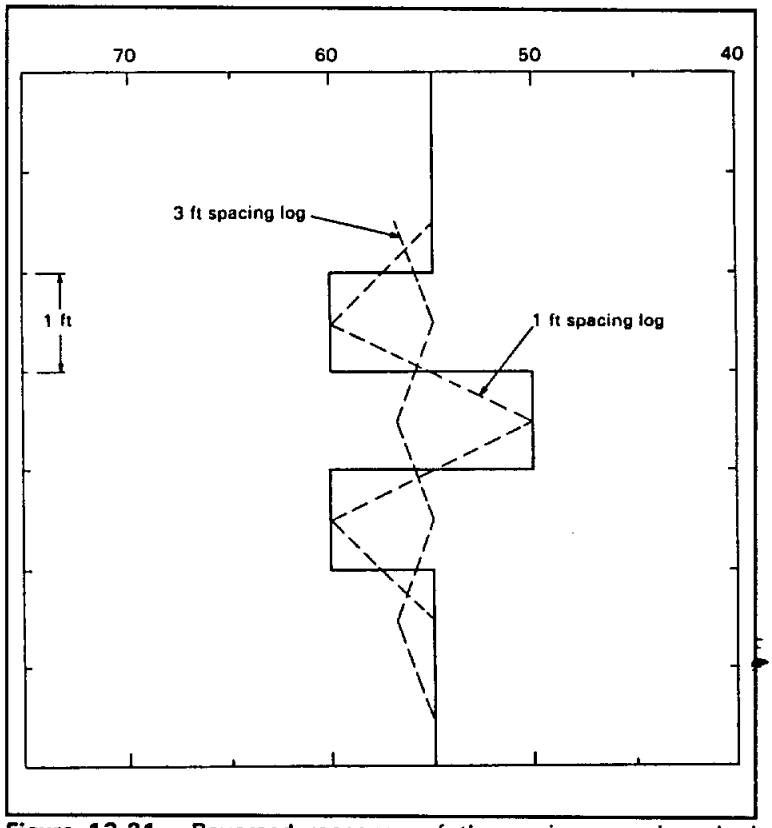

Figure 13-21. Reversed response of the sonic curve in a bed thinner than the receiver spacing (From Etnyre, 1989).

Depth of investigation and vertical resolution. Vertical resolution is the distance between the two receivers (normally 2 feet). Beds thinner than this distance are detected by the tool, but the log values will not be accurate and may trend in the opposite direction of the actual travel time (Figure 13-21). Jorden and Campbell (1986) detail other problems with thin bed interpretation.

Figure 13-21 also illustrates that at bed boundaries there is a transition in travel time values equal to the distance between the two receivers. The bed boundary is the mid-point of the transition zone.

Travel time measurements are not affected by formations outside the detector spacings (Etnyre, 1989). The sonic tool is the only porosity tool with this characteristic. This contributes to its excellent vertical resolution, which is better than any other porosity tool.

The sampling rate is a function of the logging speed and the rate at which the transmitter emits sound waves. An average sampling rate is every few inches. At 20 pulses per second a compensated tool makes 5 measurements per second, which for a logging speed of 60 feet per minute is a measurement every 2.4 inches.

Depth of investigation ranges from 5 to 40 inches into the formation (Serra, 1984). Most of the time the actual depth is from 8 to 12 inches (Hilchie, 1982). Depth of investigation is predominately a function of wavelength which, in turn, is a function of velocity and frequency. The longer the wavelength the deeper the penetration. In formations (normally shales) that have altered zones next to the borehole, the depth of investigation can be increased beyond the altered zone by using a long spaced sonic tool. This is only necessary if the sonic log is to be incorporated into a seismic study.

Log presentation. Sonic logs are a recording versus depth of the time it takes a sonic wave to travel 1 vertical foot of formation. The measurements are called **interval transit time, interval travel time, transit time, travel time, Δt (delta t)**, or **t**. The unit of measurement is microseconds (μs or μsec) per foot. Using microseconds rather than seconds makes the values whole numbers. Δt is the reciprocal of velocity in feet per second. The relationship between the two is expressed by the following equation:

$$\Delta t = \frac{10^6}{velocity} \qquad \textbf{(13-4)}$$

Interval transit time is normally presented across Tracks 2 and 3 (Figure 13-22). Transit time increases to the left, which means that porosity also increases to the left. The scale is linear and normally is either 140 to 40 μsec/ft or 150 to 50 μsec/ft.

Conventional log presentations often include integrated travel time (TTI). It is recorded in the depth column as a series of horizontal tic marks. Each tic is 1 millisecond, with a larger tic every 10 milliseconds. TTI, which is the one-way vertical travel time of a sound wave through the subsurface, is useful in interpreting seismic sections. TTI multiplied by 2 yields the travel time recorded on seismic sections.

Borehole corrections. There are no environmental corrections for the sonic log. "Acoustic log readings must be either accepted at face value, or qualitatively discounted as invalid or nonrepresentative" (Jorden and Campbell,1986).

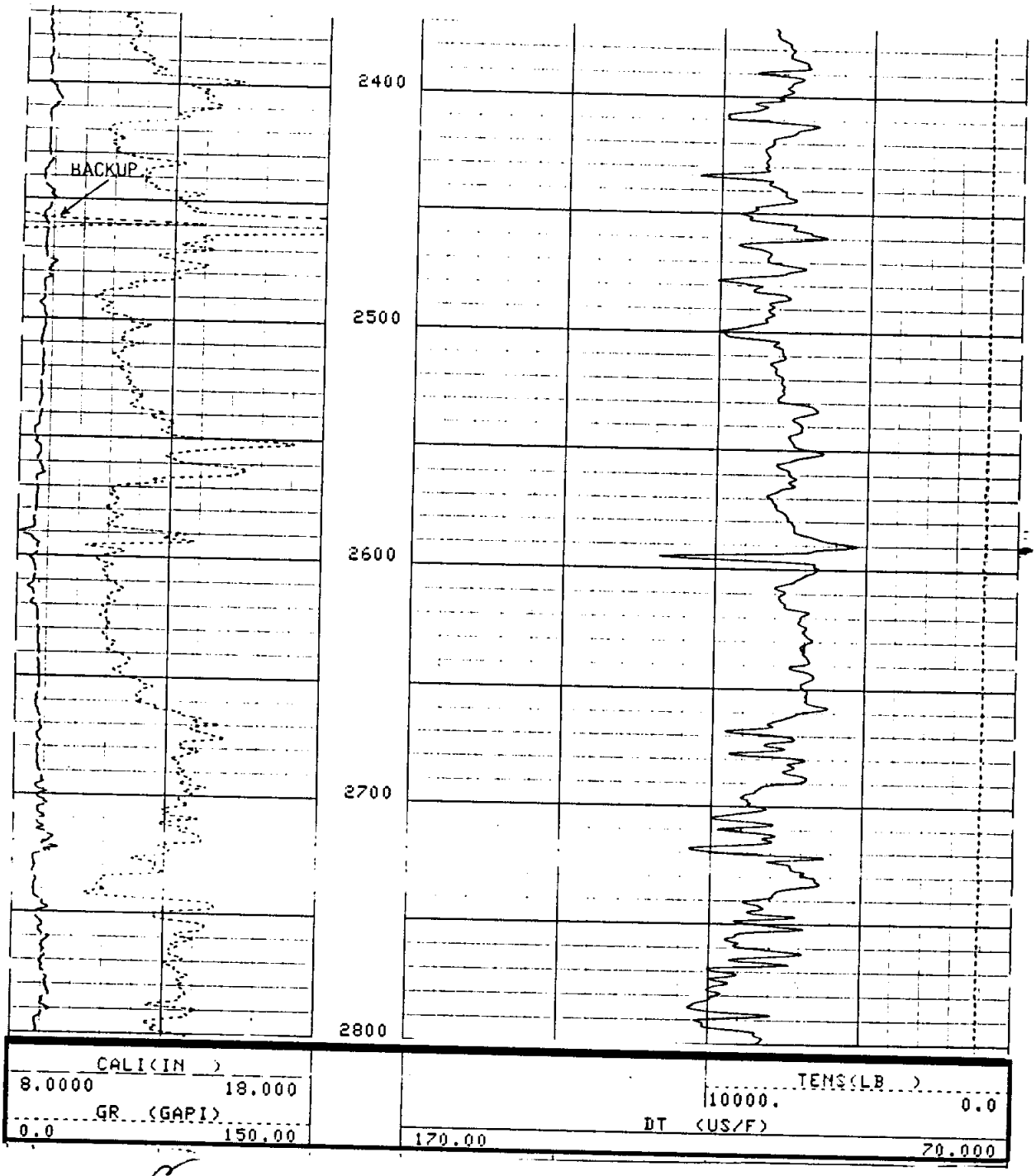

Figure 13-22. A typical sonic log presentation. Δt increases to the left, which corresponds to increasing porosity. The caliper is not very sensitive because it is built into the centralizer. In this well Δt, and thus porosity, decrease with depth. This is due to increasing compaction with depth. The lithology is alternating shales and sandstones. The radioactive zone at 2460 feet is a sandstone, not a shale. Shales have higher travel times than do sands. The well is the McKinley Drilling Company, Fox Creek #2, McMullen County, Texas. Bit size is 8.75 inches. Borehole fluid is native gel. Figures 13-27 a and b provide additional data on this well.

The Δt measurements of compensated tools are very accurate, to within approximately ± 0.25 μsec/ft (Dewan, 1983). However, there are conditions under which the tool will measure something other than the travel time of the compression wave in the formation. Some of these conditions are due to characteristics of the formation and are discussed in the following section. Others are the result of borehole conditions and are discussed below:

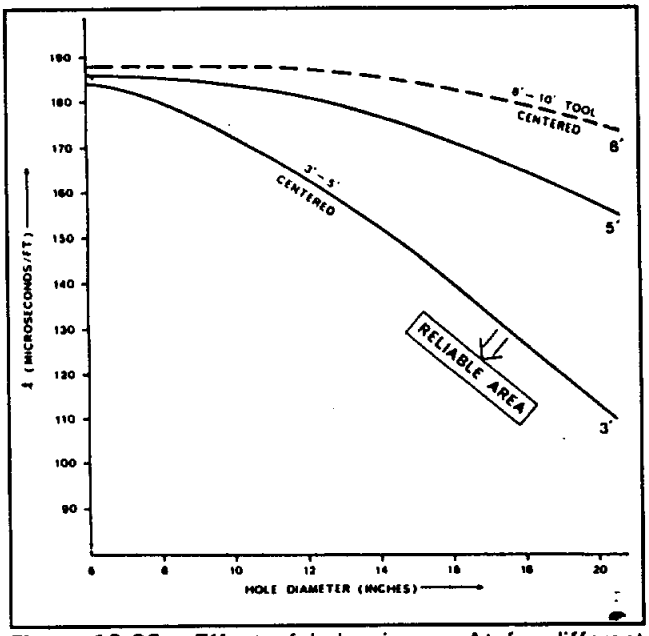

Figure 13-23. Effect of hole size on Δt for different transmitter-near receiver spacings (From Goetz et al.,1979, in Serra, 1984).

1. If the borehole diameter is large enough, the compression wave traveling through the borehole fluid will arrive first. The diameter at which this will occur is a function of the transmitter-near receiver spacing and the travel time of the formation (Figure 13-23). Figure 13-23 reveals that conventional sonic tools are not reliable in formations with high travel times (e.g. unconsolidated sands) once the borehole diameter exceeds 14 inches. In such cases the only alternative is to run the tool eccentralized (Serra, 1984). According to this chart long spaced tools are not affected by borehole diameter. However, the long spaced sonic in Figures 12-12a and 12-12b is reading the travel time of the drilling mud in a 15 inch borehole.

2. Noise in the borehole can trigger the receivers. Such noise can be generated by the centralizers scraping against the borehole wall, excessive logging speed, and the absence of centralizers. Noise yields erroneous travel times that appear on the log as sharp spikes. If the far receiver is triggered, the travel time is be too short by as much as 75μsec/ft (Dewan, 1983). Triggering the near receiver gives a travel time that is too long. Road noise is minimized by not activating the receivers for a fixed time following transmitter fire. Therefore, the far receiver is more likely to

measure noise. Some modern tools have circuits that eliminate road noise. Long spaced tools are more susceptible to noise.

3. If the sound wave is too weak to trigger the far receiver, the receiver skips that cycle and triggers on a subsequent one. Cycle skipping creates spiky increases in travel time usually over 1 foot or less of log depth (Jorden and Campbell, 1986). The increase in travel time varies from 5 to 37.5 μsec/ft, depending on which cycle triggers the receiver and whether one or both of the far receivers cycle skip (Serra, 1984). Cycle skipping will be caused by anything that strongly attenuates the sound wave, such as gas in either the mud column or the formation, fractures, tool malfunction, or improper centralization of the tool. It can also be caused by setting the detection threshold (bias) of the receivers too high. The sound wave will not activate the receiver unless it has an energy level (amplitude) that exceeds the threshold value for which the receiver has been set. Some of the very latest sonic tools have smoothing circuits that eliminate cycle skips. Long spaced tools are more susceptible to cycle skipping.

4. Microfractures in a formation (usually shales or carbonates) will result in abnormally long travel times. The fractures can be drilling-induced or natural.

Interpretation. Δt is predominately a function of lithology, texture, porosity, pore fluid, and pressure. It is very sensitive to lithologic and textural changes, which makes it one of the best logs for correlation. In combination with another porosity log, the sonic log can be used to identify lithology. Compaction trends can be identified, usually by observing how the travel time of shale decreases with depth. Overpressured zones show up as decreases in the slope of the compaction trend with increasing depth. The main use of the log, however, is to calculate porosity.

M. R. J. Wyllie, et al. (1956) proposed the first practical transform for relating travel time to porosity in sedimentary rocks. The Wyllie time-average equation is an empirical equation based on laboratory observations of the travel time of sound in rocks of varying porosities. It is a linear weighted-average relationship that assumes that the total travel time (hence the name Δt) of a formation is equal to the sum of the travel times in all the pores and rock matrix traversed by the compression wave. The equation

models Δt as a function of porosity, lithology, and pore fluid. The relationship between the four is as follows:

$$\Delta t=\phi\Delta t_f+(1-\phi)\Delta t_{ma} \qquad \textbf{(13-5)}$$

Where:

Δt = *travel time on the log in μsec/ft*
Δt_f = *travel time of the pore fluid in μsec/ft*
Δt_{ma} = *travel time of the matrix in μsec/ft*
ϕ = *porosity in decimals*

Equation 13-5 can be rearranged to solve for porosity (Equation 13-6), which is how the Wyllie transform is normally presented:

$$\phi = \frac{\Delta t-\Delta t_{ma}}{\Delta t_f-\Delta t_{ma}} \qquad \textbf{(13-6)}$$

Table 13-3 lists compressional wave transit times for common lithologies and fluids. Although each lithology has a range of travel times, normally an average Δt_{ma} is used in porosity calculations. There is some variation in the logging literature as to what the average Δt_{ma} values actually are, but the differences are usually only a couple of μsec/ft. The average values used in Table 13-3 yield porosity values that are within ± 2 pu of true porosity, even when the travel time falls somewhere else within the range of values for that lithology.

Table 13-3 also shows that the travel times of fresh and saline water are considerably different. Most log analysts automatically use 189 μsec/ft, but 205 μsec/ft should be used for fresh-water aquifers. In fresh water a Δt_f of 189 μsec/ft yields porosity values that are about 3 pu too high (Figure 13-24).

Chartbooks contain graphical solutions of Equation 13-6. The straight solid lines in Figure 13-25 are graphical solutions of the Wyllie transform for various lithologies. The chart uses a Δt_f of 189 μsec/ft.

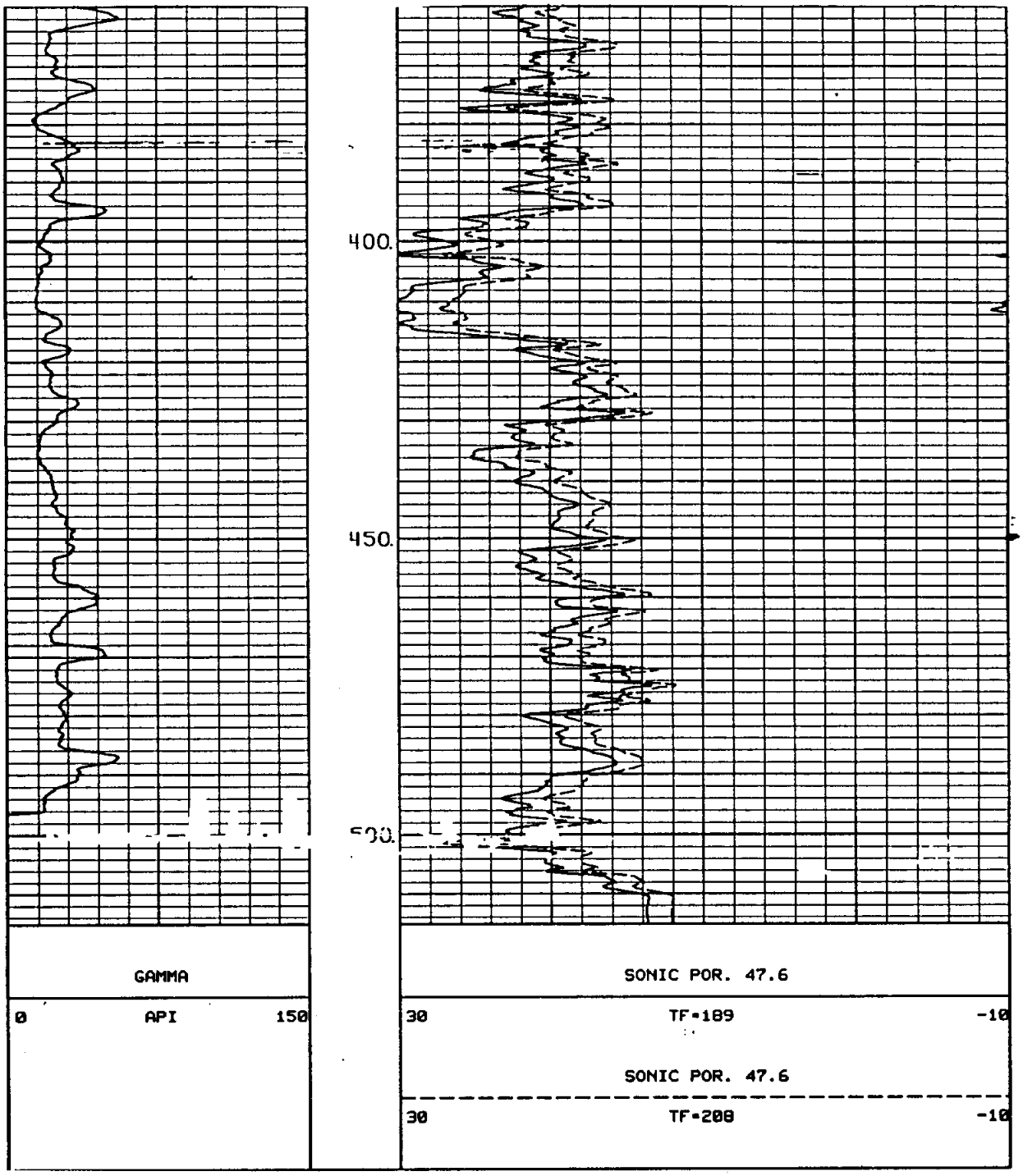

Figure 13-24. Comparison of sonic porosities calculated with the Δt_f's of fresh and saline water. The salt water value for Δt_f (189 μsec/ft), which is commonly used in oilfield logging, yields porosity values that are approximately 3 pu too large when the pore water is fresh. The Δt_f used for fresh water (208 μsec/ft) is too high. 205 μsec/ft is a better value. However, there is little difference between porosity values calculated with the two. Porosities were calculated with the Wyllie time average equation. Bit size is 6 inches. The borehole fluid is fresh formation water. The aquifer is a Cretaceous limestone in South Texas.

TABLE 13-3. Δt_{ma} AND Δt_f VALUES OF COMMON LITHOLOGIES AND FLUIDS.

Mineral/Fluid	Average Δt_{ma} or Δt_f μsec/ft	Range Δt_{ma} or Δf
Air		
Methane, 15 psi		
Oil		
Water, pure (25° C)		
Water, 100,000 ppm NaCl, 15 psi		
Oilfield water; drilling mud		
Water, 150,000 ppm NaCl, 15 psi		
Shale		170.0-60.0
Sandstones (compacted)	54.0	55.5-51.3
Quartz	55.1	55.5-54.7
Gypsum	53.0	53.0-52.5
Anhydrite		50.0
Limestone	47.6	47.6-43.5
Calcite	46.5	47.6-45.5
Dolomites	43.5	43.5-38.5
Dolomite	44.0	45.0-40.0

(Compiled from Serra, 1984 and Schlumberger, 1989.)

Shale laminae within a sandstone increase the sonic porosity values by an amount proportional to the bulk volume fraction of laminae (Schlumberger, 1989). Jorden and Campbell (1986) contains a good review of shale corrections. However, the porosity values of consolidated, compacted sandstones with 15 to 25 percent porosity are not significantly affected by disseminated shale (Schlumberger, 1989).

Gas in a formation increases the travel time, yielding porosity values that are too high. The shallower the formation, the greater the discrepancy.

The Wyllie transform models clean, consolidated, compacted formations with uniformly distributed small pores (i.e. consolidated sandstones and carbonates with interparticle or intercrystalline pore geometries). Through the years many log analysts have disregarded these prerequisites and indiscriminately applied the transform to other rock types such as uncompacted, unconsolidated sands and vuggy-moldic carbonates. In such cases considerable modification must be made to the Wyllie equation in order to obtain accurate porosity values. This problem is of considerable importance to ground-water/environmental logging because many aquifers are either uncompacted sands or vuggy-moldic carbonates.

The Wyllie transform calculates too high a porosity in unconsolidated, uncompacted sands. These sands usually have a travel time in excess of 100 μsec/ft; it can be as high as 150 μsec/ft. The adjacent shales often have travel times greater than 100 μsec/ft. The shallower the formation, the higher the travel times in both the shales and the sands.

Correct porosity values for uncompacted sands are obtained by dividing the porosities obtained in Equation 13-6 by an empirically derived compaction correction factor (B_{cp} or C_p). A more correct term would be lack of compaction correction factor. The dashed straight lines in Figure 13-25 are correction factors. B_{cp} ranges from 1.0 to 1.8 and is never less than 1.0. It can be calculated from the travel time of the shales adjacent to the sand or by dividing sonic porosity by true porosity (other porosity logs or core porosities). However, if another source of porosity measurements is available, there is really no need to recalculate sonic porosity. When the sonic log is the only porosity log available, B_{cp} can be calculated from the travel time of the adjacent shales. This technique works well as long as the travel time of the shale has not been affected by washouts or shale hydration (Hilchie, 1982). The correction factor is calculated from the following equation:

$$B_{cp} = \frac{\Delta t_{sh}}{100 \mu sec/ft} \qquad (13\text{-}7)$$

Where:

B_{cp} = *compaction correction factor*

Δt_{sh} = *travel time in the shale adjacent to the sand in* μ*sec/ft*

Dewan (1983) recommends that when travel time exceeds 110 μsec/ft a different porosity tool be used to calculate porosity.

In carbonates with scattered, isolated vuggy-moldic porosity the calculated sonic porosity will be too low. This is because the first compression wave to arrive at the receiver is the one that travels along the part of the borehole wall that has the smallest number of vuggy-moldic pores. Thus the travel time measurement, in effect, avoids pore spaces that are scattered around the rest of the borehole. There is no way to adjust

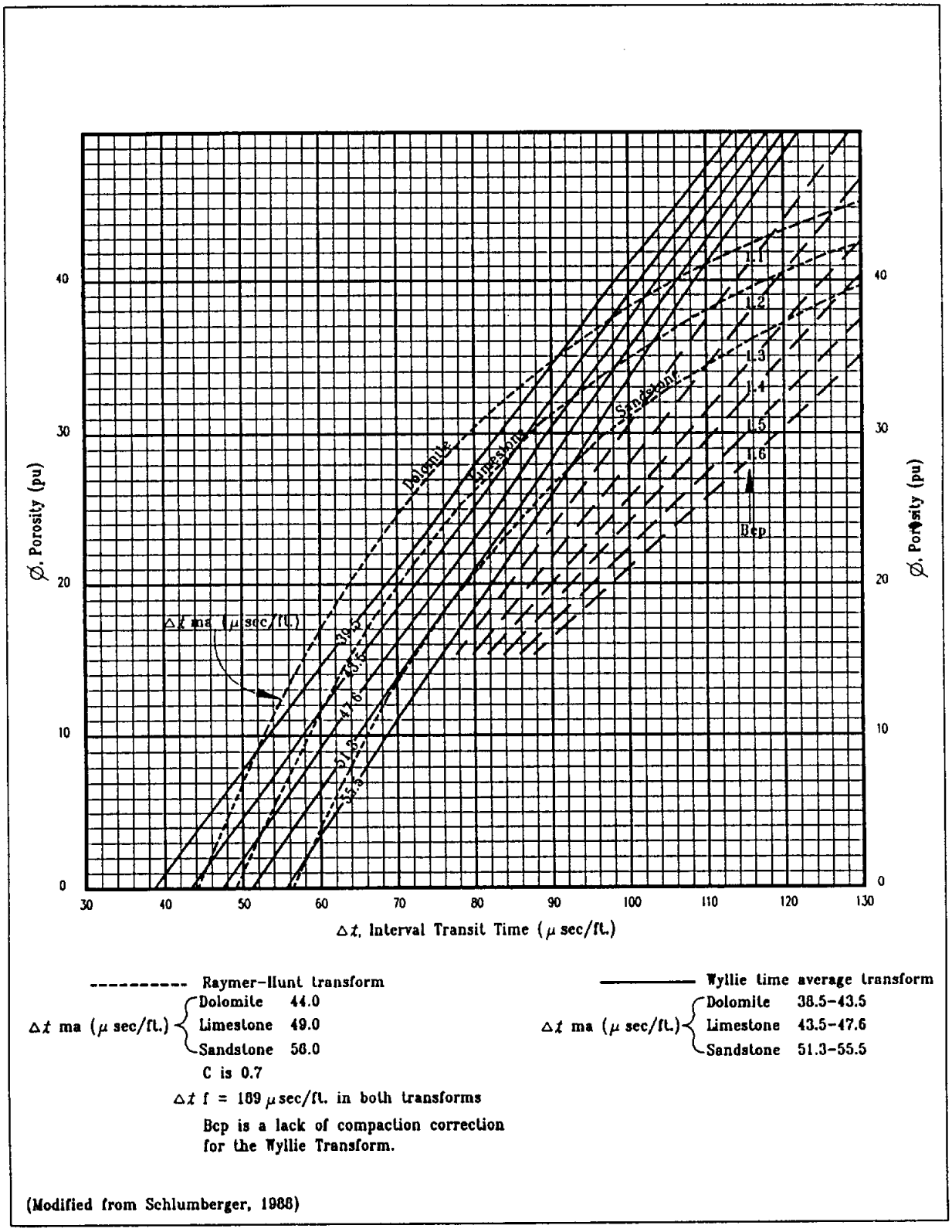

Figure 13-25. Graphs for calculating sonic porosity from the Wyllie time average and Raymer-Hunt transforms (From Schlumberger, 1988).

sonic porosities for this effect. For these types of carbonates density or neutron porosities will be closer to true porosity because these logs are affected by all the pores in the volume of rock investigated by the tool. But, the difference between density and/or neutron and sonic porosity can be used as a qualitative indicator of the amount of scattered vuggy-moldic porosity in the formation (Figure 13-26). When the vuggy/moldic pores are very abundant, the pore system becomes homogenous and the sonic measures true porosity (Hilchie, 1982). In logging literature scattered vuggy-moldic porosity is called secondary porosity.

The shortcomings of the Wyllie transform have been known for a number of years. Various other transforms have been proposed, but they are much more complicated and require the input of variables that are not readily available. Jorden and Campbell (1986) have succinct summaries of the Gassmann and Biot models.

In 1980 Raymer, Hunt, and Gardner proposed a transform that has gained fairly widespread popularity. It is referred to as both the Raymer-Hunt and the Hunt-Raymer equation. It is empirical, based on extensive field observations. Unfortunately, the data base used to derive the transform is not documented.

The Raymer-Hunt transform cannot be quantified with a single equation. The authors proposed different equations for 0 to 37 pu, 37 to 47 pu, and 47 to 100 pu. One form of the equation for the 0 to 37 pu range is

$$\Delta t = (1-\phi)^2 \Delta t_{ma} + \phi \Delta t_f \qquad \textbf{(13-8)}$$

Most log analysts use a simplified approximation of Equation 13-8:

$$\phi = C \frac{\Delta t - \Delta t_{ma}}{\Delta t} \qquad \textbf{(13-9)}$$

Values of C range from 0.625 to 0.7, depending on the log analyst. Δt_f is factored into C (Bateman, 1985). Figure 13-25 uses Equation 13-9 and a C of 0.7 for the Raymer-Hunt graphs. This figure also serves to document the differences between porosities calculated by the Wyllie and the Raymer-Hunt transforms.

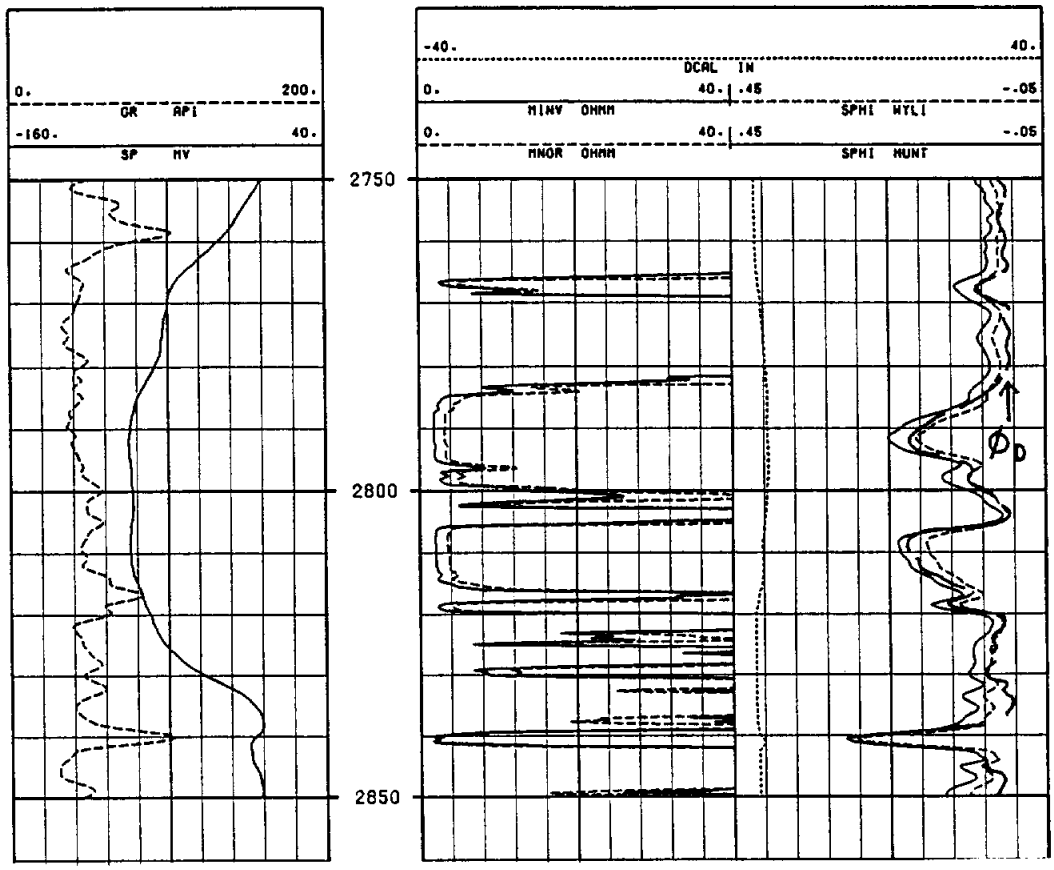

Figure 13-26. Comparison of sonic porosities calculated with the Wyllie and Raymer-Hunt transforms. The two sonic curves, along with density porosity ϕ_D, are in Track 3. The Raymer-Hunt transform yields porosities that are too high. The Wyllie equation porosities are more in line with the density values. In high porosity zones the Wyllie porosities are less than density porosities, a possible indication of isolated, vuggy-moldic porosity. Thin section analysis of the core confirms this observation (Collier, 1988). The lithology is limestone. Figure 8-33 gives additional details on this well.

Raymer, et al. maintain that their transform has three advantages over the Wyllie equation:

1. It provides superior transit time-porosity correlation over the entire porosity range (0 to 100 pu).

2. It provides accurate porosities in unconsolidated, uncompacted sandstones without using a lack of compaction factor (Figures 13-27 a and b).

3. A single Δt_{ma} value is used for each lithology: 56 μsec/ft for sandstone, 49 μsec/ft for limestone, and 44 μsec/ft for dolomite.

Although the Raymer-Hunt transform is applied to all lithologies, it is best suited for unconsolidated, uncompacted sands. In carbonates it often gives porosity values that are a few pu too high, while the Wyllie transform gives the correct values (Figure 13-26). Both transforms have variables (C for Raymer-Hunt and Δt_{ma} for Wyllie), and log analysts differ on the most appropriate values for these variables. The problems associated with sonic porosity transforms further illistrate the superiority of the density tool.

Other Porosity Tools

Four other tools have been utilized to a limited degree as porosity tools. The tools are predominately used in petroleum logging or are being developed for this market.

The microlog was originally developed as a porosity tool. However, it soon became obvious that it was not suited for this task. The microlog was subsequently marketed as a permeability indicator. It is a good "permeability" log and numerous micrologs have been run in the Trinity aquifer through the years for this purpose. Unfortunately, porosity calculations from these logs are very tenuous. The **Recommended use** section under **NONFOCUSED PAD MICROELECTRODE TOOLS** in Chapter 8 elaborates on microlog porosity calculations.

The dielectric tool is a relatively new logging tool that uses electromagnetic energy to detect water-filled porosity. Only the major logging companies have the log and there are no slimhole versions. Two types of tools are available: a high frequency, shallow investigating (1 to 5 inches) pad device and a low frequency, deep investigating (15 to 45 inches) mandrel tool. Atlas Wireline uses the name Dielectric Log for both tools. Schlumberger calls their high frequency tool an Electromagnetic Propagation Tool (EPT) and their low frequency tool a Deep Propagation Tool (DPT). Collier (1989) is an assessment of the tool as a ground-water porosity log.

Theoretically, dielectric tools would be excellent porosity tools. They do not have radioactive sources, the dielectric response is not affected by the amount of compaction and consolidation of the rock, and low frequency tools can be run in nonmetallic casing. In practicality, however, they have serious limitations:

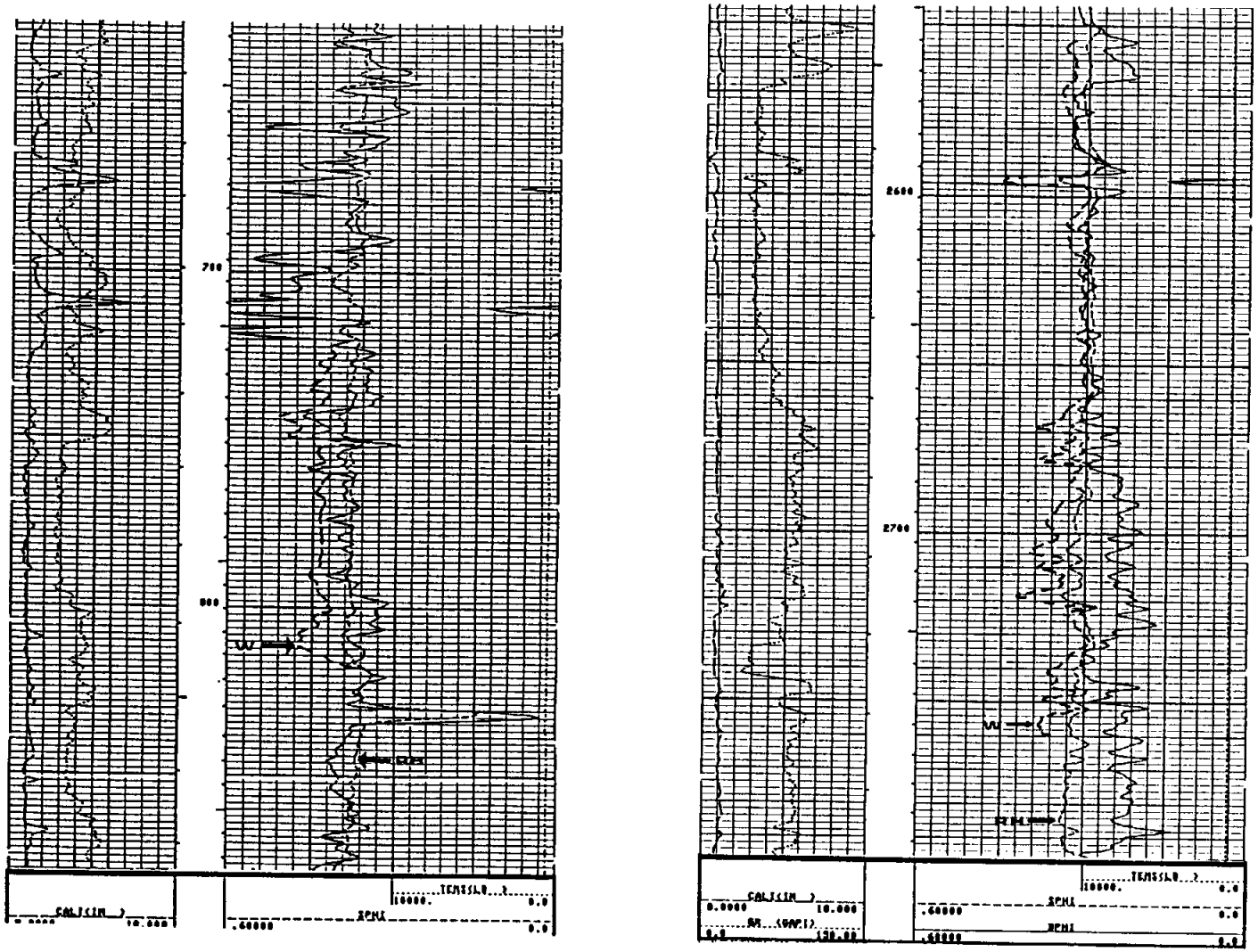

Figure 13-27 a & b. A comparison of the effect of compaction on porosities calculated with the Wyllie (W) and Raymer-Hunt (RH) transforms. At shallow depths (e.g. 750 to 790 feet) the Raymer-Hunt transform adequately corrects for a lack of compaction in the sandstones, while the Wyllie equation yields porosities that are too high. However, at deeper depths (e.g. 2600 to 2650 feet) the sandstones are compacted and both transforms calculate correct porosities. Density porosity is assumed to be true porosity. Figure 13-22 contains additional information on this well.

1. High frequency tools are severely affected by borehole rugosity (Figure 13-28).

2. Low frequency tools have a vertical resolution of about 8 feet.

3. The tools are not widely available, and low frequency tools are especially scarce.

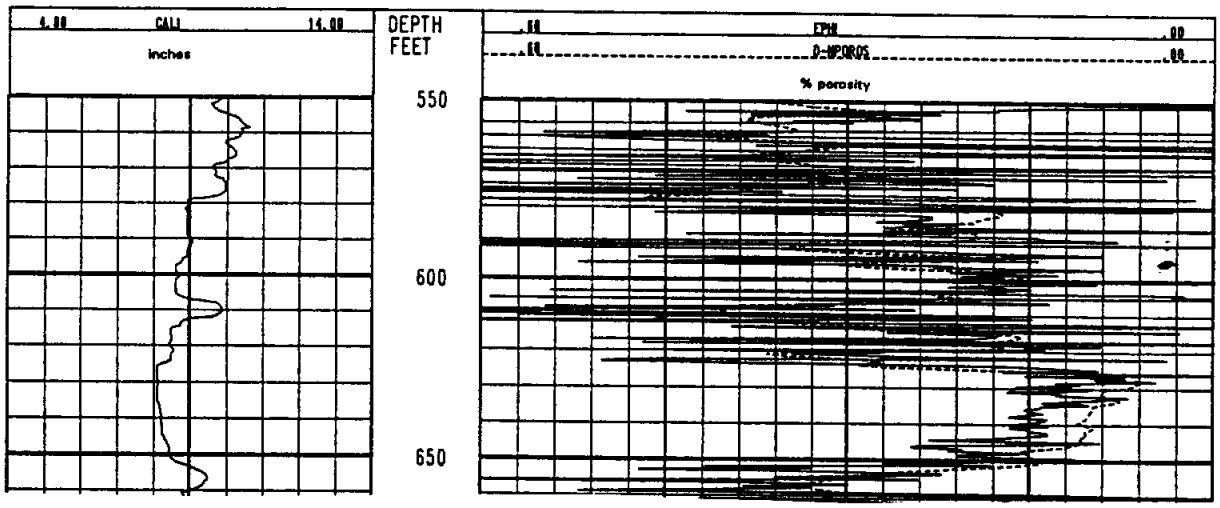

Figure 13-28. A comparison of porosity values calculated with an electromagnetic propagation tool (EPHI) and a density-neutron crossplot (D-NPOROS). The EPHI was calculated using a limestone matrix. The lithology is limestone and dolomite. Borehole rugosity is causing the spikes on the EPHI. Intervals with little borehole rugosity, such as the Regional Dense Member (626 to 646 feet), have fairly accurate EPHI values. The accuracy of the EPI values in this interval, which is a shaly limestone, could be improved by correcting for the effect of shale. The log is the Edwards Aquifer. Figures 9-22, 13-5, 13-8, 13-32, and 13-33 provide additional data on this well..

The Magnetic Resonance Imaging Log (MRIL) is presently under development as both a porosity and a permeability log. The tool utilizes spin-echo techniques to measure hydrogen content. The profile of the echoes relaxation is then transformed into a quantitative measure of porosity, free fluid porosity, and bulk-volume irreducible, a surface-to-volume index. In addition, the tool can make other measurements, including T1, the spin-lattice relaxation. T1 is strongly related to the permeability of a rock. Coates, et al. (1991) summarizes ground-water applications of the tool. Figure 13-29 is an example of the log.

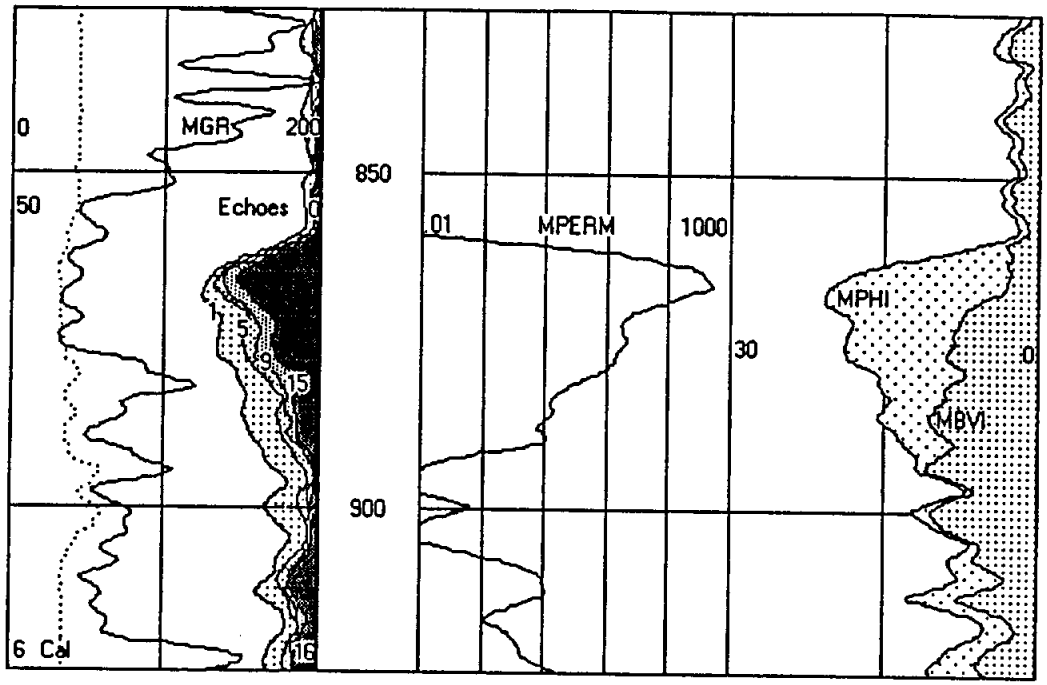

Figure 13-29. Magnetic Resonance Imaging Log (MRIL). Track 1 contains three curves: caliper (Cal), gamma ray (MGR), and amplitude of pulse-echoes (echoes). Echo spacings of 1, 5, 9, and 15 ms are recorded on a scale of 50 to 0.0 mv. Track 2 contains a calculated permeability curve (MPERM) plotted on a logarithmic scale of 0.01 to 1000 md. Track 3 contains two calculated curves: porosity (MPHI) and bulk-volume irreducible water (MBVI). The well is the Texas Water Development Board, Brady #2, McCulloch County, Texas (state well number 42-62-910). The formations are the Wilberns and Riley. The lithology is quartz sandstone with varying amounts of hematite, goethite, glauconite, calcite, dolomite, feldspars, and clay minerals. Bit size is 7⅞. Rm is 23.4 ohm-meters at 44° F and Rmf is 15.8 at 45° F.

An option for obtaining a limited number of discrete porosity measurements is wireline sidewall coring. Percussion and drilled sidewall tools are available. Recovery is sometimes poor in unconsolidated formations, and in low porosity sedimentary rocks, good recovery can only be obtained with drilled cores. Drilled sidewall cores yield accurate porosity and permeability values. The percussion coring process can significantly distort the pores of the samples. Permeability can be significantly altered,

either up or down, but porosity values are fairly accurate. Percussion sidewall cores analyzed for this project had porosity values within 3 pu of the log porosities (Figure 13-3 a and b). Sidewall cores can be thin sectioned and analyzed for such things as mineralogy, pore geometries, and qualitative permeability (Figures 13-30 and 13-31).

Figure 13-30. Photomicrograph of a thin section of a percussion sidewall core. The rock is a fossiliferous, calcite cemented, very fine to fine grained quartzarenite. Fossil fragments are the nuclei of the poikilotopic calcite. Calcite cementation has significantly reduced the porosity. Petrographic examination of the sidewall core explained why this zone has less porosity than surrounding sandstones (Figure 13-3). The sidewall coring process has fractured some grains and distorted the pore geometries. Porosity was impregnated with blue epoxy as part of the thin sectioning process. Magnification is 100x. The bar is 0.1mm.

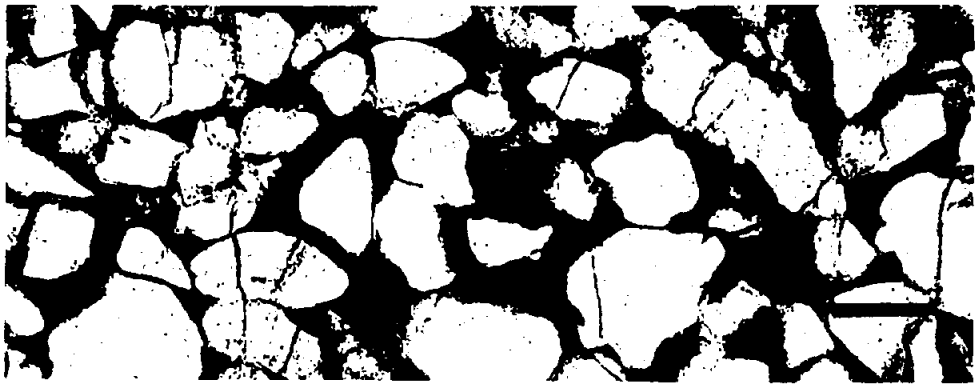

Figure 13-31. Photomicrograph of a thin section of a percussion sidewall core. The rock is a shaly, fine grained quartzarenite. Authigenic clay fills the pores and has significantly reduced permeability. Liquid permeability is 150 md. Sample depth is 3172 feet. The well is the J.L. Myers, Ladonia #2, Fannin County, Texas. Many of the grains were fractured by the coring process. Magnification is 100x. The bar is 0.1mm.

Porosity Crossplots

All porosity tools are affected by lithology, with each tool responding differently to a particluar lithology. This complicates single-log porosity calculations when the lithology is unknown and/or two or more mineralogies are present. However, if two or more porosity logs are available, these same differences can be utilized in a crossplot of the two measurements to solve for porosity and lithology.

Porosity crossplots are available for all of the various two-tool and three-tool combinations. Two-tool crossplots are the more common type, with density-neutron crossplots (Figure 13-32) the most common. All major logging companies and all comprehensive log analysis computer programs have crossplot charts.

The following guidelines should be observed when using porosity crossplots:

1. Crossplo
only be u
2. Neutron
limestone
3. Sonic po
4. Density porosity is input as apparent limestone porosity or as ρ_b.

3. Two-tool crossplots can only discriminate two-mineral mixtures; three-tool crossplots can identify three.

4. Two-tool crossplots cannot identify which two minerals comprise the mixture (i.e. the lithology could be dolomite/sandstone or dolomite/limestone). However, a general knowledge of the local geology usually allows one of the possibilities to be chosen as the most plausible one.

Figure 13-32 is a density-neutron crossplot of an Edwards Aquifer well. The lithology is limestone and dolomite, with minor amounts of chert and shale. Figure 13-33 is a more useful presentation of the data than can be gleaned from the density-neutron crossplot in Figure 13-32.

Sonic (Acoustic)

The sonic tool is used to calculate porosity, pick bed boundaries, and identify abnormally pressured formations. In conjunction with another porosity tool, it can be used to determine lithology. In conjunction with the density tool it is used to create synthetic seismograms and to calculate rock mechanical properties such as Poisson's ratio and Young's modulus.

Specialized sonic tools have been developed to identify fractures (Variable Density Log), evaluate cement bond quality (Cement Bond Log), and image the borehole (Borehole Televiewer). Research is presently underway to develop methods to calculate permeability from the sonic . Efforts are underway to develop accurate cased hole sonic porosity tools, but presently the tool works much better in open holes. Normal sonic tools only operate in liquid-filled holes.

The sonic was the first porosity tool. Popular in the 1950's, it has been supplanted in oilfield logging by the density-neutron combination. In ground-water/environmental investigations, however, it is more widely utilized. This is probably due in large part to the ease and safety (no radioactive source) with which it can be operated.

Modern conventional tools carry a variety of names: Borehole Compensated Acoustic (AC) for Atlas Wireline, Borehole Compensated Sonic (BCS) for Gearhart, Compensated Acoustic Velocity (CAV) for Welex and Halliburton, and Borehole Compensated Sonic Log (BHC) for Schlumberger. Each company also has a Long Spaced Sonic and a Full Wave Sonic, as well as various other specialized sonic tools. Jorden and Campbell (1986) contains succinct summaries of the different types of sonic tools. Slimhole sonic tools are available and a few are compensated. Slimhole full wave sonic tools are also available.

Tool theory. Ordinary sonic tools utilize a transmitter(s) and receivers to measure the velocity of sound in a formation. The transmitter generates 10 to 60 times a second a high frequency (20 to 40 kilohertz) sound wave that travels out in all directions through the tool, borehole fluid, and formation. This sound wave actually consists of several different types of waves: compression (P, pressure, or longitudinal), shear (S or transverse), Rayleigh, and Stonely. Under normal conditions, the first component of the wave to arrive at a receiver is that part of the compression wave which struck the borehole wall at the critical angle and traveled vertically through

the formation (Figure 13-19). This is the only wave of interest to ordinary sonic tools and it is the wave used to calculate porosity. Other sonic tools record the amplitude, attenuation, travel time, and/or frequency of the various components of the wave train.

The sonic tool measures the time it takes a sound wave to travel from the transmitter to each receiver. The difference between the two values, divided by the receiver spacing, is the time it takes for the compression

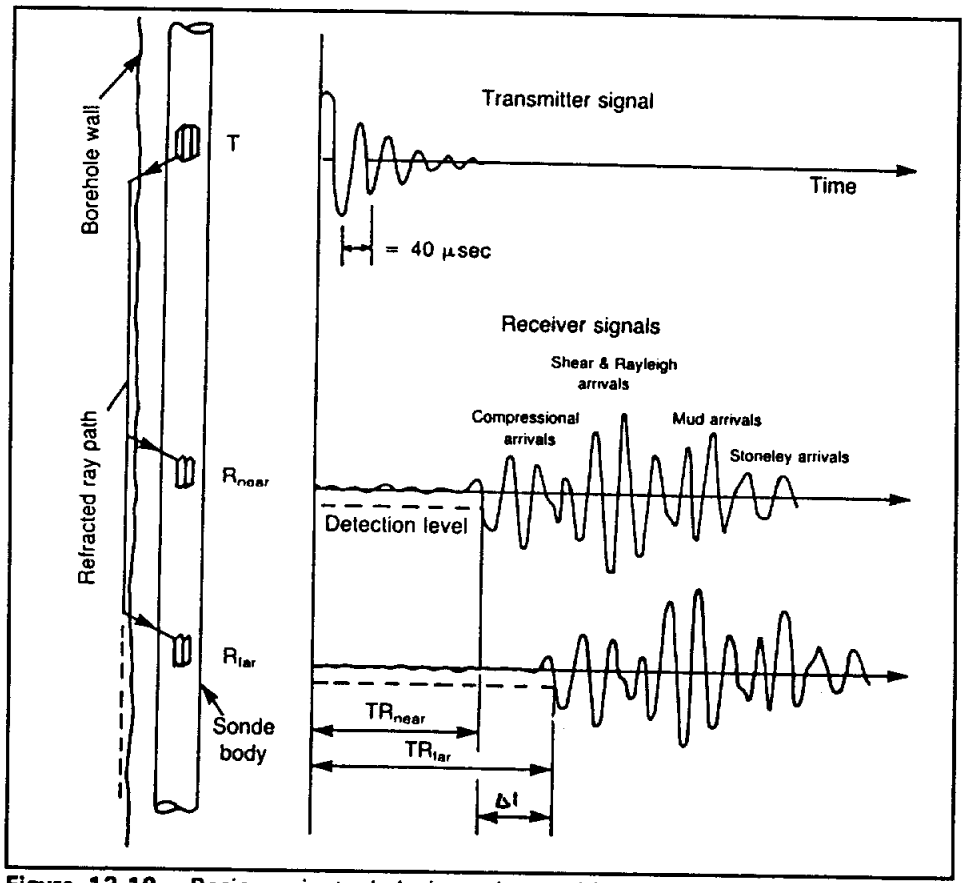

Figure 13-19. Basic sonic tool design, along with an acoustic wavetrain. The compression wave activates the receivers (Modified from Dewan, 1983).

wave to travel 1 foot in the formation. This calculation assumes that the distance from the borehole wall to each receiver is the same. The only way to be assured of this is to compensate the tool.

Tool design. Modern conventional tools and some slimhole tools are compensated. The standard design used to be a double array of one

transmitter and two receivers inverted to each other (Figure 13-20). Averaging the two measurements factors out errors in calculating sonic velocity due to washouts and tilted tools. Today some sonic tools are compensated by other methods, but the result is the same. In severe washouts compensated sonic measurements are less affected than are other porosity tools.

Most modern tools use piezoelectric ceramic crystals as the transmitting transducers. Electric current is used to physically deform the crystal, thus producing a sound wave. The receivers are also transducers, except in this case they convert acoustic energy to electrical energy.

Typically the distance between the transmitter and the near receiver is 3 feet, but it can be up to 10 feet. The distance between the two receivers is normally 2 feet, but spacings of 1 to 3 feet are used. The tool is constructed in such a way as to attenuate the sound wave traveling the length of the tool. Slots in the steel housing or a rubber insert in the housing are commonly used to accomplish this.

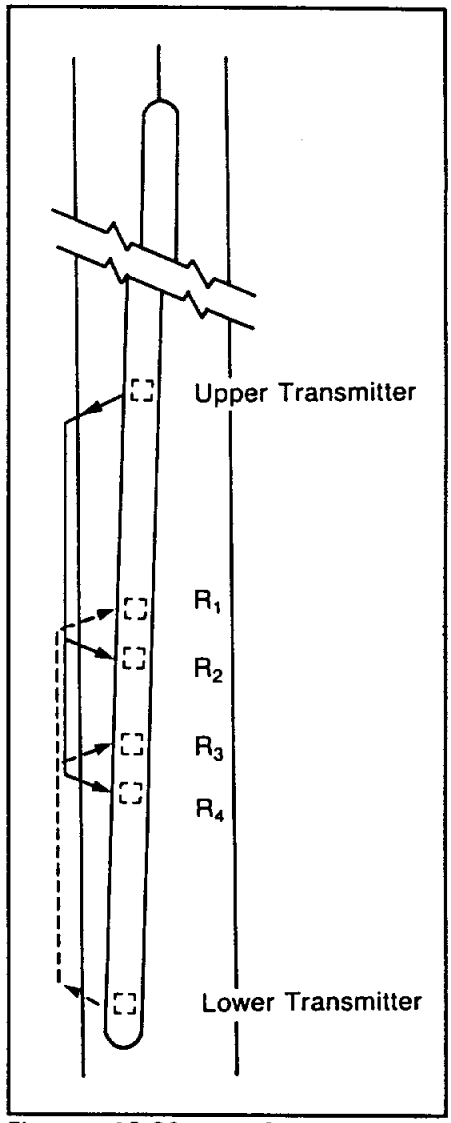

Figure 13-20. One type of compensated sonic tool (From Schlumberger, 1989).

Jorden and Campbell (1986) list the specifications of conventional sonic tools. Their book contains one of the best available discussions of sonic logging. Included is a detailed discussion of single-transmitter/dual-receiver tools, which is a common type of slimhole tool.

Sonic tools perform best when centralized in the borehole. One of the centralizers is also utilized as a caliper. The centralizers are normally bow springs, which means that the caliper measurement is not very sensitive. (Chapter 11 discusses calipers in detail.)

Calibration. There is very little in the way of calibrations to be done to the tool. A good quality-control check on the tool is to measure its response

in uncemented steel casing. It should be 57 μsec/ft. However, upon entering casing the travel time may not immediately jump to this value. The engineer may first need to adjust for the drastic change in signal amplitude created by going from open to cased hole (Dewan,1983).

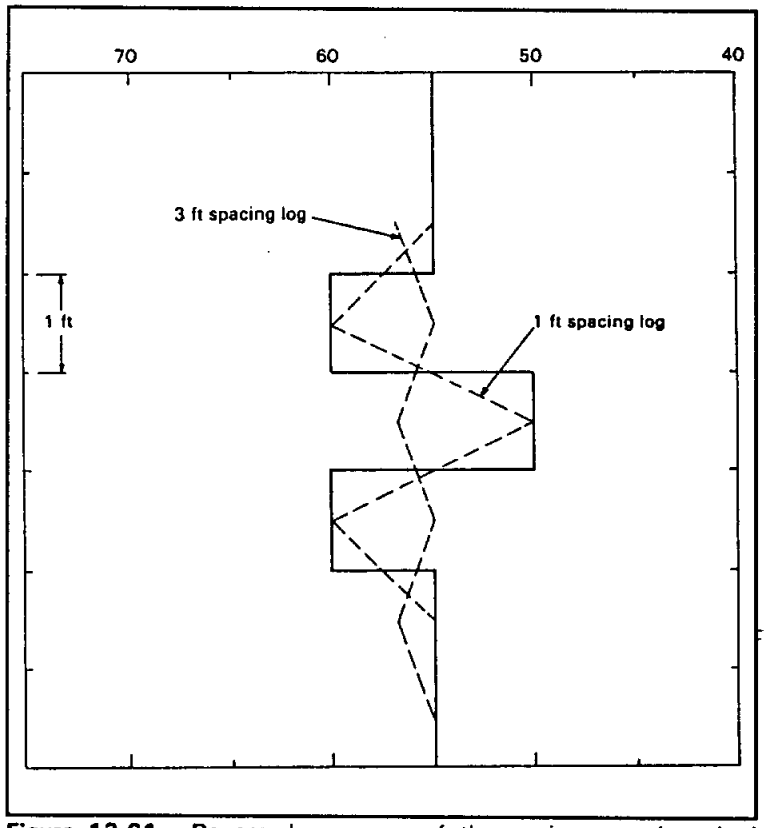

Figure 13-21. Reversed response of the sonic curve in a bed thinner than the receiver spacing (From Etnyre, 1989).

Depth of investigation and vertical resolution. Vertical resolution is the distance between the two receivers (normally 2 feet). Beds thinner than this distance are detected by the tool, but the log values will not be accurate and may trend in the opposite direction of the actual travel time (Figure 13-21). Jorden and Campbell (1986) detail other problems with thin bed interpretation.

Figure 13-21 also illustrates that at bed boundaries there is a transition in travel time values equal to the distance between the two receivers. The bed boundary is the mid-point of the transition zone.

Travel time measurements are not affected by formations outside the detector spacings (Etnyre, 1989). The sonic tool is the only porosity tool with this characteristic. This contributes to its excellent vertical resolution, which is better than any other porosity tool.

The sampling rate is a function of the logging speed and the rate at which the transmitter emits sound waves. An average sampling rate is every few inches. At 20 pulses per second a compensated tool makes 5 measurements per second, which for a logging speed of 60 feet per minute is a measurement every 2.4 inches.

Depth of investigation ranges from 5 to 40 inches into the formation (Serra, 1984). Most of the time the actual depth is from 8 to 12 inches (Hilchie, 1982). Depth of investigation is predominately a function of wavelength which, in turn, is a function of velocity and frequency. The longer the wavelength the deeper the penetration. In formations (normally shales) that have altered zones next to the borehole, the depth of investigation can be increased beyond the altered zone by using a long spaced sonic tool. This is only necessary if the sonic log is to be incorporated into a seismic study.

Log presentation. Sonic logs are a recording versus depth of the time it takes a sonic wave to travel 1 vertical foot of formation. The measurements are called **interval transit time, interval travel time, transit time, travel time, Δt (delta t)**, or t. The unit of measurement is microseconds (μs or μsec) per foot. Using microseconds rather than seconds makes the values whole numbers. Δt is the reciprocal of velocity in feet per second. The relationship between the two is expressed by the following equation:

$$\Delta t = \frac{10^6}{velocity} \qquad \textbf{(13-4)}$$

Interval transit time is normally presented across tracks 2 and 3 (Figure 13-22). Transit time increases to the left, which means that porosity also increases to the left. The scale is linear and normally is either 140 to 40 μsec/ft or 150 to 50 μsec/ft.

Conventional log presentations often include integrated travel time (TTI). It is recorded in the depth column as a series of horizontal tic marks. Each tic is 1 millisecond, with a larger tic every 10 milliseconds. TTI, which is the one-way vertical travel time of a sound wave through the subsurface, is useful in interpreting seismic sections. TTI multiplied by 2 yields the travel time recorded on seismic sections.

Borehole corrections. There are no environmental corrections for the sonic log. "Acoustic log readings must be either accepted at face value, or qualitatively discounted as invalid or nonrepresentative" (Jorden and Campbell,1986).

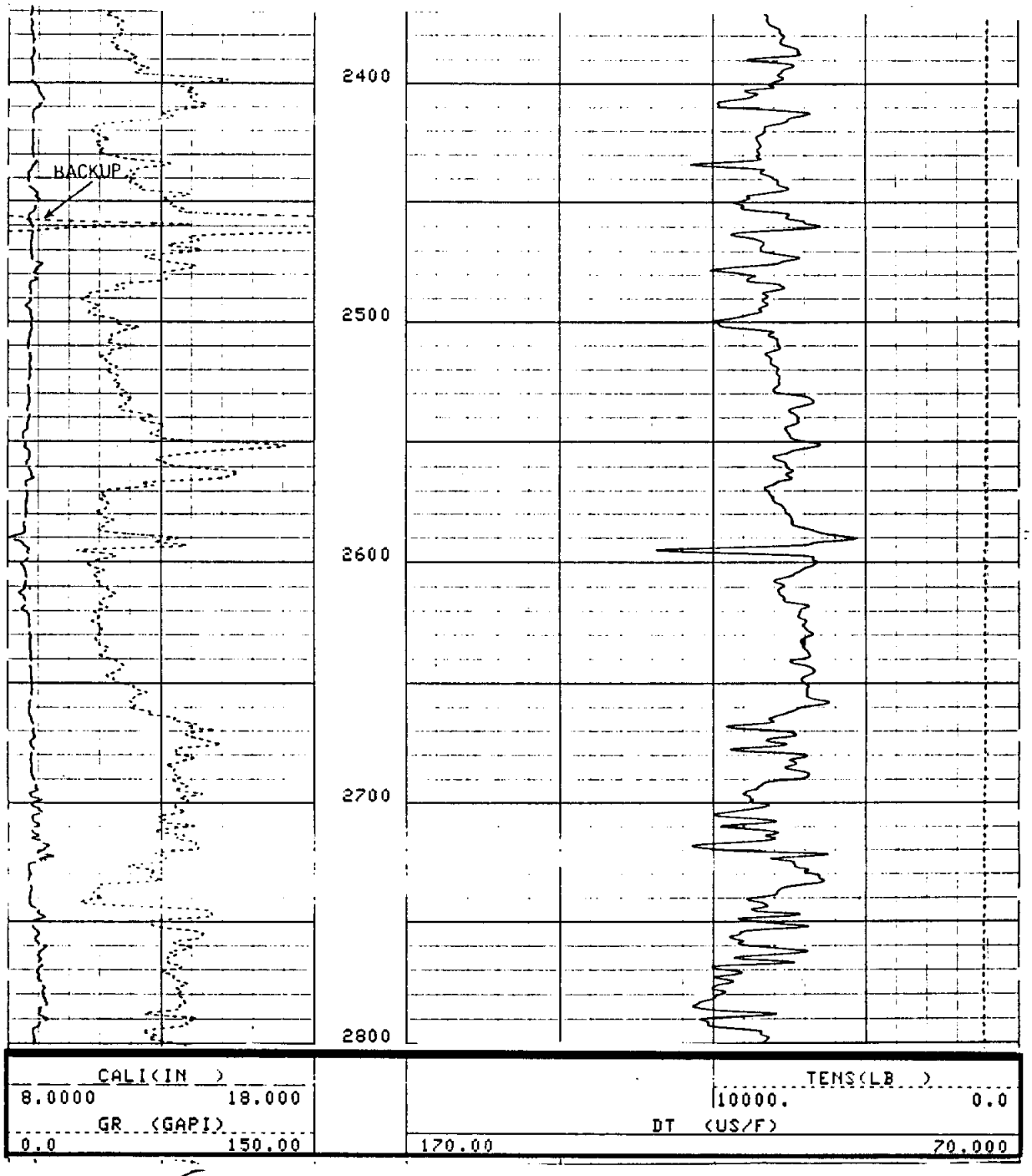

Figure 13-22. A typical sonic log presentation. Δt increases to the left, which corresponds to increasing porosity. The caliper is not very sensitive because it is built into the centralizer. In this well Δt, and thus porosity, decrease with depth. This is due to increasing compaction with depth. The lithology is alternating shales and sandstones. The radioactive zone at 2460 feet is a sandstone, not a shale. Shales have higher travel times than do sands. The well is the McKinley Drilling Company, Fox Creek #2, McMullen County, Texas. Bit size is 8.75 inches. Borehole fluid is native gel. Figures 13-27 a and b provide additional data on this well.

The Δt measurements of compensated tools are very accurate, to within approximately ± 0.25 μsec/ft (Dewan, 1983). However, there are conditions under which the tool will measure something other than the travel time of the compression wave in the formation. Some of these conditions are due to characteristics of the formation and are discussed in the following section. Others are the result of borehole conditions and are discussed below:

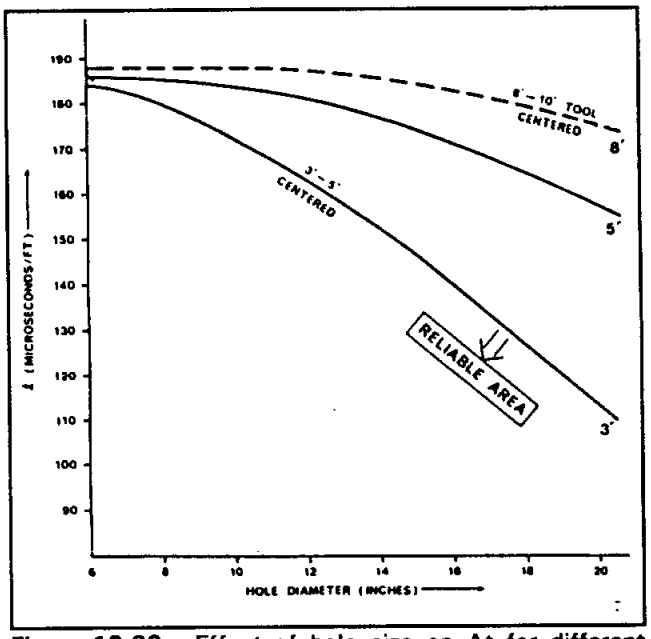

Figure 13-23. Effect of hole size on Δt for different transmitter-near receiver spacings (From Goetz et al.,1979, in Serra, 1984).

1. If the borehole diameter is large enough, the compression wave traveling through the borehole fluid will arrive first. The diameter at which this will occur is a function of the transmitter-near receiver spacing and the travel time of the formation (Figure 13-23). Figure 13-23 reveals that conventional sonic tools are not reliable in formations with high travel times (e.g. unconsolidated sands) once the borehole diameter exceeds 14 inches. In such cases the only alternative is to run the tool eccentralized (Serra, 1984). According to this chart long spaced tools are not affected by borehole diameter. However, the long spaced sonic in Figures 12-12a and 12-12b is reading the travel time of the drilling mud in a 15 inch borehole.

2. Noise in the borehole can trigger the receivers. Such noise can be generated by the centralizers scraping against the borehole wall, excessive logging speed, and the absence of centralizers. Noise yields erroneous travel times that appear on the log as sharp spikes. If the far receiver is triggered, the travel time will be too short by as much as 75μsec/ft (Dewan, 1983). Triggering the near receiver gives a travel time that is too long. Road noise is minimized by not activating the receivers for a fixed time following transmitter fire. Therefore, the far receiver is more likely to

measure noise. Some modern tools have circuits that eliminate road noise. Long spaced tools are more susceptible to noise.

3. If the sound wave is too weak to trigger the far receiver, the receiver skips that cycle and triggers on a subsequent one. Cycle skipping creates spiky increases in travel time usually over 1 foot or less of log depth (Jorden and Campbell, 1986). The increase in travel time varies from 5 to 37.5 μsec/ft, depending on which cycle triggers the receiver and whether one or both of the far receivers cycle skip (Serra, 1984). Cycle skipping will be caused by anything that strongly attenuates the sound wave, such as gas in either the mud column or the formation, fractures, tool malfunction, or improper centralization of the tool. It can also be caused by setting the detection threshold (bias) of the receivers too high. The sound wave will not activate the receiver unless it has an energy level (amplitude) that exceeds the threshold value for which the receiver has been set. Some of the very latest sonic tools have smoothing circuits that eliminate cycle skips. Long spaced tools are more susceptible to cycle skipping.

4. Microfractures in a formation (usually shales or carbonates) will result in abnormally long travel times. The fractures can be drilling-induced or natural.

Interpretation. Δt is predominately a function of lithology, texture, porosity, pore fluid, and pressure. It is very sensitive to lithologic and textural changes, which makes it one of the best logs for correlation. In combination with another porosity log, the sonic log can be used to identify lithology. Compaction trends can be identified, usually by observing how the travel time of shale decreases with depth. Overpressured zones show up as decreases in the slope of the compaction trend with increasing depth. The main use of the log, however, is to calculate porosity.

M. R. J. Wyllie, et al. (1956) proposed the first practical transform for relating travel time to porosity in sedimentary rocks. The Wyllie time-average equation is an empirical equation based on laboratory observations of the travel time of sound in rocks of varying porosities. It is a linear weighted-average relationship that assumes that the total travel time (hence the name Δt) of a formation is equal to the sum of the travel times in all the pores and rock matrix traversed by the compression wave. The equation

models Δt as a function of porosity, lithology, and pore fluid. The relationship between the four is as follows:

$$\Delta t=\phi\Delta t_f+(1-\phi)\Delta t_{ma} \qquad \textbf{(13-5)}$$

Where:

Δt = *travel time on the log in μsec/ft*
Δt_f = *travel time of the pore fluid in μsec/ft*
Δt_{ma} = *travel time of the matrix in μsec/ft*
ϕ = *porosity in decimals*

Equation 13-5 can be rearranged to solve for porosity (Equation 13-6), which is how the Wyllie transform is normally presented:

$$\phi = \frac{\Delta t-\Delta t_{ma}}{\Delta t_f-\Delta t_{ma}} \qquad \textbf{(13-6)}$$

Table 13-3 lists compressional wave transit times for common lithologies and fluids. Although each lithology has a range of travel times, normally an average Δt_{ma} is used in porosity calculations. There is some variation in the logging literature as to what the average Δt_{ma} values actually are, but the differences are usually only a couple of μsec/ft. The average values used in Table 13-3 yield porosity values that are within ± 2 pu of true porosity, even when the travel time falls somewhere else within the range of values for that lithology.

Table 13-3 also shows that the travel times of fresh and saline water are considerably different. Most log analysts automatically use 189 μsec/ft, but 205 μsec/ft should be used for fresh-water aquifers. In fresh water a Δt_f of 189 μsec/ft yields porosity values that are about 3 pu too high (Figure 13-24).

Chartbooks contain graphical solutions of Equation 13-6. The straight solid lines in Figure 13-25 are graphical solutions of the Wyllie transform for various lithologies. The chart uses a Δt_f of 189 μsec/ft.

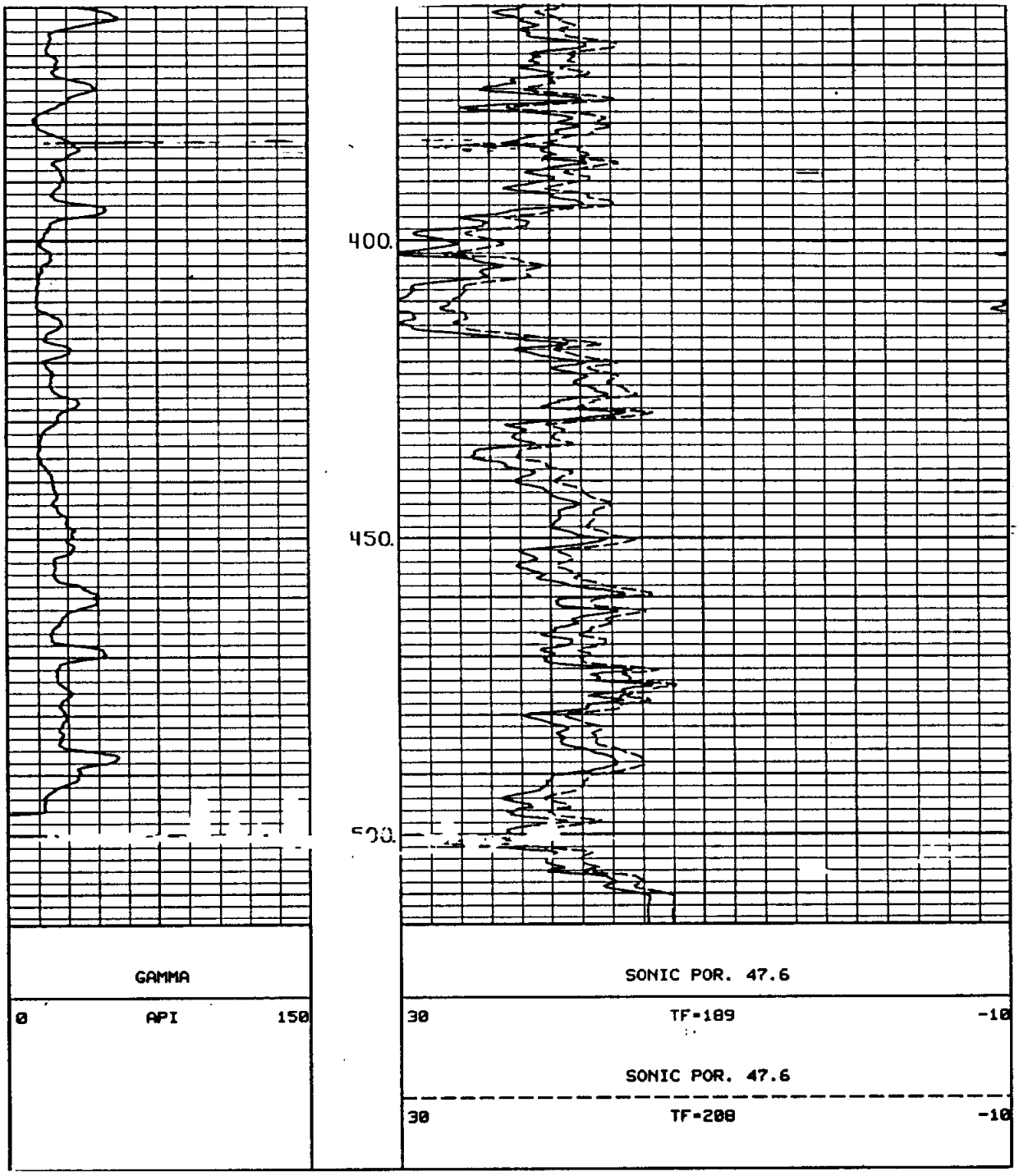

Figure 13-24. Comparison of sonic porosities calculated with the Δt_f's of fresh and saline water. The salt water value for Δt_f (189 μsec/ft), which is commonly used in oilfield logging, yields porosity values that are approximately 3 pu too large when the pore water is fresh. The Δt_f used for fresh water (208 μsec/ft) is too high. 205 μsec/ft is a better value. However, there is little difference between porosity values calculated with the two. Porosities were calculated with the Wyllie time average equation. Bit size is 6 inches. The borehole fluid is fresh formation water. The aquifer is a Cretaceous limestone in South Texas.

TABLE 13-3. Δt_{ma} AND Δt_f VALUES OF COMMON LITHOLOGIES AND FLUIDS.

Mineral/Fluid	Average Δt_{ma} or Δt_f μsec/ft	Range Δt_{ma} or Δf
Air		
Methane, 15 psi		
Oil		
Water, pure (25° C)		
Water, 100,000 ppm NaCl, 15 psi		
Oilfield water; drilling mud		
Water, 150,000 ppm NaCl, 15 psi		
Shale		170.0-60.0
Sandstones (compacted)	54.0	55.5-51.3
Quartz	55.1	55.5-54.7
Gypsum	53.0	53.0-52.5
Anhydrite		50.0
Limestone	47.6	47.6-43.5
Calcite	46.5	47.6-45.5
Dolomites	43.5	43.5-38.5
Dolomite	44.0	45.0-40.0

(Compiled from Serra, 1984 and Schlumberger, 1989.)

Shale laminae within a sandstone increase the sonic porosity values by an amount proportional to the bulk volume fraction of laminae (Schlumberger, 1989). Jorden and Campbell (1986) contains a good review of shale corrections. However, the porosity values of consolidated, compacted sandstones with 15 to 25 percent porosity are not significantly affected by disseminated shale (Schlumberger, 1989).

Gas in a formation increases the travel time, yielding porosity values that are too high. The shallower the formation, the greater the discrepancy.

The Wyllie transform models clean, consolidated, compacted formations with uniformly distributed small pores (i.e. consolidated sandstones and carbonates with interparticle or intercrystalline pore geometries). Through the years many log analysts have disregarded these prerequisites and indiscriminately applied the transform to other rock types such as uncompacted, unconsolidated sands and vuggy-moldic carbonates. In such cases considerable modification must be made to the Wyllie equation in order to obtain accurate porosity values. This problem is of considerable importance to ground-water/environmental logging because many aquifers are either uncompacted sands or vuggy-moldic carbonates.

The Wyllie transform calculates too high a porosity in unconsolidated, uncompacted sands. These sands usually have a travel time in excess of 100 μsec/ft; it can be as high as 150 μsec/ft. The adjacent shales often have travel times greater than 100 μsec/ft. The shallower the formation, the higher the travel times in both the shales and the sands.

Correct porosity values for uncompacted sands are obtained by dividing the porosities obtained in Equation 13-6 by an empirically derived compaction correction factor (B_{cp} or C_p). A more correct term would be lack of compaction correction factor. The dashed straight lines in Figure 13-25 are correction factors. B_{cp} ranges from 1.0 to 1.8 and is never less than 1.0. It can be calculated from the travel time of the shales adjacent to the sand or by dividing sonic porosity by true porosity (other porosity logs or core porosities). However, if another source of porosity measurements is available, there is really no need to recalculate sonic porosity. When the sonic log is the only porosity log available, B_{cp} can be calculated from the travel time of the adjacent shales. This technique works well as long as the travel time of the shale has not been affected by washouts or shale hydration (Hilchie, 1982). The correction factor is calculated from the following equation:

$$B_{cp} = \frac{\Delta t_{sh}}{100 \mu sec/ft} \qquad (13\text{-}7)$$

Where:

B_{cp} = *compaction correction factor*

Δt_{sh} = *travel time in the shale adjacent to the sand in* μsec/ft

Dewan (1983) recommends that when travel time exceeds 110 μsec/ft a different porosity tool be used to calculate porosity.

In carbonates with scattered, isolated vuggy-moldic porosity the calculated sonic porosity will be too low. This is because the first compression wave to arrive at the receiver is the one that travels along the part of the borehole wall that has the smallest number of vuggy-moldic pores. Thus the travel time measurement, in effect, avoids pore spaces that are scattered around the rest of the borehole. There is no way to adjust

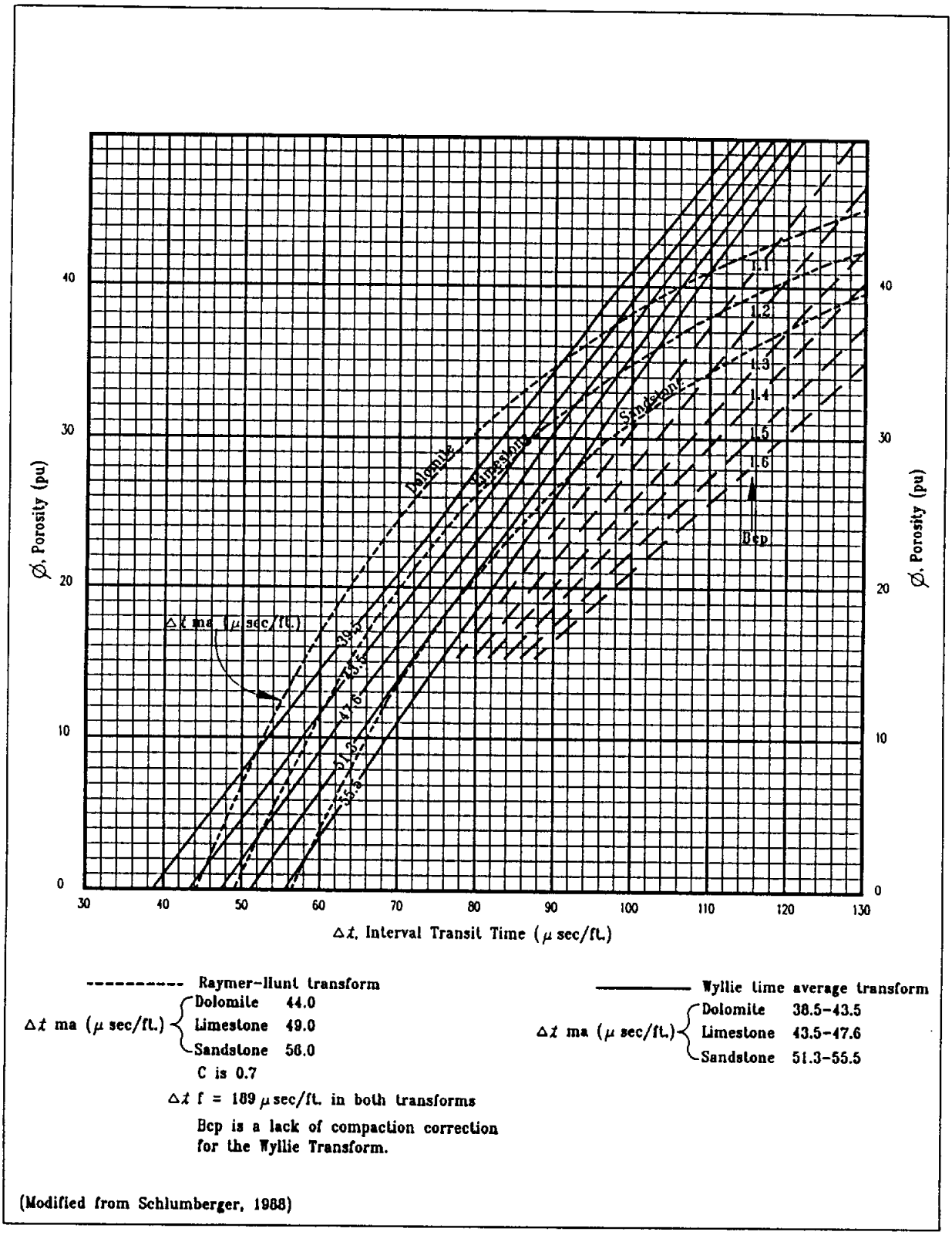

Figure 13-25. Graphs for calculating sonic porosity from the Wyllie time average and Raymer-Hunt transforms (From Schlumberger, 1988).

sonic porosities for this effect. For these types of carbonates density or neutron porosities will be closer to true porosity because these logs are affected by all the pores in the volume of rock investigated by the tool. But, the difference between density and/or neutron and sonic porosity can be used as a qualitative indicator of the amount of scattered vuggy-moldic porosity in the formation (Figure 13-26). When the vuggy/moldic pores are very abundant, the pore system becomes homogenous and the sonic measures true porosity (Hilchie, 1982). In logging literature scattered vuggy-moldic porosity is called secondary porosity.

The shortcomings of the Wyllie transform have been known for a number of years. Various other transforms have been proposed, but they are much more complicated and require the input of variables that are not readily available. Jorden and Campbell (1986) have succinct summaries of the Gassmann and Biot models.

In 1980 Raymer, Hunt, and Gardner proposed a transform that has gained fairly widespread popularity. It is referred to as both the Raymer-Hunt and the Hunt-Raymer equation. It is empirical, based on extensive field observations. Unfortunately, the data base used to derive the transform is not documented.

The Raymer-Hunt transform cannot be quantified with a single equation. The authors proposed different equations for 0 to 37 pu, 37 to 47 pu, and 47 to 100 pu. One form of the equation for the 0 to 37 pu range is

$$\Delta t = (1-\phi)^2 \Delta t_{ma} + \phi \Delta t_f \qquad \textbf{(13-8)}$$

Most log analysts use a simplified approximation of Equation 13-8:

$$\phi = C \frac{\Delta t - \Delta t_{ma}}{\Delta t} \qquad \textbf{(13-9)}$$

Values of C range from 0.625 to 0.7, depending on the log analyst. Δt_f is factored into C (Bateman, 1985). Figure 13-25 uses Equation 13-9 and a C of 0.7 for the Raymer-Hunt graphs. This figure also serves to document the differences between porosities calculated by the Wyllie and the Raymer-Hunt transforms.

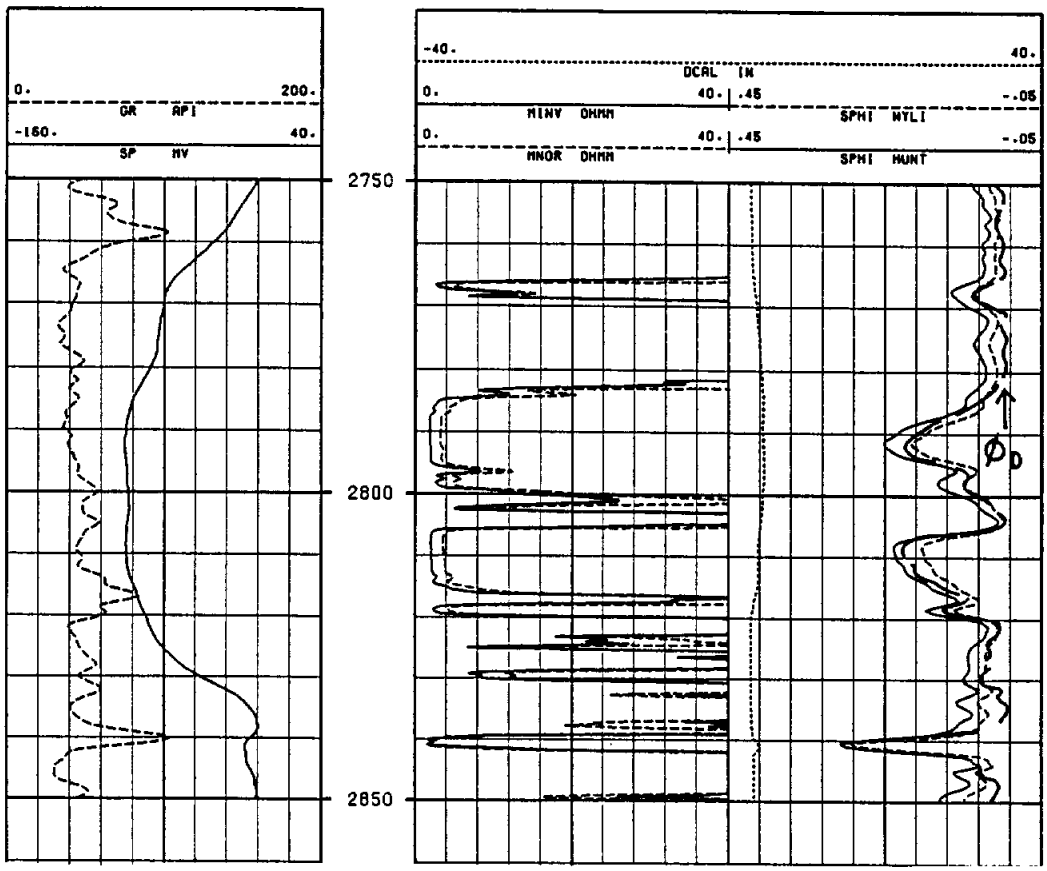

Figure 13-26. Comparison of sonic porosities calculated with the Wyllie and Raymer-Hunt transforms. The two sonic curves, along with density porosity ϕ_D, are in Track 3. The Raymer-Hunt transform yields porosities that are too high. The Wyllie equation porosities are more in line with the density values. In high porosity zones the Wyllie porosities are less than density porosities, a possible indication of isolated, vuggy-moldic porosity. Thin section analysis of the core confirms this observation (Collier, 1988). The lithology is limestone. Figure 8-33 gives additional details on this well.

Raymer, et al. maintain that their transform has three advantages over the Wyllie equation:

1. It provides superior transit time-porosity correlation over the entire porosity range (0 to 100 pu).

2. It provides accurate porosities in unconsolidated, uncompacted sandstones without using a lack of compaction factor (Figures 13-27 a and b).

3. A single Δt_{ma} value is used for each lithology: 56 μsec/ft for sandstone, 49 μsec/ft for limestone, and 44 μsec/ft for dolomite.

Although the Raymer-Hunt transform is applied to all lithologies, it is best suited for unconsolidated, uncompacted sands. In carbonates it often gives porosity values that are a few pu too high, while the Wyllie transform gives the correct values (Figure 13-26). Both transforms have variables (C for Raymer-Hunt and Δt_{ma} for Wyllie), and log analysts differ on the most appropriate values for these variables. The problems associated with sonic porosity transforms further illistrate the superiority of the density tool.

Other Porosity Tools

Four other tools have been utilized to a limited degree as porosity tools. The tools are predominately used in petroleum logging or are being developed for this market.

The microlog was originally developed as a porosity tool. However, it soon became obvious that it was not suited for this task. The microlog was subsequently marketed as a permeability indicator. It is a good "permeability" log and numerous micrologs have been run in the Trinity aquifer through the years for this purpose. Unfortunately, porosity calculations from these logs are very tenuous. The **Recommended use** section under **NONFOCUSED PAD MICROELECTRODE TOOLS** in Chapter 8 elaborates on microlog porosity calculations.

The dielectric tool is a relatively new logging tool that uses electromagnetic energy to detect water-filled porosity. Only the major logging companies have the log and there are no slimhole versions. Two types of tools are available: a high frequency, shallow investigating (1 to 5 inches) pad device and a low frequency, deep investigating (15 to 45 inches) mandrel tool. Atlas Wireline uses the name Dielectric Log for both tools. Schlumberger calls their high frequency tool an Electromagnetic Propagation Tool (EPT) and their low frequency tool a Deep Propagation Tool (DPT). Collier (1989) is an assessment of the tool as a ground-water porosity log.

Theoretically, dielectric tools would be excellent porosity tools. They do not have radioactive sources, the dielectric response is not affected by the amount of compaction and consolidation of the rock, and low frequency tools can be run in nonmetallic casing. In practicality, however, they have serious limitations:

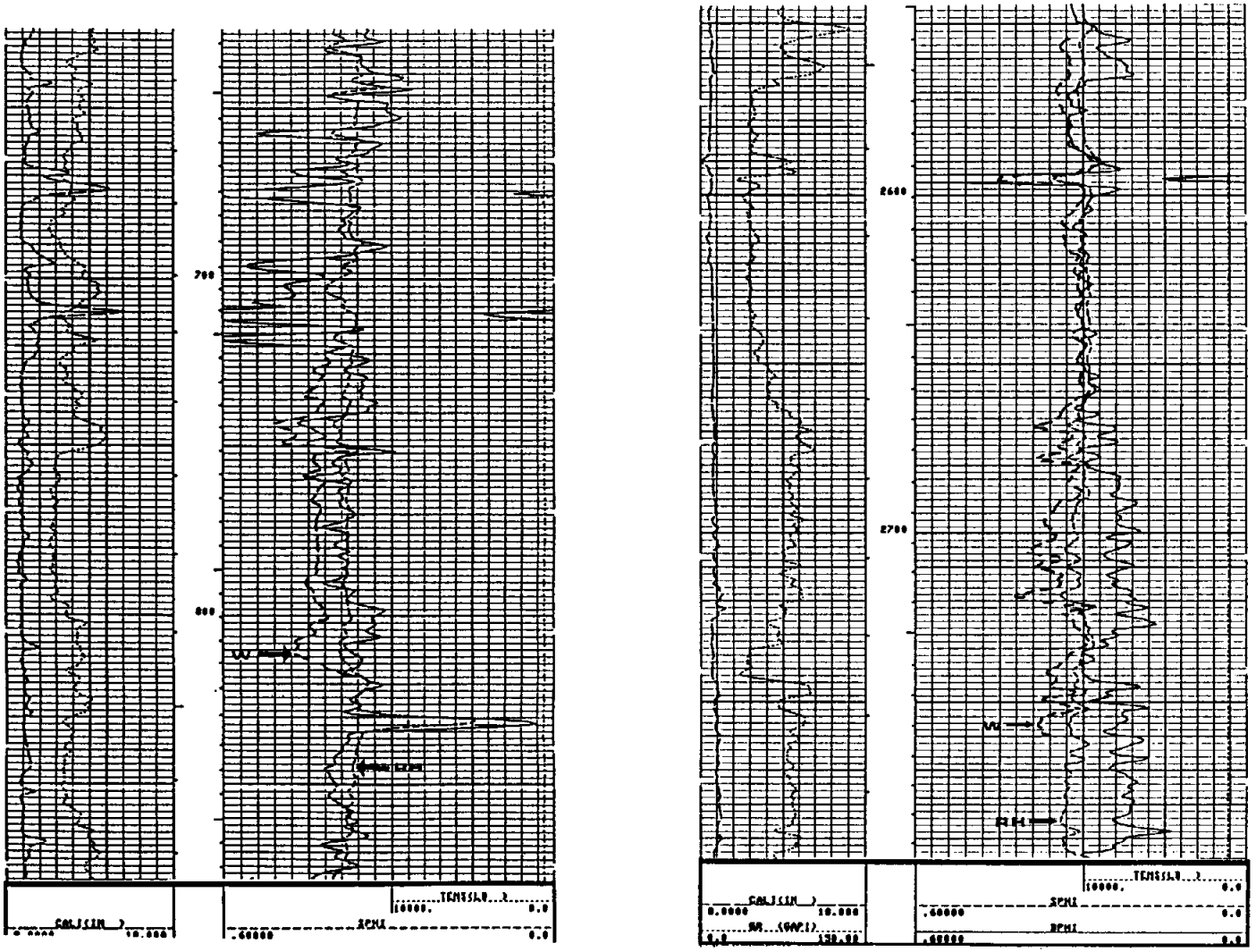

Figure 13-27 a & b. A comparison of the effect of compaction on porosities calculated with the Wyllie (W) and Raymer-Hunt (RH) transforms. At shallow depths (e.g. 750 to 790 feet) the Raymer-Hunt transform adequately corrects for a lack of compaction in the sandstones, while the Wyllie equation yields porosities that are too high. However, at deeper depths (e.g. 2600 to 2650 feet) the sandstones are compacted and both transforms calculate correct porosities. Density porosity is assumed to be true porosity. Figure 13-22 contains additional information on this well.

1. High frequency tools are severely affected by borehole rugosity (Figure 13-28).

2. Low frequency tools have a vertical resolution of about 8 feet.

3. The tools are not widely available, and low frequency tools are especially scarce.

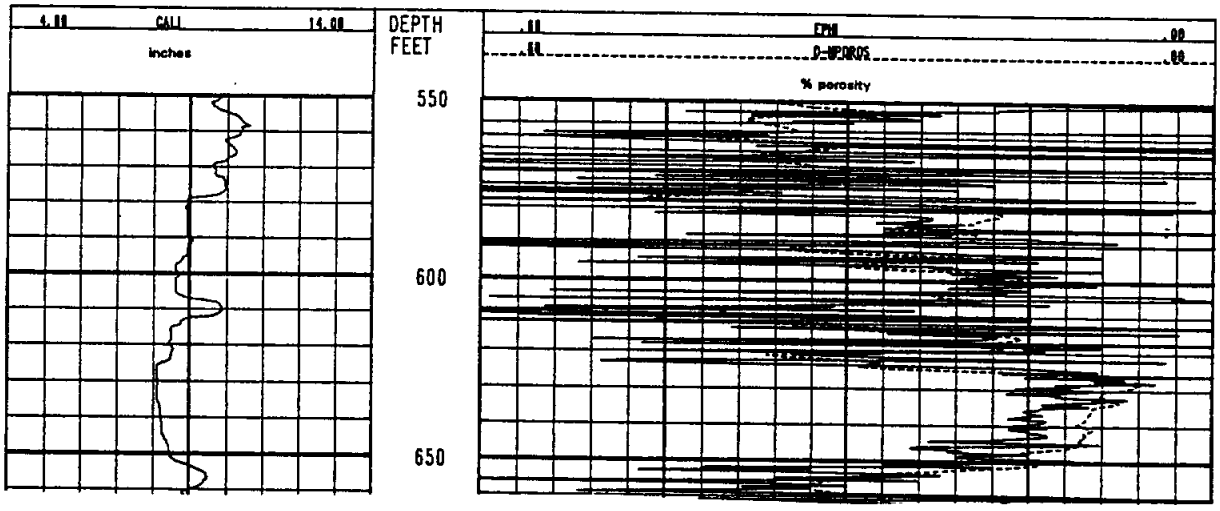

Figure 13-28. A comparison of porosity values calculated with an electromagnetic propagation tool (EPHI) and a density-neutron crossplot (D-NPOROS). The EPHI was calculated using a limestone matrix. The lithology is limestone and dolomite. Borehole rugosity is causing the spikes on the EPHI. Intervals with little borehole rugosity, such as the Regional Dense Member (626 to 646 feet), have fairly accurate EPHI values. The accuracy of the EPI values in this interval, which is a shaly limestone, could be improved by correcting for the effect of shale. The log is the Edwards Aquifer. Figures 9-22, 13-5, 13-8, 13-32, and 13-33 provide additional data on this well..

The Magnetic Resonance Imaging Log (MRIL) is presently under development as both a porosity and a permeability log. The tool utilizes spin-echo techniques to measure hydrogen content. The profile of the echoes relaxation is then transformed into a quantitative measure of porosity, free fluid porosity, and bulk-volume irreducible, a surface-to-volume index. In addition, the tool can make other measurements, including T1, the spin-lattice relaxation. T1 is strongly related to the permeability of a rock. Coates, et al. (1991) summarizes ground-water applications of the tool. Figure 13-29 is an example of the log.

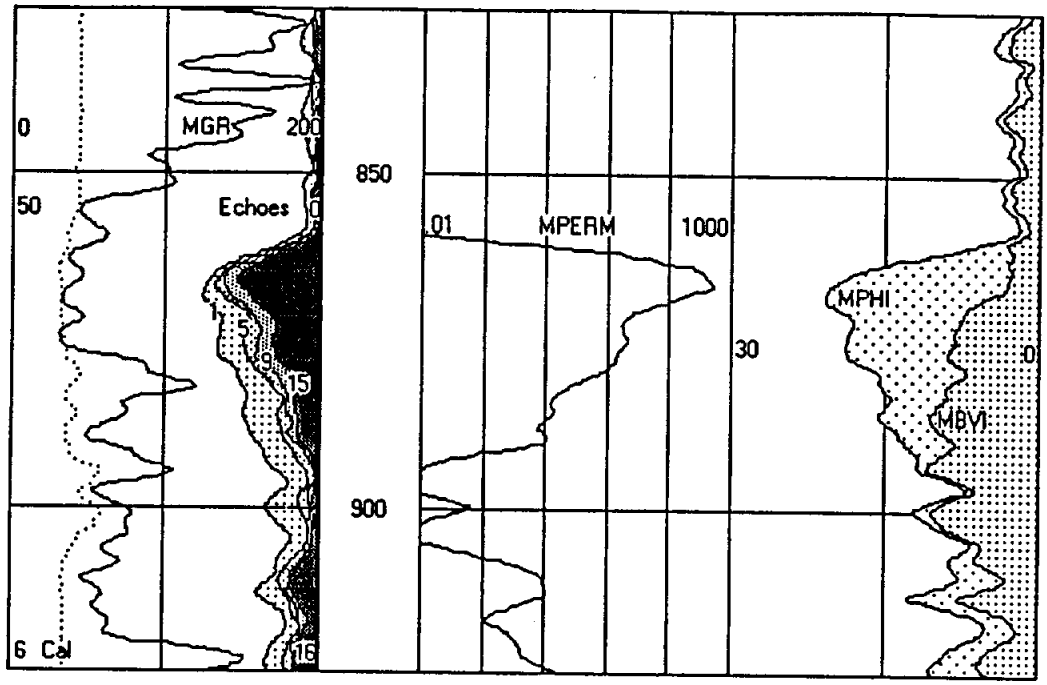

Figure 13-29. Magnetic Resonance Imaging Log (MRIL). Track 1 contains three curves: caliper (Cal), gamma ray (MGR), and amplitude of pulse-echoes (echoes). Echo spacings of 1, 5, 9, and 15 ms are recorded on a scale of 50 to 0.0 mv. Track 2 contains a calculated permeability curve (MPERM) plotted on a logarithmic scale of 0.01 to 1000 md. Track 3 contains two calculated curves: porosity (MPHI) and bulk-volume irreducible water (MBVI). The well is the Texas Water Development Board, Brady #2, McCulloch County, Texas (state well number 42-62-910). The formations are the Wilberns and Riley. The lithology is quartz sandstone with varying amounts of hematite, goethite, glauconite, calcite, dolomite, feldspars, and clay minerals. Bit size is 7⅞. Rm is 23.4 ohm-meters at 44° F and Rmf is 15.8 at 45° F.

An option for obtaining a limited number of discrete porosity measurements is wireline sidewall coring. Percussion and drilled sidewall tools are available. Recovery is sometimes poor in unconsolidated formations, and in low porosity sedimentary rocks, good recovery can only be obtained with drilled cores. Drilled sidewall cores yield accurate porosity and permeability values. The percussion coring process can significantly distort the pores of the samples. Permeability can be significantly altered,

either up or down, but porosity values are fairly accurate. Percussion sidewall cores analyzed for this project had porosity values within 3 pu of the log porosities (Figure 13-3 a and b). Sidewall cores can be thin sectioned and analyzed for such things as mineralogy, pore geometries, and qualitative permeability (Figures 13-30 and 13-31).

Figure 13-30. Photomicrograph of a thin section of a percussion sidewall core. The rock is a fossiliferous, calcite cemented, very fine to fine grained quartzarenite. Fossil fragments are the nuclei of the poikilotopic calcite. Calcite cementation has significantly reduced the porosity. Petrographic examination of the sidewall core explained why this zone has less porosity than surrounding sandstones (Figure 13-3). The sidewall coring process has fractured some grains and distorted the pore geometries. Porosity was impregnated with blue epoxy as part of the thin sectioning process. Magnification is 100x. The bar is 0.1mm.

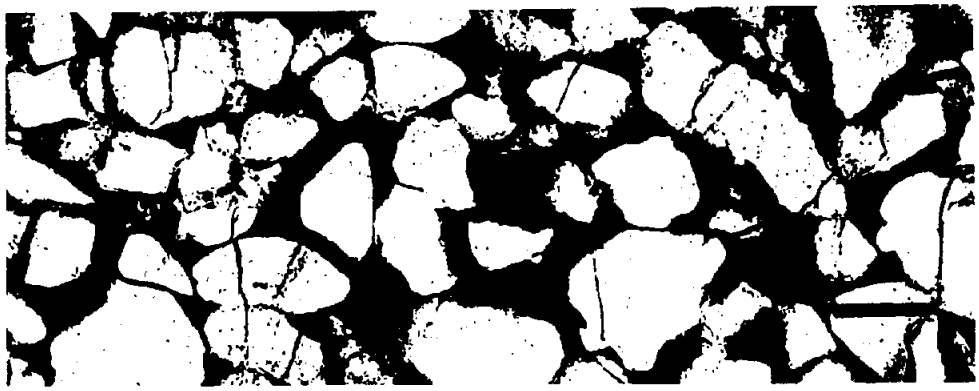

Figure 13-31. Photomicrograph of a thin section of a percussion sidewall core. The rock is a shaly, fine grained quartzarenite. Authigenic clay fills the pores and has significantly reduced permeability. Liquid permeability is 150 md. Sample depth is 3172 feet. The well is the J.L. Myers, Ladonia #2, Fannin County, Texas. Many of the grains were fractured by the coring process. Magnification is 100x. The bar is 0.1mm.

Porosity Crossplots

All porosity tools are affected by lithology, with each tool responding differently to a particluar lithology. This complicates single-log porosity calculations when the lithology is unknown and/or two or more mineralogies are present. However, if two or more porosity logs are available, these same differences can be utilized in a crossplot of the two measurements to solve for porosity and lithology.

Porosity crossplots are available for all of the various two-tool and three-tool combinations. Two-tool crossplots are the more common type, with density-neutron crossplots (Figure 13-32) the most common. All major logging companies and all comprehensive log analysis computer programs have crossplot charts.

The following guidelines should be observed when using porosity crossplots:

1. Crossplo
only be u
2. Neutron
limestone
3. Sonic po
4. Density porosity is input as apparent limestone porosity or as ρ_b.

page 341 -- last sentence on this page: The phrase "than can be gleaned" has to refer back to something else in the sentence -- Joe tried to add in something for it to refer back to. (The author may have a better choice than my wording on this, I prefer to use "as presentation" as that change).

3. Two-tool crossplots can only discriminate two-mineral mixtures; three-tool crossplots can identify three.

4. Two-tool crossplots cannot identify which two minerals comprise the mixture (i.e. the lithology could be dolomite/sandstone or dolomite/limestone). However, a general knowledge of the local geology usually allows one of the possibilities to be chosen as the most plausible one.

pair and and

Figure 13-32 is a density-neutron crossplot of an Edwards Aquifer well. The lithology is limestone and dolomite, with minor amounts of chert and shale. Figure 13-33 is a more useful presentation of the data than can be gleaned from the density-neutron crossplot in Figure 13-32.

and provides more information

A quick substitute for a two-tool porosity crossplot is to plot the two porosity curves on the same log at the same scale using the same matrix (Figure 13-8). When the curves overlay, the lithology is the same as that used in the porosity calculation. The curves separate as the lithology varies, and often the lithology can be identified by the direction and amount of separation. The mid-point between the two curves is a good approximation of true porosity when porosity is greater than 10 percent (Hilchie, personal communication, 1992).

Porosity crossplots are a very powerful lithology indicator and a great aid in determining accurate porosity values. They are one of the best reasons for running calibrated porosity tools.

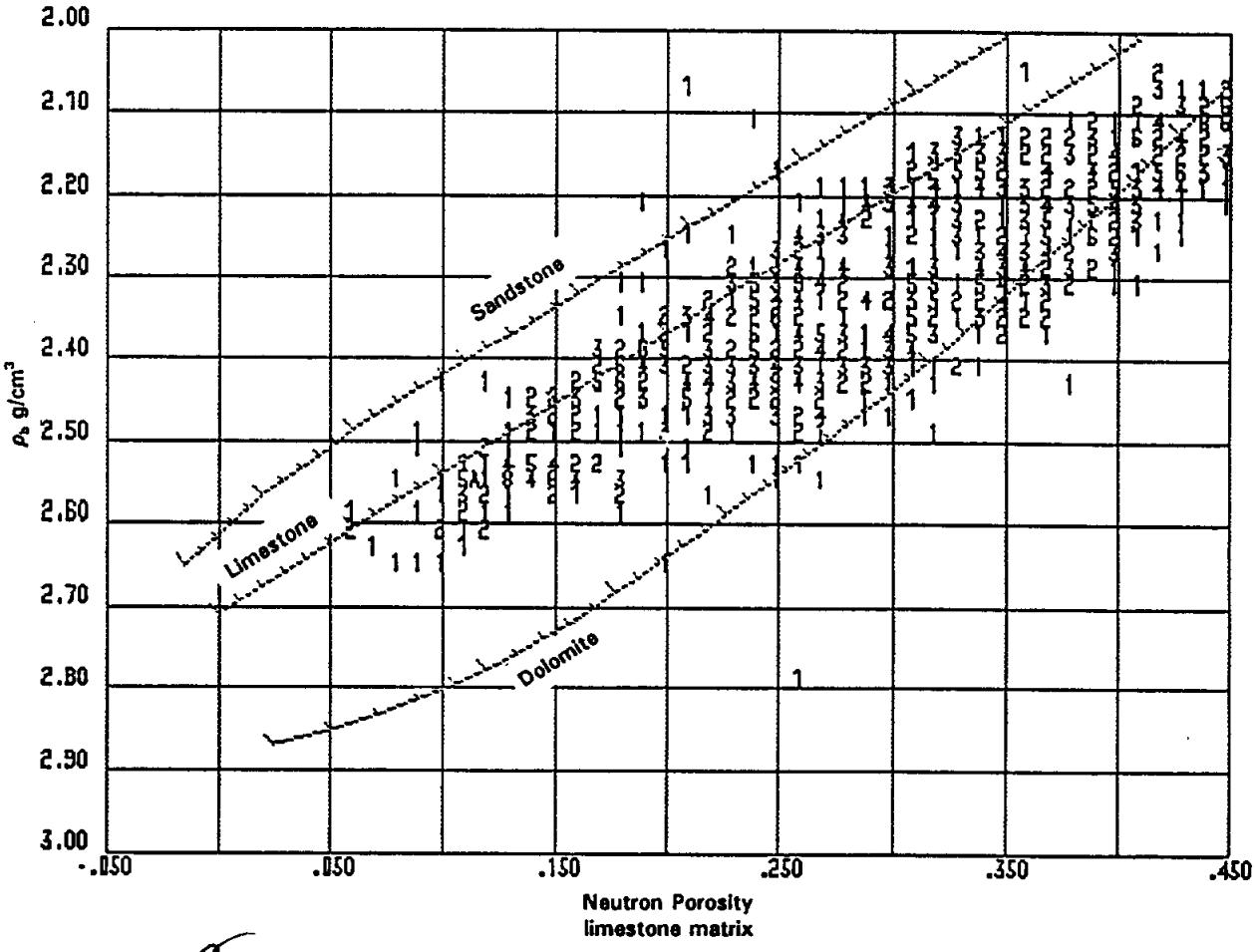

Figure 13-32. A density-neutron crossplot. The sampling interval is 0.5 feet. The numbers on the graph denote the occurrences of a particular point. The lithology is predominately limestone, dolomite, or a mixture of the two. Minor amounts of shale and chert are also present. Points that plot at isolated extremes are either other mineralogies or erroneous measurements. The well is the Edwards Aquifer. Figures 9-22, 13-5, 13-8, 13-28, and 13-33 provide additional data on this well.

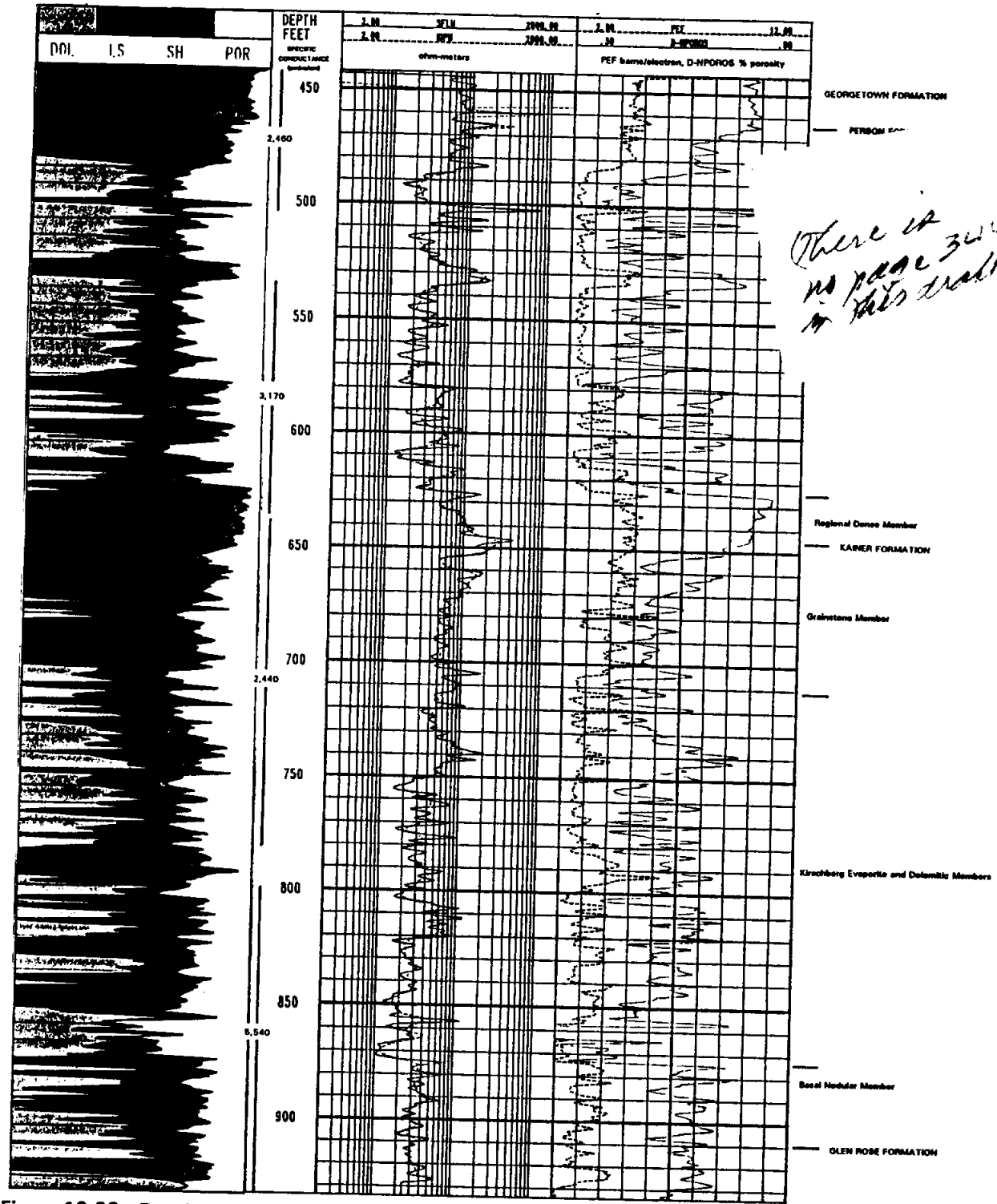

(There is no page 344 in this draft)

Figure 13-33. Density-neutron crossplot porosity and lithology calculated from the porosity logs. Track 1 contains a lithology-porosity column calculated from the density, neutron and gamma ray logs. Track 2 contains unaveraged spherically focused (SFLU) and deep phasor induction (IDPH) logs. Track 3 contains photoelectric factor (PEF) and density-neutron crossplot porosity (D-NPOROS) curves. The depth column contains depth intervals and specific conductances of selected water samples collected during the drilling. Formation and member boundaries are marked to the right of Track 3. The log is the Edwards Aquifer. Figures 9-22, 13-5, 13-8, 13-28, and 13-32 provide additional data on this well.

TECHNIQUES FOR CALCULATING Cw AND TDS FROM LOGS

Chapter 14

Assessment of ground-water quality usually centers around measurements of total dissolved solids (TDS) and specific conductance (Cw). Well logs are used to calculate Cw and then TDS is estimated from previously established TDS-Cw graphs. Sometimes other water properties such as chloride content and total hardness can be estimated from similar graphs. In some cases, TDS can be estimated directly from the log data. Unfortunately, trace elements such as iron, fluoride, and nitrates cannot be detected.

While it has been documented in other studies that determination of Cw and TDS from logging data is feasible (Chapter 1), many ground-water researchers have had little success applying the techniques. Both the cause and effect of this is the fact that most ground-water logging literature has only a cursory discussion of the subject.

This chapter is a discussion of seven techniques for calculating Cw and TDS from logging data. The first three (TDS-Ro Graphs, Ro_c-TDS Graphs, and Field Formation Factor) are empirical relationships that must be derived from the available data in a localized geographic areas (e.g. a county). The last four (Formation Factor Equation, Ro-Porosity Graphs, Resistivity Ratio Method, and SP) are stand-alone techniques that calculate Rw. This chapter also contains guidelines for accurate Cw calculations and a discussion of sources of logs in Texas.

Considerable variation exists in the logging literature for two terms important to this discussion. When reading logging literature, one should remember that:

1. Water that naturally saturates a formation is referred to as **formation water, connate water,** or **interstitial water.** The term formation water is used herein.

2. The term water resistivity (Rw), not water conductivity (Cw), is used in virtually all logging literature. This chapter also uses Rw. The relationship between the two terms is discussed in Chapter 2 and is restated here:

$$Rw\ (ohm\text{-}m) = \frac{10{,}000}{Cw}\ (\mu mhos/cm) \qquad (12\text{-}1)$$

GUIDELINES FOR Cw and TDS CALCULATIONS

The accuracy of Cw and TDS calculations will be greatly improved if:

1. The logging tools are suitable for the borehole conditions and the petrophysical properties of the aquifer being analyzed.

2. The technique for calculating Rw is compatible with the chemical composition of the water being analyzed and the available log data.

3. The logging data are accurate.

Suitable Tools and Techniques

Logging tools and water quality calculation techniques must be selected according to the chemical composition of the ground water, the petrophysical properties of the aquifer, and the borehole conditions. The choice of logging tools, especially for resistivity tools, has considerable bearing on the accuracy of the data. It also determines which analytical techniques can be used. It is essential for one to be familiar with the applications and limitations of the various resistivity tools (Chapters 8 and 9) and to remember that:

1. Most logging tools and techniques are designed for clean (shale-free), "normal" sedimentary rocks (quartz-rich sandstones, limestones, and dolomite). Analysis of shaly formations may require modifications to the techniques.

2. All resistivity tools are not created equal. They must be compatible with the type of aquifer and borehole being logged. For example, induction tools are not the best choice for logging aquifers with resistivities greater than 100 ohm-meters and/or zones (beds or porous intervals) less than 5 to10 feet thick. Guard or Latero tools provide better vertical resolution and more accurate resistivity values in such circumstances (Chapters 8 and 9).

3. The SP curve is good for quantitative work only in thick, clean sands. SP values are too low if the formation (sandstone or carbonate) is thin, shaly, highly resistive, or deeply invaded (see Guyod, 1966; Alger and Harrison, 1988; Sciacca, 1989; Chapter 12).

4. Most of the techniques for determining ground-water quality utilize either an SP or a deep resistivity curve. The techniques have been borrowed, with little or no modification, from the petroleum logging industry. Application of the techniques to ground-water studies has largely been unsuccessful because oilfield waters are radically different from ground waters. Petroleum logging techniques assume that formation waters have high salinities (more than 50,000 ppm TDS) with predominately monovalent NaCl ions. Ground waters, on the other hand, usually have much lower salinities and a significant concentration of divalent calcium and magnesium ions. The responses of SP and resistivity tools must be interpreted differently for each of the two water types (Chapter 12).

Accurate Log Data

Log data accuracy is a major area of weakness for the ground-water logging industry. The petroleum logging industry has devoted considerable attention to data accuracy (see any detailed logging text and in particular Helander, 1983; Bateman, 1985). Unfortunately, this expertise has not been sufficiently utilized by the ground-water industry. Ground-water logging articles that mention the subject provide little in the way of guidelines for correcting log values.

Log data accuracy was addressed as each tool was discussed in Chapters 8 to 13. The subject is so critical to Cw and TDS calculations that a few points need to be reemphasized:

1. The accuracy of log data will be greatly improved by running a logging suite which is compatible with the borehole conditions and the petrophysical properties of the aquifer.

2. Resistivity values may require corrections for bed thickness, borehole diameter, mud resistivity, and mud filtrate invasion (Chapters 8 and 9).

3. Tool calibration and quality control are essential for obtaining valid data. Merkel and Snyder (1977), Hallenburg (1980), Hill (1986), Hodges (1988), Collier (1988), and Sciacca (1989) discuss various aspects of these two important subjects.

4. The correct assumption must be made about what part of the borehole a particular resistivity tool is investigating. Most Cw and TDS calculations utilize Ro, which in water wells is equivalent to Rt. Variations in logging tool responses and borehole conditions mean that R_o is not always what is being measured. Either deep mud filtrate invasion (not likely to occur in shallow and/or highly porous clastic aquifers) or insufficient depth of investigation by the resistivity tool (more likely to be the case) is usually the reason an incorrect value is used for R_o. The Resistivity Ratio Method requires both R_o and R_{xo} (the resistivity of the flushed zone). In the case of R_{xo}, the resistivity tool is supposed to measure a thin zone very close to the borehole wall. If the tool reads too deep or too shallow, the resistivity will not be R_{xo}.

ACQUIRING LOGGING DATA

Fresh Water Aquifers

When studying the fresh water portion of Texas aquifers, most of the logs will be from water wells and most of the wells will have at least one water analysis. Virtually none of the logs will be hydrocarbon tests. Oil companies are required to set surface casing through fresh water aquifers and they generally do not log before setting surface casing. Openhole logs run through casing cannot be used to determine water quality.

Water well borehole geophysical logs are scattered around the ground-water industry. Unfortunately, there is no single, easily accessible source. The following firms are sources of logs:

1. **Texas Water Commission, Central Records, Ground-Water Technical File.** This is the largest collection of water well logs in Texas. Water well drilling contractors sometimes submit logs on a voluntary basis, so coverage is by no means complete. Data are filed by county and by complete or partial state well number. Without a state well number, data on a particular well are not

easily accessible. It can be very time consuming to track down large numbers of logs.

2. **Texas Water Commission, Water Rights and Uses Division, Surface Casing Unit.** This file consists mainly of oilfield logs. However, it does contain a small number of fresh-water logs. Some are logs from water wells, the rest are oilfield logs that penetrated fresh water formations.

3. **Water well drilling contractors.** Irrigation and domestic wells are rarely logged. Conversely, virtually all municipal, rural water supply, and industrial wells are. Drilling contracts usually contain a clause requiring borehole geophysical logs. Drilling companies meet the requirement by subcontracting to a logging service company. Drilling contractors generally retain copies of these logs. The older drilling firms have amassed extensive log files. Access to the logs varies from company to company.

4. **Ground-water consulting firms.** These firms have a limited number of logs and generally consider their data proprietary.

5. **Petroleum Information Corporation (PI).** PI is the main broker for oilfield logs. They carry some water well logs, but the logs are not identified as such. Water well drilling contractors do not routinely release their logs to PI. They only release the ones that PI requests, which are usually the wells logged by the major commercial logging companies. Consequently, PI carries only a small percentage of available water well logs.

6. **Logging companies.** Major logging companies, except for Schlumberger, retain their logs for only a few months. Schlumberger started archiving tapes of logging jobs as of 1987. Presently, about 50 percent of all jobs are archived (at no fee to the client). The client may request that a logging job be archived. If the client releases the data, anyone can purchase a copy of the tape. However, Schlumberger does not archive hard copies of the logs and it takes sophisticated logging software to make a hard copy from a tape. Smaller logging companies sometimes keep hard copies of all their logs (e.g. Tejas). However, they do not make a practice of furnishing copies of the logs in their files. In

fact, the logs archived by any logging company are proprietary and cannot be released without the consent of the client.

Saline Water Aquifers

Log coverage of the saline water portions of Texas aquifers is much more complete. In fact, too much data will be the problem in some of the petroleum-producing areas of the state. The majority of the logs will be from hydrocarbon tests and very few of the logs will have accompanying water analyses. When searching for logs, one should check the following sources:

1. **Petroleum Information Corporation (PI).** PI is the premier source of oilfield logs. They sell copies of the logs, or one may borrow logs from a PI log library.

2. **Petroleum log libraries.** Scattered around Texas are numerous public and private membership petroleum log libraries. Some libraries cover the entire state, while others only cover a particular geographic area. In public log libraries, logs can be examined in-house for a flat per-day fee or they may be checked out by members.

3. **Texas Water Commission, Water Rights and Uses Division, Surface Casing Unit.** This agency has over 250,000 logs from throughout the state. The logs are filed by county and are keyed to county land/ownership maps. It is easy to locate logs from a particluar geographic area. Logs may be copied from the file, though lending logs is not a normal function of the agency.

4. **Bureau of Economic Geology, Geophysical Log Facility.** This agency is the repository for oilfield logs collected by the Railroad Commission. Since 1986, oil companies have been required to submit a log for each new well. The regulation is worded so that any wireline log is acceptable. Thus, the log which is sumbmitted may be of a type that is of no value for water-quality calculations. The regulation further states that the log must be of the producing interval. Some operators, therefore, submit a partial log, rather than a log of the entire borehole. The end result is that many of these logs may not be suitable for ground-water studies. The Geophysical Log Facility also has a large number of pre-1986 logs.

These logs are from the Railroad Commission and the Bureau of Economic Geology files.

5. **Ground-water firms.** Water well drilling contractors and ground-water consulting firms have few such logs.

EMPIRICAL RELATIONSHIPS FOR ESTIMATING TDS AND RW

TDS-Ro Graphs

Under ideal conditions, it is possible to accurately estimate TDS directly from an Ro value. An Ro value is plotted on a previously established TDS-Ro graph and the corresponding TDS value is read directly off the graph. The procedure is as follows:

1. Construct a TDS-Ro graph using data from wells closest to the well being analyzed. Ideally, the data should also be from the same stratigraphic unit. In reality, well control is usually sparse and the stratigraphy of any aquifer(s) from which water samples were analyzed is not always identified . For these reasons, the data collected during this project (Volume II, Section 5) were processed by counties. Data plotted by counties often has a high correlation coeffecient because the majority of the wells are from the same aquifer (Figure 14-1).

2. Logarithmic scales are recommended. They allow a wider range of values to be plotted on a single graph (Figures 14-1 and 14-2) and the curve fit is a straight line.

3. The deepest reading resistivity curve (64" normal, deep induction, lateral, or deep laterolog) is used for Ro.

    a. An average Ro value is selected for the aquifer. Figures 8-25, 8-26, and 9-21 discuss how to select average resistivity values. If there is more than 10 percent variation in the resistivity of the zone, it may be worth plotting the highest and lowest average values, Ro High (Ro_H) and Ro Low (Ro_L). This was done, as necessary, for the graphs in Volume II, Section 5.

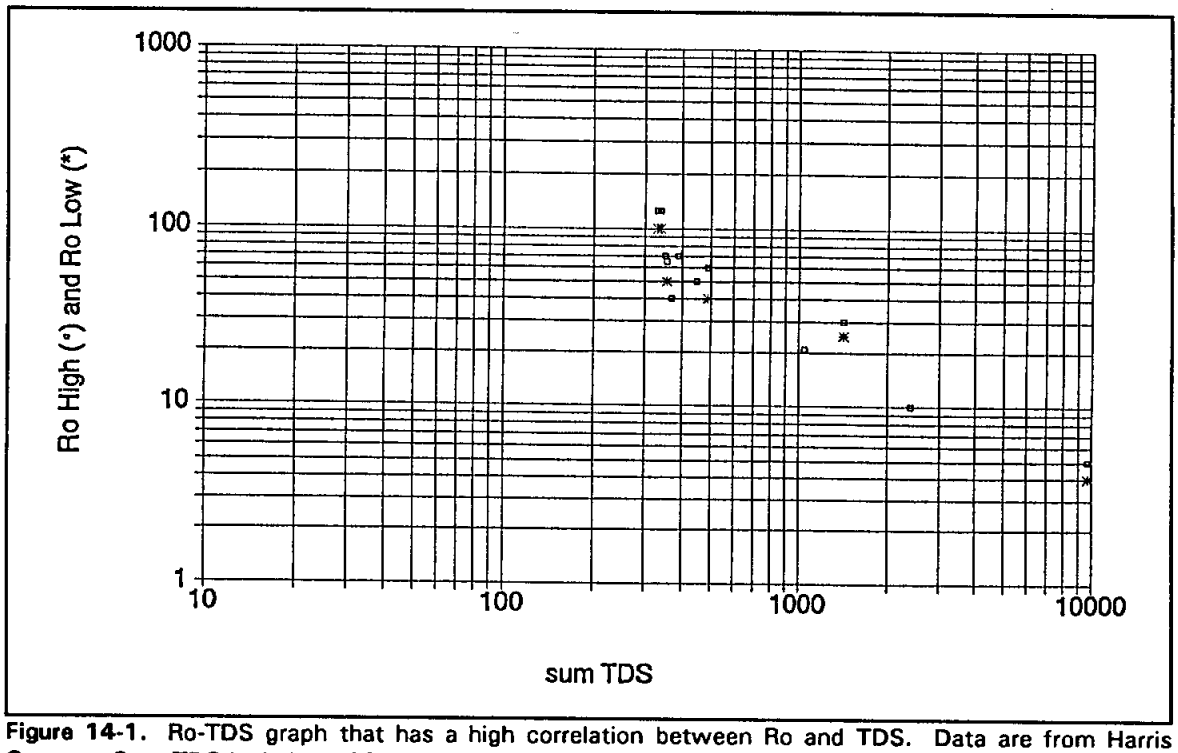

Figure 14-1. Ro-TDS graph that has a high correlation between Ro and TDS. Data are from Harris County. Sum TDS includes 100 percent of the bicarbonate value.

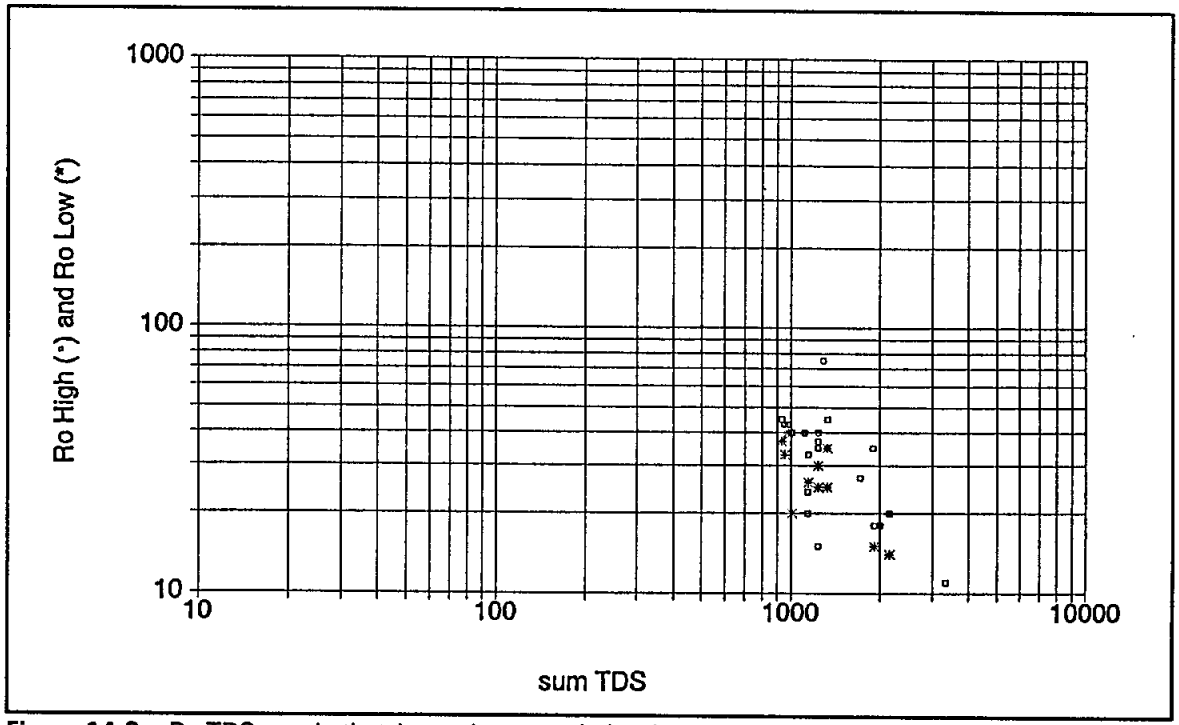

Figure 14-2. Ro-TDS graph that has a low correlation between Ro and TDS. Data are from Dallas County. Sum TDS includes 100 percent of the bicarbonate value.

b. If borehole conditions warrant, an environmental correction should be made to the resistivity value on the log (Ra) before it is used as Ro and plotted on the graph. (Chapters 8 and 9 discuss environmental corrections for each resistivity tool.)

4. TDS values should include 100 percent of the bicarbonate value.

5. A line-fitting routine can be applied to the data, but is not necessary. If there is much scatter, the equation of the line does not give an accurate TDS value. It is better to simply plot new Ro values on the graph and to look at the range of corresponding TDS values (Figure 14-2).

This technique has one serious limitation: it requires Ro values to be solely a function of water salinity (TDS). This condition exists only in shale-free sandstone aquifers that have approximately the same porosity. Such conditions normally are approximated only in sandstones that are consistent in lithology, unconsolidated to semi-consolidated, Tertiary or younger, and less than about 1000 feet deep (aquifers such as the Gulf Coast and Carrizo-Wilcox). Sandstones from the same depositional facies and a limited geographical area give the best correlation.

TDS-Ro graphs do not work as well for consolidated sandstones and carbonates such as the Trinity, North-Central Texas Paleozoic formations, Edwards, and Ellenburger. Several of the graphs in Section 5 of Volume II substantiate this fact. Figure 14-2 is an example of a poor correlation. In these types of aquifers porosity can vary considerably within a well and from well to well. In such cases, Ro is a function of both porosity and TDS, so there is no consistent correlation between Ro and TDS. The water quality calculation must account for the effect of porosity on Ro (Ro_c-TDS Graphs, Field Formation Factor, Water Saturation Equation, and Ro-Porosity Graphs) or factor it out (Rxo-Ro Ratio).

Few Ro-TDS graphs have been published. Guo (1986) and Fogg and Blanchard (1986) are the only examples this author found. Guo applied the technique to Quaternary alluvial sand aquifers in the North China Plain (Figure 14-3). The one graph that he published does have a high correlation between TDS and Ro values.

Fogg and Blanchard constructed a TDS-Ro graph for the Carrizo-Wilcox aquifer system in the Sabine Uplift area of Texas (Figure 14-4). The correlation is only fair (0.80) and the graph is a good example of the inaccuracy of this technique. An Ro of 30 ohm-meters could represent a TDS anywhere from 300 to 1400 mg/l and a TDS of 1400 mg/l could have an Ro ranging from 10 to 40 ohm-meters. The scatter is probably due, in large part, to variations in porosity. Grouping the data according to smaller geographical areas would probably improve the correlation. Also, the graph would be much easier to interpret if the data had been plotted as whole numbers.

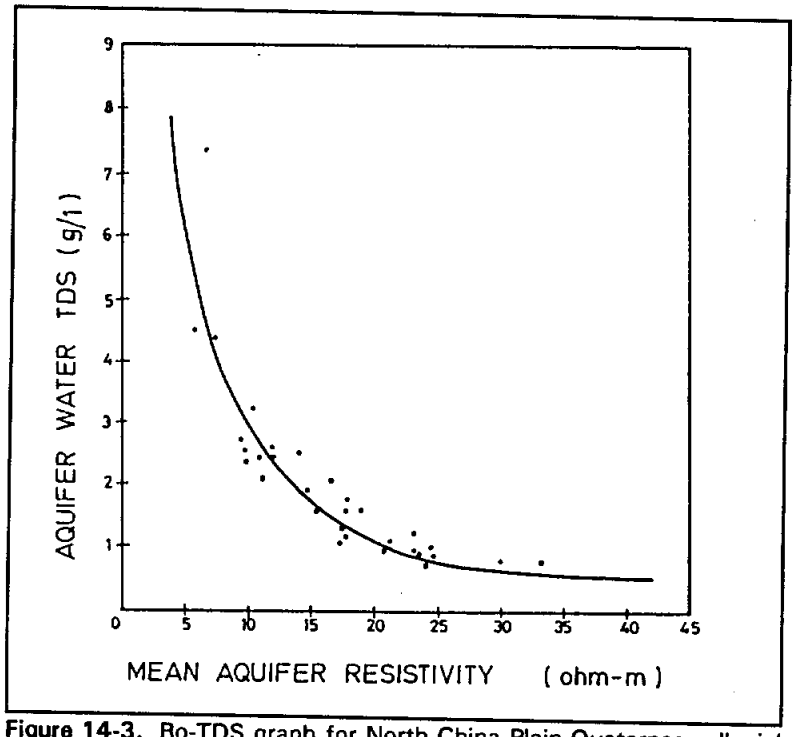

Figure 14-3. Ro-TDS graph for North China Plain Quaternary alluvial sands (Guo, 1986). g/l x 1000 = mg/l

Ro-TDS graphs were constructed from the data base assembled for this project. Ro values are from Section 3 and TDS values are from the Sum TDS column of Section 2 of Volume II. The data was plotted by counties. Forty-eight counties had enough data for a graph (Volume II, Section 5, Figures 5-1 to 5-48). Each graph contains 2 to 20 data sets.

Thirty-six graphs had sufficient data to judge the quality of the curve fit: 33 percent (Brazos, Cherokee, Denton, Ellis, Harris, Hidalgo, Hunt, McMullen, Milam, Rusk, Shelby, and Wood) had a good fit, 47 percent (Anderson, Angelina, Collin, Dallas, Dimmit, El Paso, Fannin, Freestone, Gonzales, Grayson, Jefferson, Montgomery, Nacogdoches, Smith, Tarrant, Upshur, and Van Zandt) had a fair fit, and 20 percent (Erath, Karnes, Robertson, Limestone, McLennan, Red River, and Walker) had a poor fit. The graphs are from four major Texas aquifers: Carrizo-Wilcox, Trinity, Gulf Coast, and Bolson Deposits. The Trinity has the highest percentage of poor curve fits, but it does have three counties with good curve fits.

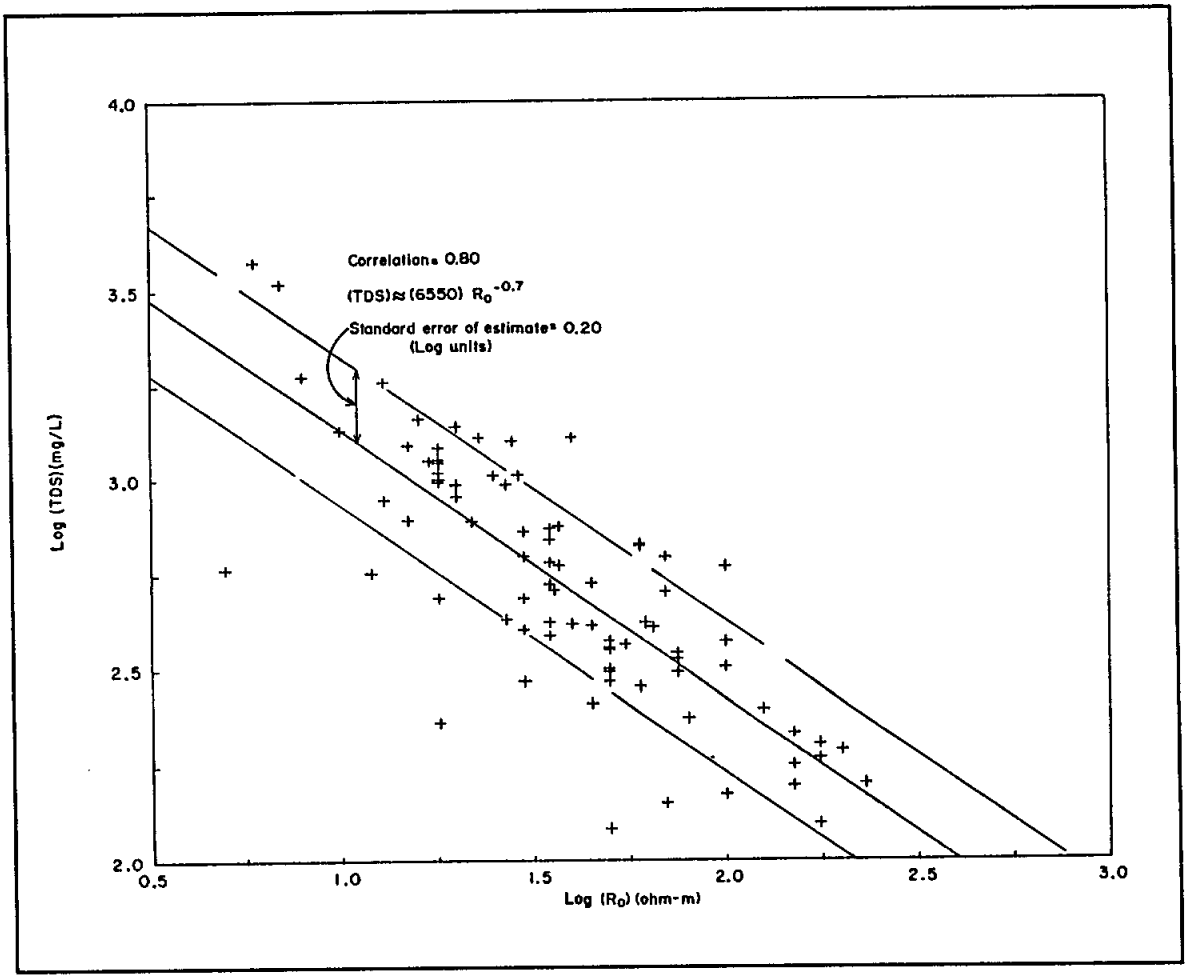

Figure 14-4. Ro-TDS graph for the Carrizo-Wilcox aquifer system, Sabine Uplift area. Ro values are from 64" normal and induction logs. Data are from water wells that are screened primarily in channel-fill sands at depths of 200 to 1,200 feet (Fogg and Blanchard, 1986). There is considerable scatter in the data. The graph would be much easier to interpret if the data had been plotted as whole numbers.

Of the twelve counties with good curve fits, nine have parallel curve fits (Figure 14-5). However, the variations in the curve fits underscore the fact that Ro-TDS graphs are site-specific and should be used with caution.

For thirty counties the data distribution was such that the Ro value(s) corresponding to 1,000 mg/l TDS could be determined from the Ro-TDS graph. Five counties had sufficient data to determine the Ro value corresponding to 10,000 mg/l TDS. Table 14-1 is a compilation of the Ro values. The data distribution for some counties was such that it was necessary to include a range of Ro values, rather than a single Ro value, in the table.

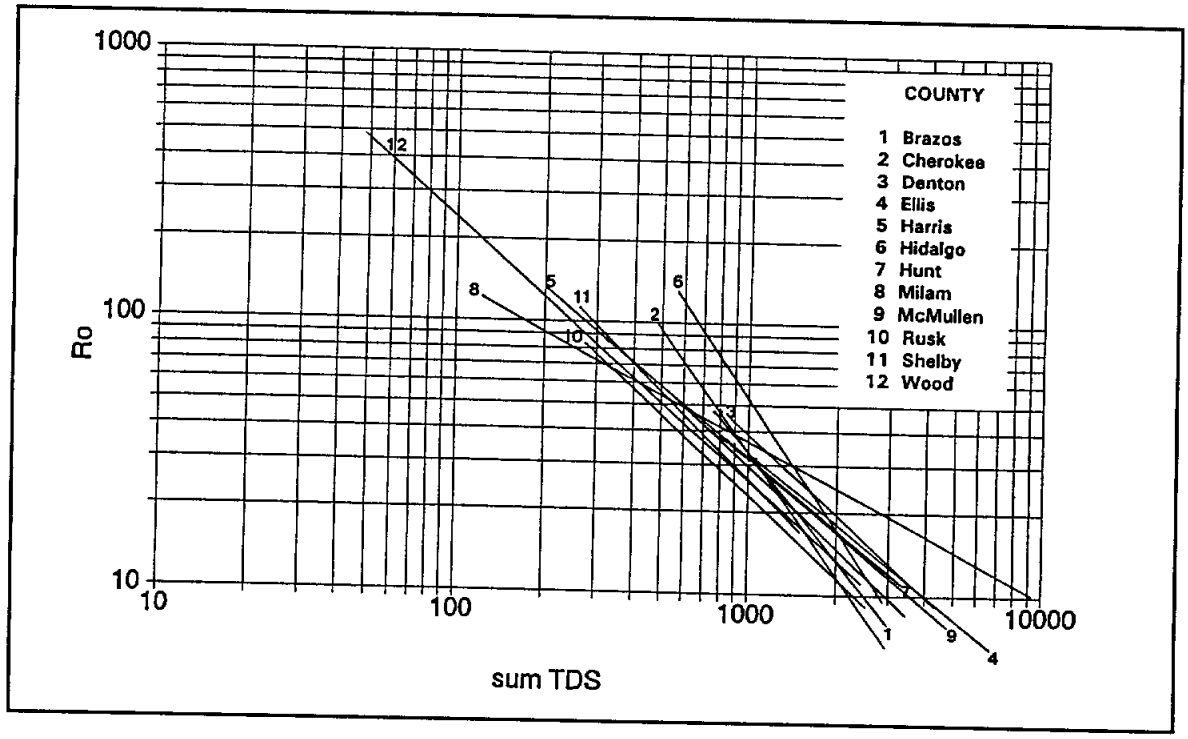

Figure 14-5. Curve fits for the Ro-TDS graphs of 12 counties. The graph of each county is in Volume II, Section 5. The correlation for each county was good, so the curve fits were "eyeballed".

Table 14-1 shows that for a TDS of 1,000 mg/l, Ro values vary considerably (15 to 45 ohm-meters). However, when grouped by aquifers, the Ro values show fairly consistent patterns. In the case of the Carrizo-Wilcox, an additional grouping by geographic area further enhanced the consistency. Ro values for 10,000 mg/l TDS, while ranging from 1 to 10 ohm-meters, are usually less than 2 ohm-meters. Table 14-1 further underscores the site-specific nature of this technique. It illustrates that using an Ro cutoff for determining a particular water salinity will usually be valid only in a limited geographic area.

When the aforementioned guidelines are followed, Ro-TDS graphs can be used with a limited amount of success to estimate TDS. The graphs are site-specific and should always be used cautiously.

Ro_c-TDS Graphs

When an aquifer extends to depths of several thousand feet, variations in Ro values at widely different depths will be, to some degree, due to the fact that formation temperature and porosity vary with depth. Alger (personal communication, 1988) proposed that the correlation

TABLE 14-1. Ro VALUES CORRESPONDING TO TDS'S OF 1000 AND 10,000 MG/L ON COUNTY Ro-TDS GRAPHS

Aquifer/County	Ro ohm-meters for 1000 mg/l TDS	Ro ohm-meters for 10,000 mg/l TDS
Huecho Bolson Aquifer		
El Paso	15	-
Carrizo-Wilcox Aquifer (North)		
Anderson	18 to 40	-
Angelina	15	1 to 2
Cherokee	20	-
Gregg	20	-
Nacogdoches	30	-
Rusk	18	-
Shelby	25	-
Smith	25	-
Wood	25	-
Carrizo-Wilcox Aquifer (Central)		
Brazos	30	-
Burleson	30	-
Freestone	40	-
Gonzales	35	-
Leon	25	-
Milam	30	10
Carrizo-Wilcox Aquifer (South)		
McMullen	30	-
Gulf Coast Aquifer		
Harris	20 to 40	5
Hidalgo	-	2 to 3
Jefferson	20	2
Kleburg	25	-
Trinity Aquifer		-
Collin	30	-
Dallas	40	-
Denton	25 to 45	-
Ellis	25 to 35	-
Fannin	45	-
Grayson	30 to 40	-
Hunt	28	-
McLennan	45	-
Tarrant	40 to 45	-

coefficient of the corresponding Ro-TDS graph could be improved by using Ro values normalized or corrected for variations in porosity and/or formation temperature. The corrected Ro value is designated Ro_c.

The temperature correction normalizes Ro values, which are at formation temperature, to equivalent Ro values at 77° F (designated as Ro_c). The procedure is as follows:

1. A geothermal gradient must be established. It can be calculated for each well or an area-wide value can be used. Most counties in Texas have geothermal gradients of 1.0 to 2.5°/ 100 feet. Columns 3 and 4 of Section 3, Volume II, list geothermal gradients for counties studies during this project. The Explanation section of Section 3 documents the geothermal gradient calculation and explains the problems associated with calculating a geothermal gradient from the bottom hole data available for many water wells.

2. The geothermal gradient is used to calculate the temperature at the depth at which Ro was measured. The equation for this calculation is listed in the explanation for Column 7 in Section 3, Volume II.

3. Ro is normalized to Ro at 77° F (Ro_c) by substituting formation temperature into Equation 2-4.

4. Ro_c is plotted versus TDS.

Temperature corrections can be made to Ro values from any type of aquifer. Alger (personal commmunication, 1988) suggested that they would be helpful when an aquifer extends below 1000 feet.

This study found that normalizing Ro values to a common temperature (77° F) did nothing to improve the curve fit of Ro_c-TDS graphs over that of the corresponding Ro-TDS graphs. This was true even for Ro values from depths of up to 4,000 feet.

Temperature corrections using both site-specific and county-wide geothermal gradients were applied to all the wells in this study (Section 3 of Volume II). Many of these wells had Ro values from depths of 2,000 to 4,000 feet. Ro_c-TDS graphs utilizing county-wide geothermal gradients were prepared for all 48 Ro-TDS graphs (Figures 14-6 and 14-7 are examples).

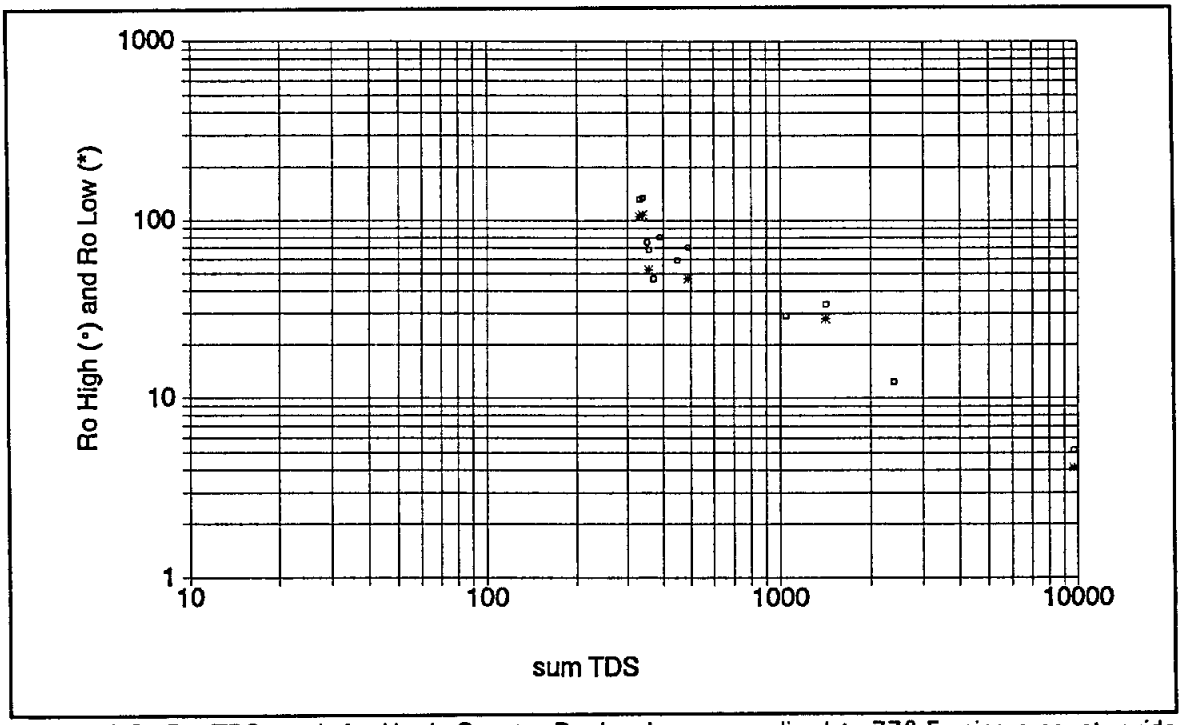

Figure 14-6. Ro_c-TDS graph for Harris County. Ro_c has been normalized to 77° F using a county-wide geothermal gradient. The curve fit is no better than that of the Ro-TDS graph (Figure 14-1).

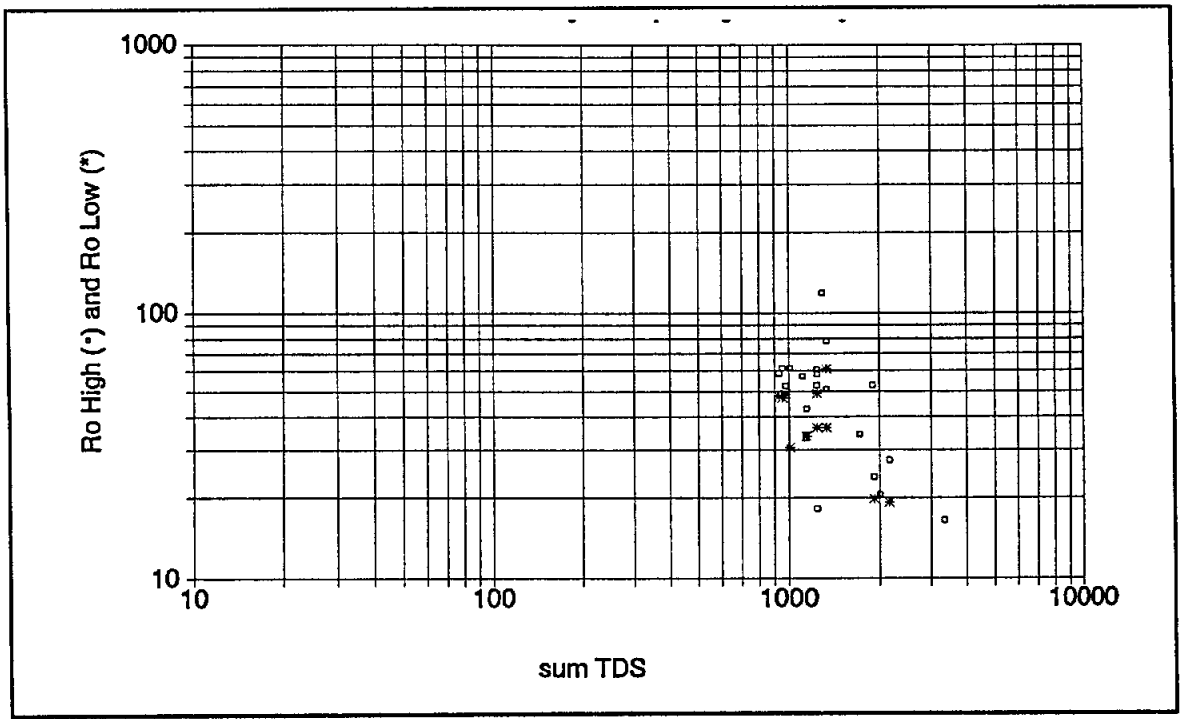

Figure 14-7. Ro_c-TDS graph for Dallas County. Ro_c was normalized to 77° F using a county-wide geothermal gradient. The curve fit is no better than that of the Ro-TDS graph (Figure 14-2).

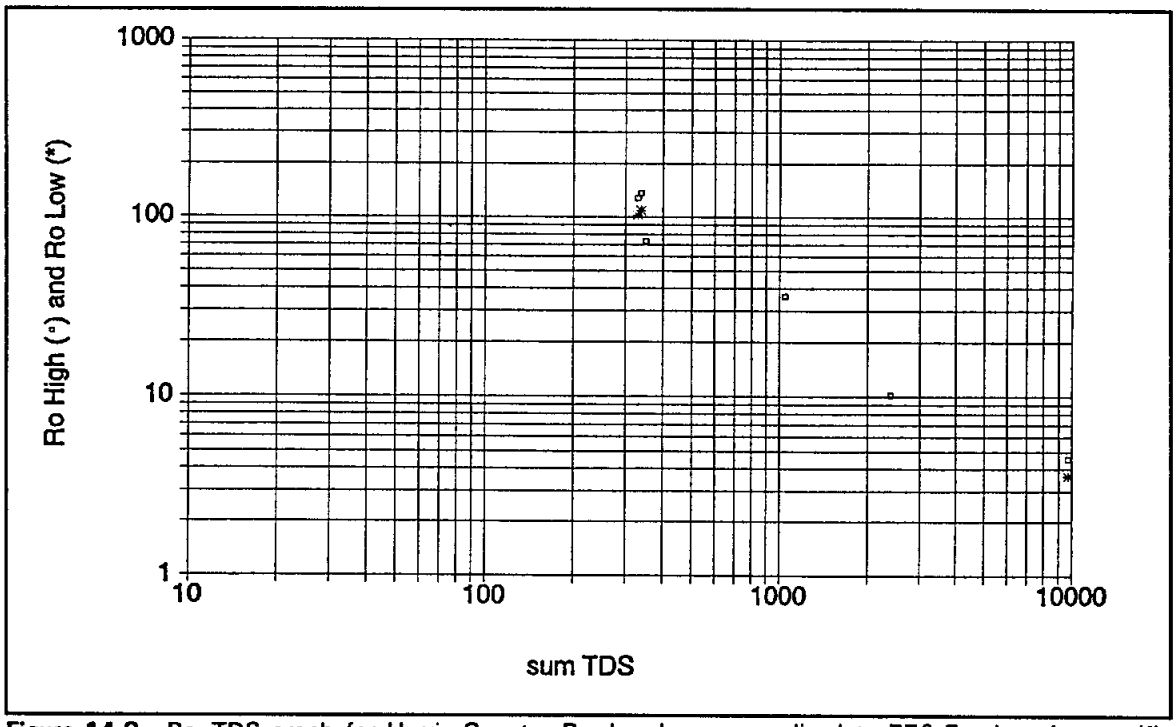

Figure 14-8. Ro_c-TDS graph for Harris County. Ro_c has been normalized to 77° F using site-specific geothermal gradients. The curve fit is no better than that of the Ro-TDS graph (Figure 14-1).

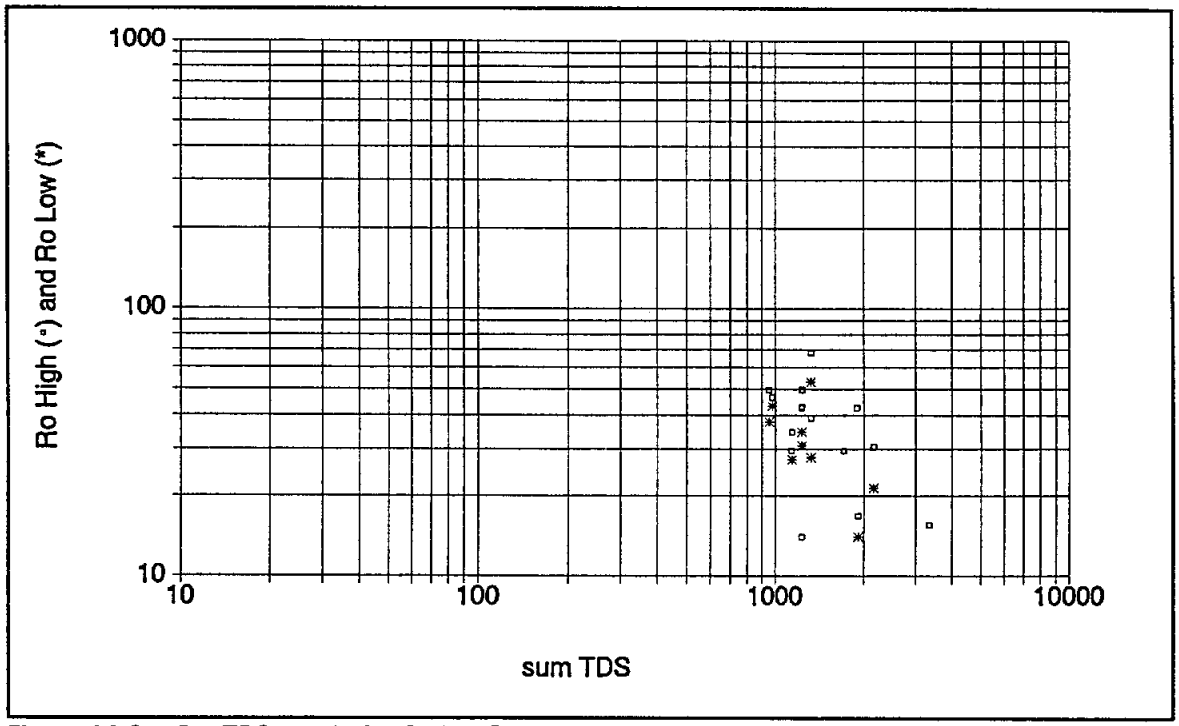

Figure 14-9. Ro_c-TDS graph for Dallas County. Ro_c was normalized to 77° F using site-specific geothermal gradients. The curve fit is no better than that of the Ro-TDS graph (Figure 14-2).

Ro_c-TDS graphs utilizing site-specific geothermal gradients were prepared for only 27 counties, since many wells lacked a bottom hole temperature (Figures 14-8 and 14-9 are examples). None of the 75 Ro_c-TDS graphs had a curve fit that was any better than the corresponding Ro-TDS graph, as illustrated by a comparison of Figures 14-1, 14-6, and 14-8 or 14-2, 14-7, and 14-9. (The rest of the Ro_c-TDS graphs were not included in this report.)

This lack of improvement in the curve fit, while due in part to inaccurate geothermal gradients, demonstrates that scatter in the curve fit is largely a function of factors other than temperature variations. Porosity variations are the most likely explanation.

Ro can also be normalized for variations in porosity due to compaction. The correction is valid only for unconsolidated sandstones in which porosity decreases with depth as a function of increasing compaction. Alger (personal communication, 1988) suggested that such Ro_c values would yield better curve fits for the portions of unconsolidated aquifers from 1,000 to 3,000 feet in depth. He considered the South Texas Carrizo-Wilcox and the Gulf Coast aquifers good candidates for the correction.

The procedure to normalize Ro for variations in porosity due to compaction is as follows:

1. A porosity value must be established for the depth that corresponds to each Ro value. This can be obtained from a porosity log of the well, if available. Unfortunately, they seldom are for water wells (see Chapter 13). The only alternative is to estimate porosity values by first establishing a porosity gradient from offsetting wells in the geographic area and depth range of the Ro values in question. As mentioned above, the porosity gradient will be valid only if porosity values are a function of compaction.

2. A formation factor (F) is calculated for each porosity value (i.e. each sample depth) using equation 14-7. Formation factor is discussed in the **Formation Factor Equation** section of this chapter.

3. A porosity value (depth) is chosen as the one to which all the rest of the data will be normalized.

4. Ro values are normalized to the common porosity (depth) value by the following equation:

$$Ro_c = Ro \times F_c / F \qquad \textbf{14-1}$$

Where:

Ro_c = Ro values corrected for variations in porosity due to compaction.
Ro = Resistivity of the uninvaded formation 100 percent saturated with water.
F_c = Formation factor of the common porosity (depth) value.
F = Formation factor corresponding to the Ro value being normalized.

5. Ro_c is plotted versus TDS.

Alger (personal communication, 1988) used density and sidewall core porosity values to calculate a porosity gradient for the Queen City and Carrizo-Wilcox in Atascosa, Karnes, LaSalle, and McMullen counties. His equation is as follows:

$$\phi = 0.40 - .00003 \times \text{depth} \pm 0.01 \qquad \textbf{14-2}$$

Where:

ϕ = porosity
depth is in feet

Equation 14-2 was used to normalize Karnes County Ro values (Section 3, Volume II). Table 14-2 contains the calculations and Figure 14-10 is a graph of the results. Only the Ro_c value from 4,300 feet had an improved curve fit. All the rest of the Ro values were from a very small depth range (700 to 1,100 feet). The scatter in the data from this interval is most plausibly explained by porosity variations that are a function of geological factors other than compaction.

In theory, the curve fit of Ro-TDS graphs should be improved by normalizing Ro for the effects of temperature and porosity variations. In practice, such was not the case for temperature normalization and porosity normalization was only slightly successful. Ro_c-TDS graphs appear to offer an advantage over Ro-TDS graphs only for porosity normalization and only when porosity is a function of compaction.

TABLE 14-2. KARNES COUNTY Ro_c VALUES NORMALIZED FOR POROSITY

Depth (feet)	Porosity from Equation 14-2	F	F_c	Ro_c High (ohm-meters) corrected to 77° F using a county-wide geothermal gradient	Ro_c High (ohm-meters) corrected to 77° F and 1000 feet
4300	0.27	10.4	5.3	29	15
1000	0.37	5.3	5.3	14	14
1000	0.37	5.3	5.3	15	15
1000	0.37	5.3	5.3	10	10
1100	0.37	5.3	5.3	6	6
700	0.38	5.0	5.3	5	5.3
800	0.38	5.0	5.3	7	7.4
800	0.38	5.0	5.3	7	7.4
700	0.38	5.0	5.3	8	8.5
800	0.38	5.0	5.3	8	8.5
700	0.38	5.0	5.3	9	9.5

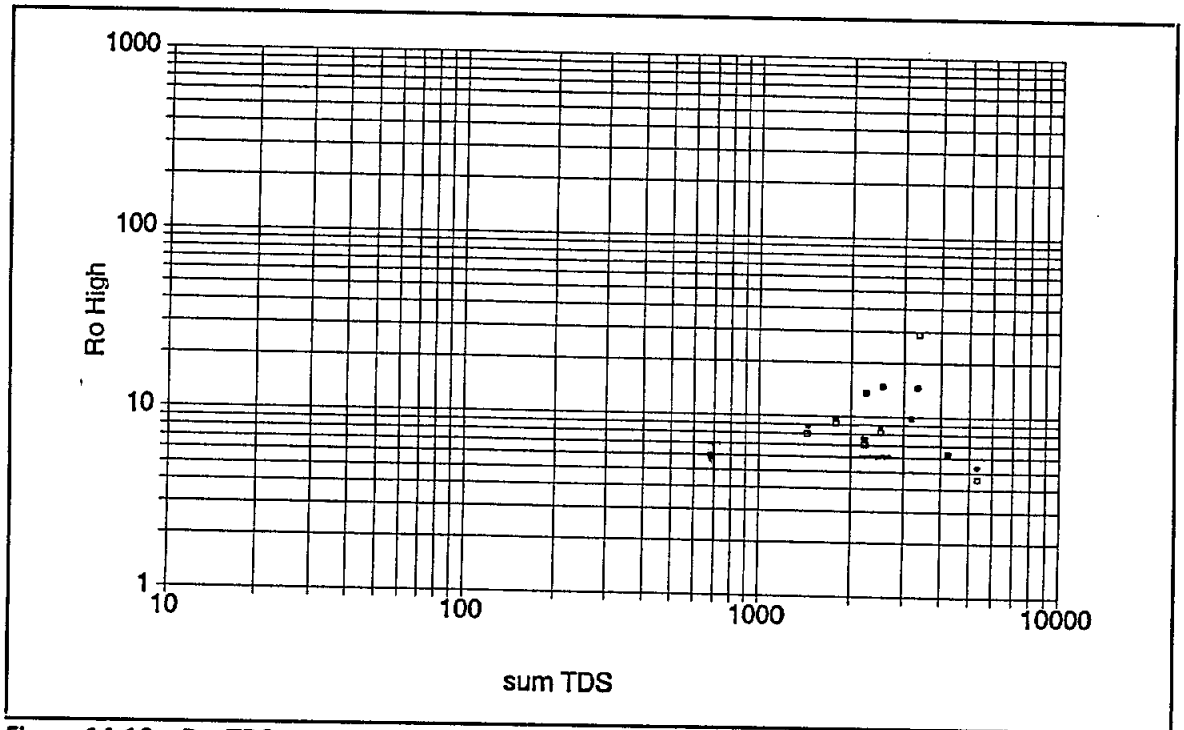

Figure 14-10. Ro_c-TDS graph for Karnes County. Ro_c High normalized to 77° F with a county-wide geothermal gradient (□) was then normalized to 1,300 feet to compensate for porosity variations (•).

Field Formation Factor (FFF)

Turcan (1962) introduced the **field formation factor (FFF)** technique as an empirical method of estimating Rw from resistivity logs. It is a slightly modified form of Archie's formation resistivity factor equation (14-5). In the FFF calculation Ro is first normalized to 77° F. This is done to negate the effects of variations in formation temperature on Ro and to calculate an Rw value at standard temperature (77° F).

There is one other significant difference between FFF and F. In fresh water (water with an Rw greater than 3 ohm-meters) FFF is less than F. In saltier water the two are equivalent. The difference between the two is due to surface conductance and is explained below. Surface conductance is explained in the **Formation Factor Equation** of this chapter.

FFF is the ratio of the Ro of a formation divided by the resistivity of the water in the formation (Rw):

$$FFF = Ro_{(@\ 77°\ F)} / Rw_{(@\ 77°\ F)} \qquad \textbf{14-3}$$

Where:

FFF = Field formation factor
$Ro_{(@\ 77°\ F)}$ = Resistivity of the uninvaded formation normalized to 77° F
$Rw_{(@\ 77°\ F)}$ = Resistivity of the formation water at 77° F

Having established the FFF of a formation, the Rw of a subsequent well can be estimated by substituting the Ro of the interval in question into a rearranged version of Equation 14-3.

$$Rw_{(@\ 77°\ F)} = Ro_{(@\ 77°\ F)} / FFF \qquad \textbf{14-4}$$

Rw is then converted to Cw (Equation 14-1). Finally, to determine TDS Cw is plotted on the appropriate TDS-Cw graph or substituted into the equation of the graph (Chapter 4 and Section 4 of Volume II).

Equation 14-4 has one serious drawback for calculating Rw: FFF is porosity dependent. Therefore, an FFF constant is valid only as long as porosity remains fairly constant (i.e., shallow, unconsolidated sands in a limited geographic area). The method worked for Turcan because he was

analyzing shallow sands in a limited area (Eocene Wilcox Group in North Louisiana). His FFF values were fairly consistent, ranging from 1.7 to 3.0.

In deeper aquifers FFF increases with depth by as much as two orders of magnitude (MacCary, 1984). MacCary calculated F's for Catahoula, Frio, Yegua, and Wilcox sandstones of the Texas Gulf Coast. Figure 14-11, a graph of his Wilcox data, illustrates how F varies with depth, sometimes by as much as a factor of 10 within a few hundred feet. The overall trend of F increasing with depth is due to porosity decreasing due to compaction. Other diagenetic processes may be contributing to the trend. The wide variations in F over small vertical intervals are probably due to variations in porosity associated with varying depositional facies. Whatever the reason(s) for the variations in F, Figure 14-11 illustrates that calculating water quality from an FFF constant is unreliable in deeper aquifers.

Alger calculated FFF's for about 400 of the wells in the data base in Section 1 of Volume II. Values range from 0.1 to 28, with most of them between 2 and 7. Wilson County is the best example of a consistent county-wide FFF value. Five values range from 5.1 to 6.2, with one value of 3.9. There is considerable variation in the values for each of the other counties, even in the Carrizo-Wilcox and Gulf Coast aquifers. Dallas County is a good example of widely ranging values. FFF's range from 4.8 to 16, reflecting porosity variations within the Trinity aquifer.

The FFF's in this data base are smaller than values calculated using Archie's formation resistivity factor/porosity equation (Equation 14-6) and a known porosity value. The difference is due to surface conductance, which lowers Ro in fresh water aquifers. Consequently, in fresh water aquifers the FFF value

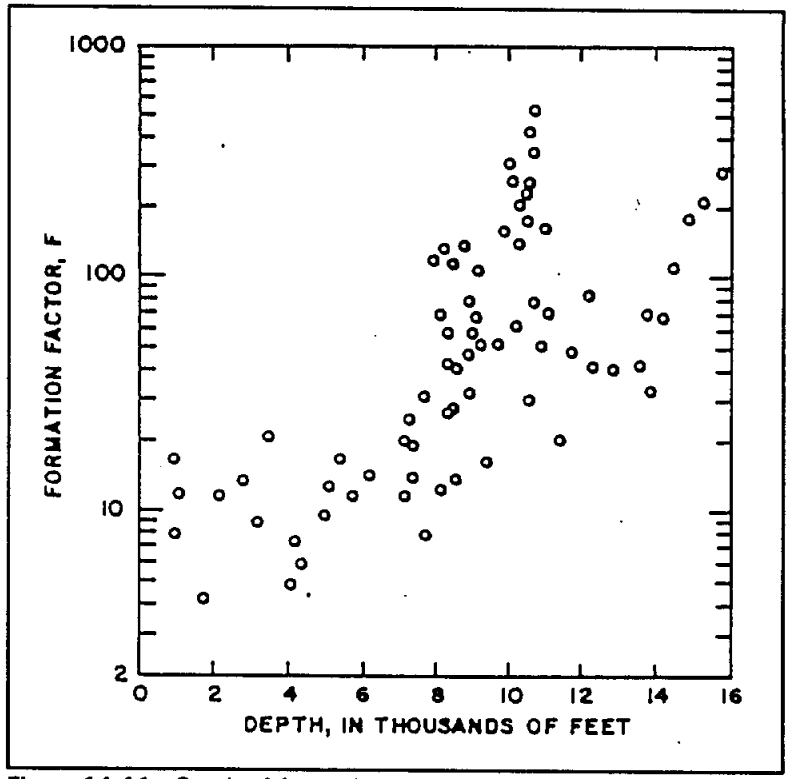

Figure 14-11. Graph of formation factor vs. depth for the Texas Gulf Coast Wilcox Group (MacCary, 1984).

calculated by Equation 14-3 is lower than an F value calculated with Equation 14-6, which is independent of Ro.

Examination of the data base in Section 1 of Volume II reveals that the FFF method of calculating water quality is not very accurate. In the absence of porosity data, an Ro-TDS graph is preferred over an FFF calculation. Indeed, a good linear fit to an Ro-TDS graph is really a plot of Equation 14-4 for varying Ro's and a constant FFF. The scatter about the linear fit demonstrates the degree to which porosity varies in the aquifer. Examination of the scatter allows one to visually take into account the effect of a change in porosity on Ro and consequently on the water quality estimation. This allows one to make a more intelligent estimation of the true water quality. An FFF calculation, on the other hand, offers no alternate interpretations and lends a false sense of accuracy to the water quality estimation.

STAND-ALONE TECHNIQUES FOR CALCULATING RW

Formation Factor Equation

Archie (1942) discovered that the resistivity of a water saturated rock (Ro) varies by a constant value as the resistivity of the formation water (Rw) changes. He quantified the relationship as:

$$Ro = F \times Rw \qquad \textbf{14-5}$$

Where:

Ro = the resistivity in ohm-meters of the formation 100 percent saturated with water
F = the formation factor, a proportionality constant
Rw = the resistivity in ohm-meters of the water saturating the formation

The proportionality constant in Equation 14-5 is called the **formation resistivity factor (F_R)** or **formation factor (F)**. F ranges from 5 to several hundred in sandstones and from 10 to several thousands in carbonates (Helander, 1983).

Archie derived Equation 14-5 by saturating core samples of different porosities (10 to 40 percent) with waters of various salinities (20,000 to 100,00 mg/l of NaCl) and then measuring Ro. He found Equation 14-5 to be valid for his entire range of porosities and salinities.

Archie also observed that Ro, and consequently F, decrease as porosity increases. He inferred that F is a function of porosity and was able to derive an empirical relationship between the two:

$$F = 1 / \phi^m \qquad \textbf{14-6}$$

Subsequent investigation by Winsauer, et. al (1952) led to the addition of a variable **a** in the numerator of Equation 14-6:

$$F = a / \phi^m \qquad \textbf{14-7}$$

Where:

F = formation factor
a = tortuosity factor
ϕ = porosity in decimal form
m = cementation exponent

In the ideal case of pore spaces that are parallel cylindrical channels, F would be inversely proportional to porosity, a and m would both equal 1, and F would equal $1/\phi$. The pore system in almost all rocks, however, departs from the ideal case. Depositional and diagenetic processes result in pore diameters of varying cross-sectional areas and pore paths of varying lengths or tortuosities. a and m quantify the degree to which the pore system departs from the ideal case. The names tortuosity factor and cementation exponent are really misnomers for a and m, because the variables are the product of several factors. For instance, Helander (1983) lists eight factors that influence m:

1. Degree of cementation
2. Shape, sorting, and packing of the particulate system
3. Type of pore system (intergranular, intercrystalline, vuggy, etc.)
4. Tortuosity of the pore system

5. Constrictions existing in porous system
6. Presence of conductive solids (clays, pyrite, etc.)
7. Compaction due to overburden
8. Thermal expansion

The pore system of natural rocks is too complicated for a and m to be measured. Instead, they are empirically derived from the best line fit of a logarithmic plot of Ro/Rw (F) and porosity in decimal form (Figures 14-12, 14-13, and 14-14). The Ro and porosity values are obtained either from core (Figure 14-12) or log (Figures 14-13 and 14-14) measurements. Rw must be known independently.

The data is plotted on three-cycle log-log paper: F on the y axis with a scale of 1.0 to 1000 and porosity on the x axis with a scale of .001 to 1.0. m is the slope of the line that fits the data (Figure 14-13) and a is the value of F when $\phi = 1.0$. a can also be expressed in terms of a rearranged version of Equation 14-7 :

$$a = F \times \phi^m \qquad \text{14-8}$$

Theoretically, a should always equal 1, since a porosity of 1.0 (100 percent) has an Ro/Rw or F of 1 and these values substituted into Equation 14-8 calculate an a of 1. In reality, a sometimes varies from 1.0. Such cases may be an artifact of the curve fitting routine or compensation for consistent variations in pore geometry (Hilchie, 1987).

Over the years a and m have been calculated for thousands of rock samples. a's of .6 to 4 and m's of 0.57

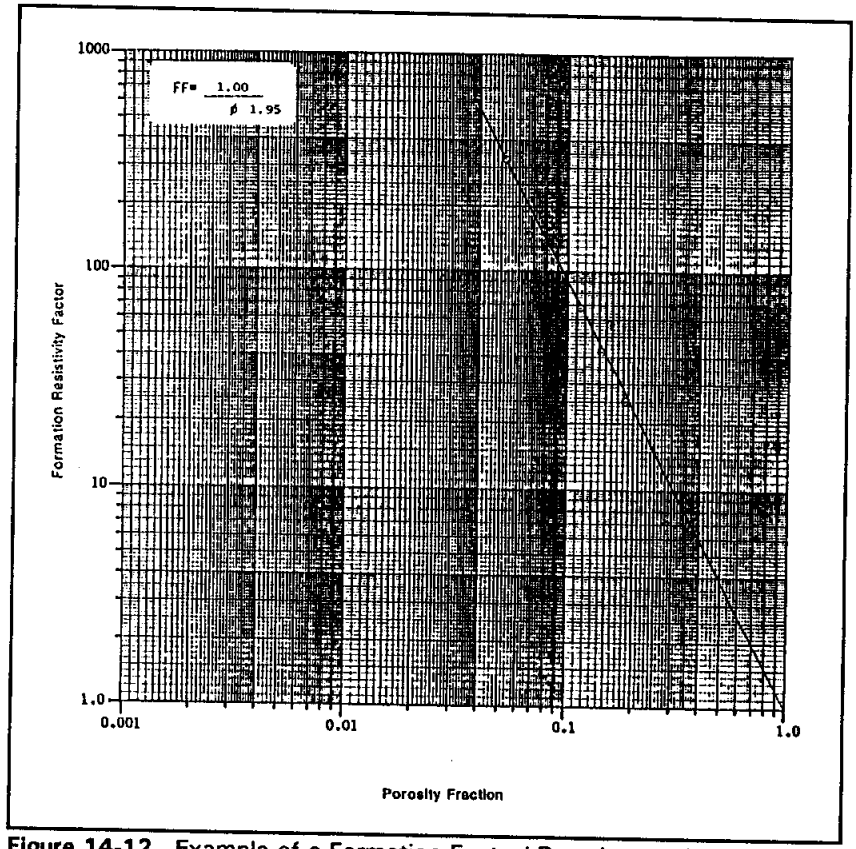

Figure 14-12. Example of a Formation Factor/ Porosity graph constructed from core data (Collier, 1988). For an a of 1, m is 1.95.

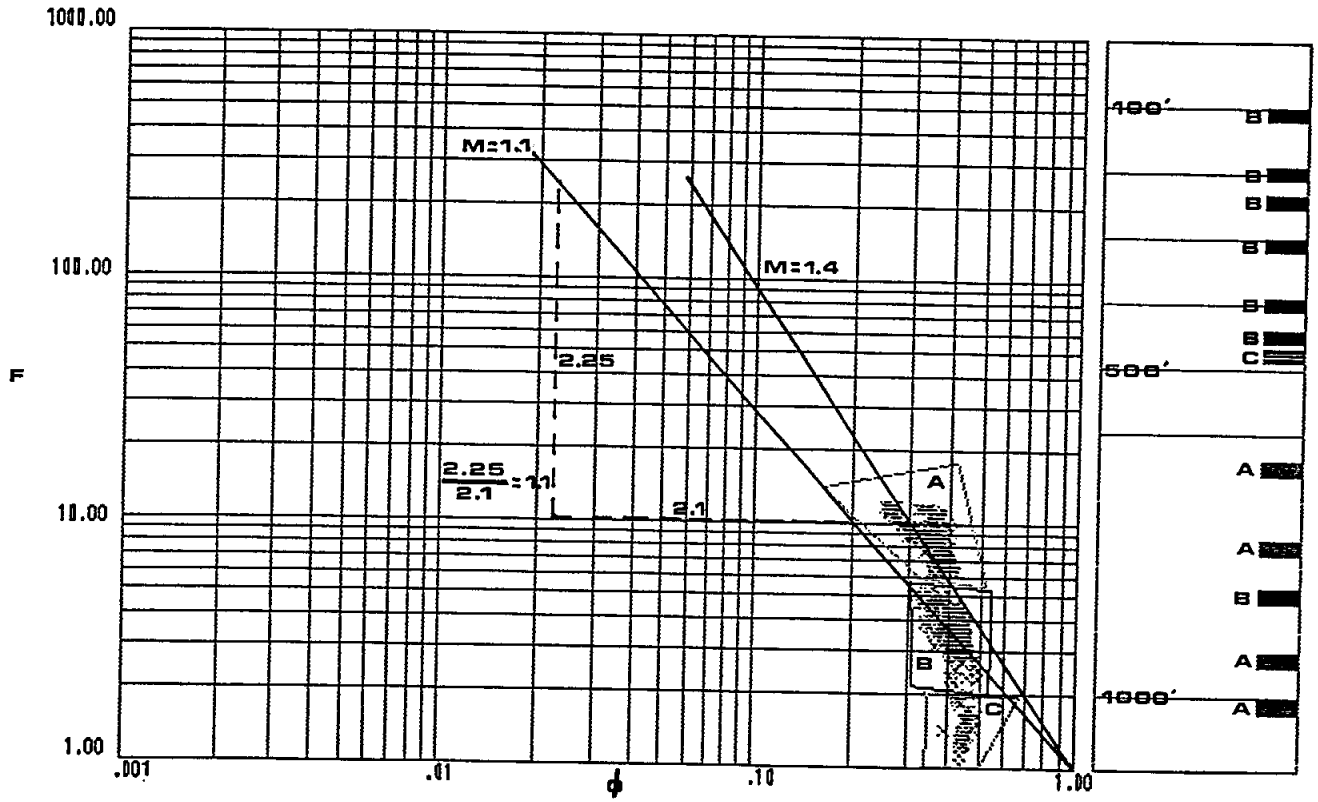

Figure 14-13. Formation Factor/Porosity graph constructed from log data. The porosity values are density-neutron crossplot porosity. The data clusters into three groups, with the two main clusters (A and B) correlating to the portion of the borehole above or below 500 feet. The column to the right of the graph is a diagram of the borehole with the intervals plotted on the graph noted by blocks. These intervals were chosen because water samples were available. The data clusters into distinct groups because of differences in the pore systems. m is 1.4 for group A and 1.1 for group B. Other differences such as water chemistry and SP behavior (refer to Plate 2) between the two intervals reinforce the conclusion of a significance difference in the petrophysical properties of the two intervals. The well was drilled in the Gulf Coast Aquifer. The well is the TWDB PUB Test Well Site F, Cameron County, Texas (state well number 88-59-411). Plates 1 to 4 and Figures 13-12 and 14-20 are also from this well.

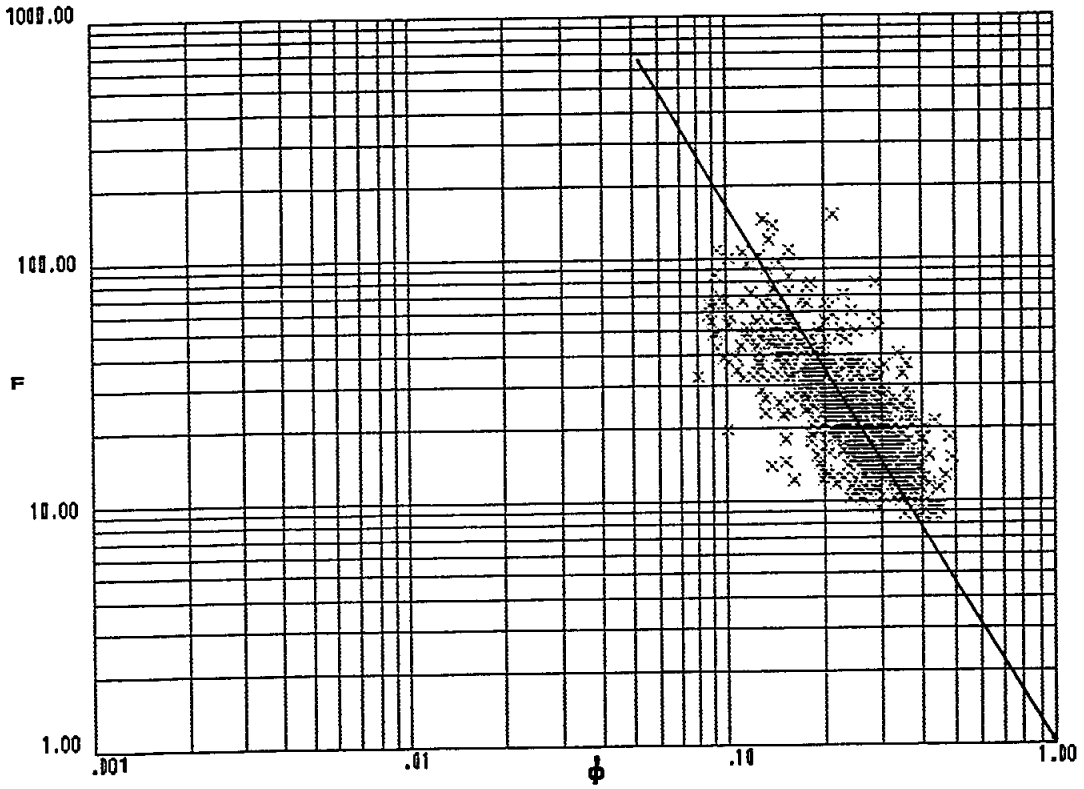

Figure 14-14. Formation Factor/Porosity graph constructed from log data. The porosity values are density-neutron crossplot porosity. The data shows a high correlation. Forcing the line fit through 1.0 on the x axis (a = 1.0) gives an m of 1.8. An m of 2 was used in the Rwa calculation for this well and yielded accurate Rw values (Poteet, Collier, and Maclay, 1992). The well is in the Edwards Aquifer, San Marcos, Texas. The well is the Edwards Underground Water District, D, Hays County, Texas (state well number 67-01-814).

to 5.4 have been documented (Porter and Carothers, 1970 and Focke and Munn, 1987). Although specific a and m values have been calculated for some formations, most of the time log analysts use one of three versions of Equation 14-7:

$$F = .62 / \phi^{2.15} \qquad \textbf{14-9}$$

was developed by researchers at Humble Oil and Refining Company (Winsauer, et. al, 1952) and is known as the Humble equation. It is used for granular formations such as sandstones with porosities of 13 to 35 percent.

$$F = .81 / \phi^{2} \qquad \textbf{14-10}$$

is known as the Tixier equation. It also applies to granular formations. It is often substituted for the Humble equation when porosity is approximately 20 to 10 percent because it is easier to calculate and the two equations are equivalent for this porosity range (Figure 14-15).

$$F = 1 / \phi^{2} \qquad \textbf{14-11}$$

is called the Archie equation. It is used for carbonates and low porosity (i.e. cemented or compacted) sandstones.

Figure 14-15 is a graphical solution of the three equations. Plate 1 demonstrates that the Humble equation is more accurate than the other two in high porosity, uncompacted sandstones (the environment of most shallow clastic aquifers, as well as the Gulf Coast and Carrizo-Wilcox aquifers).

The most accurate approach, however, is to calculate formation-specific a and m values. Many log analysts set a equal to 1 and just deal with m (Figures 14-13 and 14-14). For an a of 1, certain patterns emerge regarding m:

1. For uncemented grains m increases as sphericity decreases. m ranges from 1.3 for uncemented spheres to 1.8 for uncemented plates (Hilchie, 1982).

2. m increases as the cementation of the rock increases. m ranges from 1.3 for completely unconsolidated sands to 2.2 for well cemented sandstones (Helander, 1983).

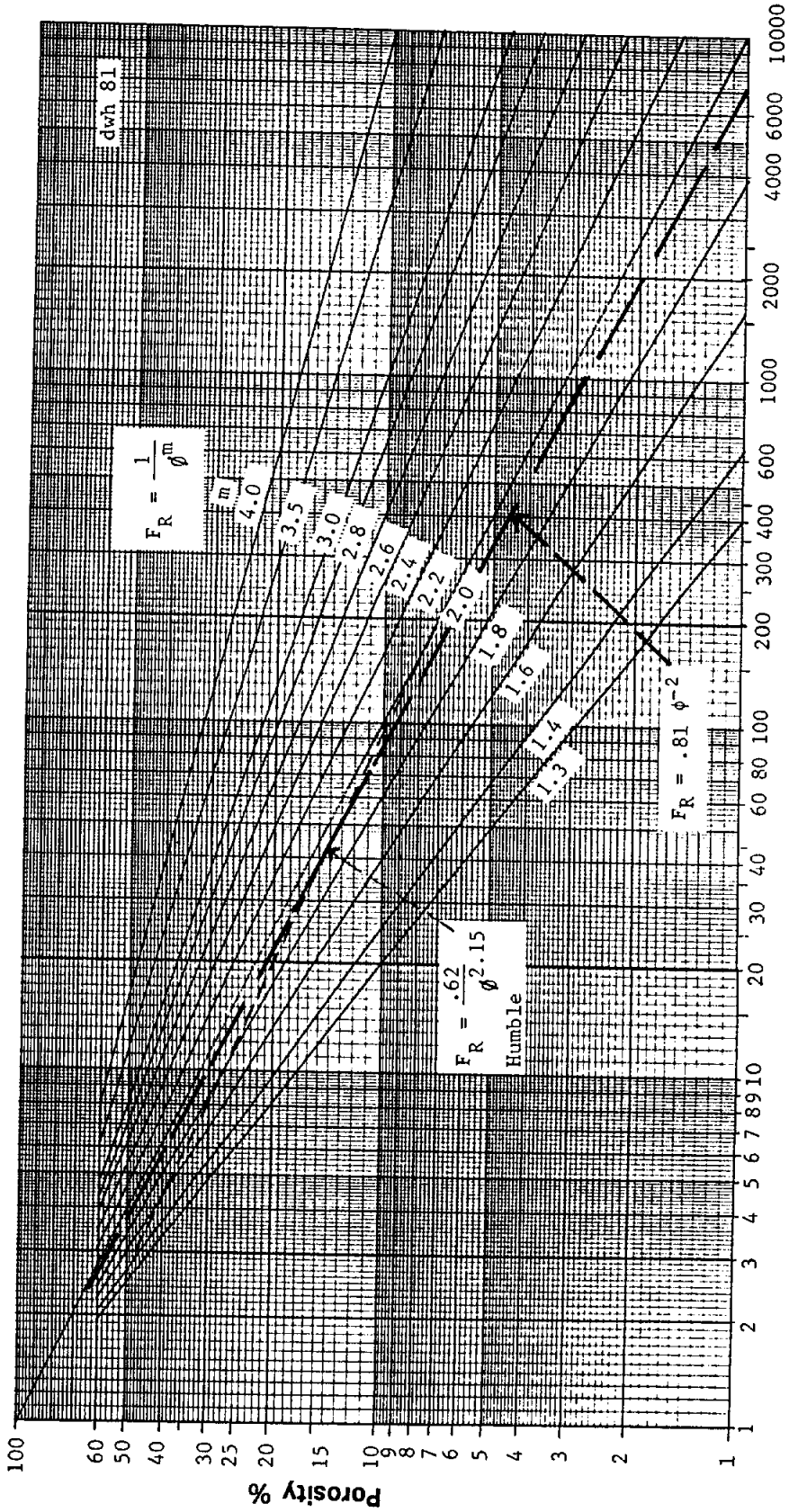

Figure 14-15. Formation Factor versus Porosity and m (modified from Hilchie, 1982). The graph is used to calculate F, given m and porosity.

3. m is 2 for carbonates with interparticle and intercrystallline porosity greater than 5 percent (Focke and Munn, 1987). Below 5 percent, m decreases as porosity decreases, down to 1.5 at 1 percent porosity.

4. For carbonates with vuggy and moldic porosity, m increases as the ratio of total porosity to vuggy/moldic porosity decreases (Towle, 1962). This is true when total porosity is greater than 5 percent. At less than 5 percent total porosity, m decreases as porosity decreases, down to about 1.3 at less than 1 percent porosity (Focke and Munn, 1987).

5. Fractures decrease m. Wide open fractures can have an m as low as 1.1 (Hilchie, 1982). This is because the pore geometry is approaching the ideal case of parallel cylindrical channels.

Rw calculated from Equation 14-5 using an F obtained from the Ro/Rw ratio in an offsetting well is the previously discussed Field Formation Factor technique. The previous discussion of F clarifies why the technique is so site specific. F will be the same in two wells only when porosity, m, and a are the same.

A much more accurate method, herein called the **Formation Factor Method**, is to substitute Equation 14-7 into 14-5 and rearrange the equation in terms of Rw:

$$Rw = Ro \times \phi^m / a \qquad \textbf{14-12}$$

This equation is called an **Rwa** calculation in petroleum logging literature. The term Rwa (apparent Rw) is used because when hydrocarbons are present in a formation Ro becomes Rt (the resistivity of the uninvaded formation with its naturally occurring fluids) and Equation 14-12 calculates an incorrect Rw value (Rwa) that is greater than Rw. The Rwa curve is an optional curve, so it is not found on many logs. It is usually placed in Track 1. The values are at formation temperature (Figure 14-16).

When the Formation Factor Equation is used to calculate water quality, Rw must be converted to 77° F. This is done by first establishing the geothermal gradient of the well (refer to the explanation for column 3 in Section 3, Volume II) and then calculating the temperature at the depth of interest (refer to the explanation for colume 6 in Section 3, Volume II). The

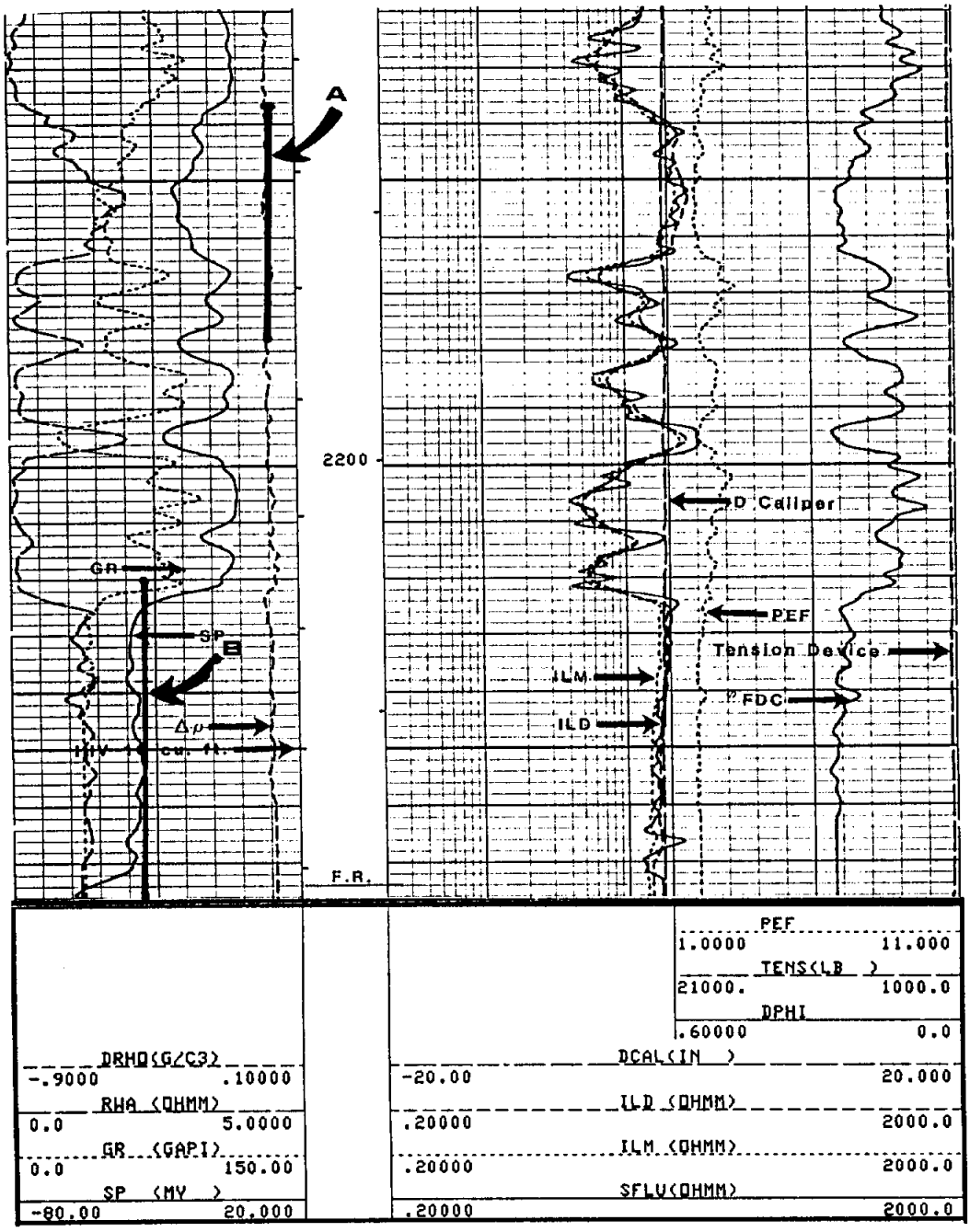

Figure 14-16. Example of a petroleum type Rwa curve. Track 1 contains an Rwa curve computed by the Formation Factor method using $1/\phi^2$ and density porosity (Track 3). Rwa values are at formation temperature. The arrows point to Rw values obtained from water samples and adjusted to formation temperature. The Rwa value of zone A is 55 percent less than the measured Rw, while the Rwa value of zone B is 40 percent less than the measured Rw. The difference between Rw measured and Rwa is greater than the difference observed in laboratory tests by Evers and Iyer (Figure 14-18) for this Rw range. However, the differences may be due to factors other than surface conductance. The gamma ray curve shows shale in the sands, which would lower Rwa. The interval is part of the Carrizo-Wilcox. The well is the McKinley Drilling Company, George Strait #1, Webb County, Texas. Rm is 5.23 ohm-meters at 90° F and Rmf is 5.87 ohm-meters at 75° F. T.D. is 2,280 feet, bottom hole temperature is 105° F, and bit size is 9⅞ inches. Density porosity was computed using a matrix density of 2.65 g/cm^3.

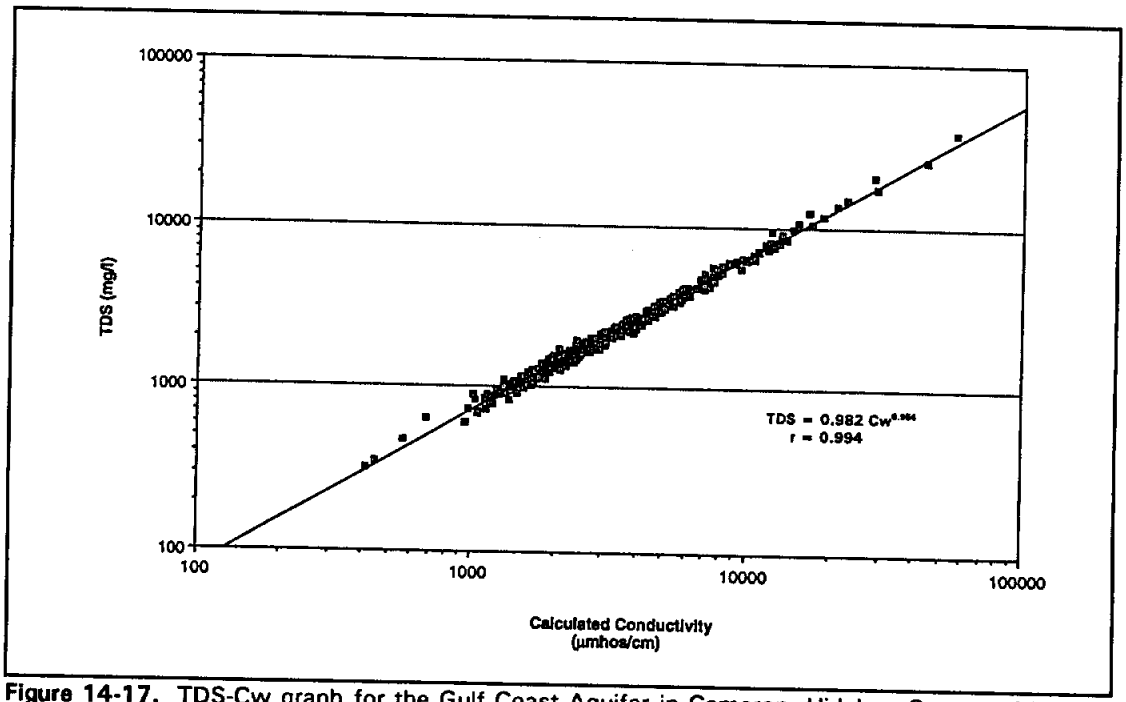

Figure 14-17. TDS-Cw graph for the Gulf Coast Aquifer in Cameron, Hidalgo, Starr, and Willacy Counties. The equation is used to calculate TDS in Plate 3. TDS includes 100 percent bicarbonate.

calculated Rw value is then converted to Rw at 77° F by substituting the formation temperature into Equation 2-4. Rw at 77 ° F is converted to Cw using Equation 14-1. Finally, Cw is converted to TDS using the appropriate TDS-Cw graph (Section 5 of Volume II). Figure 14-17 is the TDS-Cw graph for Plate 3.

Equation 14-12 will calculate accurate Rw values when the following conditions are met:

1. The formation is shale-free. Shale lowers Ro, which means that the calculated Rw will be too low.

2. The porosity value is accurate. If a single porosity log is used, the lithology must be constant. If the lithology varies, a crossplot porosity should be used (Chapter 12). The porosity log(s) must be on depth with the resistivity curve. Porosity logs are run in very few water wells. However, they are often available for post-1960 hydrocarbon tests.

3. The proper a and m values are used. Ideally, they should be calculated for the formation being analyzed. However, as discussed above, they can only be calculated if Rw is known! The

only alternative is to estimate a and m based on available geological information about the formation (sample description, porosity log, regional geology, etc.). Most of the time a should be set at 1.0 and m considered the variable. It may be advantageous to establish a range for Rw, using a high and a low value of m (Plate 1).

4. Rw is less than 2 to 3 ohm-meters at 77° F. For higher Rw's surface conductance causes the logging tool to record an Ra value that is less than Ro. There is no way to accurately correct Ra to Ro using just log data, so Ra is used for Ro in Equation 14-12. This results in a calculated Rw that is too low and Cw and TDS values that are too high. (This is the problem in Figure 14-16).

The surface conductance effect is a major drawback to using the Formation Factor Equation to calculate the water quality of aquifers with fresh to slightly saline water. Surface conductance has such a profound effect on calculated Rw values that it deserves further explanation.

Surface conductance increases the conductivity (or reduces the resistivity) of an aquifer. Chemists (McBain, et al., 1929; Urban, et al., 1935) have shown that solid surfaces in contact with aqueous solutions attract a layer of ions which, in turn, attract a layer of oppositely charged ions which, in turn, attract... The result is double layer conductivity- a more concentrated solution of predominantly positively charged ions near the surface of the solid, which has a higher conductivity than the rest of the solution. Electrical current preferentially travels through the more conductive double layer, thus making an aquifer appear to have a lower resistivity than is actually the case.

Surface conductance occurs in all aquifers, fresh or saline. Its magnitude is related to the ion concentration of the solution. In fact, surface conductance increases with increasing salinity. However, the increase in surface conductance always remains within the same order of magnitude, while the increase in water conductivity may be several orders of magnitude (McBain, et al., 1929). This means that only in fresh water aquifers will surface conductivity be a large enough percentage of the log-measured Ra value to noticeably affect Ro. For aquifers in Texas, this study found that Ro is significantly affected when Rw is greater than 2 ohm-meters (conductivity less than 5000 μmhos). This agrees with the laboratory work of Evers and Iyer (1975b) which suggests a cutoff of 3 ohm-meters (3333 μmhos).

Evers and Iyer (1975b) documented that the magnitude of surface conductance is also a function of grain size. The smaller the grain size the greater the surface conductance. Figure 14-18 is an example of two of their data sets. They also quantified the extent to which Ro is reduced as Rw increases: from a few percent at 3 ohm-meters to as much as 60 percent at 50 ohm-meters (Figure 14-18).

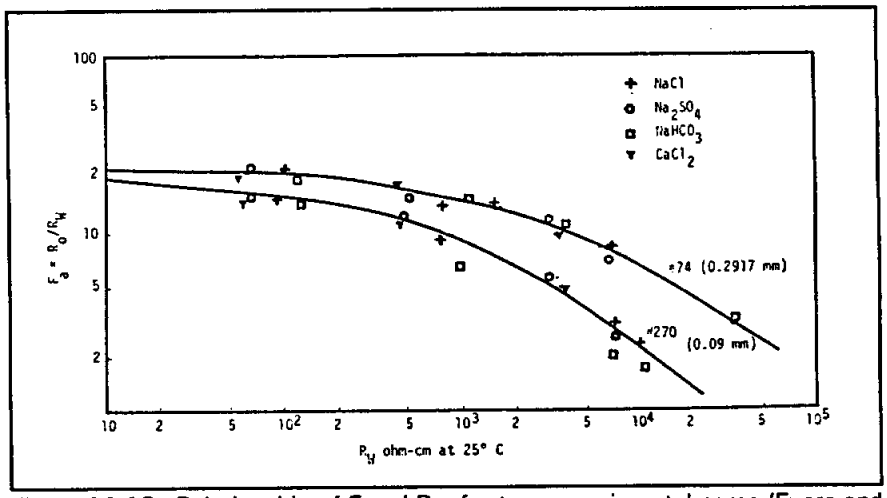

Figure 14-18. Relationship of F and Rw for two experimental cores (Evers and Iyer, 1975). Grain size is in parentheses. Note: divide the Rw values by 10 to get ohm-meters.

The amount of surface conductance is difficult to calculate from log data. There are so many factors that affect Ra (shale, borehole effects, etc.) that from log data it is very difficult to isolate and quantify the effect of surface conductance on Ra. This makes it is very difficult to establish any type of guidelines for correcting calculated Rw values. Calculations on a well in the Carrizo-Wilcox (Figure 14-16) show a much larger difference between Rwa and Rw measured than would be extrapolated from the lab data. However, other factors (e.g. shale) may be contributing to the difference.

Plates 1 to 5 are two examples of water quality calculations using the Formation Factor Equation. Plates 1 to 4 are from a well in an unconsolidated, high porosity sandstone (Gulf Coast Aquifer). Plate 5 is from a well in a high porosity carbonate (Edwards Aquifer).

Ro-Porosity Graphs

The Ro-Porosity graph, commonly known as the Pickett plot, is a graphical solution of Equation 14-12. It is a slightly modified version of a Formation Factor-Porosity graph (Figure 14-13). However, it is discussed separately in logging literature and is therefore discussed separately in this chapter.

The data is plotted on log-log paper. Ro is plotted on the x axis and porosity on the y axis. The data plots as a straight line as long as m and Rw remain constant and there is enough variation in porosity to establish a straight line. m is the negative slope of the line, the measured distance on Ro divided by the measured distance on ϕ (Figure 14-19). The point at which the line intersects the 100 percent porosity line is a $\times$ Rw at formation temperature. If a is 1 (as it usually is), the point of intersection is Rw at formation temperature.

The Ro-Porosity graph is subject to the same limitations as Equation 14-12. In many aquifers it is difficult to use the method to calculate Rw. In homogenous, high porosity aquifers there will not be enough variation in porosity to establish the slope of the line. In fresh to slightly saline aquifers the curve fit will estimate an Rw tha is too low and an m that is too high due to surface conductance. An additional complication is the accuracy of the curve fit (refer to Appendix II). However, an Ro-TDS graph should always be constructed in conjunction with the Formation Factor Equation method. Under the right circumstances (refer to the **Formation Factor Equation** section) it can be used for several purposes:

1. Rw can be estimated if m is constant, Rw is constant, and a is known (Figure 14-19).

2. m can be estimated if Rw is known and is constant (Figure 14-19).

3. Variations in m can be discerned if Rw is constant.

4. Variations in Rw can be discerned if m is relatively constant (Figures 14-20 and 14-21).

Resistivity Ratio Method

Petroleum log analysts have been using the Resistivity Ratio method to determine Rw for a number of years. Alger and Harrison (1988) proposed that the technique should be utilized more often in ground-water logging.

The Resistivity Ratio method calculates Rw by comparing the resistivity of the flushed zone (Rxo) with the resistivity of the uninvaded zone (Ro). The technique is based on four assumptions, all of which are normally valid:

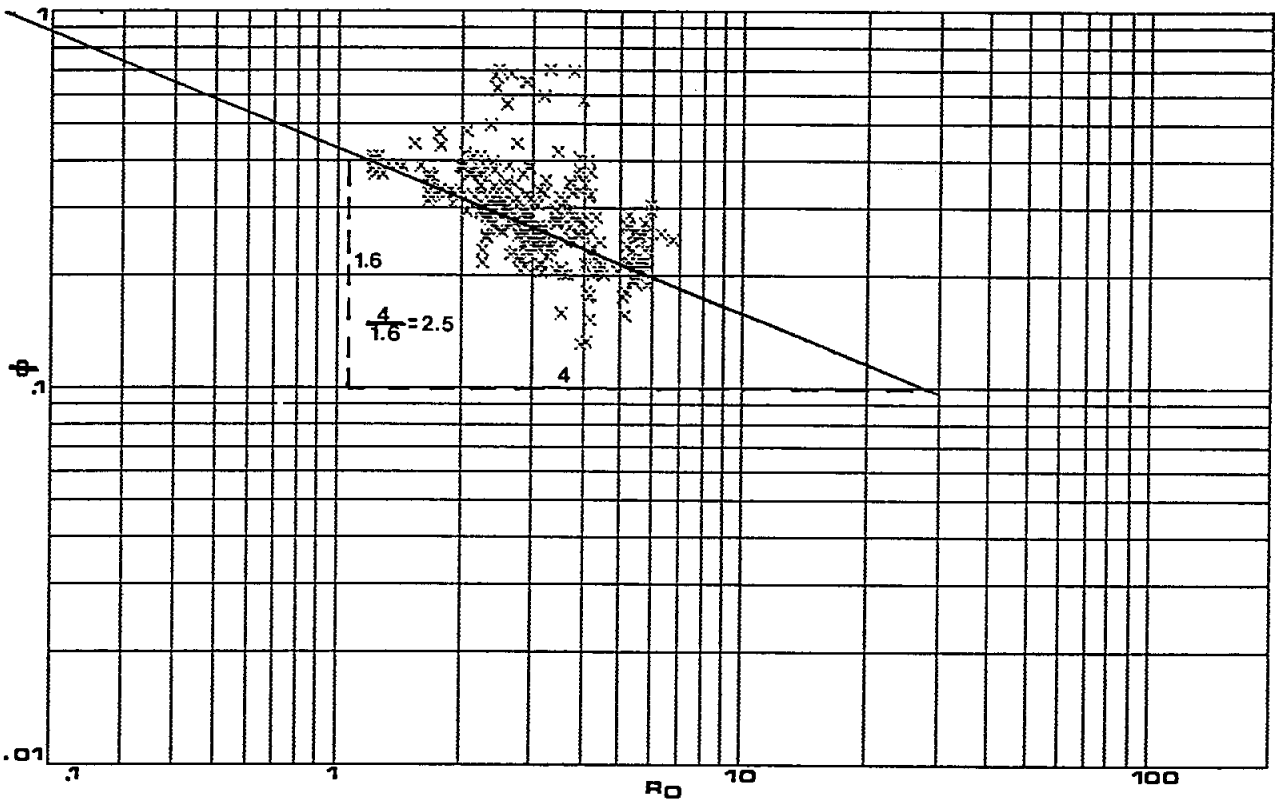

Figure 14-19. Using an Ro-Porosity plot to estimate Rw and m. Ro values are from the deep induction curve and porosity values are density-neutron crossplot porosity. The well is in the Edwards Aquifer and the data is from part of the Kirschberg Evaporite and Dolomitic Members of the Kainer Formation. The data is from an interval that has a constant Rw (1.8 ohm-meters at formation temperature). Rw is from water samples obtained during pump tests. Although there is scatter in the data, a fairly consistent pattern is present. The data is consistent enough to estimate Rw and/or m from the graph. Assuming an a of 1, a line with an Rw of 1.8 ohm-meters was fitted to the data. This line yields an m of 2.5, not an unreasonable value in a vuggy-moldic carbonate. However, an m of 2 was used in the Formation Factor Equation method and it gave accurate Rw's (Plate 5). Not knowing Rw, a best fit line through the data would yield an Rw close to the actual value. The well is the Edwards Underground Water District, A-1. Figure 13-32 and Plate 5 contain additional information on this well.

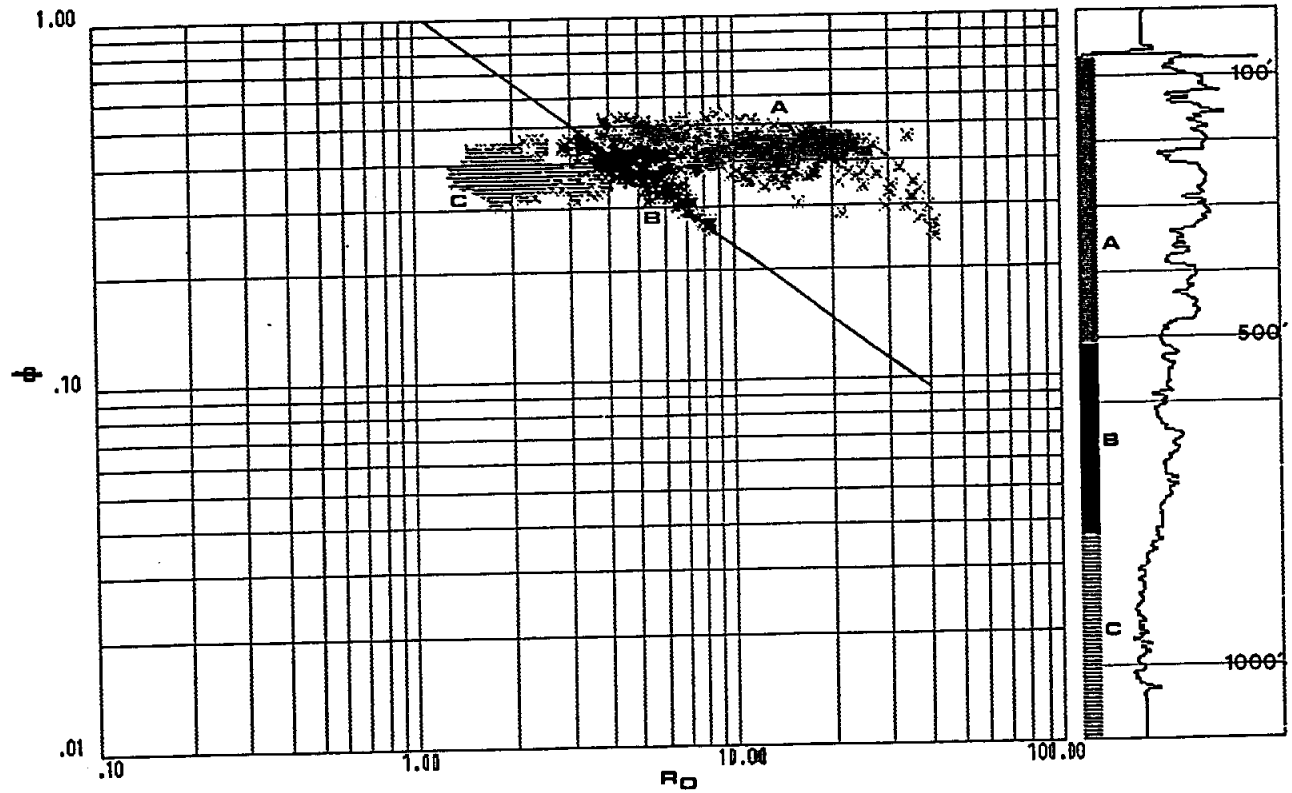

Figure 14-20. Using an Ro-Porosity graph to distinguish waters of different salinities. Ro values are from the deep induction curve and porosity values are from density-neutron crossplot porosity. The data is from the length of the entire borehole. The data cluster into three groups (A, B, and C), suggesting three different water salinities. Rw values from water samples taken during pump tests confirm three Rw ranges. The scatter in groups A and C is such that it is impossible to estimate either m or Rw. A good line fit can be drawn through group B, yielding an Rw that is too high (about 1.05 ohm-meters versus an actual Rw of about 0.54 ohm-meters at formation temperature) and an m of 1.3. This m is consistent with m's of 1.1 and 1.4 estimated from the Formation Factor-Porosity graph (Figure 14-13). The column to the right of the graph contains the deep induction curve and a few 100 foot depth markers. It also identifies the intervals in the well that correspond to the three clusters of data. The well is the TWDB PUB Test Site F, Cameron County, Texas. Refer to Figure 13-12 and Plates 1 to 4 for additional information on this welll.

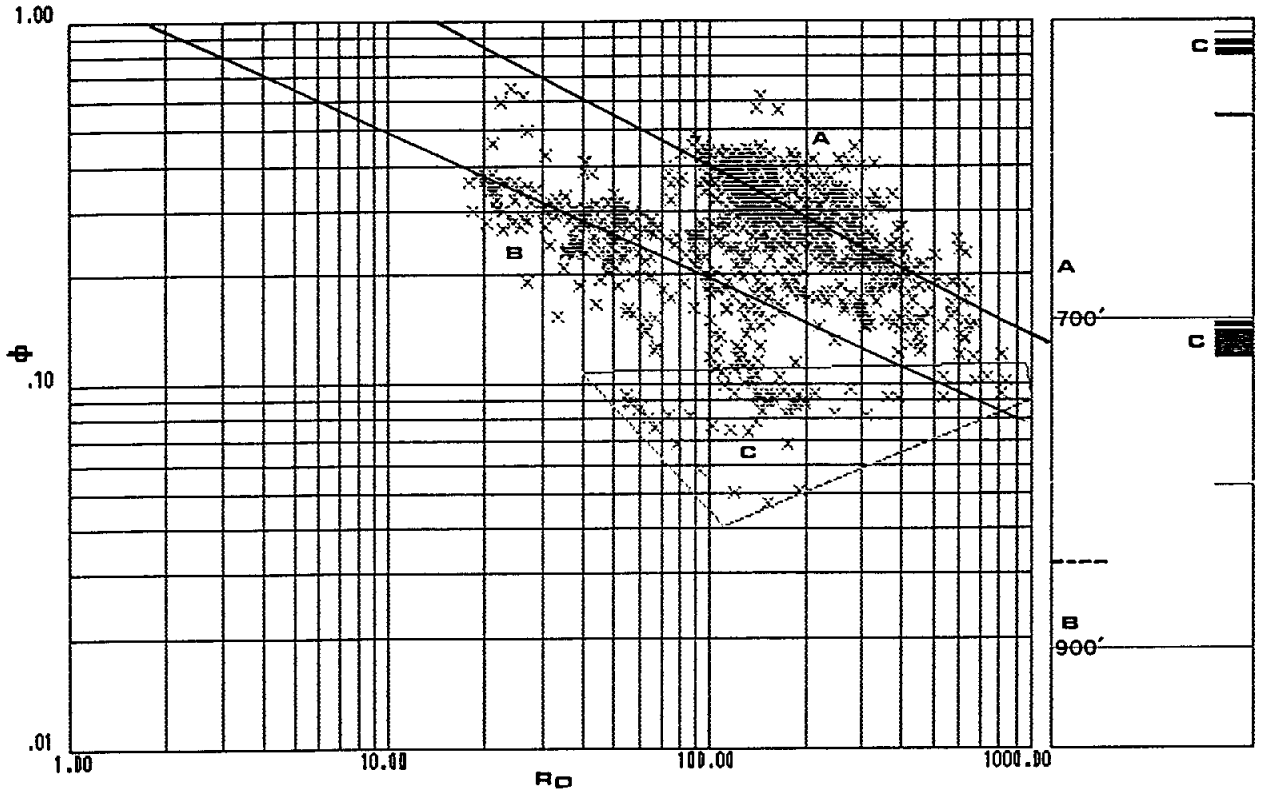

Figure 14-21. Using an Ro-Porosity graph to distinguish waters of different salinities. Ro values are from an averaged spherically focused curve and porosity values are from density-neutron crossplot porosity. The data is from the length of the entire borehole. The data cluster into three groups (A, B, and C), suggesting three different water salinities. Group C, however, is the Georgetown Formation and the Regional Dense Member of the Person Formation. Both are low porosity and very low permeability limestones. Therefore, in the case of group C the cluster represents a different pore structure, rather than a distinct water salinity. Rw values from water samples taken during pump tests confirm two Rw ranges: 16 to 17 ohm-meters for group A and 2 ohm-meters for group B. These Rw's agree closely with Rw's estimated from the graph. Group A has an m of A is 2.0 and B has an m of 2.2 (2 was used in the Formation Factor Equation). The column to the right of the graph identifies the intervals in the well that correspond to the groups. The well is in the Edwards Aquifer. It is the Edwards Underground Water District, C-1, New Braunfels, Texas (state well number 68-23-619). Poteet, Collier, and Maclay (1992) contains detailed information on the well.

1. The pore geometry and lithology of the formation near the borehole is the same as it is laterally in the formation at the depth of investigation of the deep reading resistivity tool (normally a few feet) .

2. The amount of surface conductance is the same in both the flushed and the uninvaded zones.

3. The difference between Ro and Rxo is solely a function of the difference in Rmf and Rw.

4. There is mud filtrate invasion. However, near the bottom of the hole there may not be enough invasion for a resistivity contrast between the two zones.

When the above mentioned assumptions are valid, the Formation Factor Equations for the flushed zone and the uninvaded zones (Equations 14-13 and 14-14) are equivalent (Equation 14-15). The Formation Factor Equation for the flushed zone is

$$F = Rxo / Rmf \qquad \textbf{14-13}$$

The Formation Factor Equation for the uninvaded zone is

$$F = Ro / Rw \qquad \textbf{14-14}$$

Equations 14-13 and 14-14 are equivalent, so they can be set equal to each other:

$$Rxo / Rmf = Ro / Rw \qquad \textbf{14-15}$$

The equation can then be rearranged to solve for Rw:

$$Rw = Rmf / Rxo / Ro \qquad \textbf{14-16}$$

Since F has been factored out of Equation 14-15, the Rw calculation (Equation 14-16) is independent of porosity, m, and a. Surface conductance effects are also factored out. If Rmf is adjusted to 77° F, Rw will be calculated at 77° F, thus eliminating any need to know formation temperature. The only data required for the calculation are accurate Ro, Rxo, and Rmf values.

Accurate Ro values are usually not a problem if the formation is thick and shale-free. (Chapters 8 and 9 explain how to correct resistivity curves for borehole effects.) If the formation is shaly, both Ro and Rxo must be corrected (Alger and Harrison, 1988):

$$(Rxo / Ro)^{1 / (1 - Vcl)} = (Rxo / Ro)_{clean} \qquad \textbf{14-17}$$

Where:

Rxo / Ro = log values uncorrected for shale
Vcl = clay volume
$(Rxo / Ro)_{clean}$ = log value corrected for shale

The clay volume can be calculated from either the gamma ray (Figure 10-7) or the SP curves (Equation 12-1).

Accurate Rxo values are essential. In wells with fresh-water muds and fresh-water aquifers, Rxo curves read much too high. Any subsequent Rw calculations will be too low. The appropriate borehole correction is not difficult to make, but it has usually not been applied to the Rxo curve on the log. It must be made before using the Resistivity Ratio method (refer to the **FOCUSED PAD MICROELECTRODE TOOLS** section in Chapter 9).

A greater problem with Rxo data is its availability. Rxo tools are virtually never run in water wells and they are normally utilized by the petroleum industry only in certain sections of the state, the Permian Basin being the chief area. In the absence of an Rxo curve, an Rxo value can be estimated from an Ri value obtained from a shallow reading resistivity curve (LL8, SFL, Short Guard, or Short Normal). As shown by Figure 8-3, the Short Normal reads deeper than the other three tools. Consequently, it will be the least accurate. Figure 14-22 is a nomograph correcting Ri / Ro to Rxo/ Ro for various curve combinations. The chart assumes an invasion

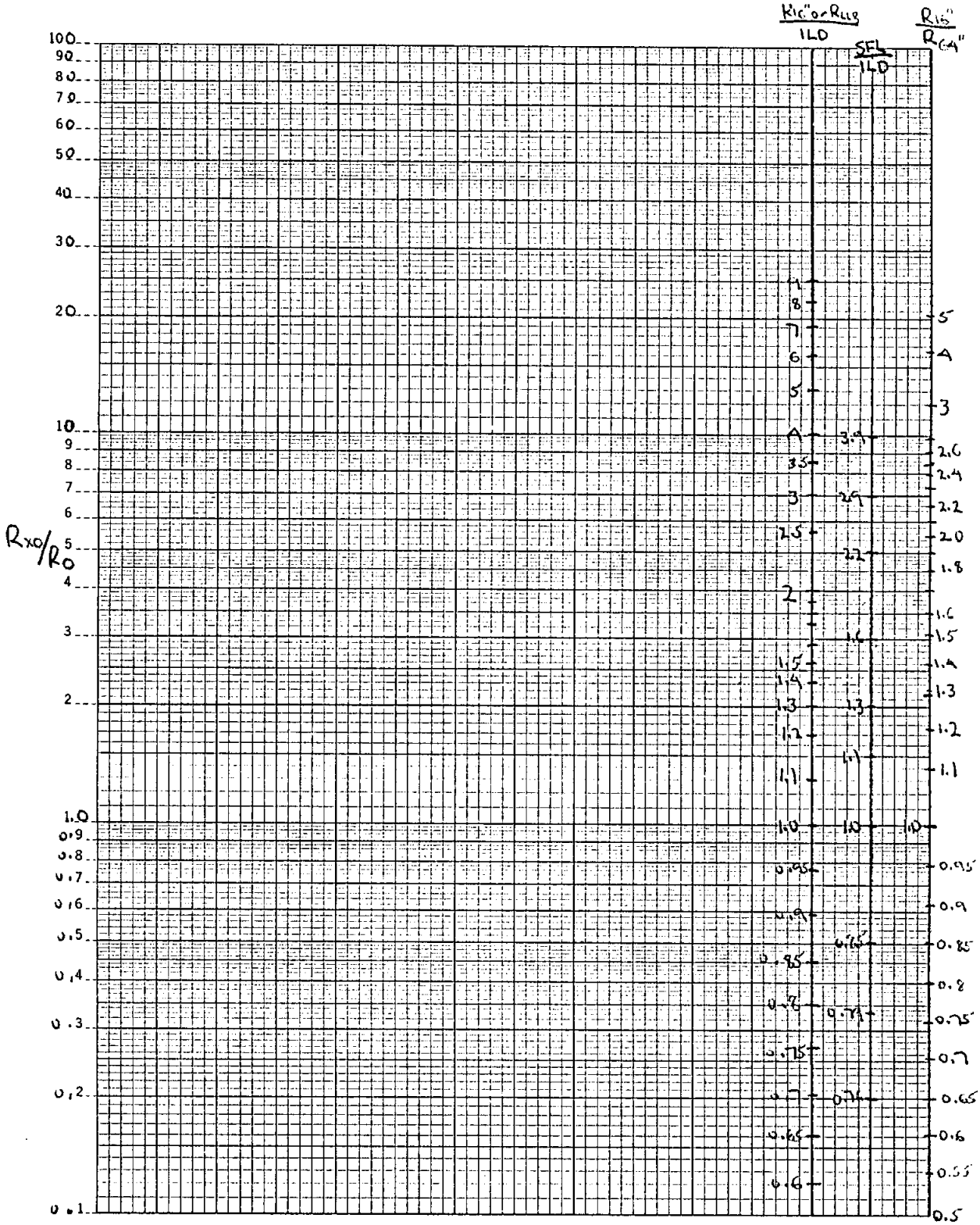

Figure 14-22. Nomograph for converting Ri / Ro to Rxo / Ro. The chart converts the most common log combinations: 16" normal / 64" normal, 16" normal / deep induction, LL8 / deep induction, and SFL / deep induction. An Ri / Ro value is entered on the appropriate line on the right side of the chart and a horizontal line is drawn to corresponding Rxo / Ro value on the left side. The chart was calculated for an invasion diameter of 20 inches, which is fairly typical for shallow, high porosity sandstones. Therefore, it contains generalized conversion factors. Bob Alger constructed the chart.

diameter of 20 inches, which is fairly typical for shallow, high porosity sandstones (Alger, personal communication). The chart, therefore, contains generalized conversion factors and the Rxo / Ro value obtained from the nomograph will usually be an estimate that has an unknown degree of accuracy. An Rw value calculated from data derived from Figure 14-22 is subject to a great deal of error.

An accurate Rmf measurement may or may not be a problem. Rm and Rmf are often measured on a sample of the drilling mud at the time of logging (refer to the **Drilling Fluid Invasion** section of Chapter 6). The values are usually included on the log header. If only Rm is measured, Rmf can be calculated from Rm. In fact, Alger (personal communication) believed that an Rmf value calculated from Rm is more accurate than a measured Rmf. This is because such a small volume of mud filtrate is available for the Rmf measurement. However, most log analysts prefer measured values (Schlumberger, 1988).

When calculating Rmf from Rm, some log analysts simply multiply Rm by 0.75. The most commonly used conversion factor is the one developed by Overton and Lipson (1958):

$$Rmf = K_m (Rm)^{1.07} \qquad \textbf{14-18}$$

The value of the constant K_m is a function of the mud weight (Table 14-3). The equation is for drilling muds with Rm in the range of 0.1 to 10 ohm-meters at 75° F. Most chart books contain a nomographs of Equation 14-18.

TABLE 14-3. K_m VALUES FOR VARIOUS MUD WEIGHTS

Mud Weight lb/gal	K_m
10	0.847
11	0.708
12	0.584
13	0.488
14	0.412
16	0.380
18	0.350

Lowe and Dunlap (1986), after reworking Overton and Lipson's data and making Rmf measurements on additional samples, developed their own conversion equation. The test data from both studies (Figure 14-23) shows that the Rmf / Rm value of muds lighter than 11 pounds per gallon is much more variable than it is for denser muds. In fact, for these lighter muds Rmf can be greater than Rm. In the wells analyzed for this study, a wide range was also observed in the ratio of Rmf to Rm and in 14 percent of the wells Rmf was greater than Rm (Section 1, Volume II).

The best policy is to accurately measure the Rm and Rmf of a circulated sample of the drilling fluid. If possible, the measurements should be taken daily during drilling because mud properties can change during the course of drilling a well. In the absence of a measured value, Rmf can be estimated from Equation 14-18. However, the calculated Rmf may be too low for muds lighter than 11 pounds per gallon.

The Resistivity Ratio method will calculate an accurate Rw, if accurate Rmf and Rxo values are available and if there is some invasion. Accurate Rw values were calculated for approximately a dozen wells analyzed during

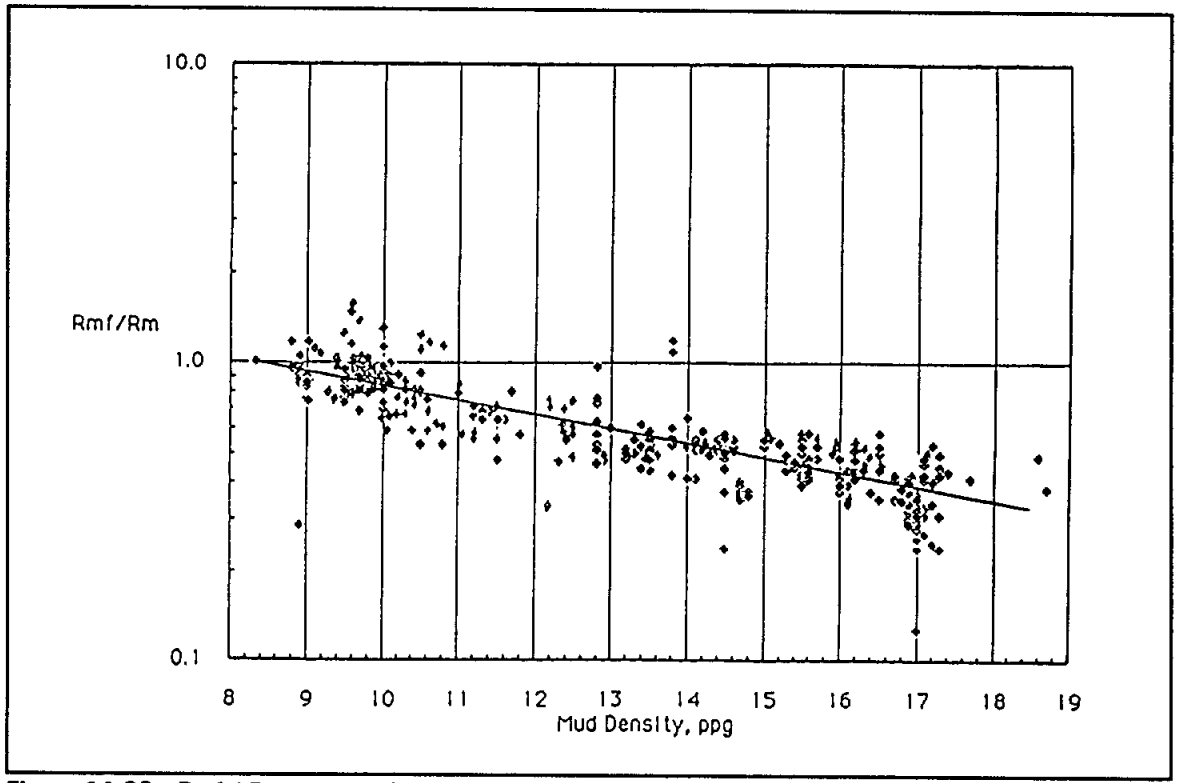

Figure 14-23. Rmf / Rm versus Mud Weight (Lowe and Dunlap, 1986). The graph includes data from Overton and Lipson (1958). The data for muds less than 11 pounds per gallon has considerable scatter.

this study (Figures 14-24 and 14-25 and Plates 2 and 3 are examples). The technique should be utilized more widely in ground-water studies, but Rxo tools must first start being run.

SP

Rw calculations from an SP curve date back to the earliest days of quantitative log analysis. Wyllie (1949) and Gondouin, et al. (1957) authored the technique. Alger (1966) elaborated on the difficulties of determining water quality with the SP curve. He also attempted to use the curve to estimate hardness (Alger and Harrison, 1988). McConnell (1983, 1985, 1988, and 1989) has been the latest to publish on the use of the SP curve in water quality calculations.

The technique requires a shale-free formation that is thick enough to have a static SP (SSP). It also assumes that static SP is solely a product of an electrochemical potential and that the shale adjacent to the formation of interest is an ideal ionic permeable membrane. (The various aspects of the SP curve are discussed in Chapter 12.) Under these conditions, SSP is related to the chemical activities of the cations in the formation water (a_w) and the mud filtrate (a_{mf}) by the formula:

$$SSP = -K \log a_w/a_{mf} \qquad \textbf{14-19}$$

For sodium chloride solutions and shales that are ideal ionic permeable membranes, K is solely a function of temperature:

$$K = 61 + 0.133\ T_{°F} \qquad \textbf{14-20}$$

For pure sodium chloride solutions that have an Rw or an Rmf of greater than 0.12 ohm-meters (83,333 μmhos/cm), resistivity is inversely proportional to the activity of the sodium ions (Figure 14-26). This means that Equation 14-19 can be rewritten as:

$$SSP = -K \log Rmf/Rw \qquad \textbf{14-21}$$

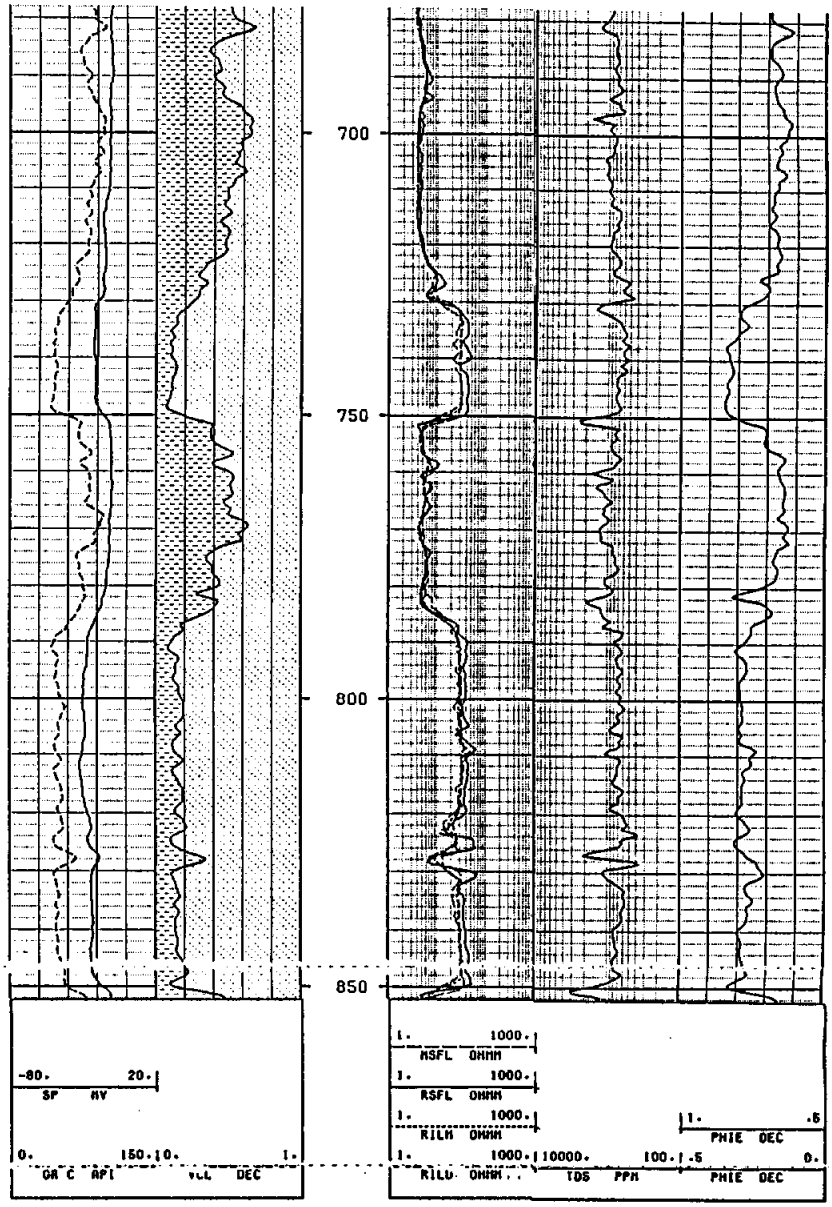

Figure 14-24. A water quality curve calculated by the Resistivity Ratio method using an Rxo curve. Track 4 contains a TDS curve calculated from Rw values obtained from the Resistivity Ratio method. Rw was converted to Cw and then TDS was calculated from Cw. The water analysis from a test hole drilled to 813 feet has a TDS of 590 mg/l. The calculated TDS of the two sands from 730 to 813 feet varies from 500 to 700 mg/l, very close to the TDS values that would give a composite TDS of 590 mg/l for the two sands. The resistivity curves nearly overlay, which indicates that Rmf and Rw are about the same. Rmf is 8.2 ohm-meters at formation temperature (82° F). Track 1 contains SP and borehole corrected gamma ray curves (GR C). Track 2 is a lithology column calculated from the gamma ray and porosity logs. The volume of clay (VCL) and the volume of quartz (dot pattern) are in decimal form (DEC). Track 3 contains microspherically focused (MSFL) and dual induction curves. Track 5 contains a density-neutron crossplot porosity curve (PHIE) in decimal form (DEC). The well is the Alsay, Cypress Creek U.D., #3, Harris County, Texas. The interval is part of the Gulf Coast Aquifer. Figure 9-14 contains additional information on this well.

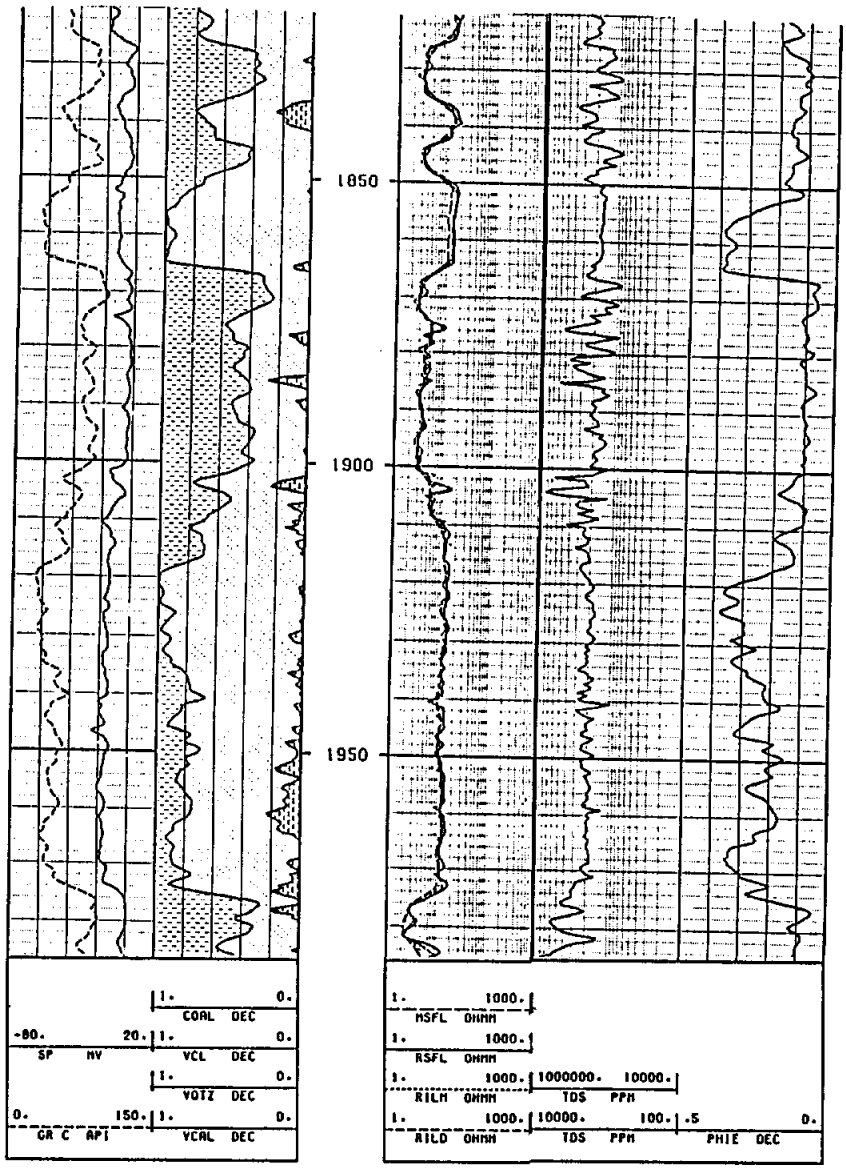

Figure 14-25. A water quality curve calculated by the Resistivity Ratio method using an Rxo curve. Track 4 contains a TDS curve calculated from Rw values obtained from the Resistivity Ratio method. Rw was converted to Cw and then TDS was calculated from Cw. The water analysis of the screened interval (1850 to 1866 and 1910 to 1974 feet) has a TDS of 2330 mg/l. The calculated TDS of the main sandstone (1910 to 1970 feet) varies from 1900 to 2100 mg/l, an error of about 10 percent. Some of the error may be due to the wrong exponent being used to convert Cw to TDS. The resistivity curves nearly overlay, which indicates that Rmf and Rw are about the same. Rmf is 3.38 ohm-meters at 81° F. Track 1 contains SP and borehole corrected gamma ray curves (GR C). Track 2 is a lithology column calculated from the gamma ray and porosity logs. The volume of clay (VCL), quartz (VQTZ), and calcite (VCAL) are in decimal form (DEC). Track 3 contains microspherically focused (MSFL) and dual induction curves. Track 5 contains a density-neutron crossplot porosity curve (PHIE) in decimal form (DEC). The well is the J.L. Myers, Bristol Water Supply #2, Ellis County, Texas. The aquifer is the Trinity. Figure 9-11 contains additional information on this well.

By rearranging Equation 14-21, Rw can be calculated:

$$Rw = Rmf/10^{(-SSP/K)} \qquad \textbf{14-22}$$

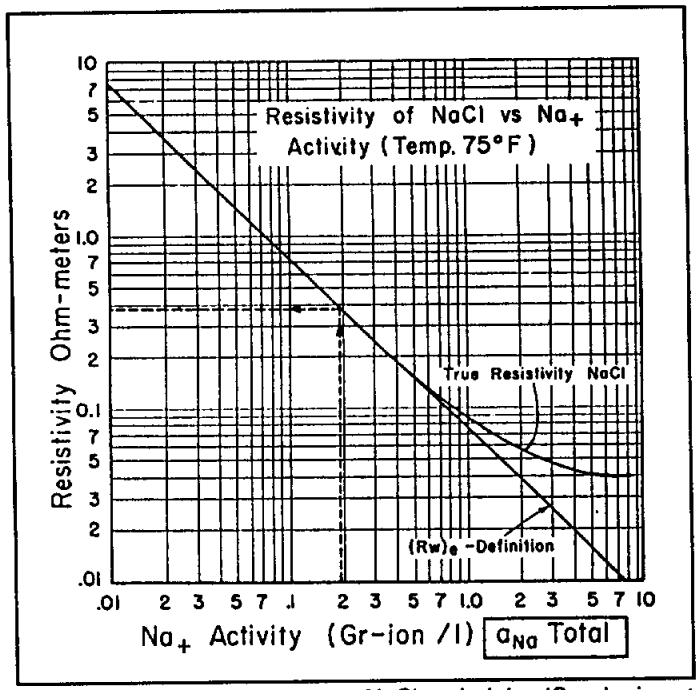

Figure 14-26. Chart of a_{Na} vs. NaCl resistivity (Gondouin, et al. 1957).

If Rw or Rmf is less than 0.12 ohm-meters (Figure 14-26), if the formation water is a type other than sodium chloride, or if polyvalent cations are present in either the formation water or the mud filtrate, Rw and Rmf are no longer inversely proportional to a_w and a_{mf}. Under any of these circumstances, Rw and Rmf in Equations 14-21 and 14-22 become **equivalent resistivities** (**Rmfe** and **Rwe**). An equivalent resistivity is the resistivity value of the sodium chloride solution that will generate the same SSP as that generated by a non-sodium chloride solution. Any basic petroleum log analysis text has a discussion of equivalent resistivities for low resistivity waters. This research was limited to non-sodium chloride waters, including those with polyvalent cations.

Polyvalent cations were found to be common in fresh to moderately saline ground waters in Texas (Section I, Volume 2). Most commonly the polyvalent cations are divalent calcium and magnesium ions. These two ions have a chemical activity that is about an order of magnitude greater than that of sodium ions (Figure 14-27). Consequently, divalent ions generate a negative SP that is much larger than the SP generated by an equivalent concentration of sodium ions. Therefore, Rwe is much lower than Rw. Rwe must be converted to Rw by means of an empirically derived correction factor.

The relationship between Rw and Rwe for a particular water type can be established if a sample of the water in question is available. The conversion factor is the ratio of the Rw of the water sample to the Rwe calculated using Equation 14-22. Figure 14-28 is a graph of Rw-Rwe

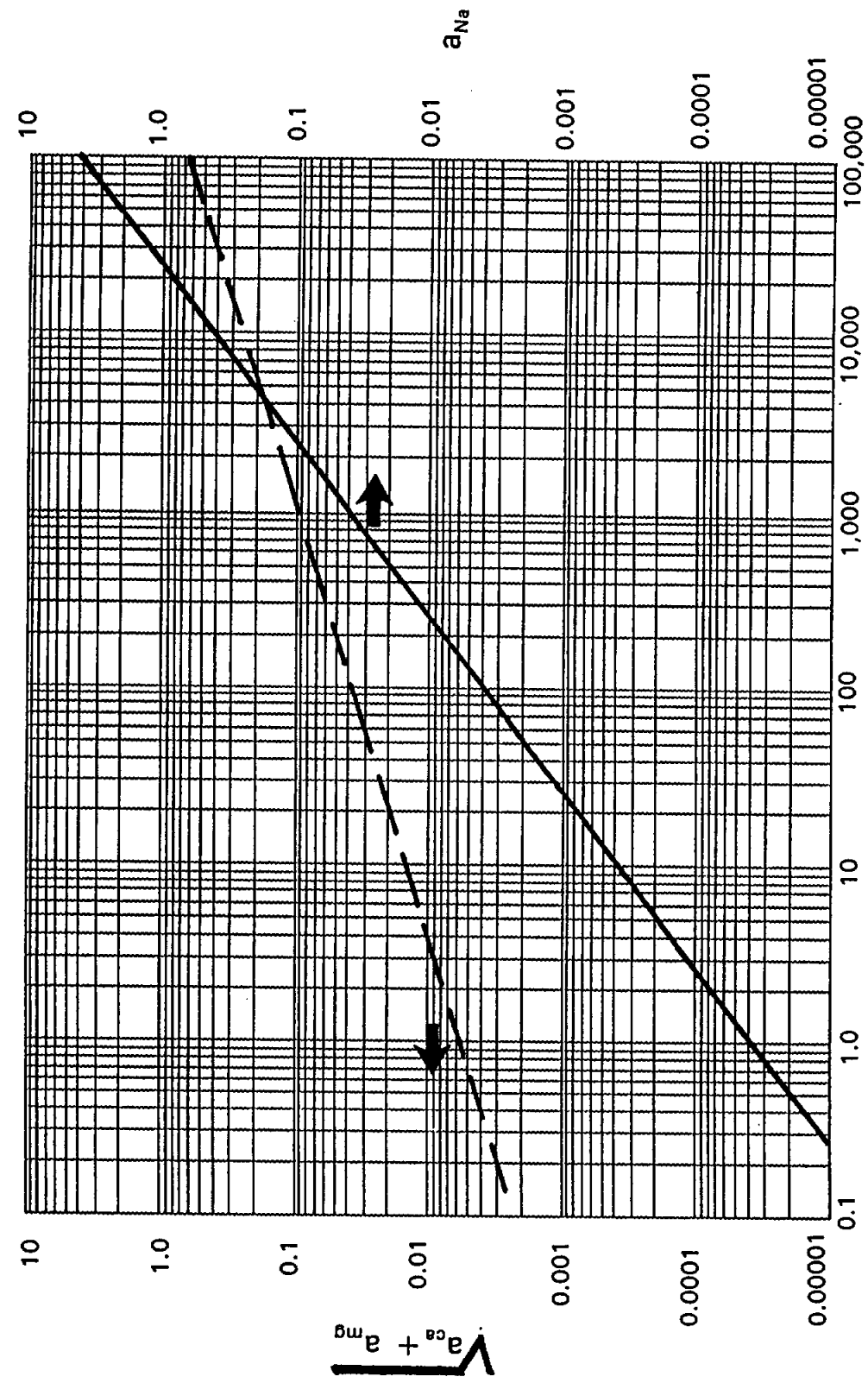

Figure 14-27. Cation concentrations vs. activities for sodium and calcium plus magnesium ions at 77° F (modified from Alger, 1966).

relationships for several pure end-member water types. Natural waters will fall somewhere in between the end members.

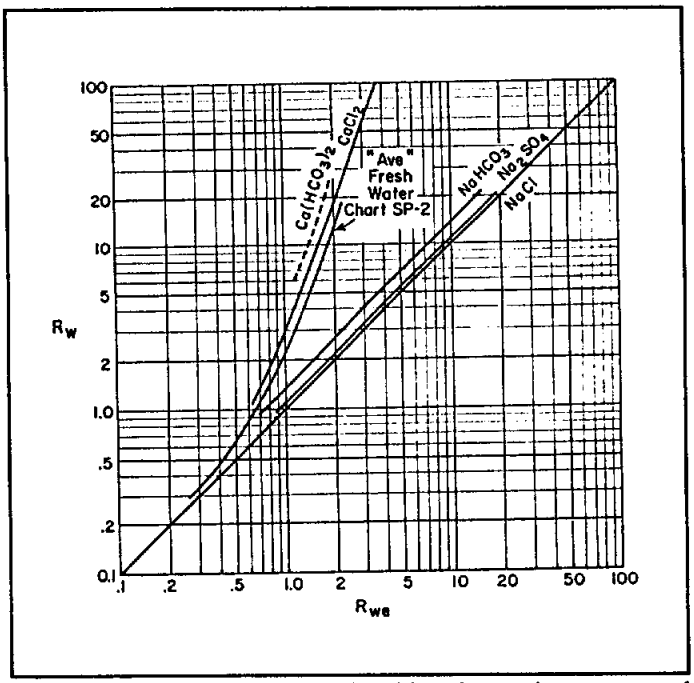

Figure 14-28. Rw-Rwe relationships for various types of waters (Schlumberger, 1972).

If a water sample is not available, the only option is to use an Rw-Rwe relationship from an offsetting well that has the same concentration of divalent ions. Unfortunately, the only way to be sure that the concentrations are the same is to have an analysis of both waters! An additional difficulty is that the water sample may not accurately reflect the chemical composition of the formation water. Mud filtrate invasion may alter the sodium/calcium/magnesium ratio of formation water passing through the invaded zone until several pore volumes of water have been produced (McConnell, 1985).

Calcium and magnesium ions can occur in mud filtrate, but the filtrate is usually a sodium chloride solution. This is because the divalent ions are preferentially adsorbed by clay platelets in the mud, while sodium ions are released into the drilling fluid (Gondouin, et al., 1957). If aquagel has been added to the drilling fluid or if long shale sections have been drilled, there is usually enough clay in the mud to adsorb any polyvalent ions (Alger and Harrison, 1988). At least, this is the assumption that has to be made, since a chemical analysis of the mud is seldom available (Alger, 1966).

There are several other conditions under which the SP curve will calculate an erroneous Rw value:

1. The presence of clay in an aquifer or a thin-bedded aquifer. Both reduce the amount of negative SP deflection, so a calculated Rw value will be too high (Plate 2).

2. An SSP with an electrokinetic potential component. SSP will be larger than expected, so a calculated Rw value will be too low.

3. A formation water and/or a mud filtrate that is predominately sodium bicarbonate. K will be less than that calculated by Equation 14-20 (Schlumberger, 1989). This will result in a calculated Rw that is too high.

4. Shales that are non-ideal membranes. Since K is a function of the cation exchange capacity of the shale (Silva and Bassiouni, 1981), it will be different than the K calculated with Equation 14-20. Unfortunately, cation exchange capacities are very seldom measured. Silva and Bassiouni (1981) recommend determining K from a previously established empirical relationship between K and shale resistivity. Shales that behave as non-ideal membranes are usually Tertiary or younger and K is less than what Equation 14-20 calculates (Alger and Harrison, 1988).

A water analysis can also be used to predict SSP. A known Rmf is converted to a_{mf} (Figure 14-26). a_w is calculated from the sum of a_{Na} and $\sqrt{a_{Ca} + a_{Mg}}$ (Figure 14-27). Equation 14-19 is then used to calculate SSP. However, such an exercise is mainly of academic interest and has little practical application in ground-water studies.

Calculating Rw from the SP curve was very unsuccessful for the wells studied in this project. This was especially true in cemented sandstones with varying porosities, such as the Trinity Aquifer. Plate 2 contains an Rw curve calculated from the SP of a well in Cameron County, Texas. The calculated Rw values are accurate down to 500 feet, but below this depth they are much too high. Possible explanations for the discrepencies are discussed in the explanation for Plate 2.

Calculating Rw from an SP curve works well for sodium chloride waters as long as the aforementioned conditions are met. If, however, the water has appreciable divalent ions, as is the case of many fresh to moderately saline ground waters, the technique is very difficult to use. It will only work if an Rw-Rwe relationship has been established. Unfortunately, the only way to establish the relationship is to first measure the Rw of a sample of the water; if a water sample is available, logging techniques are not needed! An Rw-Rwe relationship can be used from an adjacent well, as long as the calcium and magnesium concentrations are the same in both wells. But again, the only way to be sure of this is to have a water analysis from both wells. Thus Rw calculations from an SP curve in ground waters with divalent ions are only reliable after the fact.

SUMMARY AND CONCLUSIONS

Borehole geophysical techniques are a viable method of determining the water quality and hydrogeological parameters of aquifers. However, accurate answers require utilization of the correct logging suite, the appropriate interpretation technique(s), and appropriately constructed TDS-Cw graphs.

This study found a wide variety in the accuracy with which labs in Texas measure specific conductance. Some labs need to improve their calibration procedures. It was found that the Texas Department of Health's method of calculating specific conductance from diluted conductance does not give accurate values. Diluted conductance should not be substituted for measured conductance. It was documented that in the absence of a measured conductivity value, specific conductance can be accurately calculated from ionic concentrations.

Temperature-conductivity relationships for slightly to moderately saline non-NaCl type waters have not been published in either petroleum or ground-water literature. One of three equations is normally used to adjust conductivity for temperature fluctuations: Arp's, simplified Arp's, and 2 percent per ° C. Analysis of published data and laboratory experiments conducted during this project revealed that no one equation consistently yielded more accurate values. All three equations give acceptable temperature-corrected conductivity measurements, but the 2 percent per ° C equation is less likely to yield extreme values.

This study found a difference in the way labs calculate TDS. Some labs include 100 percent of the bicarbonate value, while others use 49.2 percent. Since ionic concentration governs Cw, 100 percent of the bicarbonate value should be included. Also, some labs do not document and/or perform a check on the accuracy of their TDS measurements.

TDS can be accurately estimated if Cw is known by using a TDS-Cw graph. These graphs have never been constructed for Texas ground-waters. TDS-Cw graphs were constructed for the major aquifers in the state. Also, a data base consisting of water analyses and log values from over 700 wellls in the major Texas aquifers was compiled and analyzed.

This study researched and established the proper procedure for constructing TDS-Cw graphs: guidelines for where to obtain water analyses, how to correct Cw to standard temperature (25° C), how to compute the proper TDS value, how to critique the accuracy of water analyses, and how to construct the graphs. Important conclusions include:

1. TDS should include 100 percent of the bicarbonate value.

2. The best graph is a log-log scale plot with the equation of the line fitted by reduced major axis and the equation of the line transformed to a power law.

3. Because of interionic interference, the graphs need to be established for a local area in order to conform to local water chemistry.

4. When the data is extrapolated to a TDS greater than the range of the data, TDS will be too low due to the effects of interionic interference on specific conductance.

There are two important fundamental differences between petroleum and ground-water/environmental logging:

1. Surface conductance has a significant effect on resistivity curves in ground-water logging. It was discovered that for ground-waters in Texas, surface conductance becomes a factor when Rw is greater than 2 ohm-meters.

2. SP interpretation in petroleum logging is based on sodium chloride formation water. Many of the ground-waters in Texas have calcium and magnesium, which complicates SP interpretation.

There are also important practical differences between the two types of logging. In ground-water/environmental logging, it is usually true that:

1. Bit sizes vary more, from a few inches to a few feet.

2. Poor quality drilling mud is common.

3. Little attention is paid to selecting the proper logging suite and to quality control.

4. There is a dearth of knowledge about logging techniques.

5. Slimhole logging tools are often used.

All of these factors complicates ground-water log interpretation.

Borehole geophysical tools have been run in ground-water wells since the early days of the science. However, little attention was ever paid to the subject by petroleum logging companies. Consequently, ground-water logging technology is decades behind petroleum logging. The applicability of many logging tools to ground-water studies has never been documented and guidelines for utilizing these tools in ground-water environments have never been established.

This study ran existing and new openhole logging tools in the main types of aquifers in the state (unconsolidated clastics, consolidated clastics, and carbonates). Each tool was evaluated for its applicability to ground-water/environmental studies. Guidelines were also written for using the tools in ground-water/environmental studies. The most important conclusions of this phase of the study were:

1. The single-point resistance tool, popular in environmental and mineral logging, should never be the primary resistivity tool. The tool has few strengths and several weaknesses.

2. Apart from the problem with bed definition, normal tools are ideally suited to openhole ground-water logging. The tools have been abandoned by the petroleum logging industry in favor of induction tools. However, in ground-water environments it is easier to get accurate resistivity values with normal curves than with induction curves.

3. Focused electrode (guard) tools are designed for the exact borehole environment of most water wells. The tools give accurate resistivity values and excellent vertical resolution. They should be utilized much more widely in ground-water/environmental studies.

4. The gamma ray and caliper logs are infrequently ran in water wells, but should be a standard part of every logging suite. The gamma ray provides lithology information and the caliper provides a picture

of the hole diameter. Both curves are useful in interpreting other curves.

5. Porosity logs are very seldom ran in water wells. They should be run routinely in carbonate aquifers such as the Edwards and in consolidated clastics such as the Trinity.

6. The Litho or Spectral Density tool is the porosity tool of choice. It is an excellent stand-alone porosity tool, with the ability to both identify lithology and calculate porosity.

7. Contrary to popular opinion, the sonic log will give accurate porosity values in shallow, unconsolidated formations if the correct transform is used. The Raymer-Hunt transform gives accurate porosity values in such circumstances.

8. Considerable improvement needs to be made in the quality of some slimhole logging tools. Specifically, gamma ray tools must be calibrated in API units; density and neutron tools must be calibrated in such a manner that porosity can be calcualted with the tools.

Seven techniques for calculating Cw and TDS from logs were evaluated, three empirical relationships (TDS-Ro Graphs, Ro_c-TDS Graphs, and Field Formation Factor) and four stand-alone techniques (Formation Factor Equation, Ro-Porosity Graphs, Resistivity Ratio Method, and SP). The Field Formation Factor method produced the least accurate results. Theoretically, Ro_c-TDS Graphs should be more accurate than TDS-Ro Graphs, but in reality they were not. Both types of graphs are site-specific. Ro-TDS graphs were constructed for forty-eight counties.

The Formation Factor Equation calculates accurate Rw values, as long as surface conductance is negligable (Rw less than 2 ohm-meters). The drawback is that a porosity curve is required and the cementation exponent must be accurately estimated. The Ro-Porosity Graph is simply a graphical solution of the Formation Factor Equation. The advantage is that m can be estimated and trends in water quality and m can sometimes be discerned. The Resistivity Ratio Method has the advantage of canceling the effect of surface conductance. It can, therefore, accurately calculate Rw regardless of the salinity of the water. The drawbacks are that it requires an accurate Rmf measurement and an Rxo tool. Rmf measurements are sometimes not

BIBLIOGRAPHY

Alger, R.P., 1966, Interpretation of electric logs in fresh water wells in unconsolidated formations, paper CC, *in* 7th annual symposium transactions: Society of Professional Well Log Analysts, 25 p.

Alger, R.P., and Harrison, C.W., 1988, Improved fresh water assessment in sand aquifers utilizing geophysical well logs, paper I, *in* 2nd international symposium on borehole geophysics for minerals, geotechnical, and groundwater applications [Golden, Colorado, Oct. 6-8, 1987], proceedings: Society of Professional Well Log Analysts, Minerals and Geotechnical Logging Society Chapter-at-Large, p. 99-118. Also published in 1988, *in* FOCUS conference on southwestern ground water issues [Albuquerque, New Mexico, March 23-25] proceedings: National Water Well Association, Dublin, Ohio, p. 281-309. Also published in 1988, *in* 2nd national outdoor action conference on aquifer restoration, ground water monitoring, and geophysical methods [Las Vegas, May 23-26] proceedings, volume 2: Association of Ground Water Scientists and Engineers (AAAS), p. 939-968. Later published in 1989, The Log Analyst, v. 30 (1), January-February, p. 31-44.

Allaud, L.A., and Martin, M.H., 1977, Schlumberger, the history of a technique: John Wiley & Sons, New York City, 333 p.

American Public Health Association, American Water Works Association, Water Pollution Control Federation, 1985, Standard methods for the examination of water and wastewater, (16th ed.): American Public Health Association, Washington, D.C., 1268 p.

Archie, G.E., The electrical resistivity log as an aid in determining some reservoir characteristics: Transactions AIME, v. 146, p. 54-62.

Arps, J.J., 1953, The effect of temperature on the density and electrical resistivity of sodium chloride solutions: Transactions AIME, v. 198, p. 327-330.

Baroid, 1991, Drilling fluid products for water well, mineral exploration, and geotechnical drilling: NL Baroid Corp., Houston, variously paginated.

Bateman, R.M., 1985, Openhole log analysis and formation evaluation: IHRDC Press, Boston, 647 p.

Beeson, C.M., and Wright, C.C., 1952, Loss of mud solids to formation pores: Petroleum Engineering, p. 40-52.

Bevington, P.R., 1969, Data reduction and error analysis for the physical sciences: McGraw-Hill Book Company, New York, p. 93-103.

Brown, C.E., 1988, Determination of rock properties by borehole-geophysical and physical-testing techniques and ground-water quality and movement in the Durham Triassic Basin, North Carolina: U.S. Geological Survey Professional Paper 1432, 29 p.

Brown, D.L., 1971, Techniques for quality-of-water interpretations from calibrated geophysical logs, Atlantic Coastal area: Groundwater, v. 9 (4), p. 25-38.

Clenchy, D.R., 1985, Effect of borehole diameter on log quality and interpretation--Grand Banks area, east coast Canada, paper V, *in* 10th formation evaluation symposium transactions: Canadian Well Logging Society, Calgary, 26 p.

Coates, G., Collier, H., Milligan, B., Vasilache, M., and Carter, J., in press, MRIL* an environmentally safe measure of porosity and permeability: *in* 4th international symposium on borehole geophysics for minerals, geotechnical, and groundwater applications [Toronto, Ontario, August 18-22], proceedings: Society of Professional Well Log Analysts, Minerals and Geotechnical Logging Society Chapter-at-Large.

Cohen, S.C., 1981, Relationships among the slopes of lines derived from various data analysis techniques and the associated correlation coefficient: Geophysics, v. 46 (11), p. 1606.

Collier, H.A., 1988, The effect of isolated biomoldic porosity on the log analysis of a Pennsylvanian carbonate reservoir in north Texas, paper X, *in* 29th annual symposium transactions: Society of Professional Well Log Analysts, 16 p.

_____, 1989, Assessment of the dielectric tool as a porosity device, *in* 3rd national outdoor action conference on aquifer restoration, ground

water monitoring and geophysical methods [Orlando, Florida], proceedings: National Well Water Association, Dublin, Ohio, p. 151-165. Also published in 1989 as paper L, *in* 3rd international symposium on borehole geophysics for minerals, geotechnical, and groundwater applicatons, proceedings: Society of Professional Well Log Analysts, Minerals and Geotechnical Logging Society, Chapter-at-Large, p. 183-197.

Davis, J.C., and Doveton, J.H., 1990, Overview of statistical methods in log analysis: Society of Professional Well Log Analysts computer applications workshop [Lafayette, Louisiana, June 28] course notes: Society of Professional Well Log Analysts, Houston, 19 p.

Davis, S.N., 1988, Where are the analyses?: Groundwater, v. 26 (1), p. 2-5.

Desai, K.P., and Moore, E.J., 1969, Equivalent NaCl determination from ionic concentrations: The Log Analyst v. 10 (3), p. 12-21.

Dewan, J.T., 1983, Essentials of modern open-hole log interpretation: PennWell Books, Tulsa, 361 p.

Doll, H.G., 1949, SP log: theoretical analysis and principles of interpretation: Transactions AIME, v. 179, p. 146-185.

Dresser Atlas, 1982, Well logging and interpretation techniques : Dresser Industries, Inc., Houston, variously paginated.

_____, 1985, Log interpretation charts: Dresser Industries, Inc., Houston, 157 p.

Driscoll, F.G., 1986, Groundwater and wells, (2nd ed.): Johnson Division, St. Paul, Minnesota, 1089 p.

Dunlap, H.F., and Hawthorne, R.R., 1951, The calculation of water resistivities from chemical analyses: Transactions AIME, v. 192, p. 373-375.

Dyck, J.H., Keys, W.S., and Meneley, W.A., 1972, Application of geophysical logging to groundwater studies in southeastern Saskatchewan: Canadian Journal of Earth Sciences, v. 9, p. 78-94.

Ellis, A.J., 1976, The I.A.G.C. interlaboratory water analysis comparison programme, Geochimica et Cosmochimica Acta, v. 40: Pergamon Press, Great Britain, p. 1359-1374.

Emerson, D.W., and Haines, B.M., 1974, The interpretation of geophysical well logs in water bores in unconsolidated sediments: Bulletin of Australian Society of Exploration Geophysics, v. 5 (3), p. 89-118.

Etnyre, L.M., 1984a, Practical application of weighted least squares methods to formation evaluation, part I: The logarithmic transformation of non-linear data and selection of dependent variable: The Log Analyst, v. 25 (1), p. 11-21.

_____, 1984b, Practical application of weighted least squares methods to formation evaluation, part II: Evaluating the uncertainty in least squares results: The Log Analyst, v. 25 (3). p. 11-20.

_____, 1989, Finding oil and gas from well logs: Van Nostrand Reinhold, New York, 306 p.

Evers, J.F., and Iyer, B.G., 1975a, A statistical study of the SP log in fresh water formations of northern Wyoming, paper K, *in* 16th annual symposium transactions: Society of Professional Well Log Analysts logging symposium, 8 p.

_____, 1975b, Quantification of surface conductivity in clean sandstones, paper L, *in* 16th annual symposium transactions: Society of Professional Well Log Analysts, Houston, 11 p.

Focke, J.W., and Munn, D., 1987, Cementation exponents in Middle Eastern carbonate reservoirs: SPE Formation Evaluation, v. 2 (2), p. 155-167.

Fogg, G.E., and Blanchard, P.E., 1986, Empirical relations between Wilcox ground-water quality and electric log resistivity, Sabine uplift area, *in* Geology and ground-water hydrology of deep-basin lignite in the Wilcox Group of east Texas, W.R. Kaiser, Principal Investigator, Bureau of Economic Geology, University of Texas at Austin.

Frank, R.W., 1986, Prospecting with old E-logs: Schlumberger Educational Services, Houston, 161 p.

Freeze, R.A., and Cherry, J.A., 1979, Groundwater: Prentice-Hall, Inc., Englewood Cliffs, N.J., 604 p.

Gardner, J.S., and Dumanoir, J.L., 1980, Litho-density log interpretation, paper N, *in* 21st annual symposium transactions: Society of Professional Well Log Analysts, 23 p.

Gearhart, 1981, Basic open hole seminar: Gearhart Industries, Inc., Fort Worth, variously paginated.

Glenn, E.E., and Slusser, M.L., 1957, Factors affecting well productivity - II. Drilling fluid particle invasion into porous media: Transactions AIME, v. 210, also published *in* Journal of Petroleum Technology (May), p. 132-139.

Glenn, E.E., Slusser, M.L., and Huitt, J.L., 1957, Factors affecting well productivity- I. Drilling fluid filtration: Transactions AIME, v. 210, also published *in* Journal of Petroleum Technology (May), p. 126-131.

Goetz, J.F., Dupal, L., and Bowler, J., 1979, An investigation into discrepancies between sonic log and seismic check shot velocities: unpublished.

Gondouin, M., Tixier, M.P., and Simard, G.L., 1957, An experimental study on the influence of the chemical composition of electrolytes on the S.P. curve: Transactions AIME, v. 210, also published *in* Journal of Petroleum Technology (February 1958), p. 58-70.

Guo, Y.A., 1986, Estimation of TDS in sand aquifer water through resistivity log: Ground Water, v. 24 (5), p. 598-600.

Guyod, H., 1944, Electric well logging, part 3; The single-point resistance method: The Oil Weekly, August 21, p. 44-52.

_____, 1957, Resistivity determination from electric logs: privately published, variously paginated.

_____, 1966, Interpretation of electric and gamma ray logs in water wells: The Log Analyst, v. 6, (5), p. 29-44.

Guyod, H., and Pranglin, J.A., 1959, Analysis charts for the determination of true resistivity from electric logs: Houston, 202 p.

Hallenburg, J.K., 1980, A comparison of nonpetroleum and petroleum logging, chapter E, *in* 21st annual symposium transactions: Society of Professional Well Log Analysts, 7 p.

_____, 1984, Geophysical logging for mineral and engineering applications: PennWell Books, Tulsa, 254 p.

Hansen, H.J., and Wilson, J.M., 1984, Summary of hydrogeologic data from a deep (2,678 ft.) well at Lexington Park, St. Mary's County, Maryland: Maryland Department of Natural Resources, Maryland Geological Survey, open-file report 84-02-01, 61 p.

Hartline, no date, Logging course notes: privately published, variously paginated.

Hartmann, D.J., 1975, Effect of bed thickness and pore geometry on log response, paper Y, *in* 16th annual symposium transactions: Society of Professional Well Log Analysts, 14 p.

Hassan, M., Hossin, A. and Combaz, A., 1976, Fundamentals of the differential gamma ray log interpretation technique, paper H, *in* 17th annual symposium transactions: Society of Professional Well Log Analysts, 18 p.

Helander, D.P., 1983, Fundamentals of formation evaluation: Oil and Gas Consultants International, Tulsa, 332 p.

Hem, J.D., 1982, Conductance; a collective measure of dissolved ions, *in* R.A. Minear and L.H. Keith, editors, Water analysis, v.1, Inorganic species, pt. 1: Academic Press, New York, p. 137-161.

_____, 1985, Study and interpretation of the chemical characteristics of natural water: U.S. Geological Survey Water-Supply Paper 2254, p. 1-249.

Hertzog, R., Colsen, L., Seeman, B., O'Brien, M., Scott, H., McKeon, D., Grau, J., Ellis, D., Schweitzer, J., and Herron, M., 1987, Geochemical logging with spectrometry tools, SPE-16792, in SPE annual technical

conference and exhibition, proceedings, volume omega, Formation evaluation and reservoir geology: Society of Petroleum Engineers, p. 447-460. Later published in 1989, SPE Formation Evaluation, v. 4(2), p. 153-162.

Hilchie, D.W., 1968, Caliper logging--Theory and practice: The Log Analyst, v. 9, (1), p. 3-12.

_____, 1979, Old (pre-1958) electrical log interpretation: D.W. Hilchie, Inc., Golden, Co., 161 p.

_____, 1982, revised, Applied openhole log interpretation: D.W. Hilchie, Inc., Golden, Co., variously paginated.

_____, 1987, The geologic well log interpreter notes: D.W. Hilchie, Inc., Boulder, Co., variously paginated.

_____, 1990, Wireline: a history of the well logging and perforating business in the oil fields: D.W. Hilchie, Inc., Boulder, Co., 200 p.

Hill, D.G., 1986, Geophysical well log calibration and quality control, *in* P.G. Killeen, editor, Borehole geophysics for mining and geotechnical applications [international symposium and workshop, (Toronto, Ontario, August 29-31, 1983), proceedings]: Geological Survey of Canada Paper 85-27, p. 379-392.

Hodges, R.E., 1988, Calibration and standardization of geophysical well-logging equipment for hydrologic applications: U.S. Geological Survey Water Resource Investigations Report 88-4058, 25 p.

Hounslow, A.W., 1987, Practical interpretation of water quality data, course notes: Oklahoma State University, Stillwater, Oklahoma, variously paginated.

Hurst, A., Lovell, M.A., and Morton, A.C., editors, 1990, Geological applications of wireline logs: Geological Society of London Special Publication, No. 48, 357 p.

International Critical Tables, 1928, International critical tables of numerical data, physics, chemistry and technology, v. III, prepared under the auspices of the International Research Council and the National

Acadamy of Sciences by the National Research Council of the United States of America: E.W. Washburn, editor-in-chief, New York Publishers, McGraw-Hill Book Company, Inc., p. 444.

_____, 1929, International critical tables of numerical data, physics, chemistry and technology, v. III, prepared under the auspices of the International Research Council and the National Acadamy of Sciences by the National Research Council of the United States of America: E.W. Washburn, editor-in-chief, New York Publishers, McGraw-Hill Book Company, Inc., p. 481.

Itoh, T., Miyairi, M., and Kimura, K., 1980, The high temperature well logging system for geothermal well, paper G, *in* 21st annual logging symposium: Society of Professional Well Log Analysts, 21p.

Jacobson, L.A., and Fu, C.C., 1990, Computer simulation of cased-hole density logging: SPE Formation Evaluation, v. 5 (4), p. 465-468.

Jansson, M., 1985, A comparison of detransformed logarithmic regressions and power function regressions: Geografiska Annaler, v. 67 A(1-2), p. 61-70.

Johnson, H.M., 1962, A history of well logging: Geophysics, v. 27 (4), p. 507-527.

Jones, P.H., and Buford, T.B., 1951, Electric logging applied to ground water exploration: Geophysics, v. 16, (1), p. 115-139.

Jones, T.A., 1979, Fitting straight lines when both variables are subject to error, part I; Maximum likelihood and least-squares estimation: Mathematical Geology, v. 2 (1), 25 p.

Jorden, J.R., and Campbell, F.L., 1984, Well logging I--Rock properties, borehole environment, mud and temperature logging: Society of Petroleum Engineers, Dallas, Monograph series No. 9, 167 p.

_____, 1986, Well logging II--Electric and acoustic logging: Society of Petroleum Engineers, Dallas, Monograph series No. 10, 192 p.

Jorgensen, D.G., 1988, Using geophysical logs to estimate porosity, water resistivity, and intrinsic permeability: U.S. Geological Survey, Denver, Water Supply Paper 2321, 24 p.

Keys, W.S., 1988, Borehole geophysics applied to ground-water investigations: U.S. Geological Survey open-file report 87-539, 305 p. Also published in Techniques of Water-Resources Investigations, 1990, O2-E2, 150 p.

Keys, W.S., and MacCary, L.M., 1971, Application of borehole geophysics to water-resources investigations: U.S. Geological Survey, Techniques of Water-Resources Investigations, book 2, chapter E1, 126 p.

Kienitz, C., Flaum, C., Olesen, J-R., and Barber, T., 1986, Accurate logging in large boreholes, *in* 27th annual logging symposium: Society of Professional Well Log Analysts, 21p.

Kwader, T., 1982, Interpretation of borehole geophysical logs in shallow carbonate environments and their application to ground-water resources investigations: Florida State University, unpublished dissertation, 335 p.

_____, 1984, The use of geophysical logs for determining formation water quality, *in* D.M. Neilsen and M. Curl, editors, 1984 NWWA/EPA conference on surface and borehole geophysical methods in ground water investigations, proceedings: National Water Well Association, Worthington, Ohio, p. 833-841. Later published in 1986, Ground Water, v. 24 (1), p. 11-15.

_____, 1985, Resistivity-porosity cross plots for determining in situ formation water quality--Case examples, *in* 1985 NWWA conference on surface and borehole geophysical methods in ground water investigations [Fort Worth, Texas, February 12-14], proceedings: National Water Well Association, Worthington, Ohio, p. 415-424.

_____, 1986, The use of geophysical logs for determining formation water quality: Ground Water, v. 24, (1), p. 11-15.

Labo, J., 1987, A practical introduction to borehole geophysics--An overview of wireline well logging principles for geophysicists: Society

of Exploration Geophysicists, Tulsa, Geophysical References Series, v. 2, 330 p.

Lancaster, J.R., and Atkinson, A., 1987, Computer processing of selected drilling, lithologic, and geophysical log data produces accurate permeability values and comprehensive aquifer analysis, including specific yield: COGS [Computer Oriented Geological Society] Computer Contributions, v. 3, (1), February, p. 13-36.

Logan, J., 1961, Estimation of electrical conductivity from chemical analyses of natural waters: Journal of Geophysical Research, v. 66 (8), p. 2479-2483.

Lowe, T.A., and Dunlap, H.F., 1986, Estimation of mud filtrate resistivity in fresh water drilling muds: The Log Analyst, v. 27 (2), p. 77-84.

MacCary, L.M., 1978, Interpretation of well logs in a carbonate aquifer: U.S. Geological Survey Water-Resources Investigations No. 78-88, 30 p. Later published in 1983 as, Geophysical logging in carbonate aquifers: Ground Water, v. 21 (3), p. 324-342.

_____, 1980, Use of geophysical logs to estimate water-quality trends in carbonate aquifers: U.S. Geological Survey Water-Resources Investigations, No. 80-57, 23 p.

_____, 1984, Relation of formation factor to depth of burial in aquifers along the Texas Gulf coast, *in* D.M. Nielsen and M. Curl, editors, 1984 NWWA/EPA conference on surface and borehole geophysics methods in ground water investigations, proceedings: National Water Well Association, Worthington, Ohio, p. 722-742.

Mann, C.J., 1987, Misuses of linear regression in earth sciences, *in* W.B. Size, editor, Use and abuse of statistical methods in the earth sciences: Oxford University Press, Newy York, p. 74-106.

Mark, D.M., and Church, M., 1977, On the misuse of regression in earth science: Mathematical Geology, v. 9 (1), p. 63-75.

McBain, J.W., Peaker, C.R., and King, A.M., 1929, Absolute measurements of the surface conductivity near the boundary of optically polished

glass and solutions of potassium chloride: Journal of American Chemical Society, v. 51, p. 3294-3312.

McConnell, C.L., 1983, Spontaneous potential corrections for ground-water salinity calculations; Carter County, Oklahoma, U.S.A.: Journal of Hydrology, v. 65, p. 363-372.

_____, 1985, Time dependence of the equivalent water resistivity in fresh water wells: The Log Analyst, v. 26 (3), p. 12-17.

_____, 1988, A general correction for spontaneous potential well logs in fresh water: Journal of Hydrology, v. 101 (1-4), p. 1-13.

_____, 1989, Characterization of wellhead protection areas using spontaneous potential well log analysis, paper II, *in* 3rd international symposium on borehole geophysics for minerals, geotechnical, and groundwater applications, proceedings: Society of Professional Well Log Analysts, Minerals and Geotechnical Logging Society, Chapter-at-Large, p. 671-697.

McCoy, R.L., Kumar, R.M., and Pease, R.W., 1980, Identifying fractures with conventional well logs: World Oil, v. 191 (7), Dec., p. 91-98.

Merkel, R.H., and Snyder, D.D., 1977 Application of calibrated slim hole logging tools to quantitative formation evaluation, chapter X, *in* 18th annual symposium transactions: Society of Professional Well Log Analysts, 21 p.

Miller, R.L., Bradford, W.L., and Peters, N.E., 1988, Specific conductance: theoretical considerations and application to analytical quality control: U.S. Geological Survey Water-Supply Paper 2311, p. 1-16.

Moelwyn-Hughes, E.A., 1961, Physical chemistry, (2nd ed.): Pergamon Press, New York, 1333 p.

Moore, C.V., and Kaufman, R.L, 1981, Your unsuspected problems--Fluid resistivity and water analysis, paper C, *in* 22nd annual symposium transactions: Society of Professional Well Log Analysts, Houston, 15 p.

_____, 1983, Resistivity techniques can cause unsuspected problems: World Oil, p. 49-53, 62.

Moore, E.J., 1966, A graphical description of new methods for determining equivalent NaCl concentration of chemical analysis, paper M, *in* 7th annual symposium transactions: Society of Professional Well Log Analysts, Houston, 34 p.

Moses, P.L., 1961, Geothermal gradients, drilling, and production practice: American Petroleum Institute.

National Research Council, 1928, International critical tables of numerical data, physics, chemistry and technology: McGraw-Hill Book Company, Inc., New York, v. 3, 444 p.

National Research Council, 1928, International critical tables of numerical data, physics, chemistry and technology: McGraw-Hill Book Company, Inc., New York, v. 4, 480 p.

Overton, H.L., and Lipson, L.B., 1958, Correlation of electrical properties of drilling fluids with solids content: Transactions AIME, v. 213, p. 333-336.

Peterson, B.R., 1991, Borehole geophysical logging methods for dissolved solids; a case study, *in* Ground water management: no. 5, [Las Vegas, Nevada, May 13-16], proceedings of the 5th national outdoor action conference on aquifer restoration, ground water monitoring, and geophysical methods, p. 1047-1072.

Pirson, S.J., 1963, Handbook of well log analysis for oil and gas formation evaluation: Prentice-Hall, Enlglewood Cliffs, N.J., 325 p.

Poteet, D., Collier, H., and Maclay, R., 1992, Investigation of the fresh/saline water interface in the Edwards Aquifer in New Braunfels and San Marcos, Texas: Edwards Underground Water District Report 92-02, San Antonio, Texas, 171 p.

Prensky, S.E., 1987, Geological applications of well logs--An introductory bibliography and survey of the well logging literature through September, 1986, arranged by subject and first author: The Log Analyst, parts A and B, v. 28, (1), January-February, p. 71-107, part

C, v. 28, (2), March-April, p. 219-248, (previous editions published as U.S. Geological Survey Open-File Reports 85-441, 86-170, 87-16).

Raymer, L.L., Hunt E.R., and Gardner J.S., 1980, An improved sonic transit time-to-porosity transform, paper P, *in* 21st annual symposium transactions: Society of Professional Well Log Analysts, Houston, 13 p.

Repsold, H., 1989, Well logging in groundwater development: International Association of Hydrogeologists, International Contributions to Hydrogeology, v. 9, 136 p.

Rider, M.H., 1986, The geological interpretation of well logs: John Wiley & Sons, Inc., New York, 175 p.

Rink, M., and Schopper, J.R., 1974, Interface conductivity and its implications to electric logging, paper J, *in* 15th annual symposium transactions: Society of Professional Well Log Analysts, Houston, 15 p.

Sanyal, S.K., and Jusbasche, J.M., 1979, Calculation of geothermal water salinity from well logs--A statistical approach: Geothermal Resources Council Transactions, v. 3, September, p. 613-616.

Sarma, V.V.J., and Rao, V.B., 1962, Variation of electrical resistivity of river sands, calcite, and quartz powders with water content: Geophysics, v. 27 (4), p. 470-479.

Schlumberger, 1958, Introduction to Schlumberger well logging: Schlumberger Well Surveying Corp., Houston, 176 p.

_____, 1972, Log interpretation: Volume I - principles: Schlumberger Limited, New York, New York, 112 p.

_____, 1979, Log interpretation charts: Schlumberger Well Surveying Corp., Ridgefield, Conn., 97 p.

_____, 1987, Log interpretation principles/applications: Schlumberger Educational Services, Houston, 198 p.

_____, 1988, Log interpretation charts: Schlumberger Educational Services, Houston, Document No. SMP-7006, 150p.

_____, 1989, Log interpretation principles/applications: Schlumberger Educational Services, Houston, Document No. SMP-7017, 223 p.

Sciacca, J., 1989, Operational and quality assurance considerations for borehole geophysical logging in hydrogeologic investigations, *in* 3rd national outdoor action conference on aquifer restoration, ground water monitoring and geophysical methods [Orlando, Florida], proceedings: National Water Well Association, Dublin, Ohio, p. 891-907.

Scott, J.H., 1978, A FORTRAN algorithm for correcting normal resistivity logs for borehole diameter and mud resistivity: U.S. Geological Survey, Open-File Report 78-779, 12 p.

Segesman, F., and Tixier, M.P., 1959, Some effects of invasion on the SP curve: Transactions AIME 216. Also published in 1959 *in* Journal of Petroleum Technology, p. 138-146.

Serra, O., 1984, Fundamentals of well-log interpretation, volume 1--The acquisition of logging data: Elsevier, New York, Developments in Petroleum Science, No. 15A, 423 p.

_____, 1985, Sedimentary environments from wireline logs: Schlumberger Technical Services, Paris, Document No. M-081030/SMP-7008, 211 p.

Sherman, H., and Locke, S., 1975, Depth of investigation of neutron and density sondes for 35 percent-porosity sand, paper Q, *in* 16th annual symposium transactions: Society of Professional Well Log Analysts, 14 p.

Shuter, E., and Teasdale, W.E., 1989, Application of drilling, coring, and sampling techniques to test holes and wells, chapter F1 in Collection of environmental data: U.S. Geological Survey Techniques of Water-Resources Investigations, Book 2, 97 p.

Silva, P., and Bassiouni, Z., 1981, A new approach to the determination of formation water resistivity from the SP log, paper G, *in* 22nd annual symposium transactions: Society of Professional Well Log Analysts, 14 p.

Snyder, D.D., and Fleming D.B., 1985, Well logging -- a 25-year perspective: Geophysics, v. 50 (12), p. 2504-2529.

Society of Professional Well Log Analysts, Houston Chapter, 1979, The art of ancient log analysis: Society of Professional Well Log Analysts, Houston, 131 p. + reprints of 22 classic papers.

Society of Professional Well Log Analysts, 1982, Geothermal log interpretation handbook: Society of Professional Well Log Analysts, Houston, Reprint Volume, variously paginated.

Summers, W.K., 1972, Factors affecting the validity of chemical analyses of natural water: Groundwater, v. 10 (2), p. 12-17.

Taylor, K.C., Hess, J.W., and Mazzela, A., 1989, Field evaluation of a slim-hole borehole induction tool: Ground Water Monitoring Review, v. 9 (1) p. 100-104.

Taylor, K., Molz, F., and Hayworth, J., 1988, A single well electrical tracer test for the determination of hydraulic conductivity and porosity as a function of depth, *in* 2nd national outdoor action conference on aquifer restoration, ground water monitoring and geophysical methods [Las Vegas, May 23-26], proceedings, volume 2: Association of Ground Water Scientists and Engineers (AAAS), p. 925-938.

Taylor, T.A., and Dey, J.A., 1985, Bibliography of borehole geophysics as applied to ground-water hydrology: U.S. Geological Survey Circular No. 926, 62 p.

Tittman, J., and Wahl, J.S., 1965, The physical foundations of formation density logging (gamma-gamma): Geophysics, vol. 30 (2) p. 284-294.

Towle, G., 1962, An analysis of the formation resistivity factor-porosity relationship of some assumed pore geometries, paper 3, *in* 3rd annual symposium transactions: Society of Professional Well Log Analysts.

Troutman, B.M., and Williams, G.P., 1987, Fitting straight lines in the earth sciences, *in* W.B. Size, editor, Use and abuse of statistical methods in the earth sciences: Oxford University Press, New York, p. 107-128.

Truman, R.B., Alger, R.P., Connell, J.G. and Smith, R.L., 1972, Progress report on interpretation of the dual-spacing neutron log (CNL) in the United States, paper U, *in* 13th annual symposium transactions: Society of Professional Well Log Analysts, 34 p.

Turcan, A.N. Jr., 1962, Estimating water quality from electrical logs, *in* Geological Survey Research 1962: U.S. Geological Survey Professional Paper 450-C, p. C135-C136.

_____, 1966, Calculation of water quality from electrical logs--Theory and practice: Louisiana Geological Survey, and Louisiana Department of Public Works Resources Pamphlet 19, 23 p.

Urban, F., White, H.L., and Strassner, E.A., 1935, Contribution to the theory of surface conductivity at solid-liquid interfaces: The Journal of Physical Chemistry, v. 39 (3), p. 311-330.

Veneruso, A.F., and Coquat, J.A., 1979, Technology development for high temperature logging tools, paper KK, *in* 20th annual symposium transactions: Society of Professional Well Log Analysts, 13 p.

Vonhof, J.A., 1966, Water quality determination from spontaneous-potential electric log curves: Journal of Hydrology, v. 4, p. 341-347.

Wahl, J.S., Tittman, J., Johnstone, C.W. and Alger, R.P., 1964, The dual spacing formation density log: Journal of Petroleum Technology, p. 1411-1416.

Weiss, J.S., 1987, Determining dissolved solids concentrations in mineralized ground water of the gulf coast aquifer systems using electric logs, *in* Aquifers of the Atlantic and Gulf Coastal Plain, American Water Resources Association, Monograph No. 9, J. Vecchioli and A.I. Johnson, editors, p. 139-150.

Welex, 1985, Log interpretation charts: Welex, Houston, variously paginated.

Williams, G.P., and Troutman, B.M., 1987, Algebraic manipulation of equations of best-fit straight lines, *in* W.B. Size, editor, Use and abuse of statistical methods in the earth sciences: Oxford University Press, New York, p. 129-141.

Winsauer, W.O., Shearin, H.M. Jr., Masson, P.H., and Williams, M, 1952, Resistivity of brine-saturated sands in relation to pore geometry: Bulletin of the American Association of Petroleum Geologists, v. 36 (2), p. 253-277.

Winsauer, W.O., and McCardell, W.M., 1953, Ionic double-layer conductivity in reservoir rock: Transactions AIME, v. 198, p. 129-134.

Worthington, A.E., Hedges, J.H., and Pallatt, N., 1990, SCA guidelines for sample preparation and porosity measurement of electrical resistivity samples, part I, Guidelines for preparation of brine and determination of brine resistivity for use in electrical resistivity measurements: The Log Analyst, v. 31, (1) p. 20-28.

Wyllie, M.R.J., 1949, A quantitative analysis of the electrochemical component of the SP curve: Transactions AIME, v. 186, p. 17-26.

Wyllie, M.R.J., Gregory A.R. and Gardener, L.W., 1956, Elastic wave velocities in heterogeneous and porous media: Geophysics, v. 21, (1) p. 41-70.

Yearsley, E.N., Crowder, R.E., and Irons, L.A., 1991, Monitoring well completion evaluation with borehole geophysical density logging: Ground Water Monitoring Review, v. 11 (1), p. 103-111.

ABBREVIATIONS

Appendix IV

a -	Variable used in several equations in Chapter 4; meaning varies according to the equation
a -	Tortuosity factor
A_1 -	Guard electrode
A -	Electrode
AC -	Alternating current
a_{Ca} -	Activity of the calcium ions
Al -	Aluminum
AM -	Electrode spacing of normal tools
AM ∞ -	Antiquated term for AM
a_{mf} -	Activity of the mud filtrate
a_{Mg} -	Activity of the magnesium ions
a_{Na} -	Activity of the sodium ions
AO -	Electrode spacing of lateral tools
APHA -	American Public Health Association
API -	American Petroleum Institute
a_w -	Activity of the formation water
b -	Variable used in several equations in Chapter 4: meaning varies according to the equation
B_{cp} -	Compaction correction factor (same as C_p)
BGT -	Borehole Geometry Tool
B.H.V. -	Borehole volume
BPB -	British Plaster Board
Br -	Bromide
BRC -	Balcones Research Center
C -	Conductivity
° C -	Degrees Celsius
Ca -	Calcium
Cali -	Caliper
Ca_2SO_4 -	Calcium Sulphate
CDL -	Compensated Density Log
CEC -	Cation exchange capacity
CGR -	Computed gamma ray curve minus the uranium count

CILD - Deep induction conductivity curve
Cl - Chloride
CNT-G - Epithermal/Thermal Compensated Neutron Log
CO_3 - Carbonate
Corr - Corrected
C_p - Compaction correction factor (same as B_{cp})
CPS Counts per second
CSNG - Compensated Spectral Natural Gamma Ray
Cw - Specific conductance or specific conductivity
$Cw_{Anion\ Sum}$ - Specific conductance calculated from the anion sum
$Cw_{Calculated}$ - Calculated specific conductance
$Cw_{Ion\ Conc.}$ - Specific conductance calculated from the ion concentration
$Cw_{Measured}$ - Measured specific conductance

DCAL - Differential caliper
DEC - Decimal
Δt - Travel time
Δt_f - Fluid travel time
Δt_{ma} - Matrix travel time
Δt_{sh} - Shale travel time
D.F. - Drill Floor
dh - Borehole Diameter (also d_h)
diff - Difference
DIL - Dual Induction Log
DIL-SFL - Dual Induction Log - Spherically Focused Log
DIS-EA - One version of Schlumberger's Dual Induction Tool
DLL - Dual Laterlog
DLS/DE - One version of Schlumberger's Dual Laterolog
DN - Density neutron
DNL - Dual Porosity Compensated Neutron Log
DNPOROS - Density-neutron crossplot
DPHI - Density porosity
DPT - Deep Propagation Tool
DRHO - Bulk density correction ($\Delta\rho$)

e - Bed thickness (in older literature)
E - Emitter
E_c - Electrochemical potential
E_k - Electrokinetic potential
EL - Electric log
E_{lj} - Liquid-junction potential

E log -	Electric log
E_m -	Shale membrane potential
emp -	Equivalents per million
ENPH -	Epithermal porosity
EPHI -	Electromagnetic propagation porosity
EPT -	Electromagnetic Propagation Tool
ES -	Electrical Survey
F -	A conversion factor
F -	Flouride
F -	Formation Factor
° F -	Degrees Fahrenheit
F_o -	Formation factor of the common porosity (depth) value
FDC -	Compensated Formation Density
FFF -	Field formation factor
FLUIDRES -	Fluid resistivity
FoRxo Log -	Flushed zone microelectrode tool
FR -	First reading
FR -	Fluid resistivity
F_R -	Formation resistivity factor
g -	Gram
G -	Geometric factor
GAM -	Gamma
g/l -	Grams per liter
G.L. -	Ground level
GLT -	Geochemical Logging Tool
GR -	Gamma ray
GRC -	Gamma ray corrected
GR_{cl} -	Gamma ray response in a clean zone
Gr-ion/l -	
GR_{sh} -	Gamma ray response in 100 percent shale
grain/gal. -	Grains per gallon
h -	Bed thickness
H+ -	Hydrogen ion
HCO_3 -	Bicarbonate
I -	Survey current
IDPH -	Phasor Deep Induction
IEL -	Induction Electric Log

IES - Induction Electric Survey
IFG - Instruments for Geophysics
I_{GR} - Gamma ray shale index
I.H.V. - Integrated hole volume
ILD - Deep Induction Log
ILM- Medium Induction Log
IMPH - Phasor Medium Induction
ISF - Induction Spherically Focused Log
in - Inches, also (")

J - Pseudogeometric factor

K - Constant dependent on the electrode configuration
K - Constant that is a function of temperature
K - Potassium
K.B. - Kelly bushing
KCl - Potassium chloride
KGS - Kansas Geological Society
kg/m - Kilograms per meter
K_m - Constant that is a function of the mud weight
l - length
Lat. - Lateral
lb/gal - Pounds per gallon
LDT - LithoDensity Tool
LL - Laterlog
LL3 - Laterlog 3
LL8 - Laterlog 8
LLD - Deep laterlog
LLS - Shallow laterlog
LN - Long normal
LNS - Least Normal Squares
LONG NOR - Long normal

m - Cementation exponent
M_1, M_2, M_{11}, M_2' - Monitoring electrodes
md - millidarcy
MEAS - Measured
meq/L - Milliequivalents per liter
MeV - Million electron volts
Mg - Magnesium
mg/kg - Milligrams per kilogram

mg/l - Milligrams per liter
mm - Millimeters
mmhos/m - Millimhos per meter
μmhos/cm - Millimhos per centimeter
μsec/foot - Microseconds per foot
μs - microsiemens
MINV - Microinverse
ML - Microlog
MLL - Microlaterolog
MLS - Mineral Logging Systems
Mn - Manganese
MNOR - Micronormal
MRIL - Magnetic Resonance Imaging Log
mS/m - Millisemens per meter
MSFL - Microspherically Focused Log
mv - millivolt

N - Electrode
NA - Not Available
Na - Sodium
NaCl - Sodium Chloride
$NaCl_{Equiv.}$ - Sodium Chloride equivalent
Na (diff.) - Sodium by difference
$NaHCO_3$ - Sodium bicarbonate
NAT - Natural
NGS - Natural Gamma Ray Spectometry Log (Schlumberger)
NGWA - National Ground Water Association
NO_3 - Nitrate
NPHI - Neutron porosity

O - Oxygen
O, O', OO' - Electrodes
Ω - Ohm
ohm-cm - Ohm-centimeter
ohm-m - Ohm-meter

P - Permeable bed
PC - Personal computer
Pe - Photoelectric factor
PEF - Photoelectric factor
ϕ - porosity (phi)

PHIE - Effective porosity
PI - Phasor Induction
PI - Petroleum Information Corporation
pi - π
PL - Proximity Log
ppm - Parts per million
psi - Pounds per square inch
PSP - Pseudostatic SP
pu - Porosity units
PUB - Public
PVC - Polyvinylchloride

R - Resistivity
R - Receiver
Ra - Apparent resistivity
redox- Oxidation-reduction
Ri - Resistivity of the invaded zone
R_{ID} - Deep induction resistivity
$(R_{IL})cor$ - Corrected induction resistivity
R_{ILD} - Deep induction resistivity
R_{IM} - Medium induction resistivity
Rm - Mud resistivity
Rmc - Mudcake resistivity
Rmf - Mud filtrate resistivity
Rmfe - Equivalent mud filtrate resistivity
RMA - Reduced Major Axis
Ro - Resistivity of the uninvaded formation when it is 100% saturated with water
Ro_c - Corrected resistivity of the uninvaded formation when it is 100% saturated with water
Ro_H - High Ro value
Ro_L - Low Ro value
Rs - Resistivity of shoulder beds
R_{SFL} - Resistivity of the spherically focused log
Rt - Resitivity of the uninvaded formation
Rw - Water resistivity
Rwa - Apparent water resistivity
Rwe - Equivalent water resistivity
Rxo - Resistivity of the flushed zone

S - Siemens

SBR - Shoulder bed restivity
SDL - Spectral Density Log
SFL - Spherically Focused Log
SFLA - Averaged Spherically Focused Log
SFLU - Unaveraged Spherically Focused Log
SGR - Spectral Gamma Ray
SGR - Total gamma ray count, including uranium
SH - Shale
SH NORM - Short Normal
SI - International System
SiO_2 - Silica
SMIN - Synthetic microinverse curve
SMNO - Synthetic micronormal curve
SN - Short normal
SO_4 - Sulfate
SP - Spontaneous potential or self potential
SPR - Single-point resistance
SPWLA - Society of Professional Well Log Analysts
SRG - Natural Gamma Ray Spectral Log (Gearheart)
SSP - Static SP

TD - Total depth
TDH - Texas Department of Health
TDS - Total dissolved solids
TDS_{actual} - Actual total dissolved solids
$TDS_{calculated}$ - Calculated total dissolved solids
TDS-Cw - Total dissolved solids - specific conductance
TDSMEEQU - TDS calculated using the equation of the line fitting the TDS-Cw graph and CW MEAS
Temp - Temperature
TENS - Tension
Th - Thorium
TNPH - Thermal neutron porosity
TNRIS - Texas Natural Resources Information System
TWC - Texas Water Commission
TWDB - Texas Water Development Board

U - Uranium
USGS - United States Geological Survey

var. - variation

VCAL - Volume of calcite
VCL - Volume of clay
Vmea - Voltage measured
V_{sh} - Volume of shale
VQTZ - Volume of quartz

W - Water
WC & ID - Water Control & Improvement District
WIDCO - Well Investment Development Co.
WLS - Weighted Least Squares
WSC - Water Supply Corporation

X - Variables in formulas

Y - Variables in formulas

Z - Atomic number
ZDL - Compensated Z-Densilog

2Z - Halliburton designation, electrode spacing
3iZ - Halliburton designation, electrode spacing
6FF28 - Schlumberger slimhole induction tool
6FF40 - Schlumberger deep induction curve
8FF34 - Schlumberger medium induction curve

LOGGING BOOKS

Appendix V

Modern Logging Books

Aguilera, R.: **Naturally Fractured Reservoirs**, Penn Well (1980), 703 pp. (800) 627-3212

Allaud, L. A. and Martin, M. H.: **Schlumberger, The History of a Technique**, John Wiley & Sons, Inc., New York City (1977), 333 pp.

Asquith, G. B.: **Log Analysis by Microcomputer**, Penn Well (1980), 104 pp.

Asquith, G. B. and Gibson, C.R.: **Basic Log Analysis for Geologists**, Methods in Exploration Series, AAPG, Tulsa (1982), 215 pp., AAPG, Box 979, Tulsa, Oklahoma 74101, (918) 584-2555.

Asquith, G. B.: **Handbook of Log Evaluation Techniques for Carbonate Reservoirs**, Methods in Exploration Series No. 5, AAPG, Tulsa (1985), 47 pp.

Atlas Wireline Services: **Fundamentals of Diplog Analysis**, Gulf Publishing Company, Houston (1988), 216 pp., Book Division, Dept MA, Box 2608, Houston, Texas 77252-2608, (713) 520-4444.

Bateman, R. M.: **Cased-Hole Log Analysis and Reservoir Performance Monitoring**, IHRDC Press, Boston (1984), 380 pp., IHRDC, 137 Newbury Street, Boston, Massachusetts 02116, (617) 536-0202.

Bateman, R. M.: **Log Quality Control**, IHRDC Press, Boston (1984), 398 pp.

Bateman, R. M.: **Open-Hole Log Analysis and Formation Evaluation**, IHRDC Press, Boston (1985), 647 pp.,

Brock, J.: **Analyzing Your Logs, Vol. I: Fundamentals of Open Hole Log Interpretation**, Petro-Media, Inc., Tyler (1984), 270 pp., 1729 Rose Road, Tyler, Texas 75701 (214) 592-8348, (also has video tapes).

Brock, J.: **Analyzing Your Logs, Vol. II: Advanced Open Hole Log Interpretation**, Petro-Media, Inc., Tyler (1984), 186 pp.

Brock, J.: **Applied Open-Hole Log Analysis**, Contributions in Petroleum Geology and Engineering, vol. 2, Gulf Publishing Company, Houston (1986), 292 pp.

Cased-Hole Logging, Oil and Gas Production Series, No. 5, The University of Texas at Austin, Austin (1981).

Crain, E. R.: **The Log Analysis Handbook, Vol. I--Quantitative Log Analysis Methods**, PennWell, Tulsa (1986), 684 pp.

Desbrandes, R.: **Encyclopedia of Well Logging**, Gulf Publishing Company, Houston (1985), 585 pp.

Dewan, J. T.: **Essentials of Modern Open-Hole Log Interpretation**, Penn Well, Tulsa (1983), 360 pp.

Doveton, J. H.: **Log Analysis of Subsurface Geology--Concepts and Computer Methods**, John Wiley & Sons, Inc., New York City (1986) 273 pp.

Ellis, D. V.: **Well Logging for Earth Scientists**, Elsevier Science Publishing Company, Inc., New York City (1987) 532 pp.

Etnyre, Lee M.: **Finding Oil and Gas from Well Logs**, Van Nostrand Reinhold (1989), 305 pp.

Foster, Norman H. and Beaumont, Edward A. (editors): **Formation Evaluation I: Log Evaluation**, AAPG, Tulsa, Treatise Reprint Series. 742 pp.

Foster, Norman H. and Beaumont, Edward A. (editors): **Formation Evaluation II: Log Interpretation**, AAPG, Tulsa, Treatise Reprint Series. 600 pp.

Galperin, E. I.: **Vertical Seismic Profiling and Its Exploration Potential**, P. Kennett, editor, E. Reidel Publishing Company, Dordrecht, Holland (1985).

Glossary of Terms & Expressions Used in Well Logging, second edition, Society of Professional Well Log Analysts, Houston (1984), 74 pp.

Gore, N.: **Wireline Operations**, Oil and Gas Production Series, J. Paxson, editor, The University of Texas at Austin, Austin (1984), 80 pp.

Gruner, Schlumberger, A.: **The Schlumberger Adventure**, Arco Publishing, Inc., New York City (1982).

Hallenburg, J. K.: **Geophysical Logging for Mineral and Engineering Applications**, Penn Well (1984), 264 pp.

Hearst, J. R. and Nelson, P. H.: **Well Logging for Physical Properties**, McGraw-Hill Book Company, New York City (1985), 576 pp.

Helander, D. P.: **Fundamentals of Formation Evaluation**, Oil and Gas Consultants International (OGCI) Publications, Tulsa (1983), 344 pp., OGCI, 4554 South Harvard, Tulsa, Oklahoma, 74135, (918) 742-7057.

Hilchie, D. W.: **Advanced Well Log Interpretation**, Douglas W. Hilchie Inc, Golden Co. (1989), variously paginated. 37 Perkins St., Prescott, Arizona 86301.

Hilchie, D. W.: **Applied Openhole Log Interpretation for Geologists and Engineers**, Douglas W. Hilchie Inc., Golden, Co. (1978), variously paginated.

Hilchie, D. W.: **The Geologic Well Log Interpreter**, Douglas W. Hilchie, Inc., Golden, Co., (1987), variously paginated.

Hilchie, D.W.: **Wireline: A History of the Well Logging and Perforating Business in the Oil Fields**, Boulder, Co. (1990), 200 pp.

Hill, A. Daniel: **Production Logging--Theoretical and Interpretive Elements:** Society of Petroleum Engineers, Monograph Volume 14, Dallas (1990), 154 pp., SPE Box 833836, Richardson, Tx. 75083 (800) 527-6863 (Texas) (214) 669-3377.

Hurst, A., Lovell, M. A. and Morton, A. C., editors: **Geological Applications of Wireline Logs**, Geological Society of London Special Publication (1990), No. 48, 357 pp. Order from AAPG.

Johnson, David E. and Pile, Kathryne E.: **Well Logging for the Nontechnical Person**, Penn Well (1988), 200 pp.

Jorden, J. R. and Campbell, F. L.: **Well Logging I--Rock Properties, Borehole Environment, Mud and Temperature Logging**, Society of Petroleum Engineers, Monograph Volume 9, Dallas (1984), 167 pp.

Jorden, J. R. and Cambell, F.L.: **Well Logging II--Electric and Acoustic Logging**, Society of Petroleum Engineers, Monograph Volume 10, Dallas (1986), 182 pp.

Kerzner, Mark: **Image Processing in Well Log Analysis**, IHRDC Press, Boston (1986), 140 pp.

Keys, W. Scott: **Borehole Geophysics Applied to Ground-Water Investigations**, USGS Open-File Report 87-539 (1988), 305 pp. NGWA Bookstore, Box 182039, Dept. 017, Columbus, Ohio 42018. TWI 02-E2

Kobranova, V.N. , English Translation by V.V. Kuznetsov: **Petrophysics**, Springer Verlag, New York (1990), 375 pp.

Labo, J.: **A Practical Introduction to Borehole Geophysics--An Overview of Wireline Well Logging Principles for Geophysicists**, Society of Exploration Geophysicists (1987), 330 pp., Box 702740, Tulsa, OK 74170-2740 (918) 493-3516.

Merkel, R. H.: **Well Log Formation Evaluation**, Continuing Education Course Note Series #14, AAPG, Tulsa (1983), 82 pp.

Open-Hole Logging, Oil and Gas Production Series #4, The University of Texas at Austin, Austin (1984), 87 pp.

Paillet, Frederick L. and Cheng, C.H.: **Acoustic Waves in Boreholes**, CRC Press, 000 Corporate Blvd. Boca Raton, Florida, 33431 407/994-0555 176 pp. $89.95

Pirson, S. J.: **Geologic Well Log Analysis**, third edition, Gulf Publishing Company, Houston (1983), 476 pp.

Repsold, H.: **Well Logging in Groundwater Development**, International Association of Hydrogeologist, International Contributions to Hydrogeology, v. 9, 136 pp. Verlag Heinz Heise GmbH & Co. KG (1989) 136 pp. Hannover, West Germany. Box 610407, D-3000 Hannover 61, West Germany.

Rider, M. H.: **The Geological Interpretation of Well Logs**, John Wiley & Sons, New York (1986) 175 pp.

Schlumberger: **Log Interpretation Principles/Applications**, Schlumberger Educational Services, Houston (1989), Document No. SMP-7017, variously paginated.

Schlumberger: **Cased Hole Log interpretation principles/Applications**, Schlumberger Educational Services Houston (1990), Document No. SMP-7025, variously paginated.

Sengel, E. W.: **Well Logging Handbook**, Institute for Energy Development (IED), Oklahoma City (1984), 168 pp.

Serra, O.: **Fundamentals of Well-Log Interpretation, Vol. I: The Acquisition of Logging Data**, Elsevier Science Publishing Company Inc., Developments in Petroleum Science, No. 15A, New York City (1984), 423 pp.

Serra, O.: **Fundamentals of Well-Log Interpretation, Vol. II: The Interpretation of Logging Data**, Elsevier Science Publishing Company Inc, Developments in Petroleum Science, No. 15B, Amsterdam (1986), 684 pp.

Serra, O.: **Sedimentary Environments From Wireline Logs**, Schlumberger Technical Services, Paris, Document No. M-081030/SMP-7008 (1985), 211 pp.

Theys, Phillips P.: **Log Data Acquisition and Quality Control**, Gulf Publishing, Houston (1991), 380 pp.

Tittman, J.: **Geophysical Well Logging**, excerpted from **Methods in Experimental Physics Vol. 24: Geophysics**, Academic Press, Inc., New York (1986), 175 pp.

Ward, Stanley H., editor: **Geotechnical and Environmental Geophysics, v. 1, Review and Tutorial**, Society of Exploration Geophysicists.

Ward, Stanley H., editor: **Geotechnical and Environmental Geophysics, v. 2, Environmental and Groundwater**, Society of Exploration Geophysicists.

Ward, Stanley H., editor: **Geotechnical and Environmental Geophysics, v. 3, Geotechnical**, Society of Exploration Geophysicists.

Well Log Response Chart, Penn Well (1983).

Wireline Logging Tool Catalog, second edition, Gulf Publishing Co. (1984) 450 pp.

Wireline Operations and Procedures, second edition, Vocational Training Series, American Petroleum Institute, Dallas (1983) No. 5.

Wyllie, M. R. J.: **The Fundamentals of Well Log Interpretation**, third edition, Academic Press, Inc., New York City (1963).

Old Electric Log Books

The Art of Ancient Log Analysis, Houston SPWLA (1979), 131 pp., plus reprints of 22 classic papers.
Society of Professional Well Log Analysts
6001 Gulf Freeway, Suite 129
Houston, Texas 77023 (713) 928-8925

Handbook of Well Log Analysis for Oil and Gas Foramtion Evaluation, Sylvain J. Pirson, Prentice-Hall, Inc.: Englewood Cliffs, New Jersey (1963), Chapters 7-12.

Old (pre-1958) Electrical Log Interpretation, Douglas Hilchie (1979), 163 pp.
Douglas Hilchie, Inc.
37 Perkins St.
Prescott, Az. 86301

Practical Log Analysis, a series of reprints from the Oil and Gas Journal, pp. 45-56 are on old logs.
Penn Well
Box 21288
Tulsa, Oklahoma 74121 800/627-3212

Prospecting with Old E-Logs, R. W. Frank (1986), 161 pp.
Schlumberger Educational Services
Box 2175
Houston, Texas 77252 (713) 928-4920